

**CENTRAL LIBRARY**

**Birla Institute of Technology & Science  
PILANI (Rajasthan)**

Call No. 629.1323  
D95A v.5

Accession No. 41718





# Aerodynamic Theory

**A General Review of Progress**

Under a Grant of the Guggenheim Fund  
for the Promotion of Aeronautics

**William Frederick Durand**

Editor-in-Chief —

**Volume V**

Div. N · Dynamics of the Airplane · B. Melvill Jones

Div. O · Airplane Performance · L. V. Kerber

With 133 Figures



Berlin · Julius Springer · 1935



**All rights reserved**  
**Printed in Germany**

## GENERAL PREFACE

During the active life of the Guggenheim Fund for the Promotion of Aeronautics, provision was made for the preparation of a series of monographs on the general subject of Aerodynamic Theory. It was realized that in its highly specialized form, as developed during the last twenty-five years, there was nowhere to be found a fairly comprehensive exposition of this theory, both general and in its more important applications to the problems of aeronautic design. The preparation and publication of a series of monographs on the various phases of this subject seemed, therefore, a timely undertaking, representing, as it is intended to do, a general review of progress during the past quarter century, and thus covering substantially the period since flight in heavier than air machines became an assured fact.

Such a present taking of stock should also be of value and of interest as furnishing a point of departure from which progress during coming decades may be measured.

But the chief purpose held in view in this project has been to provide for the student and for the aeronautic designer a reasonably adequate presentation of background theory. No attempt has been made to cover the domains of design itself or of construction. Important as these are, they lie quite aside from the purpose of the present work.

In order the better to suit the work to this main purpose, the first volume is largely taken up with material dealing with special mathematical topics and with fluid mechanics. The purpose of this material is to furnish, close at hand, brief treatments of special mathematical topics which, as a rule, are not usually included in the curricula of engineering and technical courses and thus to furnish to the reader, at least some elementary notions of various mathematical methods and resources, of which much use is made in the development of aerodynamic theory. The same material should also be acceptable to many who from long disuse may have lost facility in such methods and who may thus, close at hand, find the means of refreshing the memory regarding these various matters.

The treatment of the subject of Fluid Mechanics has been developed in relatively extended form since the texts usually available to the technical student are lacking in the developments more especially of interest to the student of aerodynamic theory. The more elementary treatment by the General Editor is intended to be read easily by the average technical graduate with some help from the topics comprised in Division A. The more advanced treatment by Dr. Munk will call

for some familiarity with space vector analysis and with more advanced mathematical methods, but will commend itself to more advanced students by the elegance of such methods and by the generality and importance of the results reached through this generalized three-dimensional treatment.

In order to place in its proper setting this entire development during the past quarter century, a historical sketch has been prepared by Professor Giacomelli whose careful and extended researches have resulted in a historical document which will especially interest and commend itself to the study of all those who are interested in the story of the gradual evolution of the ideas which have finally culminated in the developments which furnish the main material for the present work.

The remaining volumes of the work are intended to include the general subjects of: The aerodynamics of perfect fluids; The modifications due to viscosity and compressibility; Experiment and research, equipment and methods; Applied airfoil theory with analysis and discussion of the most important experimental results; The non-lifting system of the airplane; The air propeller; Influence of the propeller on the remainder of the structure; The dynamics of the airplane; Performance, prediction and analysis; General view of airplane as comprising four interacting and related systems; Airships, aerodynamics and performance; Hydrodynamics of boats and floats; and the Aerodynamics of cooling.

Individual reference will be made to these various divisions of the work, each in its place, and they need not, therefore, be referred to in detail at this point.

Certain general features of the work editorially may be noted as follows:

1. **Symbols.** No attempt has been made to maintain, in the treatment of the various Divisions and topics, an absolutely uniform system of notation. This was found to be quite impracticable.

Notation, to a large extent, is peculiar to the special subject under treatment and must be adjusted thereto. Furthermore, beyond a few symbols, there is no generally accepted system of notation even in any one country. For the few important items covered by the recommendations of the National Advisory Committee for Aeronautics, symbols have been employed accordingly. Otherwise, each author has developed his system of symbols in accordance with his peculiar needs.

At the head of each Division, however, will be found a table giving the most frequently employed symbols with their meaning. Symbols in general are explained or defined when first introduced.

2. **General Plan of Construction.** The work as a whole is made up of *Divisions*, each one dealing with a special topic or phase of the general

subject. These are designated by letters of the alphabet in accordance with the table on a following page.

The Divisions are then divided into chapters and the chapters into sections and occasionally subsections. The Chapters are designated by Roman numerals and the Sections by numbers in bold face.

The Chapter is made the unit for the numbering of sections and the section for the numbering of equations. The latter are given a double number in parenthesis, thus (13.6) of which the number at the left of the point designates the section and that on the right the serial number of the equation in that section.

Each page carries at the top, the chapter and section numbers.

**W. F. Durand**

Stanford University, California  
January, 1934.

# GENERAL LIST OF DIVISIONS WITH AUTHORS

## Volume I.

### A. Mathematical Aids

- W. F. DURAND — Professor (Emeritus) of Mechanical Engineering, Stanford University, Calif., Member of the National Advisory Committee for Aeronautics.

### B. Fluid Mechanics, Part I

W. F. DURAND

### C. Fluid Mechanics, Part II

- MAX M. MUNK — Lecturer in Aerodynamics at the Catholic University of America, Washington, D. C., and Technical Editor of the "Aero Digest".

### D. Historical Sketch

- R. GIACOMELLI — Lecturer in History of Mechanics at the University of Rome, Italy, and Editor of "L'Aerotecnica".

with the collaboration of

- E. PISTOLESI — Professor of Mechanics at the Royal School of Engineering at Pisa, Italy, and Editor-in-Chief of "L'Aerotecnica".

## Volume II.

### E. General Aerodynamic Theory—Perfect Fluids

- TH. VON KÁRMÁN — Director of the Guggenheim Aeronautics Laboratory, California Institute of Technology, Pasadena, Calif., and formerly Director of the Aerodynamic Institute, Aachen, Germany.

- J. M. BURGERS — Professor of Aero- and Hydrodynamics at the Technische Hoogeschool at Delft, Holland.

## Volume III.

### F. The Theory of Single Burbling

- C. WITOSZYŃSKI — Professor of Aerodynamics at the Warsaw Polytechnical School and Director of the Warsaw Aerodynamic Institute, Poland.

- M. J. THOMPSON — Assistant Professor of Aeronautical Engineering at the University of Michigan, Ann Arbor, Mich.

### G. The Mechanics of Viscous Fluids

- L. PRANDTL — Professor in Applied Mechanics at the University of Göttingen, Germany, and Director of the Kaiser Wilhelm Institute for Fluid Research.

### H. The Mechanics of Compressible Fluids

- G. I. TAYLOR — Yarrow Research Professor of the Royal Society, Fellow of Trinity College, Cambridge, England.

- J. W. MACCOOLL — Research Officer, Department of External Ballistics, Ordnance Committee, Woolwich, England.

### I. Experimental Methods—Wind Tunnels

- A. TOUSSAINT — Director of the Aerodynamic Laboratory, Saint-Cyr-l'École, France.

- E. JACOBS — Associate Aeronautical Engineer, in charge of the National Advisory Committee for Aeronautics' variable-density wind tunnel, Langley Field, Virginia.

## Volume IV.

**J. Applied Airfoil Theory**

A. BETZ — Professor at the University and Director of the Aerodynamic Research Institute at Göttingen, Germany.

**K. Airplane Body (Non-Lifting System) Drag and Influence on Lifting System**

C. WIESELSBERGER — Professor of Aerodynamics and Director of the Aerodynamic Institute, Technische Hochschule, Aachen, Germany.

**L. Airplane Propellers**

H. GLAUERT<sup>1</sup> — Past Fellow of Trinity College, Cambridge, England; Principal Scientific Officer at the Royal Aircraft Establishment, Farnborough.

**M. Influence of the Propeller on other Parts of the Airplane Structure**

C. KONING — Rijks-Studiedienst voor de Luchtvaart, Amsterdam, Holland.

## Volume V.

**N. Dynamics of the Airplane**

B. MELVILL JONES — Professor of Aeronautical Engineering in the University of Cambridge, England, Member of the Aeronautical Research Committee of Great Britain.

**O. Airplane Performance**

L. V. KERBER — Former Chief Aerodynamics Branch Materiel Division, U. S. Army Air Corps, and former Chief, Engineering Section Aeronautics Branch, Department of Commerce.

## Volume VI.

**P. Airplane as a Whole—General View of Mutual Interactions Among Constituent Systems**

W. F. DURAND<sup>2</sup> — Professor (Emeritus) of Mechanical Engineering, Stanford University, Calif., Member of the National Advisory Committee for Aeronautics.

**Q. Aerodynamics of Airships**

MAX M. MUNK — Lecturer in Aerodynamics at the Catholic University of America, Washington, D. C., and Technical Editor of the "Aero Digest".

**R. Performance of Airships**

K. ARNSTEIN — Chief Engineer of the Goodyear Zeppelin Company, Akron, Ohio.

W. KLEMPERER — Research Engineer of the Goodyear Zeppelin Company, Akron, Ohio.

**S. Hydrodynamics of Boats and Floats**

E. G. BARRILLON — Director of the Naval Experimental Tank, Paris, France.

**T. Aerodynamics of Cooling**

H. L. DRYDEN — Physicist in the United States Bureau of Standards, Chief of the Aerodynamics Section, Washington, D. C.

<sup>1</sup> Deceased August 4, 1934.

<sup>2</sup> In the original plan, it was expected that this Division would be prepared by Professor M. Panetti of the R. Scuola di Ingegneria of Turin. Unfortunately, at the last, Professor Panetti found himself unable to give the needed time for this work, and in order not to delay publication, the General Editor has undertaken to prepare a brief treatment of the subject.

# CONTENTS

## DIVISION N

### DYNAMICS OF THE AIRPLANE

By **B. Melvill Jones,**

Professor of Aeronautical Engineering in the University of Cambridge, England,  
Member of the Aeronautical Research Committee of Great Britain

CHAP.		PAGE
	PREFACE . . . . .	1
I.	STEADY MOTIONS AND LIMITING ACCELERATIONS. . . . .	5
	1. Introduction <i>p. 5</i> — 2. Symmetric Flight <i>p. 5</i> .	
	A. Steady Straight Symmetric Flight . . . . .	6
	3. Principal Forces Involved <i>p. 6</i> — 4. Dimensionless Coefficients <i>p. 7</i> — 5. Horizontal Flight <i>p. 7</i> — 6. Indicated Air Speed <i>p. 9</i> — 7. Gliding Flight <i>p. 10</i> — 8. Some Aspects of the Landing Problem <i>p. 11</i> — 9. Climbing Flight <i>p. 12</i> .	
	B. Accelerated Symmetric Flight . . . . .	13
	10. Introduction <i>p. 13</i> — 11. Radius of Curvature of the Flight Path <i>p. 14</i> — 12. Minimum Radius of Curvature <i>p. 14</i> — 13. Minimum Radius of Curvature in Terms of Stalling Speed <i>p. 15</i> — 14. Minimum Radius and Rapid Manœuvres <i>p. 15</i> — 15. Apparent Gravity and Load Factors <i>p. 16</i> — 16. Measurement of Load Factors <i>p. 16</i> — 17. Maximum Load Factor <i>p. 17</i> .	
	C. Straight Asymmetric Flight . . . . .	18
	18. Steady Straight Side-slip <i>p. 18</i> — 19. Relation of Side-force to Side-slip <i>p. 18</i> — 20. Relation of Side-slip to "Bank" <i>p. 19</i> .	
	D. Circling Flight . . . . .	19
	21. The Flat Turn <i>p. 19</i> — 22. Side-slip in the Flat Turn <i>p. 20</i> — 23. The True-banked Turn <i>p. 20</i> — 24. Stalling Speed in a True- banked Turn <i>p. 21</i> — 25. Power Required in a True-banked Turn <i>p. 21</i> — 26. Horizontal Turn of Minimum Radius <i>p. 21</i> — 27. Aero- dynamic Moments <i>p. 22</i> .	
II.	SYMMETRIC OR PITCHING MOMENTS . . . . .	22
	1. Pitching Moments and Static Stability <i>p. 22</i> — 2. The Geo- metric Mean Chord <i>p. 23</i> — 3. The Air-Reactions on an Isolated Wing <i>p. 23</i> — 4. Functions of the Tail <i>p. 24</i> — 5. Fixed Tail and Elevators <i>p. 25</i> — 6. Effect of C.G. Position on Static Stability <i>p. 26</i> — 7. Dimensionless Coefficients <i>p. 27</i> — 8. C.G. Positions for Neutral Equilibrium <i>p. 27</i> — 9. A Relation Between Control and Stability <i>p. 28</i> — 10. Experiments on Complete Models <i>p. 29</i> .	
	A. Contributions of Separate Parts of the Aeroplane to Pitching Moments	29
	11. Introduction <i>p. 29</i> — 12. Pitching Moments from Tail and Wings—C.G. on Wing Chord <i>p. 30</i> — 13. Joukowski's Theoretical	

Values for  $[dk_M/dk_L]_v$  *p.* 31 — 14. Pitching Moments When the C.G. is not on Wing Chord *p.* 32 — 15. Direct Contribution of the Airscrew to Pitching Moments *p.* 34 — 16. Numerical Values—Airscrew Contribution *p.* 35 — 17. Contribution of the Body and Minor Parts to Pitching Moments *p.* 36.

B. Forces on Tail and Interference Factors . . . . . 36

18. Statement of Problem *p.* 36 — 19. Interference Between Aeroplane and Tail *p.* 37 — 20. Hinge Moments and Free Elevators *p.* 38 — 21. Wing-tail Interference *p.* 39 — 22. Airscrew-tail Interferences *p.* 40 — 23. Body-tail Interference *p.* 40 — 24. Airscrew-wing Interference *p.* 40 — 25. Interference Problems Discussed *p.* 41 — 26. Numerical Illustrations *p.* 41 — 27. Pitching Moments at Very High Speeds *p.* 42 — 28. Pitching Moments in Stalled Flight *p.* 43.

C. Pitching Moments in Circling Flight ( $M_q$ ) . . . . . 44

29. Introduction *p.* 44 — 30. The Tail in Circling Flight *p.* 44 — 31. The Derivative  $M_q$  *p.* 45 — 32. The Dimensionless Coefficient ( $k_{mq}$ ) *p.* 45 — 33. Contribution of the Wings to  $M_q$  *p.* 46 — 34. Direct Contribution of the Screw to  $M_q$  *p.* 46 — 35. Influence of Airscrew Slip-Stream on Tail *p.* 47 — 36. Numerical Illustration *p.* 47.

D. Experimental Methods of Measuring  $M_q$  . . . . . 48

37. Whirling Arm Experiment *p.* 48 — 38. The Free Oscillation Method *p.* 48 — 39. The Forced Oscillation Method *p.* 49 — 40. Relations between  $\mu$ ,  $M_q$ , and  $M_{\dot{\alpha}}$  *p.* 49 — 41. Experimental Separation of  $M_q$  and  $M_{\dot{\alpha}}$  *p.* 51 — 42. Influence of the Screw on  $M_{\dot{\alpha}}$  *p.* 52.

E. Experimental Results for  $M_q$  . . . . . 52

43. Normal Flight *p.* 52 — 44.  $M_q$  in Stalled Flight *p.* 53.

F. The Geometric Mean Chord . . . . . 54

45. Statement of Problem *p.* 54 — 46. The Geometric Mean Chord Defined *p.* 54 — 47. Example of Application to a Biplane *p.* 56 — 48. Wings of Non-Rectangular Plan Form and with Dihedral Angle *p.* 56 — 49. Twisted and Tapered Wings *p.* 57.

III. THE ASYMMETRIC OR LATERAL MOMENTS . . . . . 57

1. Introduction *p.* 57 — 2. Axes *p.* 57 — 3. Symbols *p.* 57 — 4. Dimensionless Coefficients *p.* 58 — 5. Controls *p.* 59 — 6. Independent Variables Which Govern Asymmetric Moments *p.* 59.

A. Effects of Side-Slip . . . . . 59

7. Dihedral Angle *p.* 59 — 8. Theoretical Estimates of Rolling Moments Due to Side-Slip *p.* 60 — 9. Theoretical Estimate of Yawing Moment Due to Side-Slip *p.* 61 — 10. Conversion to Chord Axes *p.* 61 — 11. Omissions in the Assumptions *p.* 61 — 12. Experimental Measurements of the Effects of Side-Slip on an Isolated Wing *p.* 62 — 13.  $k_{lv}$  in Stalled Flight *p.* 62 — 14. Effect of Side-Slip on Body, Fin and Rudder *p.* 63 — 15. Experimental Values of  $k_{lv}$  and  $k_{nv}$  for Complete Model Aeroplanes *p.* 65 — 16. Effects of Large Side-Slips *p.* 67.



B. Theoretical Estimates of Moments due to Angular Velocities of Roll and Yaw . . . . .	67
17. Moments Due to Rate of Yaw <i>p.</i> 67 — 18. The Derivatives $k_{lr}$ and $k_{nr}$ <i>p.</i> 69 — 19. Moments Due to Rate of Roll ( <i>p.</i> 70 — 20. Approximate Formulae for the Rotary Derivatives <i>p.</i> 71 — 21. Change of Axes <i>p.</i> 71 — 22. Calculations of Rotary Derivatives Using Chord Axes Throughout <i>p.</i> 72 — 23. Rotary Derivatives Due to Body, Fin and Rudder <i>p.</i> 73.	
C. Experimental Methods of Measuring the Rotary Derivatives . . .	73
24. Oscillation Methods <i>p.</i> 73 — 25. Continuous Rotation Methods <i>p.</i> 73.	
D. Discussion of the Results of Experiments on the Rotary Derivatives at Incidences of Normal Flight . . . . .	74
26. Comparison Between Oscillation and Continuous Rotation Experiments <i>p.</i> 74 — 27. Comparison Between Experiment and "Strip" Calculation <i>p.</i> 74 — 28. Influence of Body, Fin and Rudder <i>p.</i> 75 — 29. Comparison Between Model and Full Scale Experiments <i>p.</i> 75 — 30. Effect of Large Angular Velocities <i>p.</i> 75 — 31. Summary-Rotary Derivatives in Normal Flight <i>p.</i> 75.	
E. Rotary Derivatives in Stalled Flight. . . . .	76
32. Introduction <i>p.</i> 76 — 33. Theoretical Estimate of Moments Due to Finite Rates of Roll <i>p.</i> 76 — 34. Comparison Between Strip Hypothesis and of Experiments with Continuous Finite Rates of Roll <i>p.</i> 78 — 35. Comparison Between Strip Hypothesis and Experiments with Continuous Yawing <i>p.</i> 79 — 36. Comparison Between Continuous Rotation and Oscillation Experiments <i>p.</i> 80 — 37. Auto-Rotation and Wing Tip Slots <i>p.</i> 81 — 38. Collection of Typical Values for the Six Asymmetric Moment Derivatives <i>p.</i> 81.	
F. The Asymmetric Controls. . . . .	82
39. Balanced Controls <i>p.</i> 82 — 40. Aileron Rolling Moments <i>p.</i> 83 — 41. Aileron Yawing Moments <i>p.</i> 83 — 42. Ailerons and Wing Tip Slots <i>p.</i> 84 — 43. The Rudder in Normal Flight <i>p.</i> 84 — 44. The Rudder in Stalled Flight <i>p.</i> 85.	
IV. FREE FLIGHT-SIMPLE DISCUSSION . . . . .	85
1. Introduction <i>p.</i> 85 — 2. Lanchester's Idealized Flight Path <i>p.</i> 86 — 3. Equation of the Flight Path <i>p.</i> 87 — 4. Forms of the Flight Path <i>p.</i> 88 — 5. Comparison with the Path of a Real Aeroplane <i>p.</i> 89.	
A. The Slow Oscillation of Small Amplitude . . . . .	90
6. The Ideally Simple Oscillation <i>p.</i> 90 — 7. Form of the Oscillation of Small Amplitude <i>p.</i> 90 — 8. Comparison with the Oscillation of a Real Aeroplane <i>p.</i> 91 — 9. The Effect of $M_q$ on the Period <i>p.</i> 91 — 10. The Damping of the Oscillation <i>p.</i> 94 — 11. Influence of the Airscrew <i>p.</i> 95 — 12. Other Factors which Influence the Oscillation <i>p.</i> 95 — 13. Gliding and Climbing Flight <i>p.</i> 95 — 14. The Unstable Aeroplane <i>p.</i> 95.	

B. The Rapid Incidence Adjustment . . . . .	96
15. Simplifying Assumptions <i>p.</i> 96 — 16. Sudden Change of Incidence <i>p.</i> 96 — 17. Sudden Application of Elevators <i>p.</i> 98 — 18. Solutions with More Complete Assumptions <i>p.</i> 99 — 19. Discussion of the Solutions <i>p.</i> 101 — 20. Unstable Aeroplanes <i>p.</i> 102 — 21. Stable Aeroplanes <i>p.</i> 103 — 22. Dimensionless Forms of the Quadratic for $\lambda$ <i>p.</i> 103.	
C. Asymmetric Motions . . . . .	104
23. Statement of the Problem <i>p.</i> 104 — 24. The True-banked Steady Turn <i>p.</i> 105 — 25. The Steady Turn with Side-Slip <i>p.</i> 107 — 26. Ascending and Descending Steady Turns <i>p.</i> 108.	
D. Small Disturbances from Straight Flight . . . . .	109
27. Introduction <i>p.</i> 109 — 28. The Rapid Damping of Rolling Motions <i>p.</i> 110 — 29. The Slow Spiral Motion <i>p.</i> 111 — 30. More Accurate Estimate of the Spiral Motion <i>p.</i> 113 — 31. The Oscillation of a Statically Stable Aeroplane <i>p.</i> 113 — 32. The Oscillation of a Statically Neutral Aeroplane <i>p.</i> 116 — 33. The Oscillation of a Statically Unstable Aeroplane <i>p.</i> 117 — 34. The Two Possible Forms of Instability <i>p.</i> 117.	
E. The Stalled Aeroplane . . . . .	118
35. The Stalled Aeroplane-Symmetric Motion <i>p.</i> 118 — 36. The Stalled Aeroplane-Asymmetric Motion <i>p.</i> 119.	
V. THE EQUATIONS OF MOTION WITH SOLUTIONS FOR SMALL DISTURBANCES FROM STEADY SYMMETRIC FLIGHT . . . .	121
A. Axes, Symbols and Equations of Motion . . . . .	121
1. Axes <i>p.</i> 121 — 2. Orientation <i>p.</i> 122 — 3. Symbols <i>p.</i> 122 — 4. Effect of Gravity <i>p.</i> 123 — 5. The Equations of Motion <i>p.</i> 123 — 6. Dependence of the Air-Reactions on the Velocity Components <i>p.</i> 124 — 7. Influence of $\dot{W}$ on $M$ <i>p.</i> 125 — 8. Step-by-Step Methods of Solution <i>p.</i> 125 — 9. Steady Motions <i>p.</i> 126.	
B. Small Disturbances from Steady Symmetric Flight . . . . .	126
10. Historical <i>p.</i> 126 — 11. Moderate Finito Disturbances <i>p.</i> 127 — 12. Force and Moment Derivatives <i>p.</i> 127 — 13. Shortened Notation <i>p.</i> 128 — 14. The Applied Forces <i>p.</i> 128 — 15. The Mass Accelerations <i>p.</i> 129 — 16. Separation into Symmetric and Asymmetric Groups <i>p.</i> 129 — 17. The Equations of Motion Rearranged <i>p.</i> 130.	
C. Conversion to Dimensionless Form . . . . .	130
18. Introduction <i>p.</i> 130 — 19. The Parameter " $\mu$ " <i>p.</i> 131 — 20. The Dimensionless System Explained <i>p.</i> 132 — 21. The Equations of Motion in Dimensionless Form <i>p.</i> 134.	
D. The Solutions of the Equations of Motion . . . . .	135
22. Introductory <i>p.</i> 135 — 23. The Complementary Function <i>p.</i> 135 — 24. The Quartic Equation for $\lambda$ <i>p.</i> 136 — 25. The Ratios $u_1 : w_1 : q_1$ <i>p.</i> 136 — 26. The Four Arbitrary Constants <i>p.</i> 137 — 27. General Form of the Complementary Function <i>p.</i> 137 — 28. Initial Conditions <i>p.</i> 137 — 29. Solutions of the Asymmetric Group <i>p.</i> 138 — 30. Complex Roots <i>p.</i> 138 — 31. Complex Roots in the Asymmetric Equations <i>p.</i> 141.	

## E. Complete Solution with Constant Applied Control Couples . . . 141

32. No Roots Zero—Symmetric Group *p.* 141 — 33. No Roots Zero—The Asymmetric Group *p.* 142 — 34. One Root Zero—The Symmetric Group *p.* 142 — 35. One Root Zero—The Asymmetric Group *p.* 143 — 36. Two Roots Zero *p.* 144 — 37. Case of Equal Roots *p.* 144.

## VI. NUMERICAL SOLUTION OF THE SYMMETRIC EQUATIONS OF CHAPTER V. . . . . 144

1. Introduction *p.* 144 — 2. Notation and Axes *p.* 144 — 3. Evaluation of the Derivatives *p.* 145 — 4. The Force-Velocity Derivatives *p.* 146 — 5. Force-Rotary Derivatives *p.* 147 — 6. Moment-Velocity Derivatives *p.* 148 — 7. Moment-Rotary Derivatives *p.* 148 — 8. The Derivative  $m_w$  *p.* 148 — 9. Choice of Numerical Examples *p.* 149 — 10. The Derivatives *p.* 149 — 11. The Examples Specified *p.* 150 — 12. The Constants Tabulated *p.* 151.

## A. The Complementary Function . . . . . 152

13. The Equations of Motion *p.* 152 — 14. The Quartic for  $\lambda$  *p.* 152 — 15. Information from Inspection of the Quartic for  $\lambda$  *p.* 152 — 16. Values of  $\lambda$  and of the Ratio  $u_1 : w_1 : q_1$  *p.* 154.

## B. Complete Solutions and Initial Conditions . . . . . 157

17. Choice of Initial Conditions *p.* 157 — 18. Complete Solutions in Dimensionless Form *p.* 160 — 19. Conditions to which the Solutions Apply *p.* 160 — 20. The Solutions Discussed *p.* 161 — 21. Conversion to Ordinary Units *p.* 162 — 22. The Solutions In Terms of Other Variables *p.* 163 — 23. Graphs of the Solutions Plotted Against Time *p.* 163.

## C. The Graphs Discussed . . . . . 164

24. Introductory *p.* 164 — 25. Cruising Speed—Elevator Movement *p.* 164 — 26. Cruising Speed—Vertical Gust *p.* 165 — 27. Cruising Speed—Horizontal Gust *p.* 165 — 28. Slow Speed—Unstalled *p.* 165 — 29. Stalled Flight *p.* 168.

## D. Approximations Applicable to Normal Flight Only . . . . . 168

30. Statement of the Problem *p.* 168 — 31. The Quartic of  $\lambda$  *p.* 169 — 32. Equations of Motion Referred to Wind Axes *p.* 170 — 33. Gliding Flight—Engine Off *p.* 171 — 34. Numerical Values *p.* 172 — 35. The Large Quadratic Root *p.* 172 — 36. The Small Quadratic Root *p.* 173.

## E. Level Flight . . . . . 174

37. Introductory *p.* 174 — 38. Effect of Airscrew on  $m_w$  *p.* 175 — 39. Effect of Airscrew on  $m_q$  and  $m_w$  *p.* 175 — 40. The Effect of the Airscrew on  $x_w$ ,  $z_u$ ,  $z_w$  *p.* 176 — 41. The Value of  $dT/dV$  for an Airscrew *p.* 176 — 42. The Effect of Airscrew on  $x_u$  *p.* 177 — 43. Effect of Airscrew on  $m_u$  *p.* 178 — 44. Effect of Airscrew on the Coefficients  $B$ ,  $C$  and  $E$  in the Quartic for  $\lambda$  *p.* 179 — 45. Effect of Airscrew on the Damping of the Slow Motion *p.* 180 — 46. Numerical Values *p.* 180 — 47. The Effect of Freeing the Elevators *p.* 181.

VII. NUMERICAL SOLUTIONS OF THE ASYMMETRIC EQUATIONS 182

1. Introduction *p.* 182 — 2. Notation and Axes *p.* 182 — 3. Choice of Illustrative Examples *p.* 183 — 4. Cruising Speed *p.* 183 — 5. Slow Speed *p.* 184 — 6. Stalled Flight *p.* 184 — 7. Table of Dimensionless Constants *p.* 185.

A. Complementary Function . . . . . 185

8. The Equations of Motion *p.* 185 — 9. The Quartic for  $\lambda$  *p.* 185 — 10. Values of  $\lambda$  and of the Ratios  $v : p : r$  *p.* 185 — 11. The Large Real Root *p.* 187 — 12. The Small Real Root *p.* 187 — 13. The Complex Root *p.* 187.

B. Complete Solutions and Initial Conditions . . . . . 188

14. Choice of Initial Conditions *p.* 188 — 15. Complete Solutions in Dimensionless Form *p.* 188 — 16. Conditions to which the Solutions are Applicable *p.* 188 — 17. Conversion to Ordinary Units *p.* 189 — 18. Graphs of the Solutions Plotted Against Time *p.* 191.

C. The Graphs Discussed . . . . . 192

19. Initial Rate of Roll *p.* 192 — 20. Applied Control Moments *p.* 193 — 21. Applied Rolling Moment *p.* 193 — 22. Applied Yawing Moments *p.* 196 — 23. Rolling and Yawing Moments Applied Simultaneously *p.* 196 — 24. Stalled Flight *p.* 197 — 25. Uncertainty of the Values of the Derivatives in Stalled Flight *p.* 198 — 26. Scale Effect on a Thick Wing in Stalled Flight *p.* 199.

D. Information by Inspection of the Quartic for  $\lambda$  . . . . . 199

27. Condition for Complete Stability *p.* 199 — 28. The Large Root *p.* 199 — 29. The Small Root *p.* 200 — 30. Approximate Values of the Complex Roots *p.* 200 — 31. Level and Climbing Flight *p.* 201.

E. Changes of Dihedral Angle and Fin Area . . . . . 202

32. Introduction *p.* 202 — 33. Spiral Instability *p.* 202 — 34. Increasing Oscillations *p.* 202 — 35. Spinning Instability *p.* 203 — 36. Summary *p.* 203.

VIII. THE SPIN. . . . . 204

1. Introduction *p.* 204 — 2. Experimental Methods *p.* 205 — 3. Theoretical Calculations *p.* 206 — 4. Notation and the Equations of Motion *p.* 207.

A. Autorotation. . . . . 208

5. Rotation about a Fixed Axis *p.* 208 — 6. Autorotation Defined *p.* 209 — 7. Latent Autorotation *p.* 209 — 8. Autorotation Rates *p.* 210.

B. Pitching Moments . . . . . 210

9. The Centrifugal Pitching Moment *p.* 210 — 10. The Origin of the Centrifugal Pitching Moment *p.* 211 — 11. Balance of Pitching Moments *p.* 213.

C. The Remaining Degrees of Freedom . . . . . 214

12. Freedom to Slide along the Axis of Rotation *p.* 214 — 13. Freedom to Leave the Axis of Rotation *p.* 214 — 14. Two Final Degrees of Freedom *p.* 215.

CHAP.	PAGE
D. Effects of Yaw on the Spin . . . . .	215
15. The Meaning of Yaw <i>p. 215</i> — 16. The Relation between Yaw and Side-Slip <i>p. 216</i> — 17. The Effects of Yaw on Rate of Spin <i>p. 216</i> — 18. The Air Yawing Moment <i>p. 217</i> — 19. The Centrifugal Yawing Moment <i>p. 218</i> .	
E. The Free Spin of Real Aeroplanes. . . . .	219
20. Rotation Rate and Incidence <i>p. 219</i> — 21. Radius and Rate of Descent <i>p. 219</i> — 22. Load Factor and Incidence <i>p. 220</i> — 23. Critical Nature of Transition to Flat Spin <i>p. 220</i> — 24. Reasons for Failure of Ailerons and Rudder <i>p. 221</i> .	
REFERENCES . . . . .	221

## DIVISION O

## AIRPLANE PERFORMANCE

By L. V. Kerber,

Former Chief Aerodynamics Branch Material Division, U.S. Army Air Corps, and  
former Chief, Engineering Section Aeronautics Branch, Department of Commerce

CHAP.	PAGE
EDITOR'S PREFACE . . . . .	223
I. FUNDAMENTAL RELATIONS . . . . .	224
1. Introduction <i>p. 224</i> — 2. Aerodynamics <i>p. 225</i> — 3. Engine Power <i>p. 226</i> — 4. Standard Atmosphere <i>p. 226</i> .	
II. BASIC COMPUTATIONS . . . . .	227
A. Power Required . . . . .	227
1. Data Necessary <i>p. 227</i> — 2. Lift, Lift Coefficient and Speed <i>p. 227</i> — 3. Induced Drag and Equivalent Monoplane Aspect Ratio <i>p. 230</i> — 4. Profile Drag of Airfoils and Its Variation <i>p. 232</i> — 5. Structural Drag and Its Variation <i>p. 233</i> — 6. Total Drag and Power Required at Sea Level and at Altitude <i>p. 239</i> .	
B. Power Available . . . . .	243
7. Power Curves of Engines <i>p. 243</i> — 8. Choice of Propeller Diameter <i>p. 244</i> — 9. Design $v/nD$ and Maximum Efficiency <i>p. 245</i> — 10. Variation of Engine Speed and Power at Sea Level (Full Throttle) <i>p. 246</i> — 11. Variation in Propeller Efficiency <i>p. 247</i> — 12. Power Available at Sea Level and at Altitude (First Method) <i>p. 257</i> — 13. Power Available at Sea Level and Altitude (Second Method) <i>p. 248</i> .	
III. PERFORMANCE FROM POWER GRAPHS . . . . .	250
1. High Speed <i>p. 250</i> — 2. Rate of Climb <i>p. 252</i> — 3. Ceilings <i>p. 255</i> — 4. Angle of Climb <i>p. 255</i> — 5. Time of Climb <i>p. 256</i> — 6. Power Required <i>p. 256</i> (A. Power Required by Summarizing Component Drags <i>p. 257</i> — B. Power Required by Estimating $A$ Directly <i>p. 258</i> ) — 7. Power Available <i>p. 261</i> (A. Power Available from Variation of R.P.M. with Speed <i>p. 261</i> — B. Power Available from ratio of Thrust Power <i>p. 263</i> ) — 8. Performance <i>p. 264</i> .	

## NOTATION

The following table comprises a list of the principal notations employed in the present Volume. Notations not listed are either so well understood as to render mention unnecessary, or are only rarely employed and are explained as introduced. Where occasionally a symbol is employed with more than one meaning, the local context will make the significance clear.

Occasional departures from this general scheme of notation may be noted, but where such occur, the adjacent text will make the matter clear.

### DIVISION N

$X, Y, Z$	Coordinate axes; generally, $X$ longitudinal, $Y$ transverse and $Z$ vertical. Note distinction between <i>wind</i> and <i>chord</i> axes
$\Theta, \Phi, \Psi$	Angular coordinates, generally $\Theta$ displacement of $X$ axis, $\Phi$ that of $Y$ and $\Psi$ that of $Z$
$i, j$	Coordinates of c.g. relative to screw axis and plane of screw
$c$	Chord or geometrical mean chord
$H$	Metacentric ratio,      II 8
$s$	Semi-span of wing
$S$	Wing area, area in general
$\alpha$	Angle of incidence
$\alpha_0$	Angle of incidence when flying straight and steady
$\alpha_i$	Induced angle of incidence
$A_1$	Angle of incidence when $L = W$
$\beta$	Angle of yaw
$\gamma$	Dihedral angle, also $\tan^{-1} D/L$
$\varepsilon$	Angle of "downwash" at tail
$\eta$	Elevator setting
$\Theta$	Inclination of path to horizontal
$\Phi$	Angle of roll (about $X$ ); angle of bank
$\varphi$	Used for $\Phi$ when roll or bank is small
$\xi$	Angular displacement of starboard aileron
$\zeta$	Angular displacement of rudder
$U, V, W$	Velocities along $X, Y, Z$
$u, v, w$	Often or usually small variations from steady values of $U, V, W$
$V, v$	Side-slip velocity
$v$	Extra velocity in propeller slipstream
$V$	Velocity of c.g. of plane in direction of motion
$V_s$	Stalling speed
$P, Q, R$	Angular velocities about $X, Y, Z$ ,      V 4 $P$ , rate of roll $Q$ , rate of pitch $R$ , rate of yaw
$p, q, r$	Usually small variations from steady values of $P, Q, R$ . Sometimes used instead of $P, Q, R$
$\Omega$	Angular velocity of spin,      VIII
$\mathbf{v} \ \mathbf{v} \ \mathbf{v}$	Forces along axes of $X, Y, Z$

# CONTENTS

XV

CHAP.

PAGE

IV. BAIRSTOW'S METHOD . . . . .	267
1. General Outline of Method <i>p. 267</i> — 2. Speed of Climb <i>p. 269</i> .	
V. LESLEY-REID METHOD . . . . .	270
1. Introduction <i>p. 270</i> — 2. Data Required <i>p. 270</i> — 3. Description of Method. Level Flight <i>p. 271</i> — 4. Example of Performance Calculations <i>p. 274</i> .	
VI. THE OSWALD METHOD . . . . .	279
1. Parameters <i>p. 280</i> — 2. Assumptions <i>p. 281</i> — 3. Theory <i>p. 282</i> — 4. Charts <i>p. 285</i> .	
VII. EMPIRICAL-THEORETICAL METHOD . . . . .	294
VIII. LOGARITHMIC DIAGRAMS . . . . .	296
1. Introduction <i>p. 296</i> — 2. Theory <i>p. 297</i> — 3. Determination of Performance <i>p. 303</i> .	
IX. RANGE AND ENDURANCE . . . . .	305
1. Range <i>p. 305</i> — 2. Endurance <i>p. 311</i> — 3. Breguet's Formulas <i>p. 312</i> .	
X. INFLUENCE OF PRINCIPLE FACTORS ON PERFORMANCE. . . . .	315
1. Weight <i>p. 315</i> — 2. Power <i>p. 316</i> — 3. Wing Area <i>p. 317</i> — 4. Span of Equivalent Monoplane <i>p. 318</i> — 5. Airfoil Characteristics <i>p. 318</i> — 6. Parasite Resistance <i>p. 319</i> — 7. Propeller Characteristics <i>p. 319</i> — 8. Supercharging and Throttling <i>p. 320</i> — 9. Choice of Altitude Propeller <i>p. 320</i> — 10. Power Absorbed by Any Propeller <i>p. 321</i> — 11. Power Available at Sea Level from Special Propeller <i>p. 323</i> — 12. Example <i>p. 323</i> .	
XI. LIMITS OF PERFORMANCE . . . . .	324
1. Speed Range <i>p. 324</i> — 2. High Speed <i>p. 328</i> — 3. Initial Rate of Climb <i>p. 329</i> — 4. Absolute Ceiling <i>p. 330</i> — 5. Range <i>p. 332</i> — 6. Endurance <i>p. 333</i> .	
APPENDIX I. THE INDUCED DRAG OF ANY BIPLANE . . . . .	333
Equilalent Monoplane Span for any Biplane <i>p. 333</i> .	
APPENDIX II. BIPLANE WING LIFT COEFFICIENTS . . . . .	337
REFERENCES . . . . .	341
INDEX . . . . .	342

$L, M, N$	Moments about $X, Y, Z$ $L$ , Rolling moment $M$ , Pitching moment $N$ , Yawing moment
$h_1, h_2, h_3$	Moments of momenta about $X, Y, Z$
$L_0, M_0, N_0$	Couples applied by controls to disturb steady flight
$i$	Hinge moment
$t$	Time (usually seconds)
$\tau$	Dimensionless unit of time
$t$	$t/\tau$
$G$	Gap-chord ratio
$J$	$\frac{V}{n/D}$
$\lambda$	Ratio of $J$ to $J_0$ (for zero thrust)
$n$	Load factor of plane, I 17
$\sigma$	$q/q_0$ , I 6
$w$	Plane loading = $W/S$
$m$	Mass of plane
$k_L$	Lift coefficient
$K_L$	Maximum lift coefficient
$k_l$	Dimensionless coefficient of moment $L$
$k_m$	Dimensionless coefficient of moment $M$
$k_n$	Dimensionless coefficient of moment $N$
$k_M$	Dimensionless coefficient of moment in general, usually moment $M$
$k_A, k_B, k_C$	Inertia coefficients
$k_{l p}$	Dimensionless coefficient of rolling moment due to rolling
$k_{l r}$	Dimensionless coefficient of rolling moment due to yawing
$k_{l s}$	Dimensionless coefficient of rolling moment due to side-slip
$k_{n p}$	Dimensionless coefficient of yawing moment due to rolling
$k_{n r}$	Dimensionless coefficient of yawing moment due to yawing
$k_{n s}$	Dimensionless coefficient of yawing moment due to side-slip
$k_{m q}$	Dimensionless coefficient of pitching moment due to pitching
	Other coefficients made up after these models
$\mu$	$m/\rho S c$
$J$	Ratio of radius of gyration to $s$
$k_T, k_Q$	Thrust and torque coefficients of an airscrew

*With special reference to Chapters V and VI*

$p$	Dimensionless value of $p$
$q$	Dimensionless value of $q$
$r$	Dimensionless value of $r$
$t$	Dimensionless value of time
$u$	Dimensionless value of $u$
$v$	Dimensionless value of $v$
$w$	Dimensionless value of $w$
$U_1$	Used for $(u_1 + u_2)$
$U_2$	Used for $i(u_1 - u_2)$
$\lambda$	Roots of quartic equation Chapter VI and VII
$\eta$	$\lambda = \xi \pm i\eta$
$\xi$	

# DIVISION O

$m x, m n$	As subscripts signify maximum and minimum
$b$	Span of wing, II 3



$c$	Chord of wing or mean chord, also specific fuel consumption,	IX 1
$D$	Diameter, also drag	
$G$	Gap between wings	
$A$	Equivalent flat plate area,	II 5 (b)
$S$	Area or surface	
$v$	Speed in feet per second	
$V$	Speed in miles per hour	
$V_c$	Speed of climb	
$L$	Lift	
$D$	Drag, also diameter	
$D_i$	Induced drag	
$D_0$	Profile drag	
$D_P$	Parasite drag	
$q$	Dynamic head $(1/2) \rho v^2$	
$T$	Thrust, also absolute temperature	
$W$	Weight	
$P$	Power (very commonly thrust power, thp, in hp units)	
$P_T$	Thrust power	
$P_a$	Thrust available	
$P_r$	Power required	
0 and $h$	as subscripts with $P$ signify respectively, at sea level and at altitude or at altitude $H$ . Thus there may be combinations, $P_{r0}$ = power required at sea level, $P_{ah}$ = power available at altitude, etc.	
$C_L$	Lift coefficient	
$C_D$	Drag coefficient	
$C_{Di}$	Induced drag coefficient	
$C_{D0}$	Coefficient of profile drag	
$C_{DP}$	Coefficient of parasite drag	
$C_P$	Power coefficient	
$C_T$	Thrust coefficient	
$\eta$	Propeller efficiency	
E.M.A.R.	Equivalent monoplane aspect ratio,	II 1
$N, n$	Revolutions per minute, per second	
$\nu$	Kinematic viscosity	
$\rho$	Density of air	
$\sigma$	Density ratio $\rho/\rho_0$ , also Prandtl's factor,	II 3
$T$	Temperature (absolute), also thrust	

# DIVISION N

## DYNAMICS OF THE AEROPLANE

By

**B. Melvill Jones,**  
Cambridge, England

### PREFACE

Of the large amount of experimental and theoretical work on aeroplane dynamics which has been done since the beginning of the century, by far the greater part has related to the movements of aeroplanes slightly disturbed from straight steady flight on an even keel. One reason for this is that the general problem is too complicated for the available methods of analysis to yield results of practical value; another reason is that the primary purpose of an aeroplane is to fly straight and steadily from one place to another, so that it is more important to ensure that straight flying shall require a minimum of effort from the pilot, than to follow precisely the details of violent manoeuvres, in which he will necessarily have his attention firmly fixed upon the controls.

To keep the complexity of the mathematics within reasonable bounds it has generally been necessary, in the analysis, to restrict the disturbances from straight flight to infinitesimals and at first sight this may appear to limit severely the practical value of the work. Experience has shown however that despite this limitation, the analysis is capable of predicting the nature of disturbances, such as those due to moderate control movements or air gusts, with an accuracy which is sufficient for practical purposes. In fact, when the predictions are not fulfilled, the experienced worker is more likely to attribute the discrepancy to errors in the experimental data upon which the calculations are founded, than to the influence of the second order terms which have been omitted from the analysis.

These experimental data have, almost without exception, been obtained from experiments upon models of aeroplanes and their component parts supported in wind tunnels, and an elaborate experimental technique has gradually been evolved for this purpose in the various aerodynamic laboratories of the world. The experiments necessary for the complete dynamic specification of a given aeroplane are, however, so lengthy and costly that it is impracticable to carry through the whole set for more than a few typical models; but fortunately many of the

coefficients differ but little from one aeroplane to another and research has shown how others can be approximately estimated from the design. Unless therefore a new design differs so radically from conventional forms as almost to be classed as a freak, the new experiments required for its dynamic specification can be confined to those relating to a few coefficients only, or it may even be possible to make a good prediction without any special experiments whatever.

The above remarks apply to unstalled flight. Though considerable progress has been made in the study of stalled flight more research is required before the same can be said of this more complicated mode of motion.

In spite, however, of the completeness of the experimental and theoretical structure which enables results of disturbances from straight unstalled flight to be predicted with some confidence, it is undoubtedly true that, at the time of writing, calculations of this kind are very little used by any but a few research workers. It is in fact rare for anyone actually engaged upon the design and construction of aeroplanes to make direct use of computations such as those in Chapters VI and VII of this Division, or even to be familiar with the methods by which they are made. One reason at least for this state of affairs becomes obvious as soon as one tries to carry out the computations for oneself, using the published information available at the time of writing; for one then finds that the necessary experimental data must be sought in a large number of original reports of different experiments, each written more with the idea of describing the experimental method accurately than with the object of presenting the results in a form which makes them easily accessible. Moreover, since these experimental reports have been written at different times during the research campaigns which have provided them, they are of necessity partially contradictory and expressed in different ways, so that co-ordination is difficult.

In drawing up the scheme of the present treatise on aeroplane dynamics these facts were kept in mind, and it was decided to devote the greater part of the available space to a compact discussion of the experimental data, the symbolic analysis, and the numerical computations, which are required for the study of small disturbances from straight flight; rather than to follow the ramifications of research in directions which have not as yet led to results of practical value. Thus two long Chapters—II and III—are devoted entirely to a survey of the available experimental data; Chapter V states the necessary analysis, while Chapters VI and VII are devoted to numerical computations of specific examples and to discussions of the approximations in common use.

It might be supposed that, when the formal mathematical analysis has been studied and understood, the operation of filling in numerical quantities and computing the answers to a specific problem would be

a simple matter, even if somewhat laborious. This, however, is not so. To collect the coefficients necessary to define the aeroplane dynamically, to insert them in correct form and carry out the computations and, finally, to interpret the numerical results, is a more difficult task than merely to understand the symbolical analysis which, though complicated, presents no serious mathematical difficulty. In my own opinion it is the difficulty of computation rather than of mathematical analysis which has prevented designers of aeroplanes from making more use of the methods, and it is with the object of helping in some measure to overcome these difficulties that the successive stages in the working of the examples of Chapters VI and VII have been set out in detail. It is hoped that after studying these two Chapters the reader will be in a position to make similar computations for other aeroplanes with much less effort than if he were to approach the matter with a knowledge only of the symbolic analysis of Chapter V; at least he should be able, by examining the various numerical tables, to decide before starting, which terms are likely to be negligible, which require rough estimation only, and which must be accurately specified, if a final result of useful accuracy is to be obtained.

With these objects in view it was inevitable that much of Chapters V, VI and VII should contain heavy reading and be of small interest to those who desire to obtain a general idea of the reasons why aeroplanes act as they do rather than to study the elaborate processes necessary to make the best possible use of experimental data. The general calculations, moreover, take a form in which it is not easy to follow the chain of cause and effect, from the experimental coefficients with which they start, to the movements which are finally predicted and, for these reasons, Chapter IV has been interpolated into the main argument.

In Chapter IV the subject is approached from an entirely different point of view, founded more upon the work of Lanchester (Ref. 4 of Chap. V) than, as are the later Chapters, upon the work of Bryan (Ref. 5 of Chap. V). Instead of developing each aspect of the aeroplane's motion as a special case of a general scheme, various important features of the motion are successively isolated for discussion and their causes made clear by the elimination of all factors which are not of major importance in determining the particular feature under consideration. It is the hope of the author that Chapter IV will prove easy reading to anyone who has even a passing acquaintance with simple differential equations and the mathematics of harmonic oscillations with one degree of freedom; yet it will be found that it contains most of the conclusions of practical importance which occur in the later chapters, and that many of the formulae in common use for the approximate prediction of aeroplane movements can be obtained in very simple ways. Though Chapter IV is not necessary for the logical development of the argument, it is thought

that even readers who intend to study the later Chapters thoroughly will be helped by it to a clearer appreciation of their meaning.

The reader who approaches the subject for the first time may think that the dimensionless system of representing coefficients and equations, which has been adopted throughout the bulk of the work, increases rather than decreases the difficulties. If, however, he perseveres to the study of the computations of Chapters VI and VII—and when all is said and done it is the computation of specific problems that is the end and aim of the analysis—he will find that the use of dimensionless forms is amply justified. The author at least believes that, without the use of some dimensionless system, calculations such as these would stand little chance of being widely used for practical purposes.

It is perhaps not out of place to discuss very briefly the value of calculations of the kind in Chapters V, VI and VII in the general scheme of the design and development of aeroplanes. That the researches and investigations upon which they are founded have been worth doing is undoubted, since through them we have now a much clearer appreciation than we should otherwise have had of the factors which control the motions of aeroplanes; but the extent to which such computations will be used in connection with the design and production of specific types is still a matter for conjecture. It is possible that firms engaged in the pioneering side of aircraft design and production would be well repaid for the allocation of a small part of their staff to work of this kind; for it should not be difficult for anyone who understands the subject to devise printed forms which would enable the more laborious parts of the work to be carried through at a relatively low cost and, if the results are presented in some easily understandable form, as in the figures of Chapters VI and VII, it should be possible for designers and directors to be shown very clearly and without the necessity for understanding the details of the calculation, the consequences which would follow any proposed change in design.

Again it is probable that mechanical control will become increasingly popular for large long distance aeroplanes, and for anything in the nature of pioneer work in this subject, calculations of this kind are essential. No mention of the methods of extending the calculations to deal with mechanical control will, however, be found in the present work, since this is still a matter of research and what little has been published is mainly of a controversial nature, but work of the type discussed in Chapters V, VI and VII forms an essential introduction to the study of mechanical control.

Two other Chapters have not yet been mentioned. Chapter I deals with certain very simple but important characteristics of flight which depend on the necessity that resultant force must be equal to the mass acceleration of the center of gravity; it is written on the assumption

that the moments of these forces about the centre of gravity are looked after by the pilot, through the medium of his controls.

Chapter VIII deals with the steady spin, a matter which is still so much the subject of research that it was not thought advisable to deal with it in great detail. All that is attempted in this chapter is a general survey of the situation at the time of writing.

## CHAPTER I

### STEADY MOTIONS AND LIMITING ACCELERATIONS

**1. Introduction.** The motion of an aeroplane in flight is determined by the gravitational field and by the reactions which occur between it and the air through which it flies. The resultant of the gravitational attractions is represented by a force equal to the weight of the whole aeroplane acting vertically downwards through the centre of gravity; therefore the resultant of the aerodynamic reactions is conveniently represented by three mutually perpendicular force components acting through the centre of gravity and three moments acting about three mutually perpendicular axes which meet at the centre of gravity.

In general we shall require to study the motion of the centre of gravity due to the combined actions of the weight and the air-forces, together with the rotation of the aeroplane due to the action of the air-moments. The principal difficulties will be found to lie in the estimation of the air-moments, but it will be realized that these moments are under the control of the pilot who, by using his *controls*, can adjust them to the magnitudes required for the execution of any desired manoeuvre. It will therefore be convenient to begin the discussion of our subject with a brief and simple chapter dealing with the consequences which follow from the consideration that the mass acceleration of the centre of gravity must at all times equal the resultant of the weight and the air forces; assuming that the pilot will, by his acquired skill, adjust the air-moments to give the rates of change of angular momenta required by the manoeuvre under consideration.

**2. Symmetric Flight.** It will generally be assumed that the aeroplane has a plane of symmetry such as  $AB$  in Fig. 1 and it will be observed that when such an aeroplane flies symmetrically—that is

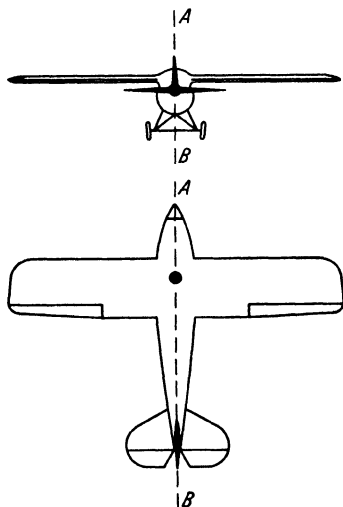


Fig. 1. The plane of symmetry of an aeroplane.

to say with the direction of motion parallel to the plane of symmetry and with no rotation about any axis parallel to the plane of symmetry—the resultant air-reaction must lie in the plane of symmetry.

It is true that a single screw aeroplane is unsymmetrical in respect to the rotation of the screw and that, even in symmetric flight, asymmetric couples arise, due to the influence of the rotating slipstream upon parts of the aeroplane and to gyroscopic couples exerted by the screw when the aeroplane is pitching. In some circumstances these asymmetric couples may become important, but it is essential for reasonable simplicity to study the behavior of the ideal symmetric aeroplane before attempting to introduce asymmetric complications.

### A. Steady Straight Symmetric Flight

**3. Principal Forces Involved.** The normal mode of progression of an aeroplane is to fly straight and at a constant speed with the plane of symmetry vertical—wings *level*—and we shall therefore begin with a discussion of the factors which control the attitude of the aeroplane to the horizontal and to the direction of motion, when flying in this way.

The resultant air-reaction now necessarily lies in the plane of symmetry and passes through the c.g. and in these circumstances it is usual

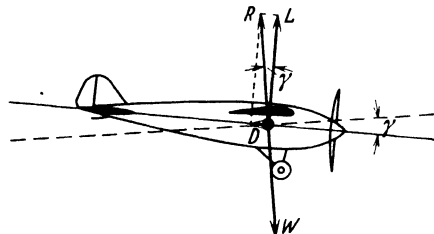


Fig. 2. Forces in steady gliding flight—engine off.

to resolve this resultant reaction ( $R$ ) (Fig. 2) into two components, perpendicular and parallel respectively to the direction of motion. The former of these is called the *lift* ( $L$ ) and the latter, when the engine is not working, is called the *drag* ( $D$ ).

The drag is always opposed to the motion, so that, when the engine is not working, the resultant air-reaction will be inclined backwards from the perpendicular to the direction of motion and, since this resultant must balance the weight and therefore be vertical, the direction of motion must be inclined downwards through an angle  $\gamma$  where  $\tan \gamma = D/L$ . The aeroplane is then said to be *gliding* with gliding angle  $\gamma$ .

When the engine is working, the airscrew thrust ( $T$ ) opposes the drag, so that the net aerodynamic force component parallel to the direction of motion may, within limits, have any value positive or negative. When the net value of this component is zero the corresponding steady straight flight path is horizontal (Fig. 3); when it is directed forwards the corresponding steady flight path is inclined upwards and the aeroplane is said to *climb*, Fig. 4.

**4. Dimensionless Coefficients.** It will often be convenient to express reactions such as  $R$ ,  $L$  and  $D$  in terms of dimensionless coefficients<sup>1</sup>,

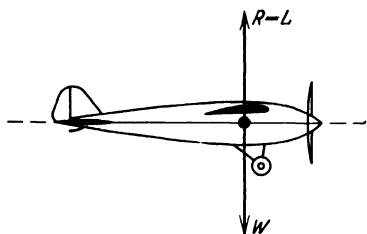


Fig. 3. Forces in steady horizontal flight.

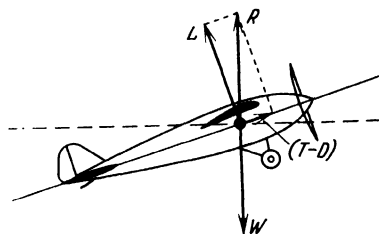


Fig. 4. Forces in steady climbing flight.

$$\text{such as } k_R = \frac{R}{\rho V^2 S} \quad k_L = \frac{L}{\rho V^2 S} \quad k_D = \frac{D}{\rho V^2 S}$$

where  $\rho$  is the air density,  $V$  the velocity of the centre of gravity relative to the air, and  $S$  the conventional wing area. The value of these dimensionless coefficients lies in the fact that, with certain limitations which need not be here discussed, they are functions of the shape and mode of motion of the aeroplane through the air, but are independent of the values of  $\rho$ ,  $V$  and  $S$ .

**5. Horizontal Flight.** In steady horizontal flight,  $R$ ,  $L$  and  $W$  are all equal (Fig. 3) and if, as a first approximation, the influence of the airscrew on lift be ignored, we can at once determine the attitude of the aeroplane for given values of  $\rho$ ,  $V$  and  $W$ , provided that we know the relationship of the lift coefficient ( $k_L$ ) to the incidence ( $\alpha$ )<sup>2</sup>.

A typical relationship for a normal aeroplane is shown in Fig. 5.

$$\text{We then have } k_L = \frac{L}{\rho V^2 S} = \frac{W}{\rho V^2 S} = \frac{w}{\rho V^2} \quad (5.1)$$

where  $w$  is the weight per unit area, or the *wing loading* of the aeroplane.

<sup>1</sup> It will be noted that, in the present Division, force coefficients generally are related to  $\rho V^2$  rather than to  $(1/2) \rho V^2$  as more commonly in other Divisions of the work.

<sup>2</sup> In symmetric flight the *incidence* is the inclination to the direction of motion through the air of an arbitrary line on the wing. This line is generally called the chord of the wing.

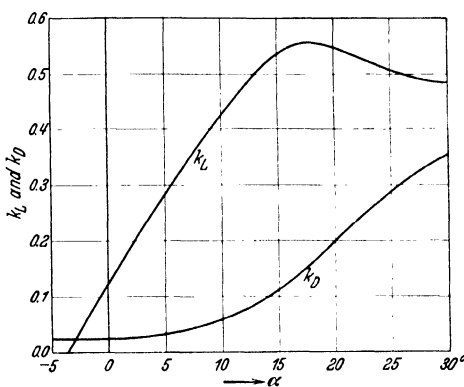


Fig. 5. Typical curves for lift and drag coefficients against incidence.



For any given value of  $w$ ,  $\rho$  and  $V$ ,  $k_L$  can be determined from (5.1) and  $\alpha$  can then be read off from a curve such as Fig. 5.

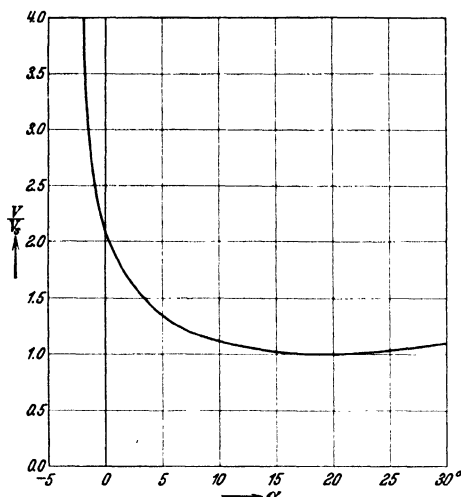


Fig. 6. Typical curves for speed against incidence— $V_S$  is the stalling speed.

It will be observed that the lift coefficient ( $k_L$ ) has a maximum value in the neighborhood of  $18^\circ$  incidence. There is thus a minimum speed at which the aeroplane can fly steadily and horizontally. This speed is called the *stalling speed* and the incidence at which it occurs is called the *stalling incidence*. We shall speak of an aeroplane flying at an incidence less than the stalling incidence as being in *normal flight*, whilst an aeroplane flying at an incidence greater than the stalling incidence will be said to be *stalled*.

Let the maximum lift coefficient be  $K_L$ , and the corresponding stalling speed  $V_S$ .

Then

$$K_L = \frac{w}{\rho V_S^2} \quad (5.2)$$

Using (5.1)  $k_L = K_L (V_S/V)^2$ .

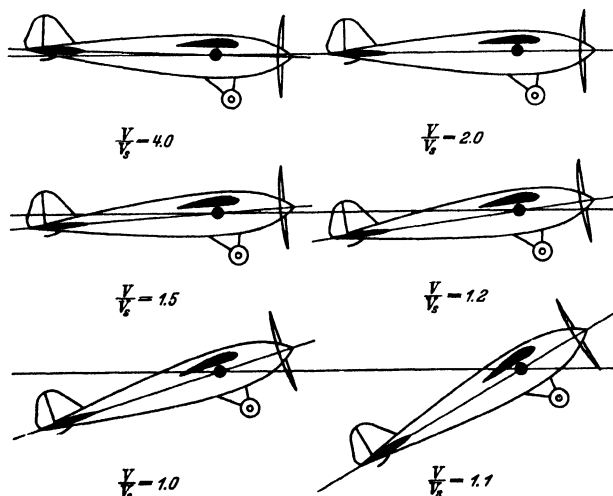


Fig. 7. Aeroplane attitudes at various speeds in steady horizontal flight— $V_S$  is the stalling speed.

From which, using Fig. 5, incidence can be determined when the ratio of the speed to the stalling speed at the height in question is known.

Figure 6 is derived from Fig. 5 and shows a typical relation between  $\alpha$  and  $V/V_S$  for horizontal flight. Figure 7 shows graphically the various attitudes in horizontal flight of an aeroplane of which the wing chord is parallel to the axis of the body and the relation between speed and incidence is as in Fig. 6.

**6. Indicated Air Speed.** The *air-speed indicator* generally used on aeroplanes is of the *pilot and static pressure* type and measures the quantity  $1/2 \rho V^2$ ; it is not a true indicator of air speed and only measures speed correctly when the air density ( $\rho$ ) has the particular value for which the instrument was calibrated. Since, however, the lift coefficient is equal to  $w/\rho V^2$  it follows that, for an aeroplane of given wing loading in steady horizontal flight, lift coefficient and therefore wing incidence are functions of the indicated speed. It is usual to calibrate these instruments for air at *normal temperature and pressure*,  $15^\circ \text{C.}$  and  $760 \text{ mm.}$  of mercury. This *standard density* is  $0.0764 \text{ lb. mass}$  or  $0.00238 \text{ slugs per cubic foot}$  and is usually given the symbol  $\rho_0$ . The ratio to the standard density, of the density of air in any other state, as for example at the low pressures found at high altitudes, is generally given the symbol  $\sigma$ , so that  $\rho = \sigma \rho_0$ . The reading of the indicator at any density other than standard will then be  $\sqrt{\sigma} V$  where  $V$  is the true speed. The expression  $\sqrt{\sigma} V$  is called the *indicated air speed*.

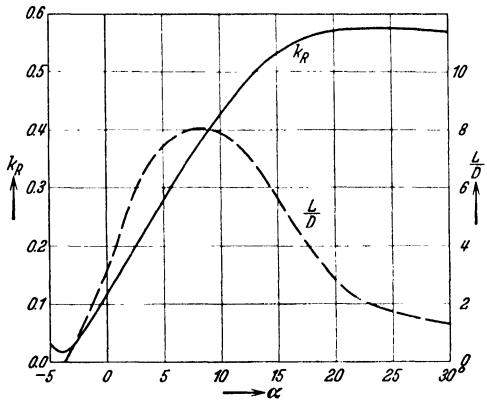


Fig. 8. Typical curves for resultant air-reaction ( $R$ ) and of the ratio of lift to drag against incidence.

To the pilot, the indicated air speed is a more real quantity than the true speed; for not only is it the quantity shown on his speed indicator, but it is the quantity which determines the characteristic behavior of his aeroplane. For example, a given aeroplane in steady horizontal flight stalls always at the same indicated air speed, no matter what the density and, as we shall see later, the maximum acceleration which the pilot can apply to his aeroplane in horizontal flight is a function of lift coefficient and therefore also a function of indicated speed.

**7. Gliding Flight.** In gliding flight we have (Fig. 2)

$$\tan \gamma = \frac{D}{L} \quad (7.1)$$

and

$$k_R = \frac{w}{\rho V^2} = K_R \left( \frac{V_S}{V} \right)^2 \quad (7.2)$$

Typical values of  $k_R$  and  $L/D$  are shown plotted against incidence in Fig. 8.

For given values of  $w$ ,  $\rho$  and  $V$ ,  $k_R$  can be found from (7.2) and  $\alpha$ ,  $\gamma$  can then be found from Fig. 8, the latter by reference to (7.1).

Typical relationships between  $\alpha$ ,  $V/V_S$  and  $\gamma$  are shown in Fig. 9.

The attitude of the aeroplane to the horizontal can be deduced from the consideration that the angle ( $\Theta$ ), made by the wing chord with the horizontal, is equal to  $\alpha - \gamma$ . In Fig. 9,  $\Theta$  is the difference between the  $\gamma$  curve and the oblique line on the diagram. When the  $\gamma$  curve is above the oblique line (as drawn), the leading edge of the wing chord is above the trailing edge. The attitudes of the gliding aeroplane and its direction of motion, as determined by Fig. 9, are shown graphically in Fig. 10, in which the thick arrows are vectors, drawn to an arbitrary scale, representing the velocity of the aeroplane.

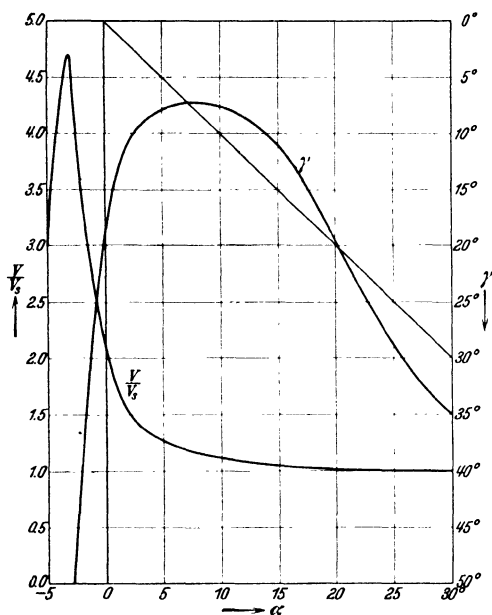


Fig. 9. Typical curves of velocity and gliding angle ( $\gamma$ ) against incidence.

Examining Figs. 9 and 10, it appears that the highest steady gliding speed occurs when the aeroplane is diving nearly vertically, so that the whole weight is supported by the drag<sup>1</sup>. This condition is described as a *terminal velocity dive*. As the incidence increases, the corresponding steady glide occurs at lower speeds and smaller values of  $\gamma$ , until, for an incidence near  $8^\circ$  and a speed of some 1.2 times stalling speed,  $\gamma$  passes through a flat minimum and then increases rapidly as the stalling angle is approached and passed. The angle  $\Theta$ , defining the aeroplane's attitude to the horizontal, changes progressively from the neighborhood of  $-90^\circ$  in the terminal velocity dive, through zero at  $7^\circ$ , to  $+4^\circ$  at

<sup>1</sup> This is not strictly correct, since the drag coefficient may not have a minimum value at zero lift, but the statement is sufficiently accurate for the present purpose.

about  $15^\circ$  incidence and then falls to zero at  $20^\circ$  incidence, which is about the highest incidence at which a normal aeroplane can be held in equilibrium by the controls.

**8. Some Aspects of the Landing Problem.** It is of interest to note here that, at incidences higher than some  $8^\circ$  to  $10^\circ$ , neither the attitude

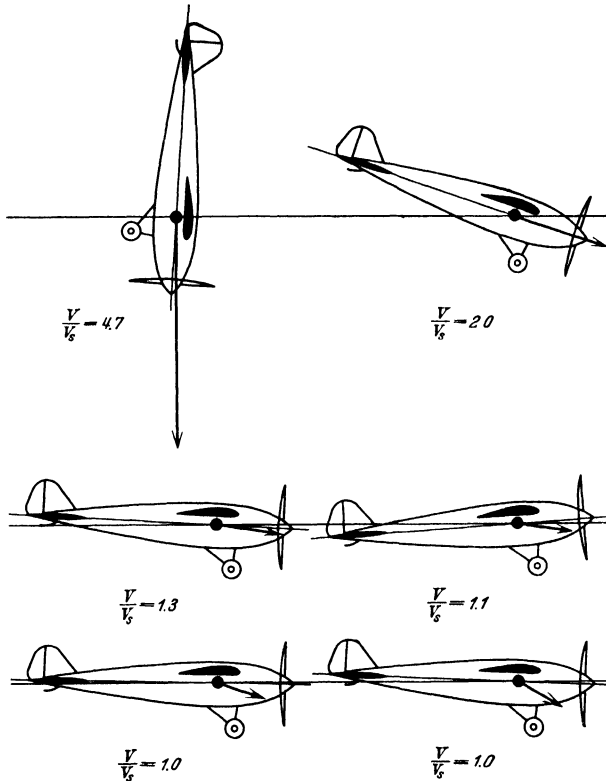


Fig. 10. Aeroplane attitudes at various speeds in steady glide with engine off— $V_s$  is the stalling speed.

of the aeroplane nor its velocity in steady flight change greatly for further changes of incidence, although the gliding angle changes rapidly. The result is that when flying at these high incidences the pilot, unless equipped with special instruments, has no effective means for rapidly ascertaining the angle of glide. This is one amongst several of the sources of danger when approaching the ground at too low a speed.

For this and other reasons which will appear later, pilots make a practice of approaching the aerodrome at speeds between 30 per cent and 40 per cent greater than the stalling speed, although, from the point of view of the reduction of the space required for landing, it would

be more advantageous to approach at lower speeds. A glance at Fig. 9 will show that at these speeds the gliding angle ( $\gamma$ ) is near its minimum and is relatively insensitive to changes of speed or incidence. This explains another difficulty in the landing of aeroplanes. The pilot dares not approach too slowly for fear of stalling and must not approach too fast for fear of over-running the aerodrome; he is therefore obliged to approach at speeds which happen to involve flat gliding angles which he is unable to modify without executing some violent unsymmetrical manoeuvre. The flat gliding angle implies the waste of much valuable space when the aeroplane has to pass over high obstacles near the aerodrome, whilst the inability to change the steady gliding angle leaves the pilot with no easy means of adjusting his rate of descent to allow for errors in estimating the point from which he started the glide. If he

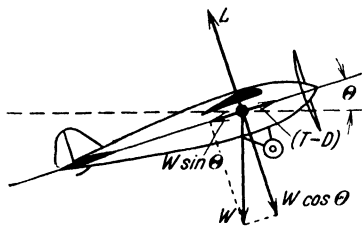


Fig. 11. Forces in climbing flight resolved perpendicularly to direction of motion.

forces the aeroplane to dive more steeply than the steady gliding angle it will merely gather speed which will have to be dissipated on reaching the level of the ground, with the result that the ultimate stopping place will generally be even further on than if he had continued the steady glide. If he pulls the nose up, the aeroplane will stall, with various unpleasant consequences that will be discussed later.

**9. Climbing Flight.** When the engine is working and the flight path is not horizontal, the attitude of the aeroplane, on the assumption that the screw does not influence lift, can be calculated as in horizontal flight, from the consideration that lift is equal to the component of the weight resolved perpendicularly to the aeroplane's velocity<sup>1</sup>.

If the inclination of this velocity to the horizontal be  $\Theta$  we have (see Fig. 11).

$$k_L = \frac{L}{\rho V^2 S} = \frac{W \cos \Theta}{\rho V^2 S} = \frac{w \cos \Theta}{\rho V^2} \quad (9.1)$$

The net forward reaction of the airscrew thrust ( $T$ ) minus the aeroplane's drag ( $D$ ) must now equal  $W \sin \Theta$ , instead of zero as in horizontal flight. When  $\Theta$  is positive the engine will therefore have to work harder than in horizontal flight, the difference appearing as gain in potential energy. The consideration of energy expenditure for flight appears, however, in the division on *Performance*, and will not, therefore, be discussed here.

The simplifying assumption that the lift coefficient is dependent on incidence only and independent of airscrew thrust, may not be sufficiently accurate and the determination of the aeroplane's attitude in

<sup>1</sup> It will be remembered that "lift" is defined as the component of the air-reaction perpendicular to the direction of motion.

steady flight then becomes a more complicated matter. If, in steady symmetric flight, the effect of changes of Reynold's number are neglected, the form of the flow about the aeroplane and therefore the magnitudes of the dimensionless coefficients, are functions of three independent variables; wing incidence ( $\alpha$ ); airscrew blade incidence, defined by  $J (= V/nD)$ , where  $n$  is the revolutions per second of the screw and  $D$  its diameter; and elevator position, defined by an angle ( $\eta$ ). If, however, the aeroplane is flying steadily without rotation, one relation between these variables is given by the condition that the moment of all the air reactions about a transverse axis through the centre of gravity must be zero. In steady flight, therefore, the number of independent variables defining the coefficients is reduced to two. If, further, the inclination of the flight path to the horizontal is specified, there will be another relation between the variables, because it is necessary that the *direction* of the resultant reaction on the whole aeroplane—including the screw—shall be vertical. In steady flight, with a given inclination of the flight path to the horizontal, the magnitude of the lift coefficient is, therefore, determined by one independent variable only. This variable can be chosen to suit the form of the calculations, but to conform with the simpler calculation considered above we may choose as independent variable the incidence ( $\alpha$ ). Given sufficient information about the action of the screw, elevators, etc., it is thus possible to prepare a curve relating  $k_L$  to  $\alpha$ , but this curve will be different for different inclinations  $\theta$  of the flight path. We can then, using (9.1) find, for any value of  $\theta$  the relation of  $V$  to  $\alpha$  in the same manner as before.

The development of methods of analyzing the relations between angle of climb and the variables  $V$ ,  $J$  and  $\alpha$  belong properly to the division on *Performance* and will not be further discussed in the present section. The matter has been mentioned in this section merely to show the lines along which the conditions for steady symmetric flight can be examined, before passing to the consideration of the way in which the aeroplane will behave when the resultant air-reaction is not vertical and equal to the weight.

## B. Accelerated Symmetric Flight

**10. Introduction.** Let us suppose that when the aeroplane is flying straight and steadily, the incidence is suddenly changed to some new value and maintained at that value. A glance at Fig. 5 will show that in normal flight, say below  $10^\circ$  incidence, changes of incidence affect the lift much more than the drag. The unbalanced force will, therefore, be nearly perpendicular to the direction of motion and its principal effect will be to curve the flight path.

In making this statement it is not implied that unbalanced forces parallel to the direction of motion are of no importance; on the contrary

it is through these and these only that changes of speed can occur, but the motion of the disturbed aeroplane, taking all factors into account, is exceedingly complicated to analyse and will be discussed from various points of view in subsequent chapters. The present preliminary survey will be confined to the consideration of the pilot's power to generate accelerations perpendicular to the direction of motion and so to curve the flight path.

**11. Radius of Curvature of the Flight Path.** Suppose that at some instant the incidence is such that the actual lift coefficient is  $k_L$ , whilst the lift coefficient which would be required for steady straight flight at that particular speed and attitude to the horizontal is  $k'_L$ . Then the unbalanced force acting upon the aeroplane, at right angles to the direction of motion of the centre of gravity, is

$$(k_L - k'_L) \rho V^2 S$$

The acceleration of the centre of gravity at right angles to the path will be  $\frac{g(k_L - k'_L) \rho V^2 S}{W}$  or  $(k_L - k'_L) \frac{g \rho V^2}{w}$

The radius of curvature of the path will be

$$\frac{V^2}{\text{acceleration}} = \frac{1}{k_L - k'_L} \cdot \frac{w}{g \rho}$$

Thus, for a given wing loading ( $w$ ) and air density ( $\rho$ ), the radius of curvature of the path depends upon the difference between the actual value of the lift coefficient and the value which would be necessary in steady flight.

**12. Minimum Radius of Curvature.** In ordinary flying the type of curvature of the flight path which is most often required is that in which the pilot's head is on the inside of the curve. This requires that  $k_L > k'_L$ . But  $k_L$  has a maximum value ( $K_L$ ), which occurs at the stalling incidence; hence the minimum possible radius of curvature depends on the difference between the maximum lift coefficient of the aeroplane and the lift coefficient which would be required for steady flight in the circumstances under consideration.

The possibility of attaining the minimum radius of curvature deduced from the above consideration depends, of course, upon the elevators being sufficiently powerful to provide the angular velocity necessary to maintain the incidence at the required value, whilst flying in the curved path. This raises questions which will be discussed in later chapters. It is not, however, difficult to provide sufficient elevator power for this purpose and so to ensure that the minimum radius of curvature available shall be limited only by the above consideration.

The lift coefficient in straight flight is small but positive when flying right-way up at high speeds in any direction, hence, when flying at high speed, the minimum available radius of curvature of the flight path

will closely approach the absolute minimum  $[w/K_L g \rho]$ . The minimum radius for any attitude to the horizontal increases as the speed decreases and becomes infinite at the stalling speed.

These remarks, it must be remembered, apply only to curvatures towards the pilot's head when the aeroplane is not inverted. If this restriction is removed, the radius may have any value down to zero; as, for example, when the aeroplane, flying nearly straight upwards, falls over on its back. In such circumstances small radii of curvature are, however, of little practical value.

Figure 5 shows that when the maximum lift coefficient is developed, the drag is very much higher than in normal flight. If, therefore, it is desired to fly in a path of small radius of curvature without excessive power expenditure or loss of speed or height, the absolute maximum lift coefficient will not be used, but one some 15 per cent or 20 per cent less and the practicable minimum radius of curvature will be correspondingly increased.

If the maximum lift coefficient ( $K_L$ ) in the above expression is to be identified with the maximum coefficient in straight flight, it must be assumed that its value is not influenced by rotation. There is reason to suppose that this may not be true, but it is probably sufficiently true for the rough estimates of minimum radius of curvature generally required. Assuming that the coefficients in curved and straight flight are identical, we may express the absolute minimum radius of curvature in a still simpler form, as follows.

**13. Minimum Radius of Curvature in Terms of Stalling Speed.** Let  $V_S$  be the stalling speed in straight horizontal flight with air density  $\rho$ .

Then

$$w = K_L \rho V_S^2$$

Hence

$$\frac{w}{K_L g \rho} = \frac{V_S^2}{g}$$

Thus the absolute minimum radius of curvature is twice the height through which the aeroplane would have to fall, *in vacuo*, to acquire a speed equal to its stalling speed in steady straight flight at the height in question. With a stalling speed of 50 m.p.h. the absolute minimum radius of curvature is about 170 feet.

**14. Minimum Radius and Rapid Manoeuvres.** These conclusions are of the greatest importance in connection with the design of craft which require power of rapid manoeuvre. They show that rapid manoeuvres involving change of direction are impossible without a fair speed range which will allow the aeroplane to fly steadily with a lift coefficient considerably lower than the maximum; and that, other things being equal, an aeroplane with a low stalling speed will be more manoeuvrable than one with a high stalling speed. These facts were well illustrated in the



late war, where the lightly loaded aeroplanes, such as the Sopwith Camel, outmanoeuvred their more heavily loaded opponents at low heights, where the speed range of both was high, but were themselves outmanoeuvred by the same opponents at greater heights where, being near their absolute *ceiling*, their speed range was much less than that of their enemies.

**15. Apparent Gravity and Load Factors.** In general, when large accelerations are occurring, the aeroplane will be flying on a curved path and will be rotating so as to maintain the necessary angle of incidence. In these circumstances the accelerations of different parts of the aeroplane will differ from the acceleration of the centre of gravity; but if the radius of curvature is large compared with the dimensions of the aeroplane these differences will be unimportant. If, as a first approximation, it is assumed that the acceleration ( $f$ ) of all parts is equal to that of the centre of gravity, then every individual mass ( $m$ ) in the aeroplane must be acted upon by a force equal to  $mf$ , in the direction of  $f$ , in addition to a force equal and opposite to its weight ( $mg$ ) which acts vertically downward. The resultant force, which must be applied to the mass to accelerate it and to balance the weight is then

$$m \times (\text{vectorial sum of } f \text{ and } -g).$$

The internal stresses within the aeroplane and pilot will thus be substantially the same as if the aeroplane were flying straight, in a gravitational field equal to the vectorial sum of  $g$  and  $-f$ . This vectorial sum is often called the *apparent gravity* in the aeroplane and its ratio to the true value of gravity is called the *load factor* ( $n$ ). Stresses in the aeroplane will then all be approximately  $n$  times as great as the corresponding stresses in steady horizontal flight at the same incidence. This approximation is widely used in calculating the stresses in aeroplanes during manoeuvres; it should not, however, be used for violent low speed manoeuvres, such as the spin, in which it may be hopelessly inaccurate, both on account of the influence of rotations upon the distribution of the air-reactions and because the accelerations of individual parts of the aeroplane may then differ widely from that of the c.g.

**16. Measurement of Load Factors.** The magnitude of the apparent gravity can be very easily measured by means of a spring-suspended weight. If the spring is hung from a universal joint its extension will be proportional to the apparent gravity; but if it has freedom of motion in one direction only, its extension measures the component of the apparent gravity in that direction. In practice it is usual to employ such an instrument to measure the component in the plane of symmetry perpendicular to the longitudinal axis of the body. In normal flight this component is practically indistinguishable either from the resultant or from the component perpendicular to the direction of motion.

**17. Maximum Load Factor.** Let  $n$  be the ratio of this component to the true gravitational field and let  $k_L$  be the lift coefficient.

$$\text{Then} \quad nW = k_L \rho V^2 S$$

Let  $k'_L$  be the lift coefficient in steady *horizontal* flight at the same speed, in air of the same density.

$$\text{Then} \quad W = k'_L \rho V^2 S$$

$$\text{Hence} \quad n = \frac{k_L}{k'_L}$$

Approximately, therefore, the load factor is simply the ratio of the actual lift coefficient to the lift coefficient in steady horizontal flight at the same speed and height. The load factors which can occur upon an aeroplane flying at a given speed cannot, therefore, exceed the ratio  $K_L/k'_L$  or  $(V/V_S)^2$ , where  $V$  is the actual speed of flight and  $V_S$  the stalling speed in straight flight with wings level<sup>1</sup>.

Whether or not this load factor can be actually reached depends upon whether the rate of rotation of the aeroplane about a transverse axis can be made sufficiently large for the stalling incidence to be reached before the speed has fallen appreciably. In the majority of aeroplanes a hard pull upon the control stick causes the necessary increase in incidence in a very short time and it is therefore possible to reach load factors not far removed from the above value.

The highest speed at which an aeroplane can travel is generally that attained in the terminal velocity dive (7) and may be between four and eight times the stalling speed. A sudden pull upon the control column at these speeds may lead, therefore, to load factors between 16 and 64 and involve forces which no reasonable aeroplane could be expected to withstand.

Aeroplanes in use at present are designed to withstand load factors ranging from 4, for large commercial craft, up to 15 for certain types of fighting machine; it has, therefore, to be assumed that the pilot will not pull violently upon the control stick when travelling at excessively high speeds. This is reasonable, because his own body cannot withstand more than certain limiting load factors, so that the amount which he will pull on the stick will be governed by his bodily appreciation of the apparent gravity.

It is of interest in this connection to note that momentary load factors up to about 11 have been recorded without permanently damaging the pilot, but that factors greater than about 4.5, if maintained for more

<sup>1</sup> Certain experiments which have been made since the above was written suggest that this generalization may not be true when the lift is very suddenly increased; it appears that, in these circumstances, the lift coefficient may temporarily exceed the maximum coefficient which can persist for any considerable time. This phenomenon, however, requires further experimental verification.

than five or six seconds, cause temporary blindness and loss of other faculties. (Refs. 1, 2, 3, 4.)

Having discussed some simple aspects of symmetric flight, steady and accelerated, we shall now consider some equally simple aspects of asymmetric flight.

### C. Straight Asymmetric Flight

**18. Steady Straight Side-slip.** Imagine an aeroplane, flying straight and symmetrically, to be rolled suddenly through an angle  $\phi$ , about an axis parallel to the direction of motion, into the attitude of Fig. 12. Suppose that immediately after the roll the direction of motion is still parallel to the plane of symmetry and that therefore the reaction of the air also lies in the plane of symmetry, as in Fig. 12. The resultant of lift and weight is now no longer zero, but is a force inclined to the plane of symmetry. This force will in time generate a velocity which will contain a component—called *side-slip*—perpendicular to the plane of symmetry and if

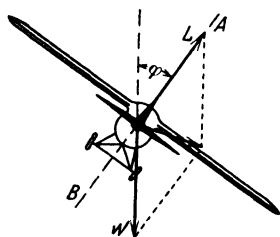


Fig. 12. Forces immediately after rolling from straight flight—no side-slip.

the attitude of the aeroplane is maintained constant, the sideslip will increase until a force component  $Y$  (positive when to starboard) perpendicular to the plane of symmetry is generated, sufficient to swing the resultant air reactions back to the vertical. This force will be called *side-force*; it is mainly due to the action of the air blowing crosswise on the body. When steady conditions have been reached, the resultant ( $R$ ) of the side-force ( $Y$ ) and the lift ( $L$ ) must equal the weight, and the lift will therefore be somewhat less than that in steady symmetrical flight at the same speed, Fig. 13.

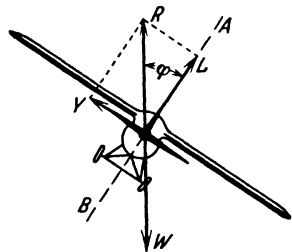


Fig. 13. Forces in a steady straight side-slip.

**19. Relation of Side-force to Side-slip.** Let the side-force coefficient be

$$k_Y = Y/\rho V^2 S$$

Then

$$k_{Y'} = -k_L \tan \phi \quad (19.1)$$

where  $k_L$  is the lift coefficient in the steady straight flight with side-slip. Let  $\beta$  (positive when side-slip is to starboard) be the angle made by the direction of motion with the plane of symmetry. It is found by wind tunnel experiment that side-force is sensibly proportional to  $\beta$  up to at least  $30^\circ$ . Side-force is also found to be very little affected by changes of incidence and its coefficient, at a given value of  $\beta$ , does not differ

greatly between different aeroplanes of conventional design. For such machines a fairly representative value is given by

$$k_Y = -0.2 \beta \quad (\beta \text{ in radians}) \quad (19.2)$$

**20. Relation of Side-slip to "Bank".** Equations (19.1) and (19.2) lead to  $\beta = 5 k_L \tan \varphi$  or, for small values, to  $\beta = 5 k_L \varphi$

Near stalling, where  $k_L$  is of the order 0.5, the angle of side-slip in slow steady flight is therefore of the order 2.5 times the angle of roll or *bank* as it is sometimes called. At higher speeds this ratio is reduced in proportion to the lift coefficient. At cruising speeds where the lift coefficient is of the order 0.20, the angle of side-slip is roughly equal to the angle of bank. These figures must be regarded merely as representative; for accurate prediction, special measurements, or estimates based on the shape of the aeroplane, are of course required.

When the side-slip becomes large—20° or over—the body of the aeroplane sets up severe turbulence in the air flow and its drag is therefore very high. At the same time the lift at a given incidence is reduced and the ratio of drag to lift therefore increases considerably. Pilots use this property of the aeroplane to increase their gliding angle without unduly reducing or increasing speed and so are able partially to overcome one of the difficulties of landing noted in 7.

## D. Circling Flight

**21. The Flat Turn.** Consider an aeroplane flying with its plane of symmetry vertical and with its centre of gravity describing, with speed  $V$ , a horizontal circle of radius  $r$  and centre  $C$  and assume that the asymmetric moments generated by this motion are balanced by suitable control settings.

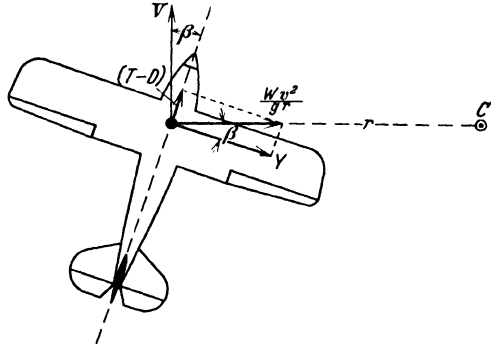


Fig. 14. Forces in a "flat turn".

The acceleration towards the centre of the circle will be  $V^2/r$ , and to maintain this acceleration a resultant horizontal air reaction directed towards  $C$  and equal to  $(W/g) (V^2/r)$  will be required. This air-reaction will be inclined to

the plane of symmetry, and to provide it, the plane of symmetry must be inclined to the direction of motion, as in Fig. 14.

The horizontal air-reactions may be resolved into a component ( $Y$ ) acting perpendicular to the plane of symmetry and a component, equal

to the difference between the airscrew thrust ( $T$ ) and the drag ( $D$ ), acting in the plane of symmetry.

Let  $\beta$  be the angle of side-slip.

Then 
$$k_Y \rho V^2 S = \frac{W}{g} \cdot \frac{V^2}{r} \cos \beta \quad (21.1)$$

**22. Side-slip in the Flat Turn.** A representative value of  $k_Y$  has been given as  $0.2\beta$  and, inserting this in (21.1) we have

$$\beta = 5 \frac{w \cos \beta}{g \rho r} \quad (22.1)$$

where  $w$  is the wing loading per unit area. The factor  $w/g\rho$  has the dimensions of length and a reasonable value corresponding to a wing loading of 8 lb. per sq. ft. in air at about 6,000 ft. above sea level, is 150 ft.

This leads to 
$$\frac{\beta}{\cos \beta} = \frac{43,000}{r} \quad (\beta \text{ in degrees}) \quad (22.2)$$

Provided that  $\beta$  is not too large,  $\cos \beta$  will be in the neighborhood of unity and therefore  $\beta$  will be inversely proportional to  $r$ . If, for example,  $r$  is 2700 feet,  $\beta$  must be in the neighborhood of  $16^\circ$ . Hence, in order to make a *flat turn*, as such a manoeuvre is called, having a radius of curvature less than half a mile, side-slip angles greater than some  $16^\circ$  are necessary. Such side-slips involve, as we have seen, heavy power losses and therefore flat turns of any but very gentle curvature are not employed, except in special circumstances.

**23. The True-banked Turn.** The usual procedure when circling is to roll—or *bank*—the aeroplane about the longitudinal axis, until the air reaction necessary both to support the weight and provide the horizontal acceleration again lies in the plane of symmetry, Fig. 15. The turn is then said to be *true-banked* and the aeroplane proceeds without side-slip.

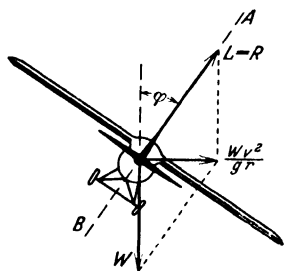


Fig. 15. Forces in a "true-banked turn".

If the angle of bank in a true-banked turn is  $\varphi$  and the radius of curvature of the path of the centre of gravity through the air is  $r$ , we

have 
$$\tan \varphi = \frac{W}{g} \cdot \frac{V^2}{r} \cdot \frac{1}{W} = \frac{V^2}{gr} \quad (23.1)$$

and 
$$k_L \rho V^2 S = W \sec \varphi \quad (23.2)$$

In horizontal circling flight the distribution of the air reactions across the span of the wing differs from that in straight flight because the outer wing moves faster than the inner. In a steady turn, however, the moments introduced from this cause will be balanced by the action of ailerons and rudder; in these circumstances it will be sufficient for a preliminary examination of the matter to suppose that the forces on the circling

aeroplane and the stresses set up thereby are the same as though it were flying straight at the same speed and incidence. On this assumption the power required and other quantities relating to a true-banked horizontal turn will be obtained, as for straight flight, but on the supposition that the weight of the aeroplane is increased in the ratio  $\sec \varphi$ : 1. The load factor ( $n$ ), for example, will equal  $\sec \varphi$ .

**24. Stalling Speed in a True-banked Turn.** The stalling speed will be given by the relation  $V_S = \sqrt{\frac{w}{\rho k_L} \sec \varphi}$

and will be  $\sqrt{\sec \varphi}$  times greater than in straight flight.

For values of  $\varphi$  equal to  $45^\circ$  and  $60^\circ$ , the stalling speed will therefore exceed that in straight flight by 19 per cent and 41 per cent respectively. This rise in the stalling speed in circling flight is a frequent cause of accidents to novices.

**25. Power Required in a True-banked Turn.** The power required for flight at high speeds is but slightly influenced by changes of weight, hence moderate true-banked turns at high speed do not call for appreciable increases of power. At lower speeds, or in steeply banked turns at any speed, considerable power losses will clearly be incurred. In particular, the minimum power for flight, which occurs at a speed not greatly in excess of the stalling speed, is very sensitive to change of weight and is therefore appreciably increased by even a moderate turn. It is therefore important to avoid any but the most gentle turns when attempting to climb at the maximum rate or to maintain height near the ceiling of the craft.

**26. Horizontal Turn of Minimum Radius.** Eliminating  $V$  between equations (23.1) and (23.2) yields

$$r = \frac{w \operatorname{cosec} \varphi}{g \rho k_L} \quad (26.1)$$

Thus, for a given angle of bank, the radius of a horizontal true-banked turn is inversely proportional to the lift coefficient and the minimum possible radius for a given angle of bank ( $\varphi$ ) is clearly,

$$\frac{w \operatorname{cosec} \varphi}{g \rho K_L} \quad (26.2)$$

This minimum approaches the absolute minimum of 12 as  $\varphi$  approaches  $90^\circ$  but the absolute minimum cannot be reached in a true-banked turn, because, in order to satisfy the relation  $k_L \rho V^2 S = W \operatorname{cosec} \varphi$ , the speed would have to increase to infinity as  $\varphi$  approaches  $90^\circ$ . If the speed does not increase in accordance with this relation the weight of the aeroplane cannot be supported, except by a side-force generated by downward side-slipping.

When the angle of bank ( $\varphi$ ) is  $60^\circ$ ,  $\sqrt{\sec \varphi} = 1.41$  and  $\operatorname{cosec} \varphi = 1.15$  so that a true-banked horizontal turn of radius less than 15 per cent

greater than the absolute minimum is possible, provided that a speed more than 41 per cent greater than the stalling speed in straight flight can be maintained whilst the lift coefficient is at its maximum value. We have seen, however, that the drag on an aeroplane flying at the incidence which gives maximum lift is very high, consequently it is much more economical of power to carry out a sharp turn with a lift coefficient somewhat lower than the maximum. Complete horizontal circles with radius no more than 20 per cent greater than the absolute minimum have been recorded.

**27. Aerodynamic Moments.** The simple considerations contained in this chapter, relating to the attitude of the aeroplane in steady flight and to the limiting accelerations which can be imposed upon it, have been discussed on the assumption that the pilot has the power and skill necessary to adjust the air-moments about axes through the c.g. to the values required by the manoeuvres considered. To proceed much further with the study of the dynamics of flight it is necessary to know something about these moments which are generated by the rotation of the aeroplane and by the action of the controls. The estimation of the magnitudes of these moments in various circumstances is the principal difficulty of our subject and the two following chapters will, therefore, be devoted to an examination of the available evidence upon which estimates of these moments can be based. Further study of the motions of the aeroplane under the combined actions of the air-forces and moments will be deferred to Chapter IV and subsequent chapters.

## CHAPTER II

### SYMMETRIC OR PITCHING MOMENTS

**1. Pitching Moments and Static Stability.** A line, such as  $YOY'$ , Fig 16, passing through the c.g. of an aeroplane and perpendicular to the plane of symmetry, will be called the *transverse axis* of the aeroplane. The total air-moment acting upon the aeroplane, about the transverse axis, will be called the *pitching moment*<sup>1</sup>—symbol  $M$ . The contribution to the pitching moment from any part of the aeroplane will be distinguished by some appropriate suffix.  $M$  is a function of many variables such as speed, air density, wing incidence and angular velocity of pitch. In steady symmetrical flight  $M$  is necessarily zero.

The partial derivative  $\partial M/\partial \alpha$  where  $\alpha$  is the wing incidence, is commonly said to define the *static pitching stability* of the aeroplane, the word *static* being introduced to indicate that the term relates to an imaginary condition in which the aeroplane is suspended in a current of air so as to be free to rotate about a *fixed* transverse axis. This partial

<sup>1</sup> Positive when it tends to raise the nose of the aeroplane.

derivative is an important factor in determining the free motion of an aeroplane when slightly disturbed from steady flight.

The pitching motion of the aeroplane is said to be statically stable, neutral or unstable, according as  $\partial M/\partial \alpha$  is negative, zero, or positive respectively. By an obvious analogy the word *weather-cock* is sometimes used instead of the word *static*, but we shall employ the shorter term.

**2. The Geometric Mean Chord.** In the conventional aeroplane of the present day the lift necessary to balance the weight is provided by a wing, or pair of wings, placed roughly one above the other, whilst the balance and control of the pitching moment is governed by a relatively small *tail* which is placed some distance behind the wings and contributes but little to the lift. Other arrangements are, of course, conceivable and have been tried, but at the present time it is true to say that all aeroplanes in common use are of the above type. The discussion which follows will relate to this type and although the methods employed can easily be adapted to other types, the approximations upon which they depend may then need modification.

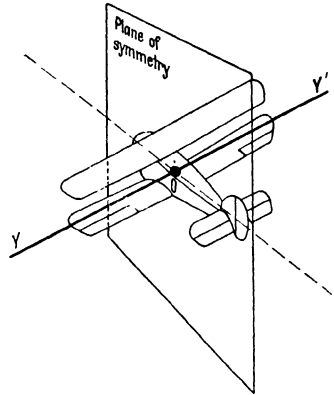


Fig. 16. The plane of symmetry and the transverse axis.

When the wings consist of more than one plane, as in a biplane, or when their plan form is not rectangular, or the profiles and incidences vary along the span, the first step in computing the pitching equilibrium and stability of the craft is to replace the actual wing system by an imaginary equivalent single wing, which may be supposed to be of rectangular plan form and to behave, as regards lift and pitching moment, in the same way as the real wing. The definition of this equivalent single wing is discussed in 46, so that it will be sufficient for the present to conduct our examination of the matter on the assumption that the lifting system consists of a single rectangular wing of uniform profile, having the *chords*<sup>1</sup> lying in a plane. The chord of this imaginary wing will be called the *geometric mean chord* of the wing system.

**3. The Air-Reactions on an Isolated Wing.** Figure 17 shows the *profile* or cross-section parallel to the plane of symmetry, of a typical modern wing, of which  $AB$  is the *chord* of length  $c$ .

If we suppose that this profile is at the plane of symmetry of a wing of rectangular plan form—aspect ratio 6—having the same profile at

<sup>1</sup> The *chord* of a wing is an arbitrary line such as  $AB$ , Fig. 17, drawn on the wing section or *profile* for the purpose of defining the width of the wing at this section and the *incidence* or orientation to the relative air stream.



all sections parallel to the plane of symmetry and having all the chords in one plane, then the arrows drawn on the diagram represent the experimentally ascertained lines of action and the relative magnitudes of the resultant air-reaction on this wing, when the incidences of the chord to the direction of the relative wind are as shown. The range of incidences— $0^\circ$  to  $10^\circ$ —covers about the whole range of normal steady flight for this wing.

Let us suppose that when the incidence is  $2.5^\circ$  corresponding to cruising conditions, the c.g. of this wing and the weight it is supporting, is located on the intersection of the chord with the line of action of the resultant force. Then it is clear that if the incidence is increased the air-reaction will pass in front of the c.g. and if it is decreased the air-reaction will pass behind the c.g. The value of  $\partial M/\partial \alpha$  will thus be positive

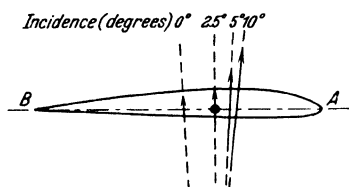


Fig. 17. The air-reactions on a typical wing.

and the equilibrium at  $2.5^\circ$  incidence will be statically unstable. Unless the c.g. is located far below this wing it will clearly be necessary to move it forward or backward to secure equilibrium at different incidences and the equilibrium in all positions within this range will be statically unstable. Although in some of the earliest flying experiments, equilibrium

at various speeds was secured by moving the c.g. in flight, this is not a convenient method and the necessity for such movement is now avoided by fixing a *tail-plane* and *elevators* some distance behind the wing, by means of which the pitching moments can be controlled and the inherent instability of the wing neutralised.

Wing forms are known and are occasionally used on which, over a wide range of incidences, the resultant reaction passes very near to a fixed point, and it is even possible, at the expense of some loss of efficiency, to find wings on which the equilibrium condition is inherently stable without assistance from a tail; but even in these circumstances a tail is always added to give the pilot control over pitching moments and to adjust for movements of the c.g. due to changes in the load distribution. Only in one or two experimental aeroplanes, which have not yet been produced in quantity, is an attempt made to dispense with the tail altogether and, in its stead, to provide the pilot with power to alter the wing form and so control the pitching moment.

**4. Functions of the Tail.** The tail has three distinct functions: fixed rigidly to the wing, it provides any required degree of static pitching stability, for the air-reaction upon it exerts a moment ( $M'$ ) about the c.g. for which  $\partial M'/\partial \alpha$  is negative: operated by the pilot through a slow irreversible mechanism, it allows equilibrium to be attained, within limits, for any incidence of the main planes and for any c.g. position:

operated through a quick acting, well balanced control, it enables unbalanced pitching moments to be generated whenever the pilot may need to produce pitching rotations.

**5. Fixed Tail and Elevators.** A common method of providing for the second and third operation above is to divide the tail into two parts called, respectively, the *fixed tail* or *stabilizer*, and the *elevators*. The fixed tail may, for example, be pivoted at *C*, Fig. 18, with the surface itself under the control of a screw jack connected with a wheel in the pilot's cockpit. By turning on this wheel the tail setting can be slowly altered, so that the angle made by the chord (*AC*) of the fixed tail with the chord of the wings can be altered through some  $5^\circ$  or  $6^\circ$ . In steady flight the incidence of the wings is (see I 5 and 9) a function of speed, and the operation of adjusting the fixed tail so as to obtain pitching equilibrium at the wing incidence appropriate to some particular speed is called *trimming* the aeroplane for that speed.

Behind the fixed tail, pivoted generally on the same axis (*C*), lie the *elevators* which, in their neutral position, continue the profile of the fixed tail, but which can be rotated quickly and easily by the pilot

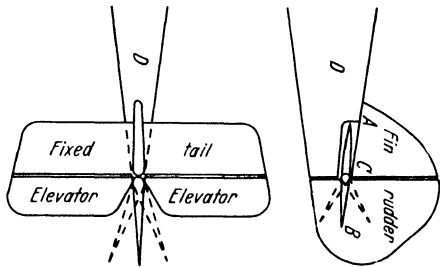


Fig. 18. Typical arrangement of tail, elevators, fin and rudder.

as shown in Fig. 18. These provide what is generally called the pitching control of the aeroplane. Because of the position of the elevators on the body (*D*) of the aeroplane, and to allow room for the rudder to swing from side to side, the elevators are generally constructed in two parts and hence are spoken of in the plural. They are, however, rigidly connected so as to move together and may be regarded as a single control organ. It will be realized that elevators situated as in Fig. 18 are very effective in performing their function of providing air-forces perpendicular to a line joining *C* to the c.g. of the aeroplane; for when they are moved, they not only experience air force themselves but, by their influence on the air flow, induce large changes in the air force on the fixed tail.

The designer will be greatly concerned with balancing the elevators, so that the air moment about *C* will be small, even when the air force which they exert is large. This balancing is carried out in a variety of ways, as for example by adjusting the position of the hinge *C*, but since, in this Division, we are concerned with the dynamics of the aeroplane under the air-reactions which come upon it and not with the practical operation of the machine, we shall not further discuss this matter of balancing controls, but will assume that the pilot has at his disposal sufficient power to place the controls in any desired position.

Though the method of plotting the line of action of the air-reaction, as in Fig. 17, is well suited to a preliminary qualitative discussion of the nature of the problems presented by the balance of pitching moments, it is not well suited to their quantitative analysis. For this purpose it is more convenient to specify the directions and magnitudes of the air-reactions by two mutually perpendicular components and their lines of action by the pitching moments about some transverse axis, such as that passing through the c.g. We shall adopt this latter method throughout the subsequent examination of the problem.

**6. Effect of C.G. Position on Static Stability.** Let the resultant air-reaction on an aeroplane flying symmetrically, be represented by the com-

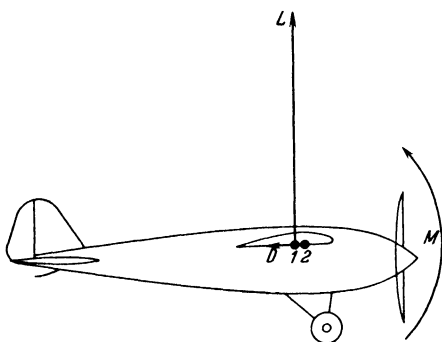


Fig. 19.

ponents, lift ( $L$ ) and drag ( $D$ ), perpendicular and parallel respectively to the direction of motion of the c.g., and by the pitching moment ( $M$ ), about the transverse axis through the c.g. When the aeroplane is flying straight and steadily with wing incidence  $\alpha_0$ , and c.g. in position (1), Fig. 19, the pitching moment  $M_1$  is necessarily zero and the static stability or instability of the equilibrium is

denoted by  $dM_1/d\alpha$ . Suppose now that a redistribution of load moves the c.g. forward through a distance  $x$  to position (2). Let  $M_2$  be the pitching moment about the new position so that

$$M_2 = M_1 - Lx$$

The aeroplane will no longer be in equilibrium at incidence  $\alpha_0$  since at this incidence  $M_1$  is zero. Suppose, however, that equilibrium is restored by an adjustment of the tail-plane or elevator which introduces an additional moment  $M_E = L_0 x$ , where  $L_0$  is the value of  $L$  when the incidence is  $\alpha_0$ . It is found experimentally that the additional moment produced in this way by a given movement of tail or elevators is substantially independent of the attitude of the aeroplane provided that the tail is not near its stalling incidence, Fig. 23 (see 18). It follows that the moment about axis (2), Fig. 19 can now be written

$$M_2 = M_1 - Lx + M_E$$

In which  $M_E$  is a constant independent of  $\alpha$ . Differentiating with respect to  $\alpha$  to obtain a measure of the static stability of the equilibrium when the c.g. is in the new position (2), gives

$$\frac{\partial M_2}{\partial \alpha} = \frac{\partial M_1}{\partial \alpha} - \frac{\partial L}{\partial \alpha} \cdot x \quad (6.1)$$

Since  $\partial L/\partial \alpha$  is essentially positive, the static pitching stability of an aeroplane in normal flight is increased by moving the c.g. forwards and decreased by moving it backwards and this increase is directly proportional to the distance through which the c.g. is moved.

We take this opportunity to note that the characteristic behaviour of an aeroplane and the approximations which are valid in normal flight—incidences less than  $10^\circ$  for a wing with profile as in Fig 2—differ so radically from those in stalled flight at higher incidences that the equations require entirely different treatment in the two conditions. Unless a specific statement is made to the contrary, it will be assumed that the equations and discussions which follow relate to normal flight.

**7. Dimensionless Coefficients.** Quantities such as  $L$  and  $M$  are dependent upon air-density ( $\rho$ ) and aeroplane velocity ( $V$ ) as well as upon the shape, size and attitude of the aeroplane. It is convenient and customary to study them in terms of the dimensionless coefficients  $k_L$  and  $k_M$  defined so that

$$k_L = \frac{L}{\rho V^2 S} \quad \text{and} \quad k_M = \frac{M}{\rho V^2 S c}$$

where  $S$  is the conventional *wing area* and  $c$  is the geometric mean chord. These dimensionless coefficients are, sensibly, functions of the form and attitude of the aeroplane only. Dividing (6.1) throughout by  $\rho V^2 S c$  gives

$$\left[ \frac{dk_M}{d\alpha} \right]_2 = \left[ \frac{dk_M}{d\alpha} \right]_1 - \frac{dk_L}{d\alpha} \cdot \frac{x}{c} \quad (7.1)$$

It is found, experimentally, that  $dk_L/d\alpha$  is sensibly independent of  $\alpha$ , being a constant in the neighborhood of 2 when  $\alpha$  is expressed in radians, and it is for many purposes convenient and is normal practice to divide (7.1) throughout by  $dk_L/d\alpha$  giving

$$\left[ \frac{dk_M}{dk_L} \right]_2 = \left[ \frac{dk_M}{dk_L} \right]_1 - \frac{x}{c} \quad (7.2)$$

The expression  $dk_M/dk_L$ —the rate of change of pitching moment with respect to lift coefficient as the incidence changes—is often used as the criterion of static pitching stability of the craft.

**8. C.G. Positions for Neutral Equilibrium.** It will be noted, by reference to (7.2) that there is some value of  $x$  for which  $[dk_M/dk_L]_2$  is zero, and this leads, after an appropriate tail adjustment, to neutral pitching equilibrium. Let this value be  $x_0$ .

Then

$$0 = \left[ \frac{dk_M}{dk_L} \right]_1 - \frac{x_0}{c}$$

with other values of  $x$ ,  $\left[ \frac{dk_M}{dk_L} \right]_2 = - \frac{x - x_0}{c}$

Dropping the suffix and writing  $(x - x_0)/c = H$ , we have  $dk_M/dk_L = -H$ , which may be written in the alternative form,

$$\frac{dk_M}{d\alpha} = - \frac{dk_L}{d\alpha} \cdot H$$

The quantity  $H$  is comparable with the *metacentric height* of a ship, that is to say it defines the distance of the c.g. from a position which gives neutral equilibrium and it is proportional to the moment which acts on the aeroplane when displaced from the equilibrium attitude. It will be shown later that the sensitivity of the static pitching stability to movements of the c.g. perpendicular to the direction of motion is small compared with the sensitivity to movements parallel to the direction of motion, or in other words, that the locus of neutral c.g. positions is a line not far removed from perpendicular to the direction of motion. Thus  $H$  is the ratio to the geometric mean chord, of the distance of the c.g. forward of the locus of neutral c.g. positions; the latter being nearly a straight line perpendicular to the direction of motion. We shall describe  $H$  as the *metacentric ratio* of the aeroplane, although this term is not in general use at the time of writing.

**9. A Relation Between Control and Stability.** In steady symmetric horizontal flight, in air of given density, wing incidence is a function of speed only: the higher the speed the smaller the incidence. A stable aeroplane, trimmed for a given speed, will therefore, at lower speeds, have to fly at a greater incidence and will be acted upon by a negative pitching moment, tending to depress the nose. At higher speeds the pitching moment will be positive. It will be necessary, therefore, to use either the elevators or the trimming mechanism to hold the nose down at high speeds and to hold the nose up at low speeds. The reverse will be true for an unstable aeroplane. Only with a neutral aeroplane will it be possible to fly steadily at various speeds without retrimming and without unbalanced forces on the controls.

This relation provides one convenient way of assessing the static pitching stability of an aeroplane in flight. The aeroplane is trimmed for some medium speed and the efforts, or control movements, required to hold it in steady flight at speeds above and below the trimmed speed are noted.

Heavy unbalanced control forces or continual retrimmings with every change of speed are objectionable in flight, hence designers try to avoid either excessive stability or instability. We shall see, when we study the stability of free flight in later chapters, that a statically stable aeroplane, when disturbed, generally oscillates slowly and with decreasing amplitude about a mean path, whereas one that is statically unstable tends to diverge more and more from the equilibrium path. Though this divergence is generally so slow that the trained pilot has no difficulty in coping with it, he is constrained by its presence to be continually attending to the controls. For these reasons the condition most generally desired is slightly on the stable side of neutrality.

The load distribution on a machine in service is subject to variations which change the position of the c.g. These variations are generally

controlled within strict limits by the airworthiness certificate of the machine. The designer generally tries to achieve a condition near neutral equilibrium at the cruising speed when the c.g. is as far back as is permitted, for this ensures stability with all other permissible load distributions. He may even accept a slight instability in the farthest back position of the c.g. in order to avoid too great stability with the usual load distribution.

**10. Experiments on Complete Models.** Sometimes the relations between the quantities  $L$ ,  $D$ ,  $M$  and the incidence  $\alpha$ , will have been determined for a model of the complete aeroplane suspended in a wind tunnel in such a way that the force components and the pitching moments about some specified transverse axis, can be measured. These measurements will usually be made at a series of values of  $\alpha$ , sufficiently close together to allow continuous curves to be drawn in which  $k_L$ ,  $k_D$  and  $k_M$  are plotted as ordinates against  $\alpha$  as common abscissa. It is then a simple process to calculate the pitching moment coefficient about any other transverse axis and so to determine  $k_M$  and  $dk_M/d\alpha$  or  $dk_M/dk_L$  for any c.g. position and any incidence. The only uncertainties introduced are those due to the difference between the *Reynolds Number* of the model experiment and the corresponding full scale flight; to inaccuracies in the model; and to possible influences of the tunnel walls upon the flow.

The making and testing of complete models is, however, a lengthy and expensive procedure and it is often necessary for the designer to estimate these quantities from published data relating to the air-reactions on the separate components of the aeroplane, such as the wings, body, tail unit and airscrew. Even when a complete model experiment is contemplated, it is generally used merely as a check on the accuracy of the estimates made from preliminary designs. The processes involved in estimating the pitching moment coefficient  $k_M$  and its derivatives are, therefore, of great practical importance and it is to the study, on broad lines, of these processes that we shall now turn.

## A. Contributions of Separate Parts of the Aeroplane to Pitching Moments

**11. Introduction.** The problem will generally present itself in the following form: given the relative positions of wings, body, airscrew and tail, with the position of the c.g., and given the forces which act on these parts separately, to estimate the pitching moment about the transverse axis through the c.g. taking into account the interferences between the various parts, each of which disturbs the flow of the air upon the others. The problem is too complicated to be precisely solved and resolves itself into an exercise in approximation. We shall approach it by considering first its simplest aspects and then consider successively additional terms, taken roughly in the order of their importance.

### 12. Pitching Moments from Tail and Wings—C.G. on Wing Chord.

We shall begin with the simple arrangement illustrated in Fig. 20 which shows a monoplane with the c.g. ( $G$ ) situated on the geometric mean chord ( $AB$ ) and with the tail-plane pivotted at a point ( $D$ ) on this chord produced.

Information respecting the air reactions on the isolated wings and tail will have been obtained without knowledge of the position of the c.g. in the particular design in contemplation, hence the lines of action of the reactions on them will have been specified by their moments about arbitrarily chosen axes. For the wings the axis commonly chosen for this purpose passes through the leading edge.

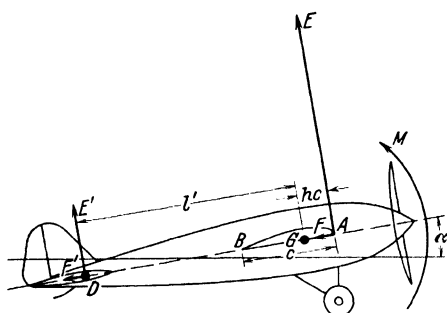


Fig. 20.

Let us suppose that the reactions on the wing are specified by the forces  $E$  and  $F$  perpendicular and parallel respectively to the chord and by the moment  $M_w$ —coefficient  $[k_M]_w$ —about the axis through  $A$ .

Let the reactions on the tail-plane in these directions be  $E'$  and  $F'$  and neglect their moment about the pivot of the tail.

Let the incidence of the wing chord ( $AB$ ) be  $\alpha$ .

Let  $AB = c$ ,  $AG = hc$  and  $GD = l'$ .

Let areas of wings and of the tail and elevators be  $S$  and  $S'$  respectively.

The force components  $E$  and  $F$  on the wings will be connected with the components  $L$  and  $D$  by the relations

$$E = L \cos \alpha + D \sin \alpha$$

$$F = D \cos \alpha - L \sin \alpha$$

which reduce, when  $D$  and  $\alpha$  are small, to the approximate form

$$E = L \quad \text{and} \quad F = D - L \alpha$$

The approximation will be sufficiently accurate for all practical purposes provided that  $L/D > 10$  and  $\alpha < 10^\circ$ ; a condition which is almost always satisfied in normal flight.

The relations between the dimensionless coefficients  $k_E$ ,  $k_F$ ,  $k_L$  and  $k_D$  will clearly be the same as those between the forces themselves, since all the force coefficients are derived through division by  $\rho V^2 S$ .

Omitting, for the present, moments contributed by the airscrew, the body, and other parts of the aeroplane, we may write the total moment  $M$  in the form

$$M = hc E + M_w - l' E'$$

or, dividing throughout by  $\rho V^2 S c$

$$k_M = h k_E + [k_M]_w - \frac{S' l'}{S c} \cdot \frac{E'}{\rho V^2 S'}$$

Write  $k'_E$  for  $E'/\rho V^2 S'$ ,  $K$  for  $S' l'/S c$  and replace  $E$  by its approximate value  $L$ , giving

$$k_M = h k_L + [k_M]_w - K k'_E \quad (12.1)$$

For equilibrium  $k_M$  is zero and (12.1) becomes

$$K k'_E = h k_L + [k_M]_w \quad (12.2)$$

which gives the value of the force coefficient ( $k'_E$ ) required from the tail.

Differentiating (12.1) with respect to  $\alpha$

$$\frac{dk_M}{d\alpha} = h \frac{dk_L}{d\alpha} + \left[ \frac{dk_M}{d\alpha} \right]_w - K \frac{dk'_E}{d\alpha} \quad (12.3)$$

For neutral equilibrium  $dk_M/d\alpha$  must also be zero, and (12.3) can

$$\text{then be written} \quad h_0 = K \frac{dk'_E}{dk_L} - \left[ \frac{dk_M}{dk_L} \right]_w \quad (12.4)$$

where  $h_0$  defines the c.g. position for neutral equilibrium.

**13. Joukowski's Theoretical Values for  $[dk_M/dk_L]_w$ .** Joukowski, from certain assumptions as to the nature of the flow, has shown that, for monoplane wings having what are now called Joukowski profiles,  $[dk_M/dk_L]_w$  is independent of incidence and equals  $-1/4$ ; this result is found by experiment to be nearly true for most monoplanes at moderate incidences<sup>1</sup>. In so far as it is true we may write (12.4) in the simpler form

$$h_0 = \frac{1}{4} + K \frac{dk'_E}{dk_L} \quad (13.1)$$

which shows that the c. g. position for neutral stability depends mainly on the tail and scarcely at all upon the form of the wing profile; for the rate of change of lift coefficient with incidence is nearly the same for all wing profiles.

Joukowski's theoretical result for the monoplane, quoted above, is equivalent to the statement that the moment coefficient about a point on the chord distant one quarter of the chord length behind the leading edge is independent of incidence: for brevity we shall describe this as the *quarter point*. This was, in fact, the way in which the proposition was first enunciated<sup>2</sup>. The magnitude of this constant coefficient is approximately determined by the curvature of the centre line of the wing profile (Ref. 1).

<sup>1</sup> For a biplane the equivalent theoretical value is

$$-\frac{1}{4} + \frac{1}{32G^2}$$

where  $G$  is the ratio of gap to chord and  $M$  is measured about the leading edge of the geometric mean chord (see 46). At moderate angles of incidence these theoretical values for biplanes agree fairly closely with the results of experiment.

<sup>2</sup> The position of Joukowski's point about which the theoretical value of the moment coefficient is independent of incidence is slightly above the chord, but it is sufficient for our purpose to assume that it is on the chord, at the quarter point.



When the c.g. lies on the quarter point the wing contributes nothing to the stability of the aeroplane; but when, as is more usual, the c.g. lies behind the quarter point the wing contributes an unstable term which has to be neutralized or overpowered by the stabilizing effect of the tail.

**14. Pitching Moments When the C.G. is not on Wing Chord.** Consider now the more general condition when the c.g. is not on the wing chord, Fig. 21.

Draw  $GN$  perpendicular to  $AB$  and let  $AN = hc$ ,  $GN = kc$ .

We must now add to the expression for the pitching moment a term  $kcF$  and to the pitching moment coefficient (12.1) and (12.2), a term  $kk_F$ . The corresponding term to be added to (12.3) or (12.4) is  $k \cdot dk_F/dk_L$ .

We proceed to expand these terms into more convenient forms.

Approximately

$$k_F = k_D - \alpha k_L \quad (14.1)$$

See 12.

Let  $-\alpha_0$  be the incidence when the lift is zero.

Let  $\alpha_i$  be the incidence induced by the trailing vortices, in accordance with the Prandtl theory of the lift of a wing of finite span. (See Division E I 11, 12; III Part C and IV 6.)

Let  $\alpha_p$  be the incidence, measured from zero lift, which would give lift coefficient  $k_L$  with two-dimensional flow about the wing profile.

$$\text{Then} \quad \alpha_p + \alpha_i = \alpha + \alpha_0 \quad (14.2)$$

$$\text{Write} \quad k_D = k_{Dp} + k_{Di} \quad (14.3)$$

where  $k_{Dp}$  is the profile drag coefficient, which may for our present purpose be assumed to be constant, and  $k_{Di}$  is the induced drag coefficient.

$$\text{Then} \quad k_{Di} = \alpha_i k_L \quad (14.4)$$

Equation (14.1) can now be rewritten, using (14.3) and (14.4)

$$k_F = k_{Dp} + \alpha_i k_L - (\alpha + \alpha_0) k_L + \alpha_0 k_L$$

$$\text{or using (14.2)} \quad k_F = k_{Dp} + \alpha_0 k_L - \alpha_p k_L$$

Now  $\alpha_p$  is sensibly proportional to  $k_L$ , so that we may write  $\alpha_p = ak_L$ , where  $a$  is a constant

$$\text{Thus} \quad k_F = k_{Dp} + \alpha_0 k_L - a k_L^2$$

and

$$\frac{dk_F}{dk_L} = \alpha_0 - 2ak_L = \alpha_i - 2\alpha_p$$

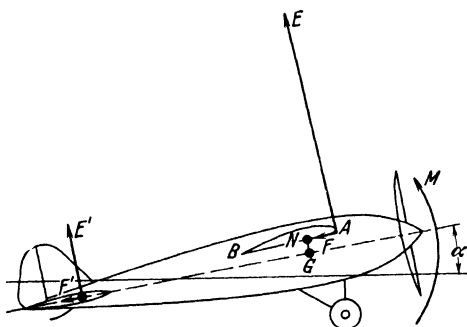


Fig. 21.

The equilibrium equation (12.2) now becomes

$$Kk'_E = [k_M]_w + k \cdot k_{Dp} + (h + \alpha_0 k) k_L - \alpha k \cdot k_L^2 \quad (14.5)$$

If we assume Joukowski's result for a monoplane, (14.5) reduces to

$$Kk'_E = k \cdot k_{Dp} + \left( h + \alpha_0 k - \frac{1}{4} \right) k_L - \alpha k \cdot k_L^2$$

This form of the equation for  $k'_E$  was first given in an unpublished paper by W. S. Farren. It is convenient for computation because it contains but one variable ( $k_L$ ).

The equation for neutral stability (12.4) becomes

$$h_0 - (2\alpha_p - \alpha_0)k_0 = K \frac{dk'_E}{dk_L} - \left[ \frac{dk_M}{dk_L} \right]_w \quad (14.6)$$

The interpretation of (14.6) is that, within the accuracy of the assumptions, the locus of neutral c.g. positions cuts the chord at the point

$$h_0 = K \frac{dk'_E}{dk_L} - \left[ \frac{dk_M}{dk_L} \right]_w$$

as is also shown by (12.4), and is a straight line inclined to the perpendicular to the chord through an angle  $(2\alpha_p - \alpha_0)$ . (See Fig. 22.)

The chord makes with the direction of motion an angle

$$\alpha = \alpha_i + \alpha_p - \alpha_0$$

Hence the locus of neutral c.g. positions is inclined to the perpendicular to the direction of motion through an angle  $(\alpha_p - \alpha_i)$  as shown in Fig. 22.

For wings of moderate thickness experiment shows that, approximately,

$$\alpha_p = 0.33 k_L \text{ for a monoplane}$$

and  $\alpha_p = 0.40 k_L$  for a biplane of normal proportions.

To a similar order of accuracy the induced incidence due to the trailing vortex system of a wing or wings of finite span is given by,

$$\alpha_i = 0.66 \frac{k_L}{A} \text{ for monoplane}$$

$$\alpha_i = 1.0 \frac{k_L}{A} \text{ for biplane,}$$

where  $A$  is the aspect ratio.

$$\text{Thus } (\alpha_p - \alpha_i) = 0.33 \left[ 1 - \frac{2}{A} \right] k_L \text{ (Monoplane)}$$

$$(\alpha_p - \alpha_i) = 0.40 \left[ 1 - \frac{2.5}{A} \right] k_L \text{ (Biplane)}$$

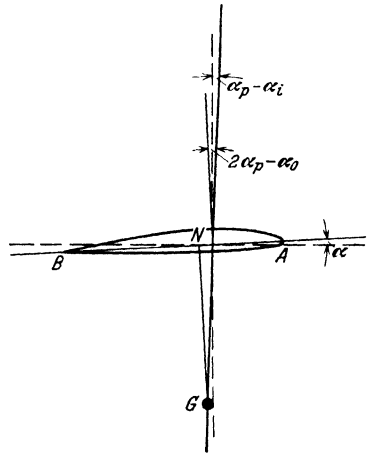


Fig. 22. Heavy line—Locus of neutral c.g. positions.  
Thin lines, perpendicular and parallel to wing chord.  
Broken lines, perpendicular and parallel to direction of motion.

A popular value of  $A$  is 6, and with this value  $(\alpha_p - \alpha_i) = 0.22 k_L$  (Monoplane) and  $0.23 k_L$  (Biplane).

A rough approximation will generally be sufficient for this angle, hence we may say, approximately, that the locus of neutral c.g. positions is inclined to the perpendicular to the direction of motion through an angle equal to  $0.22 k_L$  radians, whether for monoplanes or biplanes. This figure refers to aspect ratio 6; it rises to about  $0.27 k_L$  for aspect ratio 9 and falls to about  $0.16 k_L$  for aspect ratio 4. A representative value of  $k_L$  at cruising speed is 0.2 and, with this value and aspect ratio 6, the angle is 0.044 radians or  $2.5^\circ$ .

The locus of neutral c.g. positions is thus nearly perpendicular to the direction of motion at cruising speeds and therefore up and down movements of the c.g. (in horizontal flight) have much less influence on static pitching stability than do fore-and-aft movements. What slight influence they have is to reduce stability as the c.g. rises.

When the pivot of the tail does not lie on a line through the c.g. parallel to the wing chord a term should, strictly, be introduced into the equations to represent the moment of the force  $F'$  (Fig. 21) about the c.g. Such a term is easily introduced, but is rarely of sufficient importance to be worth considering, particularly when account is taken of the uncertainties which we shall shortly consider, arising from the interference of the wings, body and airscrew with the flow over the tail.

**15. Direct Contribution of the Airscrew to Pitching Moments.** We have next to consider the influence of the airscrew upon the pitching balance and static stability.

When the axis of the screw is parallel to the direction of motion through the air, the screw will merely exert a thrust along this axis, the moment of which about the c.g. will depend upon the distance of the c.g. from the axis. When, however, the axis of the screw is inclined to the direction of motion there is an air-reaction upon it perpendicular to the axis, which will contribute to the pitching moment, unless the c.g. happens to lie in the plane of rotation.

The forces on a screw inclined to the relative wind have been the subject of considerable theoretical investigation (Refs. 2 and 3) the main conclusions of which, in so far as they are of interest in the present connection, are well supported by experiment. It is found that the inclination of the screw does not, to a first order approximation, influence the revolutions of the engine or the thrust, but it does introduce a force in the plane of rotation, so that the screw acts as though it were a small aerofoil inclined to the wind.

Let  $F_s$  represent this force, and  $\alpha_s$  the inclination of the axis. It is shown in the reports referred to that approximately

$$F_s = \rho V^2 D^2 t \left[ \frac{kQ}{J} - \frac{1}{2} \frac{dkQ}{dJ} \right] \alpha_s$$

where  $D$  is the airscrew diameter,  $k_Q$  is the torque coefficient defined as  $Torque/\rho n^2 D^5$ ;  $n$  is revolutions per second,  $J$  stands for  $V/nD$ , and  $f$  is a numerical constant which depends on the distribution of torque along the blades.

For the screw for which the comparison between theory and experiment was made,  $f$  was 2.3 and from the nature of the calculations it is unlikely to differ widely from this figure for different screws.

If the distance of the c.g. from the plane of the screw be  $j$  (positive when c.g. behind screw) then the moment exerted by this force on the screw will be  $j \cdot F_s$  and the corresponding term to be included in the right hand sides of equilibrium equations (10.1) and (12.2) will be

$$f \frac{D^2 j}{Sc} \left[ \frac{k_Q}{J} - \frac{1}{2} \frac{dk_Q}{dJ} \right] \alpha_s \quad (15.1)$$

The corresponding term to be included in the right hand side of (12.3) and (12.4) to give the c.g. position for neutral equilibrium is

$$-f \frac{D^2 j}{Sc} \left[ \frac{k_Q}{J} - \frac{1}{2} \frac{dk_Q}{dJ} \right] \frac{d\alpha}{dk_L} \quad (15.2)$$

For, since the axis of the airscrew is fixed on the aeroplane,  $d\alpha_s/dk_L = d\alpha/dk_L$ .

The effect of the screw will, therefore, be to move the c.g. position for neutral stability forward by a distance equal to the magnitude of (15.2) multiplied by the length ( $c$ ) of the equivalent chord.

**16. Numerical Values—Airscrew Contribution.** The value of the term in the bracket of (15.2), for conventional screws, under ordinary flying conditions, is in the neighborhood of 0.02. It varies nearly in proportion to the ratio (blade area/disc area) and is rather higher for screws of high (pitch/diameter) ratio than for those in which this ratio is small. Rough estimates of its values for a two-bladed airscrew with maximum blade width about  $0.10 D$  and the value of  $J$  at cruising speed equal to about 0.65 are as follows<sup>1</sup>:

Screw idling ( $k_Q = 0$ ) . . . . .	0.016
Cruising . . . . .	0.022
Climbing. . . . .	0.025

$D^2 j/Sc$  will be at its greatest in a conventional tractor with single screw, such as the BF2b for which its value is 0.25.

Taking  $d\alpha/dk_L = 0.6$ —a figure suitable to a biplane—we see that the value of this term for the BF2b at cruising speed will be approximately,  $-2.3 \times 0.25 \times 0.022 \times 0.6 = -0.0076$ , rising to  $-0.0085$  in climbing condition and falling to  $-0.0055$  when the screw is turning freely.

<sup>1</sup> This is the airscrew of the two seater tractor biplane (BF2b) which will be used later to provide numerical examples of the magnitudes of the moments and of the motions of an aeroplane following specific disturbances.

The effect of this term will be to move the neutral c.g. position forward by a distance less than 0.01 of the mean chord, an amount which is sufficiently large to be included in the estimate of the neutral c.g. position but is not large enough to require very precise computation.

### 17. Contribution of the Body and Minor Parts to Pitching Moments.

We have now considered all the reactions which contribute to the pitching moment, with the exception of those upon the main body of the machine and such external parts as the undercarriage, wing struts, etc. The last will generally experience a drag force accompanied by very little lift, and the drags will contribute terms to the pitching moment equation; but, since these are sensibly independent of changes of incidence, they will not, as a rule, appreciably influence the static stability. The moment upon the body, on the other hand, may contribute appreciable terms both to the equilibrium and stability equations. These terms are difficult to estimate and are generally included in the estimate of the influence of the body on the terms  $k'_E$  and  $dk'_E/dk_L$  which relate to the moment exerted by the tail.

## B. Forces on Tail and Interference Factors

18. Statement of Problem. It is in the estimation of the quantities  $k'_E$  and  $dk'_E/dk_L$  that the principal difficulty lies. For this purpose the designer will probably have access to a family of curves such as those of Fig. 23.

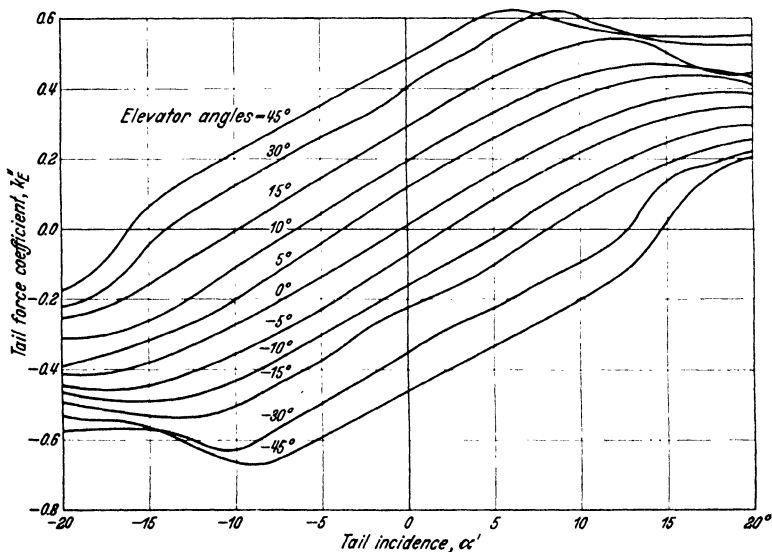


Fig. 23. Typical curves showing forces on isolated tail and elevator.

Using the conventions above described, the force on the tail when on the aeroplane will be  $k'_E \rho (V + v)^2 S'$ , where  $k'_E$  is taken from Fig. 23 at an incidence  $(\alpha + \alpha_T - \varepsilon)$ .

The force coefficient  $k'_E$  employed in the earlier calculation will thus equal  $(1 + v/V)^2 k'_E$ . For shortness we will write this in the form

$$k'_E = b k''_E$$

The derivative  $dk'_E/dk_L$ , which appears in the static stability equation (12.4), can now be written in the form,

$$\frac{dk'_E}{dk_L} = b \cdot \frac{d\alpha'}{d\alpha} \cdot \frac{d\alpha}{dk_L} \cdot \frac{dk''_E}{d\alpha'} = b \left[ 1 - \frac{d\varepsilon}{d\alpha} \right] \frac{d\alpha}{dk_L} \frac{dk''_E}{d\alpha'} \quad (19.1)$$

The terms  $b$  and  $(1 - d\varepsilon/d\alpha)$  must be estimated from laboratory experiment or previous experience;  $d\alpha/dk_L$  is known and  $dk''_E/d\alpha'$  is taken from the slopes of the curves of Fig. 23.

When estimating the tail setting necessary for equilibrium the value of  $k'_E$  required for equilibrium will be calculated from an equation such as (12.2) or (14.5). Then  $k''_E = k'_E/b$  and a line drawn at this value of  $k''_E$  parallel to the abscissa of Fig. 23 will show all the combinations of effective incidence  $(\alpha')$  and elevator setting  $(\eta)$  which will give pitching equilibrium. The tail setting  $\alpha_T$  is then found from the relation  $\alpha_T = \alpha' - \alpha + \varepsilon$ .

**20. Hinge-Moments and Free Elevators.** The moment  $(i)$  exerted by the elevators about their hinge may be represented by a coefficient  $k_i = i/\rho V'^2 S' c'$ , where  $i$  is the hinge moment in a uniform current of

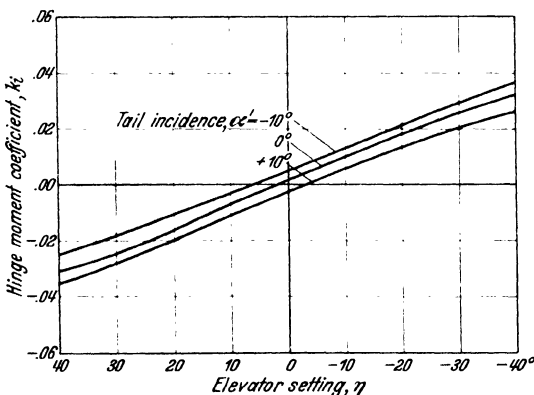


Fig. 24. Typical curves showing moments on elevator hinge.

undisturbed air of velocity  $V'$  and  $S'$  and  $c'$  are the area and chord respectively of the whole tail. An example of experimental curves showing the variations of this coefficient with incidence and elevator setting, for unbalanced elevators, is given in Fig. 24. We shall assume the actual hinge-moment of the elevator upon the aeroplane to be obtained from this coefficient by the application of the same

interference quantities  $b$  and  $\varepsilon$  as apply to the reaction on the whole tail and elevators. This assumption is not necessarily correct unless the elevators are disposed fairly evenly behind the tail, but it will be sufficient to illustrate in a simple example, the effects of freeing the elevators.

Provided that the force coefficient required from the tail is not too high, it will be observed, in Figs. 23 and 24, that both the coefficients of force and hinge-moment are sensibly linear functions of  $\alpha'$  and  $\eta$ . In normal flight therefore, it is, for most purposes, sufficiently accurate to represent Figs. 23 and 24 by the two equations

$$\begin{aligned} k_E'' &= a_1 \alpha' + a_2 \eta \\ k_i &= b_1 \alpha' + b_2 \eta \end{aligned}$$

where  $a_1$ ,  $a_2$ ,  $b_1$ ,  $b_2$  are constants.

It must, however, be remembered that this approximation is not permissible if the force coefficient on the tail approaches the maximum available.

It is sometimes necessary to examine the condition when the elevator is left free. Writing  $\eta_0$  for the value of  $\eta$  in these circumstances

$$\eta_0 = -\frac{b_1}{b_2} \alpha' + C$$

where  $C$  is a constant arising from the moment of the weight of the elevators about their hinge.

Hence 
$$k_E'' = \left[ a_1 - \frac{b_1}{b_2} a_2 \right] \alpha' + a_2 C$$

Therefore 
$$\frac{dk_E''}{d\alpha'} = a_1 - \frac{b_1}{b_2} a_2$$

whereas, with the elevators fixed we have simply  $dk_E''/d\alpha' = a_1$ .

Freeing elevators thus reduces the effectiveness of the tail in the ratio  $[1 - b_1 a_2 / b_2 a_1]$  to unity. For the system illustrated in Figs. 23 and 24,  $b_1 a_2 / b_2 a_1 = 0.3$ . Hence, on freeing the elevators of this system, the stabilizing influence of the tail is reduced in the ratio 0.7:1.

**21. Wing-tail Interference.** Many very elaborate experiments have been made, both in the laboratory and in flight, with the object of assessing the interference factors  $b$  and  $\varepsilon$  in various circumstances. It is found that the influence of the wings is almost entirely confined to the factor  $(1 - d\varepsilon/d\alpha)$ . The relation between *downwash* ( $\varepsilon$ ) and wing incidence ( $\alpha$ ) has been studied both by measurement of the direction of flow at a series of points in the neighborhood of the tail and by measurement of the force on a tail-plane separately suspended behind the wing in the position which it would occupy on a complete aeroplane. (Refs. 4 and 5.) The principal experiments, made with biplane wings, showed that, when the tail is in the conventional position, some three wing chords behind the c.g., the ratio  $d\varepsilon/d\alpha$  is slightly less than one-half, say 0.45 as an average figure. Corresponding to this figure the factor  $(1 - d\varepsilon/d\alpha)$  is therefore equal to 0.55. The downwash angle ( $\varepsilon$ ) may be considerably reduced if the wings are cut away at the centre section as is sometimes done with the object of improving the pilot's view.

**22. Airscrew-tail Interferences.** The influence of the airscrew on the tail has also been extensively studied, both alone and in combination with the wings. (Refs. 6 and 7.) It affects both  $b$  and  $\varepsilon$ . This influence is very difficult to estimate, because it depends on the precise relation of the tail to the slipstream, which is not uniform, but is of annular form with a central region not much influenced by the screw. A simple way of making a rough estimate is to find, by Froude's momentum theory, the extra velocity  $v$  in a uniform slipstream and to assume that the velocity over those parts of the tail which come within the stream is increased by this amount, whilst the direction of flow is altered by the angle  $[v/(V + v)]\alpha_s$ , where  $\alpha_s$  is the inclination of the airscrew axis to the direction of motion. This estimate is, however, very rough and the reader should consult the references or other original works for more precise information on this matter. A refinement, whereby an allowance can be made for the extra deflection of the slipstream due to the force on the inclined screw perpendicular to its axis, is given in the division on *Airscrews* (see Division L VIII 7, XII 5).

For estimating the downwash of wings and tractor screw together, the formula

$$\varepsilon = \varepsilon_1 + \frac{v}{V+v} \left[ 1 - \frac{d\varepsilon}{d\alpha} \right] \alpha_s$$

where  $\varepsilon_1$  is the downwash from the wings alone, has been suggested. This formula allows for the alteration in downwash from the wings due to the change of incidence brought about by downwash from the screw, but its physical basis is very uncertain and it gives results considerably lower than are found by experiment. The simple addition of the two sources of downwash leading to  $\varepsilon = \varepsilon_1 + \left[ \frac{v}{V+v} \right] \alpha_s$  appears to give equally good results, but this again cannot be correct for large downwashes.

**23. Body-tail Interference.** The influence of the body is generally held to be mainly on the factor  $b$ , through the slowing up of the air velocity near the roots of the tail. This factor also is very uncertain and is generally made to include any moments which act on the body itself. A value 0.7 for  $b$ , deduced more from design experience than from laboratory experiment, may be taken as roughly representing modern tractors of conventional design.

**24. Airscrew-wing Interference.** In addition to the direct influence of the screw on stability and the effect of its slipstream on the tail, there will also be a small indirect effect due to the slipstream on the main wing system. This can be roughly represented by a fictitious increase in the wing area ( $S$ ), the only sensible influence of which will be slightly to reduce the ratio  $S'/S$  and with it the static stability coefficient. We shall ignore this effect in the numerical illustration to be given later.



**25. Interference Problems Discussed.** In the presence of all these uncertainties respecting the interference factors to be applied to the tail, it will be clear that the estimation, from first principles, of the tail and elevator settings for equilibrium and of the precise position of the c.g. for neutral equilibrium, is a matter of great difficulty. Designers of experience do, however, succeed in predicting these quantities with considerable accuracy, but this is principally because the aeroplanes which they build differ but slightly from those which they have previously built and tested.

It might be thought that, with these uncertainties, the study of the various factors which determine pitching moment becomes an unprofitable exercise, having no bearing on practice, but this is not so. As in all other engineering practice, progress is made step-by-step, using the accumulated experience of past designs to predict the effect of the next step. The magnitude of the steps which can be made with reasonable certainty depends on the ability to separate the effects of different causes and on the extent to which factors of experience, such as  $b$  and  $\varepsilon$  in the present discussion, rest on sound physical bases.

Fortunately, accuracy in the prediction of the equilibrium and stability for an entirely new design is seldom essential, since it is generally possible to adjust the tail angles and c.g. positions to compensate for small errors in estimation. It is important, however, that these adjustments shall not be so large as to require partial redesign; hence efforts are continually being made to improve the experimental information upon which the coefficients of experience rest.

An additional point is worth noting. When an aeroplane has been tested and put into service and overall errors in pitching balance and stability have been corrected by adjustments to the tail and to the position of the c.g., it may often be necessary to estimate the influence of some further change, say in the position of the c.g., in the screw, or in the position and size of the tail. It may then be possible, from considerations such as those which we have been discussing, to estimate the effects of the changes with useful accuracy, despite the fact that the calculation of pitching moments from first principles may contain uncertainties much greater than the whole effect to be estimated.

**26. Numerical Illustrations.** To illustrate the relative importance of the various terms which have been under discussion, the following estimate of their numerical values has been made for a typical tractor biplane, travelling at cruising speed, when the value of the lift coefficient ( $k_L$ ) is 0.20.

With airscrew stopped and using the notation previously defined, the locus of neutral c.g. positions is given by

$$\begin{aligned}
 h_0 &= - \left[ \frac{dk_M}{dk_L} \right]_w + b \left[ 1 - \frac{d\varepsilon}{d\alpha} \right] K \frac{d\alpha}{dk_L} \frac{dk_E''}{d\alpha'} + [2ak_L - \alpha_0] k_0 \\
 h_0 &= + 0.220 + 0.70 \times [1 - 0.45] \times 0.35 \times 0.60 \times 1.7 + \\
 &\quad + [2 \times 0.4 \times 0.2 - 0.052] \times 0.04 \\
 h_0 &= + 0.220 + 0.137 + 0.004 \\
 h_0 &= 0.361
 \end{aligned}$$

When the airscrew is working, an additional term, representing the variations of force on it, perpendicular to its axis has to be added to the right hand side of this equation. The value of this term is in the neighborhood of  $-0.008$ .

The factors  $b$  and  $(1 - d\varepsilon/d\alpha)$  are also modified by the action of the slipstream on the tail. As already stated, this modification is exceedingly difficult to estimate accurately, but a very rough estimate can be made by assuming that over those parts of the tail which fall within the slipstream,  $b$  is increased by the factor  $(1 + v/V)^2$  and  $(1 - d\varepsilon/d\alpha)$  is altered to  $(1 - \frac{d\varepsilon}{d\alpha} - \frac{v}{V + v})$ .

It will be found that, using the value  $(1 - d\varepsilon/d\alpha) = 0.55$ , the net result of these two alterations is to leave the whole term representing tail influence practically unaltered for all values of  $v/V$  up to 0.3, which is the approximate value in climbing flight. For this aeroplane, therefore, the influence of the screw on static stability is sensibly confined to the term  $-0.008$ , which reduces  $h_0$  to 0.353.

This aeroplane with screw stopped thus becomes unstable when  $h > 0.361$ , and with screw working when  $h > 0.353$ . The design value for  $h$  will probably range from about 0.30 to 0.36, according to load distribution, whilst the value of  $k$  will be little influenced by changes in loading. The metacentric ratio  $H$  will, therefore, range from about zero to 0.06.

**27. Pitching Moments at Very High Speeds.** Finally it should be noted that at small values of  $k_L$ , corresponding to high speed flight, the value of  $[dk_M/dk_L]_w$  falls slightly, but definitely, below Joukowski's

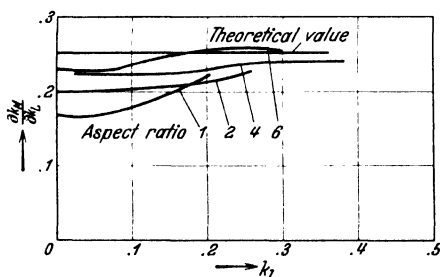


Fig. 25. Curves showing variations of  $[dk_M/dk_L]_w$  for wings of different aspect ratio.

theoretical value, which for mono-planes is one quarter. The reason for this phenomenon is not yet known, but it has been amply verified by experiment. It is particularly marked with low aspect ratios (Ref. 8).

The curves of Fig. 25 showing the values of this ratio for symmetrical aerofoils of aspect ratios 1, 2, 4, 6, give some idea of the magnitude of the variation. For

wings of aspect ratio 6 or greater this deviation from Joukowski's theory is unimportant unless the lift coefficient is less than about 0.15, corresponding to speeds greater than twice the stalling speed.

**28. Pitching Moments in Stalled Flight.** The relations which we have been considering apply to normal flight, where the lift coefficients of the tail and wings are sensibly linear functions of incidence and  $[dk_M/d\alpha]_w$  is in the neighborhood of  $-1/4$ . If the wing incidence is allowed to increase to the stalling angle and beyond, profound changes occur in the flow about the wings and in the relations between the forces and moments on the wings and tail. The lift coefficient ceases to increase with incidence and may even fall as the incidence passes the stall. The downwash ( $\varepsilon$ ) at the tail also ceases to increase and may fall in sympathy with the lift. The wing moment coefficient  $(k_M)_w$  first increases and then becomes roughly constant, and this increase, combined with the decrease in  $k_L$ , implies that the *centre of pressure* moves backward—actually to a point about 0.4 of the chord from the leading edge.

With a conventional c.g. position, say  $h = 0.33$ , the centre of pressure of the wings, after stalling, will therefore be behind the c.g., and equilibrium will require a negative, or downward, air-reaction on the tail. Unless, however, an unusually large range of tail trimming angles is provided, the effective incidence of the tail will be very high, both because the wing incidence ( $\alpha$ ) is high and because the downwash ( $\varepsilon$ ) has ceased to increase with  $\alpha$ . It may thus be impossible to provide the air-reaction on the tail necessary for equilibrium.

There will, therefore, in a conventional aeroplane, be a limiting incidence, not much greater than stalling incidence, beyond which the aeroplane will necessarily be acted upon by a negative pitching moment, which will rapidly reduce the incidence to the limiting value for equilibrium. At high incidences the stability equation (12.4) in which the various terms were differentiated with respect to  $k_L$ , has now no interest, and to examine static pitching stability in stalled flight we must return to (12.3), which is restated below with the last term expanded in accordance with 19.

$$\frac{dk_M}{d\alpha} = h \frac{dk_L}{d\alpha} + \left( \frac{dk_M}{d\alpha} \right)_w - Kb \left( 1 - \frac{d\varepsilon}{d\alpha} \right) \frac{dk'_E}{d\alpha'} \quad (28.1)$$

In normal flight, with a normal value of  $h$ , greater than 0.25, the sum of the first two terms on the right-hand side of this equation is positive, showing that the wings are producing a de-stabilizing influence which is, in a well designed aeroplane, just overpowered by the stabilizing influence of the tail, indicated by the last term. In stalled flight, the sum of the first two terms falls practically to zero, or may even become slightly negative, whilst the stabilizing influence of the tail increases, because the factor  $(1 - d\varepsilon/d\alpha)$  rises from about 0.55 in normal flight

to a value slightly greater than unity in stalled flight. In other words the downwash ceases to increase with wing incidence and the tail, therefore, becomes more effective.

If, therefore, an aeroplane can be held in pitching equilibrium, at an incidence greater than the stall, the equilibrium is, *statically*, very stable, but it must not be assumed from this that the pitching equilibrium of a stalled aeroplane in *free flight* is necessarily stable. That depends on other factors which will be considered in due course.

### C. Pitching Moments in Circling Flight ( $M_q$ )

**29. Introduction.** Hitherto we have supposed the aeroplane to be moving steadily and without rotation. We have now to consider the influence on the pitching moment, of a steady angular velocity about the transverse axis. In accordance with a system of notation which will be more fully developed in Chapter V, we shall denote this angular velocity by the symbol  $q$ . We have to consider the influence of the angular velocity  $q$  upon the pitching moment  $M$ .

An aeroplane flying with velocity  $V$  in a circular path of radius  $R$  and centre  $O$  situated in its plane of symmetry, will have an angular velocity or rate of pitch,  $q$ , such that

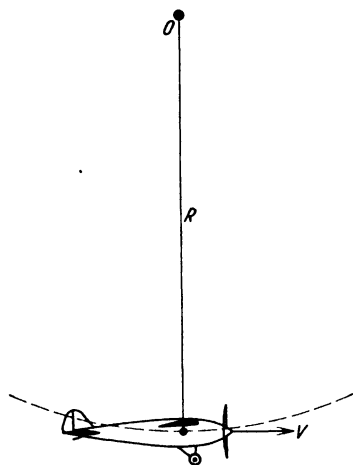
$$q = V/R$$


Fig. 26.

Continuous steady free flight of this kind without side-slip is not possible, for if the plane of the circle is horizontal there will of necessity be some side-slip occurring, whereas if the plane is inclined to the horizontal the action of gravity will differ at different parts of the circle. Nevertheless it is important to investigate the influence of  $q$  on  $M$  and for simplicity we may conceive  $q$  as occurring in a steady symmetrical motion, in which both velocity and incidence are constant.

The state of affairs conceived will be very nearly attained in a steeply banked steady horizontal turn and can be exactly achieved for a model aeroplane supported on a whirling arm and whirled around in an attitude such that the plane of symmetry coincides with the plane of rotation. One method of finding the effect of  $q$  is, in fact, to perform an experiment of this kind upon a whirling arm.

**30. The Tail in Circling Flight.** Let the c.g. of an aeroplane be travelling with velocity  $V$  while the aeroplane is rotating with angular velocity  $q$  (see Fig. 27).

Then the direction of motion of any point on the tail, distant  $l'$  behind the c.g., will make an angle  $\tan^{-1} q l' / V$  with the direction of motion of the c.g. If  $l'$  is taken to be the distance from the c.g. of a mean point on the tail, we observe that, provided  $q l'$  is not too large compared with  $V$ , the effective incidence of the tail will be increased by approximately  $q l' / V$  radians, above the incidence which it would have in the absence of  $q$ .

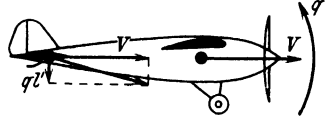


Fig. 27. Illustrating effect of rate of pitch ( $q$ ) upon incidence of tail.

We may thus anticipate that when the aeroplane is flying on a curved path with angular velocity of pitch  $q$ , the pitching moment exerted by the tail will be increased by the amount  $-\frac{\partial M'}{\partial \alpha'} \cdot \frac{q l'}{V}$  over the value in straight flight.  $\partial M' / \partial \alpha'$  is here the rate of change of the tail pitching moment with change of effective tail incidence. This anticipation is supported with reasonable accuracy by the results of experiments.

**31. The Derivative  $M_q$ .** The ratio of the pitching moment due to a small angular velocity  $q$  to the value of  $q$  which produces it is called the *rotary derivative of pitching moment due to pitching* and is given the symbol  $M_q$ . To the above order of approximation we have, due to

$$\text{tail only} \quad M_q = - \frac{\partial M'}{\partial \alpha'} \cdot \frac{l'}{V}$$

Using the notation previously developed to express the pitching moment of the tail in straight flight, we have approximately

$$\frac{\partial M'}{\partial \alpha'} = - b \rho V^2 S' l' \frac{d k_E''}{d \alpha'}$$

$$\text{or} \quad M_q = - b \rho V S' l'^2 \frac{d k_E''}{d \alpha'} \quad (\text{tail only})$$

where  $d k_E'' / d \alpha'$  stands, as before, for the slope of curves for the tail such as those in Fig. 23 and  $b$  stands for a factor of experience to allow for the shielding effect of the body on the tail.

Note that the downwash factor  $(1 - d\epsilon/d\alpha)$  does not appear in this expression, because incidence is constant in the type of motion imagined.

**32. The Dimensionless Coefficient ( $k_{mq}$ ).** It is convenient to use a dimensionless coefficient of  $M_q$ . The coefficient normally employed has the symbol  $k_{mq}$  and is defined so that

$$k_{mq} = \frac{M_q}{\rho V S c^2}$$

where  $c$ , as before, is the geometric mean wing chord. We thus have

$$k'_{mq} = - \frac{S' l'^2}{S c^2} b \frac{d k_E''}{d \alpha'} \quad (32.1)$$

The prime indicates that the symbol applies to the contribution of the tail only. A typical value for this quantity is

$$k_{mq} = -1.0 \times 0.7 \times 1.7 = -1.2$$

**33. Contribution of the Wings to  $M_q$ .** The contribution, at moderate incidences, of the wings to  $M_q$  has been calculated theoretically and the results have been found to agree reasonably closely with experiment (Ref. 9). This contribution depends mainly on the value of the c.g. coefficient  $h$  and, to a small extent, on the aspect ratio. The results of these calculations are shown in Fig. 28, from which it appears that, for normal values of  $h$  between 0.3 and 0.4, the wings contribute a term of the order one tenth that of the tail. Their contributions need not, therefore, be very accurately computed.

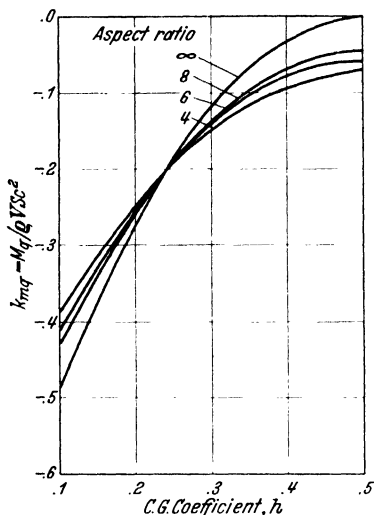


Fig. 28. Theoretical contribution of wings to  $M_q$ .

**34. Direct Contribution of the Screw to  $M_q$ .** The airscrew contributes to  $M_q$ , both directly and indirectly through the action of the slipstream on the tail. The direct effects of the forces acting on the screw itself have been calculated (Ref. 3) and, although they are not of great importance in comparison with the contribution of the tail, are here given

for convenience of reference. They can be divided into three parts, arising, respectively, from:

1. The couple acting on the screw, due to its angular velocity  $q$ .
2. The force perpendicular to the screw axis, due to velocity perpendicular to this axis, which is, in turn, due to the angular velocity  $q$ .
3. The change of thrust due to change of forward velocity arising from  $q$ .

Let  $i$  be the distance of the aeroplane's c.g. from the screw axis and  $j$  its distance from the plane of the screw.

Let the airscrew diameter be  $D$ , the thrust  $T$ , the torque  $Q$ , and the revolutions per second  $n$ .

$$\text{Let } J = V/nD$$

$$\text{As before let } k_T = T/\rho n^2 D^4 \text{ and } k_Q = Q/\rho n^2 D^5.$$

Let  $\lambda$  be the ratio of  $J$  to the value which gives zero thrust.

Then the contributions to the coefficient  $k_{mq}$  of the above three effects of  $q$  are approximately

1.  $0.05 \cdot \frac{D^4}{Sc^2} \cdot \frac{1}{J} \frac{dk_T}{dJ}$
2.  $2.3 \frac{D^2 j^2}{Sc^2} \left[ \frac{k_Q}{J} - \frac{1}{2} \frac{dk_Q}{dJ} \right]$
3.  $2 \left( \frac{i}{c} \right)^2 \frac{T}{qSV^2} \left[ 1 - \frac{2(1.325 - \lambda^3)}{(1 - \lambda^3)(2.65 + \lambda^3)} \right]$

A typical value of the first term is of the order — 0.015, which is practically negligible compared with  $k_{mq}$  due to the tail.

In level flight the third term will generally be less numerically than —0.02 so long as  $i$  is less than  $c$ , and hence in normal circumstances this term also is negligible. For very precise work involving climbing flight with a screw very much above the c.g., as in seaplanes, this term might just be appreciable.

A typical value of the second term in level flight may be of the order — 0.15. Hence this term is appreciable, though still not of great importance. The accuracy of the above formula for this term has been checked by direct experiment and reasonable agreement found (Ref. 7).

**35. Influence of Airscrew Slip-Stream on Tail.** The influence on  $M_q$  of the slipstream acting upon the tail is due to the enhanced velocity over the tail, no allowance being made for the influence of the slipstream on downwash, since, as has already been observed,  $M_q$  is to be regarded as the pitching moment due to  $q$  with incidence remaining constant. An approximate estimate of the effect of slipstream on the tail is obtained by multiplying the contribution of that part of the tail which is in the slipstream by  $(1 + v/V)^2$  where  $v$  is the estimated slipstream velocity. The contribution of slipstream to tail  $M_q$  has been measured experimentally on a simplified model aeroplane having no body and the result of the experiments agreed reasonably well with calculations by the above method (Ref. 7).

**36. Numerical Illustration.** The relative contributions of the various parts of the aeroplane to  $k_{mq}$  are illustrated in the following Table which contains rough estimates of these contributions for a typical tractor biplane in three different circumstances.

Aeroplane part	Contribution to $k_{mq}$		
	Airscrew stopped	Airscrew running in level flight	Airscrew running in climbing flight
Tail . . . . .	1.20	1.40	1.70
Wings . . . . .	0.11	0.11	0.11
Screw (Fin effect) . . . . .	0.00	0.15	0.17
Screw (Rotation effect). . . . .	0.00	0.01	0.01
Screw (Fore and aft movement) .	0.00	0.00	0.00
Total . . . . .	1.3	1.7	2.0

These rough estimates, given merely to show the order of magnitude of the various contributions, are stated without reference to wing incidence. The mean of experimental results upon complete models shows (see 43, Fig. 30) agreement with the figures for engine stopped, here given, but the experiment gives a somewhat higher value than this at zero incidence and a lower value at higher incidences.

### D. Experimental Methods of Measuring $M_q$

**37. Whirling Arm Experiment.** The determination of  $M_q$  on a complete model of an aeroplane can be carried out either on a whirling arm or by a method which involves oscillating the model in a wind tunnel. The theory of the whirling arm experiment is simple; the pitching moment ( $M_1$ ) is measured in steady circling motion on the whirling arm and the pitching moment ( $M_2$ ) is also measured on the same model fixed in a wind tunnel, the incidence in the tunnel experiment being equal to the angle between the chord of the wing and the direction of motion of the transverse axis in the whirling arm experiment.

Then  $M_q = (M_1 - M_2)/q$ , where  $q$  is the angular velocity of the whirling arm.

Technically, this experiment is very difficult, because it is difficult to prevent the whirling arm from disturbing the air in the room and so introducing errors which are large compared with the quantity to be measured.

**38. The Free Oscillation Method.** The method involving a model oscillating in a wind tunnel is theoretically more complicated but experimentally easier than the whirling arm method. Two alternative oscillation methods have been used. In both, the model oscillates about the transverse axis and measurements of the *damping* term in the oscillation are made. At first this was done by noting the natural rate of decay of the oscillation, but this method has been superseded by one in which the oscillation is *forced* from outside the tunnel. The damping term in the oscillation is not, as might be supposed, equal to the derivative  $M_q$  but the value of  $M_q$  can be deduced from it in a manner described later.

In the free oscillation method, the equation of motion may be written

$$I\ddot{\theta} + (\mu + \mu_1)\dot{\theta} + k\theta = 0$$

where  $I$  is the moment of inertia of the oscillating system,  $\mu$  is the air-damping to be measured,  $\mu_1$  represents the friction damping at the pivot, and  $k\theta$  is the restoring couple when the model is displaced through the angle  $\theta$  from the equilibrium position.

The logarithmic decrement of this oscillation, namely  $(\mu + \mu_1)/2I$ , can be ascertained by recording the amplitudes of successive swings. A repeat experiment with wing stopped allows  $\mu_1/2I$  to be determined



and, neglecting the air-damping in stationary air, the air-damping with air flowing in the tunnel is obtained from the difference of these two results.

**39. The Forced Oscillation Method.** In the more modern method, the model is supported in the tunnel with freedom to rotate about the transverse axis  $G$  (Fig. 29). A wire  $AB$ , containing a spring  $S$ , is attached to the tail at  $A$  and to an eccentric crank outside the tunnel at  $B$ . The rate of rotation of this crank is very slowly increased until the maximum synchronous oscillation of the aeroplane occurs. The amplitude and frequency of this oscillation are then observed.

The equation of motion of this system is

$$I\ddot{\theta} + (\mu + \mu_1)\dot{\theta} + k\theta = k_1 \sin pt \quad (39.1)$$

where  $k_1$  defines the amplitude of the forcing term of which the period is  $2\pi/p$ .

The steady solution of this equation after the initial disturbances have settled down is

$$\theta = \frac{k_1 \sin(pt - \epsilon)}{\sqrt{(k - Ip^2)^2 + (\mu + \mu_1)^2 p^2}}$$

where

$$\tan \epsilon = \frac{(\mu + \mu_1)p}{(k - Ip^2)}$$

The amplitude of this steady oscillation will be a maximum when

$$k - Ip^2 = \frac{(\mu + \mu_1)^2}{2I}$$

and then

$$\theta_{(\max.)} = \frac{k_1}{\mu + \mu_1} \cdot \frac{1}{\sqrt{p^2 + \frac{(\mu + \mu_1)^2}{4I^2}}}$$

The term  $(\mu + \mu_1)^2/4I^2$  is always negligible compared with  $p^2$  and hence

$$(\mu + \mu_1) = \frac{k_1}{p \cdot \theta_{(\max.)}}$$

The friction damping  $\mu_1$  is then determined by a repeat experiment with wind stopped and  $\mu$  is found by difference.

**40. Relations between  $\mu$ ,  $M_q$  and  $M_{\dot{\alpha}}$ .** The air-damping term,  $\mu$ , found by either of these methods, was for some years thought to be identical with  $M_q$ , and in the earlier published reports this assumption is made. It is now known, however, that  $\mu$  and  $M_q$  are not identical. The reason is as follows.

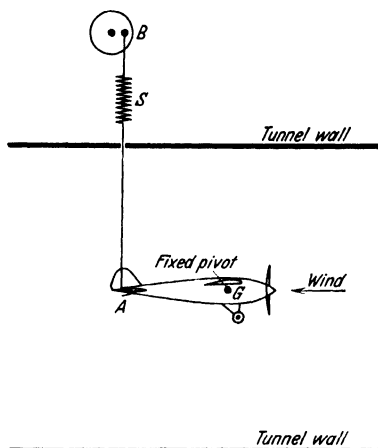


Fig. 29. Illustrating the forced oscillation experiment to find  $M_q$ .

$M_q$  is defined as the change in pitching moment due to rate of pitch, when other variables, including incidence ( $\alpha$ ), remain constant. In the oscillation experiments, however,  $\alpha$  does not remain constant; in fact  $d\alpha/dt$  is equal to  $q$ . It used to be thought that the air-reactions, though functions of incidence, are independent of rate of change of incidence, but it is now known that this is not true for the reactions on the tail in so far as they are influenced by the down wash from the wings<sup>1</sup>. There appears to be a time lag between the creation of the downwash by the wings and its action on the tail; the downwash on the tail being apparently substantially that appropriate to the lift on the wings when they were in the position occupied by the tail a fraction of a second before the tail reached that position.

If  $l'$  defines the mean distance of the tail behind the wings, the downwash at the tail will, on this supposition, be that created by the wings  $l'/V$  seconds earlier.

Let  $d\alpha$  be the increase in the incidence of the wings since they passed the position occupied by the tail at the instant under consideration. Then writing  $\dot{\alpha}$  for  $d\alpha/dt$  and assuming as a first approximation that  $\dot{\alpha}$  is constant during the time interval  $l'/V$  we have

$$d\alpha = \dot{\alpha} \frac{l'}{V}$$

Let  $d\varepsilon$  be the difference between the downwash at the tail and the downwash which would have acted there had the wing incidence been constant at the value which it has at the instant under consideration.

$$\text{Then} \quad d\varepsilon = -\frac{d\varepsilon}{d\alpha} d\alpha = -\frac{d\varepsilon}{d\alpha} \dot{\alpha} \frac{l'}{V}$$

When both angular velocity  $q$  and rate of change of incidence  $\dot{\alpha}$  are occurring, the effective incidence of the tail will differ from that in straight steady flight by an amount which is approximately represented by the expression

$$\frac{q l'}{V} - d\varepsilon$$

$$\text{or} \quad \frac{l'}{V} \left[ q + \frac{d\varepsilon}{d\alpha} \dot{\alpha} \right]$$

Now, in the oscillation experiment of previous paragraphs, both  $q$  and  $\dot{\alpha}$  are equal to  $\dot{\theta}$ , because the direction of motion of the c.g. relative to the air remains unchanged. Hence in this experiment, the increment of effective tail incidence due to  $\dot{\theta}$  is

$$\frac{l'}{V} \left[ 1 + \frac{d\varepsilon}{d\alpha} \right] \dot{\theta}$$

In the oscillation experiment, therefore, the effect of the time lag on the action of the downwash upon the tail is, according to the present assumptions, to increase the increment of effective tail incidence due to angular velocity by the factor  $\left[ 1 + \frac{d\varepsilon}{d\alpha} \right]$ .

<sup>1</sup> For a discussion of the dependence of wing reactions on  $\dot{\alpha}$  see V 6.

Writing, as before,  $M'_q$  to represent the contribution of the tail to the pitching moment due to  $q$ , with  $\alpha$  constant, we observe that that part of the air damping coefficient ( $\mu$ ) of 38 and 39 which is contributed by the tail would, if uninfluenced by  $\dot{\alpha}$ , be equal to  $M'_q$ , but that, when the influence of  $\dot{\alpha}$  upon the downwash at the tail is included, this part of  $\mu$  is increased by the factor  $\left(1 + \frac{d\varepsilon}{d\alpha}\right)$ .

Assuming that only the wings and tail contribute appreciably to  $\mu$  and that the contribution of the wings ( $M_q^0$ ) is uninfluenced by  $\dot{\alpha}$ , we have the equation

$$M_q^0 + M'_q \left(1 + \frac{d\varepsilon}{d\alpha}\right) = \mu$$

or

$$M_q = M_q^0 + M'_q = \frac{\left(\mu + M_q^0 \frac{d\varepsilon}{d\alpha}\right)}{\left(1 + \frac{d\varepsilon}{d\alpha}\right)}$$

from which  $M_q$  can be obtained in terms of  $\mu$  if  $M_q^0$  can be estimated independently, say by repeating the experiment with tail removed or by the theoretical methods of Ref. 9. Since, however,  $M_q^0$  is generally but a small fraction of  $\mu$  it is sufficiently accurate for most purposes to ignore it and to write simply

$$M_q = \frac{\mu}{\left(1 + \frac{d\varepsilon}{d\alpha}\right)}$$

**41. Experimental Separation of  $M_q$  and  $M_{\dot{\alpha}}$ .** A skeleton model, consisting of biplane wings and a monoplane tail connected together by a light structure, giving no interference with the flow over the tail, was mounted in a tunnel (see Ref. 7).

The derivative  $dM'/d\alpha'$ , the rate of change of pitching moment with effective incidence, was determined by varying the incidence of the tail, keeping the wings fixed.

The effective value of  $d\varepsilon/d\alpha$  was determined by varying the incidence of the wings and finding, for each wing incidence, the attitude of the tail which gave no lift on the tail.

The damping ( $\mu$ ) was determined for the whole model and for the wings without tail, by the method of forced oscillation.

The contribution of the tail to this damping factor was then compared with the quantity  $(dM'/d\alpha') (l'/V) \left(1 + \frac{d\varepsilon}{d\alpha}\right)$  and good agreement obtained.

In so far as it can be assumed that  $M'_q$  is equal to  $(dM'/d\alpha') (l'/V)$  this experiment indicates that the effect of the rate of change of incidence on the damping factor is given by

$$\frac{dM'}{d\alpha} = \frac{dM}{d\alpha} \cdot \frac{l'}{V} \frac{d\varepsilon}{d\alpha}$$

and that therefore

$$\mu = M_q^0 + M'_q \left(1 + \frac{d\varepsilon}{d\alpha}\right)$$

The dependence of pitching moment on rate of change of incidence, represented by the term  $M_{\dot{\alpha}}$  is of considerable practical importance, both because this term is unavoidably associated with  $M_q$  in the only experimental method of determining  $M_q$  which has yet been successfully developed, and because the derivative  $M_{\dot{\alpha}}$  has itself a considerable influence on the symmetric motions of the aeroplane in free flight. We shall find it necessary to include this term in the equations which determine the response of the aeroplane to elevator movements and other disturbances, which are developed in Chapters VI and VII.

**42. Influence of the Screw on  $M_{\dot{\alpha}}$ .** The experiment described in Ref. 5 was repeated with a tractor airscrew throwing its slipstream on wings and tail. The results were, of course, much more complicated and difficult to interpret than those of the simpler experiment without airscrew, but using arguments and methods similar to those employed in the absence of the screw, the experimental results still indicated that

$$\mu = M_q^0 + M_q' \left( 1 + \frac{d\varepsilon}{d\alpha} \right)$$

provided, of course, that  $d\varepsilon/d\alpha$  represents the rate of change of downwash due to the combined effects of wing lift and screw slipstream.

## E. Experimental Results for $M_q$

**43. Normal Flight.** Many oscillation experiments have been made in wind tunnels, to determine  $M_q$  for various aeroplanes. From a study of these it appears that an approximate estimate of  $M_q$  for an aeroplane which does not depart too far from conventional practice can be made in the following way.

Introduce a new coefficient  $k''_{mq}$  such that

$$k''_{mq} = \frac{M_q}{\rho V S' l'^2}$$

$$\text{and therefore } k_{mq} = k''_{mq} \cdot \frac{S' l'^2}{S c^2}$$

$k''_{mq}$  is thus related to  $k_{mq}$  in a simple manner, but has the advantage, for purposes of rough estimation, that it is related to the dimensions of the tail, which is responsible for about 90 per cent of its whole value. Reference to (32.1) shows that  $k''_{mq}$  may be regarded as the effective rate of change of tail force coefficient with respect to effective tail incidence,

after making an allowance, in the factor  $b$ , for the interference of the body, and a small allowance for the average contribution of the wings. It would thus be anticipated that  $k''_{mq}$  will not vary greatly from one aeroplane to another and experiment has shown this to be so.

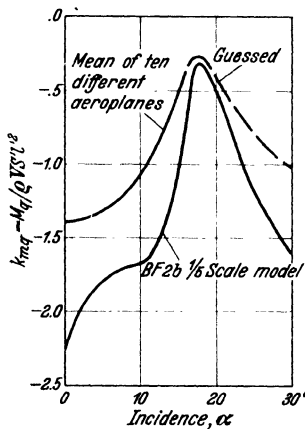


Fig. 30.

Experimental values of  $M_q$ .

In Fig. 30 the upper continuous line, covering a range of incidences from 0 deg. to 16°, is the mean of a number of experimental curves for different aeroplanes (Refs. 12, 13). The separate curves for the individual aeroplanes can be found by consulting the references. They relate to six aeroplanes of the large multi-engined land plane and sea-plane types; to two conventional war tractor biplanes and to two aeroplanes of the single engined pusher type, with tail supported on outriggers.

At the times when the reports on these experiments were written, the existence of the term  $M_{\alpha}$  had not been suspected, so that the quantities tabulated were the air damping factor ( $\mu$ ), which is now taken to be equal to  $M_q(1 + d\epsilon/d\alpha)$ . The values recorded in the original reports have therefore been divided by 1.45 which corresponds to an assumed value of 0.45 for the downwash ratio  $d\epsilon/d\alpha$  at the tail. The thick line in Fig. 30 is the mean of the values so obtained.

The majority of the experimental results for the ten aeroplanes examined in these two reports fall within 0.1 of this curve, though a few observations are more widely separated. Thus one multi-engined, seaplane gave a curve which agreed well with the mean up to about 5° incidence, but above 10° incidence the numerical value was about 0.2 greater. Also one single engined tractor biplane gave a value 0.2 above the mean at zero incidence, but agreed well at higher incidences.

On the whole it seems probable that an estimate of  $M_q$ , engine off, made from the mean curve of Fig. 30 for any of the common types of the present day, will be correct within some 10 per cent or 15 per cent for normal flight and of the right order of magnitude for incidences up to 16°.

**44.  $M_q$  in Stalled Flight.** The only experiment published at the time of writing which carries measurements of  $M_q$  up to very high incidences was performed upon a large model—8 feet wing span—of a Bristol Fighter, in the *duplex wind tunnel*, cross-section 14 feet  $\times$  7 feet, of the National Physical Laboratory of Great Britain (Ref. 14). This gave the result shown in Fig. 30. The disagreement at low incidences between this curve and the mean curve for ten aeroplanes is probably due to the interference of the wind tunnel walls of the large model. This view is supported by the fact that the downwash at the tail, which was separately measured in order to assess the factor  $(1 + d\epsilon/d\alpha)$  was much less than is usual.

The curve for the Bristol Fighter in Fig. 30 should not, therefore, be used to give a numerical estimate of  $M_q$ , even for that aeroplane; it has, however, been included in the figure because of its interesting shape at high incidences. There is apparently no doubt that the sudden fall in the numerical value of  $M_q$  at the stall is real; it has been traced to the wings, whose contribution to this derivative becomes large and positive—destabilizing—over a small range of incidence near the stall,

whilst the contribution of the tail is very little affected by the stall. This peculiar behaviour of the wings is probably due to some influence of  $q$  upon the incidence at which the flow changes characteristic of the stall occur, but the matter needs further research.

The broken line in Fig. 30 is merely a guess at what the value at high incidences may be expected to be, starting the curve from the mean curve for ten aeroplanes and continuing by analogy with the curve for the Bristol Fighter.

## F. The Geometric Mean Chord

**45. Statement of Problem.** The coefficients used in this chapter have been defined by reference to a conventional wing area ( $S$ ) and an equivalent chord ( $c$ ). It will be sufficient to define  $S$  as the sum of the areas of all the wings as they appear in a plan drawing of the aeroplane.

With a single wing of rectangular plan form having a uniform cross-section, or "profile", and coplanar chords, the equivalent chord used in the specification of pitching moment coefficients will be simply the chord of the centre section, but with wings of other forms the equivalent chord requires special definition.

For the purpose of pitching moment calculations, any line whatever in the plane of symmetry could theoretically be defined as the chord, but unless this line is carefully chosen the numerical values by which the pitching moments are specified will vary widely with different wing arrangements. It is a great convenience in design and computation if the chord can be so specified that the relation of  $k_M$  to  $k_L$  is dependent mainly on the form of the profile and to a minor extent only on the arrangement and shape of the wings.

When the wings have substantially the same profile throughout and are not twisted, it is for this reason, usual to specify the equivalent chord in such a way that the moment coefficient at any given lift coefficient is as nearly as practicable the same as it would be for a rectangular monoplane of the same profile. The equivalent chord now used in these circumstances is called the geometric mean chord and can be defined as follows.

**46. The Geometric Mean Chord Defined.** Let  $A_1B_1, A_2B_2 \dots$ , all parallel, be the chords of a group of wings as specified above.

Let  $P_1, P_2 \dots$ , be points on these chords which divide them in some given ratio, the same for all.

Let the lengths of the chords be  $c_1, c_2 \dots$  and let the co-ordinates of  $P_1, P_2 \dots$ , by reference to axes  $OX, OY$  be  $x_1, x_2 \dots, y_1, y_2 \dots$

Let the areas of the wings be  $S_1, S_2 \dots$  and let

$$S = S_1 + S_2 + \dots = \Sigma S_i$$

The geometric mean chord will be parallel to the individual chords. Let its length be  $c$  and its position be defined by a point  $P$ —coordinates  $x, y$ —which divides it in the same ratio as the individual chords are divided by  $P_1, P_2 \dots$

Then the geometric mean chord is defined so that

$$c = \frac{\Sigma c_i S_i}{S} \quad x = \frac{\Sigma x_i S_i}{S} \quad y = \frac{\Sigma y_i S_i}{S}$$

Let the forces on the separate wings be defined by the components  $X_1, X_2 \dots, Y_1, Y_2 \dots$ , passing through  $P_1, P_2 \dots$  and parallel, respectively, to the axes  $OX, OY$ ; together with the moments  $M_1, M_2 \dots$  acting about  $P_1, P_2 \dots$

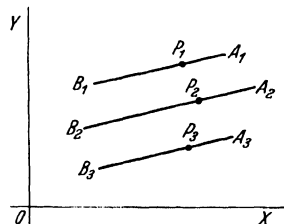


Fig. 31.

Suppose now that the dimensionless coefficients of these forces and moments are the same for all the wings, so that

$$k_x = \frac{X_1}{\rho V^2 S_1} = \frac{X_2}{\rho V^2 S_2} = \dots \quad (46.1)$$

$$k_y = \frac{Y_1}{\rho V^2 S_1} = \frac{Y_2}{\rho V^2 S_2} = \dots \quad (46.2)$$

$$k_m = \frac{M_1}{\rho V^2 S_1 c_1} = \frac{M_2}{\rho V^2 S_2 c_2} = \dots \quad (46.3)$$

The total moment of  $X_1, X_2 \dots$  about the point  $P$  will be

$$k_x \rho V^2 \Sigma S_i (y_1 - y)$$

or

$$k_x \rho V^2 (\Sigma S_i y_1 - S y)$$

which is zero by the definition of  $y$ .

Similarly the total moment of  $Y_1, Y_2 \dots$  about  $P$  will be zero.

The whole moment ( $M$ ) about  $P$  of all the forces on the individual wings will thus be

$$\begin{aligned} M &= M_1 + M_2 + \dots \\ &= k_m \rho V^2 \Sigma S_i c_i \\ &= k_m \rho V^2 S c \quad \text{by the definition of } c. \end{aligned}$$

The coefficient of this moment, defined by reference to the geometric mean chord and the total area  $S$  will, therefore, be equal to the coefficient of the individual wings.

It is easily verified that the position of the equivalent chord, according to this definition, is independent of the ratio chosen to define  $P$ .

This simple result is, of course, true only when the coefficients for individual planes are identical. If they are not identical, owing to mutual interference or to differences in the sections, or if the chords are not parallel, no such simple treatment is possible. It is usual, however, to define the equivalent chord in this simple geometrical manner whenever the various wings have the same shape and have parallel chords. For then, unless they are very close together, the simple result will

approximately be true and the deviations from it due to interferences of one wing on the other can be treated as first order corrections.

**47. Example of Application to a Biplane.** In a monoplane of Joukowski profile the moment coefficient about a point on the chord,  $1/4\ c$  behind the leading edge, has, theoretically, a constant value, say  $K_M$ . (This is not quite correct, but is sufficiently accurate for illustrative purposes.) If a biplane were made from wings of these sections and if the wings did not appreciably interfere with one another, the moment coefficient about the quarter point of the geometric mean chord would also be a constant and equal to  $K_M$ . Detailed analysis of the two-dimensional flow about a biplane has shown, however, that, due to mutual interference, the point about which the moment coefficient is constant and equal to  $K_M$  is slightly nearer to the leading edge of the equivalent chord than the quarter point (Ref. 1).

As a numerical example, in 13 the equation  $[dk_M/dk_L]_w = -1/4$  with  $M$  measured about the leading edge, was given for a Joukowski profile monoplane, whereas the value  $(dk_M/dk_L)_w = -\left(\frac{1}{4} - \frac{1}{32G^2}\right)$  was given for an equal biplane of gap/chord ratio  $G$ . These values are, of course, consistent with  $(dk_M/dk_L)_w = 0$  at points distant  $(1/4)\ c$  and  $\left(\frac{1}{4} - \frac{1}{32G^2}\right)\ c$  respectively, behind the leading edges of the chords. Thus, by adopting the geometric mean chord for the purpose of defining the total moment coefficient, the small interference effects are kept separate from the mere effects of the geometrical relations between the planes.

**48. Wings of Non-Rectangular Plan Form and with Dihedral Angle.** The geometric mean chord of a monoplane which is not of rectangular plan or does not have all the chords in one plane, is found in the same way, provided that all the chords are parallel and all the profiles are of the same shape but not necessarily the same size.

Let it be supposed that the wing is divided by a series of planes, parallel to the plane of symmetry and distant  $dz$  apart; and let the chords at these sections be of variable length ( $c_1$ ) and be projected upon the plane of symmetry.

Choose, as before, reference points on these chords, which divide them in a given ratio, the same for all; and let the co-ordinates of the projections of these reference points on the plane of symmetry be  $x_1, y_1$ .

Then, noting that the area of each strip is  $c_1\ dz$  the length of the geometric mean chord is defined as  $c = \int \frac{c_1^2 dz}{S}$  and the coordinates of its reference points are  $x = \int \frac{x_1 c_1 dz}{S}$  and  $y = \int \frac{y_1 c_1 dz}{S}$ .

If the coefficients for all the strips are identical the moment coefficient for the whole wing, defined by reference to this geometric mean



chord, will be the same as that for the individual strip, or for an equivalent rectangular wing with coplanar chords. Of course, the assumption that the coefficients are the same at all sections will not be exactly true and more detailed computation will be necessary if the dihedral angle is very large or the plan is very different from a rectangle.

When dealing with a biplane of which the wings are not rectangles with coplanar chords, the geometric mean chord of each wing will first be found and the mean chord of both wings found as already described.

**49. Twisted and Tapered Wings.** When the wings are twisted, so that the chords are not parallel, or when the profiles at different sections vary in shape, the problem of deciding on a convenient equivalent chord becomes more complex and each problem requires individual treatment.

### CHAPTER III

## THE ASYMMETRIC OR LATERAL MOMENTS

**1. Introduction.** This Chapter deals with the moments exerted by the air-reactions about axes which lie in the plane of symmetry and pass through the c.g. of the aeroplane. When a symmetrical aeroplane flies symmetrically these moments are necessarily zero; they arise only through the actions of the controls—rudder or ailerons—or as the result of asymmetric movements, such as side-slip or rotations about axes lying in the plane of symmetry.

**2. Axes.** The asymmetric moments and angular velocities are vectors which will generally be resolved into components about two mutually perpendicular axes in the plane of symmetry. The system of axes,  $OX$ ,  $OZ$  to be used for this purpose is shown in Fig. 32. Sometimes we shall choose  $OX$  parallel to the mean wing chord and shall then describe the axes as *chord axes*: at other times  $OX$  will be parallel to the projection upon the plane of symmetry of the velocity of the c.g. relative to the air, and the axes will then be described as *wind axes* because  $OX$  then coincides with the direction of the relative wind when the flight is symmetrical.

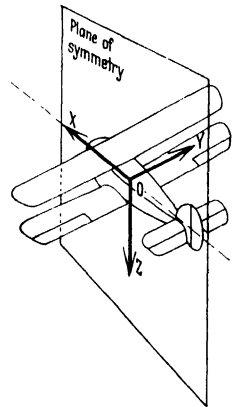


Fig. 32. Plane of symmetry and axes.

**3. Symbols.** The resultant velocity of the c.g. relative to the air receives the usual symbol  $V$  and its direction is defined by two angles: the *incidence* ( $\alpha$ ) which is the inclination to the mean wing chord of the projection of the direction of  $V$  on the plane of symmetry; and the *side-slip* angle ( $\beta$ ), which is the inclination to the plane of symmetry of the direction of  $V$ —positive when directed to starboard.

The component of  $V$  perpendicular to the plane of symmetry is called *side-slip* ( $V$ ), positive when to starboard. Note that  $V = V \sin \beta$ .

The symbols and names for the components of the asymmetric moments and angular velocities are as follows:

Axis	Positive Direction	Moment		Angular Velocity	
		Name	Symbol	Name	Symbol
$O X$	Forwards	Rolling moment	$L$	Rate of Roll	$p$
$O Z$	Downwards	Yawing moment	$N$	Rate of Yaw	$r$

Positive senses of the moments and angular velocities are defined by reference to a right handed screw when looking from the origin along the positive directions of the axes.

The choice of the positive direction of  $Z$ , downwards, may strike the reader as being peculiar; it is made to conform with the general system of notation which is fully developed in Chapter V. This system is not the only one in use at the present time, though it is the one universally adopted in England. It is difficult to devise a complete system in which all the quantities have their positive senses in what may be described as the natural directions; the one used in the present work provides a good compromise despite the fact that in it the normal lift of the wings produces a negative ( $Z$ ) force component.

It will be noticed that the symbol  $L$ , which has elsewhere been used to represent lift, is here used to represent rolling moment. This ambiguity is difficult to avoid without breaking the valuable alphabetical sequences of the complete symbolic system of Chapter V. Clash between the two symbols will, however, seldom occur; on the few occasions when it does occur the distinction will be effected by using  $L_1$  for rolling moment.

**4. Dimensionless Coefficients.** Dimensionless coefficients of rolling and yawing moments will be defined as follows:—

$$\text{Rolling Moment} \quad k_l = \frac{L}{\rho V^2 S s}$$

$$\text{Yawing Moment} \quad k_n = \frac{N}{\rho V^2 S s}$$

where  $2s$  is the span of the wings. Note the use of small  $l$  in the coefficient of rolling moment to distinguish it from the coefficient of lift.

Note here the change of form from the coefficient  $k_m = M/\rho V^2 S c$ , where  $c$  is the mean wing chord, used in Chapter II to represent the pitching moment. Pitching, rolling and yawing moments are all components of one three-dimensional vector quantity and to use one definition for the coefficients of two of these components and another for the third would be indefensible were it not that throughout the first seven

chapters the symmetric and asymmetric groups of forces and moments are treated entirely separately. In these circumstances the different definitions are convenient, and conform with modern practice. In Chapter VIII which relates to the spin, different definitions will be adopted.

**5. Controls.** The asymmetric moments are under the control of the pilot, through the medium of the *rudder* (see Fig. 18, Chapter II) and the *ailerons*; the latter enable the profiles of the wings near their outer tips to be modified so as to increase the lift on one wing while reducing that on the other. The two ailerons are always connected together by a mechanism which, for the present purpose, may be supposed rigid, so that their angular positions can be specified by a single independent variable,  $\xi$ , which is defined as the angular displacement of the starboard aileron from the neutral position—positive when the trailing edge falls. The position of the rudder, or rudders, is similarly defined by a single variable,  $\zeta$ —positive when the trailing edge moves to port.

**6. The Independent Variables Which Govern Asymmetric Moments.** With given values for the air-density ( $\rho$ ), the resultant c.g. velocity ( $V$ ) and the wing incidence ( $\alpha$ ), the asymmetric moment components are functions of the five independent variables,  $V$ ,  $p$ ,  $r$ ,  $\zeta$ ,  $\xi$ . From considerations of symmetry, these functions vanish when the independent variables are all zero and are symmetrical for positive and negative values of the variables; hence it is only necessary to find the effect of positive asymmetric variables.

A complete knowledge of the asymmetric moments would require, for each value of  $\alpha$ , a knowledge of the numerical values of both moment components for every combination of the five independent variables; such complete information is not available for any aeroplane and we shall in general consider only the values of the moments when each one of the five independent variables occurs in the absence of the other four. Except in some few instances it is necessary, in the present state of knowledge, to assume that the effect of two or more variables acting together is the sum of the effects of each acting separately.

## A. Effects of Side-Slip

**7. Dihedral Angle.** Consider first, the effect of side-slip ( $V$ ) upon the wings and assume that the chords of each half wing are in a plane, but that these planes are inclined upwards from a perpendicular to the plane of symmetry through an angle,  $\gamma$ , called the *dihedral angle* (Fig. 33).

Resolve the side-slip velocity ( $V$ ) into two components parallel and perpendicular respectively to the plane of chords of the starboard wing and neglect, for the present, the former of these components. The latter component will then alter the incidence of the starboard wing by an

angle whose circular measure is approximately  $V\gamma/V$ . The corresponding change of incidence on the port wing is then  $-V\gamma/V$ . We proceed to



Fig. 33. Dihedral angle.

consider the influence of these changes of incidence upon the rolling and yawing moments acting on the wing.

**8. Theoretical Estimates of Rolling Moments Due to Side-Slip.** Let the lift on the whole wing in symmetrical flight at speed  $V$  and incidence  $\alpha$  be  $L$ , so that the rate of change of lift with change of incidence— $V$  constant—is  $\partial L/\partial \alpha$ .

Using *wind axes* let the rolling moment exerted by the starboard half wing in symmetrical flight be  $-(1/2)LJ_1s$  where  $s$  is the semi-span of the whole wing. By symmetry the moment exerted by the port wing is  $+(1/2)LJ_1s$ .  $J_1s$  is the distance from the plane of symmetry to the line of action of the lift on each half wing.

Now let a side-slip ( $V$ ) occur which will add to the incidences of the starboard wing the approximate angles  $V\gamma/V$  and subtract a like angle from the incidence of the port wing. Neglecting the effect of the small changes in induced incidence due to the changed distribution of lift, the rolling moment on the starboard wing will be increased by the amount  $\frac{1}{2}J_1s \frac{\partial L}{\partial \alpha} \frac{V}{V} \gamma$ , while that on the port wing will be decreased by a like amount. The total rolling moment on the whole wing will therefore be  $-J_1s \frac{\partial L}{\partial \alpha} \frac{V}{V} \gamma$  the sense of which will be to raise the wing towards which the slip is occurring.

The dimensionless coefficient of this rolling moment is obtained by dividing by  $\rho V^2 S s$ , so that an estimate of the rolling moment coefficient due to side-slip is

$$k_l = -J_1 \frac{dk_L}{d\alpha} \frac{V}{V} \gamma \quad (8.1)$$

A quantity of great importance in the calculations of the motions of an aeroplane is the ratio of the rolling moment produced by side-slip to the side-slip which produces it. When the side-slip is small this ratio would be represented, in the notation of the calculus, by  $\partial L_1/\partial V$ , where  $L_1$  represents rolling moment, but for shortness it is more usual to employ the symbol  $L_v$  which is described as the derivative of rolling moment due to side-slip. The conventional dimensionless coefficient of this derivative has the symbol  $k_{lv}$  and is defined as follows:  $k_{lv} = L_v/\rho V S s$ .

and since 
$$L_v = \frac{\partial L_1}{\partial V} = \rho V^2 S s \frac{dk_l}{dV} = \rho V S s \frac{dk_l}{d(V/V)}$$

it follows that an alternative expression for  $k_{lv}$  is

$$k_{lv} = \frac{dk_l}{d(V/V)}$$

Using this notation equation (8.1) shows that a rough estimate of the derivative of rolling moment due to side-slip is

$$k_{lv} = -J_1 \frac{dk_l}{d\alpha} \gamma \quad (8.2)$$

The numerical value of  $J_1$  for a wing upon which the lift is graded uniformly across the span is  $1/2$ ; for a wing upon which the lift is graded elliptically it is  $4/3 \pi$  or  $0.425$ ; while for a wing with triangular lift grading, that is to say with lift linearly graded falling to zero at the tip, the value is  $1/3$ . The average wing has a lift grading between uniform and elliptic and a value of  $dk_l/d\alpha$  in the neighborhood of  $2$ . Hence the approximate assumptions on which (8.2) is founded would lead us to expect a value of  $k_{lv}$  slightly less than the circular measure of the dihedral angle.

**9. Theoretical Estimate of Yawing Moment Due to Side-Slip.** Arguments and assumptions similar to those used in obtaining an expression for rolling moment due to side-slip give, for the yawing moment on the wings—wind axes—the equation

$$k_{nv} = +J_1 \frac{dk_D}{d\alpha} \gamma \quad (9.1)$$

where  $k_D$  is the drag coefficient of the whole wing, and  $J_1$  now refers to the line of action of the resultant drag on each half wing. In normal flight the numerical value of this derivative is small.

**10. Conversion to Chord Axes.** The rolling and yawing moments here considered are expressed by reference to wind axes. They can be converted to chord axes by straight forward resolution. Thus if  $OX'$  (chord axes) makes an angle  $\alpha$  with  $OX$  (wind axes) and if primed symbols are used throughout temporarily to distinguish symbols referred to chord axes from those referred to wind axes, we have

$$k'_{lv} = k_{lv} \cos \alpha - k_{nv} \sin \alpha$$

$$k'_{nv} = k_{nv} \cos \alpha + k_{lv} \sin \alpha$$

Note that in normal flight, when  $\alpha$  is small and  $k_{nv}$  is small compared with  $k_{lv}$

$$k'_{lv} = k_{lv} \text{ approximately.}$$

hence

$$k'_{nv} = k_{nv} + k_{lv} \cdot \alpha \text{ approximately.}$$

In normal flight, therefore,  $k_{lv}$  will have sensibly the same numerical value whichever system of axes is used, but the value of  $k_{nv}$  will depend sensitively on the choice of axes.

**11. Omissions in the Assumptions.** These estimates of the effects of side-slip are obviously not precise, since they take no account of any effects of the component of the side-slip velocity parallel to the plane of chords of each wing, which must to some extent influence the form of the flow, particularly near the wing tips; neither do they allow for the effects of changes in the trailing vortex system when the wing is side-slipping. The simple calculation serves, however, to show the

principal reason why side-slip generates rolling moments on a pair of wings having a dihedral angle and it gives results not far different from those found by direct experiment.

**12. Experimental Measurements of the Effects of Side-Slip on an Isolated Wing.** Experiments have been made in which rolling and yawing moments due to side-slip were directly measured on a model wing in a wind tunnel (Ref. 1). The aspect ratio of this wing was 6 and the dihedral angle was varied by intervals of 2 degrees between 0 and 8°. Below 10° incidence the rolling moment was found to be sensibly proportional both to side-slip and to dihedral angle, as is suggested by (8.1) and the whole of the results for incidences less than 10° can be expressed with fair accuracy by the equation

$$k_{lv} = -0.72 \gamma \quad (12.1)$$

The greatest variation from this simple expression occurred at 10° incidence and zero dihedral angle, when the value of  $k_{lv}$  was 0.025, which is the value given by (12.1), with  $\gamma$  slightly less than 1°. At lower incidences, however,  $k_{lv}$  at zero dihedral, was practically zero.

The derivative  $dk_L/d\alpha$  for this wing was measured and found to be 2.2 so that, assuming a value of 0.45 for  $J_1$ , (8.2) reduces to  $k_{lv} = -1.0 \gamma$ . This experiment therefore showed a rolling moment due to side-slip some 30 per cent less than would be indicated by (8.2).

The experimentally determined yawing moments, expressed in chord axes, were very erratic and followed no simple law but, at the incidences of normal flight, they are small enough to be entirely neglected in calculations such as will be developed in later chapters.

**13.  $L_v$  in Stalled Flight.** At high incidences  $k_{lv}$  was found to rise to the neighborhood of about 0.2 and to be almost independent of dihedral angle. Equations (8.1) or (8.2) would suggest that, since  $dk_L/d\alpha$  falls to zero or becomes negative after stalling,  $k_{lv}$  on a stalled wing would also fall approximately to zero or change sign. Many similar experiments have, however, been made since those under discussion and all have confirmed the observation that, on stalling,  $k_{lv}$  becomes large and is scarcely influenced by changes of dihedral angle. The cause of this somewhat surprising phenomenon has been examined in an experiment in which the pressure distribution on the wing surface was measured (Ref. 2).

Figure 34 drawn from data obtained in this experiment, shows, in isometric projection, the pressure distribution at various sections of the wing when the incidence was 20° and the side-slip zero and 20° respectively. This diagram shows that in symmetrical stalled flight the intensity of lift is greater near the tip than in the middle of the wing and that when the wing is side-slipping this increased intensity of lift is accentuated on the tip towards which the slip is occurring and is elimi-

ated on the opposite tip. It seems reasonable to suppose from an inspection of these diagrams that the large rolling moment generated by side-slip upon a stalled wing is due to what may be described as differential stalling on the two tips. The effect of the relative wind component parallel to the  $Y$  axis being, apparently, to unstall the tip upon which it impinges and to cause the other tip to stall more completely than it would in symmetrical flight.

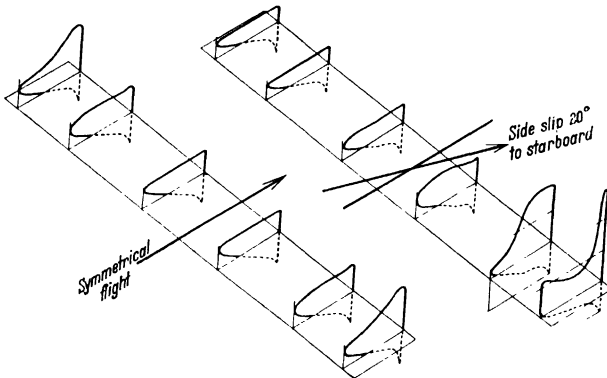


Fig. 34. Pressure distribution on a stalled wing with and without side-slip.

**14. Effect of Side-Slip on Body, Fin and Rudder.** Side-slip causes the air to impinge on the fin and rudder so as to exert a force which has a component perpendicular to the plane of symmetry. The rolling moment of this force about the  $X$  axis is nearly always negligible—except perhaps on some seaplanes—but the yawing moment about the  $Z$  axis is important. The estimation of this yawing moment from the drawings of the aeroplane is a difficult matter because the body interferes severely with the flow past fin and rudder. The sizes and positions of the fin and rudder are in practice, therefore, governed more by experience with previous aeroplanes than by any precise method of computation.

Direct measurements of the value of  $k_{nv}$  for complete model aeroplanes will be discussed later, but meantime it is of interest to make a rough estimate of the contribution of the fin and rudder alone to  $k_{nv}$ . Since this cannot be deduced effectively from experiments on isolated fins and rudders and since apparently no experiments have been made in which the forces on fins and rudders in place upon the body have been measured separately from the forces on the whole, we must fall back upon an indirect estimate. It is known from experiments on isolated fins and rudders that, in conventional designs, the air-reaction normal to the symmetric plane is roughly the same whether the rudder is rotated alone or both fin and rudder are rotated together through the same angle. We should therefore expect that when the rudder is

in place upon the aeroplane a given angular movement ( $\zeta$ ) should cause an air-reaction upon the whole fin and rudder of approximately the same amount as that caused by a side-slip angle ( $\beta$ ) equal to  $\zeta$ .

Let  $E''$  be the force on the fin and rudder, perpendicular to the plane of symmetry and let  $k'_E$  stand for the coefficient  $E''/\rho V^2 S''$ , where  $S''$  is the area of the combined fin and rudder. The yawing moment  $N$  due to the force  $E''$  on the fin and rudder can be written

$$N = k'_E \rho V^2 S'' l''$$

where  $l''$  is the effective distance behind the aeroplane's c.g.

$$\therefore k_n = \frac{N}{\rho V^2 S s} = k'_E \frac{S'' l''}{S s}$$

$S'' l''/S s$  is here a purely geometrical ratio which may be called the rudder and fin *volume coefficient*, the word volume being derived from the dimensions of the numerator and denominator of the ratio. Now

$$k_{nv} = \frac{dk_n}{d(V/V)} = \frac{dk_n}{d\beta} = \frac{dk'_E}{d\beta} \cdot \frac{S'' l''}{S s}$$

But, in so far as the above assumption is correct,  $dk'_E/d\beta$  is equal to  $dk'_E/d\zeta$  and its magnitude can therefore be estimated from experiments in which the rudder alone is moved in the absence of side-slip. There are a number of such experiments on record, (Ref. 3) the results of which can be roughly summarized by the statement that an average value of  $dk'_E/d\zeta$  is 0.7; a high value, appropriate to a fin and rudder exceptionally well placed, would be 0.9 and a low value for a badly placed fin and rudder would be 0.5.

A rough estimate of the value of  $dk'_E/d\zeta$  for a typical fin and rudder isolated in a uniform air current would be about 1.6, from which it is seen that the interference of the body with the airflow must be very severe.

If the airscrew slipstream passes over the fin and rudder it may increase their effectiveness considerably, but owing to the interference of the body with the stream the precise effect will be very difficult to estimate.

A typical value for the volume coefficient ( $S'' l''/S s$ ) is 0.05, a low value would be 0.04 and a high value 0.06. Using the figure 0.05, and a typical value for  $dk'_E/d\beta$  of 0.07, leads to a value for  $k_{nv}$  due to fin and rudder alone, of 0.035. It will appear later that a typical value of  $k_{nv}$  for the whole aeroplane is no greater than 0.010, from which it appears that most of the stabilizing effect of the fin and rudder is used to neutralize the static yawing instability of the rest of the aeroplane. The average *net* static stabilizing coefficient is thus less than one third that due to fin and rudders alone, and of the order one sixth that which would be contributed by the fin and rudder if they were acting in undisturbed air.



### 15. Experimental Values of $k_{lv}$ and $k_{nv}$ for Complete Model Aeroplanes.

Measurements of rolling and yawing moments due to side-slip have been made upon numerous models of complete aeroplanes (Ref. 4).

Figure 35 shows a few experimentally obtained curves giving  $k_{lv}$  against wing incidence for a number of models of well known aeroplanes. These results relate to axes inclined at an angle of  $-4^\circ$  to the mean wing chord, but they may, with sufficient accuracy for all practical purposes, be taken to relate to chord axes.

Dividing the values for  $k_{lv}$ , given in Fig. 35 at  $5^\circ$  incidence, by the circular measure of the dihedral angle ( $\gamma$ ) of the aeroplane to which

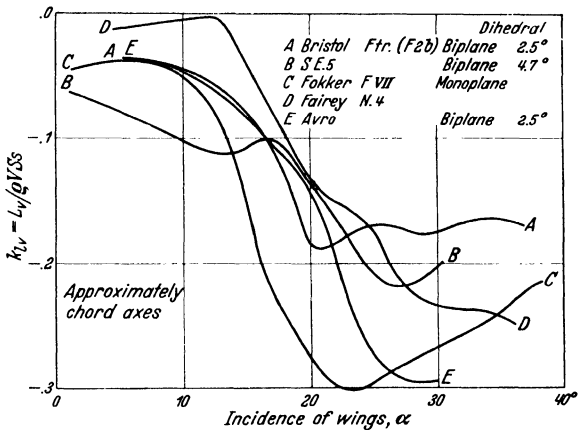


Fig. 35. Experimental curves of rolling due to side-slip for certain complete model aeroplanes.

they refer, the following figures are obtained. Bristol Fighter—0.85, Avro—0.85, S.E.5—1.0. The derivative  $dk_{lv}/d\alpha$  for these biplanes will be about 1.7 and if we assume  $J_1$  to be 0.45, Equation (8.2) would predict  $k_{lv}/\gamma = 0.77$ , a quantity which is of the correct order but on the small side. It appears therefore that while (8.2) gives predictions of the right order of magnitude, experimental measurements must be made when a high order of accuracy is required.

The very great rise, mentioned in 13, in the value of  $k_{lv}$  near the stalling angle, is well shown. It occurs on all the models and its magnitude bears no relation to dihedral angle.

Of the other aeroplanes represented in Fig. 35, the Fairley N4 has large upper wings with no dihedral and a much smaller lower wing with dihedral about  $2^\circ$ . The low value of  $k_{lv}$  in normal flight is therefore to be expected. The Fokker has a single thick wing of the peculiar, but well known, Fokker shape.

Figure 36 shows  $k_{lv}$  and  $k_{nv}$  for these same aeroplanes, plotted in the form of vector diagrams. Using chord axes,  $k_{lv}$  is plotted against  $k_{nv}$  for

various values of  $\alpha$ , which are marked on the curves. A line drawn from the origin to any point on these curves is a vector representing the magnitude and direction of the whole asymmetric moment. This form of vector diagram has the advantage of showing, at a glance, the changes in the components which would result from a change in the direction of the axes of reference.

The magnitude of the moment for a given side-slip angle ( $\beta$ ) is obtained, of course, by multiplying the length of the vector by the circular measure

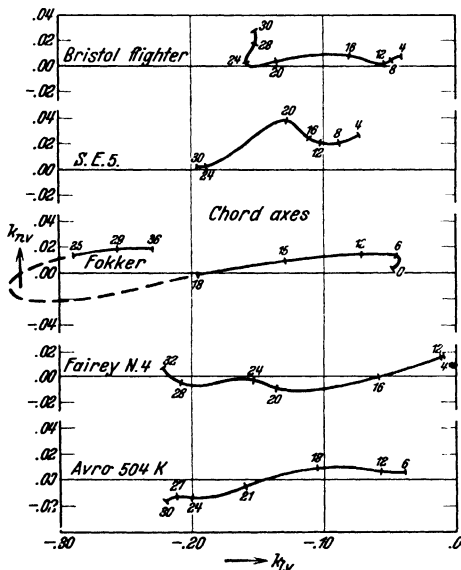


Fig. 36. "Vector diagrams" showing rolling and yawing moments due to side-slip for a number of model aeroplanes.

tionally high value (0.028) for the S.E.5 is no longer representative of modern practice.

The changes which occur in  $k_{nv}$  as the wings stall are clearly shown in Fig. 36 and it will be observed that the numerical value is, in these circumstances delicately dependent on the choice of axes of reference. Using chord axes, as in Fig. 36,  $k_{nv}$  generally becomes zero or negative—unstable—when the incidences are of the order of  $20^\circ$ , the reason being that at these incidences, the body shields the fin and rudder from the air stream.

The curves of this figure have been continued up to very high incidences, but above  $25^\circ$  incidence they are of little practical interest; steady flight above this incidence is generally impossible because the elevators are then not powerful enough to balance the pitching moments.

of  $\beta$ . The quantities here recorded were deduced from measurements of  $k_l$  and  $k_n$  when the side-slip angle ( $\beta$ ) was  $10^\circ$ . The measured values were therefore divided by 0.174, which is approximately the circular measure of  $10^\circ$ . Strictly speaking they are not therefore  $k_{lv}$  and  $k_{nv}$  since these symbols represent the ratios of infinitesimal moments to the infinitesimal angular velocities which generate them. The difference here is unimportant because the moments are approximately linear functions of angular velocity.

From these diagrams it appears that at cruising speeds—incidences under  $5^\circ$ —popular values of  $k_{nv}$  lie, as stated in 14, around about 0.01. The excep-

**16. Effects of Large Side-Slips.** Below some  $12^\circ$  incidence, rolling and yawing moments are both closely proportional to the side-slip angle, at least until  $\beta$  exceeds  $30^\circ$ . At the large incidences of stalled flight rolling moment is fairly closely proportional to sideslip until  $\beta$  exceeds some  $10^\circ$  to  $15^\circ$ , but with larger side-slip the rate of increase of the moment falls off considerably. At these high incidences also the ratio of yawing moment to side-slip becomes more positive when the side-slip is large than when it is small, so that the unstable condition indicated in Fig. 36 at high incidences and small sideslip tends to disappear when the side-slip is large, no doubt because the shielding of the fin and rudder by the body becomes less pronounced when the relative wind is blowing well from the side.

## B. Theoretical Estimates of Moments due to Angular Velocities of Roll and Yaw

We have next to consider the influence of asymmetric rotation upon asymmetric moments. With the object of displaying the factors on which these moments mainly depend, we will begin with an examination of an approximate method of calculating them when the rates of rotation are small.

**17. Moments Due to Rate of Yaw.** Consider first the wings alone. Suppose that the c.g. of the aeroplane— $O$  in Fig. 37—is moving forward, parallel to the plane of symmetry, and that the aeroplane itself is rotating with positive angular velocity  $r$  about an axis  $OZ$ , in the plane of symmetry and perpendicular to the direction of motion of  $O$ . The effect of this rotation will be to increase the velocity of the port wing and reduce that of the starboard wing. The lift and drag on the port wing will thereby be increased while, on the starboard wing, they will be decreased; the result will be a positive rolling moment and a negative yawing moment.

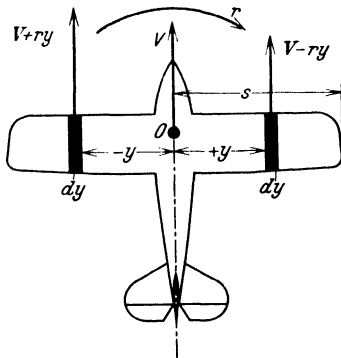


Fig. 37. Illustrating the effect of an angular velocity of yaw ( $r$ ).

To obtain an estimate of the magnitudes of these moments, suppose that the wing is divided into a series of narrow strips by planes parallel to the plane of symmetry, and that the force on each strip is the same as it would be were the whole wing moving without rotation but with velocity equal to that of a point lying on the strip and in the  $YZ$  plane. This hypothesis, which will often be employed, will be described as the *strip hypothesis*. Though it

cannot represent the facts completely, because it ignores the effects of alterations in the induced velocities near the wing which must accompany changes in lift distribution across the span, yet its consequences are worth examining.

Let the strip, Fig. 37, be distant  $y$  from the plane of symmetry and let its width be  $dy$ . Let  $c'$  be the chord of the strip and  $k'_L$  the local lift coefficient.

The velocity of a point on the strip in the  $YZ$  plane will be  $(V - ry)$  and the lift on the strip will be, approximately,

$$\rho(V - ry)^2 c' dy k'_L$$

The incidence of the strip is not altered by the additional velocity,  $(ry)$  which is parallel to  $V$ , so that, by hypothesis,  $k'_L$  is the same as the local lift coefficient at the strip when the wing is moving without rotation.

The lift on the corresponding section on the opposite side of the plane of symmetry will be  $\rho(V + ry)^2 c' dy k'_L$

The net moment of these two lifts about the  $X$  axis will therefore be

$$[(V + ry)^2 - (V - ry)^2] \rho c' y k'_L dy = 4ry^2 V \rho c' k'_L dy$$

The whole rolling moment will therefore be

$$4\rho V r \int_0^s c' y^2 k'_L dy$$

Now the whole lift on the wing may be written in either of two

alternative forms  $2\rho V^2 \int_0^s k'_L c' dy$  or  $\rho V^2 S k_L$

where  $S$  is the total area and  $k_L$  is the lift coefficient of the whole wing.

Thus 
$$\frac{S k_L}{2 \int_0^s k'_L c' dy} = 1$$

and we may write, using  $L_1$  to represent rolling moment,

$$L_1 V = 4\rho r \frac{S k_L}{2 \int_0^s k'_L c' dy} \int_0^s k'_L c' y^2 dy$$

Now the ratio of the above two integrals has the dimensions of (length)<sup>2</sup> and has a meaning which is easily visualized and conveniently expressed by a shorter notation.

Consider a curve (Fig. 38) of which the ordinates represent  $k'_L c'$  and the abscissae represent  $y$ . Such a curve defines the proportional distribution of the aerodynamic load along the span of the wing in the absence of rotation; the *load grading* as it may be called. The ratio

in question is then the square of the radius of gyration, about the axis  $y = 0$ , of the area enclosed by this curve; it therefore may reasonably be expressed by the symbols  $J_2^2 s^2$ , where  $J_2$  is the ratio of the radius of gyration of this area to the semi-span ( $s$ ).

Using this notation

$$L_1 = 2 \rho V S s^2 r k_L J_2^2$$

The dimensionless coefficient of rolling moment is defined in 4 as

$$k_l = \frac{L_1}{\rho V^2 S s}$$

Hence  $k_l = 2 J_2^2 k_L \left( \frac{r s}{V} \right)$

The quantity  $r s / V$ , which is the ratio

between the extra velocity of the wing tip due to the rotation ( $r$ ), and  $V$ , the velocity of the c.g., may be regarded as a dimensionless coefficient of  $r$  and therefore given the symbol  $k_r$  and with this notation

$$k_l = 2 J_2^2 k_L k_r$$

By a precisely similar argument

$$k_n = - 2 J_2^2 k_D k_r$$

where  $k_n$  is the coefficient of yawing moment,  $k_D$  is the drag coefficient and  $J_2 s$  is the radius of gyration of the *drag grading curve* for each half wing; this radius is not necessarily the same as that for the *lift grading curve*, but as a first approximation we shall assume that it is the same.

**18. The Derivatives  $k_{lr}$  and  $k_{nr}$ .** In subsequent chapters we shall require the derivatives  $\partial L_1 / \partial r$  and  $\partial N / \partial r$  which will be described as the derivative for *rolling moment due to yawing* and *yawing moment due to yawing*. The dimensionless coefficients of these derivatives will have the symbols  $k_{lr}$  and  $k_{nr}$  and be defined so that

$$k_{lr} = \frac{\partial L_1}{\partial r} \frac{1}{\rho V S s^2}$$

$$k_{nr} = \frac{\partial N}{\partial r} \frac{1}{\rho V S s^2}$$

Alternative expressions for these derivatives are clearly

$$k_{lr} = \frac{d k_l}{d k_r} \quad k_{nr} = \frac{d k_n}{d k_r}$$

With these definitions the above theoretical estimates can be written

$$k_{lr} = 2 J_2^2 k_L$$

$$k_{nr} = - 2 J_2^2 k_D$$

The value of  $J_2$  depends merely on load grading and it is immaterial, from the present point of view, whether this grading is due to variations in the flow at different points along the wing span, or is due to variations in the chord of the wing itself.

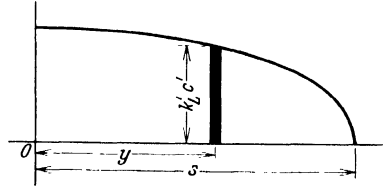


Fig. 38. Aerodynamic load grading curve for half wing.

Values of  $J_z^2$  are  $1/3$  for uniform load grading;  $1/4$  for elliptic load grading; and  $1/6$  for triangular grading. The lift grading on a rectangular wing at moderate incidences lies between uniform and elliptic and hence  $J_z^2$  in the equation for  $k_{lr}$ , with a rectangular wing, will be somewhere between 0.33 and 0.25, say in the neighborhood of 0.30.

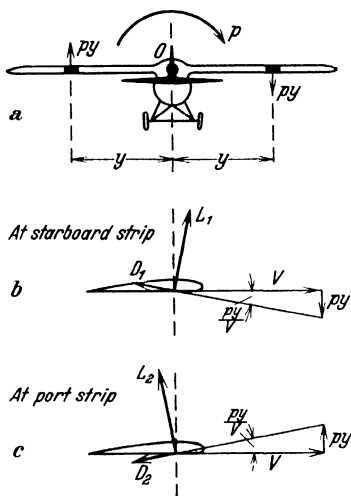


Fig. 39. Illustrating the effect of an angular velocity of roll ( $p$ ).

**19. Moments Due to Rate of Roll ( $p$ ).** Figure 39a shows an aeroplane viewed from behind. Let the c.g. be moving forwards with velocity  $V$ , parallel to the plane of symmetry—perpendicular to the paper in the figure—and let the aeroplane be rotating with a small angular velocity ( $p$ ) about an axis through  $O$  and parallel to  $V$ . To a first order approximation, the effect of this rotation upon a point distant  $y$  from  $O$  is to change the direction of its motion through an angle  $py/V$  and to leave the magnitude of its velocity unchanged.

Making assumptions similar to those of the previous section, we may suppose that the incidence of a strip of the starboard wing, distant  $y$  from the plane of symmetry, is increased by the angle  $py/V$  and we may write lift and drag on this strip in the form

$$dL = \rho V^2 c' dy \left( k'_L + \frac{dk'_L}{d\alpha} \cdot \frac{py}{V} \right)$$

$$dD = \rho V^2 c' dy \left( k'_D + \frac{dk'_D}{d\alpha} \cdot \frac{py}{V} \right)$$

where the coefficients and their rates of change with incidence are the same as those for the strip when the wing is moving without rotation, but with incidence equal to the local incidence of the strip.

The local lift and drag, as expressed above, will not, however, be perpendicular and parallel respectively to the axis of  $X$  but to the direction of motion of the strip—Fig. 39b. The force perpendicular to the direction of  $V$  will therefore be

$$dL \cdot \cos \frac{py}{V} + dD \sin \frac{py}{V}$$

$$\text{or } \rho V^2 c' dy \left[ \left( k'_L + \frac{dk'_L}{d\alpha} \cdot \frac{py}{V} \right) \cos \frac{py}{V} + \left( k'_D + \frac{dk'_D}{d\alpha} \cdot \frac{py}{V} \right) \sin \frac{py}{V} \right]$$

or, omitting small quantities of the second order

$$\rho V^2 c' dy k'_L + \rho V^2 c' dy \left[ \frac{dk'_L}{d\alpha} + k'_D \right] \frac{py}{V}$$

The force on the corresponding strip on the opposite side of the plane of symmetry will be found to be the same as above with the sign of the second term changed. The net rolling moment exerted by the two strips

is therefore 
$$-2\rho V p \int_0^s \left( \frac{dk'_L}{d\alpha} + k'_D \right) c' y^2 dy$$

Treating this expression in exactly the same way as the corresponding expression for yawing moment and using analogous notation, we obtain the first two of the four expressions below. The corresponding expressions representing the effects of rate of yaw ( $r$ ) are restated for convenience of reference.

### 20. Approximate Formulae for the Rotary Derivatives.

$$\begin{aligned} k_{lp} &= \frac{k_l}{k_p} = - \left[ \frac{dk_L}{d\alpha} + k_D \right] J_2^2 \\ k_{np} &= \frac{k_n}{k_p} = \left[ \frac{dk_D}{d\alpha} - k_L \right] J_2^2 \\ k_{lr} &= \frac{k_l}{k_r} = 2k_L J_2^2 \\ k_{nr} &= \frac{k_n}{k_r} = -2k_D J_2^2 \end{aligned}$$

Though the assumptions on which these four expressions are founded are not exact, the estimates which they give of the values of the derivatives are in many circumstances remarkably close to the measured values with which we shall presently compare them. A more precise calculation of the  $r$  derivatives for a wing with elliptic load grading, taking account of modifications to the trailing vortices has been made by C. Wieselsberger (Ref. 5), and translated into English and extended to a rectangular wing by H. Glauert (Ref. 6). The expressions there obtained involve the aspect ratio of the wing and the formula for the derivate  $k_{nr}$  takes separate account of the *profile drag* and the *induced drag*, instead of being merely concerned with the total drag, as in the simpler form. For wings of aspect ratio 6 the formulae become

$$\begin{aligned} k_{lr} &= 0.43 k_L \text{ Elliptic loading} \\ k_{lr} &= 0.49 k_L \text{ Rectangular wing} \\ k_{nr} &= 0.50 k_D \text{ (profile)} + 0.66 k_D \text{ (induced) Elliptic loading} \\ k_{nr} &= 0.67 k_D \text{ (profile)} + 0.86 k_D \text{ (induced) Rectangular wing} \end{aligned}$$

**21. Change of Axes.** The four derivatives above have been derived by reference to *wind axes*. The conversion to any other system, such as *chord axes* must now be considered.

Let  $OX$ ,  $OZ$  be chord axes and let  $OX'$   $OZ'$  be wind axes, Fig. 40. The symbols relating to the moments and angular velocity components about these axes are appended in brackets.

Let the angles  $XOX'$  and  $ZOZ'$  be equal to  $\alpha$  and let the aeroplane be rotating about  $OX$  with angular velocity  $p$ .

$$\text{Then} \quad p' = p \cos \alpha \quad r' = -p \sin \alpha$$

$$\text{And } L_p p = L' \cos \alpha - N' \sin \alpha$$

$$= (L'_p p' + L'_r r') \cos \alpha - (N'_p p' + N'_r r') \sin \alpha$$

$$= (L'_p \cos \alpha - L'_r \sin \alpha) p \cos \alpha - (N'_p \cos \alpha - N'_r \sin \alpha) p \sin \alpha$$

$$\text{or } L_p p = [L'_p \cos^2 \alpha - (L'_r + N'_p) \cos \alpha \sin \alpha + N'_r \sin^2 \alpha] p$$

Dividing through by  $p \varrho V S^2$  and forming, in a similar manner, expressions for the other three rotary derivative coefficients we obtain,

$$\left. \begin{aligned} k_{lp} &= k'_{lp} \cos^2 \alpha - (k'_{lr} + k'_{np}) \cos \alpha \sin \alpha + k'_{nr} \sin^2 \alpha \\ k_{lr} &= k'_{lr} \cos^2 \alpha + (k'_{lp} - k'_{nr}) \cos \alpha \sin \alpha - k'_{np} \sin^2 \alpha \\ k_{np} &= k'_{np} \cos^2 \alpha + (k'_{lp} - k'_{nr}) \cos \alpha \sin \alpha - k'_{lr} \sin^2 \alpha \\ k_{nr} &= k'_{nr} \cos^2 \alpha + (k'_{lr} + k'_{np}) \cos \alpha \sin \alpha + k'_{lp} \sin^2 \alpha \end{aligned} \right\} \quad (21.1)$$

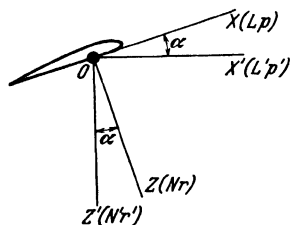


Fig. 40.

These formulae enable rotary derivatives, with respect to any system of mutually perpendicular axes lying in the plane of symmetry, to be transformed to any other similar system with the same origin, but inclined to the first system through any angle ( $\alpha$ ).

**22. Calculations of Rotary Derivatives Using Chord Axes Throughout.** If it is desired to work out a set of derivatives by reference to axes which are not *wind axes* but for

which the axis of  $X$  is inclined to the wind direction through an angle  $\alpha$ , two alternative processes are available. Either the derivatives may be computed with reference to wind axes and then transformed by the use of (21.1), or they may be worked out directly by use of the equations below, in which  $X$  and  $Z$  are the components of the aerodynamic reaction on the wing, parallel respectively to  $OX$  and  $OZ$ , when the wing is not rotating.

$$\left. \begin{aligned} k_{lp} &= \left[ \frac{dk_Z}{d\alpha} \cos \alpha + 2k_Z \sin \alpha \right] J_2^2 \\ k_{np} &= \left[ -\frac{dk_X}{d\alpha} \cos \alpha + 2k_X \sin \alpha \right] J_2^2 \\ k_{lr} &= \left[ -2k_Z \cos \alpha + \frac{dk_Z}{d\alpha} \sin \alpha \right] J_2^2 \\ k_{nr} &= \left[ 2k_X \cos \alpha - \frac{dk_X}{d\alpha} \sin \alpha \right] J_2^2 \end{aligned} \right\} \quad (22.1)$$

Note that, since  $X$  and  $Z$  in these expressions are directed forward and downward respectively, they are, when  $\alpha$  is zero, equivalent to  $-D$  and  $-L$  respectively.

The expressions (22.1) are easily deduced by noting that a rotation such as  $p$  about an axis  $OX$  inclined to the "wind" through an angle  $\alpha$



causes simultaneous changes in both the velocity and incidence of wing strips situated at a distance from the plane of symmetry.

The rotary derivatives can therefore be computed directly by reference to any desired axes. We shall, however, see shortly that experimentally determined derivatives can often be obtained by reference to some particular system of axes only, and when results so obtained have to be referred to other systems of axes, the somewhat cumbersome transformation equations (21.1) must be used.

**23. Rotary Derivatives Due to Body, Fin and Rudder.** The only important contribution of these parts is to the derivative  $N_r$ , and this contribution cannot conveniently be computed from data for isolated fins and rudders; for information on this matter we must rely upon experiments upon complete models of aeroplanes such as are discussed in the following section.

### C. Experimental Methods of Measuring the Rotary Derivatives

**24. Oscillation Methods.** All four derivatives can be measured by oscillation methods similar to those described in II 38 and 39 for the measurement of the symmetric rotary derivative  $M_q$ . Either of the methods there described can be applied unaltered to the derivatives  $L_p$  and  $N_r$ , but a modification is necessary in the application to the cross derivatives  $L_r$  and  $N_p$  (Ref. 7). The reader who desires details of this modification should consult the reference.

If the results of these oscillation experiments are to be generally applied, it is necessary to consider the extent to which the reactions are functions of rate of change of incidence as well as of incidence itself. In considering symmetric motions in Chapter II we found it necessary to take into account the influence of rate of change of incidence upon forces on the tail. This was due to the time lag between the creation of *downwash* by the wings and its action on the tail. There is no such downwash factor present to any appreciable extent in the asymmetric reactions which are now under consideration and hence the assumption is generally made that these reactions are independent<sup>1</sup> of  $d\alpha/dt$ . This assumption is probably sufficiently accurate at the incidence of normal flight, but we shall see later that it is insufficient for the consideration of stalled flight.

**25. Continuous Rotation Methods.** If a model wing in a wind tunnel is made to roll continuously about an axis parallel to the relative wind, the air-reactions upon it will be steady with respect to axes which turn with the model. With suitably arranged apparatus the moments of

---

<sup>1</sup> For further discussion on the validity of this assumption see V 6.

these air-reactions about axes fixed in the wing can be measured and the derivatives  $L_p$  and  $N_p$  determined (Ref. 8). Derivatives depending on any rotation other than about an axis parallel to the wind cannot conveniently be determined by steady rotation in a wind tunnel, because the necessary condition that side-slip should be zero or constant cannot be achieved unless the flight path is curved. The effect of rotation about any axis perpendicular to the direction of motion can, however, be determined on a whirling arm in a manner similar to that described in II 37 for the measurement of  $M_q$ . Experimentally this method is difficult, owing to the disturbance set up by the passage of the arm, the influence of which is exceedingly hard to disentangle from the effect to be measured. The technique of this whirling arm method is still undergoing development, but some few results relating to a steady rate of yaw have been published; these will be discussed in due course.

#### D. Discussion of the Results of Experiments on the Rotary Derivatives at Incidences of Normal Flight

**26. Comparison Between Oscillation and Continuous Rotation Experiments.** This comparison has been made upon a complete model of a B.F.2b (Ref. 9). In the oscillation experiments the rotations and measurements were about *chord axes* whereas in the continuous rotation experiments *wind axes* were necessarily used, but the latter have been transformed to refer to chord axes using the equations of 21. The two sets of results are compared in Figs. 42a to d (38) and show, for incidences below  $12^\circ$ , an agreement which, considering the difficult nature of the experiments, is remarkably close. The assumption, mentioned in 24, that the moments were not appreciably influenced by rate of change of incidence during the oscillation, is apparently justified so far as the experiments under discussion are concerned. The wide differences between the results at high incidences will be discussed later.

**27. Comparison Between Experiment and "Strip" Calculation.** Experiments, by the oscillation method, have been made upon the four asymmetric rotary derivatives of an 1/8 scale model of an S.E.5 aeroplane (Ref. 10), and the values so found for the three derivatives  $L_p$ ,  $L_r$ ,  $N_p$  have been compared with the results of simple strip calculations for the wings alone. With a value for  $J_z^2$  of 1/4, that is to say, assuming an elliptic aerodynamic load grading across the wing span, remarkably good agreement—within 10 per cent—was obtained over an incidence range from  $0^\circ$  to  $10^\circ$ .

A similar comparison has been made between the values of  $L_p$  and  $N_p$  obtained by strip calculation and by experiments upon the continuous roll balance, for a model of the B.F.2b. The result of this comparison for small rates of roll is given in Fig. 41a. The agreement is again good.

From these experiments it appears, therefore, that with wings of approximately rectangular plan form at the incidences of normal flight, the simple strip calculations of 17, using  $J_2^2 = 1/4$ , gives estimates of  $L_p$ ,  $L_r$ ,  $N_p$  which are in reasonably good agreement with the results of experiment either by the oscillation or by the continuous roll method.

**28. Influence of Body, Fin and Rudder.** From the above agreement we infer that the body, fin and rudders of a conventional aeroplane contribute nothing of importance to  $L_p$ ,  $L_r$ , or  $N_p$  when these are expressed in chord axes.  $N_r$  on the other hand is almost entirely due to these parts and but little influenced by the wings. The principal factors in determining this derivative are the fin and rudder. Following the method of estimating the analogous derivative  $M_q$  in Chapter II, write

$$k_{nr} = -A \frac{s''v'^2}{s^2} \quad (28.1)$$

where  $A$  is a numerical factor which includes a small allowance for wings and body of conventional form and  $s''v'^2/s^2$  is a geometrical relation defining the areas and positions of the fin and rudders. At the incidences of normal flight a value of  $A$  of the order 1.4 is representative of the principal experimental results available, which include experiments on models of the S.E.5 which had exceptional large fin and rudder and of the B.F.2b on which these organs were exceptionally small.

**29. Comparison Between Model and Full Scale Experiments.** An elaborate series of experiments to obtain the asymmetric derivatives for the B.F.2b in actual flight, at about  $10^\circ$  incidence, is described in Ref. 11. The experimental values so obtained are plotted as large circles in Fig. 42; they show good agreement with the results of model experiments except in respect of  $N_p$  for which two full scale results at nearly the same incidence differ widely between themselves and are both much larger than the model result. The cause of this discrepancy is not yet known.

**30. Effect of Large Angular Velocities.** Below  $10^\circ$  incidence, asymmetric moments are found to be closely proportional to angular velocities. Those generated by rate of roll are proportional to the rate of roll ( $p$ ), at least until  $k_p$  exceeds 0.2, a value which in actual flight corresponds to a very high angular velocity; about half that experienced in the common spin.

Experiments involving continuous rate of yaw have, up to the present, been made at one angular velocity only, corresponding to  $k_r$  equal to 0.065; but there is no reason to suppose that the proportionality in the effects of rate of yaw will be less pronounced than in the effects of rate of roll.

**31. Summary—Rotary Derivatives in Normal Flight.** Taking into account the difficult nature of the experiments and the fact that high

accuracy is not yet required or obtainable in the calculation of stability and control characteristics, it may be said that there is good agreement between the results of experiments made by the oscillation and by the continuous rotation methods.

Predictions from calculations based on the simple "strip hypothesis", with elliptic load grading across the wing span, agree well with the results of experiments on the derivatives  $L_p$ ,  $L_r$ ,  $N_p$ , but the value of  $N_r$  cannot easily be predicted and, for it, estimates must be based on experiments upon the complete body, fin and rudder.

The agreement between model and full scale experiments has been checked at  $10^\circ$  incidence only and found to be good for  $L_p$ ,  $L_r$ , and  $N_r$ , but in the case of  $N_p$  the full scale experiments agreed neither with the model results nor amongst themselves. It seems probable that this disagreement is due to some defect in the very difficult full scale experiment, but further research would be required to settle this point.

These conclusions are based on experiments on aeroplanes with biplane wings of thin profile and roughly rectangular plan form, but they probably apply, at the incidences of normal flight, to wings of other forms.

### E. Rotary Derivatives in Stalled Flight

**32. Introduction.** We pass now to the consideration of the experimental evidence relating to rotary derivatives at incidences higher than those which occur in flight, except on those rare occasions when the aeroplane is deliberately or inadvertently stalled. In spite of the rarity of these occasions it is necessary to study the changes which take place in the asymmetric air-moments at high incidences, for it is in these changes that the principal danger of flying, the loss of control following accidental stalling, is found to lie.

We have first to consider an extension of the calculations based upon *strip hypothesis* by which they can be applied to finite angular velocities in circumstances when the lifts and drags are no longer linear functions of incidence. Consideration of the calculations of 17 and 18 to find  $L_r$  and  $N_r$  referred to wind axes show no reason why the ratio of  $L$  and  $N$  to  $r$ , when  $r$  is finite, should be very different from the ratios when  $r$  is infinitesimal. On the other hand the calculations for  $L_p$  and  $N_p$  depended on the omission of small quantities of the second order and involved the rates of change of lift and drag with incidence. The following extension of the method to finite values of  $p$  is due to H. Glauert (Ref. 12).

**33. Theoretical Estimate of Moments Due to Finite Rates of Roll.** Referring back to 19, Fig. 39, let

$$\frac{py}{V} = \tan \varphi' \quad (33.1)$$

$$\text{so that} \quad \frac{p}{V} dy = \sec^2 \varphi' d\varphi' \quad (33.2)$$

When the incidence at the mid-section of the wings is  $\alpha$  that at the strips distant  $\pm y$  from the mid-section is  $\alpha \pm \varphi'$ .

Using an obvious notation and remembering that lift and drag are defined as forces perpendicular and parallel to the direction of motion, the expression for the force on strip (b) Fig. 39, perpendicular to the direction of motion of the c.g. of the aeroplane is

$$[k_L(\alpha + \varphi') \cos \varphi' + k_D(\alpha + \varphi') \sin \varphi'] \rho (V \sec \varphi')^2 c' dy$$

The corresponding force on the symmetrically placed strip is

$$[k_L(\alpha - \varphi') \cos \varphi' - k_D(\alpha - \varphi') \sin \varphi'] \rho (V \sec \varphi')^2 c' dy$$

Now, for brevity, let  $K_1$  represent the difference between the square brackets in the above expressions, so that

$$K_1 = [k_L(\alpha + \varphi') - k_L(\alpha - \varphi')] \cos \varphi' + [k_D(\alpha + \varphi') + k_D(\alpha - \varphi')] \sin \varphi'$$

Then the net contribution of both strips to the rolling moment is

$$- K_1 \rho V^2 \sec^2 \varphi' c' y dy$$

Now write  $ps/V = \tan \varphi$ , so that  $\varphi$  is the value of  $\varphi'$  at the wing tip.

Substituting for  $y$  in terms of  $\varphi'$  and integrating from wing root to tip gives:

$$\text{Total rolling moment} = - \frac{\rho V^4}{p^2} \int_0^\varphi c' K_1 \sec^4 \varphi' \tan \varphi' d\varphi'$$

Let us assume first that the plan form of the wings is rectangular so that  $c'$  is constant and therefore can be brought outside the integral sign. The wing area  $S$  is equal to  $2sc$  and, on dividing by  $\rho V^2 S s$  or  $2\rho V^2 s^2 c$  to obtain the rolling moment in coefficient form, we have

$$k_l = \frac{1}{2} \cot^2 \varphi \int_0^\varphi K_1 \sec^4 \varphi' \tan \varphi' d\varphi'$$

A similar argument gives the yawing moment coefficient

$$k_n = \frac{1}{2} \cot^2 \varphi \int_0^\varphi K_2 \sec^4 \varphi' \tan \varphi' d\varphi'$$

where

$$K_2 = [k_D(\alpha + \varphi') - k_D(\alpha - \varphi')] \cos \varphi' - [k_L(\alpha + \varphi') + k_L(\alpha - \varphi')] \sin \varphi'$$

If we can assume that the air-loading is uniform across the span and have curves of  $k_L$  and  $k_D$  against incidence for the whole wing, curves showing the values of the expressions within the integrals against  $\varphi'$  for any given value of  $\alpha$  can be prepared. Integrating these graphically up to various values of  $\varphi$  and multiplying by  $(1/2) \cot^2 \varphi$  then gives

curves of  $k_l$  and  $k_n$  against  $\varphi$  which itself defines the rate of roll: since  $\tan \varphi = ps / V = k_p$ .

If, instead of assuming  $c'$  constant and air-loading uniformly graded across the span, it is assumed that the load grading is elliptic, it can be shown by a modification of the above argument that the rolling moment coefficient is

$$k_l = -\frac{2}{\pi} \cot^2 \varphi \int_0^{\varphi} K_1 \sec^4 \varphi' \tan \varphi' \sqrt{1 - \frac{\tan^2 \varphi'}{\tan^2 \varphi}} d\varphi'$$

and that the expression for the yawing moment coefficient is similar but with  $K_2$  substituted for  $K_1$ .

The values of  $K_1$  and  $K_2$  in these last expressions are deduced from curves of lift and drag coefficients for the whole wing.

The above expressions are the same for biplanes as for monoplanes, since the extra 2 which will occur in the expressions for the moments is cancelled out when the moments are divided by  $4\rho V^2 s^2 c$  to obtain the coefficients.

**34. Comparison Between Strip Hypothesis and Results of Experiments with Continuous Finite Rates of Roll.** Using the formulae with elliptic loading in the previous section, computations have been made for the wings of a B.F.2b and compared with the results of experiments involving continuous rolling. These comparisons are shown in Figs. 41a, b and c. (Ref. 8). In Fig. 41a, calculated values of  $L_p$  and  $N_p$  are compared with the ratios of  $L$  and  $N$  to  $p$  obtained by drawing tangents at the origin to curves of experimental values of  $L$  and  $N$  against  $p$ . The smallest value of  $k_p$  in these experiments was 0.05. In Figs. 41b and c, the comparison is between the calculated and experimental values of  $L$  and  $N$  when  $k_p$  had the values 0.1 and 0.2 respectively. Considering the drastic nature of the assumptions behind the calculations and the wide range both of incidence and angular velocity covered, the agreement is remarkable.

We infer from these experiments that the simple strip hypothesis with the assumption of elliptic wing loading is sufficient to allow good estimates to be made of the rolling and yawing moments due to steady rolling—wind axes—even when the incidence is very high and the rate of roll considerable.

It must be mentioned, however, that a series of experiments were made, subsequently to those recorded in Fig. 41 using a special form of rolling balance in which the rate of roll could be made very small (Ref. 13). It was then found that when  $k_p$  was of the order 0.01 the moments on the stalled wing were of the opposite sign to the rotation and were of the order of magnitude to be expected from an unstalled wing. This state of affairs, however, persisted only at very small rates

of roll and the moments altered to the destabilizing type, indicated in Fig. 41 a, above  $20^\circ$  incidence, as soon as the rate of roll was increased much above the value 0.01. Though this peculiar behavior at very low rates of roll is theoretically interesting, it is not of great practical importance, because disturbances greater than those corresponding to  $k_p = 0.01$  are sure, sooner or later, to occur in stalled flight and then the subsequent behavior of the aeroplane will be as would be anticipated from Fig. 41,

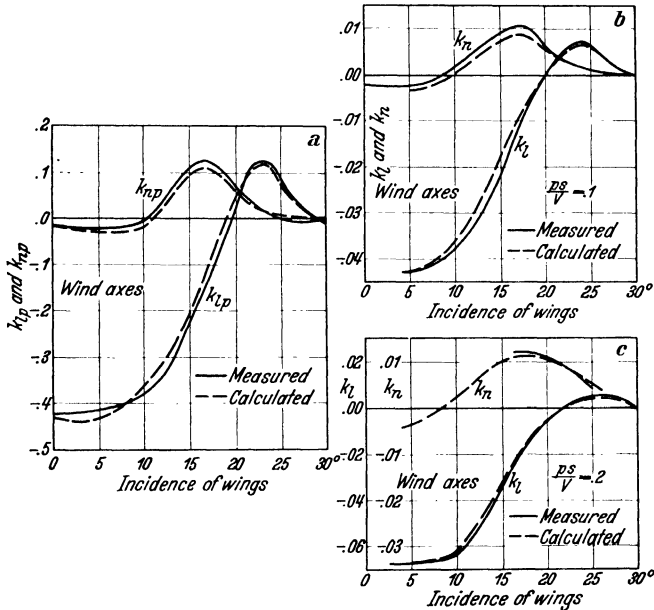


Fig. 41. Comparison between experimental and calculated values of moments due to rolling.

and will be very little influenced by the small stabilizing moments which had occurred before this slow rate of roll had been reached. In the calculations which will be made in Chapter VII upon the motions in free flight of a stalled aeroplane this anomolous behavior of the wings with very small rates of roll will be completely ignored.

**35. Comparison Between Strip Hypothesis and Experiments with Continuous Yawing.** Unlike the effects of rate of roll this comparison shows, at high incidences, a striking discrepancy between the value of  $L_r$  calculated on the "strip hypothesis" and the value found by experiment. The strip hypothesis leads to the equation

$$k_{lr} = 2 J_z^2 k_L \quad (\text{wind axes})$$

and, apart from minor changes in  $J_z^2$  due to change of distribution of lift across the span as the wing stalls, this equation indicates that the curve of  $k_{lr}$  against incidence should be of the same shape as the familiar

curve of lift coefficient against incidence; that is to say, the value of  $k_{lr}$  should rise until the stalling angle is reached and then fall slightly. Experiment, however, shows that whereas the rise of  $k_{lr}$  with incidence up to the stalling incidence is substantially that indicated by the calculation, the value after the stalling incidence is passed falls very rapidly until, at  $30^\circ$  incidence, it is not much more than one third the calculated value.

The reason for this discrepancy is easily understood. The strip hypothesis applied to find the effects of a rate of yaw, which causes a variation of velocity along the span, requires a corresponding variation of all aerodynamic pressures along the span. When, however, the wing is thoroughly stalled the *dead air* above the upper surface is practically stationary and cannot support any such pressure gradient, and the upper surface of the wing is therefore covered by air at uniform pressure. The corresponding difficulty does not arise in connection with the effects of a rolling rotation, because rolling merely changes the local incidence of each strip, and incidence changes on a stalled wing do not cause changes of pressure on the upper surface.

**36. Comparison Between Continuous Rotation and Oscillation Experiments.** This comparison for the B.F.2b aeroplane is shown in curves referred to *chord axes* in Figs. 42a to d; striking discrepancies are revealed in respect of  $N_p$  above  $12^\circ$  incidence and  $L_p$  above  $20^\circ$  incidence.

There is no reason to suppose that these discrepancies are due to experimental errors and it must therefore be inferred that the moments on a stalled rolling wing are not dependent solely on the rate of roll but depend also upon the history of the motion immediately preceding the instant under consideration. The reason for the discrepancy is probably to be found in the nature of the flow changes which occur at the stall, for there is independent evidence that the form of the air flow near the stalling angle is not a unique function of incidence, but depends on the way in which the incidence is approached. Since effects of rolling rotation depend on changes of incidence at each strip of wing they may therefore be expected to show, near the stalling point, a similar sensitivity to the history of the motion.

The curves for continuous rotation, are, as we have just seen, reasonably constant with the strip hypothesis, which requires that the extent to which the flow departs from the unstalled form should vary along the span in the same manner as it would vary in a number of wings moving steadily, without rotation, each at the local incidence of the corresponding strip of the rotating wing. The curves derived from the oscillation experiment on the other hand are reasonably consistent with the hypothesis that, the stall having once occurred, no recovery towards unstalled flow takes place during the temporary reduction of



incidence on the rising wing. This latter hypothesis would lead to a zero value for  $N_p$ —chord axes—; and assuming the value for  $l_r$  in Fig. 42c to be correct, would lead to values of  $l_p$  above  $20^\circ$  incidence, roughly as shown in the dotted line of Fig. 42a.

The problems raised in the preceding paragraph need further research for their complete elucidation; all that can be said at present is that the hypothesis suggested appears to account in a rough general manner for observed facts.

With regard to the effects of yawing rotations the results of continuous and oscillating rotations are, except for some minor variations, in reasonably good agreement.

**37. Auto-Rotation and Wing Tip Slots.** When, on an aeroplane or set of wings, the derivative  $L_p$  has a positive value as in Fig. 41a between  $19^\circ$  and  $29^\circ$  incidence, a model of the aeroplane, suspended in a wind tunnel with freedom to rotate about an axis through the c.g. and parallel to the wind, will be in unstable equilibrium; any small rotation in either direction will tend to increase until an angular velocity has been reached at which the rolling moment again falls to zero.

This phenomenon is called *auto-rotation* and is of great importance in aviation, because, when present, it renders the aeroplane dangerously unstable. It is a property possessed by nearly all wings and its elimination is one of the major problems at present before the aeronautical engineer. One method of postponing this phenomenon to incidences at which continuous flight is impossible on account of failure to balance pitching moments, is to fit slots to the front of the wing tips. These postpone the stall at the outer parts of the wings until a very high incidence. The effects of autorotation will, however, be discussed more fully in Chapters IV and VII.

**38. Collection of Typical Values for the Six Asymmetric Moment Derivatives.** Figure 42, to which reference has already been made in various connections, contains a set of typical curves for the six asymmetric moment derivatives. These relate to the B.F.2b aeroplane and probably represent the most complete set of data of the kind in existence at the time of writing. They are the result of so large an amount of experimental research, both in the laboratory and in flight, that they are not likely to be repeated in so complete a form for many different aeroplanes.

The four Figs. 42a, b, c and d, representing the four *rotary derivatives* have already been discussed in detail. Of these Figs. 42a, b, and c are probably typical of any biplane of approximately rectangular plan form and thin profile and it is probable that they are qualitatively representative of all aeroplanes. Fig. 42d on the other hand depends delicately on the exact form and size of the fin and rudder and on their relation to the body.

Figures 42e and f, relate to the effects of side-slip; the main continuous curves here relate to experiments on a model of the B.F.2b which, however, happened by accident to have a dihedral angle different from that of the full scale aeroplane on which the experiments in flight, represented by circles, were made. The short curve in Fig. 42e is corrected

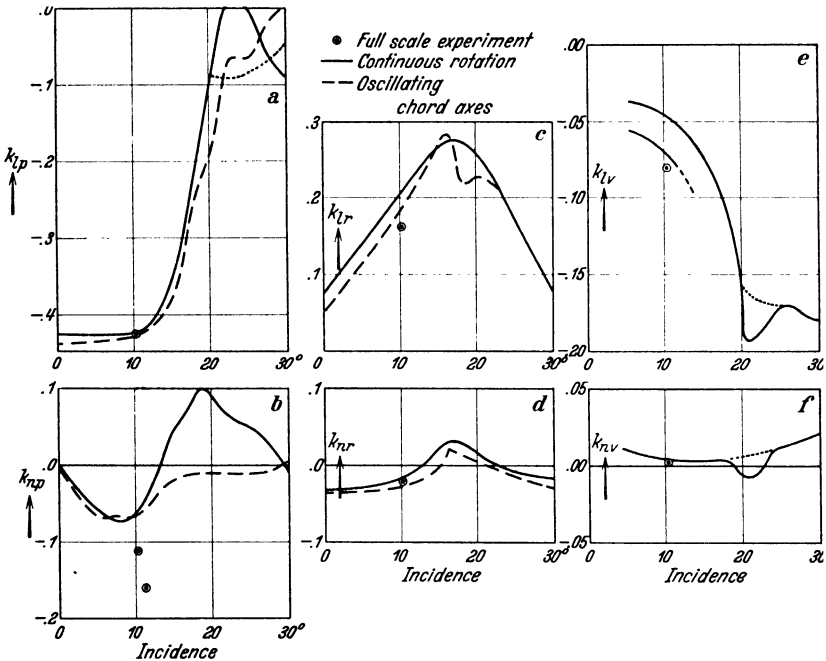


Fig. 42. The asymmetric derivatives of a typical aeroplane.

for this discrepancy and shows good agreement with the full scale experiment. The bulges in both curves in the neighborhood of 22° incidence rest on the evidence of a single experimental observation. Their validity is therefore doubtful and it is considered that the alternative dotted curves are probably nearer to the correct values.

The set of derivatives in Fig. 42 will be used as the basis of the calculation of the disturbed motion of an aeroplane which will form the main theme of Chapter VII.

## F. The Asymmetric Controls

**39. Balanced Controls.** The detailed forms of these controls vary widely according to the taste of designers but, with few exceptions, their main features are the same in all modern aeroplanes and are too well known to require special description here. Their precise forms are governed mainly by the desire to reduce the effort required to move

them when the aeroplane is in flight, by nearly balancing the moments of the air-reactions about the hinge around which they rotate. This problem of *balancing* controls does not fall within the scope of the present discussion, which is concerned with the moments of the air-reactions about the axes of the aeroplane and assumes that the pilot is able to rotate the controls to any desired position.

**40. Aileron Rolling Moments.** It will be sufficient to describe the moments exerted by a typical set of ailerons in various circumstances. Figure 43 shows the rolling moment coefficients—chord axes—exerted by the ailerons of a biplane of conventional form, the S.E.5 (Ref. 14).

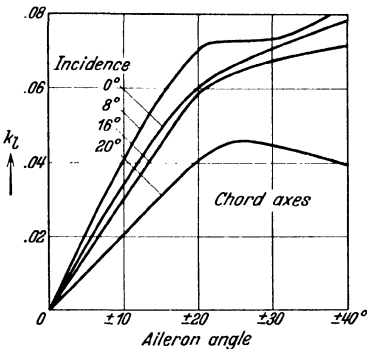


Fig. 43. Typical curves of rolling moment coefficient against aileron angle at various values of the wing incidence.

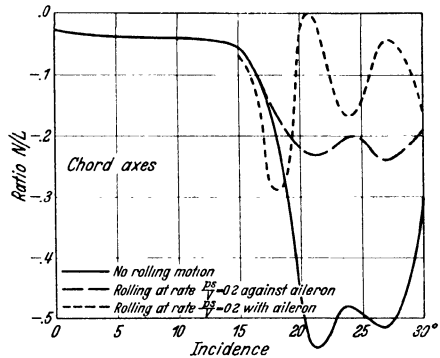


Fig. 44. Typical ratios of yawing to rolling moments—chord axes—from the ailerons of a typical biplane.

The abscissae represent the angles ( $\xi$ ), in degrees, by which the starboard aileron is moved down and the port aileron up; the ordinates represent the usual rolling moment coefficient  $k_l = (\text{rolling moment})/\rho V^2 S s$ . Curves are given for  $0^\circ$ ,  $8^\circ$ ,  $16^\circ$ , and  $20^\circ$  incidence of the wings.

Points to be noticed are: The rolling moment varies approximately in proportion to aileron angle up to  $\pm 20^\circ$  and then increases less rapidly, or may even fall; the rolling moments are not greatly affected by change of incidence of the wings up to  $16^\circ$ , but at  $20^\circ$  incidence have little more than half the value at the incidences of normal flight.

**41. Aileron Yawing Moments.** The object of the ailerons is to exert rolling moments about an axis roughly parallel to the wing chord, but the conventional ailerons of the present day generally exert in addition yawing moments about an axis perpendicular to the chord. Stated otherwise, the axis about which the ailerons generate an air-moment, instead of being parallel to the wing chord, is inclined forwards and upwards relative to the chord and consequently the effect of the ailerons is not simply to lift one wing tip and depress the other, as would be desirable, but to retard the wing tip which they are attempting to lift

and advance the tip which they are attempting to depress. The consequences of this action are discussed in Chapters IV and VII; we are here concerned with their magnitudes, some idea of which is given in Fig. 44, which was prepared from experimental measurements made on model wings of the B.F.2b (Ref. 8). In normal flight the ratio of the yawing to the rolling moment is of the order 0.03 but in stalled flight it may rise as high as 0.5, though the ratio falls considerably when the ailerons are applied whilst rolling motion is occurring.

**42. Ailerons and Wing Tip Slots.** The presence of wing tip slots, such as those mentioned in 37, in front of the ailerons, considerably improves their action at high incidences by delaying until still higher incidences the reduction of rolling moment recorded in Fig. 43 and the increase in yawing moment recorded in Fig. 44. If the slots are interconnected with the ailerons so that those in front of the raised ailerons shut whilst those in front of the depressed ailerons remain open, or if a spoiler device is employed consisting of a small projection on the upper wing surface which can be raised into the air stream when the aileron behind it is raised, the ailerons can be made to retain their effectiveness until angles of incidence are reached which are higher than can be maintained in steady flight by full use of the elevators. The failure of the ailerons in stalled flight which is illustrated in Figs. 43 and 44 can, therefore, with the help of the additional mechanisms on the wings, be eliminated at all incidences which are generally possible in steady flight. The bearing of these phenomena on the behavior of the aeroplane in flight will be discussed in later chapters.

**43. The Rudder in Normal Flight.** The rudder can be made to exert yawing moments on the aeroplane in the same way as the elevator exerts pitching moments. Generally, but not always, a fixed *fin*, analogous to the fixed *tail*, is placed in front of the rudder, to assist it in providing *static* yawing stability and to reinforce its action in producing yawing moments. So effectively does the fin serve this latter purpose that the yawing moment for a given angular movement of the rudder is, as we have already mentioned, almost as great as if both rudder and fin were rotated together.

The interference of the body of the aeroplane with the flow of air past the rudder is so severe that it is of little use attempting to estimate the rudder yawing moments from experiments upon isolated fins and rudders in an undisturbed air current; estimates must therefore be made from experiments on a complete aeroplane body with fin and rudders attached. For detailed records of experiments of this nature the reader should consult reference (3) but a rough estimate, taken from a number of such experiments, of the order of magnitude of these moments in a typical example is given below.

Adopting a procedure similar to that of 14 write

$$k_n \zeta = \frac{dk_E''}{d\zeta} \cdot \frac{S''V''}{Ss}$$

where  $k_n \zeta$  stands for the ratio of the coefficient of yawing moment ( $k_n$ ) to the angular displacement ( $\zeta$ ) of the rudder.  $dk_E''/d\zeta$  is the ratio of the coefficient of normal force on the rudder (*normal force*/ $\rho V^2 S''$ ) to the rudder angle.  $S''V''/Ss$  is the rudder and fin *volume coefficient* of 14.

Typical values of  $dk_E''/d\zeta$ , with  $\zeta$  expressed in radians, were given in 14 as 0.7 for a moderately well placed fin and rudder, 0.9 for a fin and rudder exceptionally clear of body interference and 0.5 with exceptionally severe interference.

Yawing moment is roughly proportional to rudder angle up to some  $30^\circ$ , or 0.52 radians, which is about the limit of the movement generally allowed. The maximum yawing moment coefficient which can be obtained from a typical rudder in normal flight is thus of the order

$$k_n = 0.52 \times 0.7 \times \frac{S''V''}{Ss} = 0.36 \frac{S''V''}{Ss}$$

A typical value of  $S''V''/Ss$  would be in the neighborhood of 0.05, giving a maximum moment coefficient from the rudder of 0.018. This is of course, merely a representative figure, higher or lower values are to be expected in different designs.

**44. The Rudder in Stalled Flight.** In stalled flight the rudder as a rule becomes less effective than in normal flight, because of the increased interference of the body with the air flow. A 50 per cent or even greater reduction of power is not unusual when the incidence is  $20^\circ$  and aeroplanes have been known in which, at  $30^\circ$  incidence, the rudder became entirely ineffective.

## CHAPTER IV

### FREE FLIGHT—SIMPLE DISCUSSION

**1. Introduction.** Having discussed, in the preceding chapters, the magnitude of the air-reactions which act upon an aeroplane in various circumstances, we have now to consider the movements of an aeroplane in flight under the influence of these reactions. Chapters V, VI and VII will deal with the analysis of the motion of the aeroplane when slightly disturbed from steady symmetric flight and will follow the conventional lines along which calculations are now-a-days made to investigate the stability of aircraft and their response to the controls. When these chapters are studied it will be found that although the analysis is not difficult in the mathematical sense, it is very complicated and is not well suited for giving a simple statement of the problem, or a clear grasp of the reasons why the aeroplane behaves as it does. In the present chapter, therefore, an attempt is made to deal with the general problem

of free flight in a simple way, by neglecting entirely properties of the aeroplane which in specific circumstances exert but a minor influence on its motion. Although it is possible in this way to reach very simply many of the conclusions of practical importance which emerge from the detailed analysis of later chapters, it should not be supposed that the detailed analysis is therefore valueless; on the contrary it is only from a knowledge of the details of the more complete analysis that the approximations of the present chapter can be made with confidence; moreover the methods of the succeeding chapters are generally required for quantitative computation of the behaviour of specific aeroplanes.

The reader who wishes merely to obtain a grasp of the reasons why aeroplanes behave as they do, without wishing to engage in research on the matter, or to carry out computations relating to their behaviour in certain circumstances, will, it is hoped, find what he requires in the present chapter, without the labour of studying Chapters V, VI, and VII. For the reader who intends to study those chapters the present chapter should serve as a useful introduction to more orthodox methods.

**2. Lanchester's Idealized Flight Path.** So long ago as 1908, W. F. Lanchester published a book (Chapter V, Ref. 4) upon the dynamics of free flight and in one section of this book he approached the problem by imagining an idealized aeroplane upon which the air-reaction is always perpendicular to the direction of motion and proportional to the square of the speed of the c.g. through the air. With these assumptions he was able to calculate, exactly and very simply, all possible forms which the flight path can take when it is confined to a vertical plane. Since no general solution of the equations of motion has yet been found with any more accurate assumptions, and since the solutions bear an interesting resemblance to the paths of a real aeroplane, it is worth beginning the present chapter with a consideration of Lanchester's flight paths—he called them “Phugoids”—even though they do not exactly represent the path of any real aeroplane, and though his method of analysis is quite different from that followed in the remainder of the chapter.

To visualize Lanchester's idealization more clearly we may imagine an aeroplane which has zero “drag”, or, alternatively, one on which the screw thrust is always exactly adjusted to neutralize the drag from instant to instant. To secure a lift proportional to the square of the speed, the wings must exert a constant lift coefficient, so that their incidence must be constant. This implies that the aeroplane is *statically* stable as regards pitching, that it has a negligible moment of inertia about the pitching axis, and that the length between wings and tail is small compared with the radii of curvature of the flight path. The last condition is necessary, otherwise the derivative  $M_q$  (see II 31) which defines the pitching moment generated by angular velocity of pitch, will appreciably influence the incidence. We confine attention

to the motion of this imaginary aeroplane in the vertical plane, supposing that it is always oriented symmetrically with respect to this plane.

**3. Equation of the Flight Path.** With these assumptions the external forces acting upon the aeroplane form a conservative system, because the air-reaction is always perpendicular to the direction of motion and therefore does no work. The velocity ( $V$ ) of the c.g. is therefore related to the distance  $Z$  of the c.g. below some datum level (see Fig. 45) by the equation

$$V^2 = 2gZ \quad (3.1)$$

There is evidently one flight path which is straight and horizontal, in which the air-reaction ( $L$ ) is equal to the weight ( $mg$ ), and if the distance of this path below the datum level be  $Z_1$ , we have in other flight paths, since  $L$  is by hypothesis proportional to  $V^2$  and therefore to  $Z$ ,

$$L = mg \frac{Z}{Z_1} \quad (3.2)$$

Let  $R$  be the radius of curvature of the path, positive when on the side of the path towards which the air reaction is directed. Then it is clear from Fig. 45 that if  $\Theta$  be the inclination of the path to the horizontal

$$R d\Theta = - \frac{dZ}{\sin \Theta}$$

or

$$R = \frac{dZ}{d(\cos \Theta)} \quad (3.3)$$

The total force acting perpendicular to the path is the sum of the air-reaction and the component of the weight and is therefore by (3.2)

$$mg \left( \frac{Z}{Z_1} - \cos \Theta \right)$$

The acceleration in this direction is  $V^2/R$  or, using (3.1),  $2gZ/R$  which, from (3.3), becomes

$$2gZ \frac{d(\cos \Theta)}{dZ}$$

Equating the applied force per unit mass, perpendicular to the direction of motion to the acceleration in this direction and dividing by  $g$  gives the equation,

$$2Z \frac{d(\cos \Theta)}{dZ} = \frac{Z}{Z_1} - \cos \Theta$$

This equation is easily integrated, after multiplying throughout by the integrating factor  $\frac{1}{2} Z^{-\frac{1}{2}}$ . The integral may be written

$$\cos \Theta = \frac{1}{3} \frac{Z}{Z_1} + C \left( \frac{Z_1}{Z} \right)^{1/2}$$

where  $C$  is an arbitrary constant.

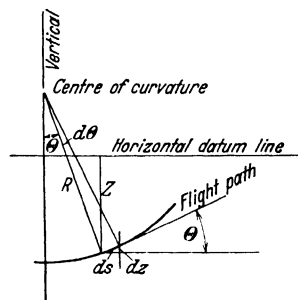


Fig. 45.

For brevity write  $\zeta$  for  $Z/Z_1$  giving

$$\cos \theta = \frac{1}{3} \zeta + \frac{C}{\zeta^{1/2}} \quad (3.4)$$

Again, using (3.3), we find

$$\frac{1}{R} = \frac{d(\cos \theta)}{dZ} = \frac{1}{3Z_1} - \frac{1}{2} C \frac{Z_1^{1/2}}{Z^{3/2}}$$

or

$$\frac{Z_1}{R} = \frac{1}{3} - \frac{1}{2} \frac{C}{\zeta^{3/2}} \quad (3.5)$$

**4. Forms of the Flight Path.** Equations (3.4) and (3.5) give the slopes and radii of curvature of the flight path at various distances below the datum level and they can be used to plot the paths with various values of the parameter  $C$  by semi-geometrical methods described in Chapter 3 of Ref. 4, Chapter V.

No real flight paths correspond to values of  $C$  greater than  $+2/3$ , for these require  $\cos \theta$  to be always greater than unity so that  $\theta$  is always imaginary.

If  $C = 2/3$  there is one unique value of  $\zeta$  only, namely unity, for which  $\theta$  is real.  $\cos \theta$  is then unity and  $\theta$  zero. This value of  $C$  corresponds, of course, to steady straight flight.

As  $C$  decreases from  $2/3$ , the range of values of  $\zeta$  greater and less than unity over which  $\theta$  is real, increases. The radius of curvature of the path is infinite when  $\zeta = (3/2 C)^{2/3}$ ; is negative when  $\zeta$  is less than this value and positive when  $\zeta$  is greater than this. With these values of  $C$  the

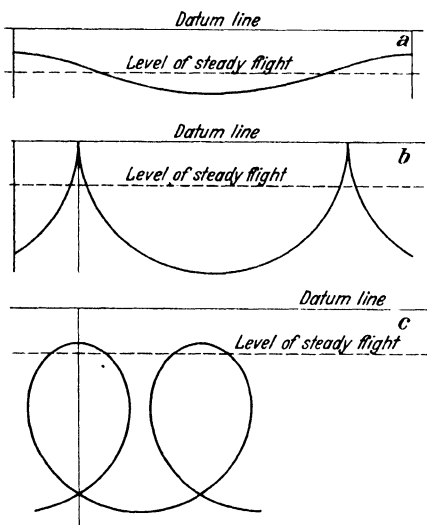


Fig. 46. Examples of Lanchester "phugoid" curves for an idealized aeroplane.

flight path is sinusoidal, the inflection points being distant  $(3/2 C)^{2/3} Z_1$  below the datum line. The radius of curvature at the highest point of the path is smaller than that at the lowest point, so that the path is not a true sine curve, but has a series of peaks, which are more or less pronounced according to the amplitude of the up and down motion. An example of a flight path of this kind is given in Fig. 46a.

As  $C$  decreases towards zero these peaks become progressively sharper and approach nearer to the datum line, until, when  $C$  is zero, they become cusps which touch the datum line; the flight path then becomes a series of semi-circles of radius  $3Z_1$  (see Fig. 46b). To follow out the assumptions accurately, the aeroplane, in this limiting case, must be supposed



to arrive at a cusp with zero velocity and pointing perpendicularly upwards, then to revolve instantaneously through  $180^\circ$  and start falling again vertically downwards on the new semi-circular path. This limiting case of course strains the assumptions severely, but pilots who have attempted a loop with insufficient speed know to their cost that something with an uncomfortable resemblance to this manoeuvre may actually occur<sup>1</sup>.

When  $C$  becomes negative,  $R$  remains permanently positive, so that the centre of curvature remains continually on the same side of the flight path which becomes a series of loops as in Fig. 46c. The larger  $C$  the more nearly circular do the loops become and the further below the datum line do the tops of the loops lie.

**5. Comparison with the Path of a Real Aeroplane.** These curves do not represent exactly the path of a real aeroplane, but that they give a good general idea of the possible motions for a freely launched rigid aeroplane can be easily verified by launching small stable paper models at various speeds. The sinuous and looped paths are easily obtained by varying the speed of launching, whilst a fair approximation to the cusps can be reached by carefully adjusting this speed. Though very interesting from a general point of view, the flight curves obtained in the above manner are not of much practical value for quantitative computation, for no one has yet devised means of modifying them to apply more accurately to a real aeroplane, except by carrying out laborious "step-by-step" computations (V 8) which have to be made afresh for every new set of initial conditions. It should also be realized that the controls are nearly always used during manoeuvres such as those indicated by the majority of these curves and the aeroplane cannot then be treated as a body of invariable form. When, for example, a loop is being made, a high speed is first attained and the stick pulled gently to avoid overstressing the aeroplane; later, when the aeroplane is inverted and moving more slowly, the stick may be pulled back hard to obtain the highest possible incidence and the smallest possible curvature while passing over the top of the loop. For these reasons there is not much object in attempting to follow, with assumptions more accurate than the foregoing, the details of violent manoeuvres such as those there considered, and, in fact, more detailed analysis has, in the main, been confined to the study of small variations from steady straight flight. It is to the study of these small disturbances that we shall now turn, observing that although, for the sake of mathematical precision the disturbances will be assumed to be infinitesimal, yet the results are found to apply with useful accuracy to disturbances of considerable magnitude.

<sup>1</sup> I once did it myself when learning to fly.

### A. The Slow Oscillation of Small Amplitude<sup>1</sup>

**6. The Ideally Simple Oscillation.** The equations of motion of Lanchester's idealized aeroplane, for infinitesimal disturbances from level flight, could of course be derived by making  $C$  in (3.4) and (3.5) differ from  $2/3$  by an infinitesimal amount, but it is easier to start again.

Using the same notation as before we have

$$V^2 = 2gZ \quad \text{and} \quad L = mg \frac{Z}{Z_1}$$

Using the symbol  $\theta$  to indicate that the inclination of the aeroplane and its flight path to the horizontal is small,  $\cos \theta$  is sensibly unity and the vertical component of the air-reaction will be sensibly equal to the resultant air-reaction ( $L$ ). The aeroplane, being now supported by a force which is proportional to the distance below a certain datum level, will, if disturbed from its equilibrium level, oscillate up and down exactly in the same way as if it were suspended upon a spring which extends under the steady weight of the aeroplane through a distance  $Z_1$ . Thus, if  $z$  be written for  $Z - Z_1$ , the vertically downward acceleration of the aeroplane at any instant is given by

$$m\ddot{z} = -mg \frac{z}{Z_1}$$

or

$$\ddot{z} + \frac{g}{Z_1} z = 0$$

The solution of which is

$$z = z_1 \cos \left( \sqrt{\frac{g}{Z_1}} t + \varepsilon \right) \quad (6.1)$$

in which  $z_1$  and  $\varepsilon$  are arbitrary constants and  $t$  represents lapse of time from some zero epoch.

The period of this oscillation is  $2\pi \sqrt{Z_1/g}$ , which is the same as that of a simple pendulum of length  $Z_1$ .

Write  $V_1$  for the velocity corresponding to the level  $Z_1$ . Then  $V_1^2 = 2gZ_1$ , and the period becomes  $\sqrt{2\pi V_1/g}$  or in foot-second units,  $0.138 V_1$  seconds.

**7. Form of the Oscillation of Small Amplitude.** Write  $V = V_1 + v$ , so that  $v$  is the variation from the mean velocity ( $V_1$ ).

Then

$$(V_1 + v)^2 = 2g(Z_1 + z)$$

Omitting small quantities of the second order this becomes

$$2V_1 v = 2gz$$

or since

$$V_1^2 = 2gZ_1$$

$$v = \sqrt{\frac{g}{2Z_1}} z$$

<sup>1</sup> The treatment, in this section, of the slow oscillation, though it differs considerably in form, is also founded upon the work of Lanchester in Ref. 3, Chapter V.

The horizontal velocity of the aeroplane is  $(V_1 + v) \cos \theta$ ; but, since  $\theta$  is small,  $\cos \theta$  differs from unity by a small quantity of the second order, so that to first order accuracy the horizontal velocity is simply  $V_1 + v$ .

The distance  $(x)$  travelled in time  $t$  is

$$x = \int (V_1 + v) dt = V_1 t + \int \sqrt{\frac{g}{2Z_1}} \cdot z dt$$

which, using (6.1), becomes

$$x = V_1 t + \sqrt{\frac{g}{2Z_1}} z_1 \int \cos \left( \sqrt{\frac{g}{Z_1}} t + \varepsilon \right) dt$$

$$\text{or} \quad x = V_1 t + \frac{1}{\sqrt{2}} z_1 \sin \left( \sqrt{\frac{g}{Z_1}} t + \varepsilon \right) + \text{constant} \quad (7.1)$$

The c.g. of the aeroplane therefore oscillates back and forth about a vertical line which travels with the mean speed  $V_1$ , the oscillation being in quadrature with, and  $1/\sqrt{2}$  times the amplitude of the vertical oscillation. Relative to axes moving with velocity  $V_1$  the aeroplane therefore describes an ellipse with major axis vertical and eccentricity  $1/\sqrt{2}$ ; the direction of rotation around the ellipse being such that the aeroplane is rising when in front of the mean position and falling when behind it. The track of the aeroplane relative to axes fixed in the air is therefore not a sine curve but is a curve of the type of Fig. 46a, in which the limb below the mean level is longer than the limb above it and the curvature above the mean level is greater than that below it.

**8. Comparison with the Oscillation of a Real Aeroplane.** The idealized aeroplane of the above calculations would, if slightly disturbed from straight level flight, continue to oscillate forever with constant amplitude and with the period given by the calculation. A real aeroplane in these circumstances generally oscillates in the manner indicated, but with a period which is considerably greater than that given by the simple calculation and an amplitude which decreases exponentially to zero. The difference is due, of course, to the various air forces and moments which have been omitted in the simple calculation. The full analysis of the motion when these forces and moments are taken into account is given in Chapters V and VI, but some of the more important effects can be investigated very simply by an extension of the methods of the preceding paragraph.

**9. The Effect of  $M_q$  on the Period.** The lengthening of the period above that given by the simple calculation is mainly due to the operation of the pitching moment due to rate of pitch—to the derivative  $M_q$  of II 31. This moment, acting sometimes in the positive and at other times in the negative sense, according to the way in which the aeroplane is pitching as it follows its sinuous path, causes the incidence to change very slightly from the constant value assumed in the simple

calculation. The nature of this change is found to be that the incidence is slightly increased during the time that the aeroplane is above the mean level and decreased while the aeroplane is below that level. The result is that while it is above the mean level the lift is greater than was assumed in the simple calculation, and while below the mean level the lift is less. The net force tending to restore the aeroplane to the mean level is thus always less than is supposed in the simple calculation and the period of the oscillation is correspondingly lengthened.

The calculation which follows shows that an approximation to the lengthening of the period is that it is increased in the ratio

$$\sqrt{1 + \frac{g}{V_1 A_1} \cdot \frac{M_q}{M_\alpha}} : 1$$

where  $A_1$  is the mean incidence of steady flight at the speed  $V_1$ , measured from that incidence at which lift is zero, and  $M_\alpha$  stands for  $\partial M / \partial \alpha$ , which is the slope of a curve of pitching moment against incidence and defines the *static* (see II 1) stability of the craft.

When the aeroplane is stable, as is assumed in the present discussion, both  $M_q$  and  $M_\alpha$  are negative and the expression under the root is greater than unity; for an aeroplane of normal stability its value is in the neighborhood of 1.7 and varies but little with change of the speed of steady flight over the normal range of speeds. It is liable, however, to increase at very high speeds, owing to the fall in the value of  $M_\alpha$  which occurs at low incidences (see II 27).

In 6 the period on the simpler assumption was found to be  $0.138 V_1$  seconds with  $V_1$  in feet per second, so that on the present more correct assumption the period becomes of the order of  $0.22 V_1$  seconds. The true period of the oscillation of a real aeroplane about a mean level cannot be accurately expressed by any simple formula of the kind under discussion, but must be worked out by an elaborate arithmetrical process described in Chapter VI and for the typical aeroplane of these calculations is found to be some 10 per cent less than is given by the approximation now under consideration.

The following simple analysis shows how this approximate formula for the period can be obtained, without recourse to the elaborate methods of later chapters. It is of interest because it shows which factors must be taken into account and which omitted in reaching the approximate formula, which, it should be noted, is identical with the approximation of VI 36 and is the approximation commonly employed in practical work.

Let  $\theta$  and  $\alpha$  represent, respectively, the small variations of the attitude and incidence of the aeroplane from the attitude and incidence of straight horizontal flight at the speed  $V_1$ . The inclination of the flight path, which in an earlier paragraph was identical with  $\theta$ , is now  $\theta - \alpha$ ,

and if, as before, the distance of the c.g. below the mean level is written  $z$ , so that  $\dot{z}$  is the downward velocity component, then

$$\dot{z} = - (V_1 + v) (\theta - \alpha) = - V_1 (\theta - \alpha)$$

since products of small quantities are negligible.

An essential point in the approximation under consideration is that, although  $\alpha$  is large enough materially to alter the lift of the aeroplane, it may be neglected in the above equation by comparison with  $\theta$ , so that we may write as an approximation

$$\dot{z} = - V_1 \dot{\theta}$$

This assumption and the neglect of moment of inertia in the equations which follow are of course justified only by comparison of the result with that of the detailed calculations of subsequent chapters.



Fig. 47.

We now have

$$q = \ddot{\theta} = - \frac{\ddot{z}}{V_1} \quad (9.1)$$

Neglecting entirely the moment of inertia of the aeroplane we have

$$M_\alpha \cdot \alpha + M_q \cdot q = 0$$

or, using (9.1)

$$\alpha = \ddot{z} \frac{M_q}{V_1 M_\alpha} \quad (9.2)$$

In normal flight, lift is closely proportional to incidence; hence we may write,

$$\text{Lift} = m C (A_1 + \alpha) V^2 = m C (A_1 + \alpha) 2 g (Z_1 + z)$$

where  $C$  is a constant.

But in steady straight flight we have

$$m g = m C A_1 2 g Z_1 \quad (9.3)$$

So that the unbalanced lift on the aeroplane at any point in its flight is

$$2 C m g [(A_1 + \alpha) (Z_1 + z) - A_1 Z_1]$$

which, omitting second order term reduces to

$$2 C m g [A_1 z + Z_1 \alpha]$$

but from (9.3)  $2 C = 1/A_1 Z_1$ .

Hence the unbalanced lift is

$$m g \left[ \frac{z}{Z_1} + \frac{\alpha}{A_1} \right]$$

or using (9.2)

$$m g \left[ \frac{z}{Z_1} + \frac{\ddot{z}}{A_1 V_1} \frac{M_q}{M_\alpha} \right]$$

Equating the unbalanced lift to the upward mass acceleration ( $-m\ddot{z}$ )

$$\text{leads to} \quad \left[ 1 + \frac{g}{V_1 A_1} \cdot \frac{M_q}{M_\alpha} \right] \ddot{z} + \frac{g}{Z_1} = 0$$

an equation which represents an undamped oscillation of period

$$2\pi \sqrt{\frac{Z_1}{g}} \sqrt{1 + \frac{g}{V_1 A_1} \cdot \frac{M_d}{M_a}} \quad (9.4)$$

**10. The Damping of the Oscillation.** As already mentioned, the oscillations of the type under consideration, in a real aeroplane, are nearly always effectively *damped*, so that they virtually disappear in the course of two or three complete periods. The factors which contribute to this damping are extremely complicated and are dealt with in detail in Chapter VI. The most important cause of the damping is the variation of drag due to the variation of speed occurring during the sinuous flight of the aeroplane; this was entirely neglected in the preceding discussion. The effect of these drag changes is found to be that while the aeroplane is falling it moves slightly faster than it would were the drag to remain constant and while rising it moves slightly slower. During the falling period therefore, the lift is higher than it otherwise would have been and during the rising period it is lower. A damping term is thus introduced and a calculation on lines similar to that of the previous paragraph shows that the net result of this addition to the equation is to

multiply the amplitude of the oscillation by an exponential term  $e^{-\frac{g}{V_1} \gamma t}$ , where  $\gamma$  is the ratio of drag to lift for the aeroplane. This term is identical with the first term ( $k_D$ ) of the elaborate expression for the damping factor obtained in VI (36.1) the difference in the symbols being due to the use of dimensionless forms in Chapter VI. Though not the only appreciable term, the above is generally the most important term in the damping and its numerical value for a normal aeroplane at cruising speed is of the order  $e^{-0.02t}$ . Due to this term alone therefore, the amplitude would be reduced one half in about every 35 seconds, or in say, slightly more than one complete period.

Hitherto the moment of inertia of the aeroplane has not entered into the estimates of period and damping of the slow oscillation; this is because the period of the oscillation is so long that the angular accelerations necessary to allow the aeroplane to follow the sinuous path are small and, if the aeroplane has appreciable stability, the changes of incidence necessary to provide the moments required to overcome the pitching inertia are so small as to be almost negligible. When the effect of moment of inertia is taken into account, it is found that the only appreciable influence which it has on the oscillations is to cause the incidence to be a little higher than it would be with no inertia during the time that the aeroplane is rising, and a little lower whilst the aeroplane is falling. The result is the addition of a small forcing, or negative-damping, term to the motion, which to some extent offsets the damping due to variations in drag. In a normal full scale aeroplane this effect is of no great importance, but by deliberately increasing the moment

of inertia of small model aeroplanes it can be made into the predominating term and will cause any small oscillation to increase indefinitely.

**11. Influence of the Airscrew.** These estimates of period and damping have ignored the variation of thrust of the screw due to changes in the aeroplane's speed. These are troublesome to calculate and are considered at some length in VI 37—46. As the speed increases, the thrust of the screw falls, so that one effect on the damping of the oscillation is the same as that of the variations of drag which we have been considering and is, from the present point of view, equivalent to an increase of the drag of the aeroplane by a quantity which depends on the details of the screw design.

The variation in the thrust of the screw with change of forward speed alters also the intensity of the slipstream from the screw and, if this slipstream passes over the tail, variations in pitching moment may arise from changes of air speed; these may have an appreciable influence both on the period and damping of the oscillation, but their further consideration is deferred to Chapter VI.

**12. Other Factors which Influence the Oscillation.** The more complete analyses of Chapter VI shows in 36 that many other influences which are not entirely negligible contribute to the damping and hence the only sound way of arriving at an accurate estimate of the damping is to carry out the complete computation. The above simplified treatment of the damping term must be regarded more as a discussion of the principal factors at work than as providing means for a quantitative estimate of the damping. As however, there is nearly always sufficient damping for practical purposes it is not generally a matter of great practical importance to arrive at a precise estimate of its amount.

**13. Gliding and Climbing Flight.** When the engine is working with either more or less power than is required for level flight the steady flight path of the aeroplane must be inclined to the horizontal, either upward or downward. The oscillations which we have been considering can take place about these inclined paths in the same way as about a level path and, unless the inclination of the path is unusually severe, its influence upon the period and damping of the oscillation is not serious, but the damping will of course be modified by the different actions of the screw in the different circumstances.

**14. The Unstable Aeroplane.** Expression (9.4) shows that the period of the oscillation becomes larger as the static stability of the aeroplane (defined by  $M_n$ ) falls towards zero. When  $M_n$  is very nearly zero the presence of the small damping term in the equations causes the motion to become aperiodic and when the aeroplane becomes statically unstable, the free flight also becomes unstable and any slight disturbance tends to increase exponentially with the lapse of time. For reasons which will

appear shortly these unstable disturbances develop relatively slowly, unless the static instability is much higher than it is likely to become in practice. The detailed analysis of an unstable condition of this kind is given in Chapter VI.

## B. The Rapid Incidence Adjustment

**15. Simplifying Assumptions.** In the previous paragraphs of the present chapter we have, with one unimportant exception, been considering the flight of a stable aeroplane which virtually has no moment of inertia, so that the incidence is always automatically adjusted to that value for which the resultant pitching moment is zero. We have now to consider what happens when, from any cause, the incidence of a real aeroplane is temporarily altered to some other value, or when the elevators are suddenly moved. We shall find that in these circumstances adjustments of direction of motion and orientation take place with such rapidity that, within less than one second, the incidence is restored nearly to the equilibrium value and the subsequent motion is of the type which we have been discussing. This rapid incidence adjustment, though completed in a very short time, is of great practical importance, for it may involve high stresses in the aeroplane and discomfort to the crew.

We shall approach the study of this motion with assumptions radically different from those of the previous sections. It will at first be assumed that the moment of inertia of the aeroplane is virtually infinite; or, if the reader prefers, that the adjustment occurs so rapidly that the aeroplane has not time to rotate appreciably in pitch. Later we shall have to modify this assumption, but the conclusions to which it leads are by no means so far from the truth as might at first sight be supposed. A second simplifying assumption is that the forward speed of the aeroplane does not change appreciably during the rapid incidence adjustment. In the present connection this assumption is sufficiently near the truth for practical purposes and will not need subsequent modification.

**16. Sudden Change of Incidence.** We shall consider an aeroplane of mass  $m$  for which the lift at a speed  $V_1$  is proportional to the incidence  $(A_1 + \alpha)$ , where  $A_1$  is the incidence at which the lift is equal to the weight and  $\alpha$  represents any variation of incidence from this value. If this aeroplane is at any time flying approximately horizontally with speed  $V_1$  and incidence  $(A_1 + \alpha)$ , the unbalanced upward force upon it is  $(mg/A_1) \alpha$  and the upward acceleration is  $(g/A_1) \alpha$ .

Suppose that, at zero time, the aeroplane, though still flying horizontally, has been rotated through an angle  $\theta_0$  from the attitude of steady horizontal flight, so that the incidence is  $(A_1 + \theta_0)$  and the



vertical acceleration is  $(g/A_1) \theta_0$ . This acceleration will, in time, generate a vertical component velocity to which, in the present section<sup>1</sup> we give the symbol  $w$ . If now, in accordance with our assumption the orientation of the aeroplane during the subsequent motion does not change appreciably, the change in the direction of motion at some subsequent instant will, assuming that  $w$  is small compared with  $V_1$ , have changed the incidence to  $(A_1 + \theta_0 - w/V_1)$

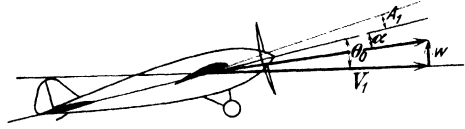


Fig. 48.

so that (see Fig. 48) 
$$\alpha = \theta_0 - \frac{w}{V_1} \quad (16.1)$$

Using  $\dot{w}$  to represent the upward acceleration, we have

$$\dot{w} = \frac{g}{A_1} \alpha \quad (16.2)$$

or from (16.1) 
$$\dot{w} = \frac{g}{A_1} \left( \theta_0 - \frac{w}{V_1} \right)$$

or 
$$\dot{w} + \frac{g}{A_1 V_1} w = \frac{g}{A_1} \theta_0$$

Since  $\theta_0$  is constant, the solution of this differential equation, with the condition that  $w$  is zero at zero time is:

$$w = \theta_0 V_1 \left( 1 - e^{-\frac{g t}{A_1 V_1}} \right) \quad (16.3)$$

Typical values of  $A_1$  and  $V_1$  might be 0.1 radian and 160 feet per second, respectively, and with these values  $g/A_1 V_1$  is approximately 2.

The exponential term in (16.3) is therefore approximately halved every third of a second and has sensibly disappeared after about one second. After this, the aeroplane is left flying with incidence  $A_1$ , upon a path which is inclined upwards through an angle  $\theta_0$  and it will continue so to fly until the speed has had time to change appreciably. Ultimately, of course, variations of speed will bring about the slow oscillation previously studied.

The vertical acceleration during this rapid adjustment of incidence is given by 
$$\dot{w} = \frac{\theta_0}{A_1} \cdot g \cdot e^{-\frac{g t}{A_1 V_1}}$$

It has a maximum value at zero time when, as is otherwise obvious, its value is  $(\theta_0/A_1) g$ .

<sup>1</sup> The positive direction of vertical velocities in the present section is upward, whereas that in the previous section and in subsequent chapters is downward. Too meticulous a regard for consistency in this respect results in an artificiality of expression which detracts from the simplicity which it is the object of this chapter to achieve. Note that  $w$  in this section is identical with  $-z$  in the previous section.

The above motion is substantially that which occurs when a statically neutral aeroplane flies suddenly into air which is moving with a vertical velocity different from that of the air from which it has emerged—into what may be called a sharp edged vertical gust. The large but very transient acceleration provides the *bump* felt by occupants of an aeroplane in these circumstances.

The only important difference between the motion represented by the above expression and that of a real aeroplane which is statically neutral arises from the effect, studied in II 40, of rate of change of incidence upon pitching moment. This neither alters the initial acceleration nor the final direction of motion, but slightly modifies the form of the transition between the initial and final states (see 18).

**17. Sudden Application of Elevators.** It is of interest to consider what happens when the elevators of an aeroplane are suddenly moved to some new position and then held fixed. We may suppose that this causes an additional constant pitching moment  $M_0$  (see Fig. 49) to act upon the aeroplane, at a moment when it is flying

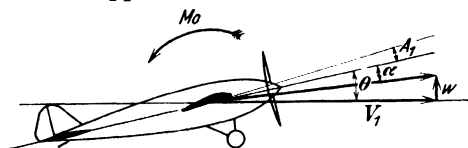


Fig. 49.

straight and steadily in a horizontal direction. For simplicity we shall first suppose that the aeroplane is statically neutral and shall neglect the pitching moment due to rate of change of incidence. The pitching moment produced by angular velocity of pitch must not, however, be neglected, since it is the principal factor which, in these circumstances, determines the form of the motion. In accordance with the notation of Chapter II, we shall write the pitching moment due to rate of pitch  $q$  in the form  $M_q \cdot q$ , where  $M_q$  is sensibly constant. The whole pitching moment acting upon the aeroplane at any instant after the constant applied moment  $M_0$  has generated an angular velocity  $q$ , is thus  $M_0 + M_q \cdot q$ . It is now, of course, no longer permissible to consider the moment of inertia to be indefinitely large, and if  $B$  is the appropriate moment of inertia of the aeroplane, we have

$$M_q \cdot q + M_0 = B\dot{q}$$

or

$$\dot{q} - \frac{M_q}{B} \cdot q = \frac{M_0}{B}$$

The solution of this equation with the condition that  $q$  is zero at zero

$$\text{time is} \quad q = -\frac{M_0}{M_q} \left[ 1 - e^{-\frac{M_q}{B}t} \right] \quad (17.1)$$

and the angular acceleration is

$$\dot{q} = \frac{M_0}{B} \cdot e^{-\frac{M_q}{B}t}$$

A typical value for  $M_q/B$  is  $-2.5$  so that it appears that the aeroplane begins to rotate with angular acceleration  $M_0/B$ , as it obviously must under the applied moment  $M_0$ ; and that this angular acceleration very rapidly dies away, and has sensibly vanished within one second; the aeroplane is then left rotating with that angular velocity which is just sufficient for the applied moment to be balanced by the moment due to the angular velocity.

If, at any instant, the angle through which the aeroplane has rotated from the attitude of steady flight be  $\theta$ , we have, as in (16.1) (see Fig. 49)

$$\alpha = \dot{\theta} = \frac{w}{V_1} \quad (17.2)$$

In which, however,  $\theta$  is now a variable whose first differential is identical with the angular velocity  $q$ .

Differentiating (17.2) with respect to time, substituting for  $w$  from (16.2) and writing  $q$  for  $\dot{\theta}$ , gives the differential equation

$$\dot{\alpha} + \frac{g}{A_1 V_1} \alpha = q \quad (17.3)$$

The variation of  $q$  with time is however, given independently by (17.1), so that using this equation, we have

$$\dot{\alpha} + \frac{g}{A_1 V_1} \alpha = -\frac{M_0}{M_q} \left[ 1 - e^{\frac{M_q}{B} t} \right]$$

For brevity write this  $\dot{\alpha} + C\alpha = G[1 - e^{-Ft}]$

where  $C$  and  $F$  are positive constants ( $M_q$  is always negative). The solution of this equation with the condition that  $\alpha$  is zero at zero time is

$$\alpha = \frac{G}{C} \left[ 1 + \frac{1}{C-F} (F e^{-Ct} - C e^{-Ft}) \right]$$

Since, as we have seen, the numerical values of  $C$  and  $F$  are of the order 2 and 2.5 respectively, the incidence very rapidly settles down to a constant  $G/C$  radians greater than that of steady straight flight.

When the incidence has become constant the direction of motion of the aeroplane is changing at the same rate as its orientation, that is to say with the sensibly constant angular velocity  $q = M_0/(-M_q)$  see (17.1) so that the aeroplane flies along the arc of a circle of radius  $(M_q/M_0) V_1$ , the curvature being upwards when  $M_0$  is positive.

On a conventional aeroplane the value of  $M_0/M_q$ , for a movement of the elevator of  $1^\circ$ , would be about 0.15 which at a speed of 150 feet per second would give a flight path with radius of curvature of about one thousand feet. The aeroplane will continue to fly in this path until an appreciable alteration has occurred in the forward speed. The subsequent motion in a particular case is shown in the illustrations to Chapter VI.

**18. Solutions with More Complete Assumptions.** When the aeroplane is not statically neutral, or when the effect on pitching moment of rate of

change of incidence is not neglected, the equations become more complicated, but the result is not very different from that of the simpler assumption. Retaining the assumption of constant forward speed, let us write for the pitching moment the expression  $M_0 + M_q \cdot q + M_\alpha \cdot \alpha + M_{\dot{\alpha}} \cdot \dot{\alpha}$  where  $M_q$ ,  $M_\alpha$  and  $M_{\dot{\alpha}}$  are sensibly constants.  $M_\alpha$  stands, as before, for  $\partial M / \partial \alpha$ ; a derivative which defines the static stability or instability of the aeroplane.  $M_{\dot{\alpha}}$  stands for  $\partial M / \partial \dot{\alpha}$  and indicates the dependence of pitching moment upon rate of change of incidence. The latter derivative was seen in II 40 to occur because the effective downwash near the tail is more nearly equal to that caused by the wings as they passed the position now occupied by the tail, than to that being generated by them at the instant under consideration.

It is now necessary to satisfy simultaneously the differential equations

$$\dot{\alpha} + \frac{g}{A_1 V_1} \alpha = q$$

$$B\dot{q} = M_0 + M_q \cdot q + M_\alpha \cdot \alpha + M_{\dot{\alpha}} \cdot \dot{\alpha}$$

which on rearranging become

$$\left. \begin{aligned} \dot{\alpha} + \frac{g}{A_1 V_1} \alpha - q &= 0 \\ -\frac{M_{\dot{\alpha}}}{B} \dot{\alpha} - \frac{M_\alpha}{B} \alpha + \dot{q} - \frac{M_q}{B} q &= \frac{M_0}{B} \end{aligned} \right\} \quad (18.1)$$

For brevity rewrite this

$$\left. \begin{aligned} \dot{\alpha} + C\alpha - q &= 0 \\ D\dot{\alpha} + E\alpha + \dot{q} + Fq &= G \end{aligned} \right\} \quad (18.2)$$

where  $C$ ,  $D$ ,  $F$  are positive constants,  $E$  is positive for a statically stable aeroplane and negative for one which is statically unstable, while  $G$  represents the applied moment.

If  $G$  is zero the solution of simultaneous differential equations of this type is known to be of the form  $\alpha = \alpha_1 e^{\lambda t}$ ,  $q = q_1 e^{\lambda t}$ , where  $\alpha_1$ ,  $q_1$  and  $\lambda$  are constants. Substituting these expressions in (18.2) and dividing by  $e^{\lambda t}$  gives the two simultaneous algebraic equations

$$\begin{aligned} (\lambda + C)\alpha_1 - q_1 &= 0 \\ (D\lambda + E)\alpha_1 + (\lambda + F)q_1 &= 0 \end{aligned}$$

Eliminating the ratio  $\alpha_1/q_1$  leaves

$$(\lambda + C)(\lambda + F) + (D\lambda + E) = 0$$

which may also be written

$$\lambda^2 + (C + F + D)\lambda + CF + E = 0 \quad (18.3)$$

This quadratic has two roots, say  $\lambda_1$  and  $\lambda_2$ . Corresponding to the root  $\lambda_1$  we have, from the first of (18.2)

$$q_1 = (\lambda_1 + C)\alpha_1$$

Corresponding to  $\lambda_2$  we have (say)

$$q_2 = (\lambda_2 + C)\alpha_2$$

The complete solution can therefore be written

$$\begin{aligned}\alpha &= \alpha_1 e^{\lambda_1 t} + \alpha_2 e^{\lambda_2 t} \\ q &= (\lambda_1 + C) \alpha_1 e^{\lambda_1 t} + (\lambda_2 + C) \alpha_2 e^{\lambda_2 t}\end{aligned}$$

In which  $\alpha_1$  and  $\alpha_2$  are arbitrary constants, which can be adjusted to fit any two conditions of the motion at zero time.

The complete solution when  $G$  is not zero is found by adding to the solution with  $G$  zero any particular integral whatever, and the simplest form of such a particular integral occurs when  $\alpha$  and  $q$  are constant. In this case the particular integral is

$$C\alpha - q = 0$$

$$E\alpha + Fq = G$$

whence 
$$\alpha = \frac{G}{E + CF} \quad q = \frac{CG}{E + CF}$$

The complete solution is therefore

$$\left. \begin{aligned}\alpha &= \alpha_1 e^{\lambda_1 t} + \alpha_2 e^{\lambda_2 t} + \frac{G}{E + CF} \\ q &= (\lambda_1 + C) \alpha_1 e^{\lambda_1 t} + (\lambda_2 + C) \alpha_2 e^{\lambda_2 t} + \frac{GC}{E + CF}\end{aligned} \right\} \quad (18.4)$$

**19. Discussion of the Solutions.** With a normal aeroplane the values of  $\lambda_1$  and  $\lambda_2$  are either real and negative or, if they are complex, the real part is negative. In the former case the exponential terms obviously die away in time and in the latter case the two terms together represent a damped harmonic oscillation which also disappears in the course of time. In either case the values of  $\alpha$  and  $q$  ultimately become constant and, after a sufficient time, the aeroplane is flying in a circular path as with the simpler assumptions of 17; but, unless  $E$  is zero, the curvature of this path is appreciably different from that of a neutral aeroplane.

If  $E$  and  $D$  are both zero, (18.3) shows that the roots become  $-C$  and  $-F$  and the motion is that examined more simply in 17.

The constant  $D$ , which defines the pitching moment due to rate of change of incidence, does not appear in the steady part of the motion but merely in the values of  $\lambda$ . The simple discussion of 16 therefore gave the correct answer for the final steady motion of a statically neutral aeroplane, but did not give the intermediate stages of the motion quite correctly for any aeroplane in which the tail is in the downwash from the wings.

The constant  $E$  defines the static stability of the aeroplane, which has been shown in II 8 to depend upon the value of the metacentric ratio ( $H$ ). A typical relation between  $E$  and  $H$  (corresponding roughly with the values 2 and 2.5 used above as illustrative of the magnitudes of  $C$  and  $F$ ) would be  $E = 100 H$ . Again, from the definition of  $D$  and  $F$  it appears that  $D/F = M_a/M_q$  and this ratio was shown in II 43 to be of

TABLE 1.

$H$	1	2
— .10	— 6.4	+ 0.8
— .05	— 5.7	0.0
— .03	— 5.3	— 0.4
.00	— 4.6	— 1.1
.031	— 2.8	— 2.8
.05	— 2.8 ±	1.4i

the order  $1/2$  for a normal aeroplane. Inserting these numerical values into (18.3), we obtain

$$\lambda^2 + 5.7 \lambda + 5 + 100 H = 0$$

The roots of this equation for various interesting values of  $H$  are given in Table 1.

**20. Unstable Aeroplanes.** From this table we observe that so long as the c.g. of the aeroplane which it represents is distant less than 0.05 of the mean wing chord behind the locus of neutral c.g. positions, the motion, in so far

as it is represented by the present assumptions, does not become unstable. In Chapter VI it will be seen that whenever  $H$  is negative the motion does become unstable, but unless the negative value appreciably exceeds a value corresponding to the figure 0.05 in the present example, the instability is slow in developing and is of a type which depends on changes in the forward speed. In the present simple analysis it has, of course, been assumed that no changes occur in the forward speed and hence this slowly developing type of instability has not been revealed.

Aeroplanes have often been in general use with the c.g. so placed that  $H$  is negative, but the negative value is rarely so great as to make the rapid adjustment of the aeroplanes to sudden disturbances become unstable. So long as the negative value of  $H$  does not appreciably exceed the critical value at which this occurs, the unstable aeroplane, though it cannot be left indefinitely to look after itself, is reasonably easy to fly, because the unstable motions develop so slowly that the pilot's reactions are amply rapid to deal with them.

By some pilots, moderately unstable aeroplanes are even preferred to aeroplanes which are completely stable, because they are more sensitive to the elevator control. For example, using the numerical values previously adopted, the constant term  $GC/(E + FC)$  in (18.4) becomes (for a stable aeroplane with  $H = +0.03$ ),  $GC/8$ , whereas for an unstable aeroplane (with  $H = -0.03$ ) it becomes  $GC/2$ . Thus, after the preliminary transition stage represented by the exponential terms of (18.4), the unstable aeroplane settles down to a circular path in which it is turning four times as fast as the stable aeroplane. It is true that with the unstable aeroplane one of the exponential terms decays more slowly than with the stable aeroplane, but even so this term becomes unimportant after some two seconds and henceforward the angular velocities are in the ratio stated above.

Though a moderate negative value of the metacentric ratio is, for these reasons, not necessarily disadvantageous, a high negative value such as — 0.10 in Table 1 may make the aeroplane almost unmanageable, even by a skilled pilot; for it introduces a positive root of the order

unity into the quadratic for  $\lambda$  and this involves an exponential term in the solution, which more than doubles itself every second.

**21. Stable Aeroplanes.** When the aeroplane is statically stable and the positive value of  $H$  exceeds about 0.03, the roots of the quadratic become complex and the motion represented is of the damped harmonic form, but even when  $H$  has the high value of 0.05 the motion is seen from Table 1 to be so heavily damped that its oscillatory nature is scarcely apparent. Thus, in this example, the period is  $2\pi/\sqrt{1.4}$  or about 5 seconds, whilst the amplitude is reduced to less than one tenth of its value in every second. The second half swing and subsequent swings of this oscillation are therefore inappreciable.

**22. Dimensionless Forms of the Quadratic for  $\lambda$ .** The numerical values used to illustrate the previous paragraphs relate to one particular type of aeroplane flying at one particular speed in air of one particular density. It is therefore of interest to manipulate the quadratic (18.3) for  $\lambda$  into a form which shows how the numerical values of the roots change from one aeroplane to another and from one flight condition to another. For this purpose we shall force the equation into a dimensionless form consistent with the system which will be employed throughout later chapters and by doing so we shall, in addition to throwing light on the problem in hand, introduce the reader in a simple manner to the very powerful system of dimensionless representation which will be met later.

In what follows, we shall assume for simplicity that  $D = 1/2 F$  and shall use the notation of Chapter II to write

$$F = -\frac{Mq}{B} = k_{mq} \frac{\rho V_1 S c^2}{B}$$

$$E = -\frac{M\alpha}{B} = aH \frac{\rho V_1^2 S c}{B}$$

$$C = \frac{g}{A_1 V_1} = a \frac{\rho V_1 S}{m}$$

where  $a$  is the rate of change of lift coefficient with incidence and  $k_{mq}$  is a dimensionless coefficient which was discussed in II §2.  $S$  and  $c$  are the area and mean chord of the wings and  $m$  is the mass of the aeroplane<sup>1</sup>. The third substitution above is obtained by observing that in steady flight, weight is equal to lift and therefore, since  $a$  is sensibly constant

$$mg = a A_1 \rho V_1^2 S$$

We introduce also three new symbols, the meanings of which will be discussed presently

$$\tau = \frac{m}{\rho V_1 S} \quad \mu = \frac{m}{\rho S c} \quad k_B = \frac{B}{m c^2}$$

<sup>1</sup> The reader will, of course, distinguish between the use of  $m$  as a subscript for  $k$  and as denoting the *mass* of the aeroplane.

Then, after multiplying throughout by  $\tau^2$  (18.3) can be written

$$(\lambda\tau)^2 + \left[ a + 1.5 \frac{k_{mq}}{k_B} \right] \lambda\tau + \frac{a}{k_B} [k_{mq} + \mu H] = 0 \quad (22.1)$$

This may be regarded as a quadratic equation in  $(\lambda\tau)$  of which it will be observed that the coefficients contain only dimensionless quantities.  $\tau$  is a quantity which has the dimensions of time, so that  $(\lambda\tau)$  has zero dimensions. The value of  $\tau$  sets a time scale to the motion, for if the dimensionless coefficients are unchanged, the two values of  $\lambda$  which correspond to the roots of this equation are inversely proportional to  $\tau$ ; thus, when  $\tau$  is large the values of  $\lambda$  are small and the period of the oscillation and the time required for damping are proportionally long. In later chapters notation will be simplified by expressing times as ratios to the time  $\tau$ , but for the present it is unnecessary to pursue this idea further.

Of the quantities which make up the coefficients of the quadratic;  $a$  varies but little from one aeroplane to another;  $k_{mq}$  was shown, in II 43 to depend principally upon the size and length of the tail and not to vary very greatly from one aeroplane to another;  $k_B$  is the square of the ratio of the radius of gyration to the mean wing chord;  $H$  is the metacentric ratio with which the reader is already familiar; while  $\mu$  is an interesting quantity which has not appeared before but which will appear frequently in later chapters.

From the definition of  $\mu$ , it is the ratio of the mass of the aeroplane to the mass of a quantity of air of density  $\rho$  and volume  $Sc$ , or it may be regarded as defining the ratio of the average density of the aeroplane to the density of the air through which it flies. The peculiar interest of  $\mu$  lies in the fact that aeroplanes having the same external form and load distribution behave in similar manners if, and only if, the value of  $\mu$  is the same for all. The time scales of the similar motions which they can then perform are in the ratio of the values of  $\tau$ . In the present chapter these properties of  $\mu$  and  $\tau$  are displayed in relation to one particular type of motion only. The general proof for all types of motion begins in V 18. The way in which  $\mu$  is associated with  $H$  in (22.1) shows that, in the motion represented, the effects of changes of  $\mu$  and of c.g. position can be represented by a single parameter,  $\mu H$ . The larger the value of  $\mu$  the more sensitive therefore does an aeroplane become to the precise value of the metacentric ratio, and the nature of the immediate response to gusts and to movements of the elevators is, in the main, determined by the two quantities  $\mu H/k_B$  and  $k_{mq}/k_B$ .

### C. Asymmetric Motions

**23. Statement of the Problem.** We have now to study, in a simple manner, the various kinds of asymmetric motion which are possible for an aeroplane. These involve angular velocities of roll ( $p$ ) and yaw ( $r$ )



about the  $X$  and  $Z$  axes respectively, and side-slip ( $V$ ) perpendicular to the plane of symmetry; they are maintained by rolling moments ( $L$ ) and yawing moments ( $N$ ) about the  $X$  and  $Z$  axes and side forces ( $Y$ ) perpendicular to the plane of symmetry (see Fig. 50).

The moments which act upon the aeroplane when it is moving asymmetrically have been discussed in Chapter III and the notation and results of that chapter will be employed. In general it will be assumed that the forces which act upon the aeroplane whilst it is rotating or moving in simple ways, such as side-slipping without rotation, or rolling without yawing or side-slipping, can be added together to give the forces in complicated motions involving all three types of movement. This cannot be exactly true, but it gives reasonably correct results for motions of moderate violence in which the directions and magnitudes of the velocities of the aeroplane's extremities do not differ very widely from the velocity of the c.g.

We shall in the present chapter be concerned mainly with manoeuvres which are regarded as infinitesimal disturbances from straight symmetric flight, or with manoeuvres of moderate violence. The violent manoeuvre of spinning will be dealt with along different lines in Chapter VIII.

**24. The True-banked Steady Turn.** The simplest motion to be considered is the steady *true-banked* horizontal turn in which the aeroplane is *banked*, or rolled about the  $X$  axis, until there is no side-slip. The balance of forces in this type of turn has been discussed in I 23, it remains to consider the balance of moments. We shall suppose first that the  $X$  axis is horizontal and use  $\Phi$  for the angle of bank (see Fig. 51).

Let the angular velocity about a vertical axis be  $\Omega$  and let it be represented by a vertical vector, the positive direction of which is downward, and corresponds to a turn to starboard.

This vector will have components

$$\begin{aligned} p &= 0 \\ q &= \Omega \sin \Phi \\ r &= \Omega \cos \Phi \end{aligned}$$

along the axes of  $X$ ,  $Y$ ,  $Z$ , respectively.

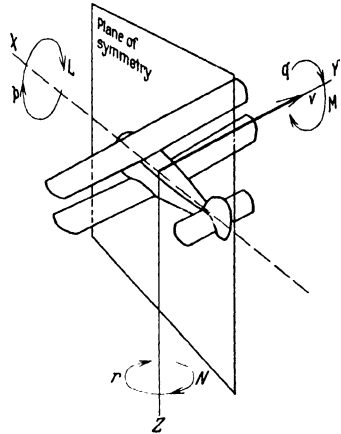


Fig. 50.

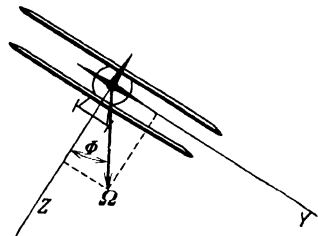


Fig. 51.

The angular velocity of pitch ( $q$ ) will cause additional pitching moments, which may be written  $M_q \cdot q$ , to act on the aeroplane and we shall assume that a symmetric rotation such as  $q$  generates no asymmetric moments and conversely that asymmetric rotation produces no symmetric moments.

To keep the aeroplane turning steadily it will be necessary for the pilot to move his elevator so as to apply a pitching moment given by

$$M_0 + M_q \cdot q = 0$$

or

$$M_0 = -M_q \Omega \sin \Phi$$

Since  $M_q$  is negative and  $\Omega$  and  $\Phi$  are always of the same sign,  $M_0$  is positive, or in other words the control stick has to be held in a farther back position during a banked turn than in straight flight at the same speed. As the turn becomes sharper and sharper and the bank steeper,  $\sin \Phi$  approaches unity and in the steeply banked turn becomes indistinguishable from unity.

An important difference should here be noted between aeroplanes which are longitudinally stable and those which are unstable. During the turn the balance of forces requires incidence to be higher than in straight flight at the same speed (see I 23) and therefore a stable aeroplane, which is correctly trimmed for straight flight will experience, on a turn, a negative pitching moment and the pilot will have to exert a large positive pitching moment to overcome both this and the moment due to the angular velocity of pitch. On the unstable aeroplane the pitching moment due to the increased incidence will be positive and help the pilot to overcome the opposing moment due to the angular velocity. Other things being equal an unstable aeroplane can, therefore, be held in a steady banked turn with less control effort than a stable one and, since the normal method of changing direction quickly is to use a steeply banked turn, this difference may have considerable practical importance. The phenomenon under discussion is the same as that discussed in relation to curved flight in a vertical plane in 20.

The angular velocity of yaw ( $r$ ) will cause a rolling moment ( $L_r r$ ) and a yawing moment ( $N_r r$ ) to act upon the aeroplane and in a steady turn, these must be neutralized by the moments  $N_0$  and  $L_0$  applied by the controls, in accordance with the equations,

$$\text{therefore} \quad \left. \begin{aligned} L_0 + L_r r &= 0^1 \\ N_0 + N_r r &= 0 \\ L_0 &= -L_r \Omega \cos \Phi \\ N_0 &= -N_r \Omega \cos \Phi \end{aligned} \right\} \quad (24.1)$$

<sup>1</sup> For strict accuracy the right hand side of the rolling moment equation should contain a term (VIII 4)

$$\frac{1}{2} \Omega^2 (C - B) \sin 2 \Phi,$$

Moments such as  $L_0$  and  $N_0$  and derivatives such as  $L_r$  and  $N_r$  were expressed in Chapter III in terms of dimensionless coefficients as follows

$$\begin{aligned} L_0 &= k_{l0} \varrho V_1^2 S s & L_r &= k_{lr} \varrho V_1 S s^2 \\ N_0 &= k_{n0} \varrho V_1^2 S s & N_r &= k_{nr} \varrho V_1 S s^2 \end{aligned}$$

where  $S$  and  $s$  are the area and semi-span of the wings.

In terms of these coefficients (24.1) becomes

$$\left. \begin{aligned} k_{l0} &= -k_{lr} k_\Omega \cos \Phi \\ k_{n0} &= -k_{nr} k_\Omega \cos \Phi \end{aligned} \right\} \quad (24.2)$$

where  $k_\Omega$  stands for  $\frac{\Omega s}{V_1}$ .

The necessary control setting for a steady true-banked horizontal turn can be obtained from these equations using values of  $k_{lr}$  and  $k_{nr}$  taken from experiments such as those recorded in III 38 and relations between  $k_{l0}$  and  $k_{n0}$  and the control settings from experiments such as those recorded in III 40.

For a conventional aeroplane in normal flight  $k_{lr}$  is positive while  $k_{nr}$  is negative. The rolling moment required for a steady true-banked turn will therefore be of opposite sign from the turn but the yawing moment will be of the same sign. Thus in a true-banked turn the control stick must be held against the bank to prevent the turn from becoming over-banked, whilst the controls must exert a net yawing moment in the sense to prevent the flight path from straightening out. The position of the rudder in the steady turn will depend, of course, upon the strength of the yawing moment exerted by the ailerons when they are set to maintain the correct bank.

**25. The Steady Turn with Side-Slip.** If the aeroplane is not correctly banked for the turn, side-slip will occur, to an extent which can be calculated along the lines of I 22. If this side-slip be  $v$  the control moments necessary for steady turning are obtained from the equation

$$\left. \begin{aligned} L_0 + L_r r + L_v v &= 0 \\ N_0 + N_r r + N_v v &= 0 \end{aligned} \right\} \quad (25.1)$$

or in terms of dimensionless coefficients

$$\left. \begin{aligned} k_{l0} &= -k_{lr} k_\Omega \cos \Phi - k_{lv} \frac{v}{V_1} \\ k_{n0} &= -k_{nr} k_\Omega \cos \Phi - k_{nv} \frac{v}{V_1} \end{aligned} \right\} \quad (25.2)$$

If the turn is under-banked  $v$  will be of opposite sign to  $\Omega$ . Likewise  $k_{lv}$  is always negative and  $k_{nv}$  generally positive; hence, in an under-banked turn, aileron control will have to be applied even more powerfully

where  $C$  and  $B$  are the moments of inertia about the  $Z$  and  $Y$  axes respectively. This term represents the moment required to hold the aeroplane against the action of centrifugal force, which is greater on the outer than on the inner wing. It is negligible in normal flight, although in the spin, terms of this type may rise to primary importance.

than in a true-banked turn, in the direction to prevent the bank from increasing. A stronger yawing moment than in the banked turn is also required in the sense to prevent the turn from stopping. It will be obvious from these considerations that the application of rudder alone, with ailerons neutral, will not only cause an aeroplane to turn, but will ultimately cause it to bank into the turn and that, unless the ailerons are applied against it, the turn will in time become over-banked.

Returning to (25.1), and eliminating  $v$  we have

$$(L_v N_r - L_r N_v) \Omega \cos \Phi = L_0 N_v - N_0 L_v \quad (25.3)$$

an equation from which can be found the steady angular velocity  $\Omega$  appropriate to any combination of applied control moments. Note that if  $(L_v N_r - L_r N_v)$  is small, small applied control moments only will be required for a given steady rate of turn. If this expression is zero, steady turns of any angular velocity can continue indefinitely without applied moments, and no finite steady rate of turn is possible with any applied moments however small they may be. In this special case the equilibrium of straight flight is neutral and the steady turns must be such that the side-slip is related to the rate of turn by the equation

$$\Omega \cos \Phi = -\frac{N_r}{N_v} = -\frac{L_r}{L_v}$$

$L_r$  is always positive and  $L_v$  always negative; therefore  $v$  must be of the same sign as  $r$  in this neutral type of motion; that is to say the side-slip must be inwards towards the centre of the circular path. Again, since  $N_r$  is negative,  $N_v$  must be positive, so that steady circling without control moments can only occur on an aeroplane which is statically stable for rotations about the  $Z$  axis—for one having static directional stability as it is generally called.

**26. Ascending and Descending Steady Turns.** When an aeroplane turns steadily whilst ascending or descending, so that each portion describes a helical path about a vertical axis, the component angular velocities about the three axes, become respectively

$$\left. \begin{aligned} p &= -\Omega \sin \Theta \\ q &= \Omega \cos \Theta \sin \Phi \\ r &= \Omega \cos \Theta \cos \Phi \end{aligned} \right\} \quad (26.1)$$

where  $\Theta$  is the angle between the  $X$  axis and the horizontal, positive when the nose points upwards, and  $\Phi$  is the angle through which the aeroplane must be rolled about the  $X$  axis to bring it from the position with wing tips level to its attitude in the steady turn. The reader who is not familiar with direction cosines in solid geometry can verify these equations by first resolving the vertically downward vector of angular velocity into components  $(-\Omega \sin \Theta$  and  $\Omega \cos \Theta)$  parallel and perpendicular respectively to the  $X$  axis. The former of these is  $p$  and the latter can be again resolved into components  $q$  and  $r$ , as in (26.1).

We now assume that the symmetric angular velocity component ( $q$ ) does not appreciably influence the asymmetric moments ( $L$  and  $N$ ), and conversely that the asymmetric moments ( $p$  and  $r$ ) do not influence the symmetric moment ( $M$ ). This assumption is certainly true for very small values of  $\Theta$  and  $\Phi$ , and is probably true enough for practical purposes for most of the possible forms of unstalled flight. With this assumption, we may write for turns without sideslip

$$\left. \begin{aligned} M_0 + M_q \cdot q &= 0 \\ L_0 + L_p \cdot p + L_r \cdot r &= 0 \\ N_0 + N_p \cdot p + N_r \cdot r &= 0 \end{aligned} \right\} \quad (26.2)$$

in which the centrifugal moments mentioned in 24 are, as before, too small to be of practical importance.

Using (26.1), (26.2) becomes

$$\left. \begin{aligned} M_0 &= -\Omega M_q \cos \Theta \sin \Phi \\ L_0 &= \Omega [L_p \sin \Theta - L_r \cos \Theta \cos \Phi] \\ N_0 &= \Omega [N_p \sin \Theta - N_r \cos \Theta \cos \Phi] \end{aligned} \right\} \quad (26.3)$$

From these equations it appears that the elevator movement required for a climbing or descending turn is less than for a horizontal turn of the same bank, but that the difference is not noticeable unless  $\Theta$  is large.

Again since  $L_p$  is of opposite sign to  $L_r$ , the aileron movement required for a climbing turn will be greater, and that for a descending turn less, than for a horizontal turn, zero movement being required when  $\tan \Theta = \frac{L_r}{L_p} \cos \Phi$ . The factor  $L_r/L_p$  is generally of the order  $-1/3$ , hence with a moderate angle of bank the ailerons will be about neutral in a true-banked descending helix with  $\Theta = -18^\circ$ . In a climbing turn with  $\Theta$  of the order  $+18^\circ$  the necessary aileron movement will be about double that in a horizontal turn of the same bank. The ratio  $N_r/N_p$  is, in normal flight, of the order  $-3$ , hence it appears from the third of (26.3) that the yawing moment necessary in a steady true-banked turn is much less influenced by the angle of ascent or descent than is the rolling moment. The rudder position will however be influenced by the necessity of neutralizing yawing moments generated by the ailerons.

When side-slip occurs in climbing or descending turns its effects are similar to those discussed for horizontal turns.

## D. Small Disturbances from Straight Flight

**27. Introduction.** The behaviour of the aeroplane following a slight asymmetric disturbance from steady symmetric flight can be examined theoretically and is of considerable interest; the conclusions though strictly true for infinitesimal departures from straight flight only, are in reasonably good agreement with the actual behavior of the aeroplane

even when the departures from straight flight are considerable. The detailed analysis of infinitesimal asymmetric disturbances from steady flight is more fully worked out in Chapters V and VII, but, as with the symmetric disturbances, it is possible, knowing the result of the detailed analysis, to explain many of the principal features of the motion in a relatively simple manner by disregarding those factors which are of minor importance in respect of the aspect of the motion under consideration.

**28. The Rapid Damping of Rolling Motions.** The dominant factor in the asymmetric motions of an aeroplane in normal flight is the high negative value of the derivative  $L_p$ . This derivative defines the rolling moment ( $L$ ) which opposes any angular velocity of roll ( $p$ ) through the increase of effective incidence near the falling wing tips and the corresponding decrease near the rising tip. This moment is so large that it very rapidly checks any rate of roll which is not being maintained by some applied rolling moment and it ensures that the rate of roll in any manoeuvre will be small unless very large rolling moments are applied to the aeroplane.

To estimate the time taken by the derivative  $L_p$  to destroy any rolling motion which is not being otherwise maintained, we may safely neglect all other factors but the moment due to this derivative and the moment of inertia about the  $X$  axis, and thus write, simply

$$A \dot{p} = L_p \cdot p$$

The solution of this is

$$p = p_1 e^{-\frac{L_p}{A}t}$$

where  $p_1$  is the value of  $p$  at zero time.

A typical value of  $L_p/A$  is  $-7$  so that the rate of roll ( $p$ ) is reduced to about one half value every tenth of a second and virtually disappears in about one third of a second.

If a rolling moment  $L_0$  is suddenly applied to an aeroplane the equation of motion for the first second or thereabouts after the application is sufficiently represented by

$$A \dot{p} = L_p \cdot p + L_0$$

of which the solution, subject to the condition that  $p$  is zero at zero

time, is

$$p = -\frac{L_0}{L_p} \left( 1 - e^{-\frac{L_p}{A}t} \right)$$

Thus, within a third of a second, the aeroplane is rolling with that angular velocity for which the opposing rolling moment ( $L_p \cdot p$ ) is equal to the applied rolling moment. These numerical values explain certain well known peculiarities of aeroplane flight very clearly. Thus, on applying the ailerons, the aeroplane appears to start rolling just as though it

had no moment of inertia, and for an interval of a second or so rolls at a rate which is directly proportional to aileron movement. Subsequently the motion is complicated by other moments which arise from the fact that a rolling motion cannot persist for long without causing either side-slip or yawing rotation, either of which themselves generate a rolling moment which modifies the motion. Again an aeroplane flying through disturbed air on a windy day experiences sudden rolling motions or *bumps* which will be familiar to everyone who has flown in bad weather. This happens whenever the aeroplane flies into air which has a vertical velocity gradient across the wing span, or which is rotating about an axis parallel to the direction of motion. These *bumps* are of course due to the aeroplane taking up the mean angular velocity of the air into which it flies with a suddenness which is indicated by the high negative value of  $L_p/A$ .

Since the influence of the moment of inertia ( $A$ ) upon the motion of an aeroplane in normal flight is confined to about one fifth of a second following any change in the applied moments, it is practicable to neglect this moment of inertia altogether when studying motions which develop relatively slowly.

**29. The Slow Spiral Motion.** Another interesting feature of the disturbed asymmetric motion of an aeroplane can be studied in a simple manner by returning to (25.3), from which it was deduced that, when  $L_r N_r - L_v N_v$  is zero, steady circling flight is possible without applied control moments, provided the ratio of side-slip to rate of turn has the value

$$-\frac{N_r}{N_v} \quad \text{or} \quad -\frac{L_r}{L_v}$$

In any normal aeroplane of the present day  $L_v N_r - L_r N_v$  is very nearly zero, hence aeroplanes can fly steadily in a circle with the lateral controls nearly in the neutral positions.

In general, of course,  $L_v N_r - L_r N_v$  is not exactly zero and therefore the circling motion with controls neutral is not quite steady but the curvature of the path and the angle of bank tend to increase or decrease slowly, according to the sign of this expression. The more detailed calculations carried through in later chapters with typical numerical values, indicate the factors which can be ignored in a simplified study of this motion. Thus, if the aeroplane is not statically unstable ( $N_v$  not negative) a fair approximation, to the exponential term which governs this motion can be obtained by neglecting entirely the moments of inertia of the aeroplane, the side-force due to side-slip, and that part of the acceleration perpendicular to the plane of symmetry which is due to the rate of change of side-slip ( $\dot{\psi}$ ). We suppose in other words that both the radius of the spiral path and the angle of bank change so slowly that the moments necessary to maintain the angular accelerations are negligible, and that the acceleration can, with sufficient accuracy be taken to be simply

the centripital acceleration ( $V_1 \Omega$ ) acting horizontally. Using small  $\varphi$  to indicate that the angle of bank is small and equating applied force perpendicular to the plane of symmetry to mass acceleration in this direction we have, on these assumptions

$$mg \sin \varphi = m V_1 \Omega \cos \varphi = m V_1 r \cos^2 \varphi$$

$$\text{or } \varphi \text{ being small} \quad g \varphi = V_1 r \quad (29.1)$$

The motion therefore must satisfy the following three simultaneous equations:

$$\left. \begin{aligned} L_p p + L_r r + L_v v &= 0 \\ N_p p + N_r r + N_v v &= 0 \\ g p - V_1 \dot{r} &= 0 \end{aligned} \right\} \quad (29.2)$$

Where the third equation is obtained by differentiating (29.1) and noticing that  $\dot{\varphi} = p$ .

The solution is of the form

$$p = p_1 e^{\lambda t} \quad r = r_1 e^{\lambda t} \quad v = v_1 e^{\lambda t}$$

where  $p_1, r_1, v_1, \lambda$  are constants.

Substituting these values in (29.2) and eliminating  $p_1, r_1, v_1$  gives

$$\lambda = - \frac{g}{V_1} \frac{L_v N_r - L_r N_v}{L_v N_p - L_p N_v}$$

The value of this expression is unchanged by substituting the dimensionless coefficient of the derivatives for the derivatives themselves, and of these only  $L_v$  and  $N_v$  vary much from one aeroplane to another. Hence, inserting typical values for the other derivatives taken from Fig. 42, III 38, at cruising incidence, we have

$$\lambda = - \frac{g}{V_1} \frac{(-.03)k_{lv} - (.11)k_{nv}}{(-.04)k_{lv} - (-.43)k_{nv}} \quad (29.3)$$

The value of  $k_{lv}$  for the particular aeroplane of Fig. 42 was approximately  $-0.05$ , hence this aeroplane will be spirally neutral if

$$k_{nv} = - \frac{.03}{.11} (-.05) = .0136$$

which is about the value actually shown in Fig. 42. If, for the sake of example, we take a somewhat smaller value for  $k_{nv}$ , say 0.010 we have

$$\lambda = - \frac{g}{V_1} \frac{.0015 - .0011}{.0020 + .0043} = - .063 \frac{g}{V_1}$$

At a cruising speed of 100 miles per hour  $V_1/g = 4.6$  seconds and therefore  $\lambda = -0.014$ .

If this aeroplane is set to turn steadily with angle of bank  $\varphi_1$ , and appropriate side-slip, the controls will be very nearly neutral and if they are then placed exactly neutral it will begin to recover an even keel according to the equation

$$\varphi = \varphi_1 e^{-.014 t}$$

The recovery will thus be very gradual, the bank being reduced to one half value in, approximately, 50 seconds.



If, on the other hand,  $k_{nv}$  is greater than 0.135, the banked turn will tend to increase, but unless the value of  $k_{nv}$  is unusually large this increase will be so slow that the instability will scarcely be noticeable unless the aeroplane is left entirely to itself for a considerable time.

It is clear from the form of (29.3) that the larger  $k_{lv}$ , that is to say the greater the dihedral angle, the greater can be the directional static stability without spiral instability developing. It is of interest to see what happens when  $k_{lv}$  is zero, that is, approximately, when the wings have no dihedral angle. In this case,

$$\lambda = -\frac{g}{V_1} \frac{-.11}{.43} = .25 \frac{g}{V_1}$$

or at 100 miles per hour  $\lambda = 0.055$

and the bank is approximately doubled every 13 seconds.

In general it appears that large dihedral angle and low directional static stability are favourable to spiral stability.

**30. More Accurate Estimate of the Spiral Motion.** A more accurate estimate of the value of  $\lambda$ , which is identical with the first approximation obtained in VII 29 as the result of the more detailed analysis of Chapter VII, is obtained by including the moment of inertia ( $C$ ) about the  $Z$  axis and the side-force  $Y_v \cdot v$ , but still neglecting the moment of inertia ( $A$ ) about the  $X$  axis and that part ( $\dot{v}$ ) of the lateral acceleration which is due to rate of changes of side-slip. The equations of motion now become

$$\begin{aligned} L_p p + L_r r + L_v v &= 0 \\ N_p p + N_r r - C \dot{r} + N_v v &= 0 \\ m g p - m V_1 \dot{r} + Y_v \dot{v} &= 0 \end{aligned}$$

Treating these three simultaneous equations in a similar manner to those of (29.2) we obtain a quadratic for  $\lambda$  in which, however, the term containing  $\lambda^2$  is negligibly small compared with the other two terms. Neglecting this small term leaves the following value for  $\lambda$

$$\lambda = -\frac{g}{V_1} \frac{L_v N_r - L_r N_v}{L_v N_p - L_p N_v - \frac{Y_v}{m V_1} (L_p N_r - L_r N_p) - \frac{g}{V_1} C L_v}$$

This more accurate expression for  $\lambda$  also vanishes when  $L_v N_r = L_r N_v$  as it obviously must do from the fact that in these circumstances the turn can continue indefinitely without either increasing or decreasing.

It appears from Table 5, VII 29, that, in the examples which were correctly worked out, this approximation agreed with the correct value within about 10 per cent, which is probably near enough for all practical purposes, particularly as the critical condition for neutral equilibrium is given correctly by the approximate formula.

**31. The Oscillation of a Statically Stable Aeroplane.** The more complete analysis of Chapters V and VII shows that, in addition to the

quickly and slowly developing modes of motion which we have been considering, the solutions of the asymmetric equations of motion contain a mode which generally takes the form of a damped oscillation with a period of some 5 or 6 seconds. This oscillation involves rolling, yawing and side-slipping in comparable proportions and, except in special circumstances, it is not easy to find any simple expressions for either the period or the damping, which will do more than indicate the order of their magnitude. The detailed analysis of Chapter VII, based on typical numerical values, shows that all the derivatives—with the exception of  $Y_p$  and  $Y_r$  which are never important—have appreciable influences upon this motion and that any attempt to represent the damping factor in the oscillation by a single general formula leads to excessive complications. In the present simplified discussion we shall therefore confine ourselves to a consideration of the nature of this oscillation and of the factors which mainly control it, without attempting to evolve a simple working formula by which it can be represented.

Imagine first an aeroplane pivoted about the  $Z$  axis, which is itself held fixed perpendicular to the relative wind: an aeroplane in fact arranged as a weather-cock. When the inclination of the plane of symmetry to the direction of a wind of strength  $V_1$  is  $\psi$ , then the side-slip velocity ( $v$ ) relative to the air is

$$v = -V_1 \psi \quad (31.1)$$

In conformity with the system of notation with which we are now familiar, write  $r$  for the angular velocity about the fixed  $Z$  axis, so that  $r = \dot{\psi}$  and let  $C$  be the moment of inertia about the  $Z$  axis.

The equation of the motion when the aeroplane is disturbed from the attitude in which  $\psi$  is zero is

$$N_v v + N_r r = C \dot{r}$$

or

$$-N_v V_1 \psi + N_r \dot{\psi} = C \dot{\psi}$$

Treating  $V_1$  as constant the solution of the equation is of the form

$$\psi = \psi_1 e^{\lambda t}$$

where  $\psi_1$  and  $\lambda$  are constants and  $\lambda$  is a root of the equation

$$\lambda^2 - \frac{N_r}{C} \lambda + \frac{N_v V_1}{C} = 0 \quad (31.2)$$

As an illustration we shall choose, for typical values of the constants in this equation, numbers which correspond with the values used in the detailed illustration, which is worked out in Chapter VII<sup>1</sup>.

With these values (31.2) becomes

$$\lambda^2 + 0.34 \lambda + 1.53 = 0$$

the roots of which are

$$-0.17 \pm 1.22 i$$

<sup>1</sup> The actual numbers employed will not be the same as those of Table 1 of Chapter VII because in that chapter the dimensionless system of calculation is employed.

The pivotted aeroplane therefore oscillates according to the equation

$$\psi = \psi_1 e^{-.17 t} \cos(1.22 t + \epsilon)$$

where the amplitude, defined by  $\psi_1$ , and the phase, defined by  $\epsilon$  are dependent on the initial conditions.

When an aeroplane with appreciable static (or weather-cock) directional stability ( $N_v$  positive) is disturbed from steady free flight by, for example, a rotation about the  $Z$  axis, a yawing oscillation of a type similar to that indicated by the above equation is set up, but the oscillation is complicated by the fact that the  $Z$  axis is not fixed either in position or direction. Both the yawing rotations and the side-slips occurring in this oscillation generate rolling moments, through the intermediary of the derivatives  $L_r$  and  $L_v$  respectively, so that the aeroplane rolls as well as yaws; further the whole aeroplane can be accelerated from side to side and so the side-slip cannot be represented simply by  $\psi V_1$  as in (31.1).

In a normal aeroplane with adequate directional static stability, the angles of side-slip ( $\beta$ ), roll ( $\varphi$ ) and yaw ( $\psi$ ) in the oscillation are all of the same order of magnitude, the period of the oscillation does not differ greatly from that of the simple oscillation of (31.2), but the damping is considerably greater. To illustrate these points the damping and period obtained by the simple equation are compared in Table 2 with the values obtained by the more precise methods of Chapter VII. The comparison is with the "neutral" and "unstable" cases at  $3^\circ$  incidence in Tables 3 and 4 in Chapter VII<sup>1</sup>.

TABLE 2. Comparison between damping and period of an oscillation with fixed  $Z$  axis and oscillation in free flight. (Aeroplane directionally stable.)

	Period: Seconds	Time to reduce amplitude by one-half: Seconds
Fixed $Z$ axis . . . . .	5.1	4.1
Free flight (Zero dihedral angle) . . . . .	5.0	2.1
Free flight (With dihedral angle) . . . . .	4.5	2.3

The agreement as regards period is remarkably close for the aeroplane without dihedral angle and the simple calculation gives a period of the correct order of magnitude even when the aeroplane has a dihedral angle. The true damping is, however, about twice as great as that of the simple oscillation.

<sup>1</sup> The words "neutral" and "unstable" refer to the slowly developing mode of motion and not to the oscillation under discussion; they are here used merely to identify the appropriate parts of Tables 3 and 4.

**32. The Oscillation of a Statically Neutral Aeroplane.** If the static directional stability, as defined by  $N_v$ , becomes small, zero, or negative, the above method of obtaining some insight into the nature of the asymmetric oscillation becomes meaningless. When  $N_v$  is zero the aeroplane pivotted on a fixed  $Z$  axis, would be in neutral equilibrium, while with  $N_v$  negative it would be unstable. The oscillation of the free aeroplane does not, however, disappear when  $N_v$  is zero, nor does the free aeroplane become unstable when this quantity is negative, unless the negative value is sufficiently large. To obtain some insight into the nature of the motion when  $N_v$  is zero, consider the hypothetical case

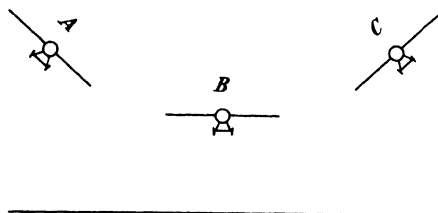


Fig. 52.

in which  $N_p$  is also zero, so that neither rolling nor side-slip can cause any yawing moment. If the aeroplane is now supposed to be rolled through an angle  $\varphi$  from steady flight, it will begin to side-slip and the side-slip will, through the intermediary of the derivative  $L_v$ , exert rolling moments tending to raise the

wing towards which the slip is occurring; and since there are no yawing moments the  $X$  axis will remain fixed in direction.

The aeroplane, seen from behind, will thus slip from position  $A$  to position  $B$ , and be carried by its momentum into position  $C$ , from which it will slip back again towards  $B$ . During the slipping, however, the side-force  $Y_v \cdot v$  will continually oppose the motion so that the oscillation will eventually be damped out. The equations controlling this motion are as follows:

$$\left. \begin{aligned} L_p p + L_v v &= A \dot{p} \\ mg\varphi + Y_v v &= m v \end{aligned} \right\} \quad (32.1)$$

For the reasons given in 28 we may, as a first approximation, neglect the term  $A \dot{p}$  and, if the second equation of (32.1) be differentiated with respect to time, we have

$$\left. \begin{aligned} L_p p + L_v v &= 0 \\ mgp - m\ddot{v} + Y_v \dot{v} &= 0 \end{aligned} \right\}$$

writing  $p = p_1 e^{\lambda t}$ ,  $v = v_1 e^{\lambda t}$  gives

$$\left. \begin{aligned} L_p p_1 + L_v v_1 &= 0 \\ mgp_1 + (-\lambda^2 + Y_v \lambda) v_1 &= 0 \end{aligned} \right\}$$

Eliminating the ratio  $p_1/v_1$  gives

$$\lambda^2 - Y_v \lambda + g \frac{L_v}{L_p} = 0$$

Taking values corresponding to the "stable" case ( $N_v = 0$ ) in Table 1, Chapter VII, this becomes,

$$\lambda^2 + 0.17\lambda + 0.15$$

And the solution can be written

$$\varphi = \varphi_1 e^{-.085t} \cos (.38 t + \varepsilon)$$

This represents an oscillation of some 17 seconds period which takes 8.2 seconds to reduce to half amplitude.

This simple calculation does not, of course, represent the facts unless  $N_p$  is zero, which it is very unlikely to be. Figure 42, III 38, shows in fact that, in normal flight,  $N_p$  is negative, and detailed calculations show that its influence on the motion is materially to increase the damping and reduce the period. Thus the calculations of Chapter VII give, for the true oscillation with  $N_p$  zero, a period of 10 seconds and a reduction to half amplitude in 3 seconds, so that the simple calculation has done no more than indicate the nature of the oscillation.

**33. The Oscillation of a Statically Unstable Aeroplane.** If  $N_v$  becomes negative and the aeroplane therefore statically unstable, the motion becomes exceedingly difficult to follow by any simple argument. The effect, as shown by detailed calculation, is that the damping of the oscillation decreases and the period increases as the numerical value of the negative  $N_r$  increases, until eventually the oscillation becomes undamped; a small further increase of the negative  $N_r$  causes the amplitude of the oscillation to grow very rapidly and still further increase causes the oscillation to break up into two exponential terms, one of which has a large positive exponent and corresponds to rotation which increases continually in one direction with great rapidity. The precise values of  $-N_r$  at which these changes occur depend of course upon the values of the other derivatives, and the only one of these over which the designer has much control is  $L_r$ , which depends mainly upon the dihedral angle between the wings. It is shown in VII 34 that the negative value of  $N_r$  necessary to cause the oscillation to persist indefinitely is nearly proportional to  $L_r$  and that with reasonable values of  $L_p$  the margin by which  $N_v$  can be on the negative side of zero is not great.

**34. The Two Possible Forms of Instability.** Comparing these conclusions with those of 29 it will be observed that the aeroplane can become unstable laterally in two ways. If the directional *static* stability is too great, free flight will become *spirally* unstable, whereas if *static* instability is too great an increasing oscillation will develop. The margin between these two forms of instability depends directly on the dihedral angle, being greater the greater the angle. Both forms of instability must be avoided if the aeroplane is to be left entirely to itself, but if it is to be continually controlled, a slight spiral instability is relatively unimportant. On the other hand the undamped oscillation which arises when the aeroplane has too great a static instability is probably very detrimental to comfortable flying; indeed, it is probable that an adequate amount

of damping for this oscillation is necessary for comfortable flying in bumpy weather, but this is a matter which would repay further investigation.

### E. The Stalled Aeroplane

**35. The Stalled Aeroplane—Symmetric Motion.** The simplified discussions of the present chapter have related exclusively to normal flight, that is to say, to flight at speeds considerably above the stalling speed, and, therefore, to angles of incidence well below the stalling incidence. Subject to this condition, the general characteristics of the motions remain the same for all speeds and incidences, but if the speed drops to something near the stalling speed and the incidence rises to near or above the stalling incidence, profound changes occur in all the derivatives and the character of the motion following any disturbance or application of the controls entirely changes. The behaviour of the aeroplane now becomes much more difficult to follow by simple arguments such as are used in the present chapter, and although considerable research has been done upon aeroplanes flying in this state, the motions are so complicated and differ so much from one aeroplane to another that they cannot as yet be said to be thoroughly understood, although a good deal is known about the causes of the principal characteristics of many of them. Numerical solutions of the motions, based on the data of Chapters II and III, are worked out in Chapters VI and VII. And we shall here give no more than a brief sketch of some of the more important factors governing these motions.

The principal change which occurs to the symmetric forces when the aeroplane stalls is that the resultant force upon it ceases to increase with incidence and may even fall as the incidence increases; the direction of this force changes from nearly perpendicular to the direction of motion to nearly perpendicular to the wing chord, and since the incidence is high this implies a large increase of drag. Further, the line of action of this resultant moves backwards until it cuts the wing chord at a point not far in front of its middle point.

A result of these changes was shown in II 28 to be that the static stability of the aeroplane becomes very great and it becomes impossible, upon an aeroplane of conventional type, to maintain equilibrium about the axis of pitch when the incidence rises much above the stall. Steady stalled flight is therefore, for such aeroplanes, confined to a range of incidences between say  $18^\circ$  and  $25^\circ$ , and if the incidence temporarily rises above the higher limiting value, it must very quickly fall again. When flying stalled within this range the pilot has some control over incidence, but owing to the greatly increased static stability, he has, when he requires to produce a given incidence change, to move his elevator much more roughly than in normal flight. Moreover, since he

cannot, by changing incidence, make any large change in the magnitude of the resultant air-reaction, he has no direct control over vertical acceleration and cannot immediately cause any appreciable change in his vertical velocity. All that he is able to do is to alter the direction of the resultant air-reaction by altering the attitude of his wing.

In a steady stalled glide with engine off, the resultant air-reaction must be vertical and, therefore, the wing chord must be nearly horizontal (see Fig. 10, I 7). If, when the aeroplane is in such a glide, the stick is thrust forward, the nose will be depressed and the resultant air-reaction, which remains nearly perpendicular to the wing chord, will be inclined forward and the speed will begin to increase; this increased speed will cause the resultant force to increase and the consequent upward acceleration will reduce the downward speed of the aeroplane. If the operation is correctly timed, a landing without shock from a stalled glide is possible, but between the moment when the stick is first pushed forward and the moment when the vertical velocity is reduced to zero, a considerable time must elapse and a large loss of height (generally more than 100 feet) is inevitable. Landing from a stalled glide is therefore a matter of great difficulty and at present is rarely attempted.

Small symmetric disturbances of the stalled aeroplane from straight flight can, of course, be worked out by the methods of Chapters V and VI, provided that the values of the derivatives are all known; but when the incidence is near the critical angle there is still much uncertainty with regard particularly to the influence of the rate of pitch ( $q$ ) upon the pitching moment and resultant force. It is indeed not yet certain whether the variations of the forces which act upon the aeroplane when near the critical incidence can be represented adequately by simple derivatives of the kind used in this and later chapters, for there is some evidence that the incidence at which the stall occurs may be influenced by the previous motion of the aeroplane. This whole matter is at present the subject of research and it would be unprofitable to discuss it further in the present chapter.

**36. The Stalled Aeroplane—Asymmetric Motion.** The asymmetric motions of a stalled aeroplane are even more complicated than the symmetric motions, but they have been more thoroughly studied on account of the importance of designing aeroplanes which do not easily develop the involuntary spinning motion which has caused so many disasters. A glance at Fig. 42, III 38, will show that all the derivatives change their values drastically, either at or shortly beyond the stall. The most important change is the reduction of the derivative,  $L_p$ , from the large negative value which it has in normal flight, to zero, or even to a positive value. This change removes the predominating factor which prevents the occurrence of rapid rolling motions in normal flight and, as a consequence, the most noticeable characteristic of stalled flight

is the high angular velocity of roll which can occur. It has been observed in III 37 that when a stalled aeroplane is rolled steadily about an axis through the c.g. and parallel to the relative wind, it may, and generally does, experience a rolling moment of the same sign as the direction of roll [ $L_p$ , positive when referred to wind axes (see III 2)]. Such an aeroplane, when pivoted about a fixed axis parallel to the wind, is in unstable equilibrium and, once rotation starts in either sense it will continually increase until an angular velocity is reached at which the rolling moment is again zero. Such a property clearly suggests instability in free flight and although it has lately been shown that complete stability in free flight is compatible with a very small positive value of  $L_p$ , it is generally true to say that an appreciable positive value of  $L_p$  leads to instability of a peculiarly violent kind.

Another important feature of stalled flight is the very great rise in the numerical value of the derivative  $L_v$  which occurs as the stalling angle is passed (see Fig. 42, III 38). This, coupled with the high value of  $L_r$  which occurs when the incidence does not greatly exceed the stalling incidence, makes the rolling motion of the aeroplane, flying near the critical stalling incidence, very sensitive to any yawing motion which may occur. For when the aeroplane yaws—that is, rotates about the  $Z$  axis—a side-slip occurs towards the advancing wing and large moments are generated which tend to raise the advancing wing.

The rolling of stalled aeroplanes can therefore be very powerfully controlled by the rudder provided the rudder has sufficient power to yaw the aeroplane in any desired direction, but it does not follow that it is easy to control a stalled aeroplane with any degree of precision by the use of the rudder alone, for the destabilizing effect of the derivative  $L_p$  causes any oscillation which may be started to increase rapidly in amplitude and a negatively damped oscillation of this kind is always difficult to control. Nevertheless it has been amply demonstrated both theoretically and practically that the provision of adequate rudder power is one of the essential factors of good control when in the stalled state.

This same property of extreme sensitivity to yawing motion is the primary cause of the failure of conventional ailerons to control the motions of a stalled aeroplane for they, as seen in III 41, exert not only the rolling moment which is required from them, but a yawing moment retarding the wing which they are attempting to raise. This yawing moment generates yawing rotations and side-slips both of which ultimately cause rolling moments which eventually overpower the direct aileron action.

Another consequence of sensitivity to yawing motion is that when, as shown by the full line in Fig. 42, III 38, the derivative  $N_p$  becomes large and positive after stalling, any rolling motion ( $p$ ) which may be occurring, of itself generates a yawing motion, which in turn causes



rolling moments in the sense to increase the original rolling motion still further. A powerful destabilizing term may thus be added to the equations of motion.

The combination of a violent instability, involving rapid rolling and yawing motions, with the failure of aileron control, renders a stalled aeroplane of normal design almost uncontrollable except in the hands of very experienced pilots and makes anything like controlled manoeuvres impossible. The cure, indicated by detailed study of the motion on the lines of Chapter VII, is to prevent the wing tips from stalling until incidences have been reached which are considerably beyond those which can be steadily maintained by full use of the elevators. This can be done by the use of the Handley Page wing tip slot mentioned in III 37, or it is possible that a partial success sufficient for many practical purposes can be achieved without slots by careful shaping of wing tips and a delicate adjustment of the derivative which depends upon fin and rudder area, but into these ramifications of modern research it is not proposed to enter since no final conclusions have yet been reached.

The lateral stability of the stalled aeroplane is discussed in more detail in VII 24 *et. seq.* where it is shown that the problem may be complicated by the fact that the moments acting upon the aeroplane depend upon the history of the motion as well as upon the motion at the instant in question. The difference between some of the derivatives, particularly  $N_p$  as obtained by oscillation and continuous rotation experiments respectively, is probably due to this cause, and the motion of the aeroplane may therefore have to be regarded as controlled by different sets of derivatives according as to whether it is oscillatory or involves continuous rotation in one direction.

## CHAPTER V

# THE EQUATIONS OF MOTION WITH SOLUTIONS FOR SMALL DISTURBANCES FROM STEADY SYMMETRIC FLIGHT

## A. Axes, Symbols, and Equations of Motion

1. Axes. The general equations representing the motion of an aeroplane are usually referred to axes which are fixed in the aeroplane and therefore move with it; we shall choose these axes as follows<sup>1</sup>:

The origin  $O$  lies on the centre of gravity of the aeroplane;  $OX$ ,  $OZ$  lie in the plane of symmetry and  $OY$  is perpendicular to it.  $OX$  lies roughly along the body, but its exact direction will be chosen to suit the convenience of each specific problem.

<sup>1</sup> The reader will find this section easier to follow if he provides himself with a small model aeroplane upon which he can visualize the axes and the various component rotations.

The names of these axes will be:—

$OX$  Longitudinal axis  
 $OY$  Transverse axis  
 $OZ$  Normal axis.

The positive directions are:—

$OX$  Forward  
 $OY$  To starboard  
 $OZ$  Towards the undercarriage of the aeroplane.

The axes will be *right handed*; that is to say the positive sense of a component rotation or couple about any axis will be determined by reference to a right handed screw, when facing the positive direction of the axis.

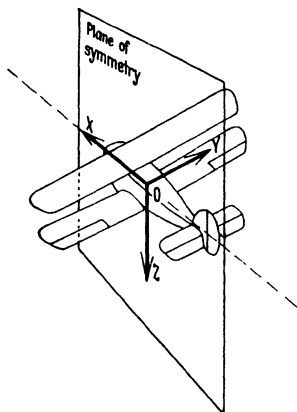


Fig. 53. Plane of symmetry and axes.

**2. Orientation.** The orientation of the aeroplane in space will be specified by three angular coordinates  $\Theta, \Phi, \Psi$ . When these are all zero  $OZ$  is vertical,  $OX$  and  $OY$  are horizontal and  $OX$  points in some specified direction in the horizontal plane. Any other orientation of the aeroplane is then reached by three consecutive rotations, of which the sequence is important.

Rotation (1). About  $OZ$ , through angle  $\Psi$ , until  $OX$  lies in the vertical plane containing its ultimate position.

Rotation (2). About  $OY$ , through angle  $\Theta$ , until  $OX$  points in its final direction.

Rotation (3). About  $OX$ , through angle  $\Phi$ , until aeroplane has the required orientation.

Using terms current in air navigation the foregoing precise statement may be loosely interpreted as follows:—

Zero orientation corresponds to horizontal flight on some assigned compass bearing with wings level. In order to reach the position which it is desired to specify, the aeroplane is:—

*First.* Rotated in azimuth to the required compass course.

*Second.* Pitched to the desired climbing or diving angle.

*Third.* Rolled to the desired angle of bank.

The positive senses of these rotations are:—

Azimuth rotation to starboard.

Pitch upwards.

Roll to starboard (starboard wing depressed).

This more picturesque statement is precise only when  $OX$  happens to coincide with the direction of motion, but it may serve to give a clearer idea of the processes imagined in the definition of  $\Theta, \Phi, \Psi$ .

**3. Symbols.** Symbols which will be used to represent the components of the velocity of the centre of gravity of the aeroplane and of its angular

velocity, together with the components of the aerodynamic forces and couples, and the moments and products of inertia of the aeroplane are collected below:—

Velocity and Force Components.

Axis . . . . .	$X$	$Y$	$Z$
Velocity . . . . .	$U$	$V$	$W$
Force . . . . .	$X$	$Y$	$Z$
Name . . . . .	Longitudinal	Lateral	Normal
Positive Direction . . . . .	Forward	Starboard	Downwards

Angular Velocity and Moment Components.

Axis . . . . .	$X$	$Y$	$Z$
Angular velocity . . .	$P$	$Q$	$R$
Moment . . . . .	$L$	$M$	$N$
Name . . . . .	Rolling	Pitching	Yawing
Positive Sense . . . . .	Starboard wing down	Nose up	Nose to Starboard

**4. Effect of Gravity.** In addition to the air-reaction upon the aeroplane the gravitational field exerts a force through the c.g. whose components along the axes are found by multiplying the weight by the direction cosines of the vertical. If  $m$  is the mass of the aeroplane and  $g$  the strength of the gravitational field these components are:—

$$\begin{aligned} & -mg \sin \Theta \quad \text{along } OX \\ & mg \cos \Theta \sin \Phi \quad \text{along } OY \\ & mg \cos \Theta \cos \Phi \quad \text{along } OZ. \end{aligned}$$

Moments and Products of Inertia.

Axis . . . . .	$X$	$Y$	$Z$
Moment of Inertia . .	$A$	$B$	$C$
Product of Inertia . .	$D$	$E$	$F$
Moment of momentum	$h_1$	$h_2$	$h_3$

**5. The Equations of Motion.** Equating mass acceleration along each axis to the appropriate component of the applied force, and equating rate of change of moment of momentum about each axis to the appropriate applied moment, we obtain six equations which must be satisfied throughout the motion of the aeroplane.

$$\left. \begin{aligned} m [\dot{U} - VR + WQ] &= X - mg \sin \Theta \\ m [\dot{V} - WP + UR] &= Y + mg \cos \Theta \sin \Phi \\ m [\dot{W} - UQ + VP] &= Z + mg \cos \Theta \cos \Phi \\ h_1 - h_2 R + h_3 Q &= L \\ h_2 - h_3 P + h_1 R &= M \\ h_3 - h_1 Q + h_2 P &= N \end{aligned} \right\} \quad (5.1)$$

where  $h_1, h_2, h_3$ , are given by the following equations:—

$$\left. \begin{aligned} h_1 &= AP - FQ - ER \\ h_2 &= BQ - DR - FP \\ h_3 &= CR - EP - DQ \end{aligned} \right\} \quad (5.2)$$

#### 6. Dependence of the Air-Reactions on the Velocity Components.

Given the shape of the aeroplane and the properties of the air through which it moves the air-reactions  $X, Y, Z, L, M, N$ , depend upon the motion of the aeroplane relative to the air; that is to say upon the six variables,  $U, V, W, P, Q, R$ , and their rates of change with respect to time. In practice, the principal difficulty lies in determining the relationships between  $X, Y, \dots$  and  $U, V, \dots$  but even could these relationships be exactly determined the solution of the equations, in any general form, becomes immensely complicated and drastic approximations and restrictions of generality have to be made before solutions can be obtained in a form sufficiently simple for practical use.

The first approximation which is always made before attempting to handle the equations is to neglect, with one exception, any dependence of the reactions on the rates of change of the variables  $U, V, \dots$ . It is assumed, in fact, that the reactions depend solely upon the instantaneous motion of the aeroplane and not upon the rate at which the motion is changing, or upon the history of the motion. This assumption cannot be exactly true. It is now known, for example, that when the incidence of the wings changes suddenly from one steady value to another, the lift approaches asymptotically to the steady value appropriate to the new incidence and does not become sensibly constant until the aeroplane has moved through a distance of the order of ten wing chord lengths from its position when the change occurred. Assuming, for example, a chord of 7 feet and a speed of 100 miles an hour, the time required to travel ten chords is of the order 0.5 second, so that oscillations or other motions involving important changes of incidence in times considerably less than half a second cannot be accurately calculated on the assumption that the air-reactions depend only upon the instantaneous values of the velocities.

Considerably more research than has yet been done will be required before effects due to this cause can be incorporated into calculations of aeroplane movements and we shall ignore them in the following calculations. The reader should, however, bear in mind the fact that those parts of the solutions which involve important changes of incidence while the aeroplane travels only one or two chord lengths may, on this account, give a somewhat inaccurate statement of the true motion. This warning is particularly important when dealing with flight conditions near the stalling angle, where such information as is available indicates that the dependence of the air-reaction upon the history of the motion may be more marked than in normal flight.

**7. Influence of  $\dot{W}$  on  $M$ .** One exception must, however, be made to the rule that the instantaneous values only of the velocity components will be held to influence the air-reactions. It was observed in II 40 that the rate of change of incidence influences the pitching moment on account, apparently, of the time lag between the generation of downwash by the wings and the effect of that downwash on the tail. Now  $U$  and  $W$  are functions of incidence and hence, if we are to introduce this effect into the equations, terms representing the effects of  $\dot{U}$  and  $\dot{W}$  upon  $M$  must be retained. In those circumstances which we shall choose for analysis the effect of  $\dot{U}$  upon rate of change of incidence will be small and therefore the only term which will be retained to represent this effect will be the term representing the effect of  $\dot{W}$  upon  $M$ .

**8. Step-by-Step Methods of Solution.** Though the general solution of the equations, even with the approximation discussed above, is too complicated to have much practical value, it is practicable, though at the expense of great labour, to reach an approximate solution for any particular set of initial conditions, by a method known as step-by-step integration. In this method the aeroplane is supposed at zero time, to be moving with certain specified values of  $U, V, W, P, Q, R$  and the values of the air-reaction  $X, Y, Z, L, M, N$  appropriate to this motion are then computed and inserted in the equations; the instantaneous values of  $\dot{U}, \dot{V}, \dot{W}, \dot{P}, \dot{Q}, \dot{R}$  are thus obtained. The changes in  $U, V \dots$  in some chosen small time interval can now be computed, on the assumption that  $\dot{U}, \dot{V} \dots$  remain constant during this interval. The new values of  $U, V \dots$  at the end of the interval are then used as the initial values for the next interval and the process repeated indefinitely.

If the time intervals chosen for this operation are sufficiently small the process can be given any degree of accuracy required, but it is obviously very laborious and, when completed, relates solely to the chosen initial conditions. It is, therefore, useful only when a specific problem is to be attacked and cannot be used to give a general survey of possible types of motion unless numerous calculations are made, which start from systematically varied initial conditions. Except by the expenditure of very great labour the method cannot, therefore, be made to take the place of the more general solution shortly to be discussed, though it may be useful in certain circumstances in which the latter becomes impracticable.

Step-by-step computations, using the full equations of motion, have been made by several investigators, with the object of following the descent of an aeroplane from steady stalled flight into the spin (Refs. 1 and 2). Each separate calculation of this type required months of computation and in most cases no more than one or two initial conditions have been attempted. The practical value of the results has been

severely limited by lack of knowledge as to the relationship between the air-reactions and the aeroplane's motion when all the components  $U$ ,  $V$ ,  $W$ ,  $P$ ,  $Q$ ,  $R$  are large.

An extensive series of step-by-step computations on the restricted problem presented by moderately small lateral disturbances of an aeroplane from steady straight flight have also been made (Ref. 3) in order to investigate the reasons for the difficulty of controlling a stalled aeroplane. This particular problem is, as will be seen, susceptible to general treatment, provided that disturbances are infinitesimal, but the step-by-step method was used to carry the investigation into regions where, although the majority of second order terms were negligible, certain of the moments were non-linear functions of the disturbances.

Step-by-step solutions of the equations, though they may have important practical applications, are of no great theoretical interest, since they merely require careful systematization on obvious lines. We shall not discuss them further, but proceed to the study of the general solutions which become practicable when the complication is reduced by restriction to certain relatively simple types of motion.

**9. Steady Motions.** Very great simplifications result when all dotted symbols are omitted from the equations so that the motion which they represent is steady. Steady motion, since it implies that the attitude of the aeroplane to the vertical shall not change, is necessarily of a spiral or helical nature. Steady motions at the incidences of normal flight have been discussed in IV 23 to 27 whilst the spin which is a steady helical motion with high wing incidence is considered in Chapter VIII.

## B. Small Disturbances from Steady Symmetric Flight

**10. Historical.** The solutions of the equations of motion when the movements of the aeroplane are limited to infinitesimal disturbances of a symmetrical aeroplane from steady straight symmetric flight have been extensively studied by many investigators, beginning about the year 1900 with Lanchester (Ref. 4), who first surveyed the ground, using unconventional mathematical methods, which were, however, sufficiently powerful to reveal many of the broad conclusions now used in practical aeronautics<sup>1</sup>. Later Bryan (Ref. 5) developed the solutions along the more conventional mathematical lines which are generally employed at the present time and which will be discussed in the present chapter. Bryan showed how the solutions could be made to depend on a number of experimentally ascertained constants or *derivatives*, as they will be called, which define the aerodynamic properties of the aeroplane. About the year 1912, Bairstow (Ref. 6) and others, at the National Physical Laboratory, developed the experimental technique necessary

<sup>1</sup> A discussion on the lines of Lanchester's methods will be found in Chapter IV.

to determine these derivatives and showed how the essential features of practical interest could be extracted from the rather elaborate solutions which arise, even in these restricted circumstances. In 1920 Bairstow published (Ref. 7) a comprehensive treatise on the subject in which he extended the solutions to more complicated motions and to the movements of airships. Since that date numerous treatises have been written, dealing mainly with the detailed application of the equations to practical problems, but apart from a general adoption of a dimensionless form for the equations, which was originally proposed by H. Glauert (Ref. 8) in 1927, the mathematical side of the matter has undergone no important change. The principal advance since 1912 has lain in the development of the experimental technique required to determine the *derivatives* necessary for the quantitative solutions of the equations, and in the accumulation of data; matters which have been discussed in Chapters II and III.

**11. Moderate Finite Disturbances.** Before proceeding to study the solutions to these equations we note that although they apply strictly to infinitesimal disturbances only, the results obtained are found to apply with fair accuracy to finite disturbances which are sufficiently large to make the conclusions drawn of great practical interest. Thus, with some exceptions, which will be noted in due course, it is true to say that an aeroplane which is stable to small disturbances from steady equilibrium flight is also stable to disturbances of moderate magnitude, such as may be met when flying through air of normal *bumpiness*. Also the effects of finite applications of the controls in steady straight flight are at least of the same type as those indicated by the solutions for infinitesimal control applications. The restriction of the mathematical processes to infinitesimal disturbances does not, therefore, restrict the general value of the solution so much as might at first be supposed.

Put otherwise; the second order terms, which are neglected in the mathematical solutions, do not seriously influence the motions, even when the disturbances are of the moderate finite amounts which occur frequently in ordinary flight.

**12. Force and Moment Derivatives.** A consequence of restricting disturbances from straight steady flight to infinitesimals is that each component of the air-reaction, such as  $X$ , can be expressed in the form

$$X = X_1 + \frac{\partial X}{\partial U} dU + \frac{\partial X}{\partial V} dV + \frac{\partial X}{\partial W} dW + \frac{\partial X}{\partial P} dP + \frac{\partial X}{\partial Q} dQ + \frac{\partial X}{\partial R} dR$$

where  $X_1$  is the value of  $X$  in steady flight and  $\partial X/\partial U$  etc. are partial derivatives;  $dU$  etc. being the variations of  $U$  etc. from steady flight. It is here assumed that  $X$  is not dependent on the rate of change of velocity components such as  $\dot{W}$ . We have, however, agreed (see 6) to ignore such effects with the exception of the effect of  $\dot{W}$  on  $M$

which will, in the equation for  $M$ , introduce an eighth term,  $\frac{\partial M}{\partial \dot{W}} d\dot{W}$ .

The equations will thus contain 37 derivatives such as  $\partial X/\partial U$ , each of which could conceivably be determined by experiments on the aeroplane itself or upon a small model; alternatively the derivatives may, in favourable circumstances, be approximately computed from a knowledge of the motion of the air about the aeroplane.

The assumption that the aeroplane has a plane of symmetry and that the steady motion about which the disturbances occur is symmetrical with regard to that plane, immediately reduces 18 of these derivatives to zero. For the disturbances such as  $dU$ ,  $dV\dots$  and the reactions such as  $X$ ,  $Y$ , ... can be divided into a symmetric group  $dU$ ,  $dW$ ,  $dQ$ ;  $X$ ,  $Z$ ,  $M$ , and an asymmetric group  $dV$ ,  $dP$ ,  $dR$ ;  $Y$ ,  $L$ ,  $N$ . Now no symmetric disturbance can cause an unsymmetric reaction and, therefore, the nine *cross* derivatives such as  $\partial Y/\partial U$  etc. are all zero. Again, the effect of an asymmetric disturbance upon a symmetric reaction must, by symmetry, be independent of the sign of the disturbance and therefore such derivatives as  $\partial X/\partial V$  must be zero when  $V$  is zero; but  $V$ ,  $P$ ,  $R$ , are all zero in steady symmetric flight, hence the nine *cross* derivatives of this type must also vanish.

**13. Shortened Notation.** In the interest of brevity we shall now adopt the following notation. Forces, moments, velocities, and angles relating to the steady motion about which the infinitesimal disturbances are to occur, will be represented by capital letters with a suffix—for example  $\Theta_1$ . Small variations from the steady motion will be represented by small letters. Thus, when the aeroplane is slightly disturbed from steady flight,  $\Theta = \Theta_1 + \theta$ ,  $U = U_1 + u$  etc. We note that the rates of change with respect to time of the capital letters are the same as those of the small letters; for example  $\dot{U} = \dot{U}_1 + \dot{u} = \dot{u}$ , since  $U_1$  is constant. Note also that  $V_1$ ,  $P_1$ ,  $Q_1$ ,  $R_1$ ,  $\Phi_1$  are all zero from considerations of symmetry. Finally we shall use symbols such as  $X_u$  to represent derivatives of the type  $\partial X/\partial u$  when the values of the derivatives for small disturbances from the steady motion are under consideration.

**14. The Applied Forces.** Using this notation the right hand sides of (5.1) become:—

$$\left. \begin{array}{l} X_1 - mg \sin \Theta_1 + X_u u + X_v v + X_q q - mg \cos \Theta_1 \theta \\ Y_1 \quad \quad \quad + Y_v v + Y_p p + Y_r r + mg \cos \Theta_1 \varphi \\ Z_1 + mg \cos \Theta_1 + Z_u u + Z_v v + Z_q q - mg \sin \Theta_1 \theta \\ L_1 \quad \quad \quad + L_v v + L_p p + L_r r + L_0 \\ M_1 \quad \quad \quad + M_u u + M_v v + M_q q + M_{\dot{w}} \dot{w} + M_0 \\ N_1 \quad \quad \quad + N_v v + N_p p + N_r r + N_0 \end{array} \right\} \quad (14.1)$$

where  $L_0$ ,  $M_0$ ,  $N_0$ , in the last three equations, represent infinitesimal couples—if there are any—applied by the controls to disturb the



aeroplane from steady flight. The corresponding terms  $X_0$ ,  $Y_0$ ,  $Z_0$ , have been omitted, because there is no means of applying them; the action of the controls in producing direct forces of this type being negligible compared with their action in producing moments.

The first two columns of these expressions represent the applied forces and moments in steady flight and therefore their sum is zero. The remaining terms represent the net applied forces and moments acting upon the disturbed aeroplane and can, therefore, be directly equated to the mass accelerations and rates of change of momenta.

**15. The Mass Accelerations.** These mass accelerations and rates of change of momenta are given on the left hand sides of (5.1). Remembering that  $V_1$ ,  $P_1$ ,  $Q_1$ ,  $R_1$ ,  $\Phi_1$  are all zero, that  $\dot{U}$ ,  $\dot{V}$ ... are the same as  $\dot{u}$ ,  $\dot{v}$ ...; that the products of inertia  $D$  and  $F$  are zero and that the products of infinitesimals can be omitted, the left hand sides of (5.1) reduce to

$$\left. \begin{aligned} m [\dot{u} + W_1 q] \\ m [\dot{v} + U_1 r - W_1 p] \\ m [\dot{w} - U_1 q] \\ A \dot{p} - E \dot{r} \\ B \dot{q} \\ C \dot{r} - E \dot{p} \end{aligned} \right\} \quad (15.1)$$

**16. Separation into Symmetric and Asymmetric Groups.** The six equations are now divisible into two groups of three, such that neither group contains any variable which occurs in the other. Thus the first, third and fifth equations contain only symmetric variables, whereas the second, fourth, and sixth contain only asymmetric variables. These groups can be treated entirely separately and will be so treated in the following analysis, under the names *Symmetric* or *Longitudinal* and *Asymmetric* or *Lateral* equations, respectively. Regrouped in this way they are stated below.

#### *Symmetric or Longitudinal Equations*

$$\left. \begin{aligned} m [\dot{u} + W_1 q + g \cos \Theta_1 \theta] &= X_u u + X_w w + X_q q \\ m [\dot{w} - U_1 q + g \sin \Theta_1 \theta] &= Z_u u + Z_w w + Z_q q \\ B \dot{q} &= M_u u + M_w w + M_q q + M_{\dot{w}} \dot{w} + M_0 \end{aligned} \right\} \quad (16.1)$$

#### *Asymmetric or Lateral Equations*

$$\left. \begin{aligned} m [\dot{v} + U_1 r - W_1 p - g \cos \Theta_1 \varphi] &= Y_v v + Y_p p + Y_r r \\ A \dot{p} - E \dot{r} &= L_v v + L_p p + L_r r + L_0 \\ C \dot{r} - E \dot{p} &= N_v v + N_p p + N_r r + N_0 \end{aligned} \right\} \quad (16.2)$$

The symmetric group relates to pitching rotations combined with variations in velocity in the symmetric plane, which in this case is vertical. The three variables consist of two linear velocity components and one angular velocity component.

The asymmetric group relates to rolling and yawing rotations combined with side-slip, the three variables consisting of two angular velocity components and one linear velocity component.

Of the constants;  $\Theta_1$ ,  $W_1$ ,  $U_1$ , together define the attitude, the inclination of the motion to the horizontal, and the wing incidence of the aeroplane in steady flight.  $A$ ,  $B$ ,  $C$  and  $E$  define the distribution of the total mass  $m$  about the centre of gravity, while the derivatives on the right hand sides of the equations define the aerodynamic properties of the aeroplane.

It is obvious that the symmetric group of movements, even when finite, could occur without generating asymmetric movements. If, however, the reverse is to be true and asymmetric movements are to generate no symmetric movements, the disturbances must for strict accuracy be infinitesimal as is here assumed. We have seen, from considerations of symmetry, that if both groups of disturbances are infinitesimal, they will proceed entirely independently of one another, and therefore the solutions of each can be considered without reference to the other.

**17. The Equations of Motion Rearranged.** Before proceeding to the solution of these equations it is convenient to rearrange their terms so as to bring variables of a like kind together and to replace  $\theta$  by the equivalent expression  $\int q dt$  and  $\cos \Theta_1 \varphi$  by the equivalent terms  $\cos \Theta_1 \int p dt + \sin \Theta_1 \int r dt$ . This substitution is legitimate because  $\varphi$  is always infinitesimal so that the only velocity component which influences  $\theta$  is  $\dot{q}$ ; also the rate of change of  $\cos \Theta_1 \varphi$ —the angle made by  $OY$  with the horizontal—is clearly  $\cos \Theta_1 \dot{p} + \sin \Theta_1 \dot{r}$ .

With these rearrangements and substitutions the equations of motion become

$$\left. \begin{aligned} m\dot{u} - X_u u & - X_w w + (mW_1 - X_q)q + mg \cos \Theta_1 \int q dt = 0 \\ -Z_u u + m\dot{w} & - Z_w w - (mU_1 + Z_q)q + mg \sin \Theta_1 \int q dt = 0 \\ -M_u u - M_w \dot{w} & - M_w w + B\dot{q} - M_q q = M_0 \end{aligned} \right\} \quad (17.1)$$

$$\left. \begin{aligned} m\dot{v} - Y_v v + (-mW_1 - Y_p)p & - mg \cos \Theta_1 \int p dt + \\ & + (mU_1 - Y_r)r - mg \sin \Theta_1 \int r dt = 0 \\ -L_v v + A\dot{p} - L_p p & - E\dot{r} - L_r r = L_0 \\ -N_v v - E\dot{p} - N_p p & + C\dot{r} - N_r r = N_0 \end{aligned} \right\} \quad (17.2)$$

### C. Conversion to Dimensionless Form

**18. Introduction.** It will ultimately be necessary, before practical use is made of (17.1), (17.2) and their solutions, to give numerical expression to the various terms involved, and experience has shown that it is then a great convenience to arrange that the numbers which appear

in the computations relate to dimensionless quantities—mere ratios—rather than to quantities, such as forces in pound units, velocities in feet per second, etc. The reasons why this is so will appear as we proceed and it is unnecessary to enumerate them here. It will be convenient, therefore, to throw the equations into dimensionless form before proceeding to their solution. There are many ways in which this can be done, but we shall adopt a form originally suggested by H. Glauert (Ref. 8) which is extensively used and is probably the most convenient which has yet appeared.

**19. The Parameter “ $\mu$ ”.** From dimensional considerations alone it can be deduced that the subsequent motion of an aeroplane of given shape which, at a given instant, was in a given attitude, flying in a given direction with velocity  $V$ , is dependent upon the value of two parameters only, which may be written  $m/\rho l^3$  and  $V^2/lg$  respectively, where  $\rho$  is the density of the air,  $g$  is the acceleration due to gravity and  $l$  is some representative length which defines the size of the aeroplane; for example, the span of the wings<sup>1</sup>. Two similar aeroplanes which at any instant are flying similarly will, if these two parameters have the same value for each, continue to travel similarly, though their sizes, masses and velocities may be very different and though the atmospheres through which they fly may have very different densities.

The parameter  $m/\rho l^3$  defines the ratio of the average density of the aeroplane to the density of the air. The inertias both of the air and of the aeroplane enter into the problem and must clearly bear the same ratio to one another in each case if the motions are to be similar. It will be more convenient to write this parameter in the alternative form  $m/\rho S l$ , where  $S$  is the conventional wing area. For brevity we shall give to it the symbol  $\mu$ . Thus  $\mu = m/\rho S l$ .

The parameter  $V^2/lg$  is the well known criterion of similarity for similar mechanisms of any kind moving under the influence of gravity. When this parameter is the same for two geometrically similar motions the accelerations of corresponding parts bear the same ratio to the gravitational field in each case.

In general these two parameters are independent of one another, but in our problem of small disturbances from steady flight, in which we shall make  $V$  the resultant velocity of steady flight, they are related by the consideration that the resultant aerodynamic reaction in steady flight must equal the aeroplane's weight and they therefore reduce to a single parameter only. One of the principal advantages of Glauert's

<sup>1</sup> Strictly, it is necessary to take into account also the parameter  $\rho V l/\mu$ , where  $\mu$  is the coefficient of viscosity of the air. Except in special circumstances, however, wide variations of this parameter will not appreciably influence the motion. The reader is referred to Division G and Division I Part 2 for further information on this point.

dimensionless system is that it separates out this parameter ( $\mu$ ) from the other quantities in the equations of motion and their solutions.

Let the resultant air-reaction on the aeroplane in steady straight flight be  $k \rho V^2 S$ , in which expression  $k$ , being dependent on incidence only, has the same value for all similar aeroplanes flying similarly. Since this resultant force is necessarily vertical

$$k \rho V^2 S = mg$$

and therefore

$$\frac{V^2}{lg} = \frac{\mu}{k}$$

giving a simple relation between the two parameters. The symbol  $k$  will be required in the analysis. It may be described as the *coefficient of resultant air-reaction* and is equal to the lift coefficient for the whole aeroplane divided by the cosine of the inclination to the horizontal of the steady flight path.

**20. The Dimensionless System Explained.** The easiest way of understanding Glauert's dimensionless form of the equations of motion is to begin by observing that the equations can be used equally well with any consistent system of units; that is to say, with any system in which Newton's law relating force to mass acceleration is expressed as an equality. Let us now imagine a system in which the fundamental units are

$$\begin{array}{llll} \text{Unit of Mass} & . & . & . & m \\ \text{Unit of length} & . & . & . & l \\ \text{Unit of time} & . & . & . & \tau \end{array} \quad \begin{array}{l} m \\ \rho V^2 S \end{array} \quad \begin{array}{l} l \\ \mu \frac{l}{V} \end{array}$$

so that in this system the mass of the aeroplane and the representative length are represented by unity and time intervals appear as ratios to the time required for the aeroplane to travel a distance  $\mu l$  whilst flying with the velocity  $V$  of the steady motion about which the small disturbances are to occur.

To be consistent with these fundamentals the units which would have to be used to express the various quantities which appear in the equations are then as given in Table 1, in which it will be observed that all the quantities in the second and third columns are constants which must be known for the aeroplane before any calculation can be undertaken.

Now suppose that every quantity in (17.1), (17.2) is divided by the appropriate expression in the third column of Table 1. This process reduces the equations to the dimensionless form which we require and since it is equivalent to expressing the equations in terms of the consistent system of units in Table 1, it does not destroy their validity. In order to avoid the unnecessary repetition of numerous symbols we now adopt the shortened notation of Table 2, in which column 1 shows the new symbols, column 2 the meaning of each symbol in terms of symbols previously employed, and column 3 shows the relation of some of the

new symbols to the dimensionless coefficients of the type employed in previous chapters. All expressions on one row of this table are exact equivalents.

TABLE 1.  
Units Employed in the Dimensionless System.

Quantity	Unit	Alternative Expression for Unit
Mass . . . . .	$m$	$m$
Length . . . . .	$l$	$l$
Time . . . . .	$\tau$	$\frac{m}{\rho V S}$
Velocity . . . . .	$\frac{l}{\tau}$	$\frac{V}{\rho V S}$
Angular Velocity . . . . .	$\frac{l}{\tau^2}$	$\frac{\mu}{V}$
Acceleration . . . . .	$\frac{l}{\tau^2}$	$\frac{\mu l}{\rho V^2 S}$
Force . . . . .	$\frac{m l}{\tau^2}$	$\frac{\mu}{\rho V^2 S}$
Moment . . . . .	$\frac{m l^2}{\tau^2}$	$\frac{\mu}{\rho V^2 S l}$
Moment of Inertia . . . . .	$m l^2$	$m l^2$
Force-Velocity derivatives . . .	$\frac{m}{\tau}$	$\frac{\rho V S}{\rho V S}$
Force-Rotary derivatives . . .	$\frac{m l}{\tau}$	$\frac{\rho V S l}{\rho V S l}$
Moment-Velocity derivatives . .	$\frac{m l}{\tau}$	$\frac{\rho V S l}{\rho V S l}$
Moment-Rotary derivatives . .	$\frac{m l^2}{\tau}$	$\frac{\rho V S l^2}{\rho V S l^2}$
Moment-Acceleration derivatives	$\frac{m l}{\tau}$	$\frac{\rho S l^2 \mu}{\rho S l^2 \mu}$

TABLE 2. Symbols Used in the Dimensionless Form of the Equations of Motion.

1	2	3
$t$	$\frac{1}{\tau} \cdot t$	
$w$	$\frac{\mu}{V} \cdot w$	
$\dot{w}$	$\frac{m \mu}{\rho V^2 S} \cdot \dot{w}$	
$q$	$\frac{\mu l}{V} \cdot q$	
$k_A$	$\frac{A}{m l^2}$	
$k_B$	$\frac{B}{m l^2}$	
$k_C$	$\frac{C}{m l^2}$	
$x_w$	$\frac{-X_w}{\rho V S}$	$-k_{xw}$
$x_q$	$\frac{-X_q}{\rho V S l}$	$-k_{xq}$
$m_w$	$\frac{-M_w}{\rho V S l k_B}$	$\frac{k_{mw}}{k_B}$
$m_{\dot{w}}$	$\frac{-M_{\dot{w}}}{\rho S l^2 k_B}$	$\frac{k_{m\dot{w}}}{k_B}$
$m_q$	$\frac{-M_q}{\rho V S l^2 k_B}$	$\frac{k_{mq}}{k_B}$
$m_0$	$\frac{M_0}{\rho V^2 S l k_B}$	$\frac{k_{m0}}{k_B}$
$\Omega$	Angle between X axis and direction of motion	

The quantities represented by  $k_A$ ,  $k_B$ ,  $k_C$ , will be called the *inertia coefficients* of the aeroplane. The table does not contain all the symbols involved in the calculations, but merely a single representative of each type. For example, the quantity which would be represented in the new notation by  $l_v$  corresponds to a moment caused by a velocity and is of the same type as  $m_w$  which, appears in the table. The entries in columns 2 and 3, which would correspond to  $l_v$  would be  $-L_v/(\rho V S l k_A)$  and  $-k_{lv}/k_A$  respectively, the appropriate inertia coefficient being used for each moment component.

Some explanation is called for to justify the use of two different kinds of dimensionless coefficient to represent the derivatives, as in columns 1 and 3 of Table 2. In dynamical calculations the type exemplified by  $m_w$  in column 1 are the more convenient, since by their use unnecessary repetition of the inertia coefficients and the minus sign in the equation is avoided. On the other hand, when discussing experiments or calculations to ascertain the values of these coefficients, the moments of inertia of the aeroplanes for which the coefficients are to be used are not known and it would be intolerable to make the recorded values dependent on arbitrary inertia coefficients. Even when the computations are made with a view to application to some definite aeroplane, rather than, as is more usual, to acquire information for general application, it will be realized that the inertia coefficients of the aeroplane are not fixed quantities, but vary with every change of loading. For these reasons coefficients of the type  $k_{mw}$ , which depend solely upon the external form of the aeroplane and on the wing incidence, are used throughout Chapters II and III, which discuss their magnitude, whilst the alternative form of column 1 are used in the present and subsequent chapters, which deal with their effect upon the aeroplane's motion. As regards the force derivatives  $k_{xu}$ ,  $x_u$  etc. the two types are identical except for the change of sign, but the appropriate symbol is employed to avoid the unnecessary mixing of symbols of different types in one calculation.

**21. The Equations of Motion in Dimensionless Form.** When this process has been carried through and the substitution of the symbols of column 1, Table 2 has been made, the equations of motion take the form (21.1), (21.2) below.

$$\left. \begin{aligned} \dot{\mathbf{u}} + x_u \mathbf{u} &+ x_w \mathbf{w} + (\mu \sin \Omega + x_q) \mathbf{q} + \mu k \cos \Theta_1 \int \mathbf{q} dt = 0 \\ z_u \mathbf{u} + \dot{\mathbf{w}} + z_w \mathbf{w} + (-\mu \cos \Omega + z_q) \mathbf{q} + \mu k \sin \Theta_1 \int \mathbf{q} dt &= 0 \\ m_u \mathbf{u} + \frac{m_w}{\mu} \dot{\mathbf{w}} + m_w \mathbf{w} + \dot{\mathbf{q}} + m_q \mathbf{q} &= \mu \mathbf{m}_0 \end{aligned} \right\} \quad (21.1)$$

$$\left. \begin{aligned} \dot{\mathbf{v}} + y_v \mathbf{v} + (-\mu \sin \Omega + y_p) \mathbf{p} - \mu k \cos \Theta_1 \int \mathbf{p} dt + \\ + (\mu \cos \Omega + y_r) \mathbf{r} - \mu k \sin \Theta_1 \int \mathbf{r} dt &= 0 \\ l_v \mathbf{v} + \dot{\mathbf{p}} + l_p \mathbf{p} - \frac{E}{A} \dot{\mathbf{r}} + l_r \mathbf{r} &= \mu l_0 \\ n_v \mathbf{v} - \frac{E}{C} \dot{\mathbf{p}} + n_p \mathbf{p} + \dot{\mathbf{r}} + n_r \mathbf{r} &= \mu n_0 \end{aligned} \right\} \quad (21.2)$$

In this form of the equations the numerical values of all the symbols used are entirely independent of the units employed and all the constants but  $\mu$  depend solely upon the shape, mass distribution, attitude, and direction of motion of the aeroplane. The influence upon the equations of the size, velocity, and mass of the aeroplane and of the density of the air through which it flies are all represented in the single parameter  $\mu$ . The variables  $\mathbf{u}$ ,  $\mathbf{v}$ , etc. and  $t$  are written in bold face type

to indicate that they are expressed in terms of the units  $m, l, \tau$ . The solutions will contain  $u, v$ , etc. expressed as functions of  $t$  and will apply equally to all aeroplanes of given shape moving initially in a given way and having the given value of  $\mu$ . When it is desired to convert the solutions so as to apply to a specified flight of a specified aeroplane in terms of specified units, it is merely necessary to multiply  $u, v, w$ , by  $V/\mu$ ;  $p, q, r$ , by  $V/\mu l$ , and  $t$  by  $\tau$  (or  $m/q VS$ ); where  $\mu, V, l, S$  relate to the specified flight and are expressed in terms of the specified units.

## D. The Solutions of the Equations of Motion

**22. Introductory.** The solutions of these equations of motion follow the usual procedure for linear, differential equations, the two groups being handled separately but on similar lines. For brevity we shall, throughout, handle the solutions in terms of the symbols appropriate to the symmetric or longitudinal group, noting in passing any small differences in procedure which may be necessary when the method is applied to the asymmetric group.

**23. The Complementary Function.** We proceed first to find the *complementary function*, that is to say the solution when the applied couples represented by  $l_0, m_0, n_0$  are zero. It is known that the solutions of equations of this type are such that the variables are related to their differential coefficients and integrals with respect to time, in the following manner.

$$\dot{u} = \lambda u; \quad \dot{v} = \lambda v; \quad \dot{q} = \lambda q; \quad \int q dt = \lambda^{-1} q \quad (23.1)$$

where  $\lambda$  is a real or complex constant having the same value for each variable.

It follows that the solutions can be written in the form

$$u = u_1 e^{\lambda t}; \quad v = v_1 e^{\lambda t}; \quad q = q_1 e^{\lambda t}; \quad \theta = \int q dt = \lambda^{-1} q_1 e^{\lambda t} \quad (23.2)$$

in which  $u_1, v_1, q_1$ , are real or complex constants.

Replace  $\dot{u}, \dot{v}, \dot{q}, \int q dt$  in (21.1) by the equivalent expressions of (23.2), thus reducing the differential equations to three algebraic equations having three unknowns, namely  $\lambda$  and the two ratios  $u_1/q_1$  and  $v_1/q_1$ , of which the last two may be written in the alternative form  $u_1: v_1: q_1$ . The unknown  $\lambda$  and the ratios  $u_1: v_1: q_1$  are thus determinate.

For convenience of reference we shall here make this substitution in both groups of equations, although we shall, as stated above, proceed subsequently in terms of the variables of the first group only. The result of this substitution is as given below.

$$\left. \begin{aligned} (\lambda + x_u) u_1 + x_w w_1 + (\mu \sin \Omega + \mu k \cos \Theta_1 \lambda^{-1} + x_q) q_1 &= 0 \\ z_u u_1 + (\lambda + z_w) w_1 + (-\mu \cos \Omega + \mu k \sin \Theta_1 \lambda^{-1} + z_q) q_1 &= 0 \\ m_u u_1 + \left( \frac{m_w}{\mu} \lambda + m_w \right) w_1 + (\lambda + m_q) q_1 &= 0 \end{aligned} \right\} \quad (23.3)$$

$$\left. \begin{aligned} (\lambda + y_r) \mathbf{v}_1 + (-\mu \sin \Omega - \mu k \cos \Theta_1 \lambda^{-1} + y_p) \mathbf{p}_1 + \\ + (\mu \cos \Omega - \mu k \sin \Theta_1 \lambda^{-1} + y_r) \mathbf{r}_1 = 0 \\ l_v \mathbf{v}_1 + (\lambda + l_p) \mathbf{p}_1 + \left(-\frac{E}{A} \lambda + l_r\right) \mathbf{r}_1 = 0 \\ n_v \mathbf{r}_1 + \left(-\frac{E}{C} \lambda + n_p\right) \mathbf{p}_1 + (\lambda + n_r) \mathbf{r}_1 = 0 \end{aligned} \right\} \quad (23.4)$$

The bold face letters are here the unknowns and it will be remembered that they are expressed in terms of the appropriate units in Table 1.  $\lambda$ , of course, need not have the same value in the two independent groups, but it has not been considered necessary to emphasize this by employing different symbols.

For brevity rewrite (23.3) in the form

$$\left. \begin{aligned} a_1 \mathbf{u}_1 + b_1 \mathbf{w}_1 + c_1 \mathbf{q}_1 &= 0 \\ a_2 \mathbf{u}_1 + b_2 \mathbf{w}_1 + c_2 \mathbf{q}_1 &= 0 \\ a_3 \mathbf{u}_1 + b_3 \mathbf{w}_1 + c_3 \mathbf{q}_1 &= 0 \end{aligned} \right\} \quad (23.5)$$

$a_1, b_1, c_1 \dots$  are here constants involving the, as yet, unknown constant  $\lambda$  and the various constants in the equations of motion. For future reference the values of  $a_1, b_1, c_1 \dots$  will be found by comparing (23.3) and (23.5). A similar shortened notation will be used in relation to (23.4).

**24. The Quartic Equation for  $\lambda$ .** Eliminate the ratio  $\mathbf{u}_1 : \mathbf{w}_1 : \mathbf{q}_1$  from (23.5), leaving the determinantal equation

$$\begin{vmatrix} a_1 & b_1 & c_1 \\ a_2 & b_2 & c_2 \\ a_3 & b_3 & c_3 \end{vmatrix} = 0 \quad (24.1)$$

which, on expansion, will be found to contain the single unknown ( $\lambda$ ) raised to every integral power from 0 to 4. This quartic for  $\lambda$  has four roots, say  $\lambda_1, \lambda_2, \lambda_3, \lambda_4$ , which may all be real or which may become complex in pairs.

**25. The Ratios  $\mathbf{u}_1 : \mathbf{w}_1 : \mathbf{q}_1$ .** Insert these four roots in turn into any two of (23.3) and for each value of the root find the corresponding value of the ratios  $\mathbf{u}_1 : \mathbf{w}_1 : \mathbf{q}_1$ .

The fact that  $\lambda_1$  is a root of the quartic ensures that the same ratios  $\mathbf{u}_1 : \mathbf{w}_1 : \mathbf{q}_1$  will be found whichever pair of (23.3) is chosen for this purpose.

Choosing the first two equations we have

$$\frac{\mathbf{u}_1}{b_1 c_2 - b_2 c_1} = \frac{\mathbf{w}_1}{c_1 a_2 - c_2 a_1} = \frac{\mathbf{q}_1}{a_1 b_2 - a_2 b_1} \quad (25.1)$$

Thus, for example, throughout the *mode* of motion corresponding to the root  $\lambda_1$ , the portions of the variables  $\mathbf{u}, \mathbf{w}, \mathbf{q}$ , which are given by this mode must be in the ratio given by (25.1) when the numerical value of this root is inserted in the quantities  $a_1, b_1 \dots$ . Since there are four roots to (24.1) there are four independent modes of motion which satisfy (24.1), with the right hand sides zero, in each of which  $\lambda$  and the ratios  $\mathbf{u} : \mathbf{w} : \mathbf{q}$  have definite values, different in each mode.



**26. The Four Arbitrary Constants.** For brevity write

$$\left. \begin{aligned} w_1 &= \frac{c_1 a_2 - c_2 a_1}{b_1 c_2 - b_2 c_1} u_1 = \alpha_1 u_1 \\ q_1 &= \frac{a_1 b_2 - a_2 b_1}{b_1 c_2 - b_2 c_1} u_1 = \beta_1 u_1 \end{aligned} \right\} \quad (26.1)$$

where the suffixes applied to the symbols  $u_1$ ,  $w_1$ ,  $q_1$ ,  $\alpha_1$ , and  $\beta_1$  indicate that they relate to the root  $\lambda_1$ .

The mode of motion corresponding to  $\lambda_1$  can now be written in the form  $u = u_1 e^{\lambda_1 t}$ ;  $w = \alpha_1 u_1 e^{\lambda_1 t}$ ;  $q = \beta_1 u_1 e^{\lambda_1 t}$

in which  $u_1$  is the only arbitrary constant and  $\alpha_1$ ,  $\beta_1$  are ratios indicated in (26.1). Since there are four roots of the quartic for  $\lambda$  there will be four such arbitrary constants.

**27. General Form of the Complementary Function.** Any combination of the four modes corresponding to the four roots of the equation for  $\lambda$  will satisfy (21.1) with  $m_0$  zero and the complementary function in its most general form can therefore be written

$$\left. \begin{aligned} u &= u_1 e^{\lambda_1 t} + u_2 e^{\lambda_2 t} + u_3 e^{\lambda_3 t} + u_4 e^{\lambda_4 t} \\ w &= \alpha_1 u_1 e^{\lambda_1 t} + \alpha_2 u_2 e^{\lambda_2 t} + \alpha_3 u_3 e^{\lambda_3 t} + \alpha_4 u_4 e^{\lambda_4 t} \\ q &= \beta_1 u_1 e^{\lambda_1 t} + \beta_2 u_2 e^{\lambda_2 t} + \beta_3 u_3 e^{\lambda_3 t} + \beta_4 u_4 e^{\lambda_4 t} \\ \theta &= \gamma_1 u_1 e^{\lambda_1 t} + \gamma_2 u_2 e^{\lambda_2 t} + \gamma_3 u_3 e^{\lambda_3 t} + \gamma_4 u_4 e^{\lambda_4 t} \end{aligned} \right\} \quad (27.1)$$

in which  $\gamma_1$ ,  $\gamma_2$ ,  $\gamma_3$ ,  $\gamma_4$  are, for uniformity of notation, written instead of  $\beta_1/\lambda_1$ ,  $\beta_2/\lambda_2$ ,  $\beta_3/\lambda_3$ ,  $\beta_4/\lambda_4$ . The equation for  $\theta$  is not necessary to define the motion, but it will be required later and is added for convenience of reference.

The right hand sides of these equations contain four arbitrary constants  $u_1$ ,  $u_2$ ,  $u_3$ ,  $u_4$  and the independent variable  $t$ ; all the other quantities present can be determined by numerical computation, in accordance with the processes above described.

When the roots are all real the motion consists of the sum of four modes, each containing an arbitrary constant, and in each of which the variables increase or decrease exponentially with time, according as the root is positive or negative, but throughout the whole time remain in constant ratios to each other; the interpretation when the roots are complex will be considered later.

**28. Initial Conditions.** The equations can be made to satisfy four arbitrary initial conditions. When  $t = 0$  we have, denoting initial values by suffix 0.

$$\left. \begin{aligned} u_0 &= u_1 + u_2 + u_3 + u_4 \\ w_0 &= \alpha_1 u_1 + \alpha_2 u_2 + \alpha_3 u_3 + \alpha_4 u_4 \\ q_0 &= \beta_1 u_1 + \beta_2 u_2 + \beta_3 u_3 + \beta_4 u_4 \\ \theta_0 &= \gamma_1 u_1 + \gamma_2 u_2 + \gamma_3 u_3 + \gamma_4 u_4 \end{aligned} \right\} \quad (28.1)$$

If we suppose  $u_0, w_0, q_0, \theta_0$  to be given, we require to find  $u_1, u_2, u_3, u_4$  in terms of  $u_0, w_0, q_0, \theta_0$  and the ratios  $\alpha_1, \alpha_2 \dots \beta_1, \beta_2$  etc.

Let the determinant

$$\begin{vmatrix} 1_1 & 1_2 & 1_3 & 1_4 \\ \alpha_1 & \alpha_2 & \alpha_3 & \alpha_4 \\ \beta_1 & \beta_2 & \beta_3 & \beta_4 \\ \gamma_1 & \gamma_2 & \gamma_3 & \gamma_4 \end{vmatrix} = \Delta \quad (28.2)$$

where the symbols in the top row each represent unity but the suffixes are added for identification of the minor determinant. Let the *minor* determinant, derived by crossing out the row and column through any symbol such as  $\alpha_2$ , be represented by  $\alpha_2$ .

Then

$$\left. \begin{aligned} \Delta u_1 &= +u_0 \begin{vmatrix} 1_1 & 1_3 & 1_4 \\ \alpha_1 & \alpha_3 & \alpha_4 \\ \beta_1 & \beta_3 & \beta_4 \end{vmatrix} - w_0 \begin{vmatrix} 1_1 & 1_3 & 1_4 \\ \alpha_1 & \alpha_3 & \alpha_4 \\ \gamma_1 & \gamma_3 & \gamma_4 \end{vmatrix} + q_0 \begin{vmatrix} 1_1 & 1_3 & 1_4 \\ \alpha_1 & \alpha_3 & \alpha_4 \\ \beta_1 & \beta_3 & \beta_4 \end{vmatrix} - \theta_0 \begin{vmatrix} 1_1 & 1_3 & 1_4 \\ \alpha_1 & \alpha_3 & \alpha_4 \\ \gamma_1 & \gamma_3 & \gamma_4 \end{vmatrix} \\ \Delta u_2 &= -u_0 \begin{vmatrix} 1_2 & 1_3 & 1_4 \\ \alpha_2 & \alpha_3 & \alpha_4 \\ \beta_2 & \beta_3 & \beta_4 \end{vmatrix} + w_0 \begin{vmatrix} 1_2 & 1_3 & 1_4 \\ \alpha_2 & \alpha_3 & \alpha_4 \\ \gamma_2 & \gamma_3 & \gamma_4 \end{vmatrix} - q_0 \begin{vmatrix} 1_2 & 1_3 & 1_4 \\ \alpha_2 & \alpha_3 & \alpha_4 \\ \beta_2 & \beta_3 & \beta_4 \end{vmatrix} + \theta_0 \begin{vmatrix} 1_2 & 1_3 & 1_4 \\ \alpha_2 & \alpha_3 & \alpha_4 \\ \gamma_2 & \gamma_3 & \gamma_4 \end{vmatrix} \\ \Delta u_3 &= +u_0 \begin{vmatrix} 1_1 & 1_2 & 1_4 \\ \alpha_1 & \alpha_2 & \alpha_4 \\ \beta_1 & \beta_2 & \beta_4 \end{vmatrix} - w_0 \begin{vmatrix} 1_1 & 1_2 & 1_4 \\ \alpha_1 & \alpha_2 & \alpha_4 \\ \gamma_1 & \gamma_2 & \gamma_4 \end{vmatrix} + q_0 \begin{vmatrix} 1_1 & 1_2 & 1_4 \\ \alpha_1 & \alpha_2 & \alpha_4 \\ \beta_1 & \beta_2 & \beta_4 \end{vmatrix} - \theta_0 \begin{vmatrix} 1_1 & 1_2 & 1_4 \\ \alpha_1 & \alpha_2 & \alpha_4 \\ \gamma_1 & \gamma_2 & \gamma_4 \end{vmatrix} \\ \Delta u_4 &= -u_0 \begin{vmatrix} 1_1 & 1_2 & 1_3 \\ \alpha_1 & \alpha_2 & \alpha_3 \\ \beta_1 & \beta_2 & \beta_3 \end{vmatrix} + w_0 \begin{vmatrix} 1_1 & 1_2 & 1_3 \\ \alpha_1 & \alpha_2 & \alpha_3 \\ \gamma_1 & \gamma_2 & \gamma_3 \end{vmatrix} - q_0 \begin{vmatrix} 1_1 & 1_2 & 1_3 \\ \alpha_1 & \alpha_2 & \alpha_3 \\ \beta_1 & \beta_2 & \beta_3 \end{vmatrix} + \theta_0 \begin{vmatrix} 1_1 & 1_2 & 1_3 \\ \alpha_1 & \alpha_2 & \alpha_3 \\ \gamma_1 & \gamma_2 & \gamma_3 \end{vmatrix} \end{aligned} \right\} \quad (28.3)$$

Inserting these values for  $u_1, u_2, u_3, u_4$  in (27.1) gives a complete statement of the motion following any four given initial conditions.

**29. Solutions of the Asymmetric Group.** In the solution of the asymmetric group the equation  $\dot{\varphi} = \rho + r \tan \Theta_1$  replaces the simpler equation  $\dot{\theta} = q$  of the symmetric group. The solutions of the asymmetric group therefore take the form

$$\left. \begin{aligned} v &= v_1 e^{\lambda_1 t} + v_2 e^{\lambda_2 t} + \dots \\ \rho &= \alpha_1 v_1 e^{\lambda_1 t} + \alpha_2 v_2 e^{\lambda_2 t} + \dots \\ r &= \beta_1 v_1 e^{\lambda_1 t} + \beta_2 v_2 e^{\lambda_2 t} + \dots \\ \varphi &= \gamma_1 v_1 e^{\lambda_1 t} + \gamma_2 v_2 e^{\lambda_2 t} + \dots \end{aligned} \right\} \text{etc.} \quad (29.1)$$

where  $\gamma_1 = \lambda^{-1} [\alpha_1 + \beta_1 \tan \Theta_1]$  etc.

Apart from this variation in the expression for  $\varphi$  the computations for the asymmetric group follow exactly the same procedure as for the symmetric, although, of course, the numbers involved may be very different.

**30. Complex Roots.** The four roots of (24.1) may become complex in pairs. It will be sufficient to examine the treatment of one pair of complex roots.

Let  $\lambda_1 = \xi + i\eta; \quad \lambda_2 = \xi - i\eta$

where  $\xi$  and  $\eta$  are real quantities and  $i$  stands for  $\sqrt{-1}$ . The solutions

then become

$$\left. \begin{aligned} u &= e^{\xi t} [u_1 e^{i\eta t} + u_2 e^{-i\eta t}] + \text{etc.} \\ w &= e^{\xi t} [w_1 e^{i\eta t} + w_2 e^{-i\eta t}] + \text{etc.} \\ q &= e^{\xi t} [q_1 e^{i\eta t} + q_2 e^{-i\eta t}] + \text{etc.} \\ \theta &= e^{\xi t} [\theta_1 e^{i\eta t} + \theta_2 e^{-i\eta t}] + \text{etc.} \end{aligned} \right\} \quad (30.1)$$

These can be rewritten in either of two alternative forms, both of which are of interest.

One of these forms is

$$u = 2 \sqrt{u_1 u_2} e^{\xi t} \cos \left[ \eta t - \tan^{-1} i \frac{(u_1 - u_2)}{u_1 + u_2} \right] + \text{etc.}$$

which, with three similar equations for  $w$ ,  $q$ ,  $\theta$ , show that the two modes combine to take the form of a damped oscillation.

Now the ratios  $u_1:w_1:q_1$  and  $u_2:w_2:q_2$  are given by (25.1). Let us suppose that, corresponding to the root  $\lambda_1 = \xi + i\eta$  we have

$$\frac{u_1}{\mu_u + i\nu_u} = \frac{w_1}{\mu_w + i\nu_w} = \frac{q_1}{\mu_q + i\nu_q} = a, \text{ (say)} \quad (30.2)$$

The  $\mu$ 's and  $i\nu$ 's being the real and imaginary parts of expressions such as  $a_1 b_2 - a_2 b_1$ , after inserting the complex value of the root.

The corresponding ratios for the root  $\lambda_2 = \xi - i\eta$  are easily seen to be

$$\frac{u_2}{\mu_u - i\nu_u} = \frac{w_2}{\mu_w - i\nu_w} = \frac{q_2}{\mu_q - i\nu_q} = b, \text{ (say)} \quad (30.3)$$

Multiplying (30.2) and (30.3) yields

$$\frac{u_1 u_2}{\mu_u^2 + \nu_u^2} = \frac{w_1 w_2}{\mu_w^2 + \nu_w^2} = \frac{q_1 q_2}{\mu_q^2 + \nu_q^2} = ab \quad (30.4)$$

Also 
$$\tan^{-1} i \frac{u_1 - u_2}{u_1 + u_2} = \tan^{-1} \frac{\nu_u}{\mu_u} = \tan^{-1} i \frac{a - b}{a + b}$$

Now  $a$  and  $b$  are complex quantities which are complementary to one another, but are otherwise arbitrary, hence we may write  $ab = c$  and  $\tan^{-1} i (a - b)/(a + b) = \varepsilon$ , where  $c$  is a real arbitrary constant and  $\varepsilon$  is a real arbitrary angle. The first three of (30.1) can therefore be written in the form.

$$\left. \begin{aligned} u &= 2c \sqrt{\mu_u^2 + \nu_u^2} e^{\xi t} \cos \left[ \eta t + \tan^{-1} \frac{\nu_u}{\mu_u} - \varepsilon \right] + \text{etc.} \\ w &= 2c \sqrt{\mu_w^2 + \nu_w^2} e^{\xi t} \cos \left[ \eta t + \tan^{-1} \frac{\nu_w}{\mu_w} - \varepsilon \right] + \text{etc.} \\ q &= 2c \sqrt{\mu_q^2 + \nu_q^2} e^{\xi t} \cos \left[ \eta t + \tan^{-1} \frac{\nu_q}{\mu_q} - \varepsilon \right] + \text{etc.} \end{aligned} \right\} \quad (30.5)$$

Thus the pair of complex roots correspond to an oscillation of period  $2\pi/\eta$  and logarithmic increment  $\xi$ . The amplitude and phase of this oscillation are arbitrary but the ratios of the magnitude of the components and the phase differences between them are determinate and are as indicated above.

For the purposes of numerical computation a more convenient form of the solution with complex roots is as follows.

$$u = e^{\xi t} [(u_1 + u_2) \cos \eta t + i(u_1 - u_2) \sin \eta t] + \text{etc.}$$

with three similar equations for  $w$ ,  $q$ , and  $\theta$ .

From (30.2) and (30.3) we have

$$\begin{aligned} w_1 + w_2 &= \frac{\mu_w + i\nu_w}{\mu_u + i\nu_u} u_1 + \frac{\mu_w - i\nu_w}{\mu_u - i\nu_u} u_2 \\ &= \frac{\mu_u \mu_w + \nu_u \nu_w}{\mu_u^2 + \nu_u^2} (u_1 + u_2) + i \frac{\mu_u \nu_w - \mu_w \nu_u}{\mu_u^2 + \nu_u^2} (u_1 - u_2) \end{aligned}$$

which may be written

$$\mathbf{w}_1 + \mathbf{w}_2 = A_1 \mathbf{U}_1 + A_2 \mathbf{U}_2$$

similarly

$$i(\mathbf{w}_1 - \mathbf{w}_2) = A_1 \mathbf{U}_2 - A_2 \mathbf{U}_1$$

where  $\mathbf{U}_1 = \mathbf{u}_1 + \mathbf{u}_2$ ;  $\mathbf{U}_2 = i(\mathbf{u}_1 - \mathbf{u}_2)$ , whilst  $A_1$  and  $A_2$  stand for the appropriate expressions involving  $\mu$ 's and  $\nu$ 's.

In a similar manner we have

$$\mathbf{q}_1 + \mathbf{q}_2 = B_1 \mathbf{U}_2 + B_2 \mathbf{U}_2$$

$$i(\mathbf{q}_1 - \mathbf{q}_2) = B_1 \mathbf{U}_2 - B_2 \mathbf{U}_1$$

The fourth equation for  $\theta$  is transformed as follows

$$\begin{aligned} \theta &= \int \mathbf{q} d\mathbf{t} = \int [\mathbf{q}_1 e^{(\xi + i\eta)t} + \mathbf{q}_2 e^{(\xi - i\eta)t}] d\mathbf{t} + \text{etc.} \\ &= \frac{e^{\xi t}}{\xi^2 + \eta^2} [(\xi - i\eta) \mathbf{q}_1 e^{i\eta t} + (\xi + i\eta) \mathbf{q}_2 e^{-i\eta t}] + \text{etc.} \\ &= \frac{e^{\xi t}}{\xi^2 + \eta^2} [(\mathbf{q}_1 + \mathbf{q}_2) \xi - i(\mathbf{q}_1 - \mathbf{q}_2) \eta] \cos \eta t + \{i(\mathbf{q}_1 - \mathbf{q}_2) \xi + \\ &\quad + (\mathbf{q}_1 + \mathbf{q}_2) \eta\} \sin \eta t + \text{etc.} \\ &= \frac{e^{\xi t}}{\xi^2 + \eta^2} \{[(B_1 \xi + B_2 \eta) \mathbf{U}_1 + (B_2 \xi - B_1 \eta) \mathbf{U}_2] \cos \eta t + \\ &\quad + [(B_1 \xi + B_2 \eta) \mathbf{U}_2 - (B_2 \xi - B_1 \eta) \mathbf{U}_1] \sin \eta t\} + \text{etc.} \end{aligned}$$

It will be convenient now to write

$$C_1 = \frac{B_1 \xi + B_2 \eta}{\xi^2 + \eta^2}; \quad C_2 = \frac{B_2 \xi - B_1 \eta}{\xi^2 + \eta^2}$$

The solution can be written as follows

$$\left. \begin{aligned} \mathbf{u} &= e^{\xi t} [\mathbf{U}_1 \cos \eta t + \mathbf{U}_2 \sin \eta t] + \text{etc.} \\ \mathbf{w} &= e^{\xi t} [(A_1 \mathbf{U}_1 + A_2 \mathbf{U}_2) \cos \eta t + (A_1 \mathbf{U}_2 - A_2 \mathbf{U}_1) \sin \eta t] + \text{etc.} \\ \mathbf{g} &= e^{\xi t} [(B_1 \mathbf{U}_1 + B_2 \mathbf{U}_2) \cos \eta t + (B_1 \mathbf{U}_2 - B_2 \mathbf{U}_1) \sin \eta t] + \text{etc.} \\ \theta &= e^{\xi t} [(C_1 \mathbf{U}_1 + C_2 \mathbf{U}_2) \cos \eta t + (C_1 \mathbf{U}_2 - C_2 \mathbf{U}_1) \sin \eta t] + \text{etc.} \end{aligned} \right\} \quad (30.6)$$

where  $\mathbf{U}_1$  and  $\mathbf{U}_2$  are arbitrary and the values of  $A_1$ ,  $A_2$ ,  $B_1$ ,  $B_2$ ,  $C_1$ ,  $C_2$  are collected, for convenience of reference, as follows:

$$\left. \begin{aligned} A_1 &= \frac{\mu_u \mu_w + \nu_u \nu_w}{\mu_u^2 + \nu_u^2} \\ A_2 &= \frac{\mu_u \nu_w - \mu_w \nu_u}{\mu_u^2 + \nu_u^2} \\ B_1 &= \frac{\mu_u \mu_q + \nu_u \nu_q}{\mu_u^2 + \nu_u^2} \\ B_2 &= \frac{\mu_u \nu_q - \mu_q \nu_u}{\mu_u^2 + \nu_u^2} \\ C_1 &= \frac{B_1 \xi + B_2 \eta}{\xi^2 + \eta^2} \\ C_2 &= \frac{B_2 \xi - B_1 \eta}{\xi^2 + \eta^2} \end{aligned} \right\} \quad (30.7)$$

The values of  $\mathbf{U}_1$ ,  $\mathbf{U}_2$  are found from the initial conditions by making  $t$  zero in the same way as when all roots are real. Thus when one pair of roots is imaginary and the other real the initial conditions yield

$$\left. \begin{aligned} \mathbf{u}_0 &= \mathbf{U}_1 + \mathbf{0} + \mathbf{u}_3 + \mathbf{u}_4 \\ \mathbf{w}_0 &= A_1 \mathbf{U}_1 + A_2 \mathbf{U}_2 + \alpha_3 \mathbf{u}_3 + \alpha_4 \mathbf{u}_4 \\ \mathbf{q}_0 &= B_1 \mathbf{U}_1 + B_2 \mathbf{U}_2 + \beta_3 \mathbf{u}_3 + \beta_4 \mathbf{u}_4 \\ \theta_0 &= C_1 \mathbf{U}_1 + C_2 \mathbf{U}_2 + \gamma_3 \mathbf{u}_3 + \gamma_4 \mathbf{u}_4 \end{aligned} \right\} \quad (30.8)$$

from which  $\mathbf{U}_1$ ,  $\mathbf{U}_2$ ,  $\mathbf{u}_3$ ,  $\mathbf{u}_4$  can be found as before.

**31. Complex Roots in the Asymmetric Equations.** The corresponding solutions for the asymmetric equations take a similar form with, again, a slight modification in the fourth equation. If the form be

$$\left. \begin{aligned} \mathbf{v} &= e^{i\mathbf{t}} [ \mathbf{V}_1 \cos \eta \mathbf{t} + \mathbf{V}_2 \sin \eta \mathbf{t} ] + \text{etc.} \\ \mathbf{p} &= e^{i\mathbf{t}} [ (A_1 \mathbf{V}_1 + A_2 \mathbf{V}_2) \cos \eta \mathbf{t} + (A_1 \mathbf{V}_2 - A_2 \mathbf{V}_1) \sin \eta \mathbf{t} ] + \text{etc.} \\ \mathbf{r} &= e^{i\mathbf{t}} [ (B_1 \mathbf{V}_1 + B_2 \mathbf{V}_2) \cos \eta \mathbf{t} + (B_1 \mathbf{V}_2 - B_2 \mathbf{V}_1) \sin \eta \mathbf{t} ] + \text{etc.} \\ \varphi &= e^{i\mathbf{t}} [ (C_1 \mathbf{V}_1 + C_2 \mathbf{V}_2) \cos \eta \mathbf{t} + (C_1 \mathbf{V}_2 - C_2 \mathbf{V}_1) \sin \eta \mathbf{t} ] + \text{etc.} \end{aligned} \right\} \quad (31.1)$$

in which  $\mathbf{V}_1$  and  $\mathbf{V}_2$  are arbitrary. The values of  $A_1$ ,  $A_2$ ,  $B_1$ ,  $B_2$  are related to the appropriate  $\mu$ 's and  $\nu$ 's exactly as for the symmetric group, but the values of  $C_1$ ,  $C_2$  are

$$C_1 = \frac{1}{\xi^2 + \eta^2} [(A_1 \tilde{\xi} + A_2 \eta) + (B_1 \tilde{\xi} + B_2 \eta) \tan \Theta_1]$$

$$C_2 = \frac{1}{\xi^2 + \eta^2} [(A_2 \tilde{\xi} + A_1 \eta) + (B_2 \tilde{\xi} + B_1 \eta) \tan \Theta_1]$$

## E. Complete Solution with Constant Applied Control Couples

**32. No Roots Zero—Symmetric Group.** The above are the general solutions of (21.1), (21.2) when the right hand sides are zero, that is to say, with suitable adjustments of the four arbitrary constants, they can be made to represent all possible motions of the aeroplane when acted upon by no forces or moments other than those represented on the left hand sides of these equations. This solution is described as the *complementary function* of (21.1), (21.2). To find the possible motions of the aeroplane under the action of constant applied moments, such as are indicated on the right hand sides of these equations, we find any solution whatever of the whole equations and add it to the complementary function. This single solution contains, of course, no arbitrary constant and is called a particular integral of the equation. When none of the roots are zero the simplest particular integral is that solution in which the motion is steady; that is to say the solution—in the symmetric case—of the following three simultaneous algebraic equations:

$$\left. \begin{aligned} x_u \mathbf{u} + x_w \mathbf{w} + \mu k \cos \Theta_1 \theta &= 0 \\ z_u \mathbf{u} + z_w \mathbf{w} + \mu k \sin \Theta_1 \theta &= 0 \\ m_u \mathbf{u} + m_w \mathbf{w} &= \mu m_0 \end{aligned} \right\} \quad (32.1)$$

which is obtained from (21.1) by omitting all terms involving  $\dot{\mathbf{u}}$ ,  $\dot{\mathbf{w}}$ ,  $\dot{\theta}$  ( $\mathbf{q}$ ), or  $\dot{\mathbf{q}}$ .

Let the solution of this be  $u = u'$ ,  $w = w'$ ,  $\theta = \theta'$ , where  $u'$ ,  $w'$ ,  $\theta'$  are constants whose magnitude varies in proportion to  $m_0$ .

The complete solution of (21.1) is obtained by adding the particular integral to the complementary function and is, therefore,

$$\left. \begin{aligned} u &= u' + u_1 e^{\lambda_1 t} + u_2 e^{\lambda_2 t} + u_3 e^{\lambda_3 t} + u_4 e^{\lambda_4 t} \\ w &= w' + \alpha_1 u_1 e^{\lambda_1 t} + \alpha_2 u_2 e^{\lambda_2 t} + \alpha_3 u_3 e^{\lambda_3 t} + \alpha_4 u_4 e^{\lambda_4 t} \\ q &= \beta_1 u_1 e^{\lambda_1 t} + \beta_2 u_2 e^{\lambda_2 t} + \beta_3 u_3 e^{\lambda_3 t} + \beta_4 u_4 e^{\lambda_4 t} \\ \theta &= \theta' + \gamma_1 u_1 e^{\lambda_1 t} + \gamma_2 u_2 e^{\lambda_2 t} + \gamma_3 u_3 e^{\lambda_3 t} + \gamma_4 u_4 e^{\lambda_4 t} \end{aligned} \right\} \quad (32.2)$$

where  $u_1, u_2, u_3, u_4$  are arbitrary,  $t$  may be regarded as the independent variable and the numerical values of all other symbols on the right hand sides are known.

If the initial values of  $u, w, q, \theta$  are known the corresponding values of the arbitrary constants are found, as before by making  $t$  zero and solving the four simultaneous linear equations.

**33. No Roots Zero—The Asymmetric Group.** The particular integral—steady motion—of the asymmetric group is obtained from (21.2) by making  $\dot{v}, \dot{p}, \dot{r}, \dot{q}$  all zero and since  $\dot{q} = p + r \tan \Theta_1$  we must put  $p = -r \tan \Theta_1$ . Since also, in (21.2),  $\int [p \cos \Theta_1 + r \sin \Theta_1] dt$  is equivalent to  $q \cos \Theta_1$  the required particular integral is the solution of

$$\left. \begin{aligned} y_v v + [\mu (\cos \Omega + \sin \Omega \tan \Theta_1) + y_r - y_p \tan \Theta_1] r - \mu k \cos \Theta_1 q &= 0 \\ l_v v + [l_r - l_p \tan \Theta_1] r &= \mu l_0 \\ n_v v + [n_r - n_p \tan \Theta_1] r &= \mu n_0 \end{aligned} \right\} \quad (33.1)$$

Let the solutions of this be  $v = v'$ ,  $r = r'$ ,  $q = q'$  and therefore  $p' = r' \tan \Theta_1$ . Then the complete solution of (21.2) is

$$\left. \begin{aligned} v &= v' + v_1 e^{\lambda_1 t} + \text{etc.} \\ p &= -r' \tan \Theta_1 + \alpha_1 v_1 e^{\lambda_1 t} + \text{etc.} \\ r &= r' + \beta_1 v_1 e^{\lambda_1 t} + \text{etc.} \\ q &= q' + \gamma_1 v_1 e^{\lambda_1 t} + \text{etc.} \end{aligned} \right\} \quad (33.2)$$

in which  $v_1, v_2, v_3, v_4$  are arbitrary and are found in terms of the initial disturbances by making  $t$  zero.

**34. One Root Zero—The Symmetric Group.** When the constant term in the quartic for  $\lambda$  happens to be zero one of the roots is zero and the complementary function contains one mode in which the variables do not change with time. The particular integral with  $u_1, w_1, \theta_1$  constant then does not exist or, stated in another way, if the root is regarded as becoming vanishingly small, the corresponding values of  $u_1, w_1, \theta_1$  become infinitely large. The simplest form of the particular integral is then

$$\left. \begin{aligned} u &= a t \\ w &= w' + \alpha_1 a t \\ q &= \gamma_1 a \\ \theta &= \theta' + \gamma_1 a t \end{aligned} \right\} \quad (34.1)$$

where  $\alpha_1, \gamma_1$  have the same values as in the mode corresponding to the zero root and  $w', \theta', a$  are constants. These constants are found by substituting from (34.1) in (21.1), observing that all terms containing  $t$  vanish identically; because, on dividing them throughout by  $t$  the remainder is identical with (23.3) when  $\lambda$  is zero and the variables  $n, w, q, \theta$  are in the ratio  $1:\alpha_1:0:\gamma_1$  which, in this special case causes the three equations to vanish identically.

The result of this substitution is

$$\begin{aligned} x_w w' + [1 + \gamma_1 \mu \sin \Omega + \gamma_1 x_q] a + \mu k \cos \Theta_1 \theta' &= 0 \\ z_w w' + [\alpha_1 - \gamma_1 \mu \cos \Omega + \gamma_1 z_q] a + \mu k \sin \Theta_1 \theta' &= 0 \\ m_w w' + \left[ \frac{m_w}{\mu} \alpha_1 + \gamma_1 m_q \right] a &= \mu m_0 \end{aligned}$$

from which  $w', a, \theta'$  can be found in terms of  $m_0$ . The complete solution is then

$$\begin{aligned} u &= at + u_1 + u_2 e^{\lambda_1 t} + \text{etc.} \\ w &= w' + \alpha_1 at + \alpha_1 u_1 + \alpha_2 u_2 e^{\lambda_2 t} + \text{etc.} \\ q &= \gamma_1 \alpha + \beta_2 u_2 e^{\lambda_2 t} + \text{etc.} \\ \theta &= \theta' + \gamma_1 at + \gamma_1 u_1 + \gamma_2 u_2 e^{\lambda_2 t} + \text{etc.} \end{aligned}$$

**35. One Root Zero—The Asymmetric Group.** The process of solving the asymmetric group of equations in this special case follows similar lines but is more complicated. The simplest form of the particular

$$\text{integral is now } \left. \begin{aligned} r &= at \\ p &= \gamma_1 a - r' \tan \Theta_1 - \beta_1 \tan \Theta_1 at \\ r &= r' + \beta_1 at \\ q &= q' + \gamma_1 at \end{aligned} \right\} \quad (35.1)$$

where  $\beta_1$  and  $\gamma_1$  have the same values as in the mode corresponding to the zero root and  $r', q', a$  are constants to be determined. The expression for  $p$  in the above is obtained from the relation  $p + r \tan \Theta_1 = q = \gamma_1 a$ .  $r', q', a$  are next found by substituting (35.1) in (21.2) and noting that terms containing  $t$  vanish identically leaving (35.2) below.

$$\left. \begin{aligned} [1 - \gamma_1 \mu \sin \Omega + \gamma_1 y_p] a + [\mu (\cos \Omega + \sin \Omega \tan \Theta_1) + y_r - y_p \tan \Theta_1] r' - \mu k \cos \Theta_1 q &= 0 \\ \left[ -\beta_1 \left( \tan \Theta_1 + \frac{E}{A} \right) + \gamma_1 l_p \right] a + [l_r - l_p \tan \Theta_1] r' &= \mu l_0 \\ \left[ \beta_1 \left( 1 + \frac{E}{A} \tan \Theta_1 \right) + \gamma_1 n_p \right] a + [n_r - n_p \tan \Theta_1] r' &= \mu n_0 \end{aligned} \right\} \quad (35.2)$$

The complete solution then takes the form

$$\begin{aligned} v &= at + v_1 + v_2 e^{\lambda_1 t} + \text{etc.} \\ p &= \gamma_1 a - r' \tan \Theta_1 - \beta_1 \tan \Theta_1 at - \beta_1 \tan \Theta_1 v_1 + \alpha_2 v_2 e^{\lambda_2 t} + \text{etc.} \\ r &= r' + \beta_1 at + \beta_1 v_1 + \beta_2 v_2 e^{\lambda_2 t} + \text{etc.} \\ q &= q' + \gamma_1 at + \gamma_1 v_1 + \gamma_2 v_2 e^{\lambda_2 t} + \text{etc.} \end{aligned}$$

**36. Two Roots Zero.** When two roots of the quartic for  $\lambda$  are zero, as may sometimes occur when dealing with the asymmetric equations for stalled motion, the particular integral involves both linear and quadratic terms in  $t$ . The process is then somewhat complicated, but follows similar lines to those when one root only is zero.

**37. Case of Equal Roots.** One other special case, that of two roots equal, requires attention, though it is of less practical importance than the case of one root zero.

Let there be two equal roots  $\lambda_1$ , then the symmetric solution takes the form

$$\begin{aligned} u &= [u_1 + u_2 t] e^{\lambda_1 t} + u_3 e^{\lambda_2 t} + u_4 e^{\lambda_3 t} \\ w &= \alpha_1 [u_1 + u_2 t] e^{\lambda_1 t} + \alpha_3 u_3 e^{\lambda_2 t} + \alpha_4 u_4 e^{\lambda_3 t} \\ q &= \beta_1 [u_1 + u_2 t] e^{\lambda_1 t} + \beta_3 u_3 e^{\lambda_2 t} + \beta_4 u_4 e^{\lambda_3 t} \\ \theta &= \gamma_1 \left[ -\frac{u_2}{\lambda_1} + u_1 + u_2 t \right] e^{\lambda_1 t} + \gamma_3 u_3 e^{\lambda_2 t} + \gamma_4 u_4 e^{\lambda_3 t} \end{aligned}$$

the asymmetric solutions in this case take the same form but with the modification arising from the fact that the relation  $\dot{\varphi} = p + r \tan \Theta_1$  replaces  $\dot{\theta} = q$ .

The solutions in the preceding sections have been given in a general form, which it is hoped will prove useful to readers who intend to carry out for themselves numerical computations of the type illustrated in Chapters VI and VII. In this general form they are inevitably somewhat complicated, but it will be realized, after reading Chapters VI and VII, that in any particular computation they can as a rule be greatly simplified by choosing conditions in which some of the quantities, such as  $\Omega$  or  $\Theta$ , are zero and by neglecting quantities, such as  $E$ ,  $y_p$ ,  $y_r$  which may be too small to influence the motion appreciably.

## CHAPTER VI

### NUMERICAL SOLUTION OF THE SYMMETRIC EQUATIONS OF CHAPTER V

**1. Introduction.** In this chapter the equations which were developed in Chapter V to represent the motion of an aeroplane subjected to infinitesimal symmetric disturbances from steady symmetric flight are studied, with regard to the numerical values of the quantities involved for a typical aeroplane. The movements following on certain initial disturbances are first computed and displayed graphically and then the approximations commonly employed when a rough survey only of the nature of the motion is required, are discussed with numerical examples.

**2. Notation and Axes.** The notation of Chapter V will be used, with the exception that the representative length used in defining dimension-



less coefficients will now be specified as the mean wing chord (II 45) and given the symbol  $c$  instead of the symbol  $l$ , which was used in Chapter V for some unspecified representative length. For the convenience of the reader, some of the salient features of the system of notation are now restated.

Capital letters with suffix (1) such as  $U_1, \Theta_1$ , etc. stand for values in the steady motion. Plain capitals such as  $U, \Theta$ , etc. stand for the values in disturbed motion. The differences between the disturbed and steady motion are represented by small letters, thus:—

$$U = U_1 + u; \quad \Theta = \Theta_1 + \theta; \text{ etc.}$$

All disturbances from the steady motion will be regarded as infinitesimal, so that the prefix  $d$  of the calculus may or may not be attached to a small symbol without altering its meaning; thus  $du$  has the same meaning as  $u$ . The small symbols such as  $u$  will be generally employed, for brevity, but the prefix  $d$  will be attached when it is desirable to indicate that some standard process of the differential calculus is being used. As in Chapter V, the symbol  $V$  will be used for the resultant velocity of the *c.g.* of the aeroplane during the steady motion.

Before proceeding to solve the equations it is necessary to choose the direction of the  $X$  and  $Z$  axes which, in Chapter V, were defined merely as lying in the plane of symmetry. Later in the present chapter it is convenient to choose the  $X$  axis parallel to the direction of motion, so as to make  $\Omega = 0$ , but for the present it will be more convenient to make the  $X$  axis parallel to the wing chord and so have it fixed permanently in the aeroplane, no matter what the incidence of the steady motion may be. These axes will be called *chord axes*.

With this choice of axes the angle  $\Omega$  between the  $X$  axis and the direction of the steady flight becomes equal to the wing incidence; we shall therefore change this symbol to  $A_1$  and write  $A = A_1 + \alpha$ , where  $A$  is the incidence in disturbed motion, and  $\alpha$  the difference between the incidence in disturbed motion and the incidence in steady motion. Note that the rate of change of incidence with respect to time may be written either  $\dot{A}$  or  $\dot{\alpha}$ , and that differential coefficients with respect to incidence may be written either  $\frac{d}{dA}$  or  $\frac{d}{d\alpha}$ .

**3. Evaluation of the Derivatives.** We have next to consider the methods by which the various derivatives of  $V$  (21.1) can be evaluated numerically. These derivatives are to some extent influenced by the

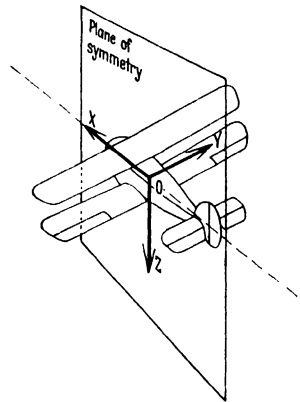


Fig. 54. Plane of symmetry and axes.

airscrew, but for simplicity we shall carry out the detailed computation for a gliding aeroplane with airscrew stopped or turning idly and controls held fixed. The influence of the airscrew will be considered later.

**4. The Force-Velocity Derivatives.** The four derivatives  $x_u, x_w, z_u, z_w$  depend upon the values of the lift and drag coefficients for the whole aeroplane and upon their rates of change with incidence. We have now to obtain expressions for these derivatives in terms of lift and drag.

From the definition of  $x_u$  we have

$$-\rho V S x_u = \frac{\partial X}{\partial U} = \frac{\partial}{\partial U} [\rho V^2 S k_x] = \rho S \left[ k_x 2 V_1 \frac{\partial V}{\partial U} + V_1^2 \frac{\partial k_x}{\partial U} \right]$$

$$\begin{aligned} \text{Therefore} \quad & -x_u = k_x 2 \frac{\partial V}{\partial U} + V_1 \frac{\partial k_x}{\partial U} \\ \text{Similarly} \quad & -x_w = k_x 2 \frac{\partial V}{\partial W} + V_1 \frac{\partial k_x}{\partial W} \end{aligned} \quad (4.1)$$

The suffix (1) indicates that the values relate to the steady motion.

Now

$$V^2 = U^2 + W^2$$

Therefore

$$V_1 dV = U_1 dU + W_1 dW$$

Hence

$$\begin{aligned} \frac{\partial V}{\partial U} &= \frac{U_1}{V_1} = \cos A_1 \\ \frac{\partial V}{\partial W} &= \frac{W_1}{V_1} = \sin A_1 \end{aligned} \quad (4.2)$$

and

Again, if  $dA$  is the change of incidence due to small changes  $dU$  and  $dW$  in the velocity components  $U$  and  $W$ , which may be supposed to occur whilst the orientation of the aeroplane remains unchanged, then, by resolving perpendicularly to the direction of the steady motion, it is easily seen that

$$V_1 dA = -dU \sin A_1 + dW \cos A_1$$

$$\text{Therefore} \quad \frac{\partial A}{\partial W} = \frac{\cos A_1}{V_1}; \quad \frac{\partial A}{\partial U} = -\frac{\sin A_1}{V_1} \quad (4.3)$$

Since  $k_x$  is a function of  $A$  only we may now write

$$\begin{aligned} V_1 \frac{\partial k_x}{\partial U} &= V_1 \frac{\partial k_x}{\partial A} \frac{\partial A}{\partial U} = -\frac{dk_x}{dA} \sin A_1 \\ V_1 \frac{\partial k_x}{\partial W} &= V_1 \frac{\partial k_x}{\partial A} \frac{\partial A}{\partial W} = +\frac{dk_x}{dA} \cos A_1 \end{aligned} \quad (4.4)$$

Using (4.1) and (4.2) and applying a similar process to  $z_u$  and  $z_w$

$$\begin{aligned} \text{we find} \quad & x_u = -2 k_x \cos A_1 + \frac{d k_x}{d A} \sin A_1 \\ & z_u = -2 k_z \cos A_1 + \frac{d k_z}{d A} \sin A_1 \\ & x_w = -\frac{d k_x}{d A} \cos A_1 - 2 k_x \sin A_1 \\ & z_w = -\frac{d k_z}{d A} \cos A_1 - 2 k_z \sin A_1 \end{aligned} \quad (4.5)$$

We have also, by direct resolution of forces

$$\left. \begin{aligned} k_x &= -k_D \cos A_1 + k_L \sin A_1 \\ k_z &= -k_L \cos A_1 - k_D \sin A_1 \end{aligned} \right\} \quad (4.6)$$

If we possess curves relating  $k_L$  and  $k_D$  for the whole aeroplane to the wing incidence  $A$ , we can deduce from these, using (4.6) curves for  $k_x$  and  $k_z$ ; from the slopes of these we can find  $dk_x/dA$  and  $dk_z/dA$  and so obtain the derivatives from (4.5). Alternatively we may differentiate (4.6) to obtain

$$\left. \begin{aligned} \frac{dk_x}{dA} &= k_D \sin A_1 + k_L \cos A_1 - \frac{dk_D}{dA} \cos A_1 + \frac{dk_L}{dA} \sin A_1 \\ \frac{dk_z}{dA} &= k_L \sin A_1 - k_D \cos A_1 - \frac{dk_L}{dA} \cos A_1 - \frac{dk_D}{dA} \sin A_1 \end{aligned} \right\} \quad (4.7)$$

Using (4.6) and (4.7), Equation (4.5) becomes

$$\left. \begin{aligned} x_u &= 2k_D \cos^2 A_1 - \left( \frac{dk_D}{dA} + k_L \right) \cos A_1 \sin A_1 + \left( \frac{dk_L}{dA} + k_D \right) \sin^2 A_1 \\ z_u &= 2k_L \cos^2 A_1 - \left( \frac{dk_L}{dA} - k_D \right) \cos A_1 \sin A_1 - \left( \frac{dk_D}{dA} - k_L \right) \sin^2 A_1 \\ x_w &= \left( \frac{dk_D}{dA} - k_L \right) \cos^2 A_1 - \left( \frac{dk_L}{dA} - k_D \right) \cos A_1 \sin A_1 - 2k_L \sin^2 A_1 \\ z_w &= \left( \frac{dk_L}{dA} + k_D \right) \cos^2 A_1 + \left( \frac{dk_D}{dA} + k_L \right) \cos A_1 \sin A_1 + 2k_D \sin^2 A_1 \end{aligned} \right\} \quad (4.8)$$

The four derivatives can thus be obtained directly from curves of  $k_L$  and  $k_D$  against incidence. We note that when the  $X$  axis coincides with the direction of motion, which with the present choice of axes occurs when the incidence is zero, the derivatives are given by the first column on the right hand side of (4.8) with  $\cos^2 A$  unity.

**5. Force-Rotary Derivatives.** The derivative  $x_q$  is always negligible and will in future be omitted from the equations.

In normal flight the effect of  $z_q$  is small and a rough estimate of its value will be sufficient. In stalled flight there is some evidence that it may be important, but at incidences near the stall so little is known about it that we shall not include it in the numerical examples relating to stalled flight.

H. Glauert has calculated the value of  $k_{zq}$  for wings alone at small incidences (Ref. 9 of Chap. II). For our present purpose it will be sufficient to summarize his result by taking for wings alone,  $k_{zq} = -1.0$  for all positions of the c.g. between  $0.3c$  and  $0.4c$  behind the leading edge.

To estimate the contribution of the tail to  $k_{zq}$  we note that its contribution to the moment  $M$  is always  $l$  times its contribution to  $Z$ , where  $l$  is its effective distance behind the c.g. Therefore (Tail only)

$$k'_{zq} = \frac{Z_q}{\rho V S c} = \frac{1}{l} \frac{M'_q}{\rho V S c} = \frac{1}{l} \frac{M'_q}{\rho V S c^2} = \frac{c}{l} k'_{mq}$$

The contribution of the body to  $k_{zq}$  may generally be neglected, so that we have as an approximation to  $z_q$ , for the whole aeroplane in normal flight

$$z_q = -k_{zq} = 1.0 - \frac{c}{l} k'_{mq} \quad (5.1)$$

**6. Moment-Velocity Derivatives.**  $m_u$  and  $m_w$  are related primarily to the coefficient of static stability  $\partial k_M / \partial A$  of Chapter II. We have

$$-\rho V S c k_B m_u = \frac{\partial M}{\partial U}$$

From which, as for the force derivatives:

$$-k_B m_u = k_m 2 \cos A_1 - \frac{\partial k_M}{\partial A} \sin A_1$$

But, since  $k_m$  in the above equation relates to steady motion, its value is zero.

$$\text{Hence} \quad m_u = \frac{1}{k_B} \frac{\partial k_M}{\partial A} \sin A_1 = -\frac{1}{k_B} H \frac{dk_L}{dA} \sin A_1 \quad \left\{ \right. \quad (6.1)$$

$$\text{Similarly} \quad m_w = -\frac{1}{k_B} \frac{\partial k_M}{\partial A} \cos A_1 = \frac{1}{k_B} H \frac{dk_L}{dA} \cos A_1 \quad \left\{ \right.$$

where  $H$  is the metacentric ratio of II 8.

**7. Moment-Rotary Derivatives.** The value of  $k_{mq}$  has already been discussed in II 43, where it was decided that in the present state of knowledge a good estimate is obtained by writing

$$k_{mq} = \frac{S' l'^2}{S c^2} k''_{mq}$$

and taking  $k''_{mq}$  from the mean curve of Fig. 30, Chapter II.

$$\text{Thus} \quad m_q = -\frac{k_{mq}}{k_B} = -\frac{S' l'^2}{S c^2} \frac{k''_{mq}}{k_B}$$

**8. The Derivative  $m_{\dot{w}}$ .** We have agreed (see V 6) to neglect the direct effects of acceleration upon the air-reactions, even though this neglect may introduce some error into the more rapidly changing motions in the solutions of our equation. We found, nevertheless, that a term involving  $m_{\dot{w}}$  must be retained in the equations to represent the fact that the downwash felt at the tail is more nearly that generated by the wings when they passed the present position of the tail than that being generated by them at the instant under consideration. We estimate the magnitude of this term as follows:

Let  $\alpha$  be the change of incidence from the value  $A_1$  of steady flight, due exclusively to a change ( $w$ ) of the  $W$  component from the value  $W_1$  of steady flight. Then—see (4.3),

$$\frac{\alpha}{w} = \frac{\cos A_1}{V_1}$$

$\alpha$  is therefore directly proportional to  $\dot{w}$ ,

$$\text{hence} \quad \frac{\partial \alpha}{\partial \dot{w}} = \frac{\cos A_1}{V_1}$$

Now we have decided to regard the effect of  $\dot{w}$  on the pitching moment ( $M$ ) as being entirely due to the influence of  $\dot{w}$  on  $\dot{\alpha}$  and we may therefore write

$$M_{\dot{w}} = \frac{\partial M}{\partial \dot{w}} = \frac{\partial M}{\partial \dot{\alpha}} \frac{\partial \dot{\alpha}}{\partial \dot{w}} = \frac{\partial M}{\partial \dot{\alpha}} \frac{\cos A_1}{V_1}$$

But we found (II 40) that  $\partial M / \partial \dot{\alpha} = M'_q \partial \varepsilon / \partial \alpha$ , where  $\varepsilon$  is the downwash from the wings at the position of the tail, and  $M'_q$  is that part of  $M_q$  which is contributed by the tail only. Therefore,

$$m_{\dot{w}} = - \frac{M_{\dot{w}}}{k_B \rho S c^2} = - \frac{\partial \varepsilon}{\partial \alpha} \frac{M'_q}{k_B \rho V_1 S c^2} \cos A_1 = \frac{\partial \varepsilon}{\partial \alpha} m'_q \cos A_1 \quad (8.1)$$

**9. Choice of Numerical Examples.** The numerical values used in the computations will be based upon the B.F.2b or *Bristol Fighter*, a tractor biplane of conventional design in the British Royal Air Force of the war period; this aeroplane has been much used for research and therefore, its aerodynamic characteristics are exceptionally well known.

To take concrete examples it will be assumed that

Air-density . . . . .	$\rho = 0.0020$ slugs per cu. ft.
Wing area . . . . .	$S = 405$ sq. ft.
Mean wing chord . . . . .	$c = 5.17$ ft.
Aeroplane mass . . . . .	$m = 96$ slugs
Aeroplane moment of inertia . . . . .	$B = 1925$ slugs ft <sup>2</sup> .

The air-density is here appropriate to a height of about 6,000 feet above sea level and the mass of the aeroplane corresponds to a weight of about 3090 lb., giving a wing loading of 7.6 lb. per sq. ft.

With these values we have

$$\mu = \frac{m}{\rho S c} = 23.0$$

$$k_B = \frac{B}{m c^2} = 0.75$$

**10. The Derivatives.** The numerical values of those coefficients and derivatives which vary with the wing incidence are plotted in Fig. 55 over an incidence range from 0° to 30°. Figure 55a shows the lift and drag coefficients and the resultant force coefficient  $k$  which is indistinguishable from the lift coefficient below about 18° incidence. Figure 55b shows the inclination of the  $X$  axis to the horizontal, obtained by subtracting the gliding angle  $\gamma (= \tan^{-1} k_D/k_L)$  from the incidence. The remaining four figures show the nine derivatives in the form which does not contain the moment of inertia of the aeroplane. To convert these to the  $x_u$  form required for the calculation it is necessary to change the sign and divide the moment derivatives by the inertia coefficient ( $k_B$ ) which, in this case, has the value 0.75.

It will be noted that rapid changes in the values of the derivatives begin shortly after 10° incidence, which may be considered as about the highest incidence of normal flight. The range of incidences above 10° is very little used in flight, except in the last moments just before

contact with the ground, or during severe stunts. The changes characteristic of the "stall" are fully developed by about  $20^\circ$  incidence. The majority of aeroplanes have elevators sufficiently powerful to retain longitudinal equilibrium up to some  $20^\circ$ — $25^\circ$  incidence only. Steady flight above these incidences is therefore very unusual.

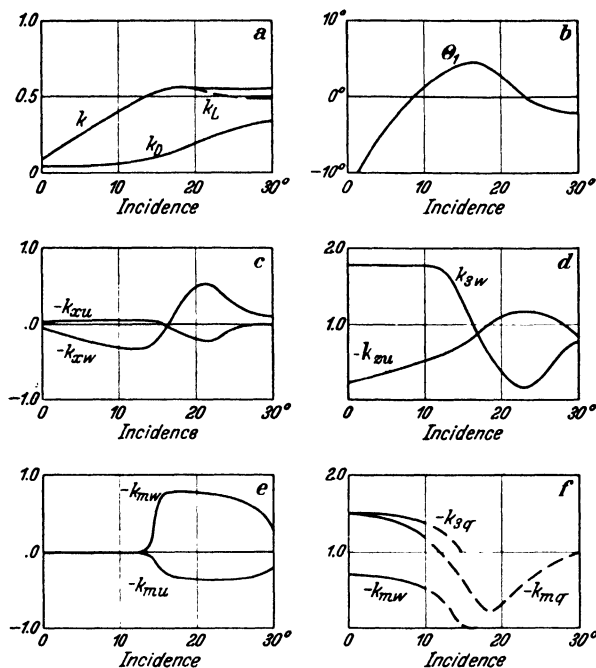


Fig. 55. Symmetric Derivatives and Coefficients of a Typical Aeroplane BF2b.

**11. The Examples Specified.** The conditions chosen to furnish illustrative examples are as follows:

1. *Gliding with incidence  $3^\circ$ .* This gives  $k_L = 0.20$  and  $V = 138$  ft. per sec., or 94 miles per hour and therefore  $\tau = m/\rho VS = 0.85$ . The gliding angle  $\gamma$  is  $10^\circ$  and the wing chord makes an angle  $\Theta_1 = -7^\circ$  with the horizontal. A pilot would describe this as a moderately steep and fast glide.

2. *Gliding with incidence  $10^\circ$ .* This gives  $k_L = 0.40$  and  $V = 98$  ft. per sec. or 66-1/2 m.p.h. and therefore  $\tau = 1.25$ .  $\gamma$  is now  $8.5^\circ$  and therefore  $\Theta_1$  is  $1.5^\circ$ . This corresponds to about the slowest speed at which the average pilot would attempt to approach a landing ground.

3. *Gliding with incidence  $20^\circ$ .* This gives  $k_L = 0.55$  and  $V = 83$  ft. per sec. or 56 miles per hour and therefore  $\tau = 1.44$ .  $\gamma$  is now  $17.5^\circ$  and  $\Theta_1$  is  $+2.5^\circ$ . This represents a fully stalled glide with the aeroplane descending very steeply.

In conditions (1) and (2) the equations will be solved for three values of the metacentric ratio, such that  $H = +.03$ ,  $H = 0$ ,  $H = -.03$ . These correspond to the aeroplane with its c.g. adjusted so as to make it statically stable, neutral and unstable, respectively. Reference to II 26 shows that on the Bristol Fighter the corresponding positions of the c.g. are distant, respectively, about  $0.33 c$ ,  $0.36 c$ , and  $0.39 c$  behind the leading edge of the mean chord. This range of c.g. positions is roughly what might be expected to occur in service, the last figure corresponding to a case of severe overloading.

Small changes of c.g. position, of this order of magnitude, do not appreciably influence any of the derivatives except  $m_w$  and  $m_u$ . These, in normal flight, will be zero when the aeroplane is statically neutral, ( $H = 0$ ), and will have values, when  $H$  is not zero, as follows:

$$m_w = H \frac{1}{k_B} \frac{dk_L}{dA} \cos A_1 = \pm 0.03 \times \frac{1}{0.75} \times 1.7 \cos A_1 = \pm 0.068 \cos A_1$$

$$m_u = -H \frac{1}{k_B} \frac{dk_L}{dA} \sin A_1 = \mp 0.068 \sin A_1$$

The upper sign refers to the stable c.g. position.

These values are not shown in Fig. 55e which may be taken to refer to an aeroplane which has the c.g. adjusted so as to make it statically neutral in normal flight.

In the stalled condition the aeroplane is essentially very stable statically and the stability is but slightly influenced by changes of c.g. position. One computation only, will therefore be made in the stalled state; for this we shall suppose the c.g. to be distant  $0.36$  of the chord from the leading edge.

## 12. The Constants Tabulated.

We have now sufficient data to evaluate all the constants which appear in the equations of motion for the seven conditions chosen for numerical solution. The numerical values of these constants are collected in Table 1, in which the alternative signs given to the values of  $m_u$  and  $m_w$  relate to the stable and unstable c.g. positions, the upper sign to the stable condition. In the neutral condition  $m_u$  and  $m_w$  are zero.

TABLE 1. Constants in the Examples Chosen for Solution.

$A_1$	$3^\circ$	$10^\circ$	$20^\circ$
$\tau$	0.85	1.25	1.44
$k$	0.20	0.40	0.55
$\Theta_1$	$-7^\circ$	$+1.5^\circ$	$2.5^\circ$
$x_u$	0.04	0.04	-0.20
$x_w$	-0.15	-0.31	+0.50
$x_q$	—	—	—
$z_u$	0.30	0.50	1.1
$z_w$	1.75	1.75	0.35
$z_q$	1.49	1.39	0?
$m_u$	$\mp 0.003$	$\mp 0.012$	-0.45
$m_w$	$\pm 0.07$	$\pm 0.07$	1.00
$m_q$	1.9	1.6	0.4?
$m_{ic}$	0.9	0.72	0?

### A. The Complementary Function

**13. The Equations of Motion.** Writing the variables in the form  $u = u_1 e^{\lambda t}$ ;  $w = w_1 e^{\lambda t}$ ;  $q = q_1 e^{\lambda t}$ , where  $u_1, w_1, q_1, \lambda$  are constant. Replacing  $\Omega$  by  $A_1$  and making  $m_0$  zero leaves the equations of motion, see V (23.3) in the form

$$\left. \begin{aligned} (\lambda + x_u) u_1 + x_w w_1 + (\mu k \cos \Theta_1 \lambda^{-1} + \mu \sin A_1 + x_q) q_1 &= 0 \\ z_u u_1 + (\lambda + z_w) w_1 + (\mu k \sin \Theta_1 \lambda^{-1} - \mu \cos A_1 + z_q) q_1 &= 0 \\ m_u u_1 + \left( \frac{m_w}{\mu} \lambda + m_w \right) w_1 + (\lambda + m_q) q_1 &= 0 \end{aligned} \right\} \quad (13.1)$$

For reference later these will be written in the shortened form

$$\left. \begin{aligned} a_1 u_1 + b_1 w_1 + c_1 q_1 &= 0 \\ a_2 u_1 + b_2 w_1 + c_2 q_1 &= 0 \\ a_3 u_1 + b_3 w_1 + c_3 q_1 &= 0 \end{aligned} \right\} \quad (13.2)$$

Values of  $\lambda$  which satisfy these simultaneous equations are obtained by expanding the determinantal equation

$$\begin{vmatrix} a_1 & b_1 & c_1 \\ a_2 & b_2 & c_2 \\ a_3 & b_3 & c_3 \end{vmatrix} = 0 \quad (13.3)$$

to give a quartic equation for  $\lambda$  which we will write in the form

$$\lambda^4 + B\lambda^3 + C\lambda^2 + D\lambda + E = 0 \quad (13.4)$$

**14. The Quartic for  $\lambda$ .** The full expressions for the coefficients of this equation, together with their numerical values for the three conditions of flight represented in Table 1 are given in Table 2. The majority of the terms in these expressions are so small that they can safely be neglected in routine calculation, in which great accuracy of computation would be meaningless on account of the uncertainties in the numerical estimation of the derivatives upon which the calculation depends. The whole of the terms have, however, been included here to enable the reader, who contemplates proceeding with similar calculations, to ascertain at the start which terms are likely to be important and which he can regard as negligible.

The figures here tabulated cover the normal ranges of incidence and c.g. position used in flight, and since aeroplanes do not differ greatly from one another in their proportions, the figures in the tables, being in dimensionless form, are roughly representative of all aeroplanes of conventional design for which the value of  $\mu$  is in the neighborhood of 23.

**15. Information from Inspection of the Quartic for  $\lambda$ .** When the numerical values of the coefficients of this quartic equation are known, as for example, in the totals of Table 2, it is possible immediately, to



obtain some information about the nature of the motion to which it refers, without actually finding the roots of the equation or examining the effects of given initial conditions.

TABLE 2. Constitution of the Coefficients of the Quartic for  $\lambda$ .

B				C			
Incidence	3°	10°	20°	Incidence	3°	10°	20°
$x_u$	.04	.04	-.20	$x_u z_w$	.07	.07	-.07
$z_w$	1.75	1.75	.35	$-x_w z_u$	.04	.16	-.55
$m_q$	1.90	1.60	.4	$m_q z_w$	3.32	2.80	.14
$-m_w z_q/\mu$	-.06	-.04		$-m_w z_q$	$\mp .10$	$\mp .09$	.00
$+m_w \cos A_1$	.90	.70		$m_q x_u$	.08	.06	-.08
Total	4.53	4.05	.55	$\mu m_w \cos A_1$	$\pm 1.61$	$\pm 1.57$	21.35
D				$-\mu m_u \sin A_1$	$\pm .00$	$\pm .05$	3.51
Incidence	3°	10°	20°	$-k m_w \sin \Theta_1$	.02	-.01	
$m_q x_u z_w$	.132	.110	-.03	$m_w x_u \cos A_1$	.04	.03	
$-m_q x_w z_u$	.086	.250	-.22	$m_w z_u \sin A_1$	.01	.06	
$-\mu m_u x_w \cos A_1$	$\mp .010$	$\mp .084$	4.82	$-m_w x_u z_q/\mu$	.00	.00	
$\mu m_w x_u \cos A_1$	$\pm .064$	$\pm .063$	4.28	Stable	5.10	4.69	24.3
$z_q m_u x_w$	$\pm .001$	$\pm .005$		Neutral	3.59	3.17	
$-z_q m_w x_u$	$\mp .004$	$\mp .004$		Unstable	2.08	1.65	
$-\mu k m_u \cos \Theta_1$	$\pm .014$	$\pm .110$	5.68	E			
$-\mu k m_w \sin \Theta_1$	$\pm .039$	$\mp .017$	-.56	Incidence	3°	10°	20°
$\mu z_u m_w \sin A_1$	$\pm .024$	$\pm .136$	8.59	$-\mu k m_u z_w \cos \Theta_1$	$\pm .024$	$\pm .193$	1.98
$-\mu z_w m_u \sin A_1$	$\pm .006$	$\pm .082$	1.23	$\mu k m_w z_u \cos \Theta_1$	$\pm .096$	$\pm .321$	13.90
$k m_w z_u \cos \Theta_1$	.053	.142		$\mu k m_u x_w \sin \Theta_1$	.000	$\pm .001$	-.13
$-k m_w x_u \sin \Theta_1$	.001	.000		$\mu k m_w x_u \sin \Theta_1$	$\pm .002$	$\mp .001$	.11
Stable	.406	.793	15.23	Stable	$\mp .122$	$\mp .514$	15.87
Neutral	.272	.502		Neutral			
Unstable	.138	.218		Unstable	-.122	-.514	

If, in the equation  $\lambda^4 + B\lambda^3 + C\lambda^2 + D\lambda + E = 0$ , the coefficients are all positive, the solution can contain no real positive root and the motion to which it relates therefore contains no mode which increases continuously as an exponential function of time. If, in addition, the quantity  $BCD - D^2 - EB^2$ , known as *Routh's discriminant* (Ref. 1) is positive, no real part of any complex root is positive and the motion contains no oscillation which increases with time. Hence if all the coefficients and Routh's discriminant are positive and not zero, any disturbance from steady flight will eventually subside and the motion be completely stable. If the coefficient  $E$  becomes zero, one of the

roots is zero and there is one mode of motion which can continue indefinitely without change, so that the equilibrium is neutral. If Routh's discriminant is zero the motion contains an oscillation which can continue without change and the equilibrium is neutral in this special sense. If one of the coefficients or Routh's discriminant becomes negative, then there is present, respectively, either an increasing exponential term or an increasing oscillation and, in general, disturbances will increase until the condition of small displacement, implicit in the equation, ceases to apply.

16. Values of  $\lambda$  and of the Ratio  $u_1:w_1:q_1$ . We shall, however, proceed to solve the quartics indicated in Table 6 to find the values of the four roots<sup>1</sup>  $\lambda_1, \lambda_2, \lambda_3, \lambda_4$  and the corresponding ratios  $u_1:w_1:q_1, u_2:w_2:q_2, u_3:w_3:q_3, u_4:w_4:q_4$ , which are found by inserting the appropriate value of the root into any two of the three equations of motion and then eliminating  $u_1, w_1$  and  $q_1$  in turn. We shall use the first and third equations for this purpose because, in this manner, we shall have to deal with the fewest terms. The values found can then be inserted into the second equation to provide a useful check on the arithmetical accuracy of the solutions up to this stage; this has been done but the check figures are not here given.

The required ratios may be written

$$\frac{u_1}{b_1 c_3 - b_3 c_1} = \frac{w_1}{c_1 a_3 - c_3 a_1} = \frac{q_1}{a_1 b_3 - a_3 b_1}$$

Expand the denominators of these ratios and arrange in descending powers of  $\lambda$  as in the following scheme:

$$\left. \begin{array}{l} u: \quad B_u \lambda + C_u + D_u \lambda^{-1} \\ w: A_w \lambda^2 + B_w \lambda + C_w + D_w \lambda^{-1} \\ q: A_q \lambda^2 + B_q \lambda + C_q \end{array} \right\} \quad (16.1)$$

<sup>1</sup> Quartic equations with numerical coefficients and at least one pair of real roots are easily solved by trial and error as follows. Guess a value for the root; substitute this value for  $\lambda$  and work out the value of the expression  $\lambda^4 + B\lambda^3 + C\lambda^2 + D\lambda + E = \Delta$  (say). If this value is not zero, make a second guess which by inspection is expected to give a value more nearly zero. Plot  $\Delta$  against the guessed roots and draw a line through the two points to cut the axis of zero  $\Delta$ . If the original guess has been made with discrimination the abscissa at this point will closely approximate to one of the roots. As a check insert this new value in the quartic expression and plot as before; if the new point does not lie on the axis, draw a curve through the three points now available and produce, if necessary, to cut the axis. With a little practice, and particularly when solving series of quartics, two real roots, if they exist, can be discovered in this way with very little labour. Combining these into a quadratic expression and dividing into the quartic expression gives the other quadratic roots. The accuracy with which the first roots have been determined is indicated by the smallness of the remainder after this division. If there are no real roots it is necessary first to reduce the quartic to cubic form by methods which can be found in any treatise on algebra. One root of this cubic must be real and can be found as above.

TABLE 3. Quantities which Determine the Ratios Between the Variables.

$B_u$				$C_u$				$D_u$			
Incidence	3°	10°	20°	Incidence	3°	10°	20°	Incidence	3°	10°	20°
$x_w$	— .150	— .310	.5	$x_w m_q$	— .285	— .495	.20	$-\mu k m_w \cos \Theta_1$	$\mp .318$	$\mp .642$	$-12.6$
$-m_w \sin A_1$	— .045	— .122		$-\mu m_w \sin A_1$	$\mp .080$	$\mp .273$	— 7.81				
Totals	— .195	— .432	.5	$-k m_w \cos \Theta_1$	— .178	.288					
				Stable	— .543	— 1.06	— 7.61				
				Neutral	— .463	— .783					
				Unstable	— .383	— .510					
$B_w$				$C_w$				$D_w$			
Incidence	3°	10°	20°	Incidence	3°	10°	20°	Incidence	3°	10°	20°
$-x_u$	— .04	— .04	.20	$\mu m_u \sin A_1$	$\mp .003$	$\mp .047$	— 3.52	$\mu k m_u \cos \Theta_1$	$\mp .014$	$\mp .110$	— 5.68
$-m_q$	— 1.90	— 1.60	— .40	$-x_u m_q$	— .076	— .064	.08				
Totals	— 1.94	— 1.64	— .20	Stable	— .079	— .111	— 3.44				
				Neutral	— .076	— .064					
				Unstable	— .073	— .017					
$A_q$				$B_q$				$C_q$			
Incidence	3°	10°	20°	Incidence	3°	10°	20°	Incidence	3°	10°	20°
$m_w/\mu$	.039	.031	0	$m_w$	$\pm .072$	$\pm .070$	1.0	$x_u m_w$	$\pm .002$	$\pm .0028$	— .20
				$m_w x_u/\mu$	.000	.0013		$-x_w m_u$	.000	$\mp .0037$	.225
				Stable	$\pm .072$	$\pm .071$	1.0	Stable	$\pm .002$	— .0009	.025
				Neutral		$\pm .0013$		Neutral			
				Unstable	— .072	— .069		Unstable	— .002	$\pm .0009$	

$A_w = -1$

TABLE 4. The Ratios of the Variables in Each Mode.

			Incidence 3°			Incidence 10°			Incidence 20°		
			Stable		Neutral		Unstable		Stable		
Root	-- 2.7	-1.8	-.03 ± .15 i	- 3.54	-.91	-.084	0	-- .402	+.18	-.35 ± .22 i	
u:	1.10	0	-.15 ± .195 i	1.00	1.00	1.00	1.00	.370	-116.5	-.97 ± .45 i	
w:	-22.3	indef.	-.02 ± .20 i	-23.2	-3.04	-.18	-.18	-9.20	32.4	+.50 ± .28 i	
q:	1.0	0	-.001 ± .011 i	2.00	-.110	-.0003	0	1.00	1.00	-.03 ± .021	

			Stable		Neutral		Unstable		Stable		
Root	-2.0 ± .55 i	-.036 ± .34 i	-3.07	-.77	-.21	0	-3.62	+.36	-.40 ± .47 i		
u:	.103 ± .153 i	-.847 ± 1.70 i	1.0	1.0	1.0	1.0	1.0	1.0	-1.01 ± 1.00 i		
w:	-.480 ± 1.29 i	.098 ± .22 i	-7.72	-1.33	-.349	-.284	-8.33	-.410	.58 ± .53 i		
q:	-.027 ± .029 i	-.0071 ± .024 i	.53	-.038	-.0016	0.00	.750	-.018	-.026 ± .044 i		

where the coefficients  $B_u$ ,  $C_w$  etc. contain the derivatives, etc. The forms of these coefficients, together with their numerical values in the various circumstances chosen for illustration are shown in Table 3. As before the  $\pm$  sign before any term shows that its value must be taken as positive, zero or negative, according as the stable, neutral, or unstable condition is under consideration. The upper sign relates to the stable condition.

From Table 3 it is possible to obtain some idea of the importance of any particular term or derivative, in determining the ratios in which the variables occur in any particular mode, remembering, of course, that the  $A$  and  $B$  coefficients are the more important in relation to rapidly changing modes in which  $\lambda$  is large, whilst the  $C$  and  $D$  coefficients are the more important in slowly changing modes of motion, in which  $\lambda$  is small.

When the numerical values of the roots  $\lambda_1$ ,  $\lambda_2$ ,  $\lambda_3$ ,  $\lambda_4$  etc. are inserted in (16.1), using the appropriate values of the coefficients, given in Table 3, the ratios appropriate to each root are found; these are set out in Table 4. When the roots are real the numbers taken from (16.1) have been divided by a common factor in order to reduce one of them to unity.

The meaning of the complex ratios, associated with the complex roots, has been explained in V 30. It will be recalled that, writing the complex quantities tabulated in the form  $\mu + i\nu$ , the relative amplitudes of the oscillations of the three independent variables are in the ratio indicated by the values of  $\sqrt{\mu^2 + \nu^2}$  and the relative phases differ by the angles  $\tan^{-1} \nu/\mu$ .

The equations of motion have now been completely solved in general terms. They consist of exponential and oscillatory terms, or modes of motion, with known exponents and frequencies and with known ratios between the variables of each mode. The separate modes are, however, entirely independent and can be combined in any proportions whatever without violating the equations of motion. There are, in fact, four arbitrary constants at our choice, so that the modes can be combined in a way to suit any four arbitrary initial conditions.

## B. Complete Solutions and Initial Conditions

**17. Choice of Initial Conditions.** To complete the illustration the arbitrary constants have been computed to fit three different initial conditions as follows:

a) An initial value of  $u$  equal to  $u_0$  which may be visualized as occurring when the aeroplane, flying steadily, passes suddenly into a gust, blowing parallel to the  $X$  axis, which increases the velocity parallel to the  $X$  axis by an amount  $u_0$ . Alternatively the aeroplane may be conceived to have experienced a forward impulse which changes the speed parallel to the  $X$  axis by this amount.

Cruising Speed ( $k_L = 0.2$ ). Incidence =  $3^\circ$ .

TABLE 5. Complete Solutions with Given Initial Conditions.

	Initial $u_0$				Initial $w_0$				Initial $m_0$				
	$u/u_0$	$w/u_0$	$q/u_0$	$\theta/u_0$	$u/w_0$	$w/w_0$	$q/w_0$	$\theta/w_0$	$u/m_0$	$w/m_0$	$q/m_0$	$\theta/m_0$	
$e^{-2.7t}$	-.01	.126	-.0057	.0021					—	9	188	—	3.2
$e^{-1.8t}$		-.020				1.00				—	292		
$e^{-.03t} \cos .155t$	1.01	-.106	.0057	-.0021					1511	—	160	8.5	—25.0
$e^{-.03t} \sin .155t$	-.16	-.018	.0008	.0364					380	—	38	2.3	50.5
1.0									—1502	264			21.8
$e^{-3.54t}$	—	.051	.0044	.0012	-.01	.31	-.026	.0076	—	3	63	—	1.5
$e^{-.91t}$	—	.004	.0048	-.0053	-.24	.74	.027	-.0294	62	—	187	—	7.4
$e^{-.084t}$	1.049	-.187	-.0003	.0040	1.37	-.25	-.001	.0048	—8134	1444	2.5	—	30.6
1.0	—	.003		.0001	—1.12	.20		.0174	8075	—1320	9.7		21.7
$t$									649	114			9.7
$e^{-4.02t}$	—	.001	-.0036	.001	-.015	.358	-.039	.010	—	1	38	—	1.0
$e^{+.18t}$	.425	-.118	-.0036	.020	-.372	.104	.003	.018	—	932	258	8.0	44.4
$e^{-.35t} \cos .22t$	.577	.085	.0072	.019	.387	.538	.036	-.028	—	571	—	32	—
$e^{-.35t} \sin .22t$	.598	-.443	-.027	.064	1.48	-.631	-.037	.121	—	476	403	24.6	—55.7
1.0									1504	—	264		—22.0

Slow Speed ( $k_L = 0.4$ ). Incidence =  $10^\circ$ .

TABLE 5 (Continued).

	Initial $u_0$				Initial $w_0$				Initial $m_0$				
	$u/u_0$	$w/u_0$	$q/u_0$	$\theta/u_0$	$u/w_0$	$w/w_0$	$q/w_0$	$\theta/w_0$	$u/m_0$	$w/m_0$	$q/m_0$	$\theta/m_0$	
$e^{-2.0t} \cos .55t$	-.003	.128	-.013	.0058	-.147	1.018	-.0017	.0049	28	- 118	- 8.5	2.9	Stable
$e^{-2.0t} \sin .55t$	.062	-.443	.002	-.0028	-.026	.447	-.0320	.0147	47	- 392	- 8.1	- 4.9	
$e^{-.036t} \cos .34t$	1.003	-.128	.013	-.0058	.147	-.018	.0017	-.0049	697	- 87	8.5	-12.7	
$e^{-.036t} \sin .34t$	-.120	.009	.001	.0372	.095	-.013	.0015	.0043	159	- 24	3.5	23.4	
1.0									- 725	205		9.8	Neutral
$e^{-3.07t}$	-.014	.108	-.0074	.0024	-.047	.362	-.025	.0081	- 9	68	- 4.7	1.5	
$e^{-.77t}$	-.252	.335	.0096	-.0125	-.736	.980	.028	-.0366	334	- 445	-12.8	16.7	
$e^{-.21t}$	1.282	-.448	-.0021	.0099	1.810	-.635	-.003	-.0139	-4474	1559	7.3	-34.2	
1.0					1.028	.293		-.0146	4150	- 1182	10.2	16.0	Unstable
$t$	-.016	.005		.0002					- 728	207		10.2	
$e^{-3.62t}$	-.007	.064	-.0056	.0016	-.050	.418	-.038	.0104	- 5	42	- 3.8	1.0	
$e^{+.36t}$	.339	-.138	-.0062	-.0170	-.314	.129	.006	.0157	- 393	160	7.1	19.6	
$e^{-4.0t} \cos .47t$	.668	.074	.0117	.0154	.364	.444	.032	-.0261	- 327	4	- 3.3	-10.7	Stalled Flight. $k_L = 0.55$ . Incidence = $20^\circ$ .
$e^{-4.0t} \sin .47t$	.164	-.405	.0220	.0373	.813	-.241	-.006	.0451	- 10	180	11.5	-15.9	
1.0									725	- 206		- 9.9	
$e^{-.048t} \cos 4.87t$	.119	-.420	-.041	-.021	-.355	.865	-.027	.043	8.4	-20.8	.53	- 1.03	
$e^{-.048t} \sin 4.87t$	.167	-.170	.101	-.008	-.167	.115	-.208	-.006	4.2	2.2	5.0	.12	Stalled Flight. $k_L = 0.55$ . Incidence = $20^\circ$ .
$e^{-.323t} \cos .75t$	.882	.420	.041	.021	.355	.136	.027	-.043	- 2.2	0.1	- .53	1.93	
$e^{-.323t} \sin .75t$	-.435	-.164	-.036	.063	.584	.281	.026	-.018	-28.5	-13.1	- 1.50	- .12	
1.0									- 6.2	20.7		- .90	

b) An initial value of  $w$  equal to  $w_0$  corresponding to sudden passage into an up current of strength  $w_0$  flowing parallel to the  $Z$  axis. A fairly close approximation to this disturbance is a common experience in flight. Such a disturbance is colloquially described as a "bump", for reasons which will appear when the resulting motion is examined.

c) A sudden change of elevator angle sufficient to generate an unbalanced pitching moment represented by  $m_0$ .

**18. Complete Solutions in Dimensionless Form.** The numerical computations involved in finding the arbitrary constants to fit these initial conditions are heavy, they involve amongst other things, the solution of four simultaneous equations with four variables. The processes have been described in detail in V 28 *et seq.*, so that no useful purpose will be served by reproducing the elaborate arithmetic. Checks can easily be provided at various stages of the computation, by substituting back in the equations etc. and observing the precision with which they are satisfied.

Table 5 gives the coefficients of the various terms in the solutions for the three chosen types of disturbance in each of the seven conditions for which the equations have been solved.

To find from this table the form of the disturbance following any given initial disturbance the appropriate numbers are multiplied by the expressions on the extreme left of the row in which they lie and the separate terms applying to any given component of the motion are added together. For example, the component of the motion following a sudden elevator movement which produces a pitching moment represented by  $m_0$  on the neutral aeroplane flying at  $3^\circ$  incidence is given by

$$\frac{\theta}{m_0} = 1.5 e^{-3.54 t} + 7.4 e^{-.91 t} - 30.6 e^{-.084 t} + 21.7 + 9.7 t$$

The effect of two or more disturbing causes acting simultaneously is, of course, obtained by adding appropriate expressions.

**19. Conditions to which the Solutions Apply.** In the dimensionless form here adopted these solutions apply equally to all aeroplanes of the same external shape as the one chosen for examination, provided that the inertia coefficient ( $k_B$ ) and the similarity criterion ( $\mu$ ) are the same. The designer generally strives to keep  $k_B$  as low as he can and, as a matter of fact, it does not, at the present time, differ very greatly from one aeroplane to another.

The similarity criterion ( $\mu = m/\rho S c$ ) is proportional to the loading of the wings per unit area ( $mg/S$ ) and inversely proportional to the wing chord ( $c$ ). The value  $\mu = 23$ , used in these computations was, as already mentioned, from the Bristol Fighter aeroplane, for which the wing loading was 7.6 lb. per sq. ft. and the mean chord 5.17 ft. Wing loading and chord might both be twice as large as these in a modern



civil transport aeroplane and half as large as these in a light glider. In either type, therefore  $\mu$  would remain in the neighborhood of the value (23) used in the illustration. On the other hand a racing aeroplane or small military pursuit aeroplane might have wing chord less than above, with wing loading of the order 20 lb. per sq. ft., so that  $\mu$  would be roughly four times as great as here assumed. A very heavily loaded small pilotless aeroplane might have  $\mu$  even higher than this.

It will also be observed on inspecting Table 2 that, with the exception of some entirely unimportant terms containing  $m_{\dot{w}}$ ,  $\mu$  only occurs as a multiplier of the derivatives  $m_{\dot{w}}$  and  $m_u$  which are themselves proportional to the metacentric ratio ( $H$ ). This confirms the conclusion reached by more approximate methods in IV 22 that two similar aeroplanes, flying with different values of  $\mu$ , will behave, as regards small symmetric disturbances from steady flight, in a similar manner, provided that the product  $\mu H$  is the same for both. In particular the behaviour of aeroplanes which are statically neutral ( $H = 0$ ) will be sensibly independent of  $\mu$ . Table 4 shows however that if  $\mu$  is altered keeping  $\mu H$  constant, the ratios of the velocities  $u$  and  $w$  to the angular velocity  $q$  will be altered, since  $m_w$  and  $m_u$  are proportional to  $H$ .

The derivatives themselves depend on the shape of the aeroplane, but the four force-velocity derivatives  $x_u$ ,  $x_w$ ,  $z_u$ ,  $z_w$  remain substantially the same for all wings working at the same lift coefficient, provided that the coefficient is not too near the stalling value. The moment derivatives depend primarily upon the quantity  $S'l/Sc$  which defines the size and leverage of the tail, and upon the inertia coefficient ( $k_B$ ). At the time of writing neither of these factors vary widely upon conventional aeroplanes so that, in so far as their broader features are concerned, the dimensionless solutions of Table 5 apply, in a general way, to the majority of modern aeroplanes.

**20. The Solutions Discussed.** In the *stable* condition at  $3^\circ$  incidence the motion following an initial disturbance to the velocity components  $u$  or  $w$  contains two terms which decrease exponentially and very rapidly with time, and to these is added an oscillation which decreases relatively slowly. Bearing in mind the fact that  $\tau$  is generally of the order unity so that  $t$  does not differ very greatly from time in seconds, it is apparent that the two exponential terms sensibly disappear within about one second, leaving nothing but the damped oscillation. This is shown graphically in Fig. 56 m, to which we shall refer later. When, however, the disturbance takes the form of a suddenly applied constant pitching moment, represented by  $m_0$ , a uniform motion, in which the aeroplane travels in a new direction and is displaced through a definite angle of pitch from the original orientation, is added to the terms which decrease progressively with time, so that, in the course of time, the aeroplane settles down to steady motion with this new direction and orientation.

In the *neutral* condition the motion following a disturbance in the form of an initial velocity involves three exponentially decreasing terms and one steady motion. The aeroplane is displaced from its original steady motion and, being neutral, takes up a new steady motion from which it never returns to the original motion. An application of the elevators to a neutral aeroplane is seen to cause a response which ultimately settles down to a uniform pitching rotation with steady rates of change both of velocity components and of orientation.

In the case of the *unstable* aeroplane the important term is the exponential with positive exponent, for this term increases indefinitely with time and eventually dominates all the others. Any motion of this aeroplane which starts from a very small disturbance will, in time, contain nothing appreciable in comparison with this latter term.

At  $10^\circ$  incidence the motion is of the same general character as at  $3^\circ$  incidence, with the exception that the expression for the stable aeroplane now contains two damped harmonic terms. One of these is, however, so heavily damped that it is almost indistinguishable from a pair of decreasing exponentials—the difference in the forms of the solutions is thus more apparent than real.

On the *stalled* aeroplane the solutions are of an entirely different form, containing one rapid and almost undamped oscillation and one rather heavily damped oscillation of moderate period. The most important differences between the symmetric motion of stalled and unstalled aeroplanes will, however, be considered later (29). It should be noted that these solutions for the stalled aeroplane cannot, like the solutions for the unstalled aeroplane, be regarded as representative of the majority of conventional aeroplanes, because the derivatives near the stalling incidence are delicately dependent on the shape of the wing section and differ widely from one aeroplane to another.

**21. Conversion to Ordinary Units.** The dimensionless solutions require to be expressed in ordinary units before they can be conveniently interpreted in terms of any specific aeroplane flight. To do this it is necessary to know the quantities  $\mu$ ,  $c$ ,  $\tau$ . The conversion is easily affected by observing that

$$u = \frac{c}{\tau} \bar{u}; \quad w = \frac{c}{\tau} \bar{w}; \quad q = \frac{1}{\tau} \bar{q}; \quad k_{m0} = k_B m_0$$

where,  $u$ ,  $w$  and  $q$  represent quantities expressed in the same units as  $c$  and  $\tau$  whilst  $k_{m0}$  represents the conventional coefficient ( $M_0/\rho V_1^2 S c$ ) of the moment ( $M_0$ ) exerted by the controls.

From these we have

$$\begin{aligned} \frac{u}{u_0} &= \left( \frac{\bar{u}}{\bar{u}_0} \right); & \frac{q}{q_0} &= \frac{1}{c} \left( \frac{\bar{q}}{\bar{q}_0} \right); & \frac{\theta}{\theta_0} &= \frac{\tau}{c} \left( \frac{\bar{\theta}}{\bar{\theta}_0} \right) \\ \frac{u}{k_{m0}} &= \frac{c}{\tau k_B} \left( \frac{\bar{u}}{\bar{m}_0} \right); & \frac{q}{k_{m0}} &= \frac{1}{\tau k_B} \left( \frac{\bar{q}}{\bar{m}_0} \right); & \frac{\theta}{k_{m0}} &= \frac{1}{k_B} \left( \frac{\bar{\theta}}{\bar{m}_0} \right) \end{aligned}$$

The corresponding expressions which include  $w$  have not been given because they are of the same form as those which include  $u$ .

Times, in Table 5 are expressed in dimensionless form, as ratios to the time unit ( $\tau$ ). Therefore  $t = t/\tau$ , where  $t$  is expressed in the same units as  $\tau$ , e.g. in seconds.

For example, the value of  $\tau$  for the flights at  $3^\circ$  incidence—cruising speed—is 0.85 seconds; the expression at the head of the first column of Table 5 changes, therefore, from  $e^{-2.7 t}$  in the dimensionless system to  $e^{-2.7 t/0.85} = e^{-3.2 t}$ , when  $t$  is expressed in seconds.

**22. The Solutions In Terms of Other Variables.** The variables  $u$ ,  $w$ ,  $q$  completely define the motion, but they may not conveniently display the particular aspect of the motion which is under consideration.

Formulae for some of the more interesting variables dependent on  $u$ ,  $w$ ,  $q$ ,  $\theta$  are stated below.

The variation ( $\alpha$ ) of the incidence from that of steady flight ( $A_1$ ) is  $\alpha = -\frac{1}{V_1} [w \cos A_1 - u \sin A_1]$ , see 4.

The variations in the direction of the resultant velocity from the direction of steady flight are ( $\theta - \alpha$ ).

The variation ( $dV$ ) in the magnitude of the resultant velocity ( $V$ ) is  $dV = u \cos A_1 + w \sin A_1$ , see 4.

The variations in the horizontal and vertical component of the aeroplane's velocity are of interest in relation to the problem of landing. If these components be  $\bar{U}$  and  $\bar{W}$  and their variations  $\bar{u}$  and  $\bar{w}$  if, as before, dashed letters represent the values in steady flight, then, remembering that positive velocities are downward

$$\bar{U} = U \cos \Theta + W \sin \Theta; \quad \bar{W} = -U \sin \Theta + W \cos \Theta$$

Differentiating,

$$\bar{u} = (-U_1 \sin \Theta_1 + W_1 \cos \Theta_1) \theta + u \cos \Theta_1 + w \sin \Theta_1$$

$$\text{or} \quad \bar{u} = \bar{W}_1 \theta + u \cos \Theta_1 + w \sin \Theta_1$$

$$\text{Similarly,} \quad \bar{w} = -\bar{U}_1 \theta + w \cos \Theta_1 - u \sin \Theta_1$$

Another quantity of interest is the acceleration perpendicular to the  $X$  axis, for this determines the apparent weight of parts of the aeroplane and pilot. This acceleration is equal to  $-\dot{w} + U_q$ .

**23. Graphs of the Solutions Plotted Against Time.** The most convenient way of showing the form of the motion which follows any given initial disturbance is to plot the expression for the motion deduced from Table 5 against time expressed in seconds. Table 5 enables any desired aspect of the motion for any initial disturbance involving change of velocity or angular displacement, or both, to be plotted in this way, without additional computation other than that necessary to express the various quantities in terms of the desired units and in relation to specific

values of  $c$  and  $\tau$ . The reader who is sufficiently interested can plot for himself any desired component of the motion following any desired disturbance<sup>1</sup>. It will be found interesting to use various time scales; an open scale to show the rapid changes which occur in the first second and a closer scale to show the subsequent development of the motion.

From what has been said it will be clear that from graphs plotted from Table 5 a good idea can be obtained of the motion of any aeroplane in a wide variety of circumstances following the application of any initial disturbing velocity or angular displacement, provided only that  $\mu H$  and  $k_H$  do not depart too widely from the assumed values and that the aeroplane is not of an excessively unconventional form.

As an illustration we shall plot the variations with time of the two variables  $\theta$  and (acceleration/ $g$ ), of which the former shows how the motion appears to the pilot whilst the latter shows how it feels to him. The variation of these quantities, expressed in foot second units, for the aeroplane specified in 9 are plotted in Fig. 56 (a to r).

### C. The Graphs Discussed

**24. Introductory.** The curves relating to normal flight have been arranged in groups of three, each group relating to the effects on one variable, at one incidence, of some one disturbance. The three curves in each group relate respectively to the stable, neutral and unstable c.g. positions, and are distinguished by the letters  $S$ ,  $N$ ,  $U$ . The effects of a redistribution of load, which moves the c.g. forward or backward without altering any of the other properties, are thus conveniently displayed.

**25. Cruising Speed—Elevator Movement.** Figures 56a and b show the extreme sensitivity to elevator control of the aeroplane flying at its cruising speed. During the first one or two seconds the response to elevator movement is almost uninfluenced by change of c.g. position, but at four seconds the changes of  $\theta$  and of acceleration on the unstable aeroplane are about double the values in the stable case. After some four seconds from the start the response is radically different in the three cases. Figure 56m represents the same condition as Fig. 56a but with a closer time scale and it shows that the stable aeroplane oscillates with

<sup>1</sup> If great accuracy is not required, a convenient way of plotting an exponential term such as  $Ae^{\lambda t}$  is to note that, if  $\lambda$  is positive, it doubles itself every  $0.7/\lambda$  seconds, or if  $\lambda$  is negative, halves itself in this same time. The damped harmonic modes are more complicated to plot; the quickest way for a rough plot, which is all that is generally required, is as follows. Suppose that the mode to be plotted is  $e^{\xi t} A \cos \eta t$ . Draw the exponential curves  $Ae^{\xi t}$  and  $-Ae^{\xi t}$ ; mark on them points corresponding to  $t = n\pi/\eta$ , where  $n$  has values 1, 2, 3 etc; then draw by eye harmonic curves which touch the exponential curves at the appropriate points. Finally, having drawn the curves representing the various modes, add their ordinates together at convenient points to get the complete motion.

decreasing amplitude about a mean position in which the nose is raised some  $2^\circ$  above the attitude when the controls were applied. The neutral aeroplane continues to pitch at a constant rate and the unstable aeroplane to pitch at an increasing rate. These two latter motions continue until the disturbances become so large that the assumptions upon which the calculations are founded cease to be even approximately correct.

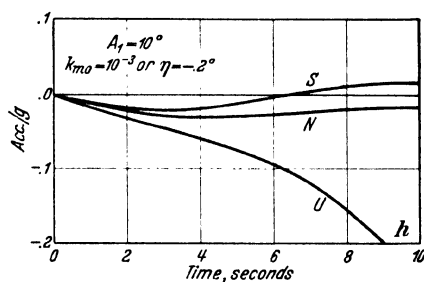
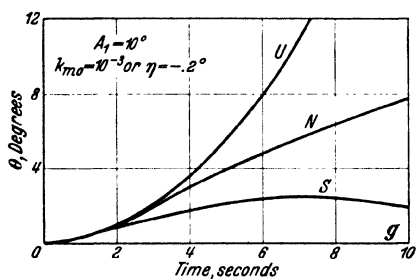
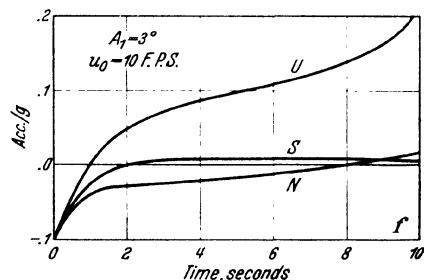
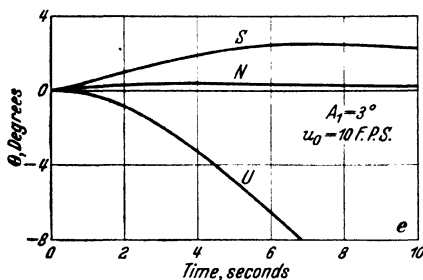
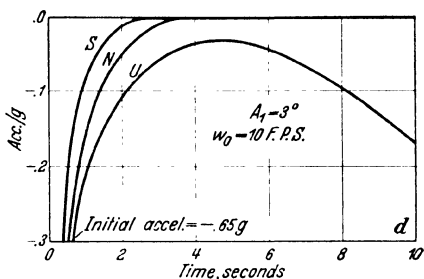
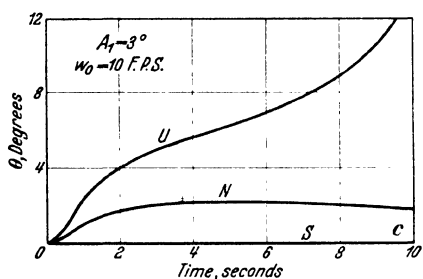
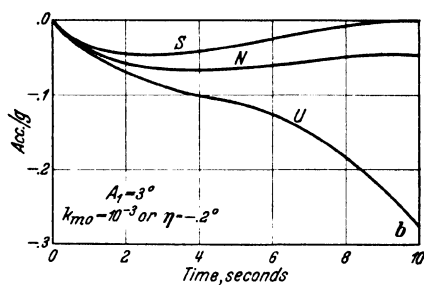
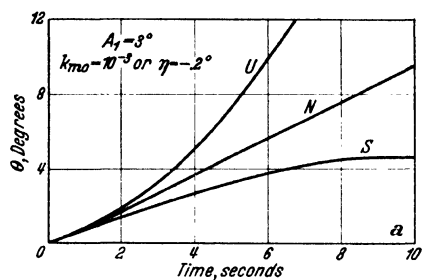
**26. Cruising Speed—Vertical Gust.** Figures 56c and d show the effect of flying into a gust of 10 ft. per sec., perpendicular to the general direction of motion. It may at first sight seem surprising that the effect of such a gust on  $\theta$  should be zero on a stable aeroplane and positive on a neutral aeroplane. This apparent anomaly is due to the derivative  $m_w$ , which allows a pitching moment to act on the neutral aeroplane before it begins to rotate and which, by an accidental combination of the values of the derivatives, neutralizes the effect of the static stability derivative  $m_w$  of the stable aeroplane.

The stable aeroplane, struck by a gust of this type, behaves in the same manner as the neutral aeroplane would do if  $m_w$  were absent. That is to say it is displaced upwards or downwards, without any change of attitude, whilst the  $w$  component dies away exponentially. It happens that during this exponential decay the  $m_w$  term exactly balances the  $m_w$  term. References to Fig. 56i will show that at  $10^\circ$  incidence this exact balance does not occur, although the curves are of the same general type as those for the lower incidences.

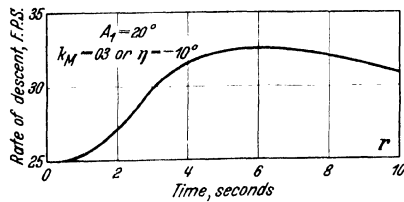
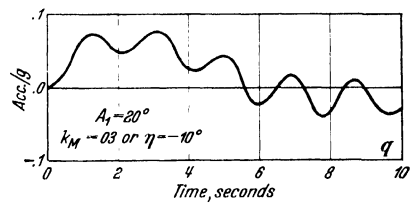
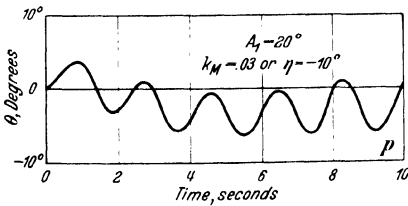
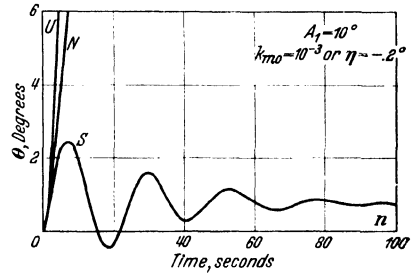
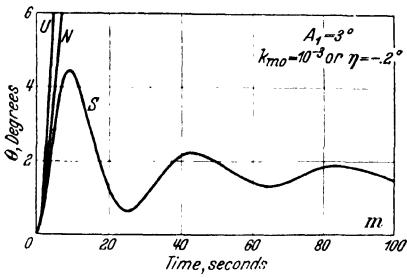
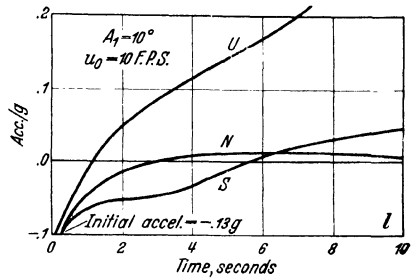
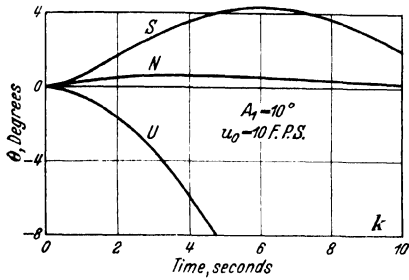
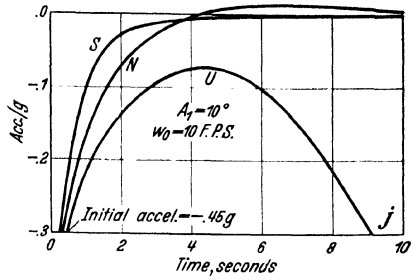
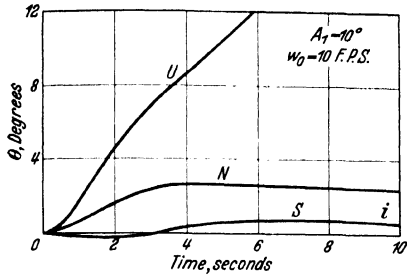
The acceleration due to the  $w$  gust is at first very large and provides what the pilot describes as the *bump* which he feels in *bumpy weather*. This acceleration falls off very rapidly to zero on the stable and neutral aeroplane and nearly to zero on the unstable aeroplane. In the last case, however, the acceleration eventually increases again as the instability makes itself felt.

**27. Cruising Speed—Horizontal Gust.** Figures 56e and f show the effect of a gust ( $u_0$ ) parallel to the  $X$  axis. The initial acceleration is much less than that due to the  $w$  gust. It is interesting to note, that, while a head on gust throws up the nose of a stable aeroplane, it causes an unstable aeroplane to dive downwards, although, of course, the first effect in every case must be to make the whole aeroplane rise slightly.

**28. Slow Speed—Unstalled.** Figures 56g to l and n, relating to slow unstalled flight, are of similar type to the diagrams relating to flight at cruising speed. The response to elevator movement is of the same order of magnitude as at cruising speed, though somewhat less in amount, both in respect of acceleration and pitching motion. The response to gusts, on the other hand, is somewhat greater, with the exception that the acceleration immediately following the onset of the  $w$  gust at the low speed is less than at the high speed. This is in accordance with normal



Figs. 56a—r. Graphs of the Disturbed



Symmetric Motion of an Aeroplane.

piloting experience; an aeroplane flying in rough weather, at low speeds, wallows about more than at high speed, but does not experience such hard bumps.

**29. Stalled Flight.** Figures 56p, q, and r relate to disturbances from steady stalled flight at  $20^\circ$  incidence. At this incidence the derivatives are rather uncertain quantities, since they depend upon the manner in which the flow-changes, characteristic of the stall, occur. The curves reproduced do not therefore, represent the motion of the real aeroplane with anything like the same precision as in normal flight, nor can the curves for one aeroplane be regarded as typical of all others. The study of the stability of stalled flight is still a matter of active research and the curves of Figs. 56, p, q and r are therefore advanced with considerable reserve; more as exercises in the solution of the equations, than as predictions of the movements of a particular aeroplane. For example, the undamped oscillation of short period does not, apparently, occur on the Bristol Fighter, but this need cause no surprise because a relatively slight increase in the derivative  $m_q$  which is only known approximately, would cause the oscillation to be rapidly damped out. Also the derivative  $z_q$ , which may be important, was omitted from the equation, because so little is known about it.

Despite these uncertainties the curves show some features of interest concerning stalled flight, which are in agreement with experience. Thus a movement of the elevators through  $10^\circ$  produces an acceleration of the same order as a movement of  $0.2^\circ$  in normal flight. The aeroplane is thus some 50 times as sensitive to its elevators in normal flight as in stalled flight, the reason being, of course, that in stalled flight it is very stable statically and the wing lift is nearly independent of incidence. What response there is to the elevators is in the wrong direction—pulling the stick back causes the aeroplane to descend faster.

Figure 56r shows how small and slow in developing is the change in vertical velocity following a large elevator movement. When it is necessary to reduce the downward velocity of a stalled aeroplane to zero—say with the object of landing without a bump—the stick must first be pushed forward, and held there till the aeroplane gathers speed and unstalls; it can then be pulled back to increase the wing lift. This process cannot be conveniently followed by the methods of the present chapter, since it requires finite velocity changes sufficient to alter the flow about the wings from the stalled to the unstalled state.

#### D. Approximations Applicable to Normal Flight Only

**30. Statement of the Problem.** When it is required to carry the solutions of the equations of motion through to the stage at which the response of the aeroplane to any given disturbance can be computed,



the process is, as the reader will have observed, very laborious. It will also have been observed that many of the terms included in the general solutions given earlier in this chapter, are numerically insignificant. It was considered expedient to give the solutions fully in order to allow the reader to see for himself which terms are negligible in any given circumstances and because, when the process of fitting solutions to initial conditions is contemplated, the labour involved is in any case so great that the extra labour of including some unnecessary terms in the coefficients of the quartic is relatively unimportant.

Though the process which has been developed earlier in this chapter will, if worked correctly, give the final answer required, it is so involved that it is not easy to trace the connection between the final answer and the separate characteristics of the aeroplane which are represented by the various derivatives included in the equations of motion. When the design of an aeroplane has been completed and it is desired to know what that aeroplane will do in given circumstances, this defect in the process of calculation may not be of great importance and it may then be reasonable to face the labour of carrying through the complete calculation with the highest accuracy practicable. When, however, it is desired merely to make a survey of the influence of given characteristics of an aeroplane upon its stability in flight, without proceeding to the study of the response to specific disturbance, it is of great importance to be able to trace the connection between individual characteristics and the resultant motion.

With regard to the response to specific disturbances no convenient means of tracing this connection has yet been devised; but when, as is more usual, the form of the solution of the quartic for  $\lambda$  in normal flight is all that is required, the omission of certain terms, which are then relatively unimportant, allows such drastic simplifications to be made, that the relation between cause and effect can be displayed with comparative ease. To this aspect of the problem we shall now direct attention.

**31. The Quartic of  $\lambda$ .** Reference to Table 2 will show that in normal flight—below  $10^\circ$  incidence—on stable or neutral aeroplanes,  $B$  and  $C$  are of the order 4, whilst  $D$  and  $E$  are less than 0.5. In these circumstances the solutions contain two large roots which are only slightly influenced by  $D$  and  $E$  and are therefore approximately the same as the roots of  $\lambda^2 + B\lambda + C = 0$ .

An approximation to the small roots can then be found as follows: Let the two quadratic factors be written

$$(\lambda^2 + B'\lambda + C') (\lambda^2 + b'\lambda + c')$$

Expanding and comparing with the original quartic gives

$$B' + b' = B; \quad C' + B'b' + c' = C; \quad B'c' + C'b' = D; \quad C'c' = E$$

As a first approximation write  $C' = C$  and  $B' = B$  and neglect terms containing small letters in comparison with those containing large letters only. This approximation gives

$$c' = \frac{E}{C} \quad \text{and} \quad b' = \frac{CD - EB}{C^2}$$

A second approximation can be obtained, if desired, by using these values of  $b'$  and  $c'$  to obtain more accurate values of  $B'$  and  $C'$  and repeating the process. This second approximation is, however, rarely used.

If, in Routh's discriminant ( $BCD - D^2 - EB^2$ ) the term  $D^2$  is neglected, the discriminant can be written  $B(CD - EB)$ . Comparing this with the approximation for  $b'$  we infer that when the sign of Routh's discriminant for a conventional aeroplane in normal flight passes from positive to negative, the slow period oscillation represented by the small quadratic root begins to increase with lapse of time.

A comparison between the correct solutions of the quartics, given in Table 3, with the solutions of the same quartics obtained by these approximate methods is of interest and is given in Table 6.

TABLE 6. Comparison Between Approximate and Correct Roots of the Quartic for  $\lambda$ .

			$\lambda_1$	$\lambda_2$	$\lambda_3$	$\lambda_4$
Incidence $3^\circ$	Stable	correct	-2.67	-1.80	-.030 $\pm$	.15 $i$
		approx.	-2.36	-1.96	-.029 $\pm$	.15 $i$
	Neutral	correct	-3.54	-.91	-.084	0
		approx.	-3.50	-1.02	-.076	0
Incidence $10^\circ$	Stable	correct	-1.99 $\pm$	.55 $i$	-.036 $\pm$	.34 $i$
		approx.	-2.02 $\pm$	.77 $i$	-.037 $\pm$	.33 $i$
	Neutral	correct	-3.07	.77	.21	0
		approx.	-2.98	-1.06	-.16	0

At cruising incidence the agreement is reasonably good, but it begins to fail at slow speeds— $10^\circ$  incidence—particularly in the neutral case. At  $10^\circ$  the incidence is a little too high for approximate methods to be applied with confidence, but it is to be noted that even at this incidence the most important item from the practical point of view, the slow motion, is given correctly for the stable condition and, although there is some discrepancy in  $\lambda_3$  for the neutral conditions, the critical change from stability to instability, defined by  $E$  zero, is necessarily given correctly.

**32. Equations of Motion Referred to Wind Axes.** For the purpose of approximate study at low incidences it is convenient to use axes in which  $OX$  is parallel to the direction of motion in steady flight, rather than *chord axes* which were used for the more detailed calculation. The former will be described as *wind axes*.

Referred to wind axes in which  $\Omega$  is zero, the equations of motion, after expressing the variables in terms of exponentials of the form  $u_1 e^{\lambda t}$  etc. and neglecting  $x_q$  and  $z_q$  become:

$$\begin{aligned} (\lambda + x_u) u_1 + x_w w_1 + \mu k \cos \Theta_1 \lambda^{-1} q_1 &= 0 \\ z_u u_1 + (\lambda + z_w) w_1 + (-\mu + \mu k \sin \Theta_1 \lambda^{-1}) q_1 &= 0 \\ m_u u_1 + \left( \frac{m_w}{\mu} \lambda + m_w \right) w_1 + (\lambda + m_q) q_1 &= 0 \end{aligned}$$

$\Theta_1$ , the angle made by the  $X$  axis with the horizontal is now the angle of climb or glide as the case may be.

**33. Gliding Flight—Engine Off.** When gliding with engine off  $\Theta_1$  is negative and numerically equal to the gliding angle, to which we give the symbol  $\gamma$ . Hence  $\Theta_1 = -\gamma$ . Unless the speed is very high  $\gamma$  will not be large and  $\cos \gamma$  may safely be taken as unity.

With the elevator held fixed and the engine off,  $m_u$  is necessarily zero; because  $M$  is zero in steady flight and change of forward velocity alone cannot alter  $M$ .

Since the angle between the  $X$  axis and the direction of motion in steady flight is now zero and since  $k_D$  in normal flight is negligible in comparison with  $dk_L/d\alpha$  we have

$$x_u = 2k_D; \quad z_u = 2k_L; \quad x_w = \frac{dk_D}{d\alpha} - k_L; \quad z_w = \frac{dk_L}{d\alpha}$$

For the present purpose it will be sufficiently accurate to assume that  $k_D$  can be expressed in the form (constant) + (constant)  $k_L^2$  so that we may write  $dk_D/dk_L = ck_L$ , where  $c$  is constant.

$$\text{From (6.1),} \quad m_w = \frac{dk_L}{d\alpha} \frac{H}{k_B}$$

where  $k_B$  is the inertia coefficient and  $H$  is the metacentric ratio. Also

$$m_q = -\frac{k_{mq}}{k_B} \quad \text{and approximately} \quad m_w = \frac{d\varepsilon}{d\alpha} m_q, \text{ see (8.2).}$$

For brevity we shall write  $dk_L/d\alpha = a$  and  $-k_{mq} = f$ . We shall treat  $a$  and  $f$  as constants, independent of incidence and we shall assign the value  $1/2$  to  $d\varepsilon/d\alpha$ .

Using these approximations and definitions we have

$$\left. \begin{aligned} x_u &= 2k_D; & x_w &= -(1-c)k_L; & x_q &= 0 \\ z_u &= 2k_L; & z_w &= a; & z_q &= 0 \\ m_u &= 0; & m_w &= \frac{aH}{k_B}; & m_q &= \frac{f}{k_B}; & m_w &= \frac{1}{2} \frac{f}{k_B} \end{aligned} \right\} \quad (33.1)$$

Omitting certain unimportant terms, the coefficients of the quartic for  $\lambda$  are

$$\left. \begin{aligned} B &= z_w + m_q + m_w \\ C &= m_q z_w + \mu m_w \\ D &= x_u C + \mu k_L m_w \sin \gamma - m_q x_w z_u + k_L m_w z_u \\ E &= \mu k_L m_w z_u \end{aligned} \right\} \quad (33.2)$$

Replacing these derivatives by their values in (33.1) and noting that  $\sin \gamma$  is sensibly equal to  $k_D/k_L$ , the relations (33.2) can be written,

$$\left. \begin{aligned} B &= a + 1.5 \frac{f}{k_B} \\ C &= \frac{a}{k_B} [f + \mu H] \\ D &= \left[ 2c + \frac{a\mu H}{k_B} \right] k_D + \frac{f}{k_B} [3 - 2c] k_L^2 \\ E &= \frac{2a\mu H}{k_B} k_L^2 \end{aligned} \right\} \quad (33.3)$$

Hence, within the accuracy of these approximations,  $B$  and  $C$  are independent of the incidence, and therefore of the speed of flight, whilst  $D$  and  $E$  are expressed in terms of constants and of lift and drag coefficients for the whole aeroplane.

**34. Numerical Values.** We shall proceed to examine these expressions with the aid of the following numerical values for the constants involved. These correspond roughly to the appropriate quantities used in the detailed computation given earlier in this chapter for a stable aeroplane.

$$\begin{aligned} a &= 1.7 & c &= 0.50 & f &= 1.3 & k_B &= 0.75 \\ H &= 0.03 & \mu &= 23 & \text{so that } \mu H &= 0.69 \end{aligned}$$

**35. The Large Quadratic Root.** The first approximation to this root depends entirely on the coefficients  $B$  and  $C$  and is therefore to the present order of accuracy independent of incidence; with the numerical values of the paragraph above we have

$$\begin{aligned} B &= 1.7 + 2.6 = 4.3 \\ C &= 2.3 (1.3 + .69) = 4.6 \end{aligned}$$

The more accurate computation—Table 2—gave  $B$  varying from 4.53 at  $3^\circ$  incidence to 4.05 at  $10^\circ$  and  $C$  varying from 5.10 at  $3^\circ$  incidence to 4.69 at  $10^\circ$ . The agreement is good enough for the purposes of a general survey of the character of the motion.

The first approximation to the large quadratic root is therefore  $\lambda^2 + 4.3\lambda + 4.6 = 0$ . This has two roots, very nearly equal, of the order of magnitude  $-2$ . If the values of the constants do not vary widely from those here assumed for illustrative purposes, the rapid motion consists either of two nearly equal exponential subsidences, or of an oscillation which is so heavily damped that its oscillatory nature is not easily apparent. In either case the rate of decay is approximately

indicated by the exponential term  $e^{-\frac{1}{2} B \frac{t}{\tau}}$ , where  $\tau$  is the unit of time of the dimensionless system and  $t$  represents time in seconds.  $\tau$  is equal to  $m/\rho V S$  and is generally of the order unity. It may rise as high as 2 on a heavily loaded aeroplane travelling slowly and fall to 0.5 on a lightly loaded aeroplane travelling fast.  $(1/2) B/\tau$  will be of the order 2

with extreme limits, say 1 and 4. The motion represented by the large root will therefore practically disappear within about one second after the disturbance which produces it. It is this motion which is felt as a bump by the occupant of the aeroplane when it meets a vertical current or when the elevator is suddenly moved.

The motion represented by the large quadratic factor will still decay even when  $H$  is negative (aeroplane statically unstable) unless the numerical value of  $-H$  becomes greater than  $f/\mu$  or, in our example, 0.06. The neutral c.g. position in this example was distant 0.36 chord length behind the leading edge of the mean chord, so that the c.g. coefficient ( $h$ ) would have to be greater than 0.42 before the motion would become unstable through the change of sign of the coefficient  $C$ . Any negative value of  $H$  leads, of course, to instability through change of sign of the coefficient  $E$ , but the instability which arises in this way is slow in developing. The practical implications of this result have been discussed in Chapter IV. It should be noted that some time before  $H$  becomes negative and large enough to make  $C$  vanish, one of the roots becomes small and the approximation that  $\lambda^2 + A\lambda + B$  is a quadratic root of the quartic ceases to be legitimate. This is illustrated in the detailed computation for the unstable case at cruising and slow speeds, Table 2.

**36. The Small Quadratic Root.** The first approximation to this root is

$$\lambda^2 + \left( \frac{D}{C} - \frac{BE}{C^2} \right) \lambda + \frac{E}{C} = 0$$

Writing this quadratic root in the form  $\lambda^2 + b'\lambda + c' = 0$ . The two roots are  $-(1/2)b' \pm i\sqrt{c' - (1/4)b'^2}$ .

We shall see that  $(1/4)b'^2$  is of the order 0.001, whereas when  $H = 0.03$ ,  $c'$  is of the order 0.02 at cruising incidence and 0.10 at  $10^\circ$  incidence. Unless, therefore, the metacentric ratio ( $H$ ) is much nearer zero than 0.03, that is to say unless the aeroplane is very nearly statically neutral, a reasonable approximation to the roots is  $-(1/2)b' \pm i\sqrt{c'}$  and the period of the slow motion is approximately  $2\pi\tau/\sqrt{c'}$  seconds.

The approximate value of the constant term is

$$c' = \frac{E}{C} = \frac{2k_L^2}{1 + \frac{f}{\mu H}}$$

Hence the period is  $\frac{2\pi\tau}{\sqrt{2}k_L} \sqrt{1 + \frac{f}{\mu H}}$  seconds or  $\sqrt{2}\pi \frac{\tau}{g} \sqrt{1 + \frac{f}{\mu H}}$ .

Since  $\tau = k_L \frac{\tau}{g}$ .

This is equivalent to the approximate expression for the period derived in IV 9.

TABLE 7.

	Periods in seconds	
	Cruising	Slow speed
$\sqrt{2} \pi \frac{V}{g}$	19.0	13.5
$\sqrt{2} \pi \frac{V}{g} \sqrt{1 + \frac{f}{\mu H}}$	33.0	22.2
From detailed calculations	30.0	23.3

A comparison between the periods given by this approximate expression, using the numerical values of 34 and the periods given by the detailed calculation is given in Table 7.

The agreement between the second and third lines is reasonably good, considering the drastic nature

of the approximations. The damping factor of the slow oscillation is  $\frac{1}{2} \left( \frac{D}{C} + \frac{BE}{C^2} \right)$ . An approximate value of this is

$$\left[ 1 + \frac{1}{2} \frac{\mu H}{f + \mu H} \right] k_D + \left[ \frac{1}{2} \frac{f(3-2e)}{a(f + \mu H)} - \frac{\mu H(a k_B + 1.5 f)}{a(f + \mu H)^2} \right] k_L^2 \quad (36.1)$$

This rather elaborate expression cannot be reduced further without loss of generality. Inserting the numerical values of 34 gives

$$[1 + .17] k_D + [.38 - .33] k_L^2 \quad \text{or} \quad 1.17 k_D + 0.05 k_L^2.$$

In the cruising condition  $k_L$  is 0.20 and we may take  $k_D$  to be 0.025<sup>1</sup> and thus get for the damping factor of the slow oscillation,

$$0.0293 + .002 = 0.031$$

In the slow speed condition  $k_L$  is 0.40 and we may take  $k_D$  to be 0.044, giving a damping factor,

$$0.052 + .0080 = 0.060$$

The agreement in respect of cruising conditions is good; the values given by the detailed calculation being 0.03. The agreement in slow flight is not so good, the detailed calculation giving 0.036. The comparison at 10° incidence has been deliberately chosen to illustrate the limit beyond which it is unsafe to employ the approximations customary for cruising incidence. On this aeroplane 10° incidence corresponds to flight about 9 m.p.h. above the stalling speed, which is a slower speed than is ever likely to be used except in stunt flying or when making an unusually slow approach to a landing ground. Even at this slow speed, however, the approximations give a moderately good estimate of the period of the slow oscillation and an estimate of the damping which is of the right order of magnitude.

### E. Level Flight

**37. Introductory.** When the engine is working, the equations of motion and their solutions differ from those in gliding flight, both because

<sup>1</sup> As the design of aeroplanes improves the drag coefficient at cruising speed becomes smaller and with it the damping of the slow oscillation.

of the influence of the airscrew on the derivatives, and because the inclination of the flight path is different from the value ( $\gamma$ ) which it has in gliding flight. The complete statement of the equations in all possible flight conditions, including climbing and partial gliding with engine on, is too complicated to be usefully included in the present discussion. We shall therefore confine our attention to the more important effects of the screw only and to level flight, which to the stability investigator is the most important condition, because it represents the state in which the aeroplane will be flying for the greater part of any long journey. The reader who has studied the methods of examining the stability of level flight should have no difficulty in applying them to climbing flight, but for information on this subject and for more detailed information about the action of the screw in level flight Ref. 2 should be consulted. When *wind axes* are used  $\Theta$  is zero in level flight and the term  $\mu k_L m_w \sin \gamma$  disappears from the coefficient  $D$  in (33.2).

This involves the disappearance of the term  $\frac{1}{2} \frac{\mu H}{f + \frac{\mu}{\mu H}} k_D$  from the damping factor [see (36.1)]. Apart from this the symbolic expression remains the same as for gliding flight except that some additional terms, involving the derivative  $m_u$  which is not in general zero when the screw is revolving, must be added. The numerical values of some of the constants will, however, be altered from their values in gliding flight.

**38. Effect of Airscrew on  $m_w$ .** The effect of the airscrew on the locus of c.g. positions which give neutral static stability has been discussed at length in II 15, 16. It was there seen that this influence is not easy to estimate; but, when it has been estimated by methods such as were there outlined, or when the neutral position has been found by experiment, the derivative  $m_w$ , which defines the static stability, will still be related to the metacentric ratio ( $H$ ) in the same way as when the screw is not running. Thus

$$m_w = \frac{d k_L}{d \alpha} \frac{H}{k_B}$$

as before; except that  $dk_L/d\alpha$  may be slightly altered by the action of the screw slipstream on the wings. We shall ignore this slight difference and assume that  $H$  is known and that  $m_w$  is obtained from  $H$  by the above equation.

**39. Effect of Airscrew on  $m_q$  and  $m_w$ .** The influence of the screw on  $m_q$  has been discussed in II 34 *et seq.* The relation  $m_w = m_q d\varepsilon/d\alpha$ , where  $\varepsilon$  is the downwash at the tail still holds approximately—(see II 42) but the value of  $d\varepsilon/d\alpha$  may be altered by the slipstream. As, however, the influence of slipstream on downwash is very uncertain, and as the effect will be relatively unimportant in the present connection, we shall, in the numerical example to follow, assume, as in gliding flight that  $m_w = (1/2)m_q$ .

**40. The Effect of the Airscrew on  $x_w$ ,  $z_w$ ,  $z_{ww}$ .** The influence of the screw on these derivatives will be regarded as negligible.

**41. The Value of  $dT/dV$  for an Airscrew.** The remaining important effects of the airscrew upon the derivatives depend upon the rate of change of thrust with change of forward speed, and this we now proceed to evaluate. Let  $T$  be the airscrew thrust and write

$$T = k'_T Q V^2 S \quad (41.1)$$

$k'_T$  will vary in some as yet unknown way with change of  $V$ . Hence

$$\text{differentiating (41.1)} \quad \frac{V_1}{T} \frac{dT}{dV} = 2 + \frac{V_1}{k'_T} \frac{dk'_T}{dV} \quad (41.2)$$

To evaluate the right hand side of this equation approximately, without entering too deeply into the detailed design of the screw, we use Bairstow's generalised equations for the thrust and torque of an airscrew (Ref. 7, Chapter V).

$$\text{These are}^1 \quad k_T = A_T (1 - \lambda^2) \quad (41.3)$$

$$k_Q = A_Q (a - \lambda^3) \quad (41.4)$$

where  $k_T = T/Qn^2 D^4$  and  $k_Q = Q/Qn^2 D^5$

$Q$  being the torque acting on the screw,  $D$  its diameter and  $n$  the revolutions per second.  $A_T$  and  $A_Q$  are constants depending on the particular screw;  $a$  is a constant, given as 1.325 for all ordinary screws, and  $\lambda$  is the ratio of the quantity  $J$ , or  $V/nD$ , to its value,  $J_0$  when the airscrew thrust is zero.

$$\text{Thus} \quad \lambda = \frac{V}{n D J_0} \quad (41.5)$$

It is now necessary to make some assumption about the variation of engine torque with  $n$ . We shall assume a constant engine torque, independent of  $n$ .

$$\text{By definition} \quad k'_T = \frac{D^2}{S J_0^2} \frac{k_T}{\lambda^2}$$

$$\text{using} \quad k'_T = \frac{D^2 A_T}{S J_0^2} \left( \frac{1 - \lambda^2}{\lambda^2} \right)$$

$$\begin{aligned} \frac{1}{k'_T} \frac{dk'_T}{d\lambda} &= - \frac{2}{\lambda(1-\lambda^2)} \\ \frac{V}{k'_T} \frac{dk'_T}{dV} &= - \frac{2}{\lambda(1-\lambda^2)} V \frac{d\lambda}{dV} \end{aligned} \quad (41.6)$$

To find  $V d\lambda/dV$  we observe that if torque ( $Q$ ) is constant (41.4) can be written

$$\frac{1}{n^2} = E (a - \lambda^3) \quad (41.7)$$

in which  $E$  is a constant.

<sup>1</sup> The reader will note the distinction between  $\lambda$  as here used and  $\lambda$ , the root of an auxiliary equation as introduced in Chapter V.



Combining (41.7) and (41.5) gives

$$V^2 = F \frac{\lambda^2}{a - \lambda^3}$$

In which  $F$  is a constant.

Differentiating, we have

$$V \frac{d\lambda}{dV} = 2\lambda \frac{a - \lambda^3}{2a + \lambda^3} \quad (41.8)$$

Combining (41.2) (41.6) and (41.8) gives finally

$$\frac{V}{T} \frac{dT}{dV} = 2 \left[ 1 - \frac{2(a - \lambda^3)}{(1 - \lambda^2)(2a + \lambda^3)} \right] \quad (41.9)$$

For brevity let us write this

$$\frac{V}{T} \frac{dT}{dV} = 2[1 - K] \quad (41.10)$$

We observe that, in so far as an airscrew can be represented by Bairstow's generalization, and engine torque is constant, the quantity  $(V/T)dT/dV$ , which defines the change of screw thrust with change of speed is a function merely of  $\lambda$ ; that is to say, of the ratio of the speed to that speed at which the thrust would fall to zero if the angular velocity were kept constant. The relation between  $(V/T)dT/dV$ ,  $K$  and  $\lambda$  is given in Table 8.

We next consider the influence of this airscrew factor  $dT/dV$  upon the derivatives using, as before, wind axes.

**42. The Effect of Airscrew on  $x_u$ .** The contribution to the derivative  $X_u$  is simply  $dT/dV$ . Therefore

$$\left. \begin{aligned} x_u &= -\frac{1}{\rho V S} X_u - 2k_D - \frac{1}{\rho V S} \frac{dT}{dV} \\ x_u &= 2k_D - k'_T \frac{V}{T} \frac{dT}{dV} \\ \text{or} \quad x_u &= 2[k_D + k'_T(K - 1)] \end{aligned} \right\} \quad (42.1)$$

Strictly, there should be included here a term representing the effect of variations of body drag due to variation of airscrew thrust. This effect is of little importance in the present connection and can, if desired, be represented by an appropriate reduction of  $k'_T$ .

Neglecting this interference effect, we note that for level flight  $k'_T = k_D$  and we have  $x_u = 2k_D K$  (level flight only).

We note, however, that  $k_D$  is here the coefficient for the whole aeroplane without its screw and is therefore less than the value, used in the gliding example, for the aeroplane with stopped screw. Since  $K$  is greater than unity the difference between  $x_u$  level flight, and  $x_u$ , gliding with engine stopped, will therefore be less than might at first sight be supposed.

**43. Effect of Airscrew on  $m_u$ .** The contribution of the screw to the derivative  $m_u$ , which is zero in gliding flight with controls fixed, arises in two distinct ways. When the screw axis does not pass through the c.g., but is distant  $i$  above it, the pitching moment exerted by the screw is  $-iT$  and its rate of change with  $u$  is  $-i dT/dV$ .

On this account we have

$$k_{mu} = -\frac{i}{\rho V S c} \frac{dT}{dV} = 2 \frac{i}{c} k'_T (K-1) \quad (43.1)^1$$

Again, the slipstream from the screw depends on thrust and when the slipstream falls on the tail, it will influence the reaction upon it and therefore the pitching moment will be influenced by the term  $dT/dV$ . When  $V$  is varied—incidence constant—the pitching moment contributed by the tail will then not vary strictly in proportion to  $V^2$ , as is necessary if equilibrium is to be preserved, and a term  $m_u$  will therefore be introduced. We will suppose that the changes in slipstream due to changes in forward speed alter the velocity over the tail but do not appreciably influence the effective incidence. With this assumption the sign of the effect we are seeking will depend on the sign of the contribution of the tail to the pitching moment; and since, in steady flight, the tail contribution is equal and opposite to that of the rest of the aeroplane, we deduce that the sign of  $m_u$ , due to slipstream on the tail, will depend upon the sign of the pitching moment on the aeroplane without its tail.

Write the pitching moment on the whole aeroplane in the form

$$M = E V^2 + F V^2 \cdot b \quad (43.1)$$

where  $E V^2$  is the moment on the aeroplane without its tail and  $F V^2 \cdot b$  is the moment contributed by the tail.  $E$  and  $F$  are constants and  $b$  is a factor representing the influence of slipstream on the tail.

Differentiating (43.1) with respect to  $V$  gives

$$\frac{dM}{dV} = 2 E V + 2 F V b + F V^2 \frac{db}{dV} \quad (43.2)$$

But since  $M$  is zero in steady flight  $E V^2 + F V^2 b = 0$  and  $\therefore F = -E/b$ .

Hence (43.2) becomes  $\frac{dM}{dV} = -E V^2 \frac{1}{b} \frac{db}{dV}$

The contribution of this term to the derivative  $k_{mu}$  is therefore

$$k_{mu} = \frac{1}{\rho V S c} \frac{dM}{dV} = -\frac{E}{\rho S c} \frac{V}{b} \frac{db}{dV}$$

Let the pitching moment coefficient on the aeroplane without tail be  $[k_m]$  so that  $[k_m] \rho V^2 S c = E V^2$

<sup>1</sup> A similar argument derives the expression given in II 34 for  $k_{mq}$ , namely  $-2 \left( \frac{i}{c} \right)^2 k'_T (K-1)$ .

Then, due to the cause under consideration

$$k_{mu} = -[k_m] \frac{V}{b} \frac{db}{dV} \quad (43.3)$$

An approximation for  $b$  which is good enough for our present purpose

$$\text{is given by} \quad b = 1 + \frac{8}{\pi} \frac{G T}{\rho V^2 D^2} = 1 + \frac{8 G S}{\pi D^2} k'_T \quad (43.4)$$

where  $G$  is the proportion of the tail which is regarded as being in the slipstream.

$$\begin{aligned} \text{Therefore} \quad \frac{V}{b} \frac{db}{dV} &= \frac{8 G S}{\pi D^2 b} V \frac{dk'_T}{dV} \text{ or, using (41.1) and (41.9)} \\ &= - \frac{8 G S}{\pi D^2 b} k'_T 2 K \end{aligned}$$

Inserting the value of  $b$  from (43.4) and using (43.3) this reduces to

$$k_{mu} = \frac{2 K [k_m]}{1 + \frac{8 G S k'_T}{\pi D^2}} \quad (43.5)$$

**44. Effect of Aircscrew on the Coefficients  $B$ ,  $C$  and  $E$  in the Quartic for  $\lambda$ .** The approximate coefficients of the large root— $B$  and  $C$ —retain the algebraic forms given in (33.3), but the numerical value of  $f$  or  $k_{mq}$  will be increased as described in II 34.

Reference to the equations of motion 32 will show that the constant term in the small root  $[E/C]$  will be altered by the addition to  $E$  of a term,  $-\mu k_L z_w m_u$ .

Thus, when the screw is running, we have, writing, as in 33,  $a$  for  $z_w$  and referring to (33.3)

$$E = \frac{2a\mu H k_L^2}{k_B} - \mu k_L a m_u$$

or, since

$$\begin{aligned} k_{mu} &= -k_B m_u \\ E &= \frac{2a\mu k_L^2}{k_B} \left[ H + \frac{k_{mu}}{2k_L} \right] \end{aligned} \quad (44.1)$$

In level flight the presence of a term  $m_u$  in the equations of motion has therefore approximately the same effect on the stability of the slow motion—small quadratic root—as an increase  $k_{mu}/2k_L$  in the meta-centric ratio  $H$ . That is to say, it is equivalent, *from the present point of view*, to a movement of the c.g. forward through a distance equal to

$$\frac{k_{mu}}{2k_L} \times (\text{mean wing chord}).$$

When the engine is working, therefore, *static stability* is no longer a direct criterion of stability in free flight; the equilibrium in *free* flight will be neutral when the c.g. is behind the locus of statically neutral c.g. positions by the above distance.

Having regard to the signs of these equations, we note that it is possible for a statically unstable aeroplane with a high aircscrew or a

lifting tail to be stable in free flight. We shall see shortly that these same factors decrease the damping of the slow motion and therefore may, in extreme circumstances, cause the slow oscillation to increase automatically and so introduce instability of a different type from that which occurs when the constant  $E$  changes sign.

**45. Effect of Airscrew on the Damping of the Slow Motion.** To determine the effect of the airscrew in level flight on the damping of the slow oscillation the expression  $(D/C - BE/C^2)$  must be evaluated. Referring back to expression (36.1) for the damping in gliding flight, the first of the two main terms is replaced by  $Kk_D$ , where  $K$  depends on the rate of change of thrust coefficient with speed and is evaluated in 41. The second main term remains algebraically unaltered, but the numerical value of  $f$ , which stands for  $k_{mq}$  is increased by the action of the slipstream. There is, in addition, a third term introduced by the presence of  $m_u$  in the equation of motion. Reference to the equations of motion (see 32) shows that the presence of  $m_u$  adds to the coefficient  $D$  a term  $-\mu m_u(x_w + k_L)$  and to  $E$ , as we have seen, a term  $-\mu a k_L m_u$ . The corresponding term to be added to the damping factor can be deduced by use of the approximations of 33 either to the form

$$[aB - Cc] \frac{\mu k_L}{c^2} m_u \quad (45.1)$$

or to the more expanded form

$$\left[ \frac{a k_B + 1.5 f}{(f + \mu H)^2} - \frac{c}{f + \mu H} \right] \frac{\mu k_L}{a} k_{mu} \quad (45.2)$$

**46. Numerical Values.** An estimated value of  $f$  or  $k_{mq}$  with airscrew working in level flight was given in II 36 as 1.7. If we suppose that  $H$  is kept at the value 0.03 by a suitable adjustment of c.g. positions we have

$$B = 1 + 1.5 \frac{f}{k_B} = 1.7 + 3.4 = 5.1$$

$$C = \frac{a}{k_B} [f + \mu H] = 2.3 [1.7 + .69] = 5.5$$

The values when gliding, engine off, were

$$B = 4.3 \quad C = 4.6$$

Hence the effect of the airscrew on the large quadratic root is to make the corresponding mode of motion disappear even more rapidly than when the screw is stopped.

The effect on the constant term of the small quadratic root was seen to be the same as that of increasing  $H$  by  $k_{mu}/2k_L$ . If the airscrew axis passes through or near to the c.g., as in the normal single engined tractor,

we have seen that

$$k_{mu} = \frac{2K[k_m]}{1 + \frac{\pi D^2}{8GSk_T}} \quad (46.1)$$

For a biplane such as the Bristol Fighter with the c.g. in the usual position we have approximately  $[k_m] = -0.025 + 0.1 k_L$ .

In level flight  $k'_T$  is equal to the drag coefficient for the aeroplane without its screw; this we shall take to be 0.020 in cruising conditions or higher speeds and 0.040 at  $10^\circ$  incidence. These figures are lower than for the actual Bristol Fighter.

Using these values of  $k'_T$  and a normal tractor screw,  $K$  becomes 1.35 at cruising or higher speed, and 1.24 at  $10^\circ$  incidence.

Inserting these values in (46.1) gives the values below.

The danger that this aeroplane may become unstable in free level flight, through the presence of a divergence in the solution, despite the possession of positive static stability becomes, therefore, serious

	$k_L$	$k_{mu}$	Equivalent to a change in $H$ of
Very high speeds . . . . .	0.10	-.0056	-.028
Cruising . . . . .	0.20	-.0018	-.004
Slow speed . . . . .	0.44	.011	.012

at high speeds only. Using the same numerical values the damping term reduces to

$$K k_D + 0.15 k_L^2 - 6 k_L k_{mu}$$

and gives the following values:

Very high speeds ( $k_L = 0.10$ )	.027 + .001 + .003 = .031
Cruising ( $k_L = 0.20$ )	.027 + .006 + .002 = .035
Slow speed ( $k_L = 0.44$ )	.050 + .029 - .029 = .050

**47. The Effect of Freeing the Elevators.** If the elevators are left free the stabilizing influence of the tail is reduced as shown in II 20. This will result in a reduction of the metacentric ratio ( $H$ ) and a corresponding reduction in  $M_q$ , but otherwise will not alter the form of the equations under consideration unless there happens to be some constant moment acting about the hinge, say for example, due to the weight of the elevators, or to the action of some spring attachment. If there is such a moment acting, the angular setting of the hinge will alter with change of speed and a contribution will be made to the derivative  $m_u$ .

Let  $m'$  be this constant moment about the hinge and  $M'$  the corresponding pitching moment produced by the change of elevator angle under the moment  $m'$ . It will generally be sufficiently accurate to assume that both hinge moment and pitching moment are linear functions of elevator angle ( $\eta$ ) and are proportional to  $V^2$ .

In symbols  $m' = a V^2 \eta$  and  $M' = b V^2 \eta$ , where  $a$  and  $b$  are constants. Therefore  $M' = (b/a)m'$  and will also be constant whatever the value of  $V$ . Write the total pitching moment  $M$  in the form

$$M = E V^2 + M'$$

where  $E$  is a constant and  $E V^2$  refers to the whole aeroplane with zero moment acting on the elevator hinge.

Then since  $M'$  is constant  $dM/dV = 2 E V$ .

But since  $M = \text{zero}$  in steady flight,  $E = -M'/V^2$ .

Hence 
$$\frac{dM}{dV} = -2 \frac{M'}{V}$$

and 
$$k_{mu} = -\frac{1}{\rho V S c} \cdot \frac{2M'}{V} = -2k'_M$$

Thus the derivative  $k_{mu}$  due to a constant moment acting about the elevator hinge is equal to minus twice the coefficient of the pitching moment due to this elevator hinge moment.

## CHAPTER VII

# NUMERICAL SOLUTIONS OF THE ASYMMETRIC EQUATIONS

**1. Introduction.** In this chapter the group of equations which were developed in Chapter V to represent the results of infinitesimal asymmetric disturbances from steady straight symmetric flight will be studied with regard to the numerical values of the quantities in a typical aeroplane. The plan of the chapter will be closely parallel with that of Chapter VI and the numerical values chosen for study will relate approximately to the same aeroplane—the Bristol Fighter. In the first part of the chapter the equations will be worked through to the point where they show the movements following certain initial disturbances occurring in flight at cruising speed, at slow speed and in stalled flight respectively. In the second part certain approximations will be discussed, which are legitimate when the incidence is not too large and estimates of periods and damping factor only are required.

**2. Notation and Axes.** The notation will be the same as in Chapters V and VI, with the exception that the representative length used in defining dimensionless coefficients will be the semi-span ( $s$ ) of the wings, instead of the mean wing chord which was used for this purpose in Chapter VI. In Chapter V, it will be remembered, this length was given the symbol  $l$  and its nature was left unspecified. The use, for the same purpose, of different lengths in the symmetric and asymmetric groups of equations would be indefensible, were it intended to study motions in which symmetric and asymmetric disturbances interact with each other, but since, in this and the previous chapter the two groups of equations are handled entirely separately, no inconvenience results from this procedure, which has certain practical advantages and is in agreement with modern usage.

The axes will be the same as those of the first part of Chapter VI, namely *chord axes* with origin at the c.g. and  $OX$  parallel to the mean wing chord. These are sufficiently near to principal axes for the product of inertia to be neglected, and it will accordingly be entirely omitted from the equations. As in Chapter VI we shall replace  $U_1/V_1$  by  $\cos A_1$  and  $W_1/V_1$  by  $\sin A_1$ ; where  $A_1$  is the incidence of steady flight,  $U_1$  and

$W_1$  are, as usual, the component velocities and  $V_1$  the resultant velocity of the c.g. in steady flight.

**3. Choice of Illustrative Examples.** In forming examples for detailed study the following numerical values will be assumed:

Air Density . . . . .	$\rho$	0.002 slugs per cu. ft.
Aeroplane wing area . . . . .	$S$	405 square feet.
Aeroplane semi-wing span . . . . .	$s$	20 feet.
Aeroplane mass. . . . .	$m$	96 slugs.
Aeroplane moment of inertia . . . . .	$A$	2600 slugs ft <sup>2</sup> .
Aeroplane moment of inertia . . . . .	$C$	4100 slugs ft <sup>2</sup> .

Using these values we have

$$\mu = \frac{m}{\rho S s} = 5.9$$

$$k_A = \frac{A}{m s^2} = 0.071$$

$$k_C = \frac{C}{m s^2} = 0.107$$

The quantities  $\rho$ ,  $S$  and  $m$  have the same values as in Chapter VI. The change in  $\mu$  from the value 23 used in Chapter VI does not correspond to any change in the aeroplane, but is consequent upon the change in the representative length used in forming dimensionless coefficients, from the mean chord (5.17 ft.) in Chapter VI, to the semi-span (20 ft.) in the present chapter.

The quantities  $k$ ,  $\tau$ , and  $\Theta$  have values which depend on the incidence of steady flight in exactly the same way as in Chapter VI.

The force-velocity derivatives  $y_p$  and  $y_r$  have a negligible influence on the motions to be studied and will be entirely omitted from the computations, but the derivative  $y_c$  cannot be neglected.

The six moment derivatives  $l_v$ ,  $l_p$ ,  $l_r$ ,  $n_v$ ,  $n_p$ ,  $n_r$  will be taken from the curves, Fig. 42 (III 38) after dividing by the appropriate inertia coefficient  $k_A$  or  $k_C$  and changing the sign. As in Chapter VI we shall study disturbances from steady flight at three incidences, representative respectively of, cruising speed, slow speed, and stalled flight. These incidences will be  $3^\circ$ ,  $10^\circ$ , and  $22^\circ$  respectively; the last being  $2^\circ$  higher than the corresponding incidence of Chapter VI in order to display the effects of changes in the derivatives which are not fully developed until this incidence is reached.

At all these three incidences the engine will be supposed to be *off* and the aeroplane gliding at the appropriate angle for steady flight at the moment when the disturbances occur.

**4. Cruising Speed.** At  $3^\circ$  incidence the values of the derivatives given in Fig. 42 III 38 make the constant term ( $E$ ) in the quartic for  $\lambda$  nearly, but not quite, zero. The solution in these circumstances is troublesome and a procedure analogous to that with the symmetric equations will be adopted. We shall suppose first that the dihedral

angle is slightly reduced, making  $k_{lr} = -.04$  instead of about  $-.05$  which would correspond to the value in Fig. 42e, while the fin and rudder are slightly increased making  $k_{nr} = +.02$ , instead of about  $.013$ . With these changes the constant term ( $E$ ) of the quartic becomes zero, and the solutions for given initial conditions can be obtained by the special method of V 35. We shall then study two other conditions, in the first of which  $k_{lr}$  is reduced to zero, leaving all other derivatives unchanged, whilst in the second  $k_{nr}$  is similarly treated. These changes correspond respectively to the elimination of the dihedral angle and of the static yawing stability respectively, and both are operations which could be performed without serious alterations in the design. The former change gives a small but manageable negative value of  $E$ , corresponding to a slowly developing *spiral* instability, the latter gives a positive value of  $E$  leading to complete stability, for, surprising though it may at first sight appear, the aeroplane can be completely stable in free flight even when it has slight static instability. This curious phenomenon is discussed more fully in 34 and 35. A study of the response of the aeroplane to its controls when in these three states will be of considerably greater interest than were one state only to be examined, even though that state happened to represent exactly the particular aeroplane under consideration.

Though the analogy between this procedure and that of Chapter VI is close, it is not exact, for in Chapter VI one quantity only, namely the metacentric ratio ( $H$ ), was altered, in order to bring the aeroplane into

TABLE 1. Dimensionless  
Constants Used in Examples.

$\mu = 5.9$   $k_A = .071$   $k_C = .107$

$A_1$	3°	10°	22°
$\Theta_1$	7°	1°	0°
$\tau$	.85	1.25	1.44
$k$	.20	.40	.55
$y_c$	.15	.15	.19
$l_r$	.56	1.05	2.4
$l_p$	6.10	6.10	.00
$l_r$	-1.75	-2.95	-3.4
$n_v$	.19	.00	-.094
$n_p$	.37	.65	-.56
$n_r$	.29	.19	.00

the stable, neutral and unstable states. In the present examples two independent derivatives  $l_r$  and  $n_r$  are successively reduced to zero in order to change the equilibrium from the neutral to unstable and stable states respectively. This difference must be borne in mind when interpreting the solution.

The stable condition has the added interest that it represents an aeroplane for which the *static directional* stability is neutral, a condition not unlikely to occur in practice if the fin and rudder are on the small side and the body on the large side.

**5. Slow Speed.** At 10° incidence the derivatives taken from Fig. 42 give a relatively large positive value of the constant

term ( $E$ ) in the quartic equation for  $\lambda$ . One solution only will, therefore, be sufficient to illustrate the changes which occur at slow speeds.

**6. Stalled Flight.** In the stalled state, at 22° incidence, one solution only will be given, representing rotary derivative values taken from continuous rotation experiments.



**7. Table of Dimensionless Constants.** The values of the constants and derivatives in the conditions chosen for computation are collected in Table 1. In this table the figures given for  $3^\circ$  incidence represent the neutral state; the stable state is derived by making  $n_v$  zero and the unstable state by making  $l_r$  zero.

### A. Complementary Function

**8. The Equations of Motion.** After writing the variables  $v$ ,  $p$ , and  $r$  in the forms  $r_1 e^{\lambda t}$ ,  $p_1 e^{\lambda t}$ ,  $r_1 e^{\lambda t}$ , where  $r_1$ ,  $p_1$ ,  $r_1$  are constant and after writing  $A_1$  for  $\Omega$  and omitting all terms containing  $y_p$ ,  $y_r$  or the product of inertia ( $E$ ) and making  $l_0$  and  $n_0$  zero, the equations of motion [V (21.2)] reduce to the three simultaneous algebraic equations below.

$$\left. \begin{aligned} (\lambda + y_r) r_1 - \mu (\sin A_1 + k \lambda^{-1} \cos \Theta_1) p_1 + \\ \quad + \mu (\cos A_1 - k \lambda^{-1} \sin \Theta_1) r_1 = 0 \\ l_v r_1 + (\lambda + l_p) p_1 + l_r r_1 = 0 \\ n_v r_1 + n_p p_1 + (\lambda + n_r) r_1 = 0 \end{aligned} \right\} \quad (8.1)$$

or, in the shortened notation,

$$\left. \begin{aligned} a_1 v_1 + b_1 p_1 + c_1 r_1 = 0 \\ a_2 v_1 + b_2 p_1 + c_2 r_1 = 0 \\ a_3 v_1 + b_3 p_1 + c_3 r_1 = 0 \end{aligned} \right\} \quad (8.2)$$

where the meanings of  $a_1$ ,  $b_1$ , etc. are found by comparison between (8.1) and (8.2).

**9. The Quartic for  $\lambda$ .** To find  $\lambda$  we eliminate the ratios  $v:p:r$  from (8.1) and arrange the result in descending powers of  $\lambda$ .

$$\lambda^4 + B\lambda^3 + C\lambda^2 + D\lambda + E = 0$$

The coefficients of this quartic are set out in full in Table 2 with their numerical values in each of the conditions chosen for illustration. As with the symmetric solutions the values of many of the terms, though negligible, have been stated in order to show their orders of magnitude. In the cruising, or  $3^\circ$  incidence column, the *neutral* total is obtained by adding the numbers as they stand, the *stable* total by omitting all terms containing  $n_r$  and the *unstable* total by omitting terms containing  $l_v$ .

**10. Values of  $\lambda$  and of the Ratios  $v:p:r$ .** The quartics for  $\lambda$  with numerical coefficients, as indicated in the *totals* of Table 2 are next solved<sup>1</sup> and the ratios between the variables which correspond to each of the four roots are found by substituting the appropriate value of the root into the second and third of (8.1) and eliminating each variable in turn. The second and third equations are chosen for this purpose because they lead to the simplest expressions for the ratios. The ratios so found can then, if desired, be inserted in the first of (8.1) to provide a check

<sup>1</sup> See Footnote (VI 16) on approximate methods of solving quartic equations.

on the arithmetic. This was actually done but the check figures are not here shown.

The expressions for the ratios  $v:p:r$  in terms of  $\lambda$  and of the derivatives are simpler than the corresponding expressions derived from

TABLE 2. Constitution of the Coefficients of the Quartic for  $\lambda$ .

B				C			
Incidence	3°	10°	22°	Incidence	3°	10°	22°
$y_v$	.15	.15	.19	$y_v l_p$	.92	.91	.00
$l_p$	6.10	6.10	.00	$y_v n_r$	.04	.03	.00
$n_r$	.29	.19	.00	$l_p n_r$	1.77	1.16	.00
Total	6.54	6.44	.19	$-l_r n_p$	.65	1.92	-1.90
D				$-\mu n_v \cos A_1$	1.12	.00	.52
Incidence	3°	10°	22°	$\mu l_v \sin A_1$	.17	1.05	5.24
$y_v l_p n_r$	.26	.17	.00	Totals Stable	3.55	5.07	3.86
$-y_v l_r n_p$	.10	.29	-.36	Neutral	4.67		
$\mu l_v n_p \cos A_1$	1.22	3.95	-7.36	Unstable	4.50		
$-\mu l_p n_v \cos A_1$	6.83	.00	.00	E			
$\mu l_v n_r \sin A_1$	.05	.20	.00	Incidence	3°	10°	22°
$-\mu l_r n_v \sin A_1$	.10	.00	-.70	$\mu k l_v n_r \cos \Theta_1$	.19	.47	.00
$\mu k l_v \cos \Theta_1$	.66	2.48	7.79	$-\mu k l_r n_v \cos \Theta_1$	-.39	.00	-1.04
$\mu k n_p \sin \Theta_1$	.03	.00	.00	$-\mu k l_v n_p \sin \Theta_1$	.03	-.03	.00
Totals Stable	2.29	7.09	-.63	$\mu k l_p n_v \sin \Theta_1$	.17	.00	.00
Neutral	9.05			Totals Stable	.22	.44	-1.04
Unstable	7.12			Neutral	.00		
				Unstable	-.22		

the symmetric equations and it is unnecessary to arrange them in tabular form as in Chapter V. They are:

$$v: \lambda^2 + (l_p + n_r) \lambda + l_p n_r - l_r n_p$$

$$p: -l_v \lambda - l_v n_r + l_r n_v$$

$$r: -n_v \lambda + l_v n_p - l_p n_v$$

The numerical values of these ratios are found by substituting the appropriate values of the derivatives taken from Table 1 and the appropriate root of the quartic for  $\lambda$ . These roots with their appropriate  $v:p:r$  ratios are given in Table 3. The meanings of the complex ratios are discussed in V 30, 31.

Table 3 defines the complementary functions of the equations in their most general form. From it we observe that there are in all cases

TABLE 3. Roots of the Quartics for  $\lambda$  and the  $v:p:r$  Ratios. Incidence 3 deg.

	Stable ( $n_v = 0$ )			Neutral			Unstable ( $l_v = 0$ )		
Root	-6.0	-.21 ± .53i	-.11	-6.0	-.26 ± 1.20i	.000	-6.0	-.29 ± 1.06i	+.031
$v:$	.046	.84 ± 3.20i	1.00	.044	.63 ± 7.03i	1.00	.045	-1.45 ± 18.6 i	1.00
$p:$	1.000	-.05 ± .30i	-.06	1.000	.32 ± .67i	.07	1.000	1.00 ± .00i	.13
$r:$	.065	.21 ± .00i	.12	.063	1.32 ± .23i	.57	.063	3.33 ± .61i	.44

	Incidence 10°			Incidence 22°		
Root	-5.8	-.30 ± 1.04i	-.065	-.44	-.16 ± 2.03i	+.57
$v:$	.015	.19 ± 5.92i	1.00	-1.24	-6.00 ± .65i	1.50
$p:$	1.000	.12 ± 1.09i	-.05	1.00	.70 ± 4.87i	1.00
$r:$	.116	.68 ± .00i	-.26	1.00	-1.36 ± .19i	1.23

two exponential modes corresponding to real roots and one oscillation corresponding to a pair of complex roots.

**11. The Large Real Root.** In normal flight one of the exponential modes decays very rapidly, the exponential term being of the order  $e^{-6t}$  which, since  $\tau$  is of the order unity, decays to about  $1/e$  of its value every sixth of a second, and, sensibly, vanishes within a small fraction of a second. The physical reason for this large root will be discussed later; for the present it is sufficient to note that it is concerned mainly with the variable  $p$ , the other two variables in this mode being of the order  $p/20$ .

**12. The Small Real Root.** The other exponential mode corresponds to a very small root and therefore decays or increases very slowly. A time of the order ten to twenty seconds is necessary for motions in this mode to decay to  $1/e$  or increase to  $e$  times their original value. An aeroplane which is unstable with respect to this mode is said to be *spirally unstable*, for reasons which we shall appreciate later. We note that this mode involves mainly  $v$  and  $r$  and contains relatively small values of  $p$ . Except when the angle of pitch ( $\theta_1$ ) is large, this is clearly inevitable in any slowly developing motion; for, if  $p$  were large the inclination of the plane of symmetry to the vertical would rapidly change and rapid changes in the action of gravity upon the aeroplane would occur.

**13. The Complex Root.** In all the examples of normal flight chosen for illustration the oscillation is heavily damped and of medium period—of the order five seconds. All three component motions are involved.

The question of the variations of the different modes with changes of the derivatives will be taken up later in this chapter, using approximate methods similar to those of Chapter VI. We proceed now to the problem of fitting these general solutions to chosen initial conditions.

## B. Complete Solutions and Initial Conditions

**14. Choice of Initial Conditions.** The following three sets of initial conditions have been chosen for further study.

- (1) An initial angular velocity of roll ( $\dot{\rho}_0$ ) so that at zero time

$$\rho = \rho_0; \text{ and } r, v, l_0, n_0 \text{ are all zero.}$$

- (2) A steady applied rolling moment (coefficient  $k_{l_0}$ ) so that at zero time

$$l_0 = \frac{k_{l_0}}{k_A}; \text{ and } \rho, r, v, n_0 \text{ are all zero.}$$

This is not necessarily the effect of a simple aileron movement, for in general, the ailerons apply yawing moments as well as rolling moments. The effect could, however, be produced by an appropriate combination of movements of ailerons and rudder.

- (3) A steady applied yawing moment (coefficient  $k_{n_0}$ ) so that at zero time

$$n_0 = \frac{k_{n_0}}{k_C}; \text{ and } \rho, r, v, l_0 \text{ are all zero.}$$

**15. Complete Solutions in Dimensionless Form.** The processes involved in fitting the solutions to initial conditions of the above types have been described in general terms in Chapter V and the detailed arithmetic will not be reproduced. As with the symmetric computation it is essential to arrange the arithmetic in a systematic manner with checks at each important stage, but no difficulty need be experienced if the directions of Chapter V are followed.

The solutions appropriate to these chosen initial conditions are given in Table 4, in which the variables are the angular displacements  $\varphi$  and  $\psi$  and the side-slip velocity  $r$ . These variables  $\varphi$  and  $\psi$  are chosen for tabulation because the motion is more easily visualized in terms of them than in terms of the variables  $\rho$  and  $r$  which were used throughout the calculations. These latter variables are related to  $\varphi$  and  $\psi$  by the equation

$$\dot{\varphi} = \dot{\rho} + r \tan \theta_1; \quad \dot{\psi} = r \sec \theta_1$$

They can therefore, if desired, be obtained by differentiating the expressions for  $\varphi$  and  $\psi$  in Table 4.

The solutions in Table 4 are arranged in the same way as in the corresponding table in Chapter VI.

**16. Conditions to which the Solutions are Applicable.** The solutions in Table 4, being in dimensionless form, apply equally to all aeroplanes of the same external form as the B.F. 2b for which they were calculated, provided that the inertia coefficients  $k_A$ ,  $k_C$  and the parameter  $\mu$  have the same values as those here assumed. The values of  $k_A$  and  $k_B$  do not vary widely from one aeroplane to another and the value of  $\mu = 5.9$  is, as we saw in VI 19 representative not only of the aeroplane chosen but of more heavily loaded larger aeroplanes and more lightly loaded smaller aeroplanes.

In the dimensionless form the derivatives do not vary greatly from one aeroplane to another, with the exception of  $l_v$  and  $n_r$ , which may vary widely and are easily altered by changing dihedral angle or fin and rudder area. More examples than have been given in Table 4 would be required to display thoroughly the effects of all possible combinations of values of  $l_r$  and  $n_r$ , but limitations of time and space do not allow more to be included. Those given are, however, sufficient to give an idea of the principal variations and to illustrate the methods.

In Table 2 it will be observed that  $\mu$  is always multiplied either by  $l_r$  or  $n_r$ . The form of the solution will therefore not be altered by a change of  $\mu$  provided that  $l_r$  and  $n_r$  are both altered in inverse proportion to  $\mu$ . From the relations in 10 however, it is clear that this change will alter the ratios of the velocity  $v$  to the angular velocities  $p$  and  $r$ .

**17. Conversion to Ordinary Units.** In order to apply the solutions of Table 4 to any particular aeroplane in terms of any desired system of units, it is necessary to know the values of  $\mu$ ,  $c$  and  $\tau$  for the flight in question. We recall that

$$v = \frac{c}{\tau} v; \quad p = \frac{1}{\tau} p; \quad r = \frac{1}{\tau} r; \quad k_{l_0} = k_A l_0; \quad k_{n_0} = k_c n_0$$

In the next paragraph we shall discuss graphs of the angles  $\varphi$  and  $\psi$  which define the orientation of the disturbed aeroplane and the side-slip angle  $\beta$  ( $= v/V_1$ ) following initial disturbances of the type included in Table 4. These are deduced from the dimensionless ratios in Table 4 in accordance with the following scheme.

$$t = \tau (t)$$

$$\begin{array}{lll} \frac{\beta}{p_0} = \frac{\tau}{\mu} \left( \frac{r}{p_0} \right); & \frac{\varphi}{p_0} = \tau \left( \frac{\varphi}{p_0} \right); & \frac{\psi}{p_0} = \tau \left( \frac{\psi}{p_0} \right) \\ \frac{\beta}{k_{l_0}} = \frac{1}{k_A} \left( \frac{r}{l_0} \right); & \frac{\varphi}{k_{l_0}} = \frac{1}{k_A} \left( \frac{\varphi}{l_0} \right); & \frac{\psi}{k_{l_0}} = \frac{1}{k_A} \left( \frac{\psi}{l_0} \right) \\ \frac{\beta}{k_{n_0}} = \frac{1}{k_c} \left( \frac{r}{n_0} \right); & \frac{\varphi}{k_{n_0}} = \frac{1}{k_c} \left( \frac{\varphi}{n_0} \right); & \frac{\psi}{k_{n_0}} = \frac{1}{k_c} \left( \frac{\psi}{n_0} \right) \end{array}$$

An example will show how Table 4 is converted so as to relate to any desired system of units. Suppose that we require an expression for the side-slip angle ( $\beta$ ) in radians, at time  $t$  seconds after a small disturbance in the form of an angular velocity of roll  $p_0$ , expressed in radians per second. We will suppose that  $n_r = 0$  and that the incidence is  $3^\circ$  so that the information comes from the first column of the first block of figures in Table 4. These figures give the dimensionless ratio  $v/p_0$  as a function of the dimensionless quantity  $t$ .

We have  $\beta/p_0 = (\tau/\mu) (r/p_0)$  also we have (Table 1)  $\mu = 5.9$  and  $\tau = 0.85$ .

Therefore  $\frac{\beta}{p_0} = 0.144 \frac{r}{p_0}$  and  $t = 1.18 t$ .

And  $\beta = p_0 \times 0.144 [0.046 e^{1.18 \times 6.0 t} \dots \text{etc.}]$

or  $\beta = p_0 \times [0.0067 e^{-7.1} \dots \dots \dots \text{etc.}]$

Incidence 3 deg.

TABLE 4. Complete Solutions with Given Initial Conditions.

	Initial $p_0$			Initial $l_0$			Initial $n_0$			
	$v/p_0$	$\varphi/p_0$	$\psi/p_0$	$v/l_0$	$\varphi/l_0$	$\psi/l_0$	$v/n_0$	$\varphi/n_0$	$\psi/n_0$	
$e - 6.0t$	.046	-.116	-.011	-.008	.028	.002	.001	-.005	.000	Stable
$e - 2.1t \cos .53t$	-.052	.162	-.019	-.171	-.211	.176	20.80	1.54	-2.20	
$e - 2.1t \sin .53t$	1.073	.067	-.116	-.76	.220	.104	2.55	-3.03	-.533	
$e - .11t$	.007	.004	-.007	-.06	-.043	.070	-26.15	-17.04	28.2	
1.0			-.001	1.79	.255	-.248	5.34	15.50	-26.0	
$t$									3.00	
$e - 6.0t$	.044	-.167	-.010	-.007	.027	.002	.001	-.005	.000	Neutral
$e - .26t \cos 1.2t$	-.088	.037	.023	-.348	-.015	.050	3.94	.092	-.594	
$e - .26t \sin 1.2t$	.453	.010	.066	.150	.028	.030	.77	-.420	-.200	
1.0	.043	.131	-.013	.355	-.012	-.052	-.3.95	-.087	.594	
$t$			.025	.043	.127	-.012	.13	.380	.081	
$t^2$						.012		2.99	.036	
$e - 6.0t$	.045	-.169	-.011	-.007	.027	.002	.002	-.008	-.001	Unstable
$e - .29t \cos 1.1t$	-.113	.010	.032	-.402	.007	.059	4.92	-.109	-.761	
$e - .29t \sin 1.1t$	.512	-.012	-.080	-.228	.011	.048	1.34	-.099	-.350	
$e + .031t$	.068	.159	.980	2.160	4.90	30.10	.34	.788	4.84	
1.0			-1.000	-.168	-4.94	-30.16	-5.26	-.671	-4.08	
$t$						-.952				

TABLE 4 (Continued).

	Incidence 10 deg.					Incidence 22 deg.				
	$v/p_0$	$\phi/p_0$	$\psi/p_0$	$r/l_0$	$q/l_0$	$q/l_0$	$r/n_0$	$\phi/n_0$	$\psi/n_0$	
$e^{-5.8t}$	.015	-.178	-.021	-.003	.031	.004	.001	-.012	.004	
$e^{-.30t} \cos 1.04t$	—	.176	.029	-.917	-.069	.087	5.65	.15	-.58	
$e^{-.30t} \sin 1.04t$	1.038	.026	-.106	-.283	.149	.053	.10	-.96	.16	
$e^{-.065t}$	.003	.002	-.012	-.034	-.023	.131	21.95	14.88	85.5	
1.0	—	—	.004	.954	.061	-.222	16.30	14.75	84.9	
$t$	—	—	—	—	—	—	—	—	5.59	
$e^{-.44t}$	—	-.146	.146	.182	.334	-.334	3.57	6.53	6.55	
$e^{+.57t}$	.170	.200	.224	.297	.348	.426	4.90	5.76	7.07	
$e^{-.16t} \cos 1.04t$	—	-.054	-.103	-.479	-.194	.026	1.99	.79	-.03	
$e^{-.16t} \sin 1.04t$	1.000	.401	-.045	-.077	-.039	-.049	.37	.11	.22	
1.0	—	—	-.287	.000	-.488	.118	10.46	13.08	-.49	
$t$	—	—	—	—	—	-.294	—	—	7.53	

### 18. Graphs of the Solutions Plotted Against Time.

Graphs illustrating the solutions in Table 4 have been plotted in Figs. 57a to m. These graphs correspond to the values of  $\tau$  and  $l$  given in Table 1 and therefore relate to the actual aeroplane, B.F.2b, flying in air of density 0.0020 slugs per cu. ft. The abscissae represent time in seconds and in order to give an air of verisimilitude to the proceedings, the scales of the ordinates have been adjusted to represent angular disturbances in degrees, due, respectively to the following causes: an initial angular velocity of roll  $p_0 = 10^\circ$  per sec.; an unbalanced rolling moment represented by  $k_{l0} = 0.001$ , and an unbalanced yawing moment represented by  $k_{n0} = 0.0001$ . The above rolling moment would be generated in normal flight by an aileron movement of roughly  $\pm 1/4$  degree and to generate the yawing moment a rudder angle of about  $1/3$  of a degree would be required. These figures relate to normal flight, the graphs for stalled flight will be discussed later. The manner in which the various modes combine to give the final curves plotted in these figures are often

most interesting and the reader who takes more than a passing interest in the subject is advised to try for himself the operation of plotting from the information in Table 4<sup>1</sup>.

### C. The Graphs Discussed

**19. Initial Rate of Roll.** Figures 57a, b and c show the motion of the aeroplane for the first 20 sec. following an initial disturbance in the form of a rate of roll ( $p_0$ ) of  $10^\circ$  per sec. The three continuous curves in each figure represent the aeroplane at  $3^\circ$  incidence, in the stable, neutral and unstable conditions defined in 4, whilst the dotted curve represents the single stable condition examined at  $10^\circ$  incidence.

During the first half second it is seen that the mode corresponding to the large root ( $\lambda = -6$ ) predominates over the others and during this period the initial rate of roll is very rapidly reduced to zero in all cases. This is due, of course, to the large positive<sup>2</sup> value of  $l_p$  possessed by all wings in normal flight, which implies a large rolling moment opposing any rapid rolling motion. We note that the motion during the first half second is much the same for all the conditions examined, because it is dominated by  $l_p$  and is but little influenced by changes of dihedral angle or of the size of the fin and rudder. During this early stage the yaw is of opposite sign from the roll, that is to say the falling wing tip moves forward relative to the c.g. This yawing motion is due to the positive value of  $n_p$  possessed by the wings in normal flight and is the principal motion which causes the positive side-slip recorded in Fig. 57c, during the first two or three seconds.

After the first rapid elimination of the rolling motion the subsequent disturbance may be considered as originating from an angular displacement ( $\varphi$ ) of a little over one degree combined with a side-slip angle ( $\beta$ ) varying from one half to one and a half degrees in the various circumstances.

In the next stage the harmonic mode plays the leading part in the motion, but is itself damped out and almost eliminated after about two complete swings, which occupy some ten to fifteen seconds. By this time the effect of the small root has become noticeable and the subsequent motion of the aeroplane depends on the sign of this root; the stable aeroplane—negative root—returns to straight flight on an even keel, the direction of motion being, by a coincidence, almost the same as that before the disturbance; the neutral aeroplane—root zero—settles down to a steady-banked turn, with slight side-slip, and the unstable aeroplane—root positive—continues to turn at a slowly increasing rate with, of course, an appropriate slow increase in the angle of bank. It

<sup>1</sup> For quick methods of plotting see footnote to VI 23.

<sup>2</sup> It will be remembered that a positive  $l_p$  corresponds to a negative value of the derivative  $\partial L/\partial p$ .



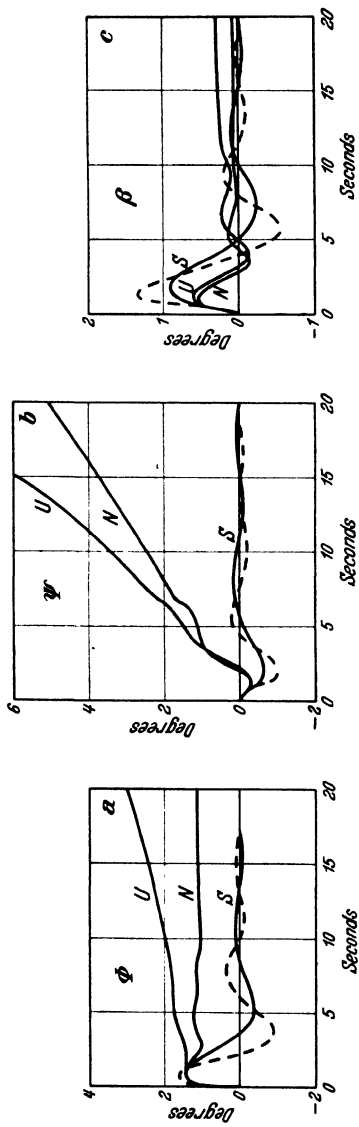
is on account of this motion that the instability resulting from a positive small root of the quartic for  $\lambda$  is often called *spiral instability*.

The dotted curves show that the motion in slow flight at  $10^\circ$  incidence is of the same character as that of the stable aeroplane at  $3^\circ$  incidence, although the quantities involved are slightly different.

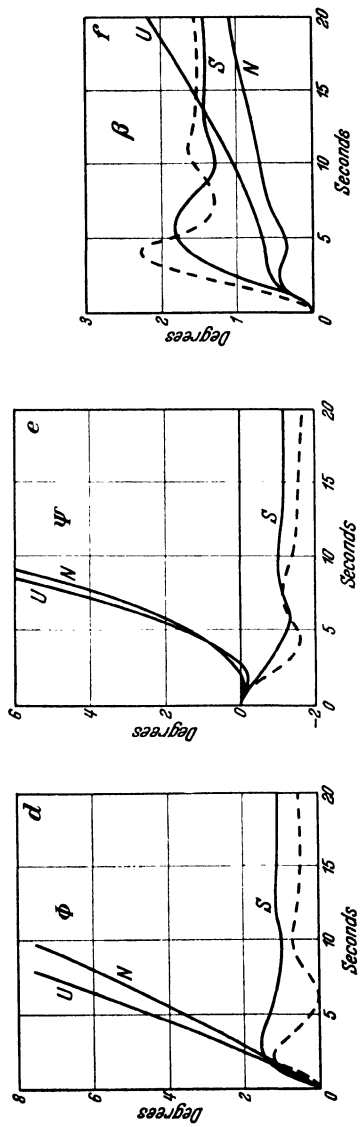
**20. Applied Control Moments.** Figure 57d to i relate to the effects of applying, by means of the controls, small rolling or yawing moments when the aeroplane is initially flying straight and steadily. Before considering these in detail we note that the disturbances caused by a rolling moment of coefficient 0.001 are of the same order of magnitude as those due to a yawing moment of 0.0001. The aeroplane is thus, speaking roughly, ten times as sensitive to yawing moments as to rolling moments. The reason for this is sufficiently obvious; after the first second or so the moments of inertia of the aeroplane have but little influence on the motion and the subsequent movements are mainly determined by the balance of applied moments against aerodynamic moments; the wings, however, are thin, flat objects with small dimensions parallel to the  $Z$  axis and they, therefore, experience smaller aerodynamic reactions when rotated about the  $Z$  axis than when rotated about the  $X$  axis. A comparison between a plan drawing and either of the elevations of an aeroplane will illustrate this point. It is on account of this property of the aeroplane that the designer, as the result of experience, provides ailerons which are roughly ten times as powerful as the rudder.

**21. Applied Rolling Moment.** Figure 57d, e and f show the effect of applying a small rolling moment, corresponding to about  $1/4$  degree up and down movement of the aileron, but without the yawing moment which the ailerons would normally generate. The effect on the stable aeroplane at  $3^\circ$  incidence is to cause it, after a preliminary oscillation damped out in from 10 to 15 secs. to fly straight and steadily with an angle of bank ( $\varphi$ ) of about  $1^\circ$ , a side-slip angle ( $\beta$ ) of  $1.5^\circ$  and a direction of motion about  $1^\circ$  to port of the original direction.

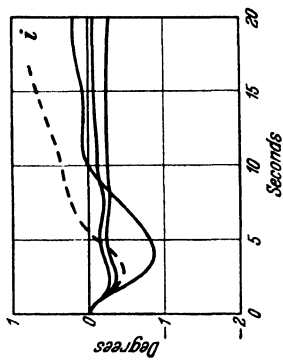
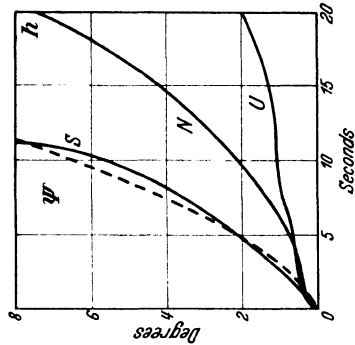
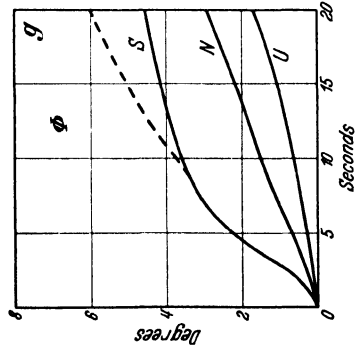
For the first two seconds after its application the rolling moment produces substantially the same effect on the aeroplane in all the three conditions examined, but after two seconds the rolling effect is much greater when the aeroplane is neutral or unstable than when it is stable. This striking difference is due to the absence of the static directional stability coefficient ( $n_r$ ) in the stable aeroplane and its presence in the other two. When this derivative is zero there is nothing to prevent the generation of large side-slips when the aeroplane is banked, and these side-slips, in turn generate rolling moments which oppose the applied moment. When, on the other hand,  $n_r$  has an appreciable negative value—aeroplane statically stable—side-slip causes the aeroplane to



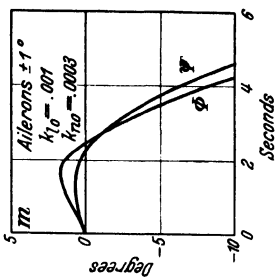
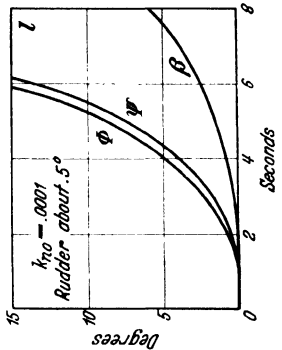
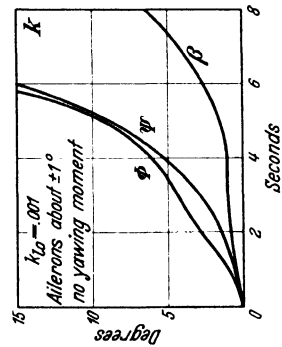
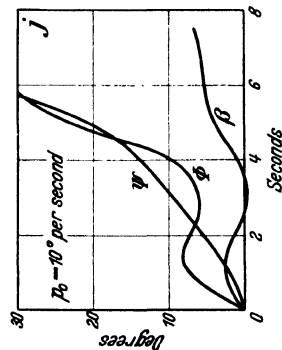
a, b and c. Initial rate of roll  $(p_*) = 10^\circ$  per second.



d, e and f. Small applied rolling moment coefficient  $(k_l)_0 = 0.001$ .



g, h and i. Small applied yawing moment of coefficient ( $k_n(0) = 0.0001$ ).



j, k, l and m. Stalled aeroplane at 22° degrees incidence.

Figs. 57 a—m. Graphs showing asymmetric motions in certain circumstance.

Heavy line = 3° incidence.  
 Broken line = 10° incidence.

$\eta$  = variations in angle of roll.

$\psi$  = variations in angle of yaw.

$\beta$  = variations in angle of side-slip.

S, stable.

N, neutral.

U, unstable.

yaw in such a way that further rapid increase of side-slip is prevented; the opposing rolling moment due to side-slip is thus greatly reduced and the applied rolling moment has more effect. These differences between the stable and the other conditions in respect of side-slips and rates of yaw are clearly shown in Fig. 57 e and f.

In the neutral case the final state is such that bank, side-slip, and rate of change of azimuth increase steadily. In the unstable case the final banked turn increases exponentially.

**22. Applied Yawing Moments.** Figure 57 g, h and i show the effect of applying a small yawing moment corresponding to about  $1/3$  degree movement of a normal rudder. In the stable condition the aeroplane is seen to be much more sensitive to this applied moment than in either the neutral or the unstable condition. This again is due to the absence of the *static* stability term ( $n_r$ ) in the stable aeroplane; with this term zero the aeroplane yaws violently under the action of the rudder; this yaw causes side-slip which generates rolling moments which rapidly bank the aeroplane.

In the unstable condition the aeroplane is seen to be even less sensitive than in the neutral condition; this is due to the absence of the  $l_r$  term—zero dihedral angle—in the former condition. When  $l_p$  is zero, side-slip generates no rolling moments, the rate of roll is less and negative side-slip is therefore greater than when  $l_r$  has the usual positive value; this again causes larger yawing moments to oppose the applied moment and hence results in a slower turn.

It is interesting to note that although the ultimate effect of a given applied yawing moment is greatest in the unstable condition and least in the stable condition, yet the magnitudes of the effects during the first twenty seconds and even longer are in the reverse order; the stable aeroplane, with its dihedral angle and small fin, being very sensitive to the rudder, whilst the unstable aeroplane with its zero dihedral and larger fin is relatively insensitive.

It is again noticeable that the aeroplane at  $10^\circ$  incidence behaves in a manner not very different from the stable aeroplane at  $3^\circ$  incidence.

**23. Rolling and Yawing Moments Applied Simultaneously.** When rolling and yawing moments are applied simultaneously, as when an ordinary aileron is used, the effect can be obtained by adding together the solutions of Fig. 57 d, e, f and Fig. 57 g, h, i in appropriate proportions. Confining attention to the first ten to twenty seconds after the application, we note that whereas the stable aeroplane with  $n_r$  zero is much less sensitive to rolling moments than the neutral or unstable aeroplanes, it is much more sensitive than the other two to yawing moments. An ordinary aileron generates, in normal flight, a yawing moment of the opposite sign to the rolling moment, and about one

tenth its magnitude (see III 42). It follows from Fig. 57 d and g, that in the stable state—positive dihedral and small fin—the yawing effect of the ailerons will indirectly neutralize their direct rolling effect and the aeroplane, under the action of its ailerons unsupported by rudder movement, will ultimately roll in the wrong direction. The unstable aeroplane—small dihedral and large fin—will not be so liable to this defect, but will be much less sensitive to its rudder.

It may at first sight be thought that ailerons which, when used alone, ultimately roll the aeroplane the wrong way, must be useless to the pilot, but this is not so, provided that the pilot is easily able, by using his rudder to neutralize the yawing moment which they generate. In normal flight this is always possible; hence, although it is better to use ailerons which do not produce appreciable yawing moments, the effect of using ailerons which, in the absence of rudder moments would roll the aeroplane the wrong way is not so serious as might be supposed. The reflexes of the trained pilot cause him always to use the rudder in sympathy with the ailerons to such an extent that he is probably unaware of what either does when the other is held fixed. These remarks are true only of normal flight. In stalled flight the adverse effects of the yawing moments produced by the ailerons are greatly increased and may lead to serious danger.

**24. Stalled Flight.** Figure 57 j, k and l show the solutions for the stalled aeroplane, with all three variables  $\varphi$ ,  $\psi$ ,  $\beta$ , plotted on the same diagram. The changes of the scales upon which the angular disturbances and the times are plotted should be noted. The motion is in all cases violently unstable owing to the presence of a large positive root in the quartic for  $\lambda$ ; the mode corresponding to these roots doubles itself every 1-3/4 secs. and very soon dominates the situation, so that the aeroplane ultimately descends into the spin, whatever the nature of the initial disturbance. The spin itself cannot, of course, be even approximately regarded as a small disturbance from straight flight, so that long before the steady spin is reached the equations cease to represent the true motion; nevertheless the initial stages of the motion leading to the spin, involving rapid yawing and rolling rotations of about equal rates, are clearly shown.

Comparison of the effects of applied rolling moment with that of applied yawing moment shows that, although the latter is slower in developing than the former, the ultimate development under an equal applied moment is, after some four seconds, about ten times as great. It was shown in Fig. 44 (III 41) that in stalled flight ailerons of normal type generate yawing moments—chord axes—between 0.2 and 0.5 times the rolling moments and of the opposite sign. From Fig. 57 j and k it is clear that any such aileron, applied without sympathetic rudder

movement, will, shortly after its application, cause the aeroplane to roll violently in the opposite direction from that intended.

Figure 57 m, obtained by adding Fig. 57 k to 57 l in correct proportions, shows the effect in stalled flight of an aileron which generated a yawing moment  $-0.30$  times the rolling moment. The disastrous consequences of this action of an aileron in stalled flight are discussed in Chapter IV, so that they will not be followed further in the present chapter.

Elaborate experiments have been made (Ref. 1) using recording gyroscopic apparatus, to determine the actual motion of a stalled aeroplane under the action of its controls. It will be sufficient to note that those carried out on the Bristol Fighter are in reasonably close agreement with the solutions here given, so that in spite of the approximations and limitations imposed on the calculations and in spite of the probable existence of *scale effects* between the results of experiments on small models and full scale aeroplanes, the solutions do represent in general character the actual motions of the full scale aeroplane in free flight, under the influence even of large control movements.

### 25. Uncertainty of the Values of the Derivatives in Stalled Flight.

The solutions here given for the stalled aeroplane are based on data obtained from continuous rotation experiments. Had they been based on data from oscillation experiments (see Fig. 42, III 38) they would have taken a very different form, involving two exponential convergencies and a practically undamped oscillation. This type of oscillation has also been recorded instrumentally on the Bristol Fighter, after it had been very carefully stalled whilst flying on an even keel with no appreciable rotation. The recorded oscillation had a very slight tendency to increase and, after developing a small but appreciable amplitude, was suddenly converted into a divergence of the type of Fig. 57 j, k, l. It, therefore, seems probable that the stalled aeroplane cannot be regarded as possessing a single set of derivatives at any given incidence, or, in other words, that the aerodynamic forces are not unique functions of the instantaneous velocities but depend also on the history of the motion. It would seem that if the disturbances start in the form of oscillations of small amplitude, in which rotations are not rapid and do not continue for any length of time in any one direction, the forces may approximate to those indicated by oscillation experiments. If, however, the amplitudes become large or, for any reason, such as a control application, the rotations continue for some time in one direction, there may be a sudden change over to a regime represented by the derivatives measured in continuous rotation experiments.

These ideas are at present conjectural, but the comparison between the theoretical solutions and the results of free flight experiments certainly suggest that they represent the truth, though possibly very roughly. More research is, however, required before any certainty can

be achieved in the analytical examination of stalled flight. The calculations discussed above have been given as examples of the application of the method to stalled conditions rather than as representing the exact behaviour of a specific aeroplane.

**26. Scale Effect on a Thick Wing in Stalled Flight.** The agreement noted above between free flight experiment and the solutions of the equations of motion based on measurements of derivatives on small models, applies to thin-wing aeroplanes for which the scale effects on the lift and drag coefficients are small. For certain thick-wing aeroplanes these scale effects are large and consequently the derivatives themselves, which depend greatly on the shapes of the curves for lift and drag against incidence, will probably be subject to large scale effects. In these circumstances agreement between solutions based on derivatives obtained at a small value of the Reynolds' number and free flight experiments in which the Reynolds' number is necessarily large, cannot be expected.

When calculations are to be made on thick-wing aeroplanes in stalled flight it will therefore, in all probability, be necessary to carry out the preliminary experiments to find the *derivatives* upon models in wind tunnels which allow of the full Reynold's number being obtained.

#### D. Information by Inspection of the Quartic for $\lambda$

**27. Condition for Complete Stability.** As with the symmetric equations of Chapter VI so with the asymmetric equations under consideration, some idea of the nature of the solutions can be obtained merely by inspecting the quartic for  $\lambda$ . Thus the motion is completely stable if all the coefficients  $B$ ,  $C$ ,  $D$ , and  $E$  are positive and Routh's *discriminant* ( $BCD - B^2E - D^2$ ) is also positive.

**28. The Large Root.** Consideration of the values of the coefficients  $B$ ,  $C$ ,  $D$ ,  $E$  in Table 2 shows that in *normal flight* there is in all cases one large root of the same order of magnitude as  $B$ , for, writing the quartic in the form  $\lambda + B + C\lambda^{-1} + D\lambda^{-2} + E\lambda^{-3} = 0$

and observing that  $B$  is of the order 6, that  $C$  and  $E$  are smaller than  $B$  and that  $D$  is never much larger than  $B$ , it follows that when the root is large the three last terms will be small compared with  $B$  and that there will therefore be a large root of the same order of magnitude as  $B$ .

A second approximation to this large root is obtained by putting  $\lambda = -B$  in the third term and neglecting the last two terms. This gives

$$\lambda = -B + C/B$$

Replacing  $B$  and  $C$  by their values in terms of the derivatives in Table 2 gives

$$\lambda = -l_p - n_r - y_v + \frac{1}{l_p} [(n_r + y_v) l_p + y_v n_r - l_r n_p + \mu (l_v \sin A_1 - n_v \cos A_1)]$$

in which the small terms  $n_r$  and  $y_v$  have been omitted from the term which multiplies the square bracket. This reduces to

$$\lambda = -l_p + \frac{1}{l_p} [y_v n_r - l_r n_p + \mu (l_v \sin A_1 - n_v \cos A_1)]$$

which, when numerical values are inserted is seen to be very nearly the same as  $\lambda = -l_p$ . Comparison between Table 1 (7) and Table 3 (10) will show that, whereas at both  $3^\circ$  and  $10^\circ$  incidences  $l_p = 6.10$  the large root is  $-6.0$  in all three cases at  $3^\circ$  incidence and  $-5.8$  at  $10^\circ$  incidence.

We have seen that the mode corresponding to the large root sensibly disappears from the motion within a small fraction of a second after the disturbance which generates it, consequently the precise value of this root is not, as a rule, of any great interest, and it is generally sufficiently accurate to assume that its value is  $-l_p$ . This assumption, however, cannot be made when the aeroplane has stalled, for then  $l_p$  is small, whereas the basis of the assumption is that  $l_p$  is large.

**29. The Small Root.** The coefficients  $B$ ,  $C$ ,  $D$  are considerably greater than unity, whereas the constant term ( $E$ ) is small, of the order  $\pm 0.2$  at  $3^\circ$  incidence. There is, therefore, a small root of approximate value  $-E/D$ , for when  $\lambda$  is small the first three terms of the quartic are small compared with the last two terms. A second approximation to this root is obtained by replacing  $\lambda$  by  $-E/D$  in the third term and neglecting the first two terms. This leads to a value of the small root  $(-E/D) [1 + CE/D^2]$ . These approximations are compared with the accurately computed small roots in Table 5.

TABLE 5. Approximate and Correct Value of the Small Root.

	First Approximation	Second Approximation	Correct Value
$3^\circ$ Incidence, stable . . . . .	—096	—11	—11
$3^\circ$ Incidence, neutral . . . . .	0	0	0
$3^\circ$ Incidence, unstable . . . . .	+031	+031	+031
$10^\circ$ Incidence . . . . .	—062	—064	—065

The first approximation is good enough for most practical purposes but slightly underestimates the value at the high incidence of  $10^\circ$ .

**30. Approximate Values of the Complex Roots.** A very rough approximation to this pair of roots is obtained by neglecting the first and last terms of the quartic and hence leaving for solution the quadratic.

$$\lambda^2 + \frac{C}{B} \lambda + \frac{D}{B} = 0$$

The roots of this quadratic are compared with the corresponding roots of the quartic in Table 6.



TABLE 6. Approximate and Correct Values of the Complex Root.

	Approximate roots	True roots
3° incidence, stable . . . .	$-.27 \pm .53i$	$-.21 \pm .53i$
3° incidence, neutral . . . .	$-.36 \pm 1.12i$	$-.26 \pm 1.20i$
3° incidence, unstable . . . .	$-.34 \pm .96i$	$-.29 \pm 1.06i$
10° incidence . . . . .	$-.39 \pm .97i$	$-.30 \pm 1.04i$

It therefore appears that, although in the examples examined the approximate solution gives a fair idea of the period of the oscillation, it definitely overestimates the damping. The value of the damping term is an important feature of this mode and hence the approximation under consideration has little practical value. The sign of this damping term, which determines whether the oscillation will increase or decrease, can be obtained from Routh's discriminant ( $BCD - B^2E - D^2$ ); the oscillation will increase if this discriminant is negative. If the magnitude of the damping term is required it must be obtained by solving the numerical quartic.

**31. Level and Climbing Flight.** When the engine is not working the attitude of the aeroplane, defined by the angle  $\Theta_1$ , is a unique function of the incidence of the wings, but when the engine is working  $\Theta_1$  depends also upon the power output. The solutions of the equations of motion involve the angle  $\Theta_1$  and therefore will depend upon the power output, or in other words upon the inclination of the steady flight path, as well as upon the incidence of the wings. The power output will also influence the derivatives through the direct and indirect action of the airscrew, but the methods of allowing for these effects of the airscrew are similar to those discussed in Chapter VI in connection with the symmetric derivatives  $m_q$  and  $m_{\dot{w}}$ , except that the complication due to the effect of the screw on the downwash from the wings is absent. We shall not, therefore, enter into a discussion of the influence of the airscrew upon asymmetric derivatives, but shall confine our attention to the effects of changes in  $\Theta_1$  which occur when the engine is working with various powers. We may suppose that the derivatives with airscrew working happen to have the values assumed in the examples previously studied in gliding flight.

The only coefficient of the quartic which is seriously influenced by changes of  $\Theta_1$  is the constant term ( $E$ ) which at the cruising incidence of 3° depends (see Table 2, 9) upon  $\Theta_1$  in the following manner,  $\cos \Theta_1$  being taken as unity.

$$\begin{aligned} \text{Stable case } n_v = 0 \quad & E = .19 - .24 \sin \Theta_1 \\ \text{Neutral case } & E = -.20 - 1.6 \sin \Theta_1 \\ \text{Unstable case } l_v = 0 \quad & E = -.39 - 1.4 \sin \Theta_1 \end{aligned}$$

In all three cases positive values of  $\Theta_1$ —steeper climbing angles—reduce  $E$  and therefore reduce the stability of the mode corresponding to the small root.

In gliding flight at  $3^\circ$  incidence,  $\Theta_1 = -7^\circ$  and  $E$  has, of course, the values of Table 2, being zero in the neutral case. In horizontal flight at this incidence  $\Theta_1 = 3^\circ$  giving,

Stable case . . . . .	$E = .18$
Neutral case . . . . .	$E = -.28$
Unstable case . . . . .	$E = -.46$

Reference to Table 2 shows that the influence of  $\Theta_1$  on  $E$  is mainly through the term  $n_v$  and therefore in the stable case in which  $n_v$  is zero its effect is small; in the other two cases, its effect is considerable.

In climbing flight, where  $\Theta_1$  may have a large positive value—say up to  $20^\circ$  in a high powered aeroplane—the destabilizing influence on an aeroplane which has large directional static stability— $n_v$  large and negative—may be very marked, but since it will be unusual for a pilot to want to abandon his controls altogether when climbing rapidly, this form of instability, which requires many seconds to make itself felt, may not be troublesome.

## E. Changes of Dihedral Angle and Fin Area

**32. Introduction.** Two only of the derivatives can be varied by minor alterations in design. These, as we have seen, are  $l_r$  which depends upon the dihedral angle between the wings and  $n_r$  which is governed by the size of the fin and rudder. In order to avoid handling small unimportant terms, which would not add to the value of an illustrative discussion, we shall assume, in studying the effect of variations of these derivatives, that  $\Theta_1$  is zero, and that the aeroplane is therefore descending at an angle of  $3^\circ$  to the horizontal.

**33. Spiral Instability.** In these circumstances

$$E = \mu k [l_v n_r - l_r n_v]$$

and therefore the slowly developing mode will be unstable unless  $[l_v n_r - l_r n_v]$  is positive. Inserting the value of  $n_r$  and  $l_r$  from Table 1 (7) at the cruising incidence of  $3^\circ$ , we find that *spiral* instability will occur unless  $.29 l_v - (-1.75) n_v$  is positive. Assuming that, as is usual,  $l_v$  is positive, the aeroplane will become unstable in respect of the small root when  $n_v$  is negative and numerically greater than  $.16 l_v$ . When  $n_v$  is negative the aeroplane is statically stable, hence, too high a degree of static stability causes spiral instability in free flight.

**34. Increasing Oscillations.** The dependence of the coefficient of the quartic on  $l_v$  and  $n_v$  at the cruising incidence of  $3^\circ$  with  $\Theta_1 = 0$  can be shown from Tables 2 p. 186 and 1 p. 184 to be as follows:

$$\begin{aligned} B &= 6.54 \\ C &= 3.38 - 5.9 n_v + .305 l_v \\ D &= 0.36 - 35.4 n_v + 3.40 l_v \\ E &= 2.05 n_v + .340 l_v \end{aligned}$$

The oscillation corresponding to the pair of complex roots becomes unstable, in the sense that its amplitude increases with time, when Routh's discriminant becomes negative. Dividing the discriminant by the constant positive term  $B$  leaves the condition for instability that  $CD - BE - D^2/B$  should be negative. Inserting the above expressions for  $B$ ,  $C$ ,  $D$  and  $E$  into this expression we find that the oscillation will increase if  $1.2 - 130 n_v + 9.2 l_v + 17 n_v^2 - 0.6 l_v^2 + 6 l_v n_v$  is negative.

The critical condition in which the oscillation will continue indefinitely without change of amplitude occurs when this expression is zero and this condition yields the following relations between  $l_v$  and  $n_v$ . The value  $l_v = 0.56$  is that used in the detailed computations of earlier paragraphs whilst 1.00 is about the highest value of  $l_v$  which is likely to occur in practice at cruising speed.

$l_v$	$n_v$
0	.009
.56	.048
1.00	.080

**35. Spinning Instability.** If the positive value of  $n_v$  increases sufficiently beyond that value which causes an increasing oscillation, the imaginary terms in the complex pair of roots will disappear; a rapidly increasing exponential mode will then occur and the aeroplane may be said to develop spinning instability. With  $l_v = .56$ , as in our illustration, the critical value of  $n_v$  at which this occurs is in the neighborhood of 0.14. But a somewhat smaller value than this will be sufficient to cause the oscillation to develop so rapidly that the motion will be almost indistinguishable from an exponential divergence.

The values of the coefficients of the quartic when  $l_v = .56$  and  $n_v = .048$  and .14 respectively are as follows:

Hence the increasing oscillation occurs whilst all the coefficients are positive, whereas the rapidly increasing exponential term does not occur until  $D$  has a considerable negative value. In the latter case the value of the positive root is about 0.3 so that this form of instability develops very rapidly, the mode doubling itself about every two seconds.

	$n_v = .048$	$n_v = .14$
$B$	6.54	6.54
$C$	3.27	2.73
$D$	.59	-2.66
$E$	.29	.48

**36. Summary.** For the asymmetric motions of the aeroplane to be completely stable the derivative  $n_v$  must lie between small negative and small positive values. If the negative value of  $n_v$  is too large—directional static stability too great—slow spiral instability will occur. If the positive value of  $n_v$  is too large, a rapidly developing type of instability will appear. When the excess of  $n_v$  over the critical value at which Routh's discriminant becomes zero is small this instability appears as an increasing amplitude of an oscillation involving rolling and yawing, but when the excess of  $n_v$  becomes relatively large, the oscillation is transformed into a rapidly increasing exponential mode. The range of stable values of  $n_v$  is nearly proportional to  $l_v$ , that is to say to dihedral angle; the range is reduced, on the spiral instability side, by increasing the angle of climb.

## CHAPTER VIII

### THE SPIN

**1. Introduction.** When an aeroplane is stalled and left to itself it may develop a rapid rolling and yawing motion, the beginnings of which have been followed in a typical instance by the detailed methods of Chapter VII and are illustrated in Fig. 57m of VII 24. If allowed to proceed unchecked this may develop into a characteristic type of motion known as the spin, in which the aeroplane descends rapidly, executing a more or less steady helical movement about a vertical axis which passes relatively close to the c.g., say between 2 and 20 feet from it, according to the type of spin which is developed. The spin is familiar to all pilots and, though it has no practical value either for military or civil purposes, it is receiving considerable attention, because it is liable to occur accidentally, either as the result of inattention on the part of the pilot or through failure to execute some manoeuvre correctly.

In the early days of flying—before 1916—the spin generally ended fatally, because what later proved the most effective means of checking it was in some respects contrary to the natural reaction of the pilot to the realization that he was diving towards the earth. About 1916 it was discovered that an effective way of checking the type of spin which was common in those days was to thrust the control stick forward and apply rudder in the sense opposed to the rotation. For sometime after this knowledge had become general, relatively few fatalities due to spinning occurred, provided that there was enough air-room for the spin to be checked and the resulting steep dive to be converted into horizontal flight; the spin then became an ordinary manoeuvre.

Some years later, about 1919, aeroplanes began to appear which developed a kind of spin which could not be checked by the control movements which had hitherto been effective, and many fatalities have since occurred through spins of this type continuing to the ground. In this new type of spin the rotation was much faster and the aeroplane's body more horizontal than in those which had been commonly observed in earlier years. For while the spins which had previously been studied occurred at a rate of about one turn in three seconds, with the body inclined at say 35 to 45 degrees to the vertical, the new and dangerous variety might have a rotation rate as high as one turn per second, with the body within 10 to 20 degrees of horizontal. Spins of every kind intermediate between these extremes have been observed, but it is reasonably representative of experience to divide them into two groups which might be described as slow-steep and fast-flat, respectively, and to say that it is from the latter group chiefly that recovery is difficult. It is not uncommon for an aeroplane to be able to spin steadily in either of two ways, one of the slow-steep and the other of the fast-flat variety,

the transition from one form to the other, when it occurs, being relatively rapid.

The reasons why the flat spin apparently became much more common after about the year 1920 have been much debated; they are probably to be found, partly in changes in the trend of design of military aeroplanes, and partly in the advent of the parachute, which greatly increased the number of survivors who could give an account of spins which had become uncontrollable. Whatever the reason, there is no doubt that, in the years following the war, the flat spin introduced a serious danger to flying, particularly in war aeroplanes, and for this reason extensive researches were set on foot in various countries the main object of which was to eliminate it from the possible modes of motion of the aeroplane. These researches have not yet reached finality, so that, in the present chapter, it would be inappropriate to do more than give a general idea of the factors which control the spin, with special reference to those which permit or prevent the occurrence of the dangerous flat spin.

**2. Experimental Methods.** Our knowledge of the forms taken by the free spin comes partly from experiments made upon full scale aeroplanes in flight, with the help of recording instruments carried within them or of cinematograph records taken from the ground, and partly from observations of small models which can now be made to spin freely and for long periods of time in an ascending air current. The full scale experiment suffers from the limitation that instrumental records cannot readily be obtained for spins of a type from which recovery is difficult, though a few isolated records of such spins have been made. The method of the free spinning model is of recent development and has added greatly to our knowledge of the form taken by the more dangerous types of spin. By this method it is now possible to study the effects on the spin of control movements, which can be started by delay action mechanisms carried on the model. The subsequent changes in the motion can then be studied in detail upon records made with high speed cinematograph cameras.

Our knowledge of the forces and moments which act in the spin upon the aeroplane or any of its parts comes from experiments in which models are constrained to rotate in wind tunnels about fixed axes, parallel to the wind in the tunnel. In the great majority of the earlier experiments the models were made to rotate about axes passing through the position of the c.g. of the aeroplane and lying in its plane of symmetry. Recently, however, the method has been extended to include observations on models rotating with their c.g. offset from the axis of rotation and in attitudes unsymmetrically disposed to the axis of rotation. It is to the extension of the rotation experiments to include these unsymmetrical attitudes and to the development of the technique of the free spinning model experiment that we owe the great strides which have been made in the study of the spin during the past few years.

**3. Theoretical Calculations.** On the theoretical side, one or two attempts have been made to trace, by step-by-step methods of calculation, the progress of an aeroplane from steady straight horizontal flight into the steady spin (Chapter V. Refs. 1 and 2). These are interesting and worth examination by those especially concerned with the study of the spin, but their usefulness is limited by the uncertainty of the data upon which they are founded.

There are also to be considered the stability of the steady spin and the power of the controls to disturb its equilibrium. Often the spin is observed not to be steady, but to involve periodic changes about an apparently steady state, or again it is found that some spins alter slowly and progressively for many turns and then begin to change at a much more rapid rate. Indeed experience in England is that the dangerous type of spin generally develops in this way. It has also been found that spins which cannot be checked by steady control movements can sometimes be stopped by moving the controls roughly and, as it were, flinging the aeroplane out of the stable equilibrium condition into which it has sunk. A few of these unsteady types of motion have been investigated, but the matter is too complicated and the results so far obtained, too slight to be included in this chapter. The following discussion relates therefore entirely to steady states.

The detailed analysis, even of the steady spin, in a form suitable for the precise prediction of the way in which an aeroplane of given design would spin with any given setting of the controls, is a matter of considerable complication, and the calculations must be based either upon wind tunnel experiments on a model of the actual aeroplane, or upon a mass of experimental data obtained from models of aeroplanes and their parts. No basis of general experimental data completely adequate for this purpose is yet available, and it seems doubtful whether it ever will become available, for the main object of studying the spin is to prevent it from occurring in any form from which recovery is difficult; and when this object has been achieved the exact prediction of the forms which spins might take, if they occurred, will become of little more than academic interest. With this consideration in mind the present chapter has been written, not with a view to displaying convenient methods for calculating the precise form which the spin will take in any given circumstances, but along lines similar to those of Chapter IV. We shall begin by studying a very simple type of motion, which may be regarded as the prototype of the real spin, and add the effects of the more important complications in successive steps, keeping the argument simple by ignoring minor factors which would have to be included in any precise statement but which do not greatly affect the final result. By this method of approach it is hoped that the reader will obtain a clear grasp of the physical ideas involved and of the relative importance of the various factors which affect the problem.

**4. Notation and the Equations of Motion.** It will however be convenient first to consider how the general equations of motion of Chapter V can be simplified to apply to the steady spin. With some modifications, which will appear as we proceed, the system of notation of previous chapters will be employed. *Chord Axes* fixed in the body will be used and treated as principal axes, so that the products of inertia,  $D$ ,  $E$ ,  $F$  of Chapter V become zero. The steady angular velocity about a vertical axis receives the symbol  $\Omega$  and the distance of the c.g. from the axis of rotation, the symbol  $R$ .

The general equations of motion of V 5 are now simplified by the omission of all dotted symbols and the first three equations, representing the balance of forces, reduce to the condition that the resultant air-force must intersect the axis of the spin and that its horizontal component must equal the centrifugal force  $mR\Omega^2$ , whilst its vertical component equals the weight ( $mg$ ).

The three equations defining the balance of moments will be found to reduce to

$$\left. \begin{aligned} L &= (C - B)qr \\ M &= (A - C)rp \\ N &= (B - A)pq \end{aligned} \right\} \quad (4.1)$$

Now since  $p, q, r$  are the components of the vector  $\Omega$  along the three axes, they can be expressed in terms of  $\Omega$  and any two angular coordinates which define the orientation of the aeroplane to the vertical. These coordinates will be specified as follows. First imagine that the aeroplane is diving with the  $X$  axis vertical and the  $Y$  and  $Z$  axes therefore horizontal. Now rotate it about the  $Y$  axis, through an angle  $\alpha$ , until the  $Z$  axis takes up its final attitude with respect to the vertical. Next rotate it about the  $Z$  axis, through an angle  $\beta$ , into its final orientation with respect to the vertical. The angle  $\alpha$  will be called the angle of pitch and be positive when the aeroplane is right way up. The angle  $\beta$  will be called the angle of yaw and be positive when the rotation from the attitude of zero yaw carries the nose of the aeroplane to the pilot's right. These angular coordinates are different in some respects from those used in earlier chapters, but they are convenient in the study of the spin. With these coordinates the component angular velocities can be expressed as follows

$$\left. \begin{aligned} p &= \Omega \cos \alpha \cos \beta \\ q &= -\Omega \cos \alpha \sin \beta \\ r &= \Omega \sin \alpha \end{aligned} \right\} \quad (4.2)$$

Inserting these values of  $p, q, r$  in (4.1) gives

$$\left. \begin{aligned} L &= -\frac{1}{2} \Omega^2 (C - B) \sin 2\alpha \sin \beta \\ M &= -\frac{1}{2} \Omega^2 (A - C) \sin 2\alpha \cos \beta \\ N &= -\frac{1}{2} \Omega^2 (B - A) \cos^2 \alpha \sin 2\beta \end{aligned} \right\} \quad (4.3)$$

These equations can be thrown into a convenient dimensionless form by dividing throughout by  $\rho V^2 S s$  to give

$$\left. \begin{aligned} k_l &= -\frac{1}{2} \mu k_\Omega^2 (k_C - k_B) \sin 2\alpha \sin \beta \\ k_m &= -\frac{1}{2} \mu k_\Omega^2 (k_A - k_C) \sin 2\alpha \cos \beta \\ k_n &= -\frac{1}{2} \mu k_\Omega^2 (k_B - k_A) \cos^2 \alpha \sin 2\beta \end{aligned} \right\} \quad (4.4)$$

in which, as in previous chapters

$$k_\Omega = \frac{\Omega s}{V} \quad \mu = \frac{m}{\rho S s}$$

$k_A, k_B, k_C$  stand, respectively for  $A, B, C$  divided by  $ms^2$ .  $k_l, k_m$  and  $k_n$  stand for  $L, M$  and  $N$  divided by  $\rho V^2 S s$  while  $\rho, S$  and  $s$  represent, as in previous chapters, the air-density, wing area and semi-wing span;  $V$  is defined as the velocity of the c.g. along the axis of the spin instead of, as before, the resultant c.g. velocity. The pitch of the helical path of the c.g. is, however, always so large compared with its radius that this difference of definition is unimportant.

The change in the definition of  $k_m$  from that of previous chapters is clearly necessary when all three components of the air-couple are included in one discussion.

## A. Autorotation.

**5. Rotation about a Fixed Axis.** In the steady free spin the moment about the axis of rotation is necessarily zero, but it is convenient to begin by considering an experiment in which an aeroplane, or its model, is constrained to rotate steadily about a fixed axis in a wind tunnel, whilst the moment necessary to maintain the rotation is measured. We shall call this moment the *spinning moment*, despite the fact that it is zero in the free spin. At first we will confine attention to the effects of rotation about an axis which passes through the c.g. and lies in the plane of symmetry of the aeroplane or its model, and is parallel to the direction of the wind in the tunnel (see Fig. 58<sup>1</sup>). Thus we begin by imagining that the motion of the aeroplane is entirely constrained, and we shall then suppose that it is given, successively, more and more degrees of freedom, until it is completely free, as in the real spin. At each stage of this imaginary process we shall consider the consequences of releasing each new degree of freedom.

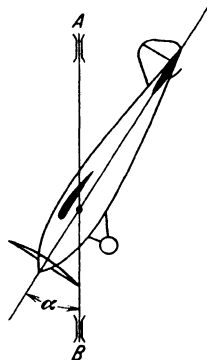


Fig. 58.

<sup>1</sup> The motions described in this chapter are more easily visualized with the aid of a small model aeroplane and a straight rod with which to represent the axis of rotation.



In this wind tunnel experiment the axis of rotation may be vertical or horizontal, but since the motion is entirely constrained, the orientation of the axis is immaterial. In the free spin the axis of rotation is necessarily vertical and, for simplicity of statement, we shall imagine that it is so in the wind tunnel experiment under discussion. In this experiment, then, the angle  $\alpha$ , which is defined in 4 as the inclination of the  $Z$  axis to the horizontal, is identical with the incidence of the wings at the centre section. This identity does not generally hold in the free spin, though the difference between  $\alpha$  and incidence is never very great.

**6. Autorotation Defined.** Figure 59 contains a typical group of curves showing the spinning moment coefficient plotted against angular velocity coefficient for a model of a particular aeroplane rotating in a wind tunnel in the manner described above and set at various angles of incidence.

In normal flight, below  $12^\circ$  incidence, the slope of the curve is large and negative, showing that powerful moments oppose the rotation; but above  $12^\circ$  incidence the slopes of all the curves near the origin, with one exception, are positive, showing that the air-moment is in the same direction as the rotation. In these latter circumstances,

the model, if free to rotate about the fixed axis but not actually rotating, would be in unstable equilibrium, for the angular velocity of any small initial rotation in either direction would increase until  $k_\Omega$  reaches the value at which the moment is again zero, when a second and stable state of equilibrium would be reached with the model rotating steadily. This phenomenon is known as *autorotation* and the angular velocity of the condition of steady free rotation will be called the *autorotation rate* of the model at the incidence in question.

**7. Latent Autorotation.** In Fig. 59 the curve corresponding to  $40^\circ$  incidence is more complicated than the others, for the slope at the origin is negative and the axis of zero moment is cut twice more, once with positive slope and once with negative slope. At this incidence the equilibrium of the non-rotating state is stable; the equilibrium when  $k_\Omega$  is approximately 0.2 is unstable, while that corresponding to  $k_\Omega = 0.75$  is again stable. If the model is given an initial angular velocity for which  $k_\Omega$  is less than 0.2 and then left free, the rotation will stop, but

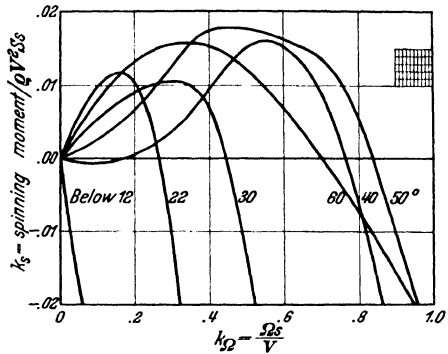


Fig. 59. The spinning moments of a model biplane. The incidence of the centre section appears on each curve.

if the initial angular velocity is greater than this it will continually increase to that of the stable equilibrium state. In these circumstances the autorotation is said to be *latent* and the angular velocity at the stable equilibrium condition is the one which is called the autorotation rate.

**8. Autorotation Rates.** Figure 60 shows the autorotation rates of the biplane of Fig. 59. These diagrams show how complicated are the factors which determine the autorotation rate, and give some idea of the very high rates which may arise, even when the aeroplane is made to rotate in an attitude which is symmetrical with respect to the axis of rotation. In the free spin the aeroplane, of course, is not necessarily

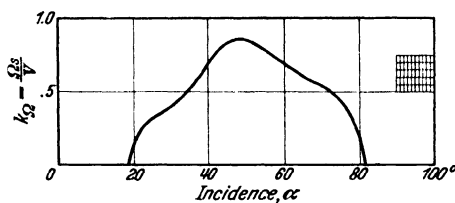


Fig. 60. The autorotation rates of a model aeroplane at various incidences.

symmetrical with respect to the axis of spin and, as we shall see, departure from the symmetrical attitude profoundly influences autorotation rate, but it will be convenient to postpone consideration of these effects until we have considered the consequences of releasing several other degrees of freedom.

Not every aeroplane can rotate so rapidly and at such high angles of incidence, whilst held in symmetrical attitudes with respect to the axis of rotation. Biplanes with small stagger can do so, but monoplanes and some biplanes with exceptionally large forward stagger of the upper planes cannot reach high rates or autorotate at high incidences, unless they are allowed certain unsymmetrical displacements which will be discussed in due course.

## B. Pitching Moments

**9. The Centrifugal Pitching Moment.** In order that an aeroplane or its model should rotate steadily about a fixed axis in the plane of symmetry, as in the motion discussed in the previous paragraphs, a certain pitching moment about an axis perpendicular to the plane of symmetry—the  $Y$  axis—must be applied to it to balance the moment exerted by the centrifugal forces (see Fig. 61) which act upon the various parts that do not lie upon the axis of rotation.

Since the word *centrifugal force* is in familiar use to represent a hypothetical force equal and opposite to that required to maintain a mass in steady circling motion, we may use the term *centrifugal moment* to represent a hypothetical moment equal and opposite to that required to maintain the aeroplane in steady rotation; and we may say that this centrifugal moment is equal to the sum of the moments of the centrifugal forces acting on all parts of the body. The air-forces acting

on the aeroplane in general exert a pitching moment and, in the experiments of the previous paragraphs, it was clearly necessary to apply some constraint to the model sufficient to exert a pitching moment which, together with the air-moment, equalled the centrifugal pitching moment.

Suppose now that this restraint is removed, and the model thus given freedom to pitch about the  $Y$  axis. It now becomes a necessary condition of steady motion that the air pitching moment shall be equal and opposite to the centrifugal moment. Equations (4.4) relate to the steady spin of entirely free aeroplanes, but we can apply the second of these equations to the specially simple motion now under consideration in which  $\beta$  is zero and we have the condition of equilibrium about the  $Y$  axis

$$k_m = -\frac{1}{2} \mu k_\Omega^2 (k_C - k_A) \sin 2\alpha \quad (9.1)$$

in which the symbol  $k_m$  represents the coefficient of the air pitching moment. Or we may express the same idea by the statement that the coefficient of the centrifugal moment is

$$\frac{1}{2} \mu k_\Omega^2 (k_C - k_A) \sin 2\alpha \quad (9.2)$$

and that, when the model is free to pitch, steady conditions require the coefficient of the air-moment to be equal and opposite to this.

This form of the expression for the centrifugal pitching moment, which involves the difference between the moments of inertia about the axes of  $Z$  and  $X$ , is the one in common use and is the most convenient for computation; but since it has been derived as a special case of the much more complicated general equations of motion (see V 5) and since it contains moments of inertia about axes with which we are not at present concerned, it may appear puzzling to readers who are not familiar with rigid dynamics. The following alternative method of deriving the expression directly for the specially simple motion under consideration may assist the reader to obtain a clearer understanding of the origin of the centrifugal pitching moment and of the parts of the aeroplane which principally contribute to it.

**10. The Origin of the Centrifugal Pitching Moment.** Consider a very simple mechanism, Fig. 62, consisting of a rod  $CD$ , pivoted at its centre of gravity  $G$  to another rod  $AB$ , which can rotate in bearings at  $A$  and  $B$ . The hinge at  $G$  is such that  $CD$  must rotate with  $AB$  while the angle ( $\alpha$ ) between the rods can be held at any desired value by a couple applied at  $G$ .

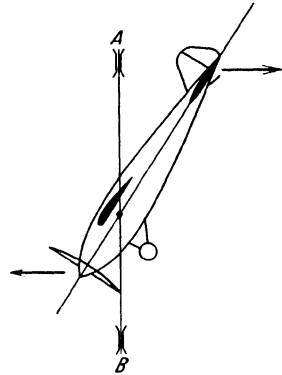


Fig. 61.

If the angular velocity of the whole about  $AB$  be  $\Omega$ , then the centrifugal force on an element of the rod  $CD$  of mass  $dm$ , distant  $x$  from  $G$  will be

$$\Omega^2 x \sin \alpha (dm)$$

The moment of this force about  $G$  will be

$$\Omega^2 x^2 \sin \alpha \cos \alpha (dm)$$

or

$$\frac{1}{2} \Omega^2 \sin 2\alpha (x^2 dm)$$

The moment exerted by the whole rod about  $G$  will therefore

$$\text{be} \quad \frac{1}{2} \Omega^2 \sin 2\alpha I$$

where  $I$  is the moment of inertia of the rod about  $G$ .

The rod, if free to rotate about  $G$ , will therefore set itself at right angles to the axis of rotation and, if constrained to remain at an angle  $\alpha$  to this axis, will experience a centrifugal couple which tends to set it at right angles to the axis and which has a maximum value ( $1/2 \Omega^2 I$ ) when  $\alpha$  is  $45^\circ$ .

Suppose now that the aeroplane is replaced by a dynamically equivalent system consisting of three rods lying along the axes  $X, Y, Z$ , whose moments of inertia about the c.g. are  $I_1, I_2, I_3$ , respectively. Then the moments of inertia of the real aeroplane are related to the moments of inertia of the rods by the equations

$$A = I_2 + I_3$$

$$B = I_3 + I_1$$

$$C = I_1 + I_2$$

When this aeroplane rotates about an axis lying in the plane of symmetry the moment (see Fig. 63) tending to set the  $X$  axis perpendicular to the axis of rotation is clearly

$$\frac{1}{2} \Omega^2 [I_1 \sin 2\alpha + I_3 \sin 2(90 + \alpha)]$$

$$\text{or} \quad \frac{1}{2} \Omega^2 \sin 2\alpha [I_1 - I_3] \quad (10.1)$$

but since  $I_1 - I_3 = C - A$ , this expression, after dividing by  $\rho V^2 S s$  to obtain the coefficient form, becomes identical with expression (9.2). A little consideration will show that the centrifugal pitching moment is unaltered when  $G$  moves away from the axis  $AB$ , provided that  $\Omega$  and  $\alpha$  are unaltered.

The form of the expression involving  $I_1 - I_3$  shows clearly which parts of the aeroplane contribute most to the centrifugal pitching moment. Thus parts such as the tail and the front of the engine, which are far from the c.g. along the  $X$  axis, tend to cause the incidence to increase and the body to set itself perpendicular to the axis of rotation, whilst parts, such as the upper wing of a biplane and the wheels of the

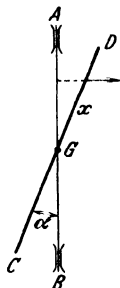


Fig. 62.

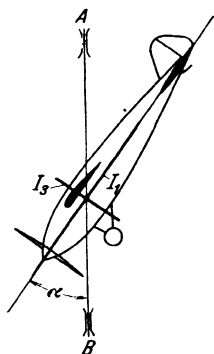


Fig. 63.

undercarriage, which are some distance from the c.g. along the  $Z$  axis, oppose this tendency. Parts, such as the wing tips, which lie near the  $Y$  axis, do not influence the centrifugal pitching moment, no matter how far they may be from the c.g. Since the length of an ordinary aeroplane from nose to tail is always much greater than its height, the centrifugal pitching moment in all normal designs acts in the sense to increase the incidence of the spin.

**11. Balance of Pitching Moments.** If the model is free to rotate about the axis defined in 5 it will do so at the autorotation rate, which is a function of incidence. With given values of  $\mu$  and  $(k_C - k_A)$ , the centrifugal pitching moment coefficient, given by the expression (9.2) then depends upon quantities which are functions of incidence only and will itself therefore be a function of incidence. The same is true of the air pitching moment coefficient which depends only upon the geometry of the motion. Figure 64 shows the form taken by these functions for the model concerned in Figs. 59 and 60. To obtain the curves for centrifugal moment the value assumed for  $(k_C - k_A)$  was 0.056, which is the value for the real aeroplane represented by this model, while four different values, marked on the curves, were assumed for  $\mu$ . The values of  $\mu$  for the real aeroplane ranged from 6 near the ground in air of standard density, to 8 in air of the density appropriate to a height of 10,000 feet.

The air pitching moment coefficient is given for three different elevator settings, corresponding to the neutral position and the two extreme settings. With aeroplanes of conventional design, in the spin, this moment is always negative; in Fig. 64 it has been plotted with sign reversed, to facilitate comparison with the centrifugal moment which opposes it.

If now we imagine that the model is free to pitch about the  $Y$  axis, then steady autorotation can only occur at those incidences at which the centrifugal and airmoments exactly balance one another; that is to say, where the appropriate curves of Fig. 64 cut one another. Thus, with  $\mu$  equal to 2, steady autorotation would be impossible with any of the three elevator settings. With  $\mu$  equal to 4, steady autorotation could occur with elevators hard up, when the incidence is either  $36^\circ$  or  $51^\circ$ , but the equilibrium at the lower incidence would be unstable; if, by

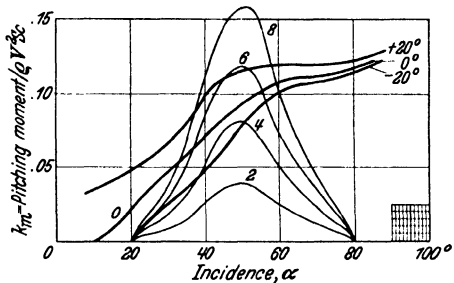


Fig. 64. Comparison between centrifugal and aerodynamic pitching moments during autorotation.

Heavy lines = Air pitching moment (signs reversed—three elevator settings).

Light lines = Centrifugal pitching moments (four values of  $\mu$ ).

some external agency, the rotation rate were raised above that corresponding to the  $36^\circ$  equilibrium condition, then the incidence would eventually rise to the stable equilibrium condition at  $51^\circ$ . With  $\mu$  equal to 6, steady autorotation could occur at  $56^\circ$  incidence with the elevators fully up and at either  $46^\circ$  or  $53^\circ$  with elevators fully down. With  $\mu$  equal to 8, steady stable autorotation could occur at incidences between  $58$  and  $60$  degrees with any elevator position between the given limits.

### C. The Remaining Degrees of Freedom

**12. Freedom to Slide along the Axis of Rotation.** So far the model has been given two degrees of freedom only and four have yet to be released before it is entirely free, as in the true spin. Suppose first that the model is allowed freedom to slide along the axis of rotation and that that axis is vertical, as in the true spin. Then, for steady conditions, it is necessary that the component of the air-reaction parallel to the axis of rotation shall equal the weight of the model. The speed  $V$  will therefore adjust itself until this balance is obtained, but the dimensionless form of (9.1) shows that the incidence and the coefficient ( $k_Q$ ) of the autorotation rate are unaffected by change of  $V$ . The sole consequence of releasing this degree of freedom is, therefore, that  $V$  becomes determinate.

To obtain an approximate estimate of  $V$  we observe that, since the majority of the wing area is stalled, the direction of the resultant force cannot depart far from the perpendicular to the wing chord, so that if this force be  $F$  we have (see Fig. 65)

$$\begin{aligned} mg &= F \sin \alpha \\ &= k_F \rho V^2 S \sin \alpha \end{aligned} \quad (12.1)$$

$$\text{or} \quad V^2 = \frac{mg}{\rho S} \cdot \frac{1}{k_F} \cdot \operatorname{cosec} \alpha$$

Now the stalling speed  $V_s$ , at the height in question, is given by the equation

$$V_s^2 = \frac{mg}{\rho S} \cdot \frac{1}{K_L}$$

where  $K_L$  is the maximum lift coefficient in straight flight.

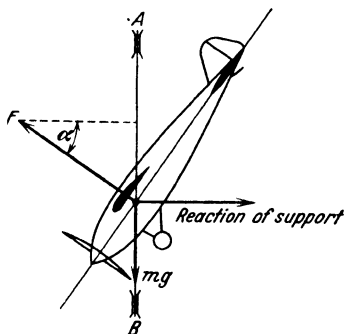


Fig. 65.

Hence

$$V = V_s \sqrt{\frac{K_L}{k_F} \operatorname{cosec} \alpha}$$

For biplanes  $k_F$  does not greatly differ from  $K_L$ , even when the autorotation speed is very high, hence, as a rough estimate only, we may write

$$V = V_s \sqrt{\operatorname{cosec} \alpha} \quad (12.2)$$

**13. Freedom to Leave the Axis of Rotation.** Now imagine that the model is given a fourth degree of freedom, for the c.g. to leave the axis

of rotation, subject to the constraint that the plane of symmetry of the model must still contain this axis. For steady rotation it now becomes necessary to satisfy (see Fig. 66) the condition that the horizontal component of the air-reaction  $F$  shall equal the centrifugal force; this condition yields the equation

$$m \Omega^2 R = F \cos \alpha \quad (13.1)$$

where  $R$  is the distance of the c.g. from the axis. Combining (12.1), (13.1)

$$\Omega^2 R = g \cot \alpha \quad (13.2)$$

from which it appears that, with a fixed value for  $\Omega$ , the flatter the spin the nearer does the c.g. approach to the axis of rotation.

**14. Two Final Degrees of Freedom.** Two degrees of freedom have still to be released before the model is completely free. We shall regard these respectively as freedom to *yaw*, or rotate about the  $Z$  axis, and release of the only remaining constraint, which is that the  $Z$  axis must pass through the axis of rotation. So far as is known at present the  $Z$  axis always passes close to the axis of rotation, and therefore release of the condition that it must intersect this axis does not greatly affect the problem. In conformity therefore with the scheme of the present chapter we shall ignore the effects of this last degree of freedom and assume that the  $Z$  axis and the axis of spin intersect. On the other hand, freedom to yaw about the  $Z$  axis, into positions which are unsymmetrical with respect to the axis of spin, has been shown by recent research to have profound effects upon the spin, and it is to the consideration of these effects that we must now direct attention.

#### D. Effects of Yaw on the Spin

**15. The Meaning of Yaw.** It is first necessary to visualize clearly what is meant by yaw about the  $Z$  axis. It may assist this visualization to imagine a model supported as in Fig. 67 by a bent rod which can rotate freely about a vertical axis  $AB$ .

This rod must be supposed to pass through the body of the model, along its  $Z$  axis, and again intersect the axis  $AB$ . Suppose now that the model can be rotated on the rod, about the  $Z$  axis, but can be prevented from

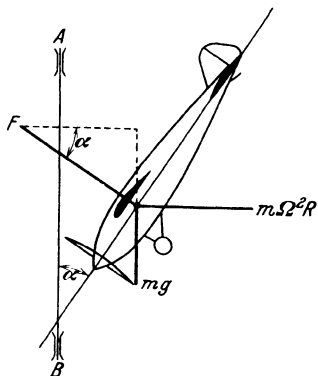


Fig. 66.

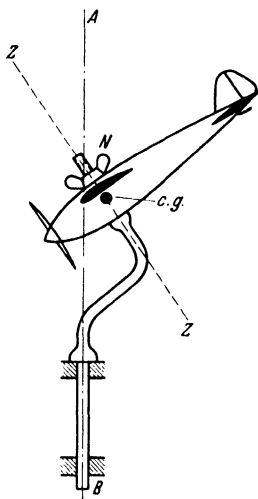


Fig. 67.

doing so by the clamping nut  $N$ . If this nut is tightened when the model is symmetrically disposed to the axis  $AB$ , so that the  $Y$  axis is horizontal, the model is then in the attitude of zero yaw, and if it rotates freely about  $AB$  in a vertical current of air, we have a picture of the motion which was discussed before the release of the last two degrees of freedom.

Now suppose that the nut  $N$  is slackened back, so that the model can be rotated through some definite angle around the rod, and is then clamped up firmly as before. This rotation about the  $Z$  axis, measured from the symmetrical attitude, is described as the *yaw* and, if the model and rod now rotate freely about the axis  $AB$  in an ascending air current, we have a picture of a spin in which yaw is not zero.

**16. The Relation between Yaw and Side-Slip.** Side-slip is defined as in previous chapters, as the component of the velocity of the c.g. perpendicular to the aeroplane's plane of symmetry. If the c.g. is on the axis of rotation,  $AB$  of Fig. 67, and the yaw is zero, there will clearly be no side-slip, but if the aeroplane is yawed to the right<sup>1</sup> there will be side-slip to the left and if yawed to the left there will be side-slip to the right. If the c.g. leaves the axis of rotation there will, however, be some side-slip, even when the yaw is zero, because of the horizontal velocity component ( $QR$ ); and since, in a free spin, the axis of spin is always in front of the c.g. this side-slip will be to the left in a right-hand spin and to the right in a left-hand spin. In general the side-slip will be the algebraic sum of the side-slip due to both these causes, the effects of which will be arithmetically additive when yaw is to the right in a right-hand spin or to the left in a left-hand spin, or in other words when the yaw is of the same sign as the rotation of the spin.

**17. The Effects of Yaw on Rate of Spin.** The importance of yaw in the spin arises from the fact that the side-slip which it causes has a profound effect upon the autorotation rate. Side-slip to the left in a right-hand spin or to the right in a left-hand spin increases the rate and will therefore be called pro-spin side-slip. Conversely side-slip in the opposite sense decreases the rate and will be called anti-spin side-slip. Similarly, yaw which causes pro-spin side-slip, namely yaw to the right in a right-hand spin or to the left in a left-hand spin, will be called pro-spin yaw, while yaw in the opposite sense will be called anti-spin yaw. Recent research has shown that practically all wing arrangements can autorotate rapidly at high incidences, if allowed to take up an attitude involving sufficient pro-spin side-slip, whilst, conversely, none can do so in attitudes involving sufficient anti-spin side-slip.

The question whether a given aeroplane can or cannot spin steadily at high incidences is therefore decided, not so much by the shape and

<sup>1</sup> When the yaw is to the right the nose of the aeroplane has swung from the symmetrical position toward the pilot's right hand.



arrangement of the wings, as by the factors which determine the angle of yaw. Aeroplanes with monoplane wings or biplane wings of exceptionally large stagger, which cannot autorotate at a high rate or at high incidences when in the symmetrical attitude of zero yaw, can only spin flat in attitudes which involve relatively large amounts of pro-spin yaw. On the other hand, biplane wings of small stagger, can autorotate at very high rates and incidences without pro-spin side-slip, and aeroplanes having this wing arrangement can, and often do, spin with appreciable anti-spin side-slip. The bearing of this distinction upon the problem of the balance of yawing moments will appear shortly.

With the very high rotation rates which are possible with any wing arrangement, given sufficient pro-spin yaw, it is impracticable to check the flat spin by providing sufficient air pitching moment to overcome the centrifugal pitching moment. There remains therefore only one practicable way in which the flat spin can with certainty be eliminated from the possible motions of conventional aeroplanes, and that is by adjusting the balance of air and centrifugal yawing moments in such a way that the aeroplane cannot spin except, in an attitude involving so large an anti-spin yaw that the rate of spin will be low.

In recent years therefore the centre of interest in the campaign to eliminate the flat spin has shifted from the autorotative properties of the wings and the balance of pitching moments, to the factors which determine the balance of yawing moments, and it is these factors which we must now briefly consider.

**18. The Air Yawing Moment.** Every part of the aeroplane, of course, contributes something to the air yawing moment, but the parts on which small modifications produce the greatest changes of yawing moment are clearly the fins, rudders and sides of the body near the tail, which are far from the  $Z$  axis and which possess large lateral velocity components due to the rotation of the spin<sup>1</sup>. In fast flat spins the direction of motion of the tail end of the body is such that the air-reactions upon effective fins in this region always exerts a moment about the axis of spin which opposes the rotation, and at the same time a yawing moment about the  $Z$  axis which tends to yaw the aeroplane in the anti-spin sense. For both these reasons fins, or their equivalent in body depth near the tail, have powerful effects in reducing the rate of rotation, provided of course that they are not so shielded by the tail and elevators as to become practically inoperative.

<sup>1</sup> The wing tips also are far from the  $Z$  axis and have large rotational velocities, but the plane of the wings is necessarily nearly perpendicular to the  $Z$  axis, and it is not practicable to make modifications in this region, which would seriously modify yawing moments in the spin, without sacrificing performance in normal flight. For experimental purposes, however, surfaces are sometimes added near the wing tips for the purpose of modifying the yawing moment.

According to the prevailing ideas at the present time, therefore, the most effective way of preventing the flat spin from developing is to provide sufficient effective fin area near the tail end of the body, and it seems that the area necessary for this purpose need not be unduly large, provided that it can be placed in a position where it will not be shielded by the tail and elevators from the direct action of the air. The principal efforts of modern research on the spin are now, therefore, directed towards finding designs for the tail end of the body which will give the desired fin effect, without departing too far from the conventional arrangements which experience has shown to be satisfactory in normal flight.

**19. The Centrifugal Yawing Moment.** A simple way of visualizing the action of the centrifugal yawing moment is to imagine, as we did with the centrifugal pitching moment, that the aeroplane is replaced by a dynamically equivalent model, consisting of three mutually perpendicular rods of moments of inertia  $I_1, I_2, I_3$ , of which  $I_1$  and  $I_2$  represent approximately the body and wings, respectively. Suppose now that this simplified model replaces the complete model in Fig. 67. Then it is not difficult to see that, as the whole arrangement spins steadily about  $AB$ , each of the rods  $I_1$  and  $I_2$ , representing the body and wings respectively, will try to rotate about the  $Z$  axis so as to set itself perpendicular to the axis of spin, that is to say, into the horizontal position occupied by the  $Y$  axis when the model is in the attitude of zero yaw. It can be shown without much difficulty that the centrifugal couple tending to move each rod into this position is given by the expression,

$$\frac{1}{2} \Omega^2 I \cos^2 \alpha \sin 2\beta$$

where  $\Omega$  is the angular velocity about  $AB$ ;  $I$  is the moment of inertia about the  $Z$  axis;  $\alpha$  is the inclination of the  $Z$  axis to the horizontal and  $\beta$  the angle through which the rod must be rotated about the  $Z$  axis to bring it from the horizontal position into the position specified.

It follows that, when the whole model spins with angle of yaw  $\beta$ , the net centrifugal couple about the  $Z$  axis tending to restore the yaw

to zero is,

$$\frac{1}{2} \Omega^2 \cos^2 \alpha [I_2 \sin 2\beta + I_1 \sin 2(\beta + 90)]$$

or,

$$\frac{1}{2} \Omega^2 (I_2 - I_1) \cos^2 \alpha \sin 2\beta$$

This expression for the centrifugal yawing moment is of course equivalent to the third equation of (4.3), and could have been derived directly from it; but it is thought that the foregoing method of derivation from first principles may give a clearer idea of the way in which the moment arises.

We are now in a position to understand the rather complicated action of the centrifugal yawing couple in the spin. If the aeroplane spins with pro-spin yaw, then the centrifugal couple will tend to increase the

yaw, and with it the rate of spin, when the inertia of the body predominates over that of the wings, but to decrease the yaw and rate of spin when the inertia of the wings predominates. On the other hand, if the aeroplane spins with anti-spin yaw, the effects of the centrifugal yawing couple on rate of spin are exactly reversed.

Now, in aeroplanes which have their engines distributed on the wings, the inertia of the wings generally predominates over that of the body, whilst in those which have long bodies and only one engine, the inertia of the body may predominate. But we have seen that monoplanes and biplanes of large stagger can, as a rule, spin flat only when there is pro-spin yaw, whilst biplanes with small stagger may, and often do, spin flat with anti-spin yaw. As a rough rule, therefore, heavy masses distributed along the wings may be expected to have an adverse effect on recovery from the spin of a biplane unless the stagger is unusually great, but a favourable effect on the spin of a monoplane. It must not, however, be assumed that this is an infallible rule, particularly in borderline cases; the exact estimate of the effects on the spin of a redistribution of mass in an aeroplane is a matter of great difficulty and complication, since both yawing and pitching centrifugal forces are in general affected. It seems, however, at the time of writing, that it should not be difficult so to design the fins and body as to provide an air yawing moment which can over-ride all the complicated effects of centrifugal moments, and thus make it unnecessary to calculate their action precisely.

### The Free Spin of Real Aeroplanes.

**20. Rotation Rate and Incidence.** We shall conclude with a brief account of phenomena which have been observed in the spin of real aeroplanes, with some comments on the bearing of the foregoing discussion upon them.

Spins have been observed with every variety of rotation rate, from that for which the coefficient  $\frac{\Omega s}{V}$  is as low as 0.3, to that corresponding to a value of  $\frac{\Omega s}{V}$  of the order 1.2 and with inclinations of the  $X$  axis to the vertical ranging from about  $30^\circ$  to  $80^\circ$ . As a rule the flatter spins are associated with the higher rotation rates, which is in conformity with our knowledge of the autorotation rates of wings in wind tunnels. Generally speaking, difficulty of recovery has not been experienced except in the flatter variety of spin.

**21. Radius and Rate of Descent.** As is to be expected from equations (12.2) and (13.2), it is found that the flatter the spin the lower is the rate of descent and the smaller the radius of the spiral path followed by the c.g. Very flat spins occur with the axis of rotation within a few feet only of the c.g. and with the rate of descent so low that impact with the ground is not always fatal to the occupants.

**22. Load Factor and Incidence.** From equation (12.1) which may be written in the form,

$$\frac{F}{mg} = \operatorname{cosec} \alpha$$

where  $F$  is the resultant air-force on the aeroplane, it appears that the apparent weight of any mass situated near the c.g. will be approximately  $\operatorname{cosec} \alpha$  times the true weight, or, in other words, that the load factor near the c.g. will be approximately  $\operatorname{cosec} \alpha$ . This load factor is probably the easiest quantity to measure in a real spin, and repeated tests have shown that it can be relied upon to give a reasonably accurate measure of incidence in accordance with equation (12.1) despite the fact that the attitude of the aeroplane is in general not exactly that assumed in this equation.

**23. Critical Nature of Transition to Flat Spin.** Equation (10.1) with the illustration in Fig. 64 of the typical values of the centrifugal and air pitching moments in an ideally simple spin, without yaw or side-slip, explains in a general way the reasons for several observed features of the spin which at first seemed very puzzling.

It appears from this illustration that, if the rotation rate remains roughly constant and high, the centrifugal pitching moment passes through a maximum value in the neighborhood of 45 degrees incidence, and round about this maximum may exceed the greatest possible air pitching moment which can be brought to bear to oppose it. It follows that after the rotation rate and incidence have worked up to sufficiently high values, the pilot may lose control of the latter which may increase suddenly to a very high value, from which recovery would be impossible without some reduction in the rotation rate. This explains in a general way the reason for the relatively sudden development of the flat spin and the failure of the elevators to effect a recovery from it; though it must be remembered that the necessary high rotation rate cannot arise unless the aeroplane can spin in an attitude involving sufficient yaw and side-slip, and that, when yaw is not zero, the exact expression for the pitching moment is more complicated than (10.1).

The tendency of the spin to pass suddenly into the dangerous flat type when the rotation rate exceeds a certain critical value is responsible for much of the difficulty which has been experienced in understanding and controlling the behaviour of aeroplanes in the past. For if the rotation rate reaches nearly, but not quite, to the critical value, no difficulty may be experienced in recovery, and the danger so narrowly avoided may not be suspected. This is probably the reason why small modifications to the controls, which were intended to give more power of recovery from the spin, sometimes made recovery more difficult, because, presumably, they enabled the critical condition to be passed. It also explains why designs which have previously given no trouble may suddenly develop a tendency to spin dangerously, after some slight modification, or when in the hands of a pilot who uses his controls in an unconventional manner.

**24. Reasons for Failure of Ailerons and Rudder.** The failure of ailerons to check a spin, whether steep or flat, is explained by the fact that any anti-spin rolling moment which they can exert is completely offset by the effects of the pro-spin yawing moment which always accompanies anti-spin rolling moment, unless the ailerons are of entirely unconventional design. Failure of the rudder, which is the most effective control for checking the flat spin, is explained, when it occurs, by the fact that it may be so shielded by the elevators from the action of the air that it cannot exert an effective yawing moment.

### References.

#### *Chapter I.*

- 1) NORTON, F. H., and ALLEN, E. T., Acceleration in Flight, U.S. N.A.C.A. Report No. 99, 1920.
- 2) NORTON, F. H., and CARROLL, T., Vertical, Longitudinal and Lateral Acceleration of an S.E. 5 Aeroplane While Maneuvering, U.S. N.A.C.A. Report No. 163, 1923.
- 3) DOOLITTLE, J. H., Accelerations in Flight, U.S. N.A.C.A. Report No. 203, 1925.
- 4) SCOTT-HALL, S., Stresses in Wing Structures. Accelerometer and Incidence Measurements in Various Maneuvers, Br. A.R.C. R. and M. 1309, 1930.

#### *Chapter II.*

- 1) GLAUERT, H., Aerofoil and Airscrew Theory, Cambridge, 1926.
- 2) HARRIS, R. G., Forces on a Propeller Due to Sideslip, Br. A.R.C. R. and M. 427, 1918.
- 3) GLAUERT, H., Stability Derivatives of an Airscrew, Br. A.R.C. R. and M. 642, 1919.
- 4) SANDERSON, C. G. D., GLAUERT, H., and JONES, J. H., Investigation of the Downwash Behind a Biplane, Br. A.R.C. R. and M. 426, 1918.
- 5) SIMMONS, L. F. G., and OWER, E., An Investigation of the Influence of Downwash on the Rotary Derivative  $M_q$ , Br. A.R.C. R. and M. 826, 1921.
- 6) SIMMONS, L. F. G., and OWER, E., An Investigation of Downwash in the Slipstream, Br. A.R.C. R. and M. 882, 1924.
- 7) SIMMONS, L. F. G., and OWER, E., An Investigation of the Influence of Downwash on the Rotary Derivative  $M_q$ , Br. A.R.C. R. and M. 883, 1923.
- 8) BRADFELD, F. B., Center of Pressure Travel of Symmetrical Section at Small Angles of Incidence, Br. A.R.C. R. and M. 1294, 1929.
- 9) GLAUERT, H., The Lift and Pitching of an Aerofoil Due to Uniform Angular Velocity of Pitch, Br. A.R.C. R. and M. 1216, 1928.
- 10) BRYANT, L. W., and IRVING, H. B., Apparatus for the Measurement of  $M_q$  on a Complete Model Aeroplane, Br. A.R.C. R. and M. 616, 1919.
- 11) RELF, E. F., and LAVENDER, T., Determination of Rotary Derivatives, Br. A.R.C. R. and M. 809, 1921.
- 12) DOUGLAS, G. P., Measurement of the Derivatives  $M_q$  and  $N_r$  for a Number of Aeroplane Models, Br. A.R.C. R. and M. 580, 1919.
- 13) RELF, E. F., and OWER, E., Experiments on Complete Models of Six Aeroplanes, Br. A.R.C. R. and M. 705, 1920.
- 14) RELF, E. F., Measurement of the Rotary Derivative  $M_q$  on the 1/5<sup>th</sup> Scale Model Bristol Fighter in the Duplex Wind Tunnel, Br. A.R.C. R. and M. 978, 1925.

#### *Chapter III.*

- 1) RELF, E. F., and LANDELLS, A., Forces and Moments on an Aerofoil Having a Dihedral Angle, Br. A.R.C. R. and M. 152 I. III., 1914.

- 2) WILLIAMS, D. H., Pressure Distribution Over a Yawed Aerofoil, Br. A.R.C. R. and M. 1203, 1928.
- 3) BRADFIELD, F. B., Pitching and Yawing Moments with Sideslip on a Model Aeroplane, Br. A.R.C. R. and M. 965, 1925.
- 4) Various Reports of Experiments in Which the Derivatives  $L_v$  and  $N_v$  Have Been Measured on Complete Model Aeroplanes, Br. A.R.C. R. and M. 831, 924, 932, 933, 965, 976, 1059, 1319.
- 5) WIESELBERGER, C., Zeitschrift für angewandte Mathematik und Mechanik, 1922.
- 6) GLAUERT, H., Calculations of the Rotary Derivative Due to Yawing for a Monoplane Wing, Br. A.R.C. R. and M. 866, 1923.
- 7) RELF, E. F., LAVENDER, T., and OWER, E., The Determination of Rotary Derivatives, Br. A.R.C. R. and M. 809, 1921.
- 8) BRADFIELD, F. B., Measurement of Rolling and Yawing Moments of Model Wings Due to Rolling, Br. A.R.C. R. and M. 787, 1921.
- 9) BRYANT, L. W., and HALLIDAY, A. S., Measurement of Lateral Derivatives on the Whirling Arm, Br. A.R.C. R. and M. 1249, 1929.
- 10) RELF, E. F., LAVENDER, T., OWER, E., and GLAUERT, H., The Determination of Rotary Derivatives, Br. A.R.C. R. and M. 809, 1921.
- 11) GARNER, H. M., and GATES, B. A., Full Scale Determination of the Lateral Derivatives of a Bristol Fighter Aeroplane, Br. A.R.C. R. and M. 987, 1925. GARNER, R. and M. 1068, 1926.
- 12) GLAUERT, H., An Investigation of the Spin of an Aeroplane, Br. A.R.C. R. and M. 618, 1919.
- 13) RELF, E. F., and LAVENDER, T., A Continuous Rotation Balance for the Measurement of  $L_p$  at Small Rates of Roll, Br. A.R.C. R. and M. 828, 1922.
- 14) IRVING, H. B., and BATSON, A. S., The Effect of Sideslip on the Aerodynamic Forces and Moments Including Those Due to the Controls for a Model SE 5 A Aeroplane, Br. A.R.C. R. and M. 831, 1922.

#### *Chapter V.*

- 1) WORKMAN, F., Analysis of the Motion of an SE 5 Aeroplane by Step-by-Step Integration, Unpublished Report of the British Aeronautical Research Committee (T 1918), 1924.
- 2) BARANOFF, A. V., and HOFF, L., Investigation of the Combined Lateral and Longitudinal Motions of an Aeroplane. Original in German, Luftfahrtforschung, March 20, 1929. Translation into English, Unpublished Report Br. A.R.C. (spin 22).
- 3) JONES, B. M., and TREVELYAN, A., Step-by-Step Calculations Upon the Asymmetric Movements of Stalled Aeroplanes, Br. A.R.C. R. and M. 999, 1925.
- 4) LANCHESTER, F. W., Aerodionetics, 1906.
- 5) BRYAN, G. H., Stability in Aviation, 1911.
- 6) BAIRSTOW, L., JONES, B. M., and THOMPSON, B. A., Investigation into the Stability of an Aeroplane, Br. A.R.C. R. and M. 77, 1913.
- 7) BAIRSTOW, L., Applied Aerodynamics, 1920.
- 8) GLAUERT, H., A Non-Dimensional Form of the Stability Equations of an Aeroplane, Br. A.R.C. R. and M. 1093, 1927.

#### *Chapter VI.*

- 1) ROUTH, E. J., Rigid Dynamics.
- 2) GATES, S. B., A Survey of Longitudinal Stability Below the Stall with an Abstract for Designers Use, Br. A.R.C. R. and M. 1118, 1927.

#### *Chapter VII.*

- 1) JONES, B. M., and MAITLAND, C. E., Lateral Motions of a Stalled Bristol Fighter Aeroplane. Br. A.R.C. R. and M. 1181, 1928 and 1286, 1929.

# DIVISION O

## AIRPLANE PERFORMANCE

By

**L. V. Kerber,**  
Washington, D. C.

### EDITOR'S PREFACE

The actual performance of an airplane furnishes the final measure of the closeness of its approach to its design characteristics. An actual airplane, however, cannot be tested in advance of construction and in the progress of a design it usually becomes necessary to make a number of estimates of performance based merely on drawings or sketches and certain general dimensions; or again to estimate the consequences of changes of specified character in a design for which the performance may be known or for which a previous estimate has been made.

In the present Division, various methods for carrying out these purposes are briefly discussed. Chapter I deals with certain general relations, followed in Chapter II by a discussion of the two basic items of power required and power available. Chapter III then gives in some detail a method by the use of computation and graphical representation, for the estimation and representation of the most important features of airplane performance.

Many variations in the development of the basic equations for performance have been developed at different times by different writers, and the next five chapters are each devoted to some one of these various methods. Additional descriptive and theoretical matter relating to these various methods may be found in the references to the general literature of the subject. Then follow chapters on Range and Endurance, on the influence of the principal Factors on performance and on what appear to be the limits of performance, assuming the present known body of aerodynamic theory, present sources of power and present available materials of construction. Illustrative examples are given freely throughout the Division, and, assuming given the basic data requisite, the interested reader should have no difficulty in applying to specific problems, the various methods herein described.

W. F. Durand.

## CHAPTER I

### FUNDAMENTAL RELATIONS

**1. Introduction.** The calculation of the performance characteristics of a proposed airplane is necessary not only to obtain reasonable assurance of the ability of the new design to meet the specified requirements, but also to discover means by which the probable performance can be improved. The investigation in the present state of the art can be made to a reasonable degree of accuracy before the construction or even the detail design is started, and thus unnecessary loss of time and expense in development of the design may be avoided.

The performance is grouped in two major parts. First, that of the airplane relative to the ground or to the air is called, simply, *performance*, and includes speeds, climbs, times to altitude, ceiling, range and endurance, take-off distance and time, roll at landing, etc. The second is the behaviour of the airplane in the air relative to its own position and the direction of its flight path. This performance comprises the stability, manoeuvrability and controllability and is called *air-worthiness*. For water machines it may include *sea-worthiness*. In the first group are involved the aerodynamics of non-accelerated flight, the characteristics of the propeller, the thermodynamics of the engine, and the effects of atmospheric changes due to a change in altitude. In the second group are involved the particular aerodynamics of the airplane when one or several conditions of flight are changing, and when the airplane is not symmetrical to the flight path. There is also included the effect of inertia due to changes in attitude.

The present Division of the work deals only with the conditions mentioned for the first group. The various methods which have been devised for dealing with this problem are all based upon some form of equation between the forces or the power required to maintain an airplane in steady flight under the particular conditions specified, and the forces or power which the engine-propeller unit is capable of delivering under corresponding conditions. The differences among and between these various methods turn upon the particular characteristics or parameters employed as independent variables and upon the various ways in which the resulting data may be represented graphically. The underlying aerodynamic assumptions are the same throughout.

No matter what method is used in computing performance, a correct estimation of the basic data, which includes the characteristics of the airfoil section, the aspect ratio selected and the manner in which the wings are combined in the case of biplanes<sup>1</sup>, must be made. The airfoil

<sup>1</sup> The cases of triplanes and multiplanes are not treated here as they are considered less efficient combinations, and are not in general use.



characteristics are fairly well standardized at present and are available from wind tunnel tests on models. The scale effect is being continually investigated by testing larger models in larger wind tunnels.

The most important item of the basic data affecting the accuracy of the performance estimate is the *parasite drag* made up of the drag of all parts other than the wings: *viz.*, fuselage, landing gear, tail surfaces, etc., and of their interference with the wings and between themselves. This interference is very often underestimated by the designer. The analysis of flight test performances shows that the interference drag may be, and actually is in many cases, as high as the sum of the drags of the component parts tested separately. The possibility of improvement of airplane performance lies principally in a decrease of the interference drag rather than in a decrease of the cross-section of the component parts. With good stream-line forms, there is little further to be gained in the resistance of the individual item. The interference effects, however, cannot be eliminated and it results that with the best stream-line forms, the interference effects are of chief residual importance. A minimum number of separate projecting parts together with compactness of form is the solution for the decrease of parasite drag.

In estimating the parasite drag, the system of summarizing individual component drags is often used, but the preferred system consists of an estimate of the equivalent flat plate area made by comparison with a number of existing airplanes for which the flat plate area has been computed from flight test performance. This system is now being used with considerable success, due undoubtedly to the elimination of innumerable possible errors in estimating the drag and mutual interference of component parts.

Determination of propeller efficiency is based on experimental results obtained partly from wind tunnel tests and partly from flight test performance. The effects of different factors are expressed by simple graphs for ready use in computing available power. From these graphs the propeller characteristics can easily be obtained for special cases such as for supercharged or throttled engines, or, when these characteristics are expressed as power or thrust coefficients, the graphs may be used directly for determination of power available.

The effect of altitude on aerodynamic forces is based on a standard variation of density with altitude. This standard is internationally recognized and is in official use in this country. The effect of altitude on the power of the engine and on the propeller engine unit is expressed by means of convenient graphs for ready use in the determination of available power.

**2. Aerodynamics.** Aerodynamic forces on the airplane are expressed in non-dimensional coefficients. Thus, the coefficient of resultant force

on an airplane wing is 
$$C_R = \frac{2R}{\rho v^2 S} \quad (2.1)$$

where:

$R$  is the resultant force on the surface (wing, tail surface, etc.) in pounds.

$S$  is the area of the surface in square feet.

$v$  is the relative velocity of the air at some distant point in feet per second.

$\rho$  is the density of the air in slugs ( $\rho = 0.00238$  at sea level where the density ratio is unity).

The *lift force*  $L$ , which is the component of the aerodynamic force perpendicular to the general direction of the on-coming air, called the flight path, has for its coefficient,

$$C_L = \frac{2L}{\rho v^2 S} \quad (2.2)$$

Similarly the *drag force*  $D$  which is the component parallel to the flight path has for its coefficient,

$$C_D = \frac{2D}{\rho v^2 S} \quad (2.3)$$

An important portion of the airplane drag is defined by the *induced drag* coefficient as expressed by the equation,

$$C_{Di} = \frac{C_L^2}{\pi (\text{E.M.A.R.})} \quad (2.4)$$

where E.M.A.R. is the *Equivalent Monoplane Aspect Ratio*, the meaning and method of calculation of which are explained at a later point.

**3. Engine Power.** The power of the engine is generally defined by the curve of brake horse power plotted against revolutions per minute. The effect of atmospheric changes (especially decrease in pressure and temperature) on the power output may be defined by empirical graphs or by mathematical formulas. The supercharging of the engine is expressed by the graph of maximum power developed at various altitudes. For throttled engines the change in power at the same revolutions per minute is considered proportional to the throttle opening, i. e., for half throttle the engine power is half that at full throttle at the same r.p.m.

**4. Standard Atmosphere.** All performance is referred to the United States standard atmosphere<sup>1</sup>.

The ratio of the air-density at altitude to the density at standard sea level is called *density ratio* and is used extensively in performance computations. The standard condition of the air at sea level corresponds to a temperature of 15° Centigrade and a pressure of 29.921 inches of mercury. A cubic foot of standard air at sea level weighs 0.07651 pounds, and its mass is 0.00238 slugs per cubic foot, denoted by  $\rho_0$  and called mass

<sup>1</sup> See Ref. 7, also Division B p. 223.

density. The mass density at any other altitude is defined by the product of  $\rho_0$  and the density ratio,  $\sigma$ . Thus, mass density at altitude  $H$

$$\rho_h = \sigma \rho_0$$

Characteristics of standard air up to 50,000 feet are given in Table 4.

## CHAPTER II BASIC COMPUTATIONS

### A. Power Required

**1. Data Necessary.** The data necessary for the computation of power required include an accurate three-view drawing of the airplane with all major dimensions, and in addition the following:

*Gross Weight*, which is the total weight of the complete airplane with its occupants and cargo and with the full capacity of fuel and oil.

*Wing Area*, which is to be measured from the projection of the actual outline on the plane of the chords, without deduction for areas blanketed by fuselage or nacelles. That part of the area so determined which lies within the fuselage or nacelles is bounded by two lateral lines that connect the intersection of the leading and trailing edges with the fuselage or nacelle, ignoring fairings and fillets. In other words, for the purpose of calculating area, a wing shall be considered to extend without interruption through fuselage and nacelles. Unless otherwise stated, wing area shall always refer to total area including ailerons.

*Characteristics of the Airfoil*<sup>1</sup>, which are represented by the polar or by the curves of lift and drag coefficients. The most convenient form of polar is that giving the lift coefficient plotted against profile drag coefficient as shown in Figs. 1 and 2.

*Equivalent Monoplane Aspect Ratio* (E.M.A.R.). This term is applied particularly to combinations of wings different from monoplanes. Its meaning is expressed as follows:

A given biplane, triplane, multiplane or sesquiplane has, for a given lift coefficient, the same induced drag coefficient as a monoplane, if its E.M.A.R. has the same value as the aspect ratio of the monoplane. For the determination of E.M.A.R. see (3.4).

**2. Lift, Lift Coefficient and Speed.** The lift of the airplane in performance calculations is considered constant and equal to the gross weight except for cases where the load is purposely altered and in calculations of the range and endurance of the airplane. In accelerated flight and in turns, the wing lift obviously differs from the weight. Furthermore, the assumption that the lift is equal to the gross weight is exact only for horizontal flight with propeller axis horizontal. In cases where the path of the airplane and the propeller axis are inclined to the horizontal, as in climb, for a given speed the wing lift (which is perpendicular to

<sup>1</sup> See Ref. 17.

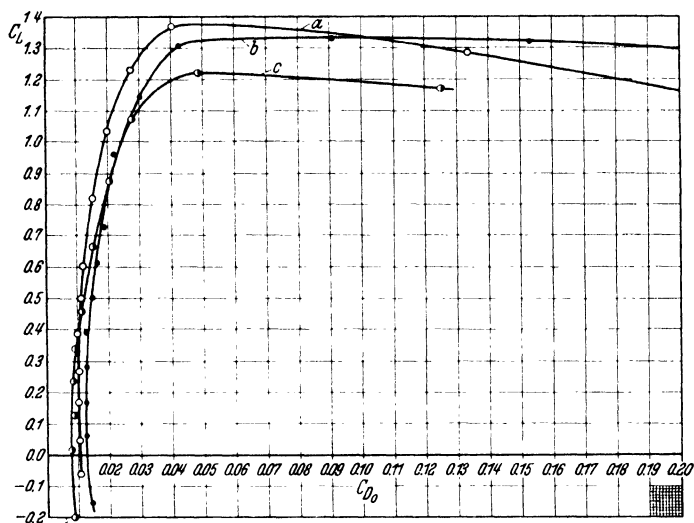


Fig. 1. Polar diagram of profile drag coefficient and lift coefficient.

*a* = Clark "Y" N.A.C.A. test, R.N. = 3,610,000,  $\alpha_{0L} = -5.08^\circ$

*b* = Gött. 387 N.A.C.A. test, R.N. = 3,470,000,  $\alpha_{0L} = -6.86^\circ$

*c* = N.A.C.A. M-6 N.A.C.A. test, R.N. = 3,660,000,  $\alpha_{0L} = -0.20^\circ$

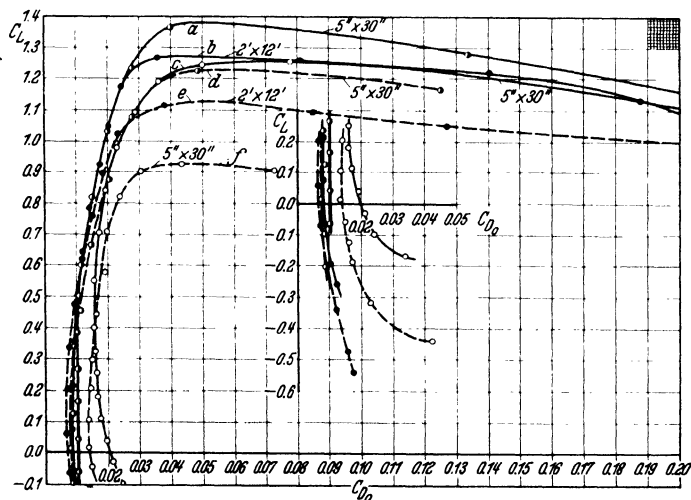


Fig. 2. Polar diagram of profile drag coefficient and lift coefficient.

*a* = Clark "Y" W.N.Y test, R.N. = 156,000  $\alpha_{0L} = -5.56^\circ$

*b* = N.A.C.A. M-6 W.N.Y test, R.N. = 156,000  $\alpha_{0L} = -1.20^\circ$

*c* = Clark "Y" N.A.C.A. test, R.N. = 3,610,000  $\alpha_{0L} = -5.08^\circ$

*d* = N.A.C.A. M-6 N.A.C.A. test, R.N. = 3,660,000  $\alpha_{0L} = -0.20^\circ$

*e* = Clark "Y" Propeller Tunnel, R.N. = 1,940,000  $\alpha_{0L} = -5.08^\circ$

*f* = N.A.C.A. M-6 Propeller Tunnel, R.N. = 1,940,000  $\alpha_{0L} = -1.00^\circ$

the flight path) is equal to the gross weight multiplied by the cosine of the angle of climb. The rest of the weight is carried by the vertical component of the thrust. This condition is known as the *helicopter effect* of the propeller. The effect of the path angle and the helicopter effect compensate each other to some extent and are neglected at least in the first approximation, but they should be included in accurate computations. The effect of this neglect on an airplane weighing 4500 pounds and powered with a 400 HP engine is an underestimation of the rate of climb at sea level by about six percent.

The lift coefficient can be expressed as a function of the wing loading, the speed of the airplane in horizontal flight and the air-density,

$$C_L = \frac{W}{S \rho v^2}$$

Forms 1a and 1b. Horsepower Required.

(1a) To be used with method (III 6 A)			(1b) To be used with method (III 6 B)	
1	$V$ m.p.h.	Includes minimum and high speeds	1	Same as 1 form 1a
2	$C_L$	$C_L = \frac{W}{S V^2 \times 0.00256}$	2	Same as 2 form 1a
3	$C_{Di}$	$C_{Di} = \frac{C_L^2}{\pi \times \text{E.M.A.R.}}$ or from Fig. 3	3	Same as 3 form 1a
4	$C_{D0}$	From Fig. 1 or 2	4	Same as 4 form 1a
5	$V$ $V_{mn}$	$V$ $V_{mn}$	5	Ratio. II (5.6) Calculated from column 2
6	$f_1$	From Fig. 6	6	$f_2$ from Fig. 8
7	$C_{Dp1}$	$C_{Dp1} = f_1 \times C_{Dp1}(V_{mx})$	7	Values of $C_{Dp}$ (H.S.) $\times f_2$
7a	$C_{Dp}$	$C_{Dp} = C_{Dp1} + C_{Dp2}$	8	Sum of values from columns 3, 4, and 7
8	$C_D$	Sum of values from columns 3, 4, and 7a	8	
9	HP required sea level	HP required $= \frac{C_D S V^3}{146\,000}$	9	Same as 9 form 1a
10	10,000 ft. $V$ m.p.h.	$1.165 \times$ values from column 1	10	Same as 10 form 1a
11	HP required	$1.165 \times$ values from column 9	11	Same as 11 form 1a
12	15,000 ft. $V$ m.p.h.	$1.261 \times$ values from column 1	12	Same as 12 form 1a
13	HP required	$1.261 \times$ values from column 9	13	Same as 13 form 1a

If  $W/S$  is expressed in pounds per square foot, speed in miles per hour and density in terms of the density ratio  $\sigma$

$$C_L = \frac{W}{S} \frac{1}{0.00256 \sigma V^2}$$

The lift coefficient, tabulated against speed, is shown in Form 1. The speeds are generally assumed in steps of 10 or 20 miles per hour, depending on the speed range and the accuracy desired, starting, however, with the minimum speed determined from the equation

$$V_{mx} = \sqrt{\frac{W}{S} \frac{1}{0.00256 C_{Lmx}}}$$

The value of  $C_{Lmx}$  should be reduced when objects such as nacelles, etc. are so placed as to interfere with the lift of the wings. The fuselage is not considered to contribute to the decrease of the maximum lift coefficient. This ruling is made because results so obtained check reasonably well free glide tests.

The column of speeds should also contain the first approximation to high speed [see (6.3)] in order to determine an approximate speed range necessary for the estimation of parasite drag variation. Tabulation of a speed 10 to 20 m.p.h. in excess of the high speed is generally sufficient. (See Form 1, column 1.)

**3. Induced Drag and Equivalent Monoplane Aspect Ratio.** In column 3 of Form 1 the induced drag coefficients are entered. This coefficient is expressed in the form:  $C_{Di} = \frac{C_L^2}{\pi(\text{E.M.A.R.})}$  [see I (2.4)]

A graph giving values of  $C_{Di}$  in terms of  $C_L$  and the E.M.A.R. is given in Fig. 3.

The value of the factor E.M.A.R. is developed as follows:

For a monoplane let:

$b$  = span from tip to tip of wing.

$c$  = mean chord = wing area  $\div b$ . Then:

Mean aspect ratio of wing =  $b^2/S = S/c^2$ .

For a biplane, let  $L_1, b_1, c_1, L_2, b_2, c_2$  denote the lift, span and mean chord of the upper and lower wings respectively.

$G$  = gap between wings.

$\sigma$  = Prandtl's factor<sup>1</sup>

For numerical values of this factor, see Fig. 4.

With this notation the fundamental Prandtl equation for induced drag is

$$D_i = \frac{1}{\pi q} \left( \frac{L_1^2}{b_1^2} + 2\sigma \frac{L_1 L_2}{b_1 b_2} + \frac{L_2^2}{b_2^2} \right) \quad (3.1)^2$$

where  $q$  is put for  $\rho v^2/2$ . We assume further that the loading of both

<sup>1</sup> Division E IV (22.6). U.S. N.A.C.A. Report No. 116, p. 200, 1921.

<sup>2</sup> Correct for best lift distribution between the two wings. See Ref. 6.

wings is the same. Then remembering that  $L_1 = C_L q b_1 c_1$  and  $L_2 = C_L q b_2 c_2$ , (3.1) becomes

$$D_i = \frac{C_L^2 q}{\pi} (c_1^2 + 2\sigma c_1 c_2 + c_2^2) \quad (3.2)$$

and again putting  $D_i = C_{Di} q S$  where  $S$  is the entire biplane area, (3.2) becomes:

$$C_{Di} = \frac{C_L^2}{\pi} \frac{c_1^2 + 2\sigma c_1 c_2 + c_2^2}{S} \quad (3.3)$$

Then putting

$$C_{Di} = \frac{C_L^2}{\pi (\text{E.M.A.R.})}$$

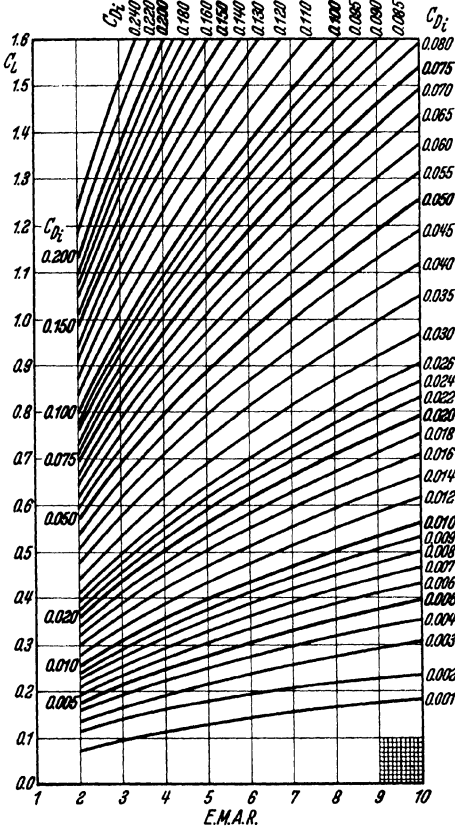


Fig. 3. Relation between coefficient of induced drag, equivalent mean aspect ratio and lift coefficient.

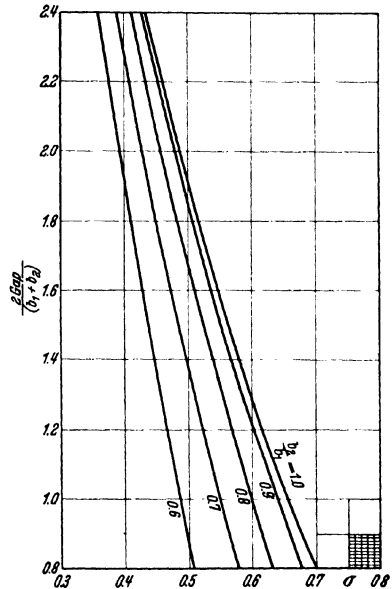


Fig. 4. Prandtl's coefficient  $\sigma$ .

whence

$$\text{E.M.A.R.} = \frac{S}{c_1^2 + 2\sigma c_1 c_2 + c_2^2} \quad (3.4)$$

If the chords are equal,  $c_1 = c_2$  and

$$\text{E.M.A.R.} = \frac{S}{2c^2(1 + \sigma)} \quad (3.5)$$

For the determination of the E.M.A.R. for any biplane, reference may be made to Appendix I and to the factors  $K$  and  $a$  as follows:

$K$  = ratio of span of equivalent monoplane to the span  $b_1$  of the longer wing.

$a = L_1 \div L = \text{Lift of longer wing} \div \text{total lift.}$

(To be assumed, or estimated from reliable data relating to similar cases.)

For any biplane in general, we shall then have

$$\text{E.M.A.R.} = \frac{(K b_1)^2}{S} \quad (3.6)$$

where  $b_1$  is the longer span, whether upper or lower. For the equivalent monoplane span, we have

$$K b_1 = \sqrt{S (\text{E.M.A.R.})} \quad (3.7)$$

**4. Profile Drag of Airfoils and Its Variation.** In column 4 of Form 1, the profile drag coefficient is entered. The profile drag of airfoils and its coefficient in the present state of the art cannot be successfully calculated, especially at higher lift coefficients. Recourse must therefore be had to the information given by tests in wind tunnels on airfoil models. The question of scale effect is still not solved. The ideal wind tunnel test will of course be on the actual size airfoil at speeds approximately those of the actual airplane. But the initial and operating costs of a wind tunnel accommodating such a full size model are very large, and, hitherto such tunnels have not been generally available. However with two tunnels in the United States<sup>1</sup> of size adequate for full scale tests either of planes as a whole or of constituent parts, and with other large tunnels projected elsewhere, information at Reynold's Numbers approaching those for full size planes in free flight is becoming available and should add definitely to our information on the subject matter of the present section.

A substitute for a full size tunnel is the compressed air tunnel where the deficiency of size is counteracted by increasing the density of the air. The criterion for the scale effect is, in any case, the Reynold's Number  $VL/\nu$  where,  $V$  is the velocity in feet per second,  $L$  the length of chord in feet and  $\nu$  the kinematic viscosity which for air at sea level has a value of 0.000159. For practical use the Reynold's Number, denoted by  $R$ , is

$$R = 9,230 L V \text{ (ft. and m.p.h.)}$$

Information on values of the profile drag for high Reynold's Numbers corresponding to full size airplanes is continually accumulating from tests made in the compressed air tunnel of the N.A.C.A.<sup>2</sup> While some designers do not accept the Reynold's Number as a criterion for scale effect, it is at least generally agreed that results obtained from tests at large values of Reynold's Numbers are more reliable than those at small values obtained in tunnels at atmospheric pressure.

Fig. 1 gives the profile drag polar of three well known airfoils tested at high Reynold's Number in the compressed air tunnel. Recently the N.A.C.A. has undertaken comparative testing of large airfoil models

<sup>1</sup> U.S. N.A.C.A. Technical Reports 300, 459; 1928, 1933.

<sup>2</sup> See Ref. 22.



of 12 foot span and 2 foot chord in the new 20 foot diameter wind tunnel at an air speed of 100 m.p.h. The Reynold's Number in that case is about half that of a full scale airplane. The results are most promising, but the number of airfoils as yet tested and the data obtainable are too limited to form any final conclusion as to whether characteristics of airfoils obtained on airfoil models of that size are the same as on full size structures. Polars for Clark Y and M-6 from the compressed air tunnel made on 5 by 30 inch models at a Reynold's Number of about 3,500,000 and those from tests on 2 by 12 foot models in the atmospheric 20 foot diameter tunnel at a Reynold's Number of about 2,000,000 are shown in Fig. 2.

The symbol for profile drag, which is considered the frictional drag of the airfoil, is  $D_0$ , and its coefficient is  $C_{D0} = \frac{2 D_0}{\rho v^2 S}$ . The profile drag coefficient is obtained from the airfoil drag coefficient by subtracting the induced drag coefficient, thus

$$C_{D0} = C_D - C_{Di}$$

**5. Structural Drag and Its Variation.** The coefficient of parasite drag,  $C_{Dp}$  is entered in column 7 or 7a of Form 1. Its estimation is one of the most difficult problems in the calculation of performance.

a) *Estimation by Summation*<sup>1</sup>. The method widely used in the past is that of summation of the resistance of the various component parts of the airplane. Tables 1, 2 and 3 give convenient forms for the tabulation of the parasite drag which includes that of struts, wires, fittings, etc. Certain other items usually omitted from wind tunnel models, such as control horns, tail skids, various exposed equipment such as radio generators, search-lights and similar items may be included in this table. In Table 2, the length  $L$  of a strut or wire may be taken as the projected length in the front elevation.

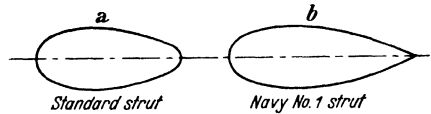


Fig. 5.

Fig. 5a and b shows two approved forms of strut section. For the strut of Fig. 5a, the resistance per foot of length at a speed of 100 m.p.h. is given approximately by the equation

$$y = 0.182 t$$

where  $y$  is the resistance in pounds and  $t$  is the maximum thickness of the strut in inches. For the strut of Fig. 5b, the corresponding equation is

$$y = 0.164 t$$

For stream-line wire the drag per foot at a speed of 100 m.p.h. is given approximately by the equation

$$y = 0.262 x - 0.161 x^2$$

where  $y$  is the drag and  $x$  is the normal diameter in inches.

<sup>1</sup> See Ref. 14.

TABLE 1. Drag of Various Items.

Item	Drag in Pounds at 100 m.p.h.
Flat plate (1 sq. ft.) . . . . .	32.8
Control horn well stream-lined . . . . .	1.0
Tail skid . . . . .	2 to 5
Compass . . . . .	4
Search-Light . . . . .	13
Radio generator . . . . .	20 to 30
Machine-gun . . . . .	20 to 30
Torpedo and gear . . . . .	20
Bomb (500 lb.) and gear . . . . .	20 to 40
Mud-guard . . . . .	5 to 10
Standard wheel with usual fairing from hub to rim (Bendix):	
26 × 3 . . . . .	7.5
28 × 4 . . . . .	10.0
30 × 5 . . . . .	12.5
32 × 6 . . . . .	16.0
36 × 8 . . . . .	24.0
44 × 10 . . . . .	36.6
54 × 12 . . . . .	54.0
Low pressure tire wheel 22 × 10. . . . .	9.25
Tail surfaces (per sq. ft.—thin) . . . . .	0.35
Tail surfaces (per sq. ft.—average thickness) . . . . .	0.40
Tail surfaces (per sq. ft.)—flat plate) . . . . .	0.30
Fuselage, square (sq. ft. of projected area) . . . . .	6 to 8 <sup>1</sup>
Fuselage, round or elliptical (sq. ft. of projected area) . . . . .	4 to 5
Fuselage, well stream-lined (no irregularities) (sq. ft. of projected area) . . . . .	3 to 4
Nacelles (sq. ft. of projected area) . . . . .	4 to 8
Radiator, free air (sq. ft. of projected area) . . . . .	15 to 20
Hull (sq. ft. of projected area) . . . . .	5.0
Hull, exceptionally clean (sq. ft. of projected area) . . . . .	4.0
Seaplane float, average shape (sq. ft. of projected area) . . . . .	5.50
Wing, tip float square (sq. ft. of projected area). . . . .	8.0
Wing, tip float average shape (sq. ft. of projected area) . . . . .	6.0
Wing, tip float well shaped (sq. ft. of projected area) . . . . .	5.0
Air-cooled engines per cylinder . . . . .	8 to 10
Landing Gears <sup>2</sup>	

Where the effect of turnbuckles and end fastenings is to be included, special information from handbook or other source should be sought.

The data on drag of struts were obtained at low Reynold's Numbers, but the models were smooth. The effect of roughness of struts at high

<sup>1</sup> The area upon which the drag of fuselages, hulls, floats, etc., should be based is the maximum cross-section area in the front view and should include all projecting sections, windshields, etc., except the wing stubs which are included in the wing drag.

<sup>2</sup> See U.S. N.A.C.A. Technical Reports Nos. 485, 1934; 518, 522, 1935.

TABLE 2. Summation of Component Parasite Drag at 100 m.p.h. (Structure).

Designation or description	Number <i>N</i>	Length <i>L</i> ft.	Size <i>t</i> in.	Total Length <i>N</i> × <i>L</i> ft.	Drag/ft. at 100 m.p.h. lb.	Drag at 100 m.p.h. lb.
1. Interplane struts . . . . .	6	5.35	1.000	32.0	0.195	6.2
2. Aileron connecting struts . . . . .	2	5.35	0.714	10.7	0.160	1.7
3. Cabane struts . . . . .	4	3.83	1.000	15.3	0.195	3.0
4. Flying wires . . . . .	6 equiv.	12.83	0.375	77.0	0.150	11.5
5. Landing wires . . . . .	4	9.17	0.313	36.7	0.140	5.1
6. Cabane wires (Lateral) . . . . .	4	3.83	0.313	15.3	0.250	3.8
7. Cabane wires (Fore and aft) . . . . .	4	3.83	0.313	15.3	0.250	3.8
8. Front outer chassis struts . . . . .	2	3.92	1.500	7.8	0.280	2.2
9. Rear chassis struts . . . . .	2	3.92	1.500	7.8	0.280	2.2
10. Front inner chassis struts . . . . .	2	5.59	2.000	11.2	0.370	4.1
11. Horizontal tail surface struts . . . . .	2	5.00	0.857	10.0	0.180	1.8
12. Fin brace wires (stream-line) . . . . .	4	5.20	0.250	20.8	0.160	3.3
13. Tail skid . . . . .	1	—	—	—	5.000	5.0
14. Control horns . . . . .	8	—	—	—	1.000	8.0
Total Structural Drag at 100 m.p.h.						61.7

TABLE 3. Summation of Component Parasite Drag at 100 m.p.h.

Designation or description of item	Number	Area sq. ft.	Drag per sq. ft. lb. at 100 m.p.h.	Drag at 100 m.p.h. lb.
Parasite drag varying with angle of attack, $P_1$ .				
1. Fuselage . . . . .	1	9.6	5.0	48.0
2. Tail surfaces . . . . .	—	65.6	0.4	26.3
Total $P_1$ at 100 m.p.h.				74.3
Parasite drag constant with angle of attack, $P_2$ .				
1. Structure (Table 2) . . . . .	1	—	—	61.7
2. Radiator (Underslung) . . . . .	1	2.5	18	45.0
3. Wheels . . . . .	2	32" × 6"	16 ea.	32.0
4. Observer's gun and mount . . . . .	1	—	—	25.0
5. Forward fixed gun, exhaust pipes, expansion tank . . . . .	—	.42 × 2 = .84	32.8	27.6
Total $P_2$ at 100 m.p.h.				191.3

Reynold's Numbers is indicated by the relatively high drag for struts wound with tape and then varnished, and by the much lower drag on struts with smooth polished metal surfaces. It is reasonable to assume that similar effects must take place on other parts of the airplane, and the condition of the finish of the exposed parts should be taken into account in determining the resistance.

The effect of protuberances on a stream-line fuselage is very great, especially if they are located near the front. As an example, it can be cited that the drag of a good stream-line body of fuselage form may be increased five-fold by mounting an uncowed radial engine. These effects must all be considered in estimating the drag of component parts<sup>1</sup>.

The drag of a fitting including its interference drag is given approximately by considering the fitting a flat plate of double its projected area. Miscellaneous projecting parts not stream-lined should be treated as fittings.

The total parasite drag must be divided into two parts, the first variable with the lift coefficient and designated  $P_1$ , the second independent of the lift and designated  $P_2$ . If there is any doubt as to the

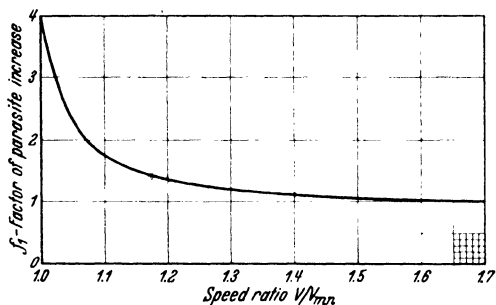


Fig. 6.

classification of the fuselage or nacelle drag, it should be put in the  $P_1$  class. The items of variable and constant drag can then be tabulated in the form shown in Table 3. The parasite drag coefficient has the form

$$C_{Dp} = \frac{2 D_p}{\rho v^2 S} \quad (5.1)$$

The variation of the  $P_1$  part of the parasite drag coefficient, designated by  $C_{Dp1}$ , is assumed to be dependent on the factor  $f_1$ , plotted against speed ratio in Fig. 6, as shown by the equation

$$C_{Dp1} \text{ at } V = C_{Dp1} \text{ at } V_{mx} \times f_1 \quad (5.2)$$

These values do not take care of interference of the fuselage with wings, landing gear, etc. In order to take care of such interference, both  $P_1$  and  $P_2$  should be increased from ten to fifteen per cent.

It is noted that the drags in the tables are given at 100 m.p.h. In order to reduce these drags to their coefficients, the following formula may be used.

$$C_{Dp} = \frac{0.039 D_p \text{ at } 100 \text{ m.p.h.}}{S} \quad (5.3)$$

When this method of summation of drags is used, the values of the ratio of speeds  $V/V_{mn}$  (where  $V$  is the speed of the airplane at sea level from column 1 and  $V_{mn}$  is the minimum speed at sea level) are entered in column 5. In column 6 are values of the factor  $f_1$  from Fig. 6. In column 7 are values of corrected variable parasite drag coefficient  $C_{Dp1}$ , where  $C_{Dp1}$  at velocity  $V$  (column 1) equals  $C_{Dp1}$  at high speed  $\times f_1$ . In column 7a is the constant value of  $C_{Dp2}$  plus  $C_{Dp1}$  corrected for velocity ratio.

<sup>1</sup> See Ref. 18.

b) *Estimation by Comparison with Similar Airplanes.* For the estimation of parasite drag a shorter and more accurate method, if used by experienced computers, is by a comparison of equivalent flat plate areas, designated by  $A$ . The whole airplane as contemplated by the design is compared with some similar airplane for which the equivalent flat plate area has been determined from actual high speed tests.

The estimate of the variation of the parasite drag coefficient, depending on the particular shape of the fuselage and the trussing, is similarly made by comparison. By referring to drawings of known airplanes, as in Fig. 7 for example, a comparison can be made with the airplane for which the performance is to be calculated, and the  $A$  estimated. For airplanes

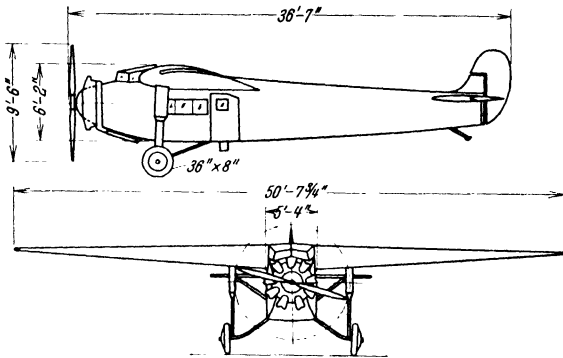


Fig. 7.

of weight less than 5,000 lbs., a formula relating weight and  $A$  representing the mean of a considerable number of examples is the following

$$A \text{ (sq. ft.)} = 0.0027 W \text{ (pounds)} \quad (5.4)$$

For heavier planes a mean value of the coefficient may be taken at 0.0031.

Where practicable, more definite information should be sought, connecting  $A$  with weight for the particular type of plane under consideration. The coefficient of parasite drag for high speed based on the wing area is

$$C_{Dp} = \frac{1.28 A}{S} \quad (5.5)$$

where 1.28 is the value of the coefficient for a flat plate moving normal to itself. Useful formulae in this connection are

$$A = (C_{Dmn} - 0.01) \frac{S}{1.28}$$

where

$$C_{Dmn} = \left( \frac{52.7}{V_{mx}} \right)^2 \frac{P_T}{S}$$

Variations of the parasite drag coefficient are illustrated in Fig. 8. The graphs in this diagram are based on the variation of parasite drag

coefficient obtained from flight tests. The basic 100 per cent value of  $C_{Dp}$  is that at high speed and the variation is in per cent of that value. The variation of  $C_{Dp}$  is then plotted against a function of the lift coefficient corresponding to limits of the speed range. The conclusion that the variation of the parasite drag is a function of the lift coefficient rather than of the angle of attack of the fuselage was reached from analysis of glides on the Sperry Messenger with different wings as tested by the N.A.C.A. and described in Ref. 11. This dependence on lift coefficient can easily be explained by considering that a large portion of the fuselage is always in the down-wash of the wings and the down-wash

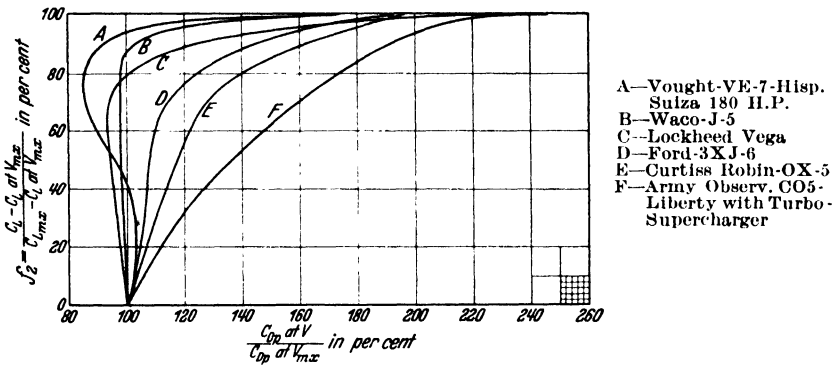


Fig. 8.

angle relative to the fuselage depends on the lift coefficient. The difference between  $C_L$  at stalling speed and  $C_L$  at high speed is considered to be 100 per cent. The method uses the assumption (supported by considerations and tests described above) that for airplanes with a speed ratio of from two to three the variation of the parasite drag depends on the ratio of differences of the respective lift coefficients as expressed in the form (see Fig. 8),

$$f_2 = \frac{C_L \text{ at speed } V - C_L \text{ at speed } V_{mx}}{C_{Lmx} - C_L \text{ at speed } V_{mx}} \quad (5.6)$$

In the tabulation and subsequent computations, as shown on Form 1 b, it is seen that the only differences are in columns 5, 6, 7 and the procedure, as indicated in 1 b, will be clear without special explanation.

In selecting the probable curve of parasite drag coefficient variation, the shape of the fuselage, particularly the front portion, the landing gear design in relation to the fuselage and to the propeller slipstream, and the relation of the wing to the rest of the airplane, must all be carefully considered. A very well stream-lined round or elliptical fuselage with well stream-lined water-cooled engine and small nose radiator will have small or negative increase of parasite drag at higher lift coefficients as

shown by the graph for the Vought VE-7 airplane. On the contrary, a fuselage with large underslung radiator with irregular projections, square corners with side turbo-supercharger and cooler near the nose of the fuselage will have a large variation in parasite drag as shown by the curve for the supercharged Liberty engined Army observation airplane. Fuselages of good stream-line shape with uncowed radial air-cooled engines have relatively higher drag at high speed, but the increase at higher lift coefficients is small and is of an appreciable magnitude only at stalling angles. This type of fuselage is represented by the curve for the Waco with J-5 engine.

The increase of the parasite drag at higher angles of attack has its detrimental effect at climbing speeds, and is partly due to the increased drag of the tail surfaces trimmed for balance at higher speeds, and partly due to greater inclination of the fuselage to the airstream. The increased angle and increased difference of speed between the slipstream of the propeller and the relative air at climbing speeds produces increased turbulence around the airplane, thus producing energy losses which finally are charged to the increase of parasite drag coefficient at lower speeds.

One of the greatest errors in estimating performance of twin or multiple engined airplanes with one or more engines stopped, is in neglecting the fact that the airplane, due to dissymmetry of the thrust, is inclined directionally to the line of flight. The drag of the fuselage, struts, and landing gear is then considerably increased, the increase depending on the angle of yaw. For round or elliptical fuselages this increase has been measured to be 15 per cent for five degrees of yaw and 45 per cent for ten degrees. For a square body of rather poor aerodynamic characteristics the increase of drag for ten degrees of yaw was over 200 per cent.

The propeller slipstream operates to increase the drag. This increase is to some extent compensated for by an increased apparent efficiency of the propeller, but the net result in general is a loss. The effect of this increase of drag is not dealt with separately, but is included in the determination of power available from the engine and is thus charged against the efficiency of the propeller.

**6. Total Drag and Power Required at Sea Level and at Altitude.** The power required at different speeds in horizontal flight at sea level is derived from the total drag, the components of which have been discussed in previous paragraphs. The procedure and sequence in tabulating the determined values is shown by Form 1.

Minimum speed is first calculated from the maximum lift coefficient, and higher speeds are assumed as explained in 2.

The first approximation of high speed is based on the fact that the high or maximum speed is the speed at which the power required for horizontal flight is exactly the same as the power delivered by the

propeller while absorbing the maximum rated brake power of the engine. This condition presupposes a propeller suitable for absorbing the rated engine power at the rated r.p.m. and at the high speed which is sought. The correct high speed is found only after the entire *power available* and *power required* curves have been determined. The first approximation to the high speed serves primarily to establish an approximate speed range for determination of the variation of the parasite drag and is sufficiently accurate for that purpose. This general program is carried forward as follows:

a) From a consideration of the airplane design and by comparison with other similar airplanes the *probable* maximum speed in miles per hour is estimated. This speed is then divided by

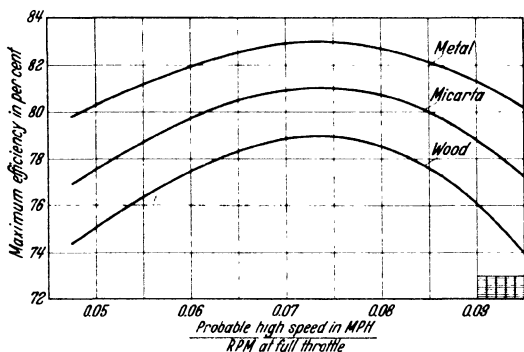


Fig. 9.

the rated r.p.m. of the engine. From the value thus obtained, the first approximation to the maximum *propeller efficiency* may be made from Fig. 9. This graph gives efficiency for metal, micarta and wood propellers with two blades. For three-bladed propellers 98 per cent, and for four-bladed propellers 96 per

cent, of the efficiency for the two-bladed propeller should be taken.

b) The first approximation of the power available at high speed is then: Rated  $h_p \times$  first approximation of propeller efficiency from (a).

c) Using again the probable high speed, the induced drag coefficient is determined from the formula,

$$C_{Di} = \frac{W^2}{(0.00256 V_1^2 S)^2 \pi (\text{E.M.A.R.})} = \frac{C_L^2}{\pi (\text{E.M.A.R.})} \quad (6.1)$$

where  $W$  is gross weight in pounds,

$S$  is wing area in square feet,

$V_1$  is probable high speed in m.p.h.

Moderate error in the approximation of the probable high speed does not seriously affect the induced drag since its value is necessarily low in comparison with values of other drag coefficients.

d) The profile drag coefficient  $C_{D0}$  corresponding to the lift coefficient for probable high speed determined in the preceding paragraph is found from polars similar to those of Figs. 1, 2.

e) The parasite drag coefficient at probable high speed,  $C_{Dp}$  is determined from the estimate of the equivalent flat plate area or from a summation of the component drags (see 5).



f) The sum of  $C_{Di} + C_{D0} + C_{Dp} = C_D$ , the total drag coefficient at probable high speed where  $C_{Di}$  is that from 3,  $C_{D0}$  from 4 and  $C_{Dp}$  from 5. This drag coefficient  $C_D$  although derived from probable high speed will be in only negligible error as compared with the drag coefficient corresponding to the first or even the second approximation of the high speed. This, of course, is not true for the actual required power expressed by the equation

$$P_r = \frac{C_D S V^3}{146\,000} \quad (6.2)$$

where  $V$ , the first approximation of high speed is an unknown quantity.

$V$  is calculated by the aid of the equation for power available as determined in (b): Thus,

$hp$  available ( $P_a$ ) = Rated  $bhp \times$  first appx. to  $\eta$ .

By equating power required to power available,

$$\frac{C_D S V^3}{146\,000} = P_a$$

the first approximation of high speed is obtained:

$$V_m = \sqrt[3]{\frac{146\,000 P_a}{C_D S}} \quad (6.3)$$

The range of speeds at sea level so established, the speeds are entered in column 1, Form 1. From speeds and wing loading, the lift coefficients

are calculated.

$$C_L = \frac{W}{0.00256 S V^2} \quad (6.4)$$

and entered in column 2. At this time the E.M.A.R. is calculated from 3 and the induced drag coefficient is found from Fig. 3 or calculated from (6.1) and entered in column 3.

The profile drag coefficient for the lift coefficient in column 2 is taken from airfoil polars obtained preferably from variable density wind tunnel test results similar to those given in Figs. 1 and 2, and is entered in column 4.

In column 5 are entered ratios as in (5.6), Form 1b.

In column 6 is entered the parasite drag variation ratio  $f$ , taken from selected curve on Fig. 8.

In column 7 is the corrected parasite drag coefficient,  $f C_{Dp}$  where the basic parasite drag coefficient  $C_{Dp}$  is derived from estimated equivalent flat plate area  $A$ , in accordance with (5.5).

Column 8 contains the sum of the drag coefficients; *i. e.*, the sum of the values in columns 3, 4 and 7 equals the total drag coefficient  $C_D$ .

In column 9 are calculated values of power required at sea level by (6.2).

While it would be possible to prepare a similar table as in Form 1, using the same procedure for all altitudes, a considerable amount of computation can be saved by using a method which consists of multiplying the sea level values of speed and of corresponding power required,

by the square root of the reciprocal of the relative density  $\sigma$  from Table 4, for the altitude selected.

TABLE 4.

*Standard Sea Level Air:*

$T = 15^\circ \text{C.}$      $W = 0.07651 \text{ lbs./cu.ft.}$      $\rho_0 = 0.00238 \text{ slugs/cu.ft.}$

$P = 29.921 \text{ ins. of Hg.}$

1 in. of Hg. = 70.732 lbs./sq.ft. = 0.4912 lbs./sq.in.

*Altitude-Pressure-Temperature Table.*

Altitude Feet	Pressure in. Hg.	Pressure lbs./sq. ft.	Tem- perature Dec. C	$\rho_0$ $\rho$	Density ratio $\frac{\rho}{\rho_0} = \sigma$	Reciprocal of square root of density ratio $\sqrt{\frac{1}{\sigma}}$
—1000	31.02	2194.1	17.0	.971	1.030	.985
— 500	30.47	2155.2	16.0	.985	1.015	.993
0	29.921	2116.4	15.0	1.000	1.000	1.000
5000	24.89	1760.5	5.1	1.161	0.862	1.077
10,000	20.58	1455.7	— 4.8	1.354	0.738	1.164
15,000	16.88	1194.0	—14.7	1.590	0.629	1.261
20,000	13.75	972.6	—24.6	1.877	0.533	1.370
25,000	11.10	785.1	—34.5	2.232	0.448	1.494
30,000	8.88	628.1	—44.4	2.674	0.374	1.635
35,000	7.04	498.0	—54.3	3.228	0.310	1.797
40,000	5.54	391.9	—55.0	4.087	0.245	2.022
45,000	4.36	308.4	—55.0	5.192	0.193	2.279
50,000	3.44	243.3	—55.0	6.592	0.152	2.568

This method of determining the power required at altitudes is based on the following aerodynamic considerations.

First, the true horizontal speeds at different altitudes for the same attitude of the airplane, that is, for the same angle of attack or the same  $C_L$ , are inversely proportional to the square roots of the relative densities.

This is shown as follows:

Let the subscript 0 denote values at sea level and the absence of subscript values at altitude. Then in general:

$$\text{Lift} = \text{weight} = \frac{1}{2} \rho v^2 C_L S$$

But weight, area and  $C_L$  (by assumption) are the same at sea level and at altitude. Hence  $\rho v^2/2$  must be the same. Hence in general under these conditions,  $v \sim \frac{1}{\sqrt{\rho}}$

$$\text{or} \quad \frac{v}{v_0} = \sqrt{\frac{\rho_0}{\rho}} \quad \text{and} \quad v = v_0 \sqrt{\frac{\rho_0}{\rho}}$$

Again Power = Drag  $\times$  Speed. But at the same attitude, the ratio  $L/D$  is the same and hence  $D$  is same at altitude and at sea level.

Hence

$$P_0 = D_0 v_0$$

$$P = D_0 v = D_0 v_0 \sqrt{\frac{\rho_0}{\rho}} = P_0 \sqrt{\frac{\rho_0}{\rho}}$$

The power will thus be proportional to the square root of the reciprocal of the relative density. Therefore, by dividing both the speed at sea level and the power required at sea level by the square root of relative density for a given altitude we obtain the true speed at altitude for the same lift coefficient, *i. e.*, same angle of attack, and the power required at that altitude corresponding to that speed. Hence, if for the same angle of attack,  $V_0$  corresponds to hp required at sea level, the true speed

at altitude,

$$V = V_0 \sqrt{\frac{1}{\sigma}}$$

will correspond to the required power

$$P_h = P_0 \sqrt{\frac{1}{\sigma}}$$

The values in columns 10 and 11, Form 1, are obtained by multiplying values from column 1 and 9 by  $\sqrt{1/\sigma}$ . It is usual to assume altitudes in steps of 5,000 or 10,000 feet up to the approximate ceiling, for which purpose columns 12 and 13, etc. are used.

## B. Power Available

Two methods for the determination of power available will be given. The first method is considered the more rational and accurate. The second is less elaborate and gives fairly good results, especially if it is used in connection with power required where the parasite drag is calculated by the summation of component drags.

Data necessary for the calculation of power available by the first method are as follows:

For the power source: number of engines, rated brake hp and corresponding r.p.m. of each engine, brake power curve plotted on r.p.m. for full throttle at standard conditions, gear ratio of the propeller hub unless a direct drive is used, whether supercharger or forced induction is used, information as to the standard altitude to which the supercharger maintains sea level power, and any other available data regarding the change of power at altitude.

For the propeller: chart of performance characteristics, and a first approximation to the high speed of the airplane.

The program is then carried forward as follows:

**7. Power Curves of Engines.** The brake horsepower is defined by the power curve at full throttle obtained on the dynamometer under standard atmospheric conditions as defined in Ref. 7. This power curve is generally furnished by the manufacturer and checked by the Government. Brake power at altitude of non-supercharged engines at constant r.p.m. is determined by the graph of Fig. 10. In the case of engines with

turbo-superchargers, the power decreases to about 80 per cent of the sea-level power (78 per cent for 20,000 foot supercharger) at the rated altitude limit of the supercharger. From this point the decrease in power is assumed the same as that of the non-supercharged engine. The altitude limit is then considered as sea level and the decrease is computed from the same graph, Fig. 10.

In the case of direct drive supercharging, remembering again that the r.p.m. are assumed constant, the power delivered to the propeller at any altitude will be equal to the sea level power of the unsupercharged engine increased by the gain in power due to the decrease in back pressure and decreased by the power absorbed by the supercharger. At sea level

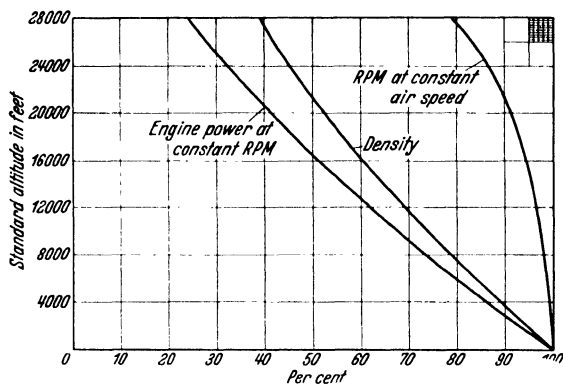


Fig. 10. Engine power, density and revolutions in relation to altitude.

the gain is, of course, zero, while some power will be required to operate the supercharger, relatively little if of the Roots type, relatively more if of the direct connected centrifugal type. It results, however, that we may assume a law of increase in both the gain of power and in the power absorbed by the supercharger in such manner that the power delivered to the propeller can be taken as increasing from sea level up, according to a linear law, and as reaching at the altitude limit, the sea level value for the non-supercharged engine. Above this limit it decreases the same as does that of the engine with turbo-supercharger. More detailed information is available in Refs. 10 and 16.

**8. Choice of Propeller Diameter<sup>1</sup>.** Various methods are available for determining the diameter of an airplane propeller, having given the power available and a sufficient selection of the operating conditions to make the problem definite. For details and practical suggestions, reference may be made to Ref. 4.

The conditions normally determining the selection of the propeller diameter are the maximum speed (first approximation), rated r.p.m. and rated power.

<sup>1</sup> See Ref. 19.

In case the propeller is to be designed for climb, the speed is taken as that approaching the speed in climb and the diameter is determined for that speed with the same rated power and r.p.m. as in the preceding case.

In the case of propeller design for a given altitude with a non-supercharged engine, the maximum power of the engine and the r.p.m. at that altitude may be determined by the use of Fig. 10 and the design may then go forward by any method appropriate to the data in hand (see Ref. 4).

**9. Design  $v/nD$  and Maximum Efficiency.** The design  $v/nD$  for any condition for which the design  $V$ ,  $N$  and  $D$  are established is:

$$\frac{v}{nD} = \frac{88 V \text{ (m.p.h.)}}{N \text{ (r.p.m.) } D \text{ (ft.)}} \quad (9.1)$$

The maximum efficiency corresponding to the design  $v/nD$  is found on the graph, Fig. 11. This graph is made for two-blade metal and wood propellers. For two-blade micarta propellers, a mean curve between metal and wooden propellers may be used. For three and four-blade propellers, multiply the maximum efficiency of two-blade propellers by 98 per cent and 96 per cent respectively. For tandem arrangements use 98 per cent of the value found for a single propeller. Calculate tip

FORM 2. Horsepower Available at Sea Level.

1	$V$ m.p.h.	Same as column 1, Form 1.
2	Per cent of design $V$	Calculated from column 1
3	Per cent of design $N$	From Fig. 12
4	$N$ r.p.m.	Values from column 3 $\times$ Design r.p.m.
4a	$N$ propeller r.p.m.	Values from column 4 $\times$ ratio of propeller to engine r.p.m. (Omit if direct drive is used)
5	hp Brake	From power curve
6	$\frac{v}{nD}$	Calculated from columns 1 and 4 or 4a and the design propeller diameter
7	Per cent of design $\frac{v}{nD}$	Calculated from column 6 and design $v/nD$
8	Per cent of maximum $\eta$	From Fig. 13
9	$\eta$	Values from column 8 $\times$ maximum propeller efficiency
10	HP Available	hp available = Brake hp $\times \eta$

speeds in the regime of design  $v/nD$ , and multiply efficiency by 97.5 per cent and 90 per cent where the tip speed is 1000 ft./sec. and 1100 ft./sec.

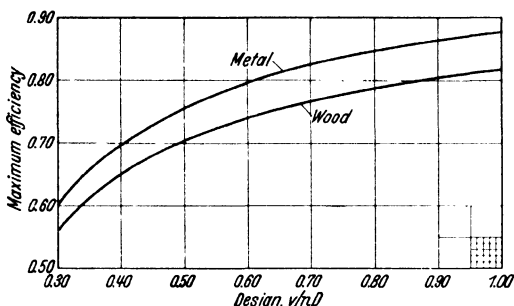


Fig. 11. Propeller efficiency in relation to values of  $v/nD$ .

Referring to Form 2 for power available, in column 1 the speeds are chosen for convenience the same as for power required in Form 1.

In column 2 are calculated percentages of speeds in relation to the design  $V$  (first approximation of high speed).

#### 10. Variation of Engine Speed and Power at Sea Level (Full Throttle).

Column 3 contains values in per cent of the average r.p.m. at sea level

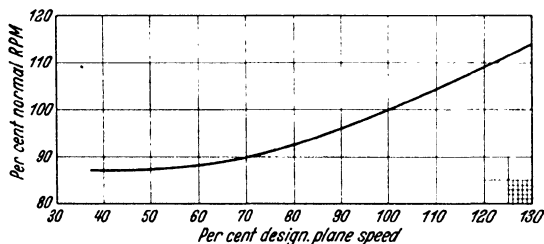


Fig. 12. Relation between per cent of normal r.p.m. and per cent of normal speed.

respectively. This correction is to be applied only at the values of  $v/nD$  where these tip speeds occur, and not to the entire efficiency curve. With these necessary values for the calculation of available power (design  $V$  or  $v$ , design  $N$  or  $n$  design hp and design  $D$ ) established, the tabulation of derived values proceeds as follows:

full throttle corresponding to values in column 2 taken from Fig. 12.

In column 4 are the r.p.m. of the engine determined from the design  $N$  and percentages in column 3. Column 4a contains r.p.m. of the propeller in the case of geared propellers. The

r.p.m. for different speeds are thus determined from the average variation of r.p.m. of many engines in different airplanes and may not correspond exactly to the r.p.m. in a particular flight test. The error in power available, incurred by using the average r.p.m. instead of the actual r.p.m. is small however, since the effects of small variation of r.p.m. on the brake power, on the  $v/nD$ , and on the propeller efficiency are compensating. That is, if the assumed r.p.m. is larger than the actual, the corresponding brake power will be larger, but at the same time the  $v/nD$  will be smaller and the corresponding propeller efficiency will be smaller. Thus the error in the assumption of the r.p.m. at a speed different from the design speed is self compensating to a considerable extent.

In column 5 is entered the brake power at sea level corresponding to the r.p.m. in column 4 taken from the power curve of the engine.

**11. Variation in Propeller Efficiency.** Equation (9.1) is used to find the various values of  $v/nD$ , taking  $V$  from column 1,  $N$  from column 4 (or 4a) and for  $D$ , the design diameter<sup>1</sup>. These values are then set in column 6.

In column 7 are percentages of the design  $v/nD$ .

In column 8 are percentages of maximum propeller efficiency corresponding to the percentages of design  $v/nD$  of column 7 taken from Fig. 13. The values on this graph are average, and were obtained from the flight tests

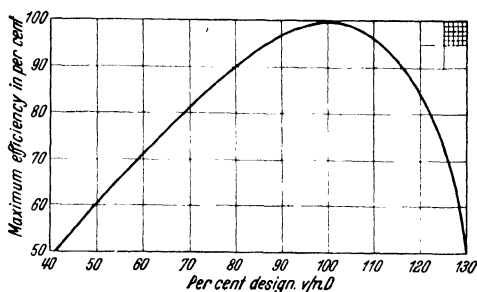


Fig. 13. Per cent maximum propeller efficiency in relation to per cent design  $v/nD$ .

of a large number of airplanes; they can be assumed to be correct at high speeds and accurate within six per cent at climbing speeds. For airplanes having a great angle of climb and for airplanes with geared engines, the recommended values of efficiency at climbing speeds are on the low side.

In column 9 are entered efficiencies of the propeller obtained by multiplying the values in column 8 by the maximum design efficiency.

**12. Power Available at Sea Level and at Altitudes (First Method).** Power available at sea level is the product of brake power, column 5, and the efficiency, column 9, and is entered in column 10.

Power available at altitude is obtained from that at sea level by using altitude factors for reduction of sea level power and r.p.m. These factors are plotted in Fig. 10. In Form 3 speeds in column 1 are taken the same as for sea level conditions, and sea level r.p.m. in column 2 is the same as column 4 in Form 2.

In column 3, engine r.p.m. at altitude is obtained by multiplying the sea level r.p.m. by the r.p.m. altitude factor taken from Fig. 10. Column 3a is used only for geared engines and contains the r.p.m. of the propeller.

In column 4 are values of sea level power of the engine at altitude r.p.m. from column 5, Form 2.

Engine power (column 5) at altitude is obtained by multiplying the power at sea level (column 4) by the power altitude factor taken from Fig. 10. The parameter  $v/nD$ , efficiency, and horsepower available,

<sup>1</sup> It may be remembered that  $v/nD = 88 V/ND$ .

FORM 3. Horsepower Available at Altitudes (Precise).

1	$V$ m.p.h.		Same as column 1, Form 1
2	$N$ r.p.m.	Sea level	From column 4, Form 2
3		Altitude	Values from column 2 $\times$ factor from Fig. 10
3a			
4	BHP	Sea level	From column 5, Form 2
5		Altitude	Values from column 4 $\times$ factor from Fig. 10
6	$\frac{v}{nD}$		Calculated from columns 1 and 3 and the design propeller diameter
7	Per cent Design $\frac{v}{nD}$		Calculated from column 6 and design $\frac{v}{nD}$
8	Per cent $\eta$ max		From Fig. 13
9	$\eta$		Values from column 8 $\times$ maximum propeller efficiency
10	HP Available at Altitude		Values from column 5 $\times$ values from column 9

in columns 6 to 10 inclusive, are found in the same manner as in the case of power available at sea level.

*Short-Cut Method.* For rapid estimation of power available at altitude

where extreme accuracy is not required, a short-cut method may be used. This consists of multiplying the values from column 10, Form 2, by the appropriate value from Fig. 14, to obtain the power available at a given altitude.

One of the advantages of the first method consists of giving information as to the r.p.m. and the propeller efficiencies. These are valuable data for the selection of propeller or propeller settings when an increase of performance at altitude is sought.

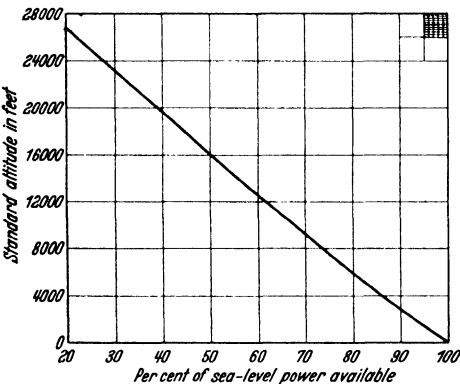


Fig. 14. Relation between altitude and per cent of sea level power available.

**13. Power Available at Sea Level and Altitude (Second Method).** The first step in this method is an approximation of high speed. This can be done by assuming a propeller efficiency by which the normal brake horsepower of the engine is multiplied to obtain the maximum horsepower available. The high speed is then found by locating the



speed on the horsepower required curve at which the horsepower required equals the approximate horsepower available.

The propeller diameter may then be estimated by the following equation:

$$D = K \sqrt[4]{\frac{bhp}{N^2 V}} \quad (13.1)$$

where

$bhp$  = normal brake horsepower

$N$  = normal engine speed (r.p.m.)

$K$  = a constant depending on the propeller, as determined from Table 5. An average compromise value for  $K$  is 300.

The design  $v/nD$  is next calculated from the values of  $V$ ,  $N$ , and  $D$  estimated above. Maximum efficiency is found for this  $v/nD$  from Fig. 11. This efficiency should be reduced for interference and high tip speed in accordance with the ratios given in 9.

The horsepower available (second approximation) is equal to the efficiency determined above, times the normal brake horsepower. The second approximation to high speed is then found from the horsepower required curve in the same manner as that used for the first approximation.

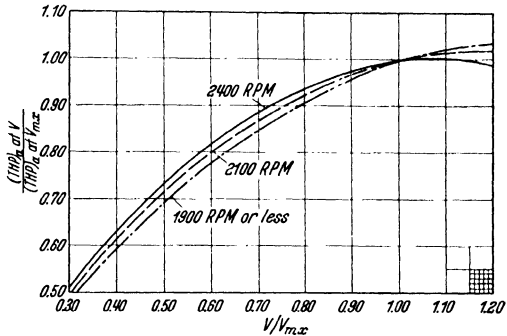


Fig. 15.

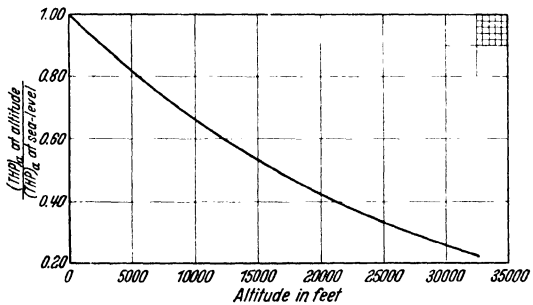


Fig. 16.

TABLE 5. Values of  $K$  in Equation for Propeller Diameter.  
Wooden Propellers. Metal Propellers.

Wooden Propellers.				Metal Propellers.				
No. of Blades		2	3	4	No. of Blades		2	3
$K$ for	Speed (optimum slip) . . . . .	285	255	240	$K$ for	Speed (optimum slip) . . . . .	280	260
	Climb (zero slip) . . . . .	320	290	270		Climb (zero slip) . . . . .	315	300
	Compromise . . . . .	305	275	260		Compromise . . . . .	300	290

Horsepower available at sea level is determined by the steps outlined in Form 4 with the use of Fig. 15. If the normal engine power is from 70 to 80 per cent of the maximum power, use the curve for 1900 r.p.m. If it is from 80 to 90 per cent, use the curve for 2100 r.p.m. and if above 90 per cent, use the curve for 2400 r.p.m.

FORM 4. Horsepower Available at Sea Level.

1	2	3	4
$V$ m.p.h.	$V$ $V_{mx}$	$\frac{P_a \text{ at } V}{P_a \text{ at } V_{mx}}$	$P_a \text{ at } V$
Same as column 1, Form 1	Calculated from column 1	From Fig. 15	Values from column $3 \times P_a \text{ at } V_{mx}$

FORM 5. Horsepower Available at Altitudes.

1	2	3	4
$V$ m.p.h.	$P_{a0}$	10,000 ft.	$P_{ah}$ 15,000 ft. etc.
Same as column 1, Form 1	From column 4, Form 4	Multiply values from column 2 by factor from Fig. 16	Multiply values from column 2 by factor from Fig. 16

Horsepower available at altitude is obtained as shown in Form 5 with the use of Fig. 16. (See also Table 13.)

## CHAPTER III

## PERFORMANCE FROM POWER GRAPHS

Practically all the performance characteristics of an airplane can be calculated directly from the power graphs, except the range and the endurance.

In the determination of performance, the curves of power required and available at sea level from Forms 1 and 2 are plotted against speed (see example, Fig. 21).

**1. High Speed.** The high speed in level flight is found at the intersection of the curve of power required and power available toward the side of higher speeds. The intersection on the low speed side which occurs in some instances is of smaller importance and corresponds to the minimum speed with power on in horizontal flight. Obviously both of these speed conditions correspond to the case where the power necessary for horizontal flight is equal to the power which the particular engine-propeller unit can transmit to the airplane in the form of thrust. It is possible of course that the airplane can travel faster than the high

speed, but the additional power then is furnished by gravity and the airplane is diving. For that reason, in checking the speeds by flight test, it is essential to fly a perfectly horizontal course. In order to insure the horizontality of the path, the speed course runs must be flown very close to the ground, at approximately 50 feet.

Similarly, the high speeds at altitude are determined from similar curves corresponding to certain altitudes, and are for reasons given above more difficult to check by flight test.

As a rule, the change of high speed with altitude is small in the first few thousand feet, but its decrease is more pronounced as the ceiling is approached. In the case of high speed airplanes or of airplanes with large speed ratio the decrease of high speed with altitude is very gradual and in some cases there is even a slight gain in speed at low altitudes. This condition occurs when, due to the rapid increase of overall lift-drag ratio at higher altitude, the power required (for same speed) is decreasing more rapidly than the power available. In the case of airplanes with modern engines with forced induction and high compression ratio this is particularly true, since the drop of the engine power at low altitude is small. Engines with forced induction are not always classed as supercharged, but they maintain their sea level power to several thousand feet of altitude.

In the case of airplanes with low speed ratio to which belongs the majority of so-called light airplanes, the high speed at altitude decreases much faster.

In the case of airplanes with supercharged engines the high speed gradually increases up to the highest altitude at which the engine maintains its sea level power.

An additional increase in high speed, and in other items of performance as well, can be gained by a controllable pitch propeller by maintaining the optimum propeller efficiency consistent with optimum power of the engine.

The minimum speed at sea level is ordinarily determined by the maximum lift coefficient of the airfoil for any except greatly underpowered airplanes, the ceiling of which is very low. If the maximum lift coefficient corresponded with the minimum power required, the minimum speed would always occur at maximum lift. However, the range of minimum required power occurs at lower lift coefficients and higher speeds, so that at or near the ceiling the power available and power required curves meet or intersect at higher speeds than stalling speed which is determined by the maximum lift coefficient. This explains the difference between minimum and stalling speeds.

On many airplanes the desired minimum and stalling speeds for slow landing cannot be reached on account of the difficulty of maintaining the airplane on even keel. Problems of lateral and directional stability

in regions of stalling angles are many and difficult to solve. Fortunately, actual airplanes can reach low landing speeds notwithstanding this limitation because of the scale effect which increases the value of maximum lift coefficient of many airfoils as compared with that obtained in the wind tunnel and used in design computations.

Reference is made here to the examples of performance determination and plot of curves on Figs. 21 and 22.

**2. Rate of Climb.** The calculation of the rate of climb is based on the difference between the power necessary for horizontal flight and that transmitted by the propeller to the airplane. The diagram of Fig. 17 shows the equilibrium of forces acting on an airplane in horizontal flight at a certain speed corresponding to a certain angle of attack. In order to support the airplane, the lift must equal the weight and the drag must be balanced by the thrust; thus the resultant of lift and drag  $R_1$  is equal and opposite to  $R_2$  which is the resultant of the thrust and the weight, the conditions of equilibrium being satisfied. The drag or the thrust multiplied by the speed denotes the horsepower necessary to keep the airplane flying horizontally. This equilibrium is expressed by

$$DV \text{ (power required)} = TV \text{ (thrust power)}$$

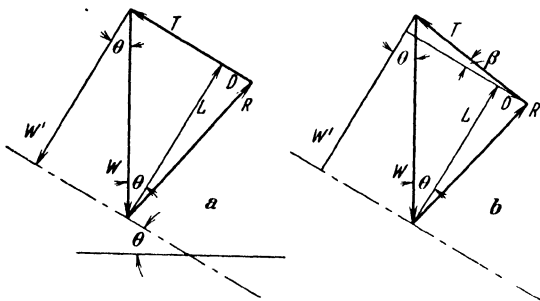


Fig. 18.

he decreases the angle of attack suitably, the speed will increase until a new condition of horizontal flight is established. Or he may decrease the angle of attack somewhat less, in which case there will be an increase of speed and a moderate angle of climb. But if he maintains the same speed, the airplane will climb at a steeper angle and with a slightly decreased angle of attack.

The conditions of equilibrium are now shown by the triangle of forces in Fig. 18a, assuming the line of thrust along the line of flight.

If the power of the engine, and therefore the thrust power, is increased by opening of the throttle, either the speed is increased, the airplane starts to climb, or both occur. The pilot has at his discretion any one of three possibilities. If by action of the elevators,

The resultant of lift  $L$  and drag  $D$  will give the resultant air-force  $R$  and there must be equilibrium between this force  $R$ , the weight  $W$  and the thrust  $T$  as shown. The weight  $W$  is now carried, in part by the vertical component of the lift  $L$  and in part by the vertical component of the resultant force (thrust minus drag) along the line of flight. As shown by the diagram we must have the following relations:

$$L = W \cos \theta \quad (2.1)$$

$$T = W \sin \theta + D \quad (2.2)$$

The decrease in the angle of attack, the speed in climb being the same as in horizontal flight, is due to the fact that if the angle remained the same and the speed the same, the lift would remain the same or  $L = W$ , instead of  $L = W \cos \theta$ . Hence the angle of attack must be reduced and in the final condition of steady flight along the climbing path the conditions of Fig. 18a will be realized.

The determination of the rate of climb is developed as follows. From (2.2), we have

$$W \sin \theta V = (T - D)V$$

or in words, the power required to lift the weight  $W$  against gravity at the speed  $V \sin \theta$  is equal to the power corresponding to the net force  $(T - D)$  acting along the flight path at the speed  $V$ . The power  $TV$  is the thrust power available, the power required against air resistance is  $DV$ , and the difference is the reserve available for lifting the plane against gravity at the vertical velocity  $V \sin \theta$ . We have therefore

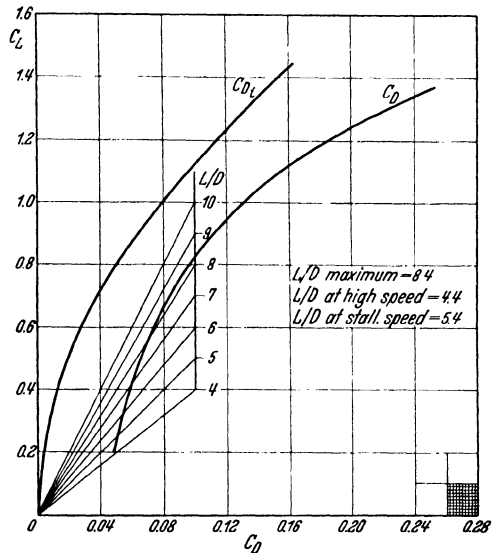


Fig. 19. Polar of complete airplane.

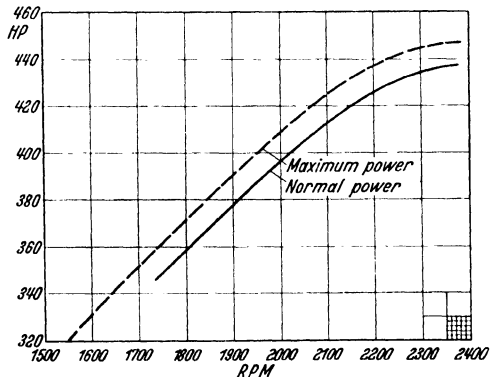


Fig. 20. Horsepower curve for 400 hp supercharged engine.

$$V \sin \theta = \frac{T V - D V}{W}$$

or otherwise

$$V \sin \theta \text{ (ft. per min.)} = \frac{\text{Reserve hp} \times 33\,000}{W} \quad (2.3)$$

In case the propeller shaft is inclined to the line of flight at an angle  $\beta$  and if it could be assumed in such case that the line of resultant force acts from the propeller on the plane along the shaft and hence inclined

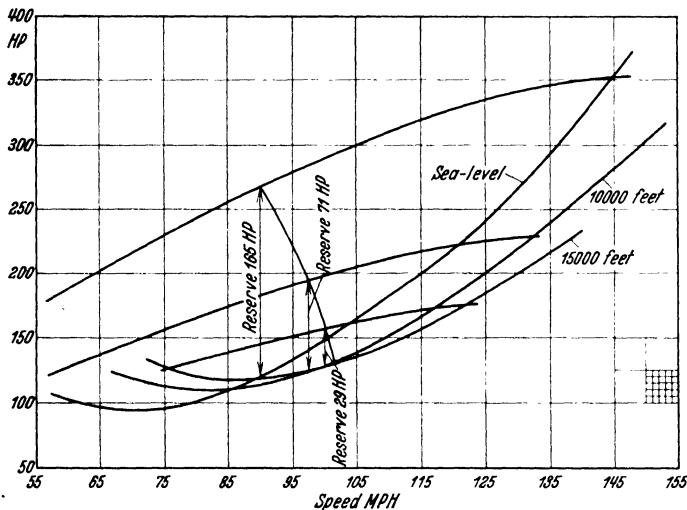


Fig. 21. Performance curves.

also at the angle  $\beta$  to the flight path, we should have the conditions of Fig. 18 b.

$$T \cos \beta - D = W \sin \theta$$

$$T \sin \beta + L = W \cos \theta$$

The determination of the actual line of thrust in such case, however, becomes very complex and it will ordinarily serve practical requirements to assume the thrust along the flight path and the conditions of Fig. 18 a.

The maximum reserve power is determined graphically, and is expressed by the maximum vertical distance between the power available and power required curves at the same speed. Its value is obtained by trial with a compass and it occurs at a certain speed where the tangents to the curves are parallel. Upon inspection of the shape of the power curves (see Fig. 21) it is apparent that small changes in speed do not appreciably change the value of the reserve power and therefore of the rate of climb. Reserve power at altitude is obtained by the same method and without any corrections due to altitude in the above formula. The horizontal speed at absolute ceiling is obtained by extrapolating points

of available and required powers corresponding to climbing speed. The intersection of these two curves denotes the only speed at which the airplane can fly at absolute ceiling. The rate of climb at sea level and at several altitudes is plotted against altitude to determine the curve of rate of climb as shown by Fig. 22. This curve is generally approximated by a straight line, although if many points are plotted, it has a somewhat upturned curvature. In performance prediction a good agreement with flight test is obtained by using a straight line passing through the

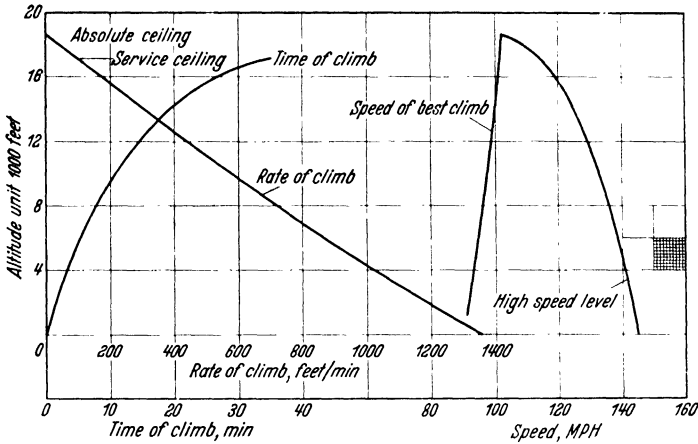


Fig. 22. Performance summary.

point of rate at ground and some point from two to five thousand feet below the ceiling.

**3. Ceilings.** The *absolute ceiling* is the altitude of zero rate and is determined by extrapolating the rate of climb curve to zero rate. Similarly the *service ceiling* is defined by the altitude where the rate is 100 feet per minute. The ceiling is a complex function of the airplane, engine, and propeller design characteristics, of which the ability of the engine to maintain its power is the most important. Low span loading with high lift-drag ratios at high lift coefficients are requisite characteristics of a high altitude airplane.

**4. Angle of Climb.** As shown in Fig. 18a, the angle of climb, important in take-off from emergency landing fields, is determined by the angle  $\theta$  where

$$\sin \theta = \frac{\text{Thrust} - \text{Drag}}{\text{Weight}}$$

Since the information on the rate of climb and speed is directly available, the following formulas are more convenient:

$$\sin \theta = \frac{\text{Rate of Climb (ft./min.)} \times 0.01136}{\text{Speed, m.p.h.}}$$

or approximately for small values of  $\theta$ ,

$$\theta \text{ deg.} = \frac{0.65 \times \text{Rate of Climb (ft./min.)}}{V \text{ (m.p.h.)}}$$

**5. Time of Climb.** Assuming a linear variation of the rate of climb against altitude, ( $dh/dt = R(1 - h/H)$ ) the shortest possible time to climb to a given altitude is calculated by the use of the equation:

$$t = 2.3 \frac{H}{R} \log_{10} \left( \frac{H}{H - h} \right), \text{ where}$$

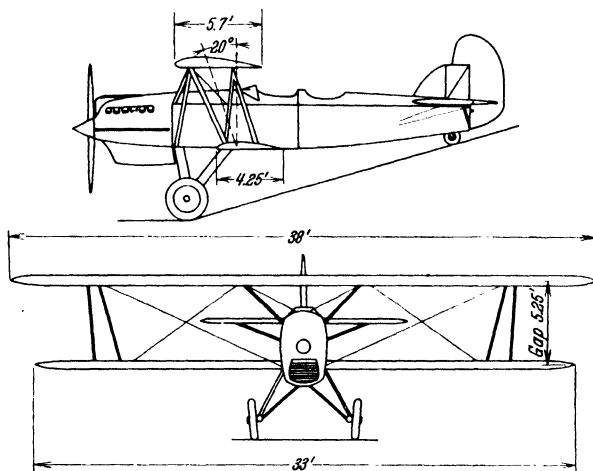


Fig. 23. Example airplane.

Weight 400 lbs.	Lower area 135 sq. ft.
Total area 350 sq. ft.	435 hp @ 2300 r.p.m.
Upper area 215 sq. ft.	$A = 9.5$ sq. ft.

$t$  is time of climb in minutes to altitude  $h$  in feet,  
 $H$  is the absolute ceiling in feet, and  
 $R$  is the maximum rate of climb at sea level in feet per minute.

#### *Example of Performance Calculations.*

The application of the procedures outlined in the preceding paragraphs is made in the following examples for which was chosen a biplane with open cockpits (Fig. 23), single bay wing cellule trussing, with large upper wing and small lower wings and with one water-cooled tractor engine non-supercharged.

Two complete examples are given for performance computations from power graphs in the following paragraphs.

**6. Power Required.** Summary of Performance No. 1, Form 6, is based on power required from Table 6, where parasite drag was obtained by summation of component drags. The power available was computed by methods used by the U.S. Navy as shown in Tables 8 and 9.



Summary of Performance No. 2, Form 6a, is based on power required from Table 7, where equivalent flat plate area  $A$  was obtained by comparison with other airplanes. The power available is computed as shown in Tables 10, 11 and 12 (see also 7).

The differences in the various characteristics determined by both of these methods are well within the accuracy of flight test results.

#### A. Power Required by Summarizing Component Drags

In Table 2 is the tabulation of data when the summation of component drags is used for determination of parasite drag. (Note slight discrepancies between results of two methods of parasite drag determination.)

The determination of power required in this case is made in Table 6, according to Form 1a.

a) Determination of values in columns 1 to 4 is as noted earlier in II 5 and 6.

b) Determination of parasite drag by summation of component parts is made in Tables 2 and 3. Due to the mutual interference, an increase of 15 per cent is made to  $D_{p1}$  and to  $D_{p2}$ , the respective values of which are 74.3 and 191.4.

TABLE 6. Horsepower Required (Parasite Drag est. by Summation).  
 $W/S = 11.42 \text{ lb./sq. ft.}$   $CD_{p1} = .00956$ .  $CD_{p2} = .02460$ .

1	2	3	4	5	6	7	8	9	10	11	12	13
$V$ m.p.h.	$C_L$	$CD_i$	$CD_0$	$V/V_{mn}$	$f_1$	$CD_{p1} \times f_1$	$CD$	HP required	@ 10,000 ft. $V$	HP required	@ 15,000 ft. $V$	HP required
57.2	1.37	.1270	.0450	1.00	4	.0382	.2348	105	66.6	122	72.2	132
70	.915	.0654	.0170	1.22	1.3	.0124	.1104	91	81.5	106	88.2	115
80	.701	.0331	.0131	1.40	1.1	.0105	.0813	100	93.2	116.5	100.8	126
90	.554	.0207	.0115	1.57	1.03	.00985	.0667	117	104.9	136	113.5	148
100	.449	.0136	.0110	1.75	1.00	.00956	.0588	141	116.5	164	126.1	178
110	.370	.0092	.0110	1.92	1.0	.00956	.0544	174	128.1	203	138.6	220
120	.311	.0065	.0105	2.10	1.0	.00956	.0512	210	139.8	245	151.3	265
130	.265	.0047	.0102	2.27	1.0	.00956	.0491	259	151.5	302	164.0	327
145.2	.212	.0030	.0100	2.54	1.0	.00956	.0472	347				

Thus  $D_{p1} = 74.3 \times 1.15 = 85.7$  pounds.

$D_{p2} = 191.4 \times 1.15 = 220.3$  pounds.

These values reduced to coefficients are [see II (5.3)]:

$$C_{Dp1} = 0.00956$$

$$C_{Dp2} = 0.02460$$

which total for high speed,  $C_{Dp} = 0.03416$  from which  $A = 9.34$  [see II (5.5)] square feet as compared with the direct estimate of  $A = 9.5$  square feet.

c) In columns 5, 6 and 7 are entered values resulting from Tables 2 and 3, in accordance with Form 1a.

d) Column 8 is the sum of the values in columns 3, 4, 7 plus the constant value of  $C_{Dp2}$ .

e) Determination of power required is made from column 8 [see II (6.2)].

f) Power required at sea level and altitudes is then plotted as in Fig. 21.

### *B. Power Required by Estimating A Directly.*

a) Data available for calculation of power required were:

Gross weight = 4,000 pounds.

Wing area (total) = 350 square feet, airfoil—Clark Y.

Upper wing: Span ( $b_1$ ) = 38 feet

Chord = 5.7 feet

Area = 215 square feet.

Lower wing: Span ( $b_2$ ) = 33 feet

Chord = 4.25 feet

Area = 135 square feet

Gap ( $G$ ) = 5.25, Stagger = 20 deg.

Engine Power: 435 bhp, 2300 r.p.m. (Fig. 20).

Metal Propeller, 2 blades.

b) Determination of interference factor  $\sigma$ :

Mean span, ( $b$ ) = 35.5 feet

Ratio of spans ( $b_2/b_1$ ) = 0.868

$G/b$  = 0.144

$\sigma$  (from Fig. 4) = 0.551.

c) Determination of equivalent geometrical chords:

$$c_1 = \frac{215}{38} = 5.66$$

$$c_2 = \frac{135}{33} = 4.09$$

d) Determination of equivalent monoplane aspect ratio, first method, assuming E.M.A.R. as in II (3.4):

$$\text{E.M.A.R.} = \frac{350}{74.2} = 4.72$$

e) Determination of E.M.A.R. (precise method) using Appendix 1, and assuming the value of the ratio  $a = 0.66$ :

$$\text{E.M.A.R.} = \frac{(K b_1)^2}{S} = \frac{(K \times 38)^2}{350}$$

$$G/b_1 = 0.138$$

$$r = 0.87$$

$$K \text{ for } r = 0.87 \text{ (by interpolation)} = 1.072$$

$$\text{E.M.A.R.} = \frac{(1.072 \times 38)^2}{350} = 4.74^1$$

f) Determination of equivalent flat plate area by direct estimate from similar airplane (see Fig. 23).

The available data were two airplanes of generally similar character, one with  $W = 2269$  pounds and  $A = 6.03$  and one with  $W = 6483$  pounds and  $A = 12.5$ . Interpolation gives an approximate value  $A = 8.8$ . Due, however, to the fact that the larger of these two planes has a closed fuselage and is very close to the lower limit of  $A$ , 0.7 square feet is added to the interpolated value, making a total of 9.5 square feet. The coefficient of parasite drag at high speed is then,

$$C_{Dp} = \frac{1.28 A}{S} = 0.03475$$

g) Determination of stalling speed at sea level: For Clark Y, maximum  $C_L = 1.37$  (in variable density tunnel at R.N. 3,610,000)

$$V = \sqrt{\frac{4,000}{0.00256 \times 1.37 \times 350}} = 57.2 \text{ m.p.h.}$$

h) Determination of high speed (first approximation):

$$\text{Rated r.p.m. } 2300$$

$$\text{Normal Brake Horsepower } 435 \text{ hp}$$

$$V/N = \frac{140 \text{ (assumed)}}{2300} = 0.061$$

First approximation of propeller efficiency from Fig. 9 yields

$$\text{Efficiency (maximum)} = 0.82$$

First approximation of power available,

$$435 \times 0.82 = 357 \text{ hp}$$

Induced drag coefficient:

From II (6.1), by substitution of numerical values,

$$C_{Di} = 0.0036$$

<sup>1</sup> The discrepancy in these two methods is small because the biplane chosen happens to have the best area distribution which Prandtl assumes. The precise method is preferable especially when a small difference in aspect ratios of the two wings occurs, which is the usual case.

TABLE 7. Horsepower Required. (*A* estimated.)  
 $W/S = 11.42 \text{ lb./sq. ft.}$  ( $C_{Dp} \text{ H.S.} = 0.03475$ ). E.M.A.R. = 4.72.

1	2	3	4	5	6	7	8	9	10	11	12	13
<i>V</i> m.p.h.	$C_L$	$C_{Di}$	$C_{D0}$	$\frac{C_L - .212}{1.158}$	$\frac{C_{Dp}}{C_{Dp} \text{ H.S.}}$	$C_{Dp}$	$C_D$	HP required S.L.	<i>V</i>	10,000 ft. HP required	15,000 ft. <i>V</i>	HP required
57.2	1.37	.127	.0450	1.0	1.72	.0598	.2318	104	66.6	121	72.2	131
70	.915	.0564	.0170	.607	.90	.0313	.1047	86.0	81.5	100	88.2	109
80	.701	.0331	.0131	.422	1.02	.0355	.0817	100.4	93.2	117	100.8	127
90	.554	.0207	.0115	.295	1.03	.0358	.0680	119	104.9	139	113.5	150
100	.449	.0136	.0110	.205	1.03	.0358	.0604	145	116.5	169	126.1	183
110	.370	.0092	.0110	.136	1.02	.0355	.0557	178	128.1	209	138.6	225
120	.311	.0065	.0105	.085	1.02	.0355	.0525	218	139.8	254	151.3	275
130	.265	.0047	.0102	.046	1.01	.0351	.0500	264	151.5	308	164.0	333
145.2	.212	.0030	.0100	0.00	1.00	.03475	.04775	351				

*A* = Equivalent Flat Plate Area. HP required = Horsepower Required. H.S. = High Speed. S.L. = Sea Level.

or, from II (6.4) we find

$$C_L = 0.288$$

and this with

E.M.A.R. = 4.73 in Fig. 3  
gives

$$C_{Di} = 0.0036 \text{ as above.}$$

Profile drag coefficient (from  
polar similar to Figs. 1, 2)

$$C_{D0} = 0.0102$$

Parasite drag coefficient [(*f*)  
above]

$$C_{Dp} = 0.03475$$

Total drag coefficient =

$$C_{Di} + C_{D0} + C_{Dp} = 0.04855.$$

First approximation of high  
speed: From II (6.3) substitut-  
ing numerical values we have

$$V_m = 145.2 \text{ m.p.h.}$$

Then correcting the first  
value of  $C_L$  we have from  
II (6.4)

$$C_L = 0.212$$

i) Determination of range  
of lift coefficients correspond-  
ing to speed range 57.2 to  
145.2 m.p.h.

$$C_{Lm} - C_L(V_m) =$$

$$= 1.37 - 0.212 = 1.158$$

taken as 100 per cent.

The values in column 5,  
Table 7, according to Form 1b,  
are then tabulated as shown.

j) Determination of vari-  
ation of  $C_{Dp}$ .

Assume variation similar to  
VE-7 from Fig. 8 and fill in  
columns 6 and 7.

k) Determination of total  
drag coefficient as in column 8.

l) Determination of power  
required at sea level as in  
column 9 [see II (6.2)].

m) Determination of power required at 10,000 and 15,000 feet.

$$\sqrt{\frac{1}{\sigma}} \text{ at } 10,000 = 1.165 \quad \sqrt{\frac{1}{\sigma}} \text{ at } 15,000 = 1.261$$

These values are used in calculating columns 10 to 13.

The polar of the whole airplane, which is used for some special investigations and in a method for performance determination based on indicated speed and indicated r.p.m. (see Chapter V), is plotted in Fig. 19. Values of  $L/D$  can also be obtained from this graph.

**7. Power Available.** Data necessary for the calculation of power available are:

Engine rated at 435 brake horsepower at 2300 r.p.m. non-supercharged without forced induction (see Fig. 20).

Propeller: Two-bladed metal.

TABLE 8. Horse power Available at Sea Level. See Form 4.

1	2	3	4
$V$ m.p.h.	$\frac{V}{V_{\max.}}$	THP av. (THP av.) <sub>0</sub>	THP av.
57.2	0.394	0.625	216
70.0	0.482	0.715	248
80.0	0.552	0.780	270
90.0	0.620	0.835	289
100.0	0.690	0.880	305
110.0	0.759	0.918	318
120.0	0.828	0.948	328
130.0	0.896	0.973	337
140.0	0.966	0.993	344
150.0	1.035	1.002	347

TABLE 9. Horsepower Available at Altitudes. See Form 5.

1	2	3	4
Air Speed $V$ m.p.h.	Sea Level THP av. (From Table 9)	.66 THP av. at altitudes 10,000 ft.	.53 THP av. at altitudes 15,000 ft.
57.2	216	143	115
70.0	248	164	132
80.0	270	178	143
90.0	289	191	153
100.0	305	201	162
110.0	318	210	169
120.0	328	217	174
130.0	337	222	179
140.0	344	227	182
145.0	346	228	183
150.0	347	229	184

#### *A. Power Available from Variation of R.P.M. with Speed.*

a) Determination of design speed.

First approximation of high speed (from power required) was 145.2 m.p.h., which may be taken as the design speed for the propeller. But considering that the high speed will not be changed appreciably if a lower design speed is assumed and that the climb at lower speeds will be improved, the design speed is assumed 98 per cent of the first approximation of high speed.

$$\text{Design } V = 145.2 \times .98 = 142.4.$$

b) Determination of propeller diameter.

$$\text{r.p.m.} = 2300, \text{ hp} = 435, V = 142.4 \text{ m.p.h.}$$

TABLE 10. Horsepower Available at Sea Level.  
Des.  $v/n D = .637$ .  $D = 8.55$  ft.  $\eta_{\max.} = 81\%$

1	2	3	4	5	6	7	8	9	10
$V$ m.p.h.	Per cent Des. $V$	Per cent Des. $N$	$N$ r.p.m.	BHP	$v/n D$	Per cent Des. $v/n D$	Per cent $\eta_{\max.}$	$\eta$	HP av.
57.2	40.2	87	2000	396.5	.295	46.3	56.0	.454	180
70	49.2	87.1	2004	397.0	.360	56.5	67.5	.547	217
80	56.2	87.8	2020	400	.408	64.0	75.5	.612	245
90	63.2	88.7	2040	401	.455	71.4	82.5	.668	268
100	70.2	89.8	2065	408	.498	78.2	88.5	.717	293
110	77.2	91.5	2105	412	.538	84.4	93.5	.757	312
120	84.2	93.8	2160	420	.572	89.8	96.8	.784	329
130	91.3	96.0	2210	426	.606	95.1	99.0	.802	342
145.2	102.0	100.5	2310	435	.647	101.6	99.8	.808	352

TABLE 11. Horsepower Available at 10,000 Ft.

1	2	3	4	5	6	7	8	9	10
$V$	$N$ Sea Level 10,000 ft.		BHP Sea Level 10,000 ft.		$v$ $n D$	Per cent Design $v$ $n D$	Per cent $\eta_{\max.}$	$\eta$	HP av. 10,000 ft.
57.2	2000	1950	390.0	264.5	.303	47.6	57.5	.466	123.3
70.0	2004	1953	390.5	265.0	.369	57.9	69.0	.559	148.2
80.0	2020	1968	392.0	266.0	.419	65.8	77.4	.627	166.8
90.0	2040	1987	395.0	268.0	.467	73.4	84.5	.685	183.7
100.0	2065	2012	400.0	271.0	.511	80.2	90.2	.731	198.2
110.0	2105	2050	405.0	274.5	.552	86.7	95.0	.770	211.5
120.0	2160	2105	412.0	279.5	.587	92.2	98.2	.796	222.6
130.0	2210	2155	420.0	284.8	.622	97.7	99.8	.809	230.0

TABLE 12. Horsepower Available at 15,000 Ft.

1	2	3	4	5	6	7	8	9	10
$V$	$N$ Sea Level 15,000 ft.		BHP Sea Level 15,000 ft.		$v$ $n D$	Per cent Design $v$ $n D$	Per cent $\eta_{\max.}$	$\eta$	HP av. 15,000 ft.
57.2	2000	1900	381	205.9	.310	48.7	58.7	.476	98.0
70.0	2004	1905	382	206.2	.379	59.5	70.7	.573	118.3
80.0	2020	1920	384	207.4	.430	67.5	79.0	.640	132.8
90.0	2040	1939	386	208.5	.479	75.2	86.2	.698	145.7
100.0	2065	1962	392	211.8	.524	82.3	91.9	.745	157.8
110.0	2105	2000	397	214.3	.566	88.8	96.5	.782	167.7
120.0	2160	2052	405	218.8	.602	94.5	99.0	.802	175.6
130.0	2210	2100	412	222.5	.638	100.0	100.0	.810	180.4

Then by any appropriate method of propeller design (see Ref. 4) we may determine suitable values as follows:

Diameter (wood propeller) 2 blades . . . . . 8.05 feet.

Diameter (metal propeller) 2 blades . . . . . 8.55 feet.

c) Determination of design  $v/nD$

$$\frac{v}{nD} = \frac{88 V}{ND} = 0.637.$$

d) Determination of maximum efficiency. From Fig. 11, for  $v/nD = 0.637$ ,  $\eta_{\max.} = 81$  per cent.

e) Determination of power available at sea level is made in Table 10, according to Form 2.

f) Determination of power available at altitudes.

(1) By precise method according to Form 3, and tabulated in Tables 11 and 12.

(2) By simplified method (short cut) using Fig. 14, and tabulated in Table 13. Factor for horsepower available at 10,000 feet is 0.68 and that for 15,000 feet is 0.535.

g) Curves of power available at sea level and at altitudes are then plotted as in Fig. 21.

TABLE 13.  
Power Available at 10,000—15,000 Ft.  
(Short-cut Method.)

1	2	3	4
$V$	HP av. Sea Level	HP av. 10,000 ft.	HP av. 15,000 ft.
57.2	180	122	100
70	217	148	116
80	243	165	130
90	267	182	143
100	292	199	156
110	311	212	166
120	329	224	176
130	341	232	182
142.4	352		

### *B. Power Available from Ratio of Thrust Power.*

a) The data required are the same as in the first method.

Engine power 435 horsepower at 2300 r.p.m., non-supercharged (see power curve, Fig. 20).

Propeller 2 blades, metal, direct drive.

b) Propeller efficiency assumed to equal 0.80 (first approximation).

Horsepower available (approximate)  $435 \times 0.80 = 348$ .

c) Determination of high speed (first approximation) from horsepower required curve and horsepower available; at 348 hp,

$$V = 145 \text{ m.p.h.}$$

d) Determination of propeller diameter: By substitution of values in II (13.1), we find  $D = 8.25$  feet

e) Determination of design  $v/nD$

$$\frac{88 V}{ND} = 0.673$$

- f) Determination of basic maximum efficiency (see Fig. 11) gives 0.817.  
 Tip speed =  $\pi \times 8.25 \times 2300/60 = 1,000$  feet per second.  
 Reduction due to tip speed 2 per cent.  
 Net efficiency  $0.817 - 0.02 = 0.797$ .
- g) Thrust horsepower available at design  $V = 145$  m.p.h.  
 Thrust horsepower available =  $435 \times 0.797 = 346$  hp  
 $V$  maximum (second approximation) from horsepower required curve = 145 m.p.h.
- h) Thrust horsepower available at sea level is derived in Table 8, from Fig. 15.
- i) Thrust horsepower available at altitudes is derived in Table 9, from Fig. 16.  
 Reduction factor for 10,000 feet is 0.66.  
 Reduction factor for 15,000 feet is 0.53.
- j) Curves of power available at sea level and at altitudes are then plotted as in Fig. 21.

**8. Performance.** The usual information given by performance estimates from power curves comprises (1) the high speed in level flight at sea level and altitudes, (2) rates of the best climb, (3) Corresponding climbing speeds at sea level and altitudes, (4) service and absolute ceilings.

FORM 6. *Summary of Performance 1.*

Power required (by summation), Table 6.

Power available at sea level (second method), Table 8.

Power available at altitude (second method), Table 9.

Altitude Feet	High Speed m.p.h.	Speed at Maximum Climb	Rate of Climb Feet per Min.	Time to Climb Min.	Angle of Climb Degrees
Sea level . . . . .	145	80	1390	0	11.3°
10,000 . . . . .	135.5	93.5	625	10.4	4.35°
15,000 . . . . .	126.5	99	314	22.4	2.05°
Serv. Ceiling 17,100 .	115	100	100	33.2	
Absol. Ceiling 18,500 .	100.5	100.5	0		0

$$\text{Angle of climb at sea level} = \frac{1390 \times 0.65}{80} = 11.3^\circ$$

$$\text{Angle of climb at 10,000} = \frac{625 \times 0.65}{93.5} = 4.35^\circ$$

$$\text{Angle of climb at 15,000} = \frac{314 \times 0.65}{99} = 2.05^\circ$$

$$\begin{aligned} \text{Time to climb to 10,000 ft.} &= 2.3 \frac{18,500}{1390} \times \log \frac{18,500}{8,500} = \\ &= 30.6 \times 0.337 = 10.3 \text{ min.} \end{aligned}$$

$$\text{Time to climb to 15,000 ft.} = 30.6 \times \log \frac{18,500}{3,500} = 30.6 \times 0.725 = 22.2 \text{ min.}$$

$$\text{Time to climb to Service Ceiling} = 30.6 \times \log \frac{18,500}{1,400} = 30.6 \times 1.12 = 33.2 \text{ min.}$$



FORM 6a. *Summary of Performance 2.*

Power required from Table 7.

Power available at sea level, Table 10.

Power available at altitude, Tables 11 and 12.

Altitude Feet	High Speed	Speed at Maximum Climb m.p.h.	Rate of Climb Feet per Min.	Time to Climb Min.	Angles of Climb Degrees
Sea level . . . . .	145.2	90	1240	0	8.95°
10,000 . . . . .	135	97.5	635	11.5	4.22°
15,000 . . . . .	126	100	270	24.5	1.69°
Serv. Ceiling 17,300 .	114.0		100	36.5	
Absol. Ceiling 18,600	101.5	101.5	0		0

$$\text{Angle of climb at sea level} = \frac{1240 \times 0.65}{90} = 8.95^\circ$$

$$\text{Angle of climb at 10,000} = \frac{635 \times 0.65}{97.5} = 4.22^\circ$$

$$\text{Angle of climb at 15,000} = \frac{270 \times 0.65}{100} = 1.69^\circ$$

$$\begin{aligned} \text{Time to climb to 10,000 ft.} &= 2.3 \frac{18,600}{1240} \times \log \frac{18,600}{8,600} = \\ &= 34.5 \times 0.334 = 11.5 \text{ min.} \end{aligned}$$

$$\text{Time to climb to 15,000 ft.} = 34.5 \times \log \frac{18,600}{3,600} = 34.5 \times 0.713 = 24.5 \text{ min.}$$

$$\text{Time to climb to Service Ceiling} = 34.5 \times \log \frac{18,600}{1,300} = 34.5 \times 1.155 = 39.9 \text{ min.}$$

The full throttle r.p.m. corresponding to the above data can be obtained directly from power curves or from curves obtained by plotting r.p.m. versus speeds on the power available at several altitudes. However, the r.p.m. are not often given in the estimates.

The actual estimates of performance are made from graphs of power required (6 A and 6 B) and power available (7 A and 7 B), calculations and plotting of which are made as previously indicated. In both of these methods the same general procedure in performance determination from graphs is employed.

The summaries of performance are tabulated in Forms 6 and 6a, corresponding to power required 6 A and power available 7 A, and power required 6 B and power available 7 B respectively.

Referring to Fig. 21 for illustration, the high speeds in level flight at full throttle at sea level and at altitudes are found at the right hand intersection of curves for required and available power corresponding to the same altitude. The abscissa of this point of intersection read on the speed scale gives the high speed at each corresponding altitude. For example, at sea level the high speed is 145 m.p.h.

The intersection, if any, of curves of power required and available at the same altitude on the left side gives the minimum possible horizontal speed with full throttle. This low speed is not always possible of realization in horizontal flight, especially at sea level, due to the inability of some airplanes to maintain sufficient lateral, longitudinal, or directional control, due to burbling of the wings. This speed is sometimes called the landing speed and may be somewhat lower than the minimum speed corresponding to maximum lift coefficient. In that case the additional lift necessary to reduce the speed below the *minimum* speed, as defined above, is furnished on one hand by the vertical component of the thrust and on the other hand by the effect of the slipstream on a portion of the wings, giving additional lift by the virtue of increased speed over that portion.

The best rate of climb is also determined from the curves of power required and available. The maximum difference between the value of power required and power available at the same speed is found by trial with a pair of dividers. This difference is called the maximum reserve power for a given altitude and it is this reserve power which permits the airplane to climb. Speeds corresponding to the maximum reserve power, and, therefore, to the best rate of climb, are the speeds at which the airplane climbs the fastest. However, these speeds are the true speeds and not the indicated speeds shown by the air speed indicator. The rates are calculated from the reserve power by (2.3).

In the example of Fig. 21, the rate of climb at sea level is

$$V \sin \theta = \frac{165 \times 33,000}{4000} = 1360 \text{ feet per minute.}$$

An absolute ceiling of 18,300 feet and a service ceiling of 16,550 feet are obtained by plotting and extrapolating the rate of climb on altitude curve to zero rate of climb. The absolute ceiling is the altitude where the rate of climb is zero, while the service ceiling is the altitude where the rate of climb is 100 feet per minute. Theoretically the absolute ceiling is never reached as it would take an infinite time to do so. The practical value (the service ceiling) can ordinarily be reached in about 45 minutes.

At the absolute ceiling, the high speed and the climbing speed reach the same value, which fact facilitates the extrapolation of high speed and climbing speed graphs near the ceiling.

In addition to the plot of Fig. 21, it is customary to plot the performance items against altitude as shown in Fig. 22.

For convenience the performance summary should also include the basic data on the airplane as follows:

Gross weight, weight, per sq. ft. of area, total area of the wings, the E.M.A.R., the equivalent flat plate area at high speed in sq. ft.,

the rated power and r.p.m. of the engine, the gear ratio, the altitude limit of the induction system, and the design speed, as well as the diameter, r.p.m., blade setting, make, and material of the propeller. It is assumed that the propeller is to absorb the rated power of the engine unless otherwise specified.

## CHAPTER IV BAIRSTOW'S METHOD

This pioneer method as developed by Bairstow (see Ref. 2) is based on the same fundamental principles as that discussed in detail in the preceding chapters. The method itself does not, however, deal with the various details for computing or estimating the power required or the power available, but assumes all such basic data in hand and ready for use directly in the performance calculations. Instead of computing and plotting the various quantities involved as functions of speed, use is made of the function  $\sigma^{1/2} v$  or  $\sigma^{1/2} V$  and to which the name of *indicated speed* is applied.

Attention is called to the following items of notation peculiar to the description of this method.

- $p$  = pitch of propeller
- $P_{B0}$  = brake power at sea level
- $P_{Bh}$  = brake power at altitude  $H$
- $f$  = altitude reduction factor for power =  $P_{Bh}/P_{B0}$

**1. General Outline of Method.** This method as given in the author's text requires or assumes as available the following:

1) Characteristic curves for the propeller, giving on the abscissa  $v/nD$  or  $v/np$  ( $p$  = pitch) the following:

$$\begin{aligned} \text{Torque coefficient } k_Q &= \frac{Q}{\rho n^2 D^5} = \frac{2\pi n Q}{2\pi \rho n^3 D^5} = \frac{550 P_{Bh}}{2\pi \rho n^3 D^5} \quad \text{or} \\ k_Q &= \frac{550 f P_{B0}}{2\pi D^5 \sigma \rho_0 n^3} = \frac{550}{2\pi D^5 \rho_0 (\sigma^{1/2} n)^2} \left( f \frac{P_{B0}}{n} \right) \quad (1.1) \end{aligned}$$

$$\text{Thrust coefficient } k_T = \frac{T}{\rho n^2 D^4} \quad (1.2)$$

Efficiency  $\eta$

2) For the plane a polar or equivalent data giving<sup>1</sup>:

$$\text{Lift coefficient } k_L = \frac{L}{\rho v^2 S} \quad (1.3)$$

$$\text{Drag coefficient } k_D = \frac{D}{\rho v^2 S} \quad (1.4)$$

3) Curves or equivalent data giving for the engine the relation at sea level between power and revolutions and at altitude the reduction

<sup>1</sup> It will be noted that the coefficients  $k_L$  and  $k_D$  are one half the values  $C_L$  and  $C_D$  used elsewhere in this work. Also it is clear that the  $D$  in the form for  $k_D$  means drag, while in the propeller coefficients  $k_T$  and  $k_Q$  it means diameter.

factor for the power, the revolutions being assumed the same, see Figs. 10 and 20.

By means of these coefficients and the usual assumption that, for small or moderate angles of climb we may take  $\cos \theta = 1$  and hence  $W = L$ , the basic equation of equilibrium in climbing flight

$$T = D + W \frac{v_c}{v} \quad [\text{see III (2.2)}]$$

may be put in the form<sup>1</sup>

$$k_T \left( \frac{v}{nD} \right)^{-2} \frac{D^2}{S} = k_D + k_L \frac{v_c}{v} \quad (1.5)$$

In the expression for lift coefficient (1.3), we put  $\rho = \sigma \rho_0$  and  $L = W$ , giving

$$k_L = \frac{W}{\rho_0 (\sigma^{1/2} v)^2 S} \quad (1.6)$$

The term  $\sigma^{1/2} v$  is called the indicated speed. It is the speed which, with the angle of attack required at altitude, would, at sea level, serve for the support of the weight  $W$ . It is less than the actual speed  $v$  at altitude in the ratio  $\sigma^{1/2}$ . Or otherwise, for the same angle of attack as at sea level and hence the same value of  $k_L$ , the speed at altitude for sustentation must be  $v_0/\sigma^{1/2}$ .

For speed in level flight,  $v_c$  in (1.5) will be zero and the first step is the assumption of a value of the indicated speed ( $\sigma^{1/2} v$ ), which from (1.6) gives a value of  $k_L$  and thence  $k_D$  from the polar of the plane. This serves in (1.5) to give a value of  $k_T (v/nD)^{-2}$  and by use of the factor  $p^2/D^2$ , a value of  $k_T (v/np)^{-2}$ .

From a curve of the values of  $k_T$  on  $v/nD$ , a curve of  $k_T (v/np)^{-2}$  on  $v/np$  is then found. The value of  $k_T (v/np)^{-2}$  found as above will then, with this curve, serve to determine  $v/np$  and  $k_T$ .

Likewise we have 
$$\sigma^{1/2} n = \frac{\sigma^{1/2} v \times n D}{D \times v} \quad (1.7)$$

Then with  $v/nD$  or  $v/np$  known, the value of  $k_Q$  is found from the curve of  $k_Q$  values; and thence from (1.1) and (1.7) the value of  $f P_{B0}/n = P_{Bh}/n$ .

Taken in this way with a specific value of  $\sigma^{1/2} v$ , it is seen that the values of  $\sigma^{1/2} n$  or  $\sigma^{1/2} N$  and of  $f P_{B0}/n$  do not in themselves, depend on  $\sigma$  or on altitude. That is, a series of values of  $\sigma^{1/2} v$ ,  $\sigma^{1/2} V$ ,  $\sigma^{1/2} n$ ,  $\sigma^{1/2} N$  and  $f P_{B0}/n$  or  $f P_{B0}/N$  will be independent of altitude directly, and hence one such set of values will serve for all altitudes. In particular the single curve of  $f P_{B0}/N$  on  $\sigma^{1/2} N$  is next plotted, as representing, in this form, the engine output power required for level flight.

The procedure for finding level speed at any specified altitude may best be followed by outlining the steps for any one altitude  $H$ . These are as follows: First from the engine data as above specified, the reduction

<sup>1</sup> In (1.5) on the left hand side,  $D$  is, of course, *diameter* and not *drag*.

factor  $f$  for the given altitude is found, thus giving for any specified value of  $N$  the relation noted above,

$$P_{Bh} = f P_{B0}$$

Then assume on trial a point on the curve of  $f P_{B0}/N$  on  $\sigma^{1/2}N$ . This will fix a value of  $\sigma^{1/2}N$  and hence the value of  $N$ . Then with this value of  $N$  and the suitable curve, find  $P_{B0}$  and thence with the value of  $f$  for the given altitude, find  $f P_{B0}$  and  $f P_{B0}/N$ . If this value agrees with that on the diagram, the point is correct and the value of  $N$  becomes known. If not, the usual method of trial and approach may be employed until a satisfactory agreement is obtained.

Otherwise and graphically, a value of  $N$  may be assumed and the value of  $\sigma^{1/2}N$  found. This and the computed value of  $f P_{B0}/N$  will determine a point on the diagram. If the point should fall on the curve, the estimate was correct. Otherwise two or three such points may be found lying on either side of the given curve, and a short curve through these points will give, at the intersection, the correct value of  $N$ .

A curve of  $\sigma^{1/2}V$  on  $\sigma^{1/2}N$  is then laid down, and from this curve the value of  $\sigma^{1/2}V$  is found and thence  $V$ .

**2. Speed of Climb.** For speed of climb, at any specified altitude  $H$ , the steps to be taken are as follows:

An air speed  $V$  or  $v$  is assumed at the specified altitude. This with the known characteristics of the plane will serve to determine  $k_D$  and  $k_L$  (again assuming  $L = W$ ).

Then from the engine data referred to previously, we may find, for an assumed value of  $N$ , the bhp at sea level and at altitude ( $P_{Bh}$ ). Next with this power output from the engine, we find from (1.1) the value of  $k_Q$  and thence from the diagram the value of  $v/n p$  and thence  $v$  and  $V$ .

A series of such values for an assumed series of values of  $N$  will furnish the data for curves giving for altitude  $H$ , the relation between  $v$  and  $N$  and between  $v$  and  $v/n D$  or  $v/n p$ . The basic propeller diagram will also give the values of  $k_T$  for any known value of  $k_Q$ . A series of such curves for a series of altitudes  $H$  will then give full data for the remaining steps.

With these curves and data, we may then, for any given value of  $H$ , determine the remaining term in (1.5) and thence the value of  $v_c$ . A series of such computations for an assumed series of values of the air speed are then plotted, giving thus the maximum rate for the given value of  $H$ .

Special features of the performance, such as the ceiling, stalling speed, time to climb to altitude, etc., develop from these basic curves and tables in the same general manner as with other methods, and need not be developed here in detail.

## CHAPTER V

### LESLEY-REID METHOD

**1. Introduction.** This method was developed by Professors Lesley and Reid, Ref. 12, and is intended to be a simplification and revision of the Bairstow method.

The method is formulated in non-dimensional coefficients and furnishes the same line of information as by the Bairstow method. Its accuracy is theoretically as high as that of any other method, but this, in common with all methods, depends on the accuracy of the original data relating to the airplane and propeller characteristics.

The method assumes that the lift and drag of the whole airplane are known throughout the flying range; it assumes also that the power, thrust and torque coefficients of the propeller and its efficiency at all values of  $v/nD$  within the flying range, are known, which of course presupposes that the propeller diameter, the setting of the blades, their form and other dimensional characteristics can be determined.

Since this method does not give the procedure for obtaining the airplane polar or the diameter and other characteristics of the propeller, these phases of the calculation must be performed according to procedures equivalent to those given in previous chapters.

Similarly to other systems of performance calculations, this method merely determines conditions for the equilibrium of acting forces in steady flight, either level or climbing.

The various items of airplane performance may be made to depend on a number of independent variables and among others on  $\sigma^{1/2}V$  and  $\sigma^{1/2}N$  as in the Bairstow method. However, the authors of the present method have made more effective use of these variables and through a somewhat different choice of coefficients and changes in the procedure, have succeeded in simplifying and shortening the Bairstow program of operations.

To the abstract quantity  $\sigma^{1/2}N$ , the name *indicated r.p.m.* is given after the analogy with  $\sigma^{1/2}V$  and its name *indicated air speed*.

**2. Data Required.** Data required before the application of this method can be made are as follows:

Wing area, gross weight, the polar of the whole airplane; a curve of brake horsepower versus r.p.m. at sea level, and the diameter and aerodynamic characteristics of the propeller. In particular the latter should include a diagram giving values of the coefficients  $C_T$ ,  $C_P$  (as defined below) plotted on  $v/nD$ .

*a) The Power Curve.* The power curve of the engine selected giving the full throttle sea level brake power against r.p.m. of the crankshaft is usually obtainable from the engine manufacturer. If the engine is

geared, a computation must be made to reduce crankshaft to propeller speed.

*b) Effect of Altitude on Power.* Many formulas based on various assumptions have been developed for the determination of variation of brake horsepower of engines with altitude, and any of them can be incorporated in this method of performance estimation. The authors recommend dependence of the altitude power on the temperature and pressure, where (for the same r.p.m.) we put

$$P_h = P_0 \times R_a \text{ (brake power)} \quad (2.1)$$

$$R_a = \frac{p_h}{p_0} \sqrt{\frac{T_0}{T_h}}$$

where  $p_h$  and  $p_0$  = barometric pressure at altitude  $h$  and at sea level.

$T_h$  and  $T_0$  = absolute temperature at altitude  $h$  and at sea level.

The terms  $p$  and  $T$  relate to the "standard atmosphere", values of which are tabulated in Table 4.

*c) Propeller Coefficients.* The following are well known non-dimensional coefficients relating to propeller performance.

$$\text{Thrust Coefficient: } C_T = \frac{T}{\rho v^2 D^2} \quad (2.2)$$

$$\text{Power Coefficient: } C_P = \frac{P}{\rho n^3 D^5} \quad (2.3)$$

where  $T$  = thrust

$P$  = power (brake)

$D$  = diameter

$v$  = speed

$n$  = revolutions

The units throughout are the foot, the pound and the second. If  $P$  is expressed in hp units, it must, of course, be multiplied by 550.

From these two coefficients we directly derive the relation

$$C_T = \frac{\eta C_P}{(v/n D)^3} \quad (2.4)$$

At sea level, where  $\rho = 0.00238$ , the power coefficient becomes:

$$C_P = \frac{231\,000 \text{ Brake hp}}{n^3 D^5} \quad (2.5)$$

For a given value of  $D$  the term  $231000/D^5$  is a constant and the

value becomes  $C_P = \frac{\text{Brake hp}}{n^3} \times \text{constant}$  (2.6)

**3. Description of Method. Level Flight.** The customary simplifications in performance computations are made as follows:

The thrust is assumed to be parallel to the flight path. Since there is no definite means of ascertaining the direction of the resultant thrust action of the propeller when its axis is inclined to the flight path and since the angle between this resultant and the flight path can be reasonably assumed to be small, neglect of the effect of this angle is justified.

The further assumption that lift equals weight ( $L = W$ ) is made for climbing flight as well as for horizontal. In climbing flight where the vertical component of the thrust carries a part of the weight, this assumption is not exact; but in the actual procedure, the resulting error, in comparison with the results of a more exact analysis, is found to be quite unimportant, especially for moderate angles of climb.

The fundamental equations for level flight are therefore:

$$L = W \quad \text{and} \quad T = D \quad (\text{drag}) \quad (3.1)$$

The coefficients for lift and drag are recalled as follows:

$$C_L = 2 \times \text{weight} \div \rho^2 v^2 S \quad (3.2)$$

$$C_D = 2 \times \text{Drag} \div \rho v^2 S \quad (3.3)$$

For  $C_L$  we then derive the value

$$C_L = \frac{2W}{\rho v^2 S} = \frac{2W}{\rho_0 \sigma v^2 S} = \frac{2W}{\rho_0 (\sigma^{1/2} v)^2 S} = \frac{391 W}{(\sigma^{1/2} V)^2 S} \quad (3.4)$$

Equating thrust from (2.2) and drag from (3.3), we find the following relation between the two coefficients:

$$C_T = \frac{C_D S}{2 D^2} \quad (3.5)$$

Referring now to the propeller diagram as noted in 2 it is seen that for any given value of  $C_T$ , the corresponding value of  $v/nD$  may be found.

It is now possible to combine the indicated air speed and the corresponding  $v/nD$  for the selected propeller of diameter  $D$  in the form:

$$\frac{\sigma^{1/2} v}{(v/nD) \times D} = \sigma^{1/2} n \quad (3.6)$$

and obtain thus an abstract but highly useful quantity which is a function of the propeller revolutions and of the relative density, *i. e.*, of the altitude. From the analogy of the form of this expression to the form of *indicated air speed*, the name selected for this function of propeller revolutions was *indicated r.p.s.* and from which we may find  $\sigma^{1/2} N$  the *indicated r.p.m.* The latter can be expressed as a function of the speed  $V$

$$\text{in the form:} \quad \sigma^{1/2} N = \frac{\sigma^{1/2} V (\text{m.p.h.}) \times 88}{(v/nD) \times D} \quad (3.7)$$

$\sigma^{1/2} N$  *Required.* Having established these formulae and assuming the needful data in hand, the first step in the calculation proper is to determine the values for a curve of required  $\sigma^{1/2} N$  on  $\sigma^{1/2} V$ . This will involve the use of (3.7), the propeller diagram, (3.5), the airplane polar and (3.4). The necessary steps may be outlined as follows:

- Assume a value of  $\sigma^{1/2} V$
- Find  $C_L$  from (3.4)
- Find  $C_D$  from Polar
- Find  $C_T$  from (3.5)
- Find  $v/nD$  from propeller diagram
- Find  $\sigma^{1/2} N$  from (3.7)



This procedure is repeated for a series of values of  $\sigma^{1/2} V$  covering the anticipated range, and the curve of  $\sigma^{1/2} N$  on  $\sigma^{1/2} V$  is then plotted.

It will be noted that this entire procedure is independent of density and therefore of altitude. Hence as noted in connection with Bairstow's method, a curve of  $\sigma^{1/2} N$  (required) on  $\sigma^{1/2} V$  is unique and holds for all altitudes.

$\sigma^{1/2} N$  Available. The indicated r.p.m. available for any indicated airspeed  $\sigma^{1/2} V$  is the maximum r.p.m. at which the engine can turn the propeller with the plane moving at the air speed  $V$ , multiplied by  $\sigma^{1/2}$ . While the indicated r.p.m. is represented by one curve for all altitudes, the available indicated r.p.m. is represented by a curve for each altitude. The labor of computation, however, may be greatly reduced by taking note of the following relation.

If we write (2.3), once for sea level and once for altitude  $h$  and divide one by the other, we shall have (assuming  $n$  the same):

$$\frac{C_{Ph}}{C_{P0}} = \frac{P_{ah}}{P_{a0}} \cdot \frac{\rho_0}{\rho_h}$$

But the value of  $P_{ah}/P_{a0}$  is expressed by the symbol  $R_a$  in (2.1) and  $\rho_0/\rho_h = 1/\sigma$ . Hence

$$C_{ph} = \frac{R_a C_{P0}}{\sigma} \quad (3.8)$$

The first step is therefore the preparation of a table of values for sea level. To this end the procedure is outlined as follows:

Assume a value of  $N$

Find  $P_{a0}$  from a curve such as that of Fig. 20

Find  $C_P$  by (2.3) or (2.6)

Find  $v/nD$  from propeller diagram

Find  $V$  from (3.7)

A series of such values will then give the curve of available  $N$  on  $V$  for sea level conditions where  $\sigma = 1$ . It is advisable to extend the table for this condition to smaller values of  $N$  than those which will directly apply to sea level flight, this for the reason that such values will be required for the determination of the curves for altitude.

Then with these results in hand the procedure for any given altitude is as follows:

Assume a value of  $N$  (one of the values in the preceding table)

Find  $\sigma^{1/2} N$

Find  $C_P$  by (3.8)

Find  $v/nD$  from propeller diagram

Find  $\sigma^{1/2} V$  by (3.7)

Then plot as before. This will give a series of curves of available  $\sigma^{1/2} N$ , one for each altitude selected.

*High Speed.* The high speed in level flight is determined by the right hand point of intersection of the curve of required  $\sigma^{1/2}N$  with that of available  $\sigma^{1/2}N$  at full throttle, both plotted on  $\sigma^{1/2}V$ . True speeds and actual r.p.m. are obtained by dividing the values indicated on the graph by values of  $\sigma^{1/2}$  corresponding to the altitudes for which the available  $\sigma^{1/2}N$  are plotted.

*Minimum Speed.* Similarly, minimum speed in level flight full throttle is determined by the left hand intersection of the indicated r.p.m. required and indicated r.p.m. available curves. Usually, at sea level and low altitude these two curves do not intersect, in which case the minimum speed is that corresponding to the maximum lift coefficient and in order to maintain horizontal flight it is necessary to throttle the engine to the indicated r.p.m. required. If full throttle r.p.m. denoted by the indicated r.p.m. available is maintained, the airplane will climb.

*Climb and Ceilings.* The formulas required are developed as follows. The conditions of equilibrium in climbing flight give

$$T = D + W \sin \theta = D + W \frac{V_c}{V} \quad [\text{see III (2.2)}]$$

where  $V_c$  = speed of climb.

Putting  $L$  for  $W$ , in accordance with the assumption of 3, expressing  $T$ ,  $D$  and  $L$  in terms of the coefficients  $C_T$ ,  $C_D$ ,  $C_L$  and then dividing through by  $\rho v^2 S/2$ , we find

$$\sin \theta = \frac{V_c}{V} = \frac{2 C_T D^2/S - C_D}{C_L} \quad (3.9)$$

$$\text{Then} \quad V_{cfm} \text{ (ft. per mt.)} = 88 \left( \frac{V_c}{V} \right) \frac{\sigma^{1/2} V}{\sigma^{1/2}} \quad (3.10)$$

The procedure to be followed for any given altitude is outlined as follows:

Assume a value of  $\sigma^{1/2}V$

Find  $\sigma^{1/2}N$  from curves for available  $\sigma^{1/2}N$ , Level Flight (Fig. 25)

Find  $v/nD$  by (3.7)

Find  $C_T$  from propeller diagram

Find  $C_L$  and  $C_D$  from Table 15.

Find  $\sin \theta = V_c/V$  by (3.9) and thence  $V_{cfm}$  by (3.10)

A series of such values for the given altitude will then give a curve from which the maximum speed of climb may be determined, as in other methods.

**4. Example of Performance Calculations.** To illustrate the Lesley-Reid method, the airplane used to illustrate the method of Chapters I, II, III, will be used.

**Data.** The polar of the whole airplane is taken from Fig. 19, and Table 7.

The propeller diameter of 8.55 feet is determined by any appropriate method (see Ref. 4).

TABLE 14. Determination of Propeller Characteristics.

1	2	3	4	5	6	7	8	9	10	11	12
$V$	% des. $V$	% des. $N$	$N$ r.p.m.	BHP	$N$ r.p.s.	$v/nD$	% des. $v/nD$	% des. $\eta_{\max}$	$\eta$	$C_P$	$C_T$
57.2	40.2	87	2000	396.5	33.3	.295	46.3	56.0	.454	.0543	.960
70	49.2	87.1	2004	397	33.4	.360	56.5	67.5	.547	.0539	.632
80	56.2	87.8	2020	400	33.7	.408	64.0	75.5	.612	.0529	.477
90	63.2	88.7	2040	401	34.0	.455	71.4	82.5	.668	.0516	.366
100	70.2	89.8	2065	408	34.4	.498	78.2	88.5	.717	.0507	.295
110	77.2	91.5	2105	412	35.1	.538	84.4	93.5	.757	.0482	.235
120	84.2	93.8	2160	420	36.0	.572	89.8	96.8	.784	.0455	.191
130	91.3	96	2210	426	36.8	.606	95.1	99	.802	.0432	.156
145.2	100	100	2300	435	38.3	.637	100	100	.810	.0392	.123

Des.  $V = 145.2$ , Des.  $v/nD = .637$ ,  $D = 8.55$  Ft., Des.  $N = 2300$ ,  
BHP rated = 435,  $\eta_{\max} = 81\%$

Plotted on Fig. 24.

Tabulation of the data may be made as in Table 14 and the plotting of  $C_P$  and  $C_T$  against  $v/nD$  is shown in Fig. 24.

Otherwise and if such data are available, the values of  $C_T$ ,  $C_P$  and  $\eta$  may be taken directly from a diagram giving results of a model propeller test.

The engine power curve used is that of Fig. 20.

*Indicated R.P.M. Required.* Determination of indicated r.p.m. required for level flight is made according to the method explained in 3

TABLE 15.  
Indicated r.p.m. Required for Level Flight.

1	2	3	4	5	6
$\sqrt{\sigma} V$	$C_L$	$C_D$	$C_T$	$v/nD$	$\sqrt{\sigma} N$
57.2	1.37	.2348	.562	.382	1540
70	.915	.1104	.264	.518	1390
80	.701	.0813	.195	.573	1436
90	.555	.0667	.160	.600	1544
100	.449	.0588	.141	.620	1660
110	.370	.0544	.131	.630	1796
120	.311	.0512	.123	.638	1935
130	.265	.0491	.118	.642	2085
145.2	.215	.0472	.113	.648	2305

$$C_T = \frac{C_D S}{2 D^2} = \frac{C_D \times 350}{2 \times 8.55^2} = 2.393 C_D$$

$$\begin{aligned} \sqrt{\sigma} N &= \frac{\sqrt{\sigma} V \times 88}{v/nD \times D} = \frac{\sqrt{\sigma} V \times 88}{v/nD \times 8.55} = \\ &= 10.29 \frac{\sqrt{\sigma} V}{v/nD} \end{aligned}$$

Plotted on Fig. 25.

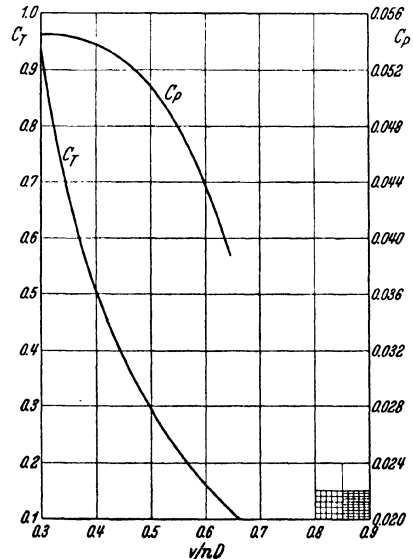


Fig. 24. Propeller coefficients plotted on  $v/nD$ .

and the values arranged as in Table 15. Substitution of numerical values in (3.4), (3.5) and (3.7) then gives,

$$C_L = \frac{4470}{(\sigma^{1/2} V)^2}$$
$$C_T = 2.39 C_D$$
$$\sqrt{\sigma} N = 10.3 \frac{\sqrt{\sigma} V}{v/n D}$$

The plot of  $\sqrt{\sigma} N$  required against  $\sqrt{\sigma} V$  at sea level is shown in Fig. 25.

*Indicated R.P.M. Available.* For the determination of indicated r.p.m. available at sea level full throttle, the power curve of Fig. 20 and the following formulas are used. From the value of  $C_P$  [see (2.3)] with  $\rho$  for sea level (0.00238) and  $D = 8.55$  we have

$$C_P = \frac{1,092,500 P}{N^3} \text{ (P in hp units)}$$

Also from (3.7)

$$\sqrt{\sigma} V \text{ (m.p.h.)} = \frac{\sqrt{\sigma} N (v/n D) D}{88} = 0.09715 \sqrt{\sigma} N (v/n D)$$

Values of  $v/n D$  versus  $C_P$  are found in Fig. 24. Tabulation of the above values is shown in Table 16, and graphic presentation of indicated r.p.m. available at sea level in Fig. 25.

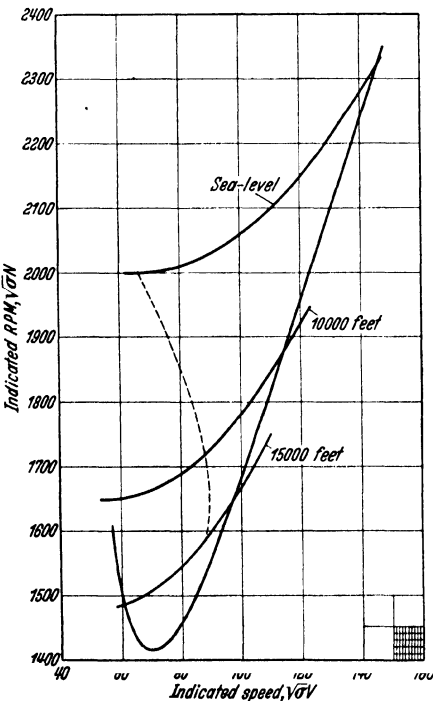


Fig. 25. Performance curves.

TABLE 16. Indicated r.p.m.  
Available at Sea Level  $\sigma = 1.0$ .

1	2	3	4	5	6
N from power curve	BHP from power curve	r.p.s. $\sqrt{\sigma} n$	$C_P$	$v/n D$	$V$
2000	396.5	33.33	.0543	.345	67.2
2020	400	33.69	.0530	.432	84.8
2050	405	34.17	.0514	.488	97.2
2100	413	35.00	.0487	.540	110.2
2150	420	35.82	.0463	.572	119.6
2200	426	36.67	.0436	.603	129.0
2250	431	37.50	.0414	.622	136.0
2300	435	38.33	.0392	.637	142.5

$$\sqrt{\sigma} n = \frac{N}{60}$$
$$C_P = \frac{\text{BHP} \times 231000}{(\text{r.p.s.})^3 \times D^5} =$$
$$= \frac{\text{BHP} \times 231000}{(\text{r.p.s.})^3 \times 45680} = 5.057 \frac{\text{BHP}}{(\text{r.p.s.})^3}$$
$$\sqrt{\sigma} V = \sqrt{\sigma} N \times \frac{v}{n D} \times \frac{D}{88} =$$
$$= 0.09715 \sqrt{\sigma} N (v/n D)$$

Plotted on Fig. 25.

For the determination of indicated r.p.m. available at altitude, the density ratio at 10,000 and 15,000 feet is found from Table 4. The altitude power factor  $R$  at constant r.p.m. is found in Fig. 10. Ratios  $R$  are calculated as follows:

At altitude 10,000 ft.,  $\sigma = 0.737$ ;  $R = 0.675$ ;  $R/\sigma = 0.916$

At altitude 15,000 ft.,  $\sigma = 0.629$ ;  $R = 0.540$ ;  $R/\sigma = 0.859$

The sequence in computing is shown in Table 17 for 10,000 feet and in Table 18 for 15,000 feet altitude. Values are then plotted in Fig. 25.

TABLE 17. Indicated r.p.m. Available at 10,000 Ft.

$\sqrt{\sigma} = .8585$ ,  $\sigma = .737$ ,  $R = .675$ ,  $R/\sigma = .916$ .

1	2	3	4	5	6	7	8
$N$	BHP	$\sqrt{\sigma} N$	$CP$	$CP$ (alt)	$v/nD$	$\sqrt{\sigma} V$	$V$ true
1925	383	1653	.0582	.0533	.425	68.3	78.6
1950	387	1674	.0572	.0524	.460	74.8	87.1
2000	396.5	1716	.0543	.0497	.524	87.5	102.0
2050	405	1760	.0514	.0471	.562	96.2	112.0
2100	413	1803	.0487	.0446	.592	103.8	121.0
2150	420	1845	.0463	.0424	.615	110.4	128.5
2200	426	1888	.0436	.0399	.635	116.6	135.8
2250	431	1930	.0414	.0379			

$$CP(\text{alt}) = CP_0 \times \frac{R}{\sigma} = \frac{\text{BHP} \times 231\,000}{(\text{r.p.s.})^3 \times D^5} \times \frac{R}{\sigma} = 5.057 \times \frac{\text{BHP}}{(\text{r.p.s.})^3} \times \frac{R}{\sigma}$$

$$\sqrt{\sigma} V = .09715 \times \sqrt{\sigma} N \times \frac{v}{nD}$$

$$V = \frac{\sqrt{\sigma} V}{\sqrt{\sigma}}$$

Plotted on Fig. 25.

TABLE 18. Indicated r.p.m. Available at 15,000 Ft.

$\sqrt{\sigma} = .7931$ ,  $\sigma = .629$ ,  $R = .540$ ,  $R/\sigma = .859$ .

1	2	3	4	5	6	7	8
$N$	BHP	$\sqrt{\sigma} N$	$CP_0$	$CP$ (alt)	$v/nD$	$\sqrt{\sigma} V$	$V$ true
1875	373	1486	.0620	.0533	.425	61.4	77.4
1900	378	1506	.0603	.0518	.478	70.0	88.3
2000	396.5	1586	.0543	.0466	.568	87.6	110.5
2100	413	1665	.0487	.0418	.620	100.3	126.4
2150	420	1705	.0463	.0398	.635	105.3	133.0
2200	426	1745	.0436				
2250	431	1785	.0414				
2300	435	1825	.0392				

Plotted on Fig. 25.

*Climb and Ceilings.* Determination of rates of climb at sea level and at altitudes is made by tabulation of the different values as shown in Table 19. Graphic presentation of the rates of climb at different indicated speeds is made in Fig. 26.

TABLE 19. Determination of Rates of Climb at Various Speeds and Altitudes.

	1	2	3	4	5	6	7	8	9	10
	$\sqrt{\sigma} V$	$\sqrt{\sigma} N$	$v/nD$	$C_T$	$C_L$	$C_D$	$\frac{(2C_T D^2)}{S}$	Col. 7— $C_D$	$\frac{V_c}{V}$	Rate $V_{c/m}$ Ft./Min.
Sea Level	80	2012	.409	.485	.698	.0830	.2028	.1198	.1717	1210
	90	2031	.456	.372	.552	.0713	.1555	.0842	.1525	1208
	100	2058	.500	.292	.447	.0628	.1221	.0603	.1350	1188
	110	2100	.539	.233	.369	.0575	.0974	.0399	.1081	1047
10,000	70	1664	.433	.422	.912	.1153	.1764	.0611	.0670	480
	80	1689	.488	.313	.698	.0830	.1308	.0478	.0685	561
	90	1728	.536	.238	.552	.0713	.0995	.0282	.0511	472
15,000	70	1508	.478	.330	.912	.1153	.1379	.0226	.0248	193
	80	1545	.533	.242	.698	.0830	.1012	.0182	.0261	232
	90	1600	.578	.192	.552	.0710	.0803	.0093	.0116	116

$$C_L = \frac{2W}{\sigma \rho_0 v^2 S} = \frac{2 \times 4000}{.00238 \times 1.466^2 \times 350} \times \frac{1}{(\sqrt{\sigma} V)^2} = \frac{4470}{\sigma V^2}$$

$$\frac{2C_T D^2}{S} = .418 C_T \quad \frac{V_c}{V} = \frac{2C_T D^2/S - C_D}{C_L}, \quad V_{c/m} = \frac{V_c}{V} \times \frac{\sqrt{\sigma} V \times 88}{\sqrt{\sigma}}$$

Plotted on Fig. 26.

Best rates of climb are defined by the peaks of the rate curves in Fig. 26 and are represented by a line connecting the peaks and extrapolated to the zero rate. From the indicated speeds located on this line the indicated r.p.m. for selected altitudes can be found on curves of indicated r.p.m. available as plotted in Fig. 25.

TABLE 20. Summary of Performance.

		Ceiling			Service 15,900	Absolute 18,800
		Sea level	@ 10,000 ft.	@ 15,000 ft.		
High Speed	Speed Indicated . .	145.5	114.5	96.5	92	79
	Speed True . . . .	145.5	134	121	118	106.5
	r.p.m. Indicated . .	2320	1885	1645	1590	1460
	r.p.m. Actual . . .	2320	2198	2070	2035	1930
	Best Rate of Climb	1200	415	140	100	0
	Speed Indicated . .	93	80	79.5	79	83
	Speed True . . . .	93	93.5	100	101.5	106.5
	r.p.m. Indicated . .	2040	1690	1540	1515	1510
	r.p.m. Actual . . .	2040	1970	1940	1937	1930

Plotting best rates against altitudes as shown in Fig. 26 and extrapolating to zero climb, the absolute ceiling of 18,000 feet and the service ceiling of 15,900 are determined.

### Summary of Performance.

In Fig. 27 the following performance curves, in addition to the above, are plotted on altitude:

High speeds from Fig. 25, climbing speeds and best rates of climb from Fig. 26, r.p.m. for high speeds from Fig. 25, r.p.m. for best climb from Figs. 25 and 26.

Extrapolating all the above curves to the absolute ceiling the performance at the service and absolute ceilings is determined and the entire summary presented in Table 20.

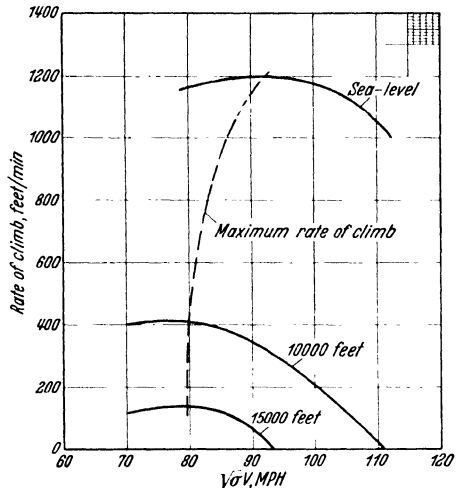


Fig. 26. Performance curves.

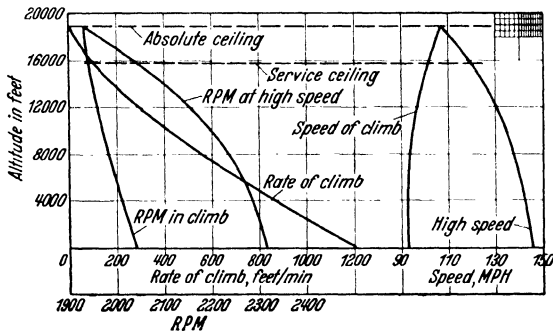


Fig. 27. Performance curves.

## CHAPTER VI

### THE OSWALD METHOD<sup>1</sup>

One of the most successful graphical methods of estimating performance is that developed at the California Institute of Technology by Mr. W. Bailey Oswald. Use of this method requires few actual computations and, if proper assumptions are made for certain values characterizing each individual airplane, the results are in good agreement with those of the best methods treated in previous chapters. The main advantage of this method is the rapidity with which it can be applied. Special charts

<sup>1</sup> OSWALD, W. BAILEY, General Formulas and Charts for the Calculation of Airplane Performance, U.S. N.A.C.A. Report No 408, 1932.

are however required for use with supercharged engines or with variable pitch propellers<sup>1</sup>. Also careful consideration must be given to the meaning of the different parameters in the case of multiple engines.

The method covers the determination of high speed, rate of climb with corresponding speeds, time to climb to different altitudes, and absolute ceiling.

**1. Parameters.** The Oswald performance estimates are made with the aid of a series of charts representing graphically the usual calculations for each individual case. The graphs are so arranged that the basic characteristic values for any airplane can be used either directly, or for the purpose of determining auxiliary values from which performance graphs can be obtained.

The basic characteristic values or parameters are the effective span loading ( $l_s$ ), the effective parasite loading ( $l_p$ ) and the thrust power loading ( $l_t$ ). These are defined as follows:

$$l_s = \frac{W}{e(Kb)^2} \quad (1.1)$$

In this expression  $W$  is the gross weight,  $b$  the span, and  $K$  the factor for the equivalent monoplane span as in II 3.  $Kb$  is therefore the equivalent monoplane span. The factor  $e$  is called the *airplane efficiency factor* and is a special coefficient introduced to take account of the cleanness of design having in view not only low drag at high speed, but also a good lift-drag ratio at climbing attitudes. The effect of an erroneous assumption of  $e$  is mostly noticeable in the determination of climb and ceiling. Due to the lack of a better definition,  $e$  might be considered a correction factor to the theoretical performance estimate in order to bring a check with flight tests. Actually  $e$  is introduced to account for the variation of parasite drag with angle of attack. It is assumed that this variation is some function of  $C_L^2$  and is therefore included in the expression for induced drag. For suggestions regarding actual values for  $e$ , see Table 23.

The parameter  $l_p$  has the value

$$l_p = \frac{W}{f} \quad (1.2)$$

where  $W$  is the gross weight and  $f$  is the sum of the equivalent flat plate area for the structure and for the profile drag of the wings at high speed. This parameter is therefore the effective parasite loading.

The parameter  $l_t$  has the value

$$l_t = \frac{W}{(\eta \text{ BHP})_{m x}} \quad (1.3)$$

This defines the ratio of the weight  $W$  to the available thrust power at high speed

$$l_w = \text{wing loading} = \frac{W}{S}$$

<sup>1</sup> See Ref. 20.



This parameter is used only in the determination of landing speed and of speed ratio.

In addition to these basic parameters, it is found convenient to make use of a combination parameter  $L$  defined as follows:

$$L = \frac{l_s l_t^{4/3}}{l_p^{1/3}} \quad (1.4)$$

Most of the performance items are plotted graphically as functions of  $L$ .

A further parameter having special relation to the propeller is defined as follows:

$$C_s = \frac{0.638 V}{(\text{BHP})^{1/5} N^{2/5}} \quad (1.5)$$

where  $V$  is speed in m.p.h.

$N$  is r.p.m.

It thus appears that some of the parameters can be obtained directly from the basic data of the airplane, some are computed, and those whose computations are more laborious are found with the aid of graphs. The compound parameters  $L$  and  $C_s$  are found on graphs.

**2. Assumptions.** The assumptions involved are in general the theoretical interpretations of the mechanics of flight and in this respect do not differ from others used in performance calculations. The accuracy of the assumptions determines the value of the performance estimate, and the result depends to a large extent upon the experience and discretion of the computer in making assumptions and applying them to the method.

Of primary importance for any successful estimate of performance is the correct assumption of the equivalent flat plate area  $A$ . Similarly the estimate of the value of minimum profile drag must be correctly made. To that end wind tunnel data on airfoils must be resorted to. Unfortunately these data obtained on small models are not entirely reliable when applied to full size airfoils and effort is being made at present to check the wind tunnel results against full flight test results in order to determine a suitable correction for the discrepancies due to scale effect, fuselage and wing interference, and slipstream effect. The standardization of profile drag for the most commonly used airfoils is thus being attempted.

The sum of the structural flat plate area  $A$ , and the wing profile drag reduced to the same terms, is denoted by a quantity  $f$ , which is the most influential factor on high speed. As previously stated, in the determination of rate of climb and ceiling, the factor  $e$  is of great importance.

The method itself does not consider the necessary increase of the wing lift due to the down load on the stabilizer, and the lift is considered equal to the gross weight. However, for high speed there is a correction graph which takes the stabilizer load into consideration, the assumption being made that the thrust axis is horizontal and that therefore no vertical

thrust component exists. In climb, the assumption is made that the vertical component of thrust is compensated by the down load on the stabilizer, and therefore no correction for either is made.

Referring to the engine propeller unit, the charts developed apply generally to all airplanes equipped with fixed metal propellers and modern motors with rated brake horsepower at (or at less than) 80 per cent r.p.m. of peak brake horsepower actually developed. The accuracy of the charts depends almost entirely upon the accuracy with which any general propeller and thrust horsepower data represent the engine-propeller unit.

It has been established from flight tests on the most modern airplanes equipped with present day engines, that the decrease in power and r.p.m. at altitudes is not as great as the accepted and used data would indicate. For that reason the graphs dealing with performance at altitude have been revised and are at a slight variance from those originally developed by the author of this method.

In order to express the variation of thrust horsepower with altitude and speed, use is made of certain ratios developed as follows:

$P$  will denote in general thrust horsepower.

The subscript 0 will denote in general, quantities at sea level and letters without altitude subscript, those at any specified altitude.

The subscripts  $mx$  and  $mn$  will denote respectively, maximum and minimum.

We may then have expressions such as the following.

$P_{a0v}$  = Thrust power available at sea level and at speed  $V$ .

$P_{av}$  = Thrust power available at altitude and at speed  $V$ .

$P_{a0v_{mx}}$  = Thrust power available at sea level and at speed  $V_{mx}$ .

We then define the following ratios,

$$T_H = \frac{P_a}{P_{a0}} \quad (2.1)$$

The ratio  $T_H$  implies the same speed in each case

$$T_V = \frac{P_{av}}{P_{av_{mx}}} \quad (2.2)$$

The ratio  $T_V$  implies the same level in each case

$$R_V = \frac{V}{V_{0\ mx}} \quad (2.3)$$

**3. Theory.** The following is a resumé of theoretical considerations underlying the development of this method. No attempt will be made to give a complete derivation of the formulae, which in many cases are of a somewhat complicated nature. The solutions of the formulae are represented by graphs. Only the basic theory and assumptions will be presented, for in this way it is felt that a clearer picture of the results obtained may be had.

The fundamental equation governing the airplane performance in climb is  $\frac{dh}{dt} = \frac{550(P_a - P_r)}{W}$  (3.1)

where  $\frac{dh}{dt}$  = rate of change in altitude.

$W$  = gross weight of the airplane.

$P_a$  = thrust horsepower available.

$P_r$  = thrust horsepower required (air-resistance)

For convenience put

$$w_r = 550 \frac{P_a}{W} = \text{rising speed.}$$

$$w_s = 550 \frac{P_r}{W} = \text{sinking speed.}$$

Then (3.1) becomes:

$$\frac{dh}{dt} = w_r - w_s \quad (3.2)$$

Through multiplication by a pair of unity factors and a rearrangement of the parts of the resulting expression (remembering that  $P_{a0} V_{mx}$  is the same as  $\eta \text{ bhp}_{mx}$ ), the value of  $w_r$  may be expressed as follows:

$$w_r = \frac{550 P_a V}{W} \cdot \frac{P_{a0} V}{P_{a0} V} \cdot \frac{P_{a0} V_{mx}}{P_{a0} V_{mx}}$$

$$\text{or} \quad w_r = \frac{550}{W} \cdot \frac{P_a V}{P_{a0} V} \cdot \frac{P_{a0} V}{P_{a0} V_{mx}} (\eta \text{ bhp})_{mx}$$

Then from (1.3), (2.1), (2.2)

$$w_r = 550 \frac{T_H T_V}{l_t} \quad (3.3)$$

For modern motors with fixed pitch metal propellers, it has been found that we may put, approximately,

$$T_H = \frac{\sigma - 0.165}{0.835} \quad (3.4)$$

$$\text{where } \sigma \text{ is the relative density} = \frac{\rho}{\rho_0} = \frac{\rho}{.00238} \quad (3.5)$$

and

$$T_V = (R_V)^m \quad (3.6)$$

where the exponent  $m$  is a function of the propeller design characteristics with suggested values as follows in terms of the parameter  $C_s$

$$m = .65 - \frac{C_s - 0.9}{7} \quad (3.7)$$

again we have

$$w_s = \frac{550 P_r}{W} = \frac{D v}{W} \quad (3.8)$$

where  $D$  = drag

$v$  = velocity in f.s.

But  $D = D_p + D_i$

where  $D_p$  = parasite drag (including profile drag)

$D_i$  = induced drag.

Let  $f$  be the equivalent flat plate area representing the sum of the structural drag and the wing profile drag. Then without further correction for variation of parasite drag with angle of attack we should have

$$D_p = 1.28 \frac{\rho v^2 f}{2} = 0.64 \rho v^2 f$$

where 1.28 is the flat plate coefficient.

There is, however, an effect due to change of angle of attack and the well known expression for induced drag with elliptical wing distribution [see I (2.4)] will not hold for the more general case. It is found possible to include both of these corrections by introducing a factor into the expression for induced drag in the form of a multiplier  $e$  for the equivalent monoplane aspect ratio  $(Kb)^2/S$ . This gives for the induced drag the value

$$D_i = \frac{2 W^2}{\pi \rho v^2 e (Kb)^2} \quad (3.9)$$

This factor  $e$  is the *airplane efficiency* factor previously referred to.

TABLE 21.

Type of Airplane	Values of $e$ Varying with "Cleanness"
Flying wing . . . . .	0.95—1.00
Cantilever Monoplane . . .	0.85—1.00
Semi-cantilever Monoplane .	0.80—0.95
Single Bay Biplane . . . .	0.75—0.95
Multiple Bay Biplane . . .	0.70—0.90

The author's suggested values for  $e$  as given with respect to the type of airplane are contained in Table 21.

Airplanes with normal amount of fairing and cowling correspond to the mean values of  $e$ .

Airplanes with square fuselages, rectangular wings, little fairing, etc., correspond to the lower values of  $e$ .

Airplanes with exceptionally well streamlined fuselages, elliptical wings and careful streamlining of projections correspond to the upper values of  $e$ .

The flight test checks on the determination of factor  $e$  show that the behaviour of the engine power at altitude plays an important part in the effect of  $e$  on calculated performance. Higher values of  $e$  should be used for airplanes with engines having smaller decrease in the power at altitudes.

The value of the term  $w_s$  thus becomes

$$w_s = 0.64 \frac{\rho f}{W} v^3 + \frac{2 W}{\pi \rho e (Kb)^2} \cdot \frac{1}{v} \quad (3.10)$$

Making use of (1.1) and (1.2) and putting in numerical values for  $\rho_0$  the value of  $w_s$  becomes

$$w_s = 0.001522 \frac{\sigma}{l_p} v^3 + 267.7 \frac{l_s}{\sigma} \cdot \frac{1}{v} \quad (3.11)$$

Putting these values of  $w_r$  and  $w_s$  in (3.2) the expression for the rate of climb becomes:

$$\frac{dh}{dt} = 550 \frac{(\sigma - 0.165)(R_V)^m}{0.835 l_t} - .001522 \frac{\sigma}{l_p} v^3 - 267.7 \frac{l_s}{\sigma} \frac{1}{v} \quad (3.12)$$

This is the fundamental equation for rate of climb, speed of climb and ceiling calculations.

**4. Charts.** The charts upon which this method are based are graphical partial solutions of the calculations involved in computing the different phases of performance. The advantage of such a system is evident, since most of the time necessary to arrive at results is consumed in application of the different formulas and in tabulating step by step the

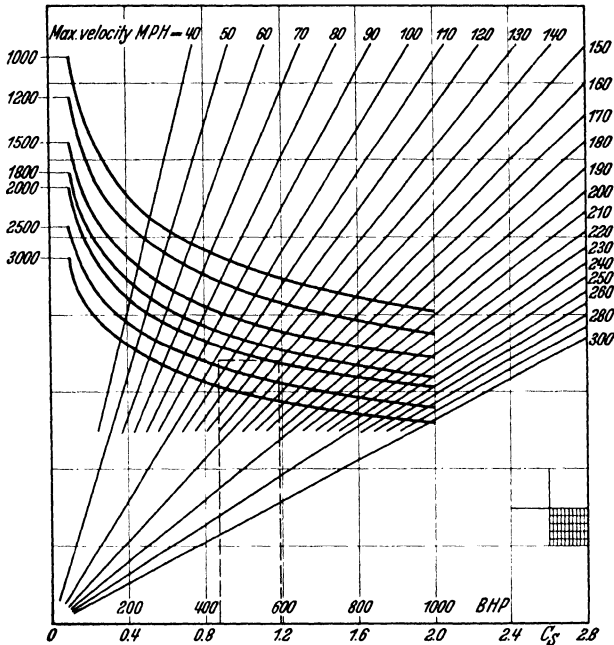


Fig. 28. Graphical chart of coefficient  $C_s$ .

resulting values computed. Most of these manipulations are repetitions of some procedure by substituting different values for each individual case. Since the accuracy of performance estimates are much more subject to the correctness of the assumptions than to the degree of arithmetical precision, the solution by interpolating on accurately traced graphs, is at least of as high a degree of accuracy as the assumptions made. However, for practical purposes the magnitude of the scales used should be sufficient to insure reasonable facility and accuracy in the interpolation and reading of the different values.

Fig. 28 gives a graphical determination of the coefficient  $C_s$ . This coefficient expresses the conditions of the engine-propeller unit at

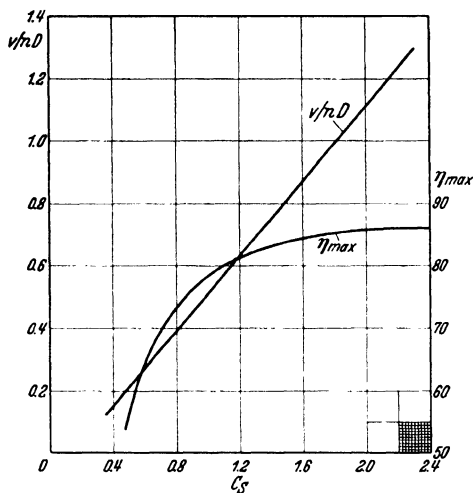
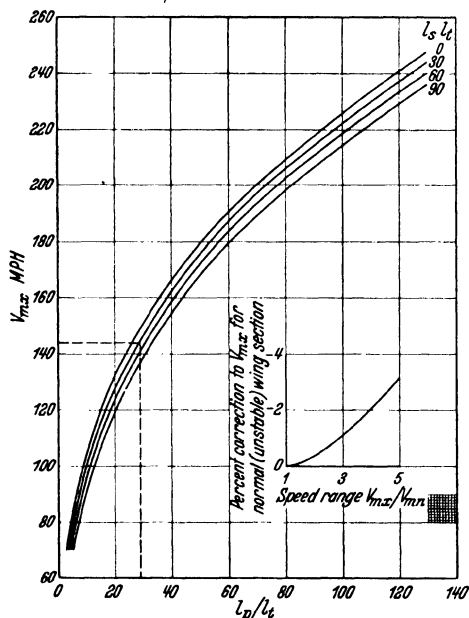


Fig. 29.

Fig. 30. Maximum velocity as a function of  $l_p/l_t$ .

maximum speed. Its determination requires an estimate, to a first approximation, of the high speed, the rated power of the engine and corresponding r.p.m. of the propeller. Fig. 28 is a plot of the equation,

$$C_s = \frac{0.638 V}{(\text{bhp})^{1/5} (\text{r.p.m.})^{2/5}}$$

For a graphical solution for  $C_s$ , first find the intersection of the bhp line with the propeller r.p.m. curve; second, draw a horizontal line through this intersection until it meets the line of speed; third, draw a vertical line through the last intersection and extend to the scale of  $C_s$ , the value of which is sought.

Fig. 29 shows the maximum efficiencies of propellers designed for a compromise of high speed and the best rate of climb, together with the corresponding  $v/nD$ , plotted against the values of  $C_s$  determined from Fig. 28. They were obtained as average values for metal propellers of good design.

Fig. 30 is for the determination of maximum speed. The conditions for level flight and maximum speed are as follows:

$$\frac{dh}{dt} = 0$$

$$\sigma = 1$$

$$(R_V)^m = 1$$

Substituting these values and putting  $1.467 V$  for  $v$  in order to express speed in miles per hour, we may put (3.12) in the form:

$$V_{mx} = 48.6 \left( \frac{l_p}{l_t} \right)^{1/3} \left( 1 - 0.332 \frac{l_s l_t}{V_{mx}} \right)^{1/3} \quad (4.1)$$

In Fig. 30,  $V_{mx}$  is plotted against  $(l_p/l_t)^{1/3}$  for different values of  $l_s/l_t$ .

The above procedure however, does not take into account the down-load on the tail necessary to balance the wing moments nor the consequent increase of lift which must be furnished by the wing at the expense of increased drag which reduces the high speed.

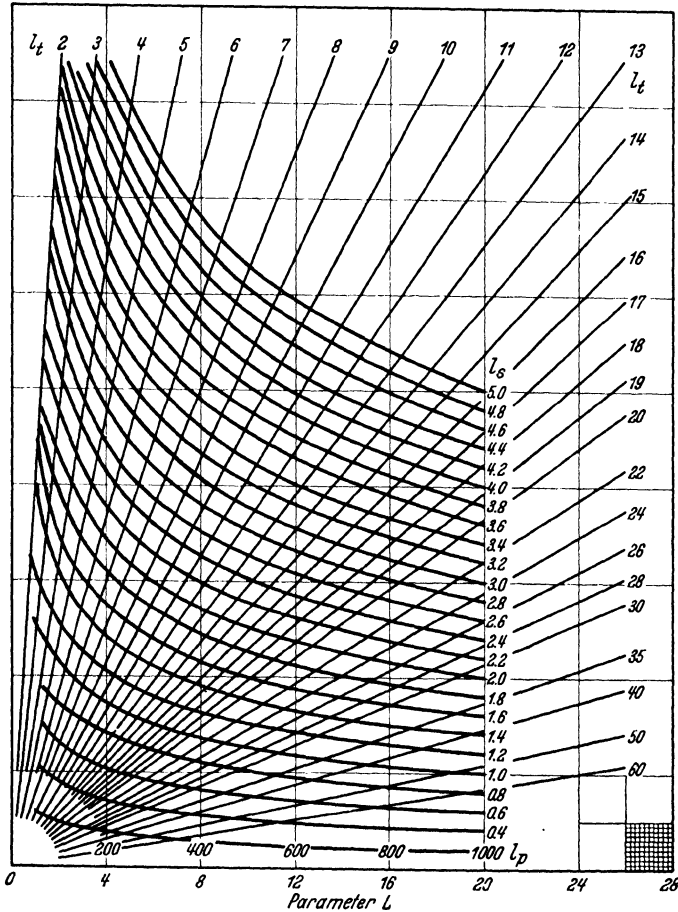


Fig. 31. Chart for determination of parameter  $L$ .

The effect of this decrease in high speed is taken care of by a correction given as a function of the ratio of the maximum to minimum speed  $V_{mx}/V_{mn}$ . This correction assumes the center of gravity location on the wing vector corresponding to the minimum speed, and on an average progression of wing vector with the increase of the speed in level flight. For a so-called "stable" airfoil or in any other case when the vectors for low and high speed pass through the center of gravity, this correction is to be omitted. The procedure in Fig. 30 is obvious.

Fig. 31 gives values of the parameter  $L$ , as expressed in the form:

$$L = \frac{l_s l_t^{4/3}}{l_p^{1/3}}$$

The primary parameters should be used in the following order:  $l_p$ ,  $l_s$ , and  $l_t$ .

Fig. 32 is for the determination of level speeds and air speeds at best climb, at various altitudes.

All speeds determined from this chart are given in percent of the high speed found from Fig. 29. The different percentages are plotted

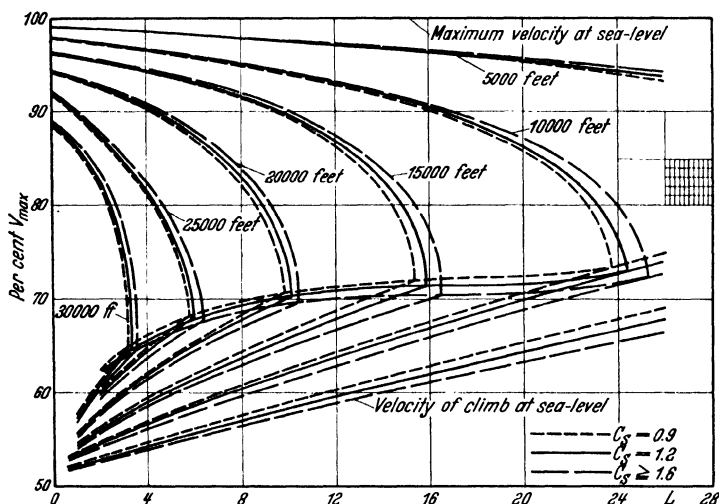


Fig. 32. Performance charts.

with the parameter  $L$  as abscissa and the graphs are calculated for different altitudes and different values of  $C_s$  as found on Fig. 28.

The formulae for this diagram are developed as follows:

In (3.12) we put  $v = 1.467 V$ , divide and multiply by  $R_V$  and make the condition  $V = R_V V_m$ . Then with a little rearrangement we have an equation in  $R_V$  as variable, in the form:

$$\frac{dh}{dt} = \frac{550}{\sigma R_V l_t} \left[ \left( \frac{\sigma - 0.165}{0.835} \right) R_V^{m+1} \sigma - \sigma^2 R_V^4 - \frac{l_s l_t}{3.014 V_m x} (1 - \sigma^2 R_V^4) \right] \quad (4.2)$$

Making the condition for level flight,  $dh/dt = 0$  and solving for  $l_s l_t / V_m x$  we find

$$\frac{l_s l_t}{V_m x} = 3.014 \left[ \frac{(\sigma - 0.165) R_V^{m+1} \sigma - 0.835 \sigma^2 R_V^4}{0.835 (1 - \sigma^2 R_V^4)} \right] \quad (4.3)$$



Again from (1.4) and solving (4.1) for  $V_{mx} l_t^{1/2}/l_p^{1/2}$  we may express the parameter  $L$  in the form

$$L = 48.6 \frac{l_s l_t}{V_{mx}} \left( 1 - 0.332 \frac{l_s l_t}{V_{mx}} \right)^{1/3} \quad (4.4)$$

Equations (4.2) and (4.3) are used to plot the curves for maximum level speeds at altitudes in per cent of the high speed  $V_m$ .

The condition for the speed corresponding to the maximum rate of climb is

$$\frac{d \left( \frac{dh}{dt} \right)}{d R_V} = 0$$

This yields the following special value of  $l_s l_t / V_{mx}$ .

$$\frac{l_s l_t}{V_{mx}} = \frac{3.014 \left[ 3 \sigma^2 R_{Vc}^4 - m R_{Vc}^m + 1 \right] \sigma \left( \frac{\sigma - 0.165}{0.835} \right)}{1 + 3 \sigma^2 R_{Vc}^4} \quad (4.5)$$

where

$$R_{Vc} = \frac{\text{speed at max. rate of climb}}{V_{0mx}}$$

The condition for speed at absolute ceiling is given by putting  $dh/dt = 0$ . This gives an equation in the same form as (4.3) but all conditions must now be understood as referring to absolute ceiling. The curve of speeds at absolute ceiling is then found as the intersection of level speeds and speeds at best rate of climb and can be determined graphically.

Fig. 33 is plotted for the determination of the best rate of climb. These curves for the best rate at different altitudes are plotted with the parameter  $L$  as abscissa. Denoting this rate by  $C_h$ , it is given indirectly by the product,  $C_h l_t$  plotted as ordinate. The actual rate is then given by dividing this product by  $l_t$ .

The values of  $C_h l_t$  are obtained by multiplying the general equation (4.2) by  $l_t$  and then substituting for  $l_s l_t / V_{mx}$  its value from (4.3).

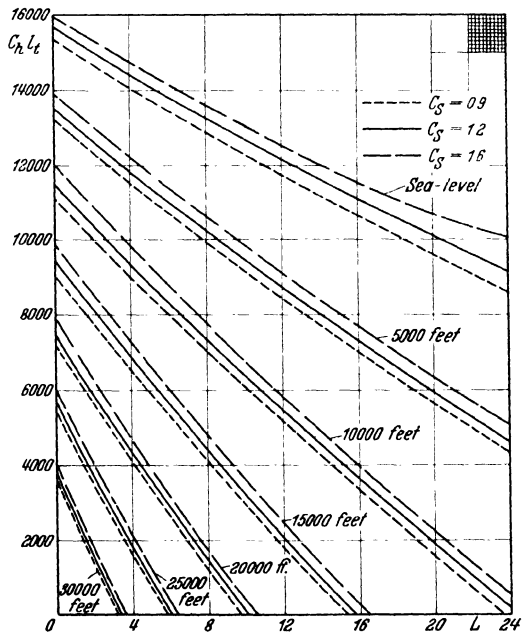


Fig. 33. Determination of best rate of climb.

The corresponding values of  $L$  come also by substituting the same values of  $l_s l_t / V_{mx}$  in (4.4).

Fig. 34, for the determination of absolute ceiling is obtained from preceding charts by a determination of the value of  $L$  at which the best

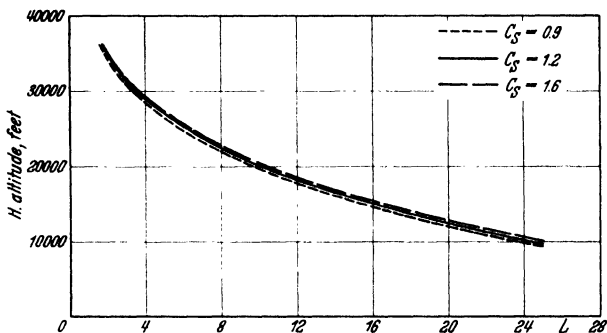


Fig. 34. Determination of absolute ceiling.

rate of climb at any one altitude is zero. The absolute ceiling is then made a function of  $L$  and  $C_s$  and plotted on a graph, the use of which is obvious.

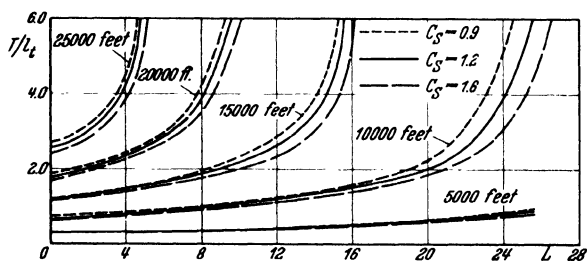


Fig. 35. Determination of minimum time to climb to altitude.

Fig. 35 is for the determination of the minimum time to climb to altitude. The minimum time necessary for a given airplane to climb from one altitude to another altitude below the absolute ceiling is expressed by the equation:

$$T = \int_{h_1}^{h_2} \frac{dh}{C_h} \quad (\text{minutes})$$

where  $C_h$  is the rate of climb. It was found convenient, in plotting the graph to use the product of  $C_h \times l_t$  instead of the rate  $C_h$ , and  $T/l_t$  instead of  $T$ . The above formula was then given the form:

$$\frac{T}{l_t} = \int_{h_1}^{h_2} \frac{dh}{C_h l_t}$$

Values of  $T/l_t$  are then plotted against  $L$  for different values of  $C_s$ . For given values of  $L$  and  $C_s$  a value of  $T/l_t$  may then be taken from the chart and this value multiplied by  $l_t$  will give the minimum time required to climb to the altitude in question.

The time to reach absolute ceiling is of course infinite as shown by extrapolation of graphs where the curves for altitude of absolute ceiling become tangent to the vertical passing through calculated  $L$ .

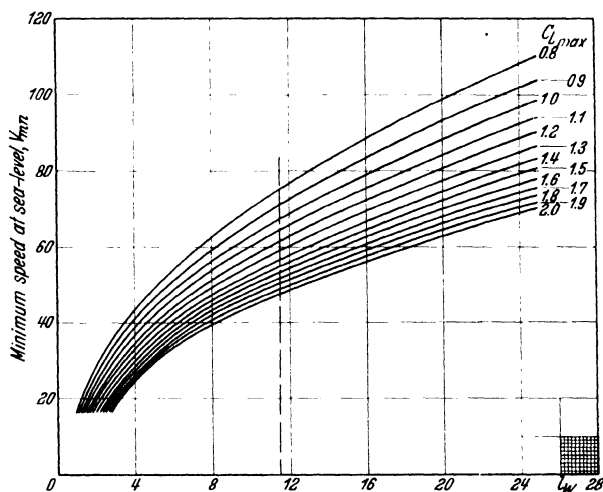


Fig. 36. Determination of landing speed.

Fig. 36 for the determination of the landing speed is not a part of the method of performance calculations explained previously, but is merely a convenient graphical method of determining landing speeds for different wing loadings and for different lift coefficients. However the values of  $V_{min}$  — minimum speed at sea level are used in Fig. 30 for determination of the speed range used in making corrections to high speed.

It is possible to extend the fundamental formulas thus developed, to the solution of other and special problems which ordinarily are not of general interest. These and detailed derivations of all equations may be found in Ref. 13.

*Example by Oswald's Method.* Data required:

$W$  = Gross weight, 4000 lbs.

$S$  = Wing area (total), 350 sq. ft.

Airfoil, Clark Y.

Upper wing, Span ( $b_1$ ) = 38 ft.

Chord = 5.7 ft.

Area = 215 sq. ft.

Lower wing, Span ( $b_2$ ) = 33 ft.  
 Chord = 4.25 ft.  
 Area = 135 sq. ft.  
 Gap ( $g$ ) = 5.25 ft. Stagger = 20 deg.  
 Engine, 435 bph. at 2300 r.p.m.  
 Propeller, 2 blades, metal.

*Assumptions:*

Equivalent flat plate  $A = 9.5$  sq. ft. (For determination of  $A$  see II 5b).

Minimum profile drag coefficient  $C_{D0} = 0.0102$  (from profile drag coefficient polar).

Equivalent monoplane aspect ratio E.M.A.R. = 4.73. (For determination of E.M.A.R. see II 3.)

Maximum lift coefficient  $C_{L \text{ max}} = 1.25$ .

*Determination of Parameters:*

Parasite loading  $l_p = \frac{W}{f}$

where  $W = 4000$ , and  $f$  is the sum of parasite and profile drags in terms of flat plate area,

$$f = 9.5 + \frac{0.0102}{1.282} \times 350 = 9.5 + 2.785 = 12.285 \text{ sq. ft.}^1$$

$$l_p = \frac{4000}{12.275} = 326$$

Span loading  $l_s = \frac{W}{e(Kb)^2} = \frac{W}{e(\text{E.M.A.R.}) \times S}$

$$l_s = \frac{4000}{0.85 \times 4.73 \times 350} = 2.842$$

Wing loading  $l_w = \frac{W}{S} = \frac{4000}{350} = 11.42$

*Thrust power loading*

$$l_t = \frac{W}{(\eta \text{ bhp})_{m \times}}$$

This parameter is obtained by successive approximations as follows: The probable high speed is arbitrarily estimated, say 140 m.p.h.

Using Fig. 28 and the power and r.p.m. of the engine, the composite parameter  $C_s$  is found as previously indicated, giving a value  $C_s = 1.18$ .

The maximum propeller efficiency corresponding to  $C_s = 1.18$  is found on Fig. 29 and is 80.5 per cent.

The power loading  $l_t = \frac{4000}{435 \times .805} = 11.43$

<sup>1</sup> In U.S. N.A.C.A. Technical Report No. 408 the text and charts are based on  $f = 1.28 A + .01 S$ .

Using this power loading, we find the ratio,

$$\frac{l_p}{l_t} = \frac{326}{11.43} = 28.5$$

and the product:  $l_s \times l_t = 2.842 \times 11.43 = 32.55$

Using Fig. 30 the speed corresponding to  $l_p/l_t = 28.5$  and  $l_s l_t = 32.55$  is  $V_{m x} = 143.5$  m.p.h. This speed is subject to a reduction depending on the speed range. The minimum speed is determined from Fig. 36 from

$$l_w = 11.42 \text{ and } C_L \text{ max} = 1.25$$

$$V_{m n} = 60 \text{ m.p.h. and}$$

the speed range  $V_{m x}/V_{m n} = \frac{140}{60} = 2.34$

The corresponding correction to this value 2.34 is found on the supplementary Fig. 30 to be  $-0.6$  per cent and the net high speed is,

$$143.5 \times 0.994 = 142.6 \text{ m.p.h.}$$

This speed is the first approximation and is very close to the probable speed estimated at 140 m.p.h. A second approximation is not necessary unless the first approximation differs from the estimated by more than 5 m.p.h. or unless a greater accuracy is required.

The next step is the determination by means of Fig. 31 of the fundamental parameter  $L$  used extensively throughout the remaining performance estimates:

Starting in Fig. 31 on scale  $l_p = 326$  and proceeding vertically to the interpolated curve of  $l_s = 2.842$ , thence horizontally to the interpolated line of  $l_t = 11.43$ ; thence vertically down to the scale of  $L$ , giving the value  $L = 10.6$ .

Now there are sufficient data to completely determine the performance from the two composite parameters  $L$  and  $C_s$  in terms of which all the performance graphs at sea level (except high speed at sea level) and at altitudes, are plotted. Horizontal speeds and speeds for best climb at

*Speeds.*

Altitude	Speeds, Level		Speeds in Climb	
	Per cent	m.p.h.	Per cent	m.p.h.
0	100	142.5	58.7	83.6
5000	97.6	138.5		
10,000	94	134.0	62.5	89
15,000	89	126.8	66.5	94.8
Abs. Ceiling	70.5	100	70.5	100

altitudes are found on Fig. 32 as percentages of the high speed at sea level found previously on Fig. 30 to be 142.5 m.p.h.

The best rates of climb are found from Fig. 33. The necessary parameters are  $L = 10.6$ ,  $C_s = 1.18$ ,  $l_t = 11.43$ , and the following table may be made, where the rate of climb is computed by:

$$\text{Rate} = \frac{C_h l_t}{11.43}$$

<i>Rate of Climb.</i>		
Altitude	$C_h l_t$	Rate (ft. per mt.)
0	12,500	1095
5,000	9,200	804
10,000	6,000	532
15,000	2,800	248

The absolute ceiling is found from Fig. 34 directly. For  $L = 10.6$  and  $C_s = 1.18$  the absolute ceiling is 19,500 ft. and the service ceiling is computed from the rate at 15,000 ft. as follows:

$$\text{S.C.} = 19,500 - (19,500 - 15,000) \times \frac{100}{248} = 17,680 \text{ ft.}$$

Minimum time to climb is determined from

<i>Time to Climb to Altitude.</i>		
Altitude	$T/l_t$	Time to Climb
5,000	.37	4.23 min.
10,000	1.1	12.55 "
15,000	2.3	26.20 "

Fig. 35 by determining first the value of  $T/l_t$ . The parameters necessary to know are  $L = 10.6$ ,  $C_s = 1.18$ , and  $l_t = 11.43$ . The following table then is made, where the time to climb is computed by,  $\text{Time} = T/l_t \times 11.43$ .

A summary of the performances obtained by Oswald's graphical method is contained in the following table:

Altitude	0	5,000	10,000	15,000	19,500
Level speeds (m.p.h.) . . .	142.5	138.5	134.0	126.8	100
Speeds in climb (m.p.h.) . .	83.6	85	89	94.8	100
Rate of climb (ft. per mt.)	1095	772	532	248	0
Time to climb (mt.) . . .	0	4.23	12.55	26.20	x

The service ceiling is 17,680 ft.

## CHAPTER VII EMPIRICAL-THEORETICAL METHOD

One of the most convenient graphical methods of performance prediction requiring practically no computation was developed in 1920, based on theoretical considerations and using basic data empirically determined from flight test results. This method is of interest because its derivation provides a valuable practice problem for the young student, and because it for the first time introduced a factor of fineness, depending on the cleanness of the design, to be used in combination with the power and wing loadings which had, until that period, been the sole criteria.

The "fineness" was taken as the measure of the relative overall efficiency of the lift-drag ratio of the complete airplane. Thus if the fineness of two airplanes is 100 and 120 respectively, it means that at any value of lift coefficient common to both, the lift-drag ratio of the latter is  $(1.2)^3$  times that of the former. Since, at a given value of the speed or lift coefficient and wing area, the horsepower required is inversely proportional to the lift-drag ratio, the second airplane could have a power loading  $(1.2)^3$  times the first. "Fineness" is hence defined as

100 times the cube root of the lift-drag ratio of an airplane relative to that of a basic airplane with a fineness of 100. By employing for the groundwork of the subsequent charts the results of a wind tunnel test on a model of the DH-4 biplane, this airplane became the basic one.

Previous purely theoretical charts yielded for the same power and wing loadings, identical performances for a large twin engined bomber as for a small cleanly designed pursuit airplane, whereas the lift-drag ratio of the latter might be as much as 100 per cent greater than that of the former. Differences in high speed at the ground would in this case be of the order of 25 per cent. A further disadvantage of these charts was the fact that the limits were not extended to the loadings coming into more recent practice.

Purely theoretical analyses of performance necessarily gave somewhat unsatisfactory results because of the lack of adequate experimental data on wings, parasite drag, interference, propellers, and engine power at altitude. The logical solution was by means of an empirical-theoretical method.

The inadequacy of previous purely empirical methods was thus overcome by taking "fineness" into account, and the main difficulties of purely theoretical methods were obviated by empirically solving for the effects of wing combinations, interference, and engine-propeller performance at altitude.

The method consisted in (a) the construction of a chart for the determination of fineness, engine-propeller performance, high speed at any

TABLE 22.

Aircraft	lb./HP	lb./Sq. Ft.	High Speed at Sea level	Fineness
Ford C-4 (3 Wasps) . . . .	8.8	15.5	135	90
Sikorsky Amphibian S-38 .	11.3	14	120	92
Martin Bomber (2 Liberties)	12.3	9.6	105	93
Ford C-7 (3 Whirlwinds) .	10.7	13.9	126	93
Atlantic C-2 (3 Whirlwinds)	14.5	14	112	95
Fokker F-10 (3 Wasps) . .	9.9	17.5	141	97
DeHaviland 4 . . . . .	9.8	8.9	120	100
Fairchild C-928 . . . . .	11.3	15.5	140	102
Fokker Super-Univ. . . . .	11.1	11.9	131	102
Fokker D-VII . . . . .	10.8	8.5	117	102
SE-5. . . . .	11.4	8.4	117	105
Vought VE-7 . . . . .	11.6	7.4	114	106
Bellanca Cargo . . . . .	13.6	14.8	139	108
Thomas Morse MB-3 . . . .	6.3	8.4	152	112
Verville Pursuit . . . . .	8.7	9.7	150	116
Spartan C-5-301 . . . . .	13.9	13.9	145	118
Lockheed. . . . .	9.3	15.3	179	120

Unless otherwise noted, aircraft are single engined.

altitude, and, in the limit of the application, absolute ceiling<sup>1</sup>; (b) in the construction of an empirical-theoretical chart for the determination of rate of climb at the ground; (c) in the use of an equation for time of climb based on a linear variation of rate with altitude; and (d) in the combination of the results of (a), (b), and (c) to construct, with the aid of cross-plotting, a performance and design chart<sup>2</sup>.

The final chart of Ref. 5 furnishes a complete picture of the variation at all altitudes, including sea level, service ceiling and absolute ceiling, of horizontal high speed, time of climb and rate of climb of any airplane with a given engine and with any combination of the three main variables, loading per horsepower, loading per square foot, and fineness.

In Table 22 is shown the wide variation in fineness of various types of aircraft, both modern and of the wartime period. Refs. 3 and 5 may be consulted for further details of this method.

## CHAPTER VIII LOGARITHMIC DIAGRAMS

**1. Introduction.** The basic principle of performance prediction by the use of logarithmic polars is that of the slide rule, that is, all multiplications and divisions, of which the majority of computations consists, can be made graphically by adding or subtracting distances on suitably made scales.

This method assumes that the usual polar of lift and drag coefficients is known or determined by some other means. It assumes also that the variation of the power of the engine and the efficiencies of the propeller are known.

It is particularly suited for a study of airplanes where one or more characteristics are varied; namely for a study of the effects of changing weight, power or wing area. The use of the charts can be extended to practically any problem of airplane performance, including the choice of the propeller best suited for any particular need.

Performance estimation by the use of logarithmic polars is probably the oldest method developed for this work and certainly antedates the original Bairstow method. It may be pointed out, however, that the fundamentals of both methods are the same. In Eiffels' original work of 1909, this method of performance estimation was used and was the only one then known to aerodynamists. The performance of famous predecessors of modern aircraft—the airplanes of the Wright brothers and of Curtiss, the Bleriot XI of English Channel fame, the Santos-

---

<sup>1</sup> Ref. 3.

<sup>2</sup> Ref. 5.



Dumont "Demoiselle", Latham's "Antoinette" and many others—was estimated by this method.

The original adaptation of the logarithmic polar diagram is credited to Eiffel's collaborator Rith, and the description may be found in Ref. 1.

The criticisms regarding the accuracy of this method are not well founded. The accuracy of this method, as of any other, using graphics for solutions, is limited only by the size of charts and the accuracy in plotting and interpolating. The charts used by Eiffel were of generous size and their accuracy was well above the precision of the basic data. The advantage of this method over any analytical method, supposedly more accurate, is that the different steps are visually apparent and if any errors are made they are easily detected, while in analytical computations if an error is made at the beginning of the calculations, it is difficult to locate or it passes unnoticed altogether.

**2. Theory.** Originally this method was designed to represent the performances of airplanes, models of which were tested in the tunnel, but of which the total weights and engine power were not definitely known. Aerodynamic characteristics obtained in the tunnel were relied upon and considered as final. The logarithmic polar diagram of the airplane was based on the tunnel tests and the lift and drag coefficients were the main constituents of the diagram.

However, for an airplane of given area, not the coefficient but the actual lift and drag per unit of speed were plotted as logarithmic coordinates. But, since the performance depends also on the actual weight of the airplane, the power of the engine and the altitude at which it flies, additional scales, in agreement with the lift and drag scales, were established.

The interdependence of the different quantities above mentioned is represented by the following equations:

$$W = LV^2 \quad (2.1)$$

$$P = DV^3 \quad (2.2)$$

In these equations it should be especially noted that  $L$  and  $D$  denote respectively the lift and the drag in pounds at a speed of one mile per hour, while  $V$  is the speed in miles per hour and  $P$  is the thrust power in mile, pound, hour units.

Then with the usual non-dimensional coefficients we shall have

$$L = C_L S \rho \frac{(1.467)^2}{2}$$

$$D = C_D S \rho \frac{(1.467)^2}{2}$$

where 1.467 is the velocity in f.p.s. for a speed of 1 m.p.h. At the sea level these values become

$$L = 0.00256 C_L S$$

$$D = 0.00256 C_D S$$

The first two equations expressed logarithmically are:

$$\log W = \log L + 2 \log V$$

$$\log P = \log D + 3 \log V$$

whence

$$\log L = \log W - 2 \log V \quad (2.3)$$

$$\log D = \log P - 3 \log V \quad (2.4)$$

From the above equations it is apparent that the logarithm of the unit lift  $L$  is the sum of  $\log W$  and  $-2 \log V$ , and that of the unit drag  $D$  is the sum of  $\log P$  and  $-3 \log V$ .

To develop a convenient graphical representation of these equations, we may proceed as follows. We first note that (2.3) is simply a statement of numerical relation between three quantities—one number is equal to the sum of two others. Suppose now that we have three values  $L_1$ ,  $W_1$  and  $V_1$  which fulfil equation (2.3). We may then write

$$\log L_1 = \log W_1 - 2 \log V_1$$

Subtract one equation from the other and we have

$$\log \frac{L}{L_1} = \log \frac{W}{W_1} - 2 \log \frac{V}{V_1} \quad (2.5)$$

This we may rewrite in the form

$$\log \frac{L}{L_1} = \log \frac{W}{W_1} + 2 \log \frac{V_1}{V} \quad (2.6)$$

These are again statements of a numerical relation between  $\log L$ ,  $\log W$  and  $\log V$ , all expressed, however, in terms of  $L_1$ ,  $W_1$  and  $V_1$  as units. It is clear, then, that at the origin of the scale for  $\log L$  we must put the number  $L_1$  (since this fulfils the condition  $\log L/L_1 = \log 1 = 0$ ) and similarly for the scales for  $W$  and  $V$ . Regarding these three quantities  $L_1$ ,  $W_1$  and  $V_1$  it is evident that we may select arbitrarily any two and having selected these, the third will follow from (2.1). These three quantities give, therefore, certain coincident values at the initial point of a diagram of graphic construction intended to represent (2.3). Exactly the same principles hold for the initial values for (2.4) except that now having fixed a value of  $V_1$ , the same value must apply for (2.4) and we have, therefore, only one arbitrary choice between  $D_1$  and  $P_1$ .

If now  $L_1$  and  $W_1$  are taken smaller than the normal run of values and  $V_1$  larger,  $L/L_1$  and  $W/W_1$  will be greater than unity and  $V/V_1$  less, with the result that all terms in (2.5) will be positive.

There will evidently be similar forms for (2.4).

$$\log \frac{D}{D_1} = \log \frac{P}{P_1} - 3 \log \frac{V}{V_1} \quad (2.7)$$

$$\log \frac{D}{D_1} = \log \frac{P}{P_1} + 3 \log \frac{V_1}{V} \quad (2.8)$$

and with a similar understanding regarding the initial values, all terms in these equations will be positive.

Referring now to Fig. 37 let the scales for  $P$  and  $D$  be laid off on  $OX$ , those for  $L$  and  $W$  on  $OY$  and that for  $V$  on a line  $OV$  inclined to  $OX$  at an angle  $\tan^{-1} 2/3$ . Then if the scales on  $OX$  and  $OY$  increase from the origin and that on  $OV$  increases toward the origin, lengths such as  $OE$  and  $OH$  may represent  $+\log (L/L_1)$  and  $+\log (W/W_1)$  while a length such as  $OG$ , or its equivalents  $AB$ ,  $CD$  or  $EF$  will represent  $+\log (V_1/V)$  or  $-\log (V/V_1)$ . Then with suitable scales for plotting these logs, it is seen that  $EH$  may represent  $2 \log (V_1/V)$  or  $-2 \log (V/V_1)$  and  $AP$  may represent  $3 \log (V_1/V)$  or  $-3 \log (V/V_1)$ . With these understandings, it follows that  $OH$ ,  $OE$  and  $EH$  will represent (2.6) while  $OP$ ,  $OA$  and  $AP$  will represent (2.8).

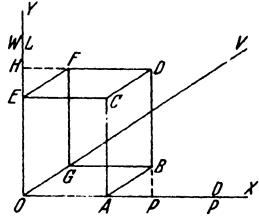


Fig. 37.

For the actual plotting of the logarithmic scales, any convenient unit may be chosen for the scales on the  $X$  and  $Y$  axes, but having adopted such a unit, that for the scale of  $\log V$  as measured along the  $Y$  axis must be twice that for  $\log L$  and  $\log W$  and hence the unit for the scale along  $OV$  must be  $\left(\sqrt{\frac{4+9}{2}}\right) \times 2 = 3.605$  times that along  $L$  and  $W$ . The same result will be reached by starting from the scales along  $D$  and  $P$ .

As noted earlier, the basic equations (2.1), (2.2) are expressed in terms of mile, pound, hour units. In placing the actual numbers on the scales, however, the logarithmic relations will be the same whatever units are employed, and the scale for  $P$  may therefore be marked directly in hp units.

Again it may be that the unit values  $L_1$ ,  $W_1$ ,  $P_1$ ,  $D_1$  will lie well outside the range of normal values and that, in consequence, there will be no object in extending these scales to values at or near the origin. In such case, coincident points on these scales are readily determined from (2.1) and (2.2) by taking  $V = V_1$  and selecting any value desired for either  $L$  or  $W$  in one case and for either  $D$  or  $P$  in the other. The scales so established will have definite values at the origin but these values may be quite outside the usual range and therefore without interest.

Thus suppose  $V_1$  is taken at 200 and  $W$  at 1000. Then from (2.1)  $L = 0.025$ . In the same manner if  $P$  is taken 100 hp = 37,500 (mile, pound, hour) units, then from (2.2),  $D = 0.004685$ . The location of  $L = 0.025$  being thus found, the location of  $L = 0.01$  or .10 readily follows and similarly for the scale for  $D$ . Fig. 38 is a diagram of scales so constructed, and shows graphically the functional dependence of the factors affecting the performance.

The effect of altitude may be expressed analytically by alterations in the basic equations.

$$W = \sigma L V^2$$

$$P = \sigma D V^3$$

where  $\sigma$  is the ratio of the density of air at altitude to that at sea level and  $L$  and  $D$  are values for sea level at speed  $V$ .

Taking logarithms we have

$$\log L = \log W - \log \sigma - 2 \log V \quad (2.9)$$

$$\log D = \log P - \log \sigma - 3 \log V \quad (2.10)$$

Then lay off from  $O$ , Fig. 39, an altitude axis  $OH$  at  $45^\circ$  to  $OP$  and on this axis lay down a scale of  $\log \sigma_0/\sigma$  ( $\sigma_0 = \sigma$  for sea level). It will thus result, in a similar manner as along the  $V$  axis, that a distance from  $O$  along  $OH$  will represent  $\log 1/\sigma = -\log \sigma$ . For the modulus

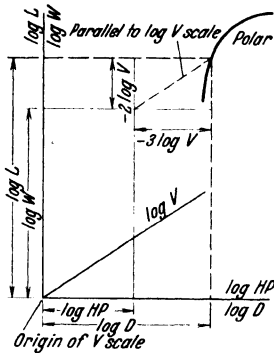


Fig. 38.

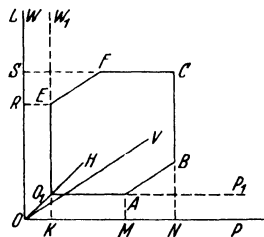


Fig. 39.

of this scale take  $\sqrt{2} = 1.414$  times that along  $OP$  and  $OW$ . Under these conditions it is readily seen that the coordinates  $ON$  and  $OS$  of a point  $C$  on the polar are made up of segments which represent the various terms of (2.9) and (2.10). Thus  $OK = -\log \sigma$ ,  $KM = \log P$ ,  $MN = -3 \log V$  and similarly for the axis of  $W$  and  $L$ . It is seen that the effect of this is to shift the origin  $O$  along  $OH$  a distance represented by  $\log 1/\sigma$ . If, therefore, from such a point  $O_1$ , auxiliary lines  $O_1P_1$  and  $O_1W_1$  are drawn, the latter may be used as axes of  $P$ ,  $D$ ,  $W$  and  $L$  and the construction will go forward as before.

With regard to the graduation of the axis  $OH$ , the distance, as noted, will represent values of  $\log 1/\sigma$ . The numbers on the scale may, however, represent actual altitudes in feet corresponding to the several values of  $\log 1/\sigma$ . For this scale the origin value will be taken as  $\sigma = 1$ ,  $1/\sigma = 1$ ,  $\log 1/\sigma = 0$  and altitude = 0 while the outer end may conveniently correspond to  $\sigma = 0.10$ . A further consideration is the range of weights, power, unit lifts and drags, and speed which should be covered. For purposes of illustration, ranges as follows may be taken:

weight, 100 to 100,000 lbs.

power, 10 to 10,000 hp

speed, 20 to 200 m.p.h.

areas, 100 to 5000 sq. ft.

$C_L$ ,  $mx = 2.0$ ,  $mn = 0.2$

$C_D$ ,  $mx = 0.100$ ,  $mn = 0.01$

$L_1$ ,  $mx = 2.0 \times 0.00256 \times 5000$  sq. ft. = 25.6

$D_1$ ,  $mx = 0.100 \times 0.00256 \times 5000$  sq. ft. = 1.28

$L_1$ ,  $mn = 0.2 \times 0.00256 \times 100$  sq. ft. = 0.0512

$D_1$ ,  $mn = 0.01 \times 0.00256 \times 100$  sq. ft. = 0.00256.

It should be noted that for any particular airplane the whole range as given above does not have to be covered, and for the same space available, the scale modulus may be enlarged and thus the accuracy of results increased.

The next step is to decide on the size of the diagram. A study of the ranges for different variables indicates that a sheet 20 by 15 inches will be sufficiently large for reasonably accurate performance estimation. The corresponding modulus distance for a group of values from 1 to its next decimal multiple (10 or .1) on the vertical and horizontal scales may be conveniently taken as 3.5 inches. For the speed scale the modulus distance will be  $3.5 \times 3.6055 = 12.615$  inches, and for the 45° altitude scale it will be  $3.5 \times 1.414 = 4.95$  inches.

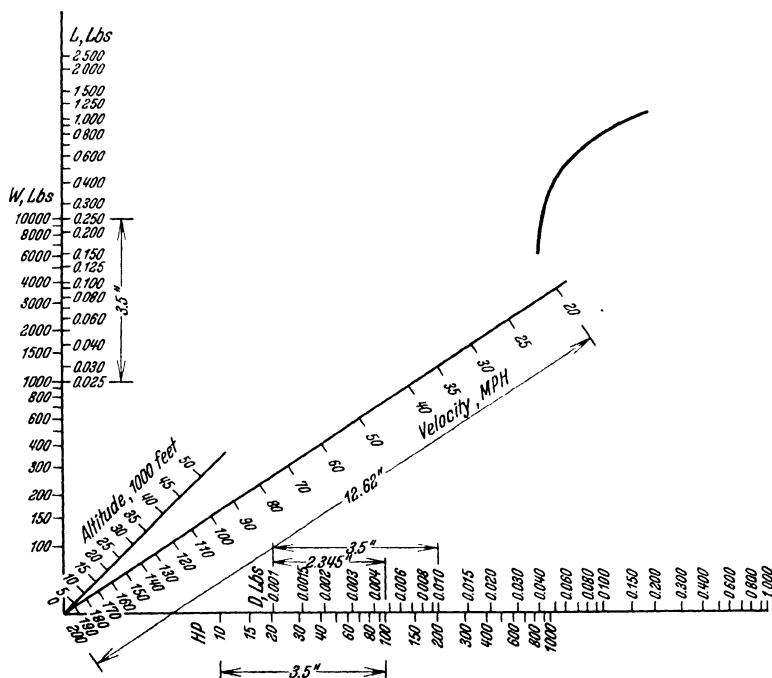


Fig. 40. Chart showing logarithmic scales.

TABLE 23. For Setting Scales for Logarithmic Polar Diagram. Basic Modulus 3.5''.

N	log N	"d" (in.)	L <sub>1</sub> (lbs.)	D <sub>1</sub> (lbs.)	W (lbs.)	HP	"d" (in.)	V M.P.H.	"d" (in.)	Density Ratio	
		Modulus 3.5"					Modulus 12.62		Modulus 4.95		
1	0	0	.1	1.00	.010	100	1000	10	100	0	.10
1.25	.0969	.339	.125	1.25	.0125	125	1250	125	125	.4796	.125
1.5	.1761	.617	.15	1.5	.015	150	1500	15	150	.872	.15
1.75	.2430	.851	.175	1.75	.0175	175	1750	175	175	1.203	.175
2.0	.3010	1.053	.20	2.0	.020	200	2000	20	200	1.149	.20
2.25	.3522	1.233	.225	2.25	.0225	225	2250	225	225	1.743	.225
2.5	.3979	1.393	.25	2.50	.025	25	250	25	250	1.970	.250
2.75	.4393	1.538	.275	2.75	.0275	275	2750	275	275	2.175	.275
3.0	.4771	1.670	.3	3.0	.030	300	3000	30	300	2.362	.30
3.5	.5441	1.904	.35	3.5	.035	350	3500	35	350	2.693	.35
4.0	.6021	2.107	.40	4.0	.040	400	4000	40	400	2.980	.40
4.5	.6532	2.286	.45	4.5	.045	450	4500	45	450	3.233	.45
5.0	.6990	2.447	.5	5.0	.050	500	5000	50	500	3.460	.50
5.5	.7404	2.591	.55	5.5	.055	550	5500	55	550	3.665	.55
6.0	.7782	2.724	.6	6.0	.060	600	6000	60	600	3.850	.60
6.5	.8129	2.845	.65	6.5	.065	650	6500	65	650	4.023	.65
7.0	.8451	2.958	.7	7.0	.070	700	7000	70	700	4.183	.70
7.5	.8751	3.063	.75	7.5	.075	750	7500	75	750	4.331	.75
8.0	.9031	3.160	.8	8.0	.080	800	8000	80	800	4.470	.80
8.5	.9294	3.253	.85	8.5	.085	850	8500	85	850	4.600	.85
9	.9542	3.340	.9	9.0	.090	900	9000	90	900	4.723	.90
9.5	.9777	3.422	.95	9.5	.095	950	9500	95	950	4.840	.95
10	1.0	3.500	1.0	10	.10	1000	10000	100	1000	4.950	1.0

Table 23 is used for making logarithmic polar scales to satisfy conditions set forth previously. In this table " $N$ " is a series of numbers proportional to the divisions desired within any one basic modulus range. Column  $d$  gives the values of  $\log N$  in terms of a basic modulus ( $3.5''$ ). The columns under  $L$ ,  $D$ ,  $W$  and  $P$  are the corresponding values of these quantities over two ranges of the factor 10. Column  $d$  gives, therefore, the distance in inches from the beginning of a modulus range to the point for the number in question. Thus the point for  $L = 0.30$  will be  $1.67''$  from the point for  $L = 0.10$  and the point for  $L = 3.0$  will be the same distance from the point for  $L = 1.0$ . The same general method is followed for the scales for  $V$  and  $\sigma$ .

TABLE 24.  
Table for Setting Scale  
for Altitudes.

Alt.	$\sigma$	$\log 10 \sigma$	$d$ (mod. 4.95'')
0	1.000	1.0	4.95 in.
5,000	.862	.9355	4.63 ..
10,000	.738	.8681	4.30 ..
15,000	.629	.7987	3.95 ..
20,000	.533	.7267	3.60 ..
25,000	.448	.6513	3.22 ..
30,000	.374	.5729	2.84 ..
35,000	.310	.4914	2.43 ..
40,000	.245	.3892	1.93 ..
45,000	.193	.2856	1.41 ..
50,000	.152	.1818	0.90 ..

The actual location of the points for  $P =$  say 100 and  $W = 1000$  may be selected according to convenience since wherever they are placed the origin values will meet the conditions previously indicated. These points located, the corresponding values for  $L$  and  $D$  are coincident and thence the points for the beginning of each modulus range on the  $L$  and  $D$  scales are found. Table 24 gives values for altitudes in feet against density. Fig. 40 indicates the character of a diagram plotted in accordance with these proportions.

**3. Determination of Performance.** The first step is to lay down, from the known characteristics of the plane, the polar diagram—that is, the points on the diagram having  $D$  and  $L$  as co-ordinates.

For the determination of sea level high speed, it is necessary to ascertain the propeller efficiency at that speed in order to find  $P$ , the available thrust horsepower ( $\text{THP} = \text{BHP} \times \eta$ ). The efficiency at high speed is usually the maximum, and the value may be determined by methods described in II 9. Likewise the BHP is found as in Chapter II and thence the THP as above.

The next step is to locate the point  $A$  of which  $W$  and  $P$  are the coordinates (see Fig. 41). A line is then drawn from this point parallel to the  $V$  axis to the point of intersection with the polar.

The length of this line laid off on the speed axis from the origin will then give the speed value. It will be remembered that  $L$  and  $D$  are directly

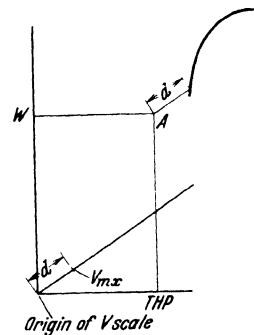


Fig. 41.





If desired, hp available and hp required, both at sea level and at altitude may be plotted on such a diagram. Thus in Fig. 43 an auxiliary speed axis is laid off from  $W$  and from a point  $a$  on this axis, representing a speed  $V$ , a horizontal line is drawn to the polar and from this point  $b$  a line parallel to the speed axis back to intersect the horizontal through  $W$  at a point  $c$ . This gives a parallelogram  $Wabc$ . If then a vertical line is drawn from  $c$  to cut  $ab$ , it is obvious that  $Wc$ , the power required for the speed  $cb$  (or  $Wa$ ), is represented by an abscissa  $ef$ , thus giving a point  $f$  on the line  $ab$ . Similar points found for other speeds will give a curve  $AB$  of power required, each point on the curve corresponding to a particular speed, determined in the manner described. If then for these same speeds and on these same lines  $ab$ , there be laid off from the axis of  $W$  and  $L$  values for the power available, we shall have a curve somewhat as shown by  $CD$ . The intersection of these curves at  $h$  will evidently give the maximum speed and power, while the upper intersection will give the minimum speed and power, similar to  $d_2$  and  $P_2$  in Fig. 42 (see also III 1).

By the use of these curves with special constructions, various other items of performance can be determined—maximum reserve power, best speed of climb, rate of climb, absolute ceiling, etc. With reference to these items, however, there is no special advantage of logarithmic plotting over determination by other methods, and the details may be left to the ingenuity of the interested reader.

The general summary of performance obtained in this manner may then be tabulated and represented graphically in the same form as for the cases discussed in Chapters III and V.

## CHAPTER IX RANGE AND ENDURANCE

Two special problems in connection with performance prediction of definite practical importance are those of the determination of the distance that can be flown, *range*, and the time of flight, *endurance*, with a given amount of fuel.

The solution of these problems, which are necessarily closely inter-related, becomes very complex if an attempt is made to take into account all possible variations in the conditions of flight. It is possible, however, to make certain simplifying assumptions which greatly reduce these difficulties.

**1. Range<sup>1</sup>.** Let us consider first the matter of range. In order to obtain maximum range it is obvious that the amount of fuel used per mile must be a minimum. This condition evidently corresponds to the least work required of the engines per mile. Since work is the product of a force times the distance through which it acts, the least work will

<sup>1</sup> See Ref. 8.

be done when the thrust, which is equal to the drag, is least. This indicates that for a given airplane with a given gross weight, there exists a definite air speed which will give the maximum range, and that such speed is that of minimum drag. Minimum drag usually occurs at from 130 per cent to 140 per cent of the stalling speed.

a) *Variables.* During a flight the value of gross weight is not constant, but decreases continually due to the consumption of fuel by the engines. As the gross weight decreases there is a proportionate decrease in wing loading, which means that when flying at a constant speed the angle of attack of the wing must be decreased. This means a decrease in drag, hence minimum drag will occur at different weights and speeds.

So far we have proceeded on the assumption that the efficiency of the engine, as well as the propeller efficiency, remains constant for every air speed. This of course is a false assumption. In the first place, in order to slow down from high speed to the speed of minimum drag, the engines must be throttled. Throttling means a decrease in thermal efficiency, or an increase of specific fuel consumption, which may outweigh in importance the decrease in drag.

A second factor which is important is propeller efficiency. The propeller is designed in a majority of cases to operate with maximum efficiency at high speed; at any lower speed the efficiency becomes reduced. This reduction is of considerable importance in the lower range of speeds.

Third, the speed and the direction of the wind relative to the ground during the flight have considerable influence on the range and must be taken into account in special cases when a long flight is anticipated over a territory with known prevailing winds, or again flying speeds must be altered during flight if it is found that the wind velocities do not correspond to those assumed in the original calculations. The so-called service range is considered in calm air. Still another variable affecting the range is that of the altitude at which the flight can be made.

For an accurate analysis of range, it is, therefore, necessary to take all of the foregoing factors into consideration. They are the ones most susceptible to logical treatment. Others, however, while important, cannot be so readily reduced to figures. Such are: variations of operating conditions of the engine during flight due to the use of mixture controls, use of the supercharger, etc.; variations in atmospheric conditions, particularly in the wind speed and direction which cannot be foreseen; deviation from the correct speed corresponding to the gross weight at any instant; deviation from the best altitude, mainly due to the difficulty of measuring the altitude accurately, and the possibility of inaccuracy in the estimation of the airplane characteristics and those of the engine and propeller upon which the whole analysis is based.

While all of these conditions have a bearing on the accurate prediction of range, their values are so uncertain that recourse is usually

had to certain simple formulas which, although not always covering all the main variables, yet have the merit of quick and easy application and are at the same time within the range of accuracy to be expected in view of the uncertainty of the basic data.

*b) Rational Method.* However, for those who so desire, a rational method of analysis may be outlined comprising the following steps:

1) Determination of the curve of total drag versus air speed for a gross weight which corresponds to full fuel load.

2) Estimation of propeller efficiency versus air speed.

3) Determination of the specific fuel consumption of the engine, in pounds per brake horse power per hour, versus air speed.

4) Combination of the foregoing curves to obtain a curve of fuel consumption expressed in pounds per mile and from that the reciprocal curve, miles per pound.

5) A repetition of the procedure so far outlined for several gross weights, including one representing the condition of empty fuel tanks.

6) Integration of a curve of maximum miles per pound versus gross weight between the limits given, to obtain the total number of miles. This represents maximum range.

7) Investigation of the effect of a head wind or following wind on the range.

Referring to step 1, the curve of drag versus speed can be obtained from a polar curve for the complete airplane either from wind tunnel tests or by estimation as outlined in previous chapters on performance computations. Then for each speed of a series of speeds selected, the lift coefficients can be calculated using the weight and wing area. The drag coefficient corresponding to the lift coefficient is then found on the polar curve and the drag calculated. A typical example of this calculation is shown in Table 25.

TABLE 25. Airplane Drag (With Full Tanks).

$V$	$C_L$	$C_D$	Drag Lbs.	$V$	$C_L$	$C_D$	Drag Lbs.
57.2	1.364	.251	736	110	.369	.057	618
70	.911	.113	496	120	.310	.054	697
80	.698	.084	482	130	.264	.051	772
90	.551	.070	508	140	.228	.050	878
100	.446	.062	556	145.2	.212	.049	926

$$C_L = \frac{2W}{\rho A V^2} = \frac{2 \times 4000}{.00238 \times 350 \times (88/60)^2 \times V^2 \text{ m.p.h.}} = \frac{4465}{V^2 \text{ m.p.h.}}$$

$$D = \frac{.00238}{2} \times 350 \times C_D \times V^2 \text{ f.p.s.} = .896 C_D V^2 \text{ m.p.h.}$$

Step 2 is somewhat more intricate. Assuming that, as outlined in preceding chapters, a performance estimate has already been prepared for the airplane in question, the following is necessary:

First, a determination is made of the r.p.m. required for level flight at various speeds (the speeds chosen for step 1 will be found convenient) from curves of indicated air speed versus indicated r.p.m. The performance method giving this information is that described in Chapter V. Second, calculations are made of the  $v/nD$  at which the propeller is operating at each speed. Third, determination is made of the propeller efficiency for each  $v/nD$ . This procedure has been explained in Chapter V and Table 26 gives an example.

It should be noted that efficiencies calculated in connection with speed and climb computations cannot be used in place of step 2, since the engine is no longer working at full throttle, and therefore the  $v/nD$  corresponding to a given speed is different.

A graph of engine performance characteristics such as would be furnished by an engine manufacturer or from dynamometer tests, contains a curve of specific fuel consumption,  $c$  versus r.p.m. Step 3 consists in taking the value from this curve at the r.p.m. required for level flight at each speed (see Table 26).

TABLE 26. Fuel Consumption per Mile and per Hour (With Full Tanks).

$V$ m.p.h.	Level r.p.m.	$v/nD$	% $\eta_{mx}$	$\eta$	$c$	lbs./mi	lbs./hr
57.2	1607	.368	57.1	.462	.580	2.46	140.6
70	1415	.510	79.1	.641	.660	1.36	95.2
80	1453	.567	87.9	.712	.645	1.16	92.8
90	1570	.590	91.5	.741	.595	1.09	98.1
100	1690	.609	94.5	.765	.555	1.07	107.0
110	1818	.624	96.7	.784	.520	1.09	120.0
120	1960	.630	97.6	.790	.500	1.18	141.5
130	2100	.638	98.9	.801	.495	1.27	165.0
145.2	2320	.645	100	.81	.532	1.62	235.0

$$v/nD = \frac{V \text{ m.p.h.} \times 88}{N \text{ r.p.m.} \times D_{ft.}} = \frac{V}{N} \times \frac{88}{8.55} = 10.3 V/N$$

$$\text{Best lbs./mi} = 1.067$$

$$\text{Best mi/lbs.} = .937$$

$$\text{Best lbs./hr} = 92.0$$

$$\text{Best hr/lbs.} = .01088$$

$$\text{lbs./mi} = \frac{c \times D}{\eta \times 375}$$

In step 4 the results so far obtained are used to convert pounds per horsepower per hour as obtained in engine tests on a dynamometer into pounds per mile and thence into miles per pound.

Let  $P$  denote the brake hp for a given speed  $V$ .

$T$  = corresponding thrust =  $D$  = drag.

$W$  = total weight = lift =  $L$ .

$c$  = specific fuel consumption = pounds of fuel per brake hph<sup>1</sup>.

$\eta$  = propeller efficiency.

$x$  = distance.

<sup>1</sup> While  $c$  is called *fuel consumption* its value should be taken to include the consumption of lubricating oil as well.

Then :

$$P = \frac{TV}{375\eta} = \frac{DV}{375\eta}$$

$Pc$  = lbs. consumption per hour

$$\frac{Pc}{V} = \frac{cD}{375\eta} = \text{lbs. per mile} \quad (1.1)$$

and

$$Pc = \frac{cDV}{375\eta} = \text{lbs. per hour} \quad (1.2)$$

Then with the mile, hour and pound as units, we have

$$\frac{dW}{dx} = - \frac{cD}{375\eta} \quad (1.3)$$

$$\frac{dW}{dt} = - \frac{cDV}{375\eta} \quad (1.4)$$

To complete the process, the foregoing steps must be repeated, using at least one and preferably two different gross weights. One of these must be the gross weight with empty fuel tanks.

The reciprocal of the values given by (1.1) will then give the miles per pound, each for the weight assumed, and the maximum of such values can be plotted against the corresponding weights, giving a curve such as Fig. 44.

In most cases a sufficient approximation will be given by making the computation for two gross weights, one corresponding to full tanks and the other to tanks empty (see Table 27) and assuming a

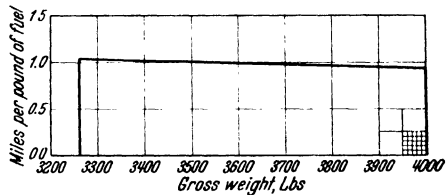


Fig. 44.

linear variation between the values for these two conditions. This procedure was followed in the case represented in Fig. 44.

TABLE 27. Drag of the Airplane and Consumption of Fuel (With Tanks Empty).

$V$	$C_L$	$C_D$	$D$	r.p.m.	$v/nD$	$\frac{\%}{\eta \max}$	$\eta$	$c$	lbs/mi	lbs/hr
70	.744	.0895	393	1415	.510	79.1	.641	.660	1.080	75.6
80	.570	.0715	410	1453	.567	87.9	.712	.645	.990	79.2
90	.450	.0625	454	1570	.590	91.5	.741	.595	.972	87.5
100	.365	.0565	506	1690	.609	94.5	.765	.555	.978	97.8
110	.301	.0530	575	1818	.624	96.7	.784	.520	1.017	111.9
120	.253	.0510	658	1960	.630	97.6	.790	.500	1.110	133.3
130	.215	.0490	742	2100	.638	98.9	.801	.495	1.222	159.0
145.2	.173	.0480	907	2320	.645	100	.810	.532	1.588	230.5

$$C_L = \frac{2 \times 3264}{.00238 \times 350 \times (88/60)^2 \times V^2 \text{ m.p.h.}} = \frac{3645}{V^2}$$

$$D = .896 C_D V^2$$

$$\text{lbs/mi} = \frac{c \times D}{\eta \times 375}$$

$$\text{Best lbs/mi} = .968$$

$$\text{Best mi/lbs} = 1.033$$

$$\text{Best lbs/hr} = 75.0$$

$$\text{Best hr/lbs} = .01333$$

The area under this curve can be found by planimeter or it may be graphically or analytically integrated. This area will then represent the maximum number of miles which may be flown with a given amount of fuel. If it is desired to investigate the effect of altitude on the range, or to find the best altitude for any gross weight, the entire calculation must be repeated for two or three different altitudes. The data on drag, propeller efficiency, specific fuel consumption and power absorbed at altitudes are obtained by methods used in performance calculations as treated previously.

To find the air speed of minimum drag a curve of power required versus speed must be drawn. The point of tangency of a line from the origin drawn tangent to this curve will give the speed of minimum drag. This can be shown as follows:

A point on the curve has as its ordinate some value of the power, which is the product of drag times speed. The corresponding abscissa is speed, so that the slope of the line from the origin through the point is  $DV/V = D$ . The line tangent to the curve will have the minimum slope of all lines from the origin meeting the curve, and hence this line will determine the point and hence the speed for minimum drag.

Here also, if no account is taken of propeller efficiency and thermal efficiency of the engine, serious errors are introduced. Therefore the power should be changed to include these factors. To this end it is desirable to plot the curve of fuel consumption in pounds per hour versus speed. Since power is the rate of doing work, it can be expressed in foot-pounds of energy per hour, and since a pound of fuel represents a definite number of foot-pounds of energy, the expression "pounds of fuel per hour" is admissible and represents power as truly as does "foot-pounds per hour". These values can be found from the curve of pounds per mile by multiplying by the corresponding speed in miles per hour (see Fig. 45).

The effect of the wind on this solution is to shift the scale of speeds by an amount equal to the wind speed. This is shown as follows.

We have the general relation

$$\frac{dW}{dt} = - \frac{cDV}{375\eta} \quad (1.5)$$

Then

$$\frac{dW}{dx} = - \frac{dW}{dt} \frac{dt}{dx} \quad (1.6)$$

If now  $dx/dt = V$ , (1.6) with (1.5) gives (1.3). But if there is a wind velocity  $V_0$  (head), we shall have  $dx/dt = (V - V_0)$  and in this case, (1.6) becomes

$$\frac{dW}{dx} = - \frac{c}{375\eta} \frac{DV}{(V - V_0)}$$

In order then that the consumption per mile over the ground may be the least, we must have  $DV/(V - V_0)$  a minimum; and reference

to Fig. 45 will show that this condition will be determined by shifting the point from which the tangent is drawn, along the speed axis to the point representing the wind speed—to the right for a head wind and to the left for a following wind.

By combining the cases of various altitudes and wind velocities a curve similar to that of Fig. 44 may be plotted from which the longest range under anticipated conditions can be determined.

**2. Endurance.** The maximum endurance of the airplane can be calculated at the same time as the range. The two problems are very similar and the basic data required are the same. The chief difference is that the endurance depends *only* on the time rate of the fuel consumption. In other words, if the factors of propeller and thermal efficiency are neglected, the power required determines the endurance. But as we have seen, these factors should be considered. This means that the ordinates of the curve of power required will have to be divided by the propeller efficiency and multiplied by the specific fuel consumption, to give pounds per hour. This has been shown to be the equivalent of power.

If the range is not one of the items required, then the power required, propeller efficiency and specific fuel consumption will have to be determined as outlined previously. If range has been calculated then the curve of pounds of fuel per hour is known or can be found from the curve of pounds per mile (in wind of zero velocity). It is only necessary then to plot similar curves for several gross weights, between the limits of full fuel load and empty tanks, plotting the reciprocal of the minimum value versus weight to give a curve of maximum hours per pound of fuel versus weight.

This curve, when integrated between the limits of weight mentioned above, determines the maximum hours of flight endurance. For an example see Figs. 45 and 46.

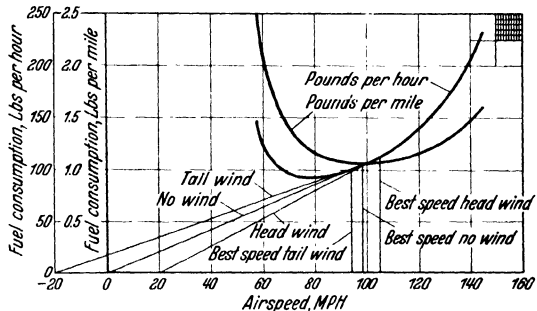


Fig. 45.

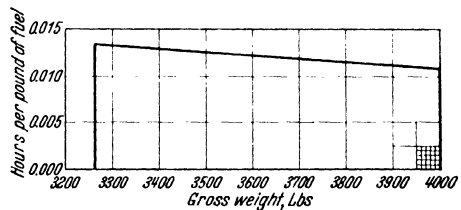


Fig. 46.

With endurance, as with the range, it is necessary to repeat the process if the effect of altitude is desired. However, it is usually sufficient to limit such calculations to one altitude. Wind has no effect on the endurance, except insofar as it brings the possibility of more difficult flying if the air is *bumpy*.

**3. Breguet's Formulas.** The methods so far outlined, while offering rational solutions, are quite laborious, and because of the uncertainties before mentioned, are not entirely dependable for comparative purposes. For these reasons it is usually preferable to use some simple approximate formulas rather than the longer methods. Breguet's formulas are most commonly used.

a) *Range.* For the computation of range the derivation is based on the following equations:

$$\text{From (1.3)} \quad \frac{dW}{dx} = -\frac{c}{\eta} \cdot \frac{D}{375}$$

$$\text{But} \quad D = L \cdot \frac{D}{L} = W \cdot \frac{C_D}{C_L}$$

$$\text{whence} \quad \frac{dW}{dx} = -\frac{c}{\eta} \cdot \frac{W}{375} \cdot \frac{C_D}{C_L} \quad (3.1)$$

$$\text{and} \quad dx = -375 \cdot \frac{\eta}{c} \cdot \frac{C_L}{C_D} \cdot \frac{dW}{W} \quad (3.2)$$

Integrating, putting in limits for  $W$  and multiplying by 2.3026 to reduce to common logarithms, we have

$$x = 863.5 \cdot \frac{\eta}{c} \cdot \frac{C_L}{C_D} \log_{10} \left( \frac{W_1}{W_2} \right) \quad (\text{miles}) \quad (3.3)$$

If  $x$  is to be the range while  $W_1$  and  $W_2$  are the weights of airplane with full fuel load and with tanks empty, the values of  $C_L/C_D = L/D$ ,  $\eta$ , and  $c$  must be average, which ordinarily are difficult to estimate. On the contrary the maximum  $L/D$  and  $\eta$  are known as is the minimum  $c$ . In order to obtain average values the known values must be multiplied by factors, the product of which will result in an overall reduction factor the value of which must be based primarily on experience. Tests seem to indicate for this reduction factor a value not far from 0.7 and introducing this we have for the maximum range,

$$x = 600 \left( \frac{C_L}{C_D} \right)_{mx} \frac{\eta_{mx}}{c_{mn}} \log_{10} \left( \frac{W_1}{W_2} \right) \quad (\text{miles}) \quad (3.4)$$

In practice it is difficult to maintain always the conditions for realizing the result indicated by this formula and for a so-called *service range* a further reduction may be made bringing the formula finally to

$$\text{Service Range} = 500 \left( \frac{C_L}{C_D} \right)_{mx} \frac{\eta_{mx}}{c_{mn}} \log_{10} \left( \frac{W_1}{W_2} \right) \quad (3.5)$$

b) *Endurance.* The basic equation for the derivation of Breguet's formula for endurance is similar to that for the range except that the derivative with time is used instead of distance.



Thus we have

$$\frac{dx}{dt} = V \quad \text{and} \quad dt = \frac{dx}{V}$$

If we can assume  $V$  constant or taken at some mean value, we may then integrate giving

$$t = \frac{x}{V} = \frac{\text{range}}{V}$$

From (3.3) this gives

$$t = \frac{863.5}{V} \cdot \frac{\eta}{c} \cdot \frac{C_L}{C_D} \log_{10} \left( \frac{W_1}{W_2} \right) \quad (3.6)$$

A more useful form, however, is developed by a somewhat different treatment. Thus omitting numerical factors we have from (1.5)

$$\frac{dW}{dt} = - \frac{cP}{\eta}$$

Substituting for the thrust power  $P$ , this becomes

$$\frac{dW}{dt} = - \frac{c C_D \rho S v^3}{2 \eta}$$

But for level flight we must have

$$W = \frac{C_L \rho S v^2}{2} \quad \text{or} \quad v = \sqrt{\frac{2W}{C_L \rho S}}$$

Substituting this value for  $v$  and reducing we have

$$dt = - \frac{\eta}{c} \frac{C_L^{3/2}}{C_D} \left( \frac{\rho S}{2} \right)^{1/2} \frac{dW}{W^{3/2}}$$

Integrating, putting in limits  $W_1$  and  $W_2$  and supplying the numerical factor we have

$$t = 1100 \frac{\eta}{c} \frac{C_L^{3/2}}{C_D} \left( \frac{\rho S}{2} \right)^{1/2} \left[ \frac{1}{W_2^{1/2}} - \frac{1}{W_1^{1/2}} \right] \text{ (hours)} \quad (3.7)$$

or

$$t = 1100 \frac{\eta}{c} \frac{C_L^{3/2}}{C_D} \left( \frac{\rho S}{2 W_1} \right)^{1/2} \left[ \left( \frac{W_1}{W_2} \right)^{1/2} - 1 \right] \text{ (hours)} \quad (3.8)$$

From (3.3) it will be noted that for maximum range the attitude of the plane should be such as to give a maximum value for  $C_L/C_D$  while for maximum endurance the attitude should be such as to make the ratio  $C_L^{3/2}/C_D$  a maximum. This will mean in general that for maximum endurance the plane will fly at a greater  $C_L$  than for maximum range and hence at a slower speed.

In formula (3.6) the propeller efficiency  $\eta$ ,  $C_L/C_D$  of the airplane,  $c$  the specific fuel consumption and  $V$  the speed are average values during the flight. Each of these values can be expressed in terms of the maximum or minimum values known from performance calculations, assigning to each a factor reducing it to an average value.

Thus for  $\eta_{mx}$  the factor is assumed to be 0.85, for  $(C_L/C_D)_{mx}$  the factor is taken at 0.9, and for  $c_{mn}$  at 1.2. The basic speed selected was

the minimum and its factor was taken as 1.25. All these factors are then combined into one giving an overall factor of 0.51.

Formula (3.6) thus becomes:

$$t = \frac{440}{V_{mn}} \cdot \frac{\eta_{mx}}{c_{mn}} \left( \frac{C_L}{C_D} \right)_{mx} \log_{10} \left( \frac{W_1}{W_2} \right) \quad (3.9)$$

A similar allowance in connection with formula (3.8) gives an overall factor of about 0.50. This formula then becomes

$$t = 550 \frac{\eta_{mx}}{c_{mn}} \left( \frac{C_L}{C_D} \right)_{mx} \left( \frac{gS}{2W_1} \right)^{1/2} \left[ \left( \frac{W_1}{W_2} \right)^{1/2} - 1 \right] \text{ (hours)} \quad (3.10)$$

**4. Examples.** Basic data for the examples of the range and endurance calculations are as follows:

Gross weight	= 4000 lbs.
Wing area	= 350 sq. ft.
Max. $L/D$	= 8.4
Speed, min.	= 57.2 m.p.h.
Max. engine power	= 435 hp at 2300 r.p.m.
Propeller dia.	= 8.55 ft. $\eta_{mx} = 0.81$ .
Weight of fuel carried	= 736 lbs. (664 lbs. gas, 72 lbs. oil).
Polar curve for the whole airplane	from Fig. 19.
For the curve of horsepower required	see Fig. 21.
Minimum specific fuel consumption	= 0.52 lb. per hph.

Results obtained by precise calculation of the range from Fig. 44 show:

Range, maximum = 725 miles in still air.

Using Breguet's formula for maximum range, (3.4) and substituting numerical values we find:

Range = 698 miles

If this is reduced in accordance with (3.5) we have

Service range = 582 miles.

The agreement is sufficiently satisfactory with a tendency of the reduction factor used to give a result on the safe side.

For endurance, the results of precise calculations from Fig. 46 show:

Endurance, max. = 9.1 hours.

Using the Breguet formula (3.9) and substituting numerical values we find:

Endurance, max. = 8.94 hours.

Or again using formula (3.10) with a maximum value of  $C_L^{3/2}/C_D$  of 7.65 derived from Fig. 19 we find:

Endurance, max. = 9.1 hours.

The agreement between the results obtained by precise calculations and by the short cut formula is obviously satisfactory.

## CHAPTER X

### INFLUENCE OF PRINCIPAL FACTORS ON PERFORMANCE

In studying the effects of various characteristics on the performance, it becomes evident that certain items of performance are affected more than others by a particular characteristic, and this fact must be borne in mind when designing an airplane for a predetermined purpose. Physical limitations are often present and hence permissible variations of the various factors must be well understood in order to arrive at a desirable compromise between structural and aerodynamical efficiencies.

The following paragraphs will deal in general with the effects on performance of varying one characteristic at a time. In practice, for developing highly efficient aircraft, often two or more factors must be simultaneously taken into account, although the importance of one may be only minor.

**1. Weight.** The weight is the primary characteristic of any airplane, especially in the effect of its variation on landing speed, climb, and ceiling. The decrease in climb and ceiling with increase in weight is more rapid than the ratio of weights would indicate. In general, two effects are present. The first is based directly on the relation

$$\text{Best rate of climb} = \frac{\text{Maximum Reserve Power}}{\text{Weight}} \times \text{const.}$$

By inspection, the rate is inversely proportional to the weight, assuming the reserve power unchanged. But since for a given climbing speed the heavier airplane must fly at a higher lift coefficient, which in turn, in the range of climbing speeds corresponds to a higher drag coefficient, the drag and consequently the required power are increased. As a result, the excess power decreases and thus the rate of climb is still further decreased. Strictly speaking, there is a slight increase in power available since the speed of best climb is higher with increased weight, but the net result, in spite of higher engine revolutions and propeller efficiency, is invariably a decrease in reserve power.

The exact variation of reserve power with weight cannot be expressed by a simple precise formula, since it depends on other characteristics of the airplane, such as wing loading, the shape of the polar, and the shape of the available power curve depending on the particular engine-propeller combination. Warner<sup>1</sup> gives an approximation which may be used in expressing the influence of weight on reserve power, as follows:

$$\text{Reserve Power} = 0.65 \text{ (Rated bhp.)} - \frac{W^{3/2}}{115 S^{1/2}}$$

<sup>1</sup> See p. 313 of Ref. 9.

The combined effect of the weight on the rate of climb can then be expressed, by the approximate formula:

$$\text{Best rate of climb at sea level} = \frac{21000 \times \text{Rated bhp}}{W} - 300 \left( \frac{W}{S} \right)^{1/2} \quad (1.1)$$

or

$$\text{Best rate of climb at sea level} = \frac{21000 \times \text{Rated bhp}}{W} - 300 W^{3/2} / S^{1/2}$$

The effect of weight changes on high speed is not great in the case of practical airplanes with a speed range of 2.5 or more, but in the case of underpowered aircraft with very high power loadings, the effect may be pronounced. Considering the polar of a military or commercial airplane, the lift coefficient for high speed is in the neighborhood of minimum drag, which is approximately constant in the range of high speed lift coefficients. Although the lift coefficient at high speed is changed by the weight change, practically no change in the drag or in the power required occurs. In fact it is possible that the speed may increase slightly with an increase in weight.

In the case of a *light* airplane or powered glider, the effect of weight on high speed is more pronounced. In this case the high speed occurs at rather high lift coefficients, in the range where there is considerable variation in the drag coefficient.

A direct effect of the variation in weight is noted on the landing speed or minimum speed of flight. This is expressed by the equation

$$V_{mn} = \sqrt{\frac{2W}{C_{Lmx} \times \rho S}}$$

from which it is evident that minimum speed varies directly with the square root of the weight.

For the effect on ceiling, Warner<sup>1</sup> gives an approximate formula which can be expressed as:

$$\text{Absolute Ceiling} = 120,000 \times \log_{10} \frac{V_{mx}}{W^{1/2}} \times \text{const.}$$

from which the effect of the weight on ceiling can roughly be estimated.

The effect of weight on ceiling is actually a combination of many effects and difficult of precise analysis by means of one equation. It will be found that the higher the ceiling of the normally loaded airplane, the greater percentage of overload it can carry before the ceiling is lowered to a practical minimum.

**2. Power.** The variation in the power of the engine, subject to the efficiency of the propeller, affects the different items of performance in varying degrees. The effect of a change in rated engine power on climb may be seen to depend on the equation.

$$\text{Rate of climb} = \frac{\text{Rated bhp} \times \text{efficiency} - \text{Power required}}{W}$$

<sup>1</sup> See p. 312 of Ref. 9.

The rate increases more rapidly than the rated bhp, because it depends on the increase of the reserve power which is the difference between power available and required. The smaller this initial difference, the greater the effect on climb of an increase in rated power, assuming power required and propeller efficiency to be unchanged.

An increase in power affects the high speed of a conventional airplane in proportion to the cube root of the power change. Denote high speed by  $V$ . Then,

$$\left. \begin{aligned} \frac{\bar{V}_2}{\bar{V}_1} &= \left( \frac{P_2}{P_1} \right)^{1/3} \text{ for conventional airplanes.} \\ \frac{\bar{V}_2}{\bar{V}_1} &> \left( \frac{P_2}{P_1} \right)^{1/3} \text{ for underpowered airplanes.} \end{aligned} \right\} \quad (2.1)$$

The reason for the difference in these two cases is based on the same arguments discussed in the paragraph on weight as affecting high speed. Minimum speed is practically unaffected by variations in the power.

Ceiling as affected by power may be calculated from Warner's approximate formula<sup>1</sup> in terms of maximum and minimum speeds.

$$\text{Ceiling } H = 120,000 \log_{10} \frac{V_{mx}}{1.6 V_{mn}} \quad (2.2)$$

Then if we put

$H_1$  and  $\bar{V}_1$  = ceiling and high speed with power  $P_1$

$H_2$  and  $\bar{V}_2$  = ceiling and high speed with power  $P_2$

$V_{mn}$  = low speed in each case

and express by (2.2) the ratio of  $H_2$  to  $H_1$  and then reduce by the aid of (2.1) we find

$$\frac{H_2}{H_1} = 1 + \frac{\log_{10} (P_2/P_1)}{3 \log_{10} (V_1/1.6 V_{mn})} \quad (2.3)$$

This equation is also readily put in the form

$$H_2 - H_1 = 40,000 \log_{10} (P_2/P_1) \quad (2.4)$$

**3. Wing Area.** An increase of wing area reduces both high and low speeds and results in an increase in rate of climb and ceiling, provided in this case, that the span of the wing has increased.

The increase in climb, and hence ceiling, is due to the fact that in this range of speeds the induced drag is of greater importance and decreases as the square of the equivalent monoplane span loading. There is, of course, a concomitant increase in skin frictional resistance as the area is increased, but this effect is overshadowed by the decrease in induced drag. Reference to (1.1) for rate of climb indicates how this is affected by changes in area.

The minimum speed varies inversely as the square root of the wing area, except as this is modified slightly by the increase in  $W$  due to increase in  $S$ .

<sup>1</sup> Loc. cit.

**4. Span of Equivalent Monoplane.** The effect of a change in equivalent monoplane span (denoted by E.M.S.) is most important in the range of take-off and climbing speeds. Assuming the area unchanged, the result is an increase or decrease in span loading. The induced drag and the horsepower required to overcome it vary directly as the square of the span loading. The effect of an increase in equivalent monoplane span is to increase the rate of climb and ceiling, with no effect on high speed, except near the ceiling. The exact effect on climb and ceiling is again complicated, depending as it does on a change in only a portion of the drag and hence power required. The simplest way to determine the effect at a given climbing speed is to compute the horsepower corresponding to the induced drag for the two cases by the equation:

$$P\Big]_{Di} = \frac{D_i v}{550} = \frac{2}{550 \pi q v^2} \left( \frac{W}{\text{E.M.S.}} \right)^2 v \text{ (ft. lb. sec.)}$$

Putting 1.467  $V$  for  $v$  ( $V$  in m.p.h.) and reducing, we have

$$P\Big]_{Di} = \frac{1}{3V} \left( \frac{W}{\text{E.M.S.}} \right)^2 \quad (4.1)$$

The difference will also be the change in reserve power and the new rate of climb can be quickly calculated.

The disadvantages of large spans are mainly structural. There is also an increased lateral inertia of the wings, and increased damping in roll and yaw and hence a decrease in maneuverability.

Extremely large aspect ratios, *i. e.*, small span loading, are used on competition gliders where large lift drag ratios are essential in order to reduce sinking velocities. Moderately large aspect ratios are used on power gliders and light airplanes, thus decreasing the induced drag in the flying range of fairly high lift coefficients. The limited power of such aircraft does not permit them to fly at low lift coefficients where the induced drag and therefore the span loading does not play an important part. High aspect ratios are also indicated for airplanes which are to operate at high altitudes. Due to lack of power, they must fly at high angles of attack and lift coefficients, where induced drag is predominant.

**5. Airfoil Characteristics.** Although thousands of airfoils have been tested in scores of tunnels with different model sizes, different turbulence characteristics, different wall effects, etc., the selection of an airfoil has been limited from experience to choice between perhaps a score of well known sections.

Except for the fact that landing speed varies inversely as the square root of the maximum lift coefficient, we are concerned chiefly with the curve of profile drag versus lift coefficient, since induced drag is not at all affected by a change in airfoil section. Most of the well known and commonly used sections have fairly low values of profile drag coefficient in the flying range. Since at climbing speed the induced drag is predominant, and at high speed the structural parasite drag, the influence

of a change in profile drag is generally of little concern. Exceptions are in the case of racers, where the parasite resistance is comparatively low, and in gliders, where a high profile drag coefficient at low or negative lift coefficients may be desired in order to limit the diving speed.

A few general rules for the selection of an airfoil can be formulated as follows:

1) Thin and double cambered airfoils are used on racing and pursuit airplanes with low power loading, where low landing speed and high ceiling may be sacrificed.

2) Airfoils of medium thickness and camber are used on present day commercial and military aircraft where general all around good performance is desired.

3) Thicker and highly cambered airfoils are used on heavily loaded aircraft where low landing speeds are desired and high speed can be sacrificed.

**6. Parasite Resistance.** A change in parasite resistance has no effect on the landing speed, affects the climb and ceiling to a moderate extent, and has its greatest influence on high speed. If profile drag of the wings is included in parasite resistance the effect of a change in the latter on high speed is shown approximately by an equation in the form,

$$V = \sqrt[3]{\frac{K}{C_{Di} + C_{Dp}}}$$

When it is considered that induced drag is negligible at high speed, we see that practically the speed varies inversely as the cube root of the parasite drag coefficient, or of the equivalent flat plate area.

At climbing speeds, although the induced drag is predominant, an increase in parasite drag results in a decrease in climb and ceiling. The effect on climb is shown by the following equations:

$$\text{Rate} = (P_a - P_r) \frac{33000}{W} \quad (6.1)$$

$$P_r = \frac{1}{3V} \left( \frac{W}{b} \right)^2 + \frac{0.00327 A V^3}{375} \quad (6.2)$$

where  $b$  = span [see (4.1)] and the second term represents all items of resistance except  $D_i$ , expressed in terms of equivalent flat plate area  $A$ . Putting (6.2) in (6.1) we have

$$\text{Rate} = \frac{33000 P_a}{W} - \frac{11000 W}{b^2 V} - \frac{0.288 A V^3}{W}$$

From this equation it is clear that the decrease in the rate of climb, the climbing speed remaining constant, is a linear function of the increase in equivalent flat plate area of parasite resistance.

**7. Propeller Characteristics.** There are in general two types of suitable propellers, the propeller designed for maximum efficiency at high speed

and the propeller designed for best climbing results. Since the high speed propeller will deliver less power at lower speeds, high speed will be obtained at the expense of climbing ability. The propeller designed for best climb will permit the engine to turn at too high an r.p.m. at high speed, and throttling will be necessary if rated r.p.m. is not to be exceeded. This will of course adversely affect the high speed. The ideal propeller is one with its pitch controllable in flight. In this case the diameter is chosen at that desirable for high speed, then at climbing speeds the pitch is decreased so that the r.p.m. is maintained.

The propeller material effects the performance in that metal propellers with their thinner sections are about 5 per cent more efficient than wooden propellers, especially in the high speed range.

In special cases the propeller is designed for high altitudes, in which case the resultant large diameter and high pitch setting do not permit the engine to develop full power at low altitudes, and therefore there results a decrease in performances at these altitudes.

**8. Supercharging and Throttling.** Both supercharging and throttling of an engine affect the amount of charge admitted to the cylinder during a working cycle, the former increasing it by forcing the intake air to the carburetor after pre-compression, and the latter decreasing it by restricting the intake air passage.

In general, the effect of supercharging is to improve rates of climb, high speeds at altitudes and the ceiling. The effect of a power increase has been discussed in 2.

**9. Choice of Altitude Propeller.** In order to realize benefit from supercharging of the engine, it is necessary that the propeller be properly designed for high altitude conditions. A propeller designed for the usual low altitude conditions and an unsupercharged engine would be worthless with a supercharged engine at altitude. For determining the propeller characteristics for good altitude performance, the following procedure may be used.

a) Determine the altitude at which the maximum performance is to be expected. This is generally the rated altitude of the supercharger. Note the corresponding density ratio.

b) Determine the engine power at rated r.p.m. at the altitude selected. A number of tests on planes with supercharged engines, both turbine and geared, indicate a gradual decrease of engine power with altitude at the rate of about one per cent per 1000 feet altitude up to about 20,000 feet and with a rate of decrease above this level of about twice this figure.

For altitudes up to 35,000 feet, and with superchargers of the character employed in these tests, the percentage of sea level rated power may therefore be taken approximately as in the following table:



Altitude	Percentage
.000	100
5,000	95
10,000	90
15,000	84
20,000	78
25,000	67
30,000	56
35,000	44

c) Compute a fictitious power which would be absorbed by the altitude propeller at sea level at rated r.p.m.

$$HP_0 = HP_{alt} \times \frac{1}{\sigma}$$

d) Estimate high speed at altitude and determine the propeller diameter, using the fictitious  $HP_0$  with any approved method of design.

e) Determine the design  $v/nD$ , efficiency and available power at the basic altitude selected, by the methods of II 9—12.

f) Available power at higher altitudes is then computed by the method of II 12 except that the basic altitude selected is considered as sea level and the altitude density ratios are taken with respect to the density at the basic altitude.

g) The power available from an altitude propeller at sea level, can be approximated as that of a propeller designed for sea level conditions for an engine of 5/6 the rated power at 90% of the rated r.p.m. If more accurate results are desired, the propeller power coefficients  $C_p$  versus  $v/nD$  must be obtained and power absorbed at various velocities and r.p.m.'s determined.

**10. Power Absorbed by Any Propeller.** The power absorbed by any propeller is expressed by the equation,

$$HP_{abs} = \frac{C_p n^3 D^5 \sigma}{232,000}$$

where  $C_p$  is the power coefficient depending on  $v/nD$  and the design characteristics of the propeller. The determination of the power coefficient when the diameter is known is carried out as shown in Table 28, wherein is given a computation for an altitude propeller designed for the example airplane specified in III 5, but with a supercharged engine. It is convenient to determine at the same time the efficiency and power available for subsequent use. From data in Table 28, the graph of Fig. 47 may be drawn.

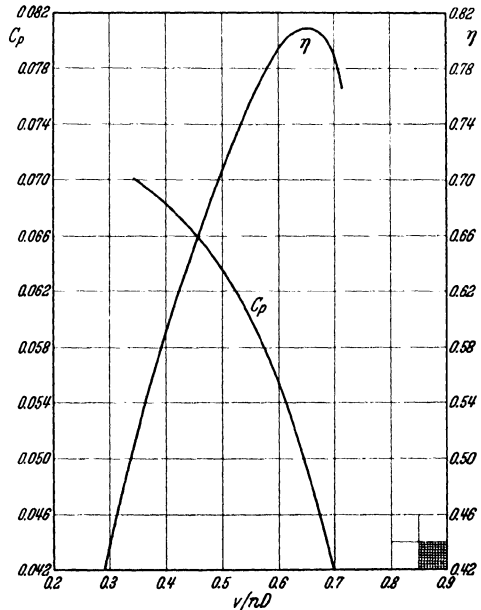


Fig. 47. Characteristics of altitude propeller for supercharged engine developing 340 hp. @ 2300 r.p.m. @ 20,000 ft.

TABLE 28. Determination of Power Coefficient and Efficiency.

$V$	% des. $V$	% des. $N$	$N$	BHP S.L.	BHP Alt.	$n$ r.p.s.	$v/nD$	% des. $v/nD$	% $\eta_{\max}$	$C_p$	$\eta$	HP Av. 20,000 Ft.
1	2	3	4	5	6	7	8	9	10	11	12	13
70	46.7	87	2000	397	310	33.3	.348	53.25	64	.0672	52.0	161
80	53.3	87	2000	397	310	33.3	.398	61.2	72.5	.0672	58.7	182
90	60	88	2025	401	313	33.75	.442	68.0	79.5	.0651	64.3	201
100	66.6	89	2050	405	316	34.18	.485	74.6	85.6	.0632	69.4	219
110	73.2	90.5	2080	410	320	34.68	.526	81.0	91	.0614	73.7	236
120	80	92.5	2130	417	326	35.5	.560	86.2	94.5	.0583	76.5	249
130	86.5	95	2180	423	330	36.32	.592	91.1	97.5	.0553	79.0	261
140	93.4	97	2240	430	336	37.32	.622	95.7	99.3	.0519	80.5	270
150	100	100	2300	435	340	38.32	.650	100.0	100	.0488	81.0	275
160	106.7	103	2370	439	343	39.5	.672	103.4	99.5	.0445	80.6	277
170	113.3	105.5	2430	445	347	40.6	.695	107.0	98	.0415	79.5	276
180	120	109	2510	446	348	41.9	.713	110.0	96	.0380	77.8	271

Column 3 is from Fig. 12.

Column 10 is from Fig. 13.

bhp at 20,000 ft. =  $435 \times 78\% = 340$  HP at 2300 r.p.m.

$$C_p = \frac{\text{bhp} \times 231000}{n^3 \times D^5 \times \sigma} = \frac{\text{bhp} \times 231000}{n^3 \times 8.85^5 \times .532} = 8.00 \frac{\text{bhp}}{n^3}$$

The power absorbed by the propeller at any altitude is computed according to the tabulation in Table 29, where the power at sea level is taken as example. In this case the density ratio is unity, but the same procedure is followed for any altitude by inserting the proper value of

TABLE 29. Power Absorbed at Sea Level by an Altitude Propeller.

Design values = 340 hp; 2300 r.p.m.; 20,000 ft.;  $D = 8.85$  ft.;  $v/nD = .65$ ;  $\eta_{mx} = 81\%$ .

	R.P.M. R.P.S. (R.P.S.) <sup>a</sup>	( <i>N</i> ) ( <i>n</i> ) ( <i>n</i> <sup>3</sup> )	1600/318 hp 26.67 18,850		1700/339 hp 28.32 22,700		1800/358 hp 30.0 27,000		1900/378 hp 31.55 31,400		2000/397 hp 33.33 37,000	
<i>v/n D</i>	<i>C<sub>p</sub></i>	<i>η</i>	<i>V</i> <sub>m.p.h.</sub>	HPab	<i>V</i>	HPab	<i>V</i>	HPab	<i>V</i>	HPab	<i>V</i>	HPab
.35	.0683	52	56	307	60	370	63.5	440				
.4	.0682	59	64.2	300	68.3	362	90.5	396				
.5	.0637	71	80.5	276	85.5	331	108.5	352				
.6	.0553	79.5		246	102.5	295	117.5	312	114.5	421	120.5	466
.65	.0493	81							124	374	130.5	414
.7	.042	79							134	310	141	354

$$\text{HP absorbed at sea level} = \frac{C_p n^3 D^5 \sigma}{232,000} = .234 C_p n^3 \quad v/nD = \frac{V}{N} \times \frac{88}{8.85} = 9.96 \frac{V}{N}$$

density ratio  $\sigma$  in the equation for absorbed power. The purpose of the system shown in Table 29 is to cover only useful ranges, i. e., within the range of brake horsepower available. Since the power absorbed by a propeller is independent of the engine power and r.p.m., it is somewhat

difficult to predict which coincident values of r.p.m.,  $v/nD$ , and  $C_p$  should be chosen, but a few trials will soon indicate the proper values for heading the columns in the table.

**11. Power Available at Sea Level from Special Propeller.** The determination of the power available from a given engine and propeller for a condition for which the propeller was not designed, consists of two steps. First must be determined the forward speeds at which the power absorbed by the propeller at a given altitude at a certain r.p.m. is equal to the engine power at the same r.p.m. A graphical solution is made

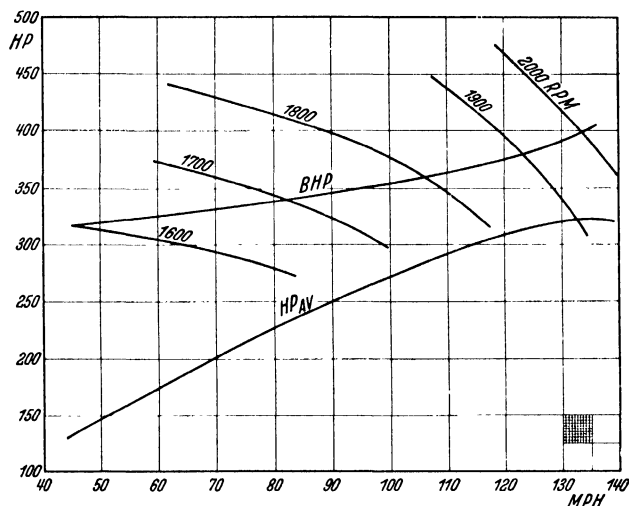


Fig. 48. Performance curves for supercharged engine with altitude propeller.

in Fig. 48 where absorbed power versus speed is plotted from Table 29 for different values of r.p.m. The engine power at the same r.p.m. is then spotted on these curves and a curve of engine brake horsepower obtained.

The second step is the determination of power available from the engine propeller group. Table 30 (p. 324) shows how  $V$  is tabulated from Fig. 48, and how it is combined with r.p.m. and diameter to determine  $v/nD$  and efficiency. The resultant horsepower available is plotted in Fig. 48.

**12. Example.** The steps in the calculation of power available from a supercharged engine with an altitude propeller are as follows:

1) Determination of propeller diameter, design  $v/nD$ , and maximum efficiency.

Propeller designed for 20,000 Ft.

Engine: 435 HP at 2300 r.p.m. at sea level (see III 7 and Fig. 20).

TABLE 30. Brake Horsepower and Power Available

From Fig. 48	R.P.M. $V$ (m.p.h.)	1600 45				1700 82			
		$v/nD$	$\eta$	BHP	HP <sub>av</sub>	$v/nD$	$\eta$	BHP	HP <sub>av</sub>
		.28	.39	318	124	.48	.684	339	232

Altitude 20,000 Ft.  $\sigma = .532$  (Table 4).

Power at 20,000 Ft. at all r.p.m. is 78% sea level (Ref. 10).

BHP @ 20,000 Ft. =  $.78 \times 435 = 340$  hp at 2300 r.p.m.

Estimated efficiency = 80%.

HP<sub>av</sub> first approximation = 272.

Probable high speed at 20,000 Ft. = 150 m.p.h.

Fictitious sea level power =  $272/.532 = 511$  hp

Diameter (511 bhp;  $N = 2300$ ;  $V = 150$  m.p.h.) = 8.85 ft.<sup>1</sup>

$$\text{Design } v/nD = \frac{150 \times 88}{2300 \times 8.85} = 0.65.$$

Efficiency max = 81%.

2) Determination of power coefficient and efficiency as in Table 28 and Fig. 47.

3) Determination of power absorbed as in Table 29 and Fig. 48.

4) Determination of power available as in Table 30 and Fig. 48.

## CHAPTER XI

### LIMITS OF PERFORMANCE

**1. Speed Range.** The present day airplane is considered the most economical type of heavier-than-aircraft. Its ultimate performance is limited to certain ranges depending on the limitations of the various separate factors on which the performance is dependent. Keeping in mind the contemporary development of aerodynamics, assuming no radical advance in engine design, the item of performance which will be most difficult to improve is the speed range.

It may be pointed out here that the Autogiro possesses a speed range which cannot be approached in the design of an airplane. But this desirable feature is now obtained in the Autogiro at the expense of cruising speed which is inferior to that of an airplane of the same weight and power.

A speed ratio of three is seldom exceeded at present in an airplane, and no appreciable increase would result even from a considerable

<sup>1</sup> Any approved method of design based on these three data may be employed. See Ref. 4.

at Sea Level. Engine-Altitude Propeller Combination.

1800 106				1900 123.5				2000 133.5			
$v/nD$	$\eta$	BHP	HPav	$v/nD$	$\eta$	BHP	HPav	$v/nD$	$\eta$	BHP	HPav
.588	.786	358	282	.647	.81	378	306	.662	.81	397	322

increase in power. This present limitation is due to the operation of no single factor, but is rather the inevitable result of the combination of all the factors existing in a practical airplane. The value of the speed ratio of an airplane may be considered a good indication of the designer's skill in compromising the available means and requirements to the best advantage.

Taking into account the present available knowledge of the aerodynamic characteristics of airfoils and streamlined bodies, of engine power available for a given engine weight and of the unit weights of structural components, it is possible to calculate the speed range within the practical limitations of these factors. Conversely, to attain higher speed ranges, it is possible to indicate what advances in these factors are necessary. Ref. 15 deals in greater detail with limiting factors.

Conditions which limit the speed range are:

- a) maximum lift coefficient and minimum drag of the airplane,
- b) the combination of airfoil and fuselage with a view to securing minimum drag at high speed,
- c) the wing loading governing a landing speed consistent with the maximum lift coefficient, and
- d) the power loading consistent with a practical structural weight.

It is noted that neither the size, weight, nor power is considered as a limiting factor, but rather a practical combination of the three.

The fundamental equations used in establishing limits (at sea level) are,

$$P (\text{THP in ft. lb. per sec.}) = (1/2) \rho C_{Dmn} S v_{mx}^3 \quad (1.1)$$

$$L \text{ at minimum speed} = W = 1/2 \rho C_{Lmx} S v_{mn}^2 \quad (1.2)$$

Putting numerical values in (1.1) and (1.2) and reducing to hp units and miles per hour, we have

$$V_{mx} = \frac{52.7}{C_{Dmn}^{1/3}} \left( \frac{PT}{S} \right)^{1/3} \quad (1.3)$$

$$V_{mn} = \frac{19.8}{C_{Lmx}^{1/2}} \left( \frac{W}{S} \right)^{1/2} \quad (1.4)$$

Assumptions at this point as to  $C_{Lmx}$  and  $C_{Dmn}$  reduce the latter equations to much simpler form.  $C_{Lmx}$  is taken at 2.5, an extremely high value undoubtedly necessitating the use of flaps or flaps and auxiliary airfoils. An alternative value of 1.5 is assumed as attainable with an ungarnished airfoil.

$C_{Dmn}$  is taken as from 0.01 to 0.07. The value of 0.01 would correspond to a flying wing. For any other airplane,

$$C_{Dmn} = \frac{1.28A}{S} + 0.01$$

where  $A$  is the equivalent flat plate area as defined in Chapter II. Substituting the above values in (1.3) and (1.4) we have, for examples,

$$V_{mx} = 245 \left( \frac{P_T}{S} \right)^{1/3} \text{ for } C_{Dmn} = 0.010 \quad (1.5)$$

$$V_{mn} = 12.6 \left( \frac{L}{S} \right)^{1/2} \text{ for } C_{Lmx} = 2.5 \quad (1.6)$$

Dividing (1.3) by (1.4), we obtain limiting values of speed range in the

$$\text{form: } \frac{V_{mx}}{V_{mn}} = K \left( \frac{S}{L} \right)^{1/2} \left( \frac{P_T}{S} \right)^{1/3} = K \left( \frac{S}{W} \right)^{1/2} \left( \frac{P_T}{S} \right)^{1/3} \quad (1.7)$$

where  $K = 2.665 (C_{Lmx}^{1/2}/C_{Dmn}^{1/3})$  and may have values as below.

Values of $K$ .			
$C_{Lmx}$	$C_{Dmn}$		
	0.010	0.035	0.070
2.5	19.4	12.8	10.16
1.5	15.2	10.00	7.95

Assuming a permissible landing speed of 70 m.p.h. the wing loading limit is set by  $C_{Lmx}$ . Taking  $C_{Lmx} = 2.5$ , the maximum wing loading is then 30 lbs./sq. ft. For simplicity we will assume the same limiting loading of 30 when  $C_{Lmx} = 1.5$ , which gives an extreme landing speed of 88.5 m.p.h. The lower limit of wing loading is arbitrarily assumed as 4 lbs./sq. ft., corresponding to minimum landing speeds of 25.0 and 32.4 m.p.h. for  $C_{Lmx} = 2.5$  and 1.5 respectively.

Substituting  $L = 30 S$  in (1.7) we have, for example

$$\frac{V_{mx}}{V_{mn}} = \frac{K}{5.48} \left( \frac{P_T}{S} \right)^{1/3} \quad (1.8)$$

Setting  $K(S/W)^{1/2} = C$ , we can construct a table of  $C$  values corresponding to the equation

$$\frac{V_{mx}}{V_{mn}} = C \left( \frac{P_T}{S} \right)^{1/3}$$

where

$$C = 2.665 \frac{C_{Lmx}^{1/2}}{C_{Dmn}^{1/3} (W/S)^{1/2}} \quad (1.9)$$

Values of $C$ .						
$C_{Lmx}$	$C_{Dmn}$					
	0.010		0.035		0.070	
2.5	3.57	9.77	2.36	6.45	1.87	5.12
1.5	2.78	7.60	1.83	5.00	1.45	3.97
	$L/S = 30$	$L/S = 4$	$L/S = 30$	$L/S = 4$	$L/S = 30$	$L/S = 4$

The value of  $P_T/S$  is dependent indirectly on the power plant and structural weight, and directly on the engine power and propeller effi-

ciency at high speed. Assumptions of power loading limits can be made by disregarding the propeller efficiency and taking the thrust power loading to vary from 4 to 25 lbs. per hp. Then,

$$\frac{P_T}{S} = \frac{P_T}{W} \cdot \frac{W}{S} \quad (1.10)$$

and 
$$\frac{V_{mx}}{V_{mn}} = C \left( \frac{P_T}{W} \cdot \frac{W}{S} \right)^{1/3} \quad (1.11)$$

If the table for  $C$  is not used, and the values of  $C_{Lmx}$  and  $C_{Dmn}$  are known, (1.11) may be written as

$$\frac{V_{mx}}{V_{mn}} = 2.665 \left( \frac{S}{W} \right)^{1/6} \cdot \left( \frac{P_T}{W} \right)^{1/3} \cdot \frac{C_{Lmx}^{1/2}}{C_{Dmn}^{1/3}} \quad (1.12)$$

An inspection of this equation shows that the main factor affecting speed range is the maximum lift coefficient. Less influential but still important are the weight per horsepower and the minimum drag. Not the least important is the wing loading, and since the latter indirectly affects the minimum drag its effect on airplanes of given structural drag is actually greater than the equation would indicate, since the lower the wing loading the lower the minimum drag coefficient. Equation (1.12) has been plotted in Figs. 49 and 50 for values of  $C_{Lmx}$  of 2.5 and 1.5 respectively.

Analyzing these figures, the maximum speed range within limits of power loading 4, wing loading 4, and  $C_{Dmn} = 0.010$ , is 9.77. Such an airplane would consist of a wing of low drag characteristics, retracted landing gear, no fuselage or tail, and with flaps and slots to attain the high  $C_{Lmx}$  of 2.5. Since in this case  $A$  is taken as zero, it is doubtful if such a machine can ever be built, because some sort of empennage would

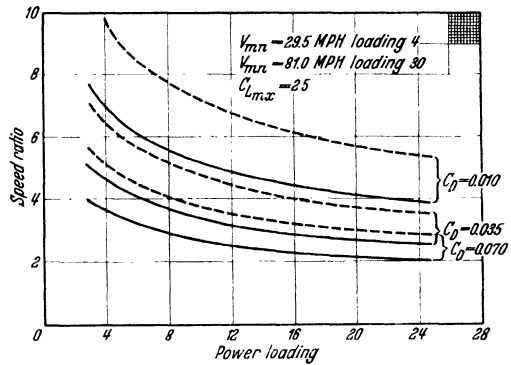


Fig. 49. Speed range.  
Dotted lines = loading 4. Full lines = loading 30.

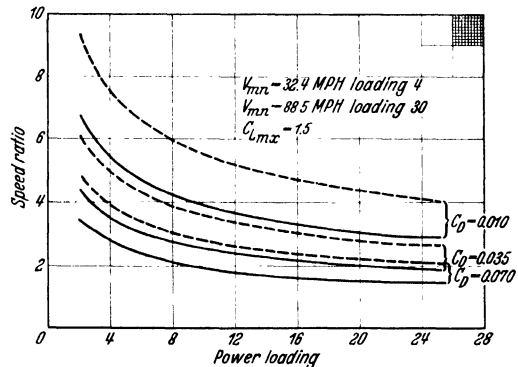


Fig. 50. Speed range.  
Dotted lines = loading 4. Full lines = loading 30.

be necessary to provide stability. Furthermore, the use of auxiliary airfoils and flaps in order to attain the high  $C_{Lmx}$  would undoubtedly have an extremely adverse effect on the assumed  $C_{Dmn}$ .

The lowest drag coefficient attainable in a commercial airplane is probably .03 with a maximum lift coefficient of 1.2, which together with a wing loading of 4 and a possible power loading of 4, would result in a more reasonable practical limiting speed ratio of 4.7.

**2. High Speed.** The conditions for limiting high speed are closely associated with those for limiting speed range treated in the above paragraphs. The limiting speed may be considered as dependent on the value of  $A$ , on the weight per horsepower of the power plant, and on the minimum permissible speed. Equation (1.3) may

be written 
$$V_{mx} = 52.7 \sqrt[3]{\frac{W/S}{(W/P_T) C_{Dmn}}}$$

in which  $W/S$ , in accordance with (1.4) will determine the landing speed.

If we assume that the most powerful power plant which will fit into the nose of a fuselage suitable for housing a pilot develops 2300 horsepower, that the landing gear will be retracted, that  $A$  cannot be reduced below a value of 1 sq.ft., that the landing speed will be limited to 100 m.p.h., that in order to realize a profile drag coefficient of the wing alone of 0.009 no auxiliary landing devices will be fitted and hence  $C_{Lmx}$  will not exceed 1.25, and that the weight per thrust horsepower can be reduced to 2.4, we may compute  $V_{mx}$  as follows:

$$\begin{aligned} \frac{W}{S} &= 32 \\ \frac{W}{P_T} &= \frac{W}{\eta P} = 2.4 \\ W &= 2.4 \times 0.80 \times 2300 = 4420 \\ S &= \frac{4420}{32} = 138 \\ C_{Dmn} &= \frac{1.28 \times 1}{138} + 0.009 = 0.01827 \\ V_{mx} &= 474 \text{ m.p.h. (under sea-level conditions).} \end{aligned}$$

If it were possible to increase  $C_{Lmx}$  to 1.75 without increasing  $C_{D0}$  of the wing alone to more than 0.01, we will find that  $S$  becomes 99,  $C_{Dmn}$  becomes 0.0229 and  $V_{mx}$  increases to only 491 m.p.h.

In the above computations, it has been further assumed that any reduction in values of  $C_{Dmn}$  due to scale effect at these high speeds is offset by an increase due to the compressibility of the air.

If the power plant above is assumed to be supercharged without any increase in weight or resistance,  $V_{mx}$  at the attitude at which sea level power is maintained will be  $\sqrt[3]{1/\sigma} V_{mx}$  at sea level.



**3. Initial Rate of Climb.** In determining the limits of rate of climb it is convenient to derive a simple formula for rate of climb in which the various factors involved appear quite clearly. As previously noted, the rate of climb is a complex function of the characteristics of the airplane and of the engine-propeller group. A simplification can be made by taking the speed and power available at the best climbing rate as a definite function of the speed and power at high speed. There is a slight variation with speed range, but this can readily be introduced.

A considerable number of flight tests of military airplanes has established the fact that for airplanes with a speed range of 3 the climbing speed is 57 per cent, and with a speed range of 2 is 63 per cent of the high speed. Expressing this variation as a linear function, we get for the speed at best climb,

$$V_c = \left(0.75 - 0.06 \frac{V_{mx}}{V_{mn}}\right) V_{mx} \quad (3.1)$$

The power required is then,

$$P_{Tr} = \frac{W V_{mx} (0.75 - 0.06 V_{mx}/V_{mn})}{375 L/D} \quad (3.2)$$

where  $L/D$  is the value at climbing speed, and may be taken approximately as the maximum  $L/D$  of the airplane.

The horsepower available at best climbing speed has been found from many flight tests to average 76 per cent of the power available at high speed. This constant may be introduced with but small error, and we may write,

$$P_{Ta} \text{ (best climb)} = 0.76 P_{Ta} \text{ (high speed)} \quad (3.3)$$

The rate of climb is

$$R_c = \frac{33\,000}{W} (P_{Ta} - P_{Tr}) \text{ (ft. per mt.)} \quad (3.4)$$

Substituting from (3.2) and (3.3) this gives

$$R_c = \frac{25,000}{W/P_{Ta} \text{ (high speed)}} - \left[66 - 5.3 \frac{V_{mx}}{V_{mn}}\right] \frac{V_{mx}}{(L/D)_{mx}} \quad (3.5)$$

The prime importance of power loading is clearly shown by this equation. The effect of high speed is not great, since its higher values are generally accompanied by higher values of  $(L/D)_{mx}$ . The effect of speed range within the limits attainable at present, is also seen to be small.

Using, for example, the hypothetical airplane of 2 we obtain, for the limiting rate of climb, by substitution in (3.5),

$$\begin{aligned} R_c &= \frac{25,000}{2.4} - (66 - 5.3 \times 4.74) \frac{474}{15} \\ &= 10,400 - 1300 = 9100 \text{ ft. per mt.} \end{aligned} \quad (3.6)$$

In the above solution  $(L/D)_{mx}$  has been estimated at 15. However an increase of 33-1/3 per cent to 20 results in only a 4 per cent increase in

rate of climb. It can furthermore be shown that an increase in speed ratio of 50 per cent also results in only a 4 per cent increase in rate. In the example cited, the second term reduces the first by only 12.5 per cent.

From (3.1) the speed along the climbing path would be,

$$R_c = (0.75 - 0.06 \times 4.74) 474 = 220 \text{ m.p.h.}$$

The angle of climb would be  $28^\circ$  corresponding to a sine of 0.470.

The foregoing calculations are based on the assumption that the propeller is of usual design, that is, for maximum efficiency at high speed. Experience shows that if a "climbing" or controllable-pitch propeller<sup>1</sup> is fitted, the first term may be increased by 25 per cent, and the second term may be reduced 15 per cent, to take into account, respectively, the increase in power available, and the decrease in power required. The latter correction is necessary because the design of the "climbing" propeller will result in best climb at a lower speed more closely approximating the speed of minimum power required. Modifying (3.6) in this manner we have,

$$\begin{aligned} R_c &= 1.25 (10,400) - 0.85 (1300) \\ &= 11,900 \text{ ft. per mt.} \end{aligned}$$

Rates of the above magnitude may be considered as optimistic limits in the light of present knowledge and calling for considerable improvement in aerodynamic, structural, and engine-propeller group characteristics.

**4. Absolute Ceiling.** The maximum absolute ceiling will be reached by an airplane fitted with an ideal supercharger by means of which the engine power will be maintained at all altitudes, and with a propeller designed to give maximum efficiency at the limiting ceiling. The horsepower available will then be,

$$P_a = \text{bhp} \times \eta = \text{thp} \quad (4.1)$$

The required power at the limiting altitude will be taken as the minimum power at sea level increased in the ratio  $\sqrt{\rho_0/\rho}$  to take account of the effect of change of density. This is justified by the consideration that the ceiling will be reached with the airplane at, or nearly at, the corresponding attitude. Furthermore it will be assumed that this attitude will be that at which maximum  $L/D$  occurs, the resultant error being negligible and giving conservative results.

$$P_{r0} (P_r \text{ at sea level}) = \frac{W}{(L/D)_{mx}} \cdot \frac{V_{mp}}{375} \quad (4.2)$$

where  $V_{mp}$  is the speed of minimum power required at sea level.  $V_{mp}$  can be expressed in terms of wing loading and the lift coefficient corresponding to maximum  $L/D$  as follows, see (1.4)

$$V_{mp} = \frac{19.8}{\sqrt{CL}} \sqrt{\frac{W}{S}} \quad (4.3)$$

<sup>1</sup> See Ref. 21.

Then for the horsepower required at altitude, we have

$$(P_r \text{ at altitude}) = \frac{0.0528W}{(L/D)_{mx}} \sqrt{\frac{W}{S}} \frac{1}{\sqrt{C_L}} \left( \frac{\rho_0}{\rho} \right)^{1/2} \quad (4.4)$$

Equating horsepower available (THP) and required, we find,

$$\left( \frac{\rho_0}{\rho} \right) = 358 C_L \frac{S}{W} \left( \frac{L}{D} \right)_{mx}^2 \cdot \left( \frac{\text{THP}}{W} \right)^2 \quad (4.5)$$

Applying this formula to a hypothetical airplane with thrust power loading of 10, wing loading of 10 and  $L/D_{mx}$  of 10.4, and assuming the corresponding lift coefficient as 0.70, we have

$$\frac{\rho_0}{\rho} = \frac{358 \times 0.70 \times 10.4^2}{10 \times 10^2} = 28.4$$

and the relative density at the ceiling is  $\rho/\rho_0 = 0.0352$ . Using the formulas in Ref. 7, we find this ceiling to be 80,600 ft. The chosen values of power and wing loading are relatively high, but in view of the structural requirements of a cabin suitable at such an altitude, and the inordinately high performance required of the supercharger, these values are probably not unduly conservative. At any rate, the above example, which must be understood to yield a result based on assumptions which cannot be met in practice, shows the tremendous effect on the ceiling of the normal decrease in power when a supercharger is not fitted, since in this case the ceiling would be only about 18,000 ft. A more practical limit will be derived later.

For the unsupercharged engine, the above formulas are considerably altered. Assuming the propeller designed for best efficiency at normal sea level engine speed, the available power at altitude can be written:

$$P_{ah} = P_{a0} \left( \frac{\rho}{\rho_0} \right)^{1.4} = \frac{W}{W/P_{a0}} \left( \frac{\rho}{\rho_0} \right)^{1.4} \quad (4.6)$$

Equating this to the horsepower required as in (4.4), and solving for  $(\rho_0/\rho)^{1.9}$  we have

$$\left( \frac{\rho_0}{\rho} \right)^{1.9} = 18.9 \left( \frac{L}{D} \right)_{mx} \cdot \left( \frac{1}{W/P_{a0}} \right) \cdot \left( \frac{C_L}{W/S} \right)^{1/2} \quad (4.7)$$

Substituting in this equation the values for the example of III 6 ( $W/P_{a0} = 7.35$ ,  $W/S = 11.42$ ,  $(L/D)_{mx} = 8.48$  and  $C_L$  at  $(L/D)_{mx} = 0.7$ ) and solving for  $\rho/\rho_0$  we find the value 0.411 which, by Table 4, corresponds to an altitude of 27,000 ft., whereas the actual ceiling is only 18,600 ft.

This discrepancy is due to a twofold engine-propeller effect. First, the engine speed at the ceiling is less than at sea level, and second, the efficiency of the propeller is less because it is operating at a value of  $v/nD$  lower than that of maximum efficiency. This combined effect can be approximated by introducing a reduction factor  $F$  which can be shown to depend on the speed range, as follows:

$$F = \frac{1.42}{\text{Speed range}} = \frac{1.42}{r} \quad (4.8)$$

The modified equation (4.7) then becomes

$$\left(\frac{\rho_0}{\rho}\right)^{1.9} = \frac{26.9}{r} \left(\frac{L}{D}\right)_{mx} \cdot \left(\frac{1}{W/P_{a0}}\right) \cdot \left(\frac{C_L}{W/S}\right)^{1/2} \quad (4.9)$$

Applying this formula to the example airplane, where  $r = 2.55$ , we find the relative density  $\rho/\rho_0 = 0.56$  corresponding to an altitude of 18,600 ft. which checks the value obtained in III 8.

Substituting in (4.9) the probable limiting values for an airplane with unsupercharged engine, *i. e.*,  $W/P_{a0} = 3$ ,  $W/S = 4$ ,  $C_L = 0.7$  and  $(L/D)_{mx} = 16.6$  and  $r = 4.7$ , we find  $\rho/\rho_0 = 0.298$  corresponding to a ceiling of about 36,000 ft., which limit can probably only be raised by the use of a satisfactory controllable-pitch propeller.

We now have two extreme cases, *i. e.*, a limiting ceiling of 36,000 ft. for an airplane with low loadings and an engine with critical altitude zero, and a limiting ceiling of 80,600 for a hypothetical airplane of higher loadings, controllable pitch propeller and critical engine supercharger altitude of 80,600 ft. To determine a practical limiting ceiling we may assume a linear variation with critical engine supercharger altitude according to the formula,

$$Y = 36,000 + \frac{h}{H} (H - 36,000)$$

where  $h$  and  $H$  are the ideal and practical values of the critical supercharger altitude. Taking these as 80,600 ft. and 30,000 ft. yields a ceiling of 53,000 ft. which does not appear to be beyond the possibilities for the near future.

**5. Range.** From IX (3.3) we have the Breguet range formula:

$$\text{Max. Range} = 863.5 \frac{C_L}{C_D} \times \frac{\eta}{c} \log_{10} \left( \frac{W_1}{W_2} \right)$$

All the factors are average values during the flight, so that a proper estimate of these will enable the limiting practical range to be computed. A ratio of total load  $W_1$  to the weight without fuel  $W_2$  of 2.6 has actually been attained by the Dewoitine D-33 long distance airplane. This might possibly be raised to 3.0 in the future.

The maximum  $C_L/C_D$  or  $L/D$  of an airplane with retractable landing gear may be as high as 20, with an average value during the flight of possibly 16 being attainable. The present  $c$  of 0.50 lb. per hph may be expected to be lowered to 0.45 by increased engine efficiency. An average value of propeller efficiency  $\eta$  of 80 per cent may be attained if a controllable-pitch propeller and engine gearing are assumed. Substituting these values, we obtain a limiting range of

$$\text{Range} = 863.5 \times 16 \times \frac{0.80}{0.45} \log_{10} 3 = 11,750 \text{ miles.}$$

If, however, the same fuel consumption conditions could be maintained at various altitudes, and the airplane flown at maximum  $L/D$  throughout the flight, the above limit would be increased in the ratio 20/16 or

$$\text{Range} = 14,700 \text{ miles.}$$

Although the value of  $L/D$  of 16 above assumed may already be realized in an airplane such as the Bernard 80 G.R., its ratio of  $W_1/W_2$  is only 2.3. Using these values, a fixed pitch propeller efficiency of 65 per cent and  $c = 0.50$ , we derive a range of 6,500 miles which may be considered as not far removed from present attainment, without the use of a controllable-pitch propeller.

**6. Endurance.** Similarly, the limiting endurance can be estimated from the Breguet formula,

$$\text{Max. Endurance} = 863.5 \frac{\eta}{c} \frac{L}{D} \frac{1}{V} \log_{10} \left( \frac{W_1}{W_2} \right)$$

Using the same values as for the range computation, and assuming an average minimum speed of 55 m.p.h. throughout the flight, we find,

$$\text{Max. Endurance} = 11,750 \div 55 = 214 \text{ hours.}$$

The endurance cannot be increased by flying at altitude, since this would require flight at a higher minimum speed.

If we assume the same values as in the last case above for range, and assume also a more reasonable figure for average speed of 70 m.p.h., we find an endurance of 93 hours, which should be attained in the near future.

## APPENDIX I THE INDUCED DRAG OF ANY BIPLANE

In Prandtl's discussion of the induced drag of multiplanes<sup>1</sup>, solutions of the fundamental equation for biplanes are given for the special case of a division of lift giving minimum induced drag. This solution may be generalized and when put in graphical form furnishes a ready determination of the equivalent monoplane span for any biplane with any lift division between the two wings. In such form, furthermore, the diagrams permit a visualization of the effect on the induced drag of improper disposition of areas in the case of wings of unequal span or chord.

**Equivalent Monoplane Span for any Biplane.** The well-known equation for the induced drag of the biplane is

$$D_i = \frac{1}{\pi q} \left[ \frac{L_1^2}{b_1^2} + 2\sigma \frac{L_1 L_2}{b_1 b_2} + \frac{L_2^2}{b_2^2} \right] \quad (1)$$

<sup>1</sup> U.S. N.A.C.A. Technical Note No. 182, also "Technische Berichte", III, No. 7, pp. 309—315.

In this formula  $L$  = lift,  $b$  = span and  $\sigma$  is the Prandtl coefficient. The subscript <sub>1</sub> is intended to refer to the longer wing which may be either the upper or the lower.

The equivalent monoplane is defined as one having the same lift and induced drag as the biplane. Let  $L = L_1 + L_2$  be its lift and  $b$  its span. Then the induced drag will be

$$D_i = \frac{1}{\pi q} \cdot \frac{L^2}{b^2}$$

$$\text{Let } L_1 = aL$$

$$L_2 = (1 - a)L$$

$$b_2 = r$$

$$b_1$$

Then equating these two values of the induced drag and reducing in terms of  $a$  and  $r$  we readily find

$$\frac{b}{b_1} = K = \frac{r}{[a^2(r^2 - 2\sigma r + 1) + 2a(\sigma r - 1) + 1]^{1/2}}$$

In Fig. 51 values of  $\sigma$  are shown graphically as a function of  $G/b_1$  and  $r$  ( $G$  = gap).

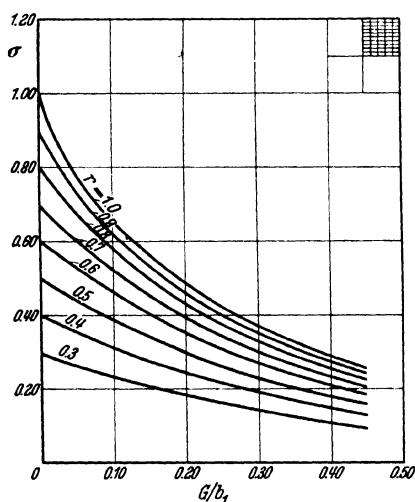


Fig. 51. Values of  $\sigma$  as a function of  $G/b_1$  and  $r$ .

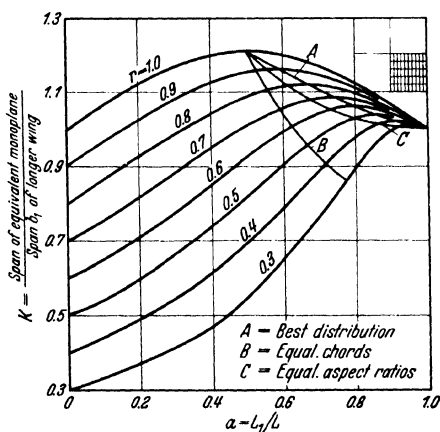


Fig. 52. Values of  $K$  as a function of  $r$  and  $a$  ( $G/b_1 = .30$ ).

In Fig. 52,  $K$  has been plotted as a function of  $r$  and  $a$  for  $G/b_1$  constant at .30. This chart is interesting in that it shows the increase in variation of  $K$  with  $a$  as  $r$  becomes increasingly less than unity. It also shows the well known fact that an equal span biplane with fifty-fifty lift distribution is the most favorable arrangement with a given span. The curve marked  $A$  intersects the values corresponding to best distribution given by Prandtl for  $G/b_1 = 0.3$ . Curve  $B$  intersects values for equal chords, and curve  $C$  intersects values for equal aspect ratios, assuming, as Prandtl

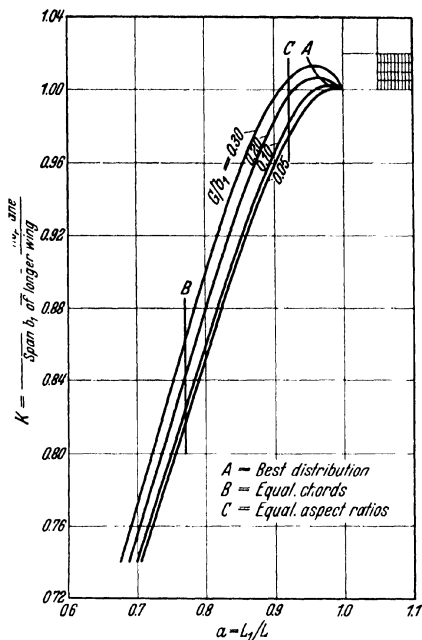


Fig. 53. Values of  $K$  as a function of  $G/b_1$  and  $a$  for  $r = 0.3$ .

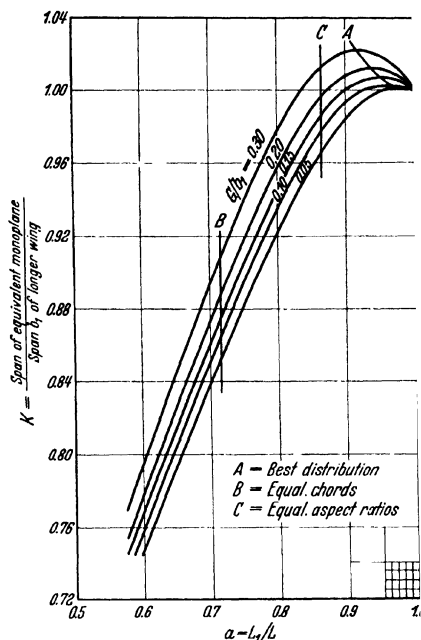
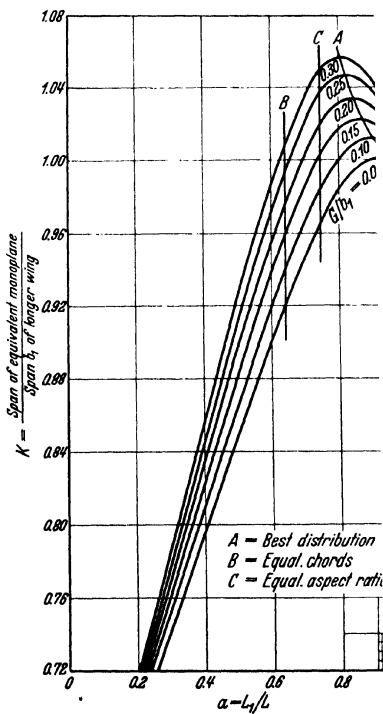
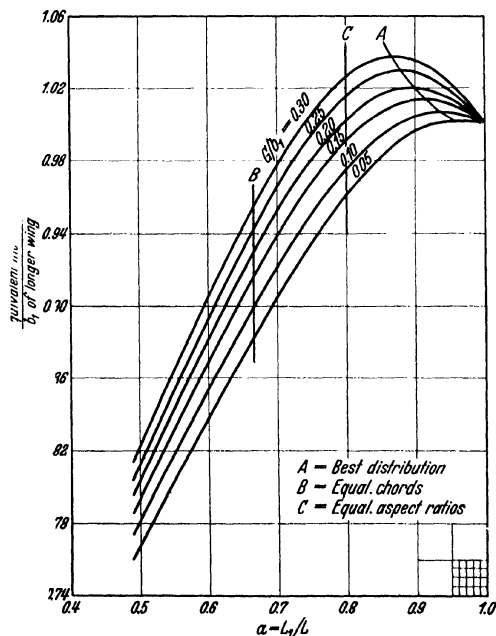


Fig. 54. Values of  $K$  as a function of  $G/b_1$  and  $a$  for  $r = 0.4$ .



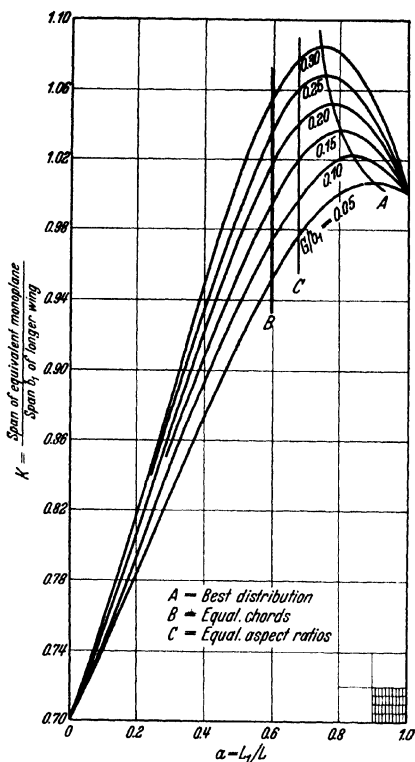


Fig. 57. Values of  $K$  as a function of  $G/b_1$  and  $\alpha$  for  $r = 0.7$ .

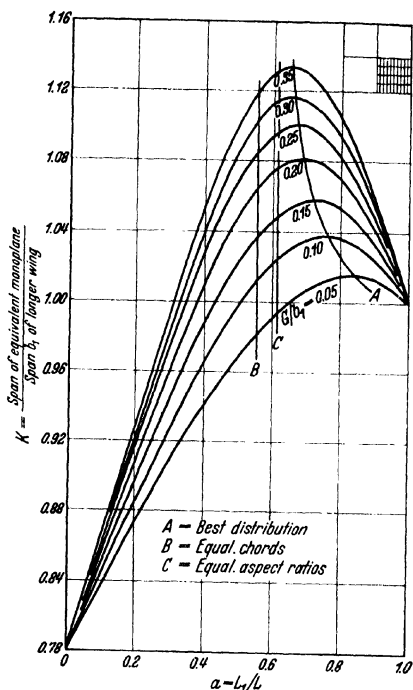


Fig. 58. Values of  $K$  as a function of  $G/b_1$  and  $\alpha$  for  $r = 0.8$ .

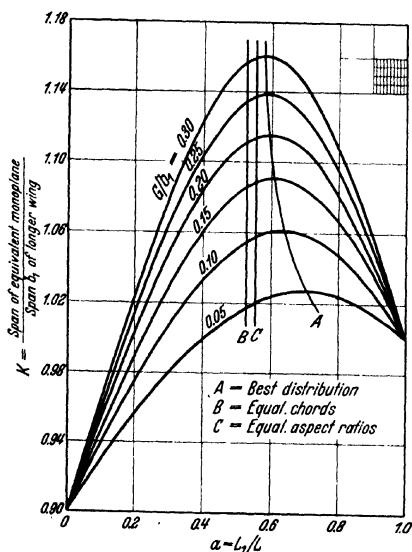


Fig. 59. Values of  $K$  as a function of  $G/b_1$  and  $\alpha$  for  $r = 0.9$ .

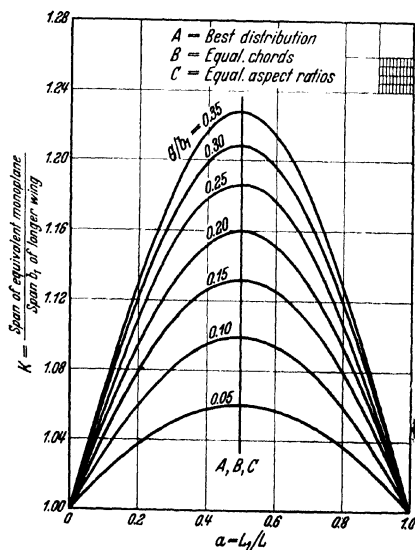


Fig. 60. Values of  $K$  as a function of  $G/b_1$  and  $\alpha$  for  $r = 1.0$ .



does, that the lifts are proportional to the areas. It should be remembered, when comparing two lift distributions, that the induced drag varies as the inverse square of the ratio of the  $K$  values.

Holding  $r$  constant,  $K$  can be found as a function of  $G/b_1$  and  $a$ , the fraction of the total lift carried by the longer wing<sup>1</sup>. Figs. 53 to 60 give values for  $r = 0.3$  to  $r = 1.0$ . Straight line interpolation may be made with good approximation for intermediate values of  $r$ .

In comparing these diagrams with the original paper by Prandtl it may be pointed out that the points indicated on the diagrams of Figs. 53—60 by the line  $A$  correspond to the values in Prandtl's diagram Fig. 6 with the following changes in notation.

$$\begin{aligned} a &= (1 - x) \text{ (Prandtl)} \\ r &= \mu \\ G/b_1 &= h/b_1. \\ K &= 1/\kappa. \end{aligned}$$

## APPENDIX II BIPLANE WING LIFT COEFFICIENTS

Two recent N.A.C.A. Technical Reports<sup>2</sup> embody a complete exposition of the latest available information as to the effects on the individual wing lift coefficients, of stagger, wing thickness, gap, decalage, overhang, unequal chords, and unequal effective areas. The purpose of this appendix is to present in summarized form a simplified practical solution for  $C_{Lu}$  and  $C_{LI}$  based on the data of these reports, except for certain practical compromises and the elimination of an inconsistency as noted later.

First are listed the known cellule and wing characteristics, followed, by computations and references to the diagrams of this appendix in the order corresponding to the quickest solution. A sample computation parallels the general presentation.

Given:

$b_u = 40$ ft.	Overall span of upper wing.
$b_l = 20$ ft.	Overall span of lower wing.
$b'_u = 40$ ft.	Net span of upper wing (overall less fuselage cut-out).
$b'_l = 17.4$ ft.	Net span of lower wing (overall less fuselage cut-out).
$S_u = 300$ sq. ft.	Gross area of upper wing <sup>3</sup> .

<sup>1</sup> Reference may be made to Appendix II for formulae giving  $C_{Lu}$  and  $C_{LI}$  whence  $a = C_{Lu}S_u/(C_{Lu}S_u + C_{LI}S_l)$ .

<sup>2</sup> DIEHL, WALTER S., Relative Loading on Biplane Wings, U.S. N.A.C.A. Technical Report No. 458; and Relative Loading on Biplane Wings of Unequal Chords, U.S. N.A.C.A. Technical Report No. 501.

<sup>3</sup> Assuming wings continuous from tip to tip.

$S_l = 76$ sq. ft.	Gross area of lower wing <sup>1</sup> .
$S'_u = 300$ sq. ft.	Net area of upper wing (gross less cut-outs).
$S'_l = 64$ sq. ft.	Net area of lower wing (gross less cut-outs).
$c'_u = 7.5$ ft. $= S'_u/b'_u$	Mean geometric chord of upper wing.
$c'_l = 44$ in. $= S'_l/b'_l$	Mean geometric chord of lower wing.
$G = 66$ in.	Distance normal to zero lift direction <sup>2</sup> .
Stagger = 44 in.	Distance parallel to zero lift direction <sup>2</sup> .
$t_l = 6.6$ in.	Maximum thickness of $c'_l$ .
$\delta = 3^\circ$ .	Decalage in degrees.

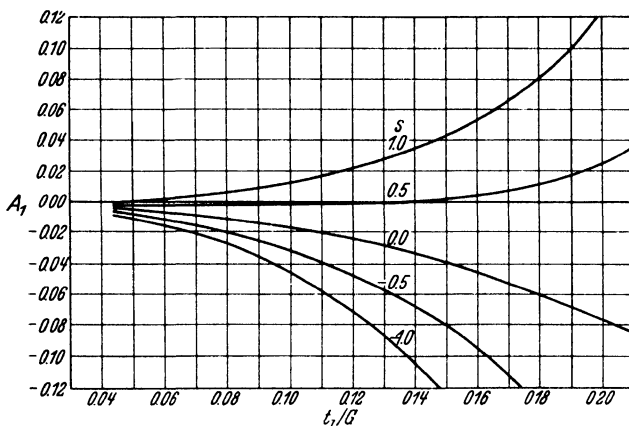


Fig. 61. Values of  $A_1$  plotted on  $t_l/G$  for constant values of stagger  $s$ .

Solution:

$$t_l/G = 0.10 = 6.6/66.$$

$$s = 1.0 = \text{stagger}/c'_l = 44/44.$$

$$A_1 = 0.012 \text{ from Fig. 61, function of } t_l/G \text{ and } s.$$

$$\frac{b_u - b_l}{b_u} = 0.50 = \frac{40 - 20}{40}$$

$$F_1 = 0.50 = 1 - \frac{b_u - b_l}{b_u}$$

$$G/c'_l = 1.5 = 66/44.$$

$$B_1 = -0.0596 \text{ from Fig. 62, function of } G/c'_l.$$

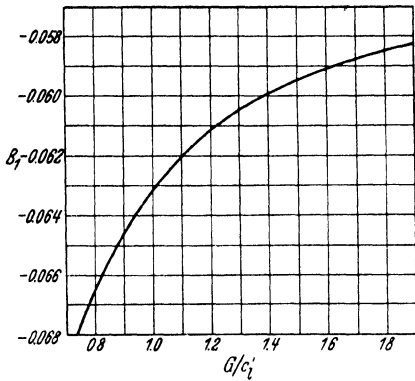
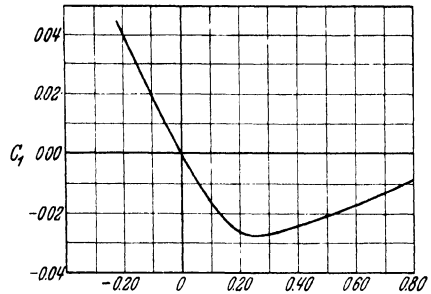
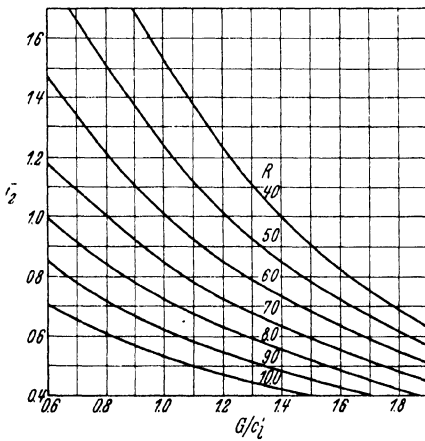
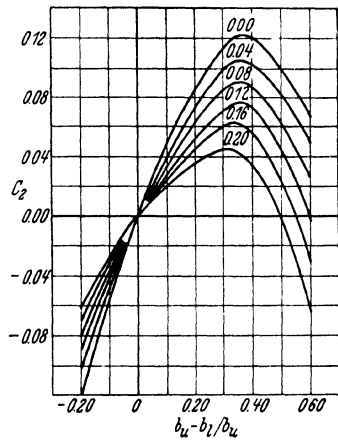
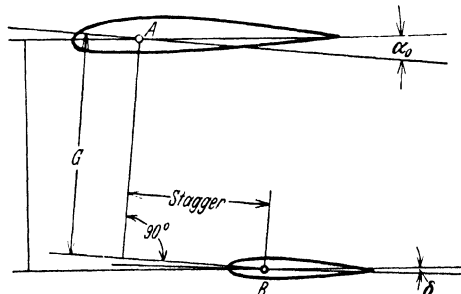
$$C_1 = -0.015 \text{ from Fig. 63, function of } \frac{b_u - b_l}{b_u}$$

$$D = c'_l/c'_u = \frac{S'_l}{S'_u} \times \frac{b'_u}{b'_l} = \frac{64}{300} \times \frac{40}{17} = 0.50.$$

$$K_1 = [F_1 (A_1 + B_1 \delta) + C_1] D \\ = [0.50 (0.012 + 3 \times (-0.0596)) + (-0.015)] 0.50 = -0.049.$$

<sup>1</sup> See footnote 3, page 337.

<sup>2</sup> Between mean aerodynamic centers of upper and lower wings as shown in Fig. 66.


 Fig. 62. Values of  $B_1$  on  $G/c'_l$ .

 Fig. 63. Values of  $C_1$  as a function of  $\frac{b_u - b_l}{b_u}$  when  $b_u > b_l$  or of  $\frac{b_l - b_u}{b_l}$  when  $b_u < b_l$ .

 Fig. 64. Values of  $F_2$  on  $G/c'_l$  for constant values of  $R$ .

 Fig. 65. Values of  $C_2$  on  $\frac{b_u - b_l}{b_u}$  for constant values of  $A_2 F_2 + B_2 \delta$ .

 Fig. 66.  $A$  and  $B$  are aerodynamic centers of upper and lower wing respectively.

$$A_2 = 0.050 + 0.17 s = 0.050 + 0.17 \times 1 = 0.22.$$

$$R = \frac{1}{2} \left[ \frac{b_u^2}{s_u} + \frac{b_l^2}{s_l} \right] = \frac{1}{2} \left[ \frac{40^2}{300} + \frac{20^2}{76} \right] = 5.3.$$

$$F_2 = 0.76 \text{ from Fig. 64, function of } R \text{ and } G/c'_l.$$

$$B_2 = 0.0186.$$

$$(A_2 F_2 + B_2 \delta) = 0.22 \times 0.76 + 0.0186 \times 3 = 0.223.$$

$$C_2 = -0.013 \text{ from Fig. 65, function of } \frac{b_u - b_l}{b_u} \text{ and } (A_2 F_2 + B_2 \delta).$$

$$K_2 = [A_2 F_2 + B_2 \delta + C_2] D = [0.223 - 0.013] 0.50 = 0.105.$$

$$E = 4.68 = S'_u/S'_l = 300/64.$$

$$C_{Lu} = (1 + K_2) C_L + K_1 = (1 + 0.105) C_L - 0.049.$$

$$C_{Lu} = 1.105 C_L - 0.049.$$

$$C_{Li} = (1 - K_2 E) C_L - K_1 E \\ = (1 - 0.105 \times 4.68) C_L - (-0.049 \times 4.68).$$

$$C_{Li} = 0.508 C_L + 0.23.$$

$$\text{When } C_L = 0, C_{Lu} = -0.049, C_{Li} = 0.23.$$

$$\text{When } C_L = 1.0, C_{Lu} = 1.056, C_{Li} = 0.738.$$

Remarks: (1) It should be noted that the methods in Technical Report No. 501 of correcting for overhang in Figs. 4 and 6 are subject to correction in that  $K_{10}$ ,  $K_{11}$  and  $K_{12}$ , as well as  $F_2 \times K_{20}$  and  $K_{21}$ , should correspond to  $c_l/c_u$  equals unity, *i. e.*, equal chords. The correction for unequal chords should have been introduced later by multiplication of the values of  $K_1$  and  $K_2$  for equal chords by the ratio of geometric chords of the lower to upper wing.

(2) Gross areas are used only for the determination of the average aspect ratio.

(3) For the case of deflected flaps an equivalent decalage should be introduced.

(4) In a correct solution the derived straight lines for  $C_{Lu}$  and  $C_{Li}$  will intersect at the corresponding value of  $C_L$  of the cellule.

(5) The use of the mean aerodynamic centers makes this method of solution applicable also to those cases where the wings incorporate sweep back and/or taper in plan form.

(6) Wings incorporating twist are a special problem not directly amenable to the procedure of this appendix.

### References

The following references, gathered here in a single list, will serve also as a brief bibliography to some of the more readily accessible literature on the subject of airplane performance.

1. EIFFEL, G., *Nouvelles Recherches sur la Résistance de l'Air et l'Aviation*, Paris, 1914.
2. BAIRSTOW, L., *Applied Aerodynamics*, London, 1920.
3. KERBER, L. V., *An Empirical-Theoretical Method für the Comparative Prediction of Airplane Performance*, Air Service Information Circular No. 68, 1920.
4. WATTS, H. C., *The Design of Screw Propellers for Aircraft*, London, 1920.
5. WEICK, R. E., *Aircraft Propeller Design*, New York, 1930.
6. KERBER, L. V., *Airplane Performance and Design Charts*, Air Service Information Circular No. 183, 1921.
7. PRANDTL, L., *Induced Drag of Multiplanes*, U.S. N.A.C.A. Technical Note No. 182, 1924.
8. BROMBACHER, W. G., *Tables for Calibrating Altimeters and Computing Altitudes Based on the Standard Atmosphere*, U.S. N.A.C.A. Technical Report No. 246, 1926; see also U.S. N.A.C.A. Technical Report No. 538, 1935.
9. DIEHL, W. S., *Three Methods of Calculating Range and Endurance of Airplanes*, U.S. N.A.C.A. Technical Report No. 234, 1926.
10. WARNER, E. P., *Airplane Design, Aerodynamics*, McGraw-Hill, 1927.
11. BAILEY, N. R., *Variation of the Brake Horsepower of Supercharged Engine, with Altitude*, Air Corps Material Division Report, Serial No. 3132, 1928.
12. DE PORT, THEO, *Variation of Parasite Drag as a Function of the Lift Coefficient*, Air Corps Material Division Report, Serial No. 3080, 1929.
13. LESLEY, E. P., and REID, E. G., *A New Method for the Prediction of Airplane Performance*, U.S. N.A.C.A. Technical Note No. 302, 1929.
14. OSWALD, W. BAILEY, *Precise Algebraic Performance Formulae and Charts*, Daniel Guggenheim School of Aeronautics, California Institute of Technology, 1930; see also U.S. N.A.C.A. Technical Report No. 408, 1932.
15. U.S. N.A.C.A. Technical Notes Nos. 340, 1930; 456, 480, 481, 1933; 525, 1935.
16. DE PORT, THEO, *Possible Limits of Airplane Performance*, Air Corps Technical Report, A.D.M. 1255, 1931.
17. U.S. N.A.C.A. Technical Report No. 384, 1931; also U.S. N.A.C.A. Technical Note No. 426, 1932.
18. U.S. N.A.C.A. Technical Note No. 412, 1932; also U.S. N.A.C.A. Technical Reports Nos. 446, 1933; 492, 1934; 530, 1935.
19. U.S. N.A.C.A. Technical Note No. 432, 1932; also U.S. N.A.C.A. Technical Reports Nos. 414, 1932; 462, 1933.
20. U.S. N.A.C.A. Technical Report No. 481, 1933.
21. Air Corps Information Circular No. 679, 1933.
22. U.S. N.A.C.A. Technical Report No. 484, 1933.
23. RELF, E. F., *Results from the Compressed Air Tunnel*, Journal of the Royal Aeronautical Society, January 1935.

## INDEX

- Accelerations, mass 129.
- Aerodynamic moments 22.
- Aileron rolling moments 83.
  - tail interference 40.
  - yawing moments 84.
- Ailerons and wing tip slots 85.
- Air reactions, dependence on velocity components 124.
  - on an isolated wing 23.
- Airscrew, contribution of to  $M_q$  46.
  - , — — — pitching moments 34, 35.
  - , influence of on  $M_x$  52.
  - , — on damping of oscillation 95.
  - slip-stream, influence of on tail 47.
  - wing interference 40.
- Air speed, indicated 9.
- Altitude propeller, choice of 320.
- Apparent gravity 16.
- Asymmetric controls 82.
  - derivatives, comparison between model and full scale experiments 75.
  - , effect of large angular velocities on 75.
  - equations 129.
  - , changes of dihedral angle and fin area 202.
  - , changes of dihedral angle and fin area, increasing oscillations 202.
  - , changes of dihedral angle and fin area, spinning instability 203.
  - , changes of dihedral angle and fin area, spiral instability 202.
- Asymmetric equations, complementary function 185.
  - , — — —, complex root 187.
  - , — — —, large real root 187.
  - , — — —, quartic for  $\lambda$  185.
  - , — — —, small real root 187.
  - , — — —, values of  $\lambda$  185.
  - , complete solutions and initial conditions 188.
  - , complete solutions and initial conditions, conditions to which applicable 188.
  - , complete solutions and initial conditions, conversion to ordinary units 189.
  - , complete solutions and initial conditions, dimensionless form 188.
  - , complete solutions and initial conditions, graphs plotted on time 191.
  - , graphs discussed 192—199.
  - , information by inspection of quartic for  $\lambda$  199.
  - , information by inspection of quartic for  $\lambda$ , complex roots 200.
  - , information by inspection of quartic for  $\lambda$ , condition for complete stability 199.
- Asymmetric equations, information by inspection of quartic for  $\lambda$ , large root 199.
  - , information by inspection of quartic for  $\lambda$ , level and climbing flight 201.
  - , information by inspection of quartic for  $\lambda$ , small root 200.
  - , numerical solutions of 182.
  - , — — —, choice of examples 183.
  - , — — —, cruising speed 183.
  - , — — —, dimensionless constants 185.
  - , — — —, slow speed 184.
  - , — — —, stalled flight 184.
  - flight, straight 18.
  - moment derivatives, typical values for 81.
  - moments 57.
  - , effects of side-slip with dihedral angle 59.
  - , estimates of rolling moments due to side-slip 60.
  - , independent variables which govern 59.
  - in relation to controls 59.
  - motion of stalled aeroplane 119.
  - motions 104.
- Atmosphere, standard 226, 242.
- Auto-rotation and wing tip slots 81.
- Axes, change of 71.
  - of reference 57, 121, 144, 182.

- Baird's method 267.  
 Bank, relation of side-slip to 19.  
 Banked, true, steady turn 105.  
 Biplane wing lift coefficients 337.  
 Body and minor parts, contribution of to pitching moments 36.  
 Body-tail interference 40.  
 Breguet's formulas 312.  
 Bump 98.
- Ceiling, absolute 330.  
 Ceilings 255.  
 Center of gravity position, effect on static stability 26.  
 — — — positions for neutral equilibrium 27.  
 Chord axes 71.  
 — — —, conversion to 61.  
 Circling flight 19.  
 — — —, pitching moments in 44.  
 — — —, tail in 44.  
 Climb, angle of 255.  
 —, rate of 252, 329.  
 —, speed of 269.  
 —, time of 256.  
 Climbing and gliding flight 95.  
 — flight 12.  
 Complementary function 135.  
 — —, general form of 137.  
 Complex roots 138, 141.  
 Continuous rotation methods for measurement of rotary derivatives 73.  
 Control and stability, relation between 28.  
 Controls, asymmetric 82.  
 —, balanced 82.
- Damping of oscillation 94.  
 —, rapid, of rolling motions 110.  
 Density ratio 226.  
 Derivative  $L_v$  in stalled flight 62.  
 —  $M_q$  45.
- Derivative  $M_q$ , experimental methods of measuring 48.  
 —  $M_{\dot{w}}$  148.  
 Derivatives, evaluation of 145.  
 —, force-rotary 147.  
 —, force-velocity 146.  
 —, moment-rotary 148.  
 —, moment-velocity 148.  
 —, numerical values of 149.  
 Diehl, Walter S. 337.  
 Dimensionless coefficient  $k_{mq}$  45.  
 — — —, numerical values 47.  
 — coefficients 7, 27, 58.  
 — —  $k_{lr}$  and  $k_{nr}$  69.  
 — form, conversion to 130, 134.  
 — system explained 132.  
 Drag, induced 230.  
 —, parasite 225.  
 —, profile 232.  
 —, structural 233.  
 —, total 239.
- Efficiency maximum and design  $v/nD$  245.  
 Elevators 25.  
 —, sudden application of 98.  
 Empirical-theoretical method 294.  
 Endurance 333.  
 — of airplanes 305, 311.  
 Engine speed and power, variation of at sea level 246.  
 Equations of motion 121, 123.  
 — — —, axes 121.  
 — — —, dependence of air reactions on velocity components 124.  
 — — —, dimensionless form 130, 134.  
 — — —, dimensionless system explained 132.  
 — — —, parameter  $\mu$  131.  
 — — —, small disturbances 126.
- Equations of motion, small disturbances, applied forces 128.  
 — — —, — — —, force and moment derivatives 127.  
 — — —, — — —, mass accelerations 129.  
 — — —, — — —, notation, shortened 128.  
 — — —, — — —, separation into symmetric and asymmetric groups 129.  
 — — —, solutions 135.  
 — — —, — — —, asymmetric group 138.  
 — — —, — — —, complementary function 135, 137.  
 — — —, — — —, complex roots 138, 141.  
 — — —, — — —, constant applied control couples 141.  
 — — —, — — —, constant applied control couples, asymmetric group, no roots zero 142.  
 — — —, — — —, constant applied control couples, asymmetric group, one root zero 143.  
 — — —, — — —, constant applied control couples, equal roots 144.  
 — — —, — — —, constant applied control couples, symmetric group, no roots zero 141.  
 — — —, — — —, constant applied control couples, symmetric group, one root zero 142.  
 — — —, — — —, constant applied control couples, two roots zero 144.  
 — — —, — — —, initial conditions 137.  
 — — —, — — —, quartic for  $\lambda$  136.  
 — — —, — — —, ratios  $u_1$ ,  $w_1$ ,  $q_1$  136.  
 — — —, — — —, step by step methods of solution 125.  
 — — —, symbols 122.

- Equivalent flat plate area 237.  
 — monoplane aspect ratio 226.  
 — — — and induced drag 230.  
 — — span for any biplane 333.  
 Experimental methods of measuring  $M_q$  48.  
 — results for  $M_q$  in normal flight 52.  
 — — — — stalled flight 53.  
 — separation of  $M_q$  and  $M_{\dot{\alpha}}$  51.  
 — values of  $k_{lr}$  and  $k_{nv}$  for complete model aeroplanes 65.  
 Experiments on complete models 29.  
 — rotary derivatives, discussion of 74.  
 — with finite rates of roll and strip hypothesis, comparison between 78.  
 — yawing and strip hypothesis, comparison between 79.  
 Fixed tail and elevators 25.  
 Flat turn 19.  
 Flight, asymmetric 18.  
 —, circling 19.  
 —, climbing 12.  
 —, free, simple discussion 85.  
 —, gliding 10.  
 —, — and climbing 95.  
 —, horizontal 7.  
 —, normal, experimental results for  $M_q$  52.  
 —, —, rudder in 84.  
 — path, equation to 87.  
 —, forms of 88.  
 — of real aeroplane, comparison with ideal 89.  
 —, radius of curvature of 14.  
 —, stalled, experimental results for  $M_q$  53.  
 —, —, rudder in 85.  
 Flight, straight, small disturbances from 109.  
 —, symmetric 5.  
 —, —, accelerated 13.  
 Force and moment derivatives 127.  
 Forced oscillation method for measuring  $M_q$  49.  
 Forces applied 128.  
 — on tail and interference factors 36.  
 Free elevators and hinge moments 38.  
 — flight, simple discussion 85.  
 — oscillation method for measuring  $M_q$  48.  
 Geometric mean chord 23, 54.  
 — — —, application to biplane 56.  
 — — — with wings non-rectangular and with dihedral 56.  
 — — — — twisted and tapered 57.  
 Gliding and climbing flight 95.  
 — flight 10.  
 Gravity, apparent 16.  
 —, effect of 123.  
 Hinge moments and free elevators 38.  
 Horizontal turn of minimum radius 21.  
 Incidence adjustment, rapid 96.  
 —, sudden change of 96.  
 Indicated air speed 9, 270.  
 — r.p.m. 272.  
 — — available 273.  
 — — required 272.  
 — speed 268.  
 Induced drag and equivalent monoplane aspect ratio 230.  
 — of any biplane 333.  
 Initial conditions 137.  
 Instability, two forms of 117.  
 Interference 36—41.  
 — between aeroplane and tail 37.  
 — factors and forces on tail 36.  
 —, numerical values 41.  
 — problems discussed 41.  
 Joukowski's theoretical values 31.  
 Lanchester's idealized flight path 86.  
 Landing problem, some aspects of 11.  
 Lesley-Reid method 270.  
 — — —, climb and ceilings 274.  
 — — —, description of 271.  
 — — —, effect of altitude on power 271.  
 — — —, example 274.  
 — — —, minimum speed 274.  
 — — —, propeller coefficients 271.  
 Lift coefficient and speed 227.  
 Limits of performance 324.  
 — — —, absolute, ceiling 330.  
 — — —, endurance 333.  
 — — —, high speed 328.  
 — — —, range 332.  
 — — —, rate of climb 329.  
 — — —, speed range 324.  
 Load factor, maximum 17.  
 — factors 16.  
 — grading curve 69.  
 Logarithmic diagrams 296.  
 — —, method of use 303.  
 — —, theory 297.  
 Maximum efficiency and design  $v/nD$  245.  
 Mean chord, geometric 23, 54.  
 Metacentric height 28.  
 Minimum radius of horizontal turn 21.



- Model aeroplanes, experimental values of  $k_{lv}$  and  $k_{nv}$  for 65.
- Models, complete, experiments on 29.
- Moment and force derivatives 127.
- Moments, aerodynamic 22.
- , asymmetric 57.
- due to finite rates of roll, estimates of 77.
- — — rate of roll 70.
- — — — yaw 67.
- , pitching 22.
- , —, contribution of separate parts to 29.
- Neutral aeroplane, statically, oscillation of 116.
- equilibrium, e.g. positions for 27.
- Non-dimensional coefficients 225.
- Notation 144.
- shortened 128.
- Numerical examples. choice of 149.
- Orientation of aeroplane in space 122.
- Oscillation and rotation experiments, comparison between 80.
- , damping of 94.
- , forced, method for measuring  $M_q$  49.
- , free, method for measuring  $M_q$  48.
- , ideal, simple 90.
- , influence of airscrew on damping of 95.
- methods for measurement of rotary derivatives 73.
- of real aeroplane, comparison with ideal 91.
- — small amplitude, form of 90.
- — statically neutral aeroplane 116.
- — — stable aeroplane 113.
- — — — unstable aeroplane 117.
- Oscillation, other factors which influence 95.
- , period of, effect of  $M_q$  on 91.
- , slow, of small amplitude 90.
- Oscillations, treatment with more complete assumptions 99.
- , — — — —, discussion of results 101.
- Oswald method 279.
- , —, assumptions 281.
- , —, charts 285.
- , —, example by 291.
- , —, parameters 280, 292.
- , —, theory 282.
- Parameter  $\mu$  131.
- Parasite drag 225.
- coefficient 240.
- Performance from power graphs 250.
- , influence of principal factors on 25.
- , influence of principal factors on airfoil characteristics 318.
- , influence of principal factors on E.M.A.R. 318.
- , influence of principal factors on parasite resistance 319.
- , influence of principal factors on power 316.
- , influence of principal factors on propeller characteristics 319.
- , influence of principal factors on supercharging and throttling 320.
- , influence of principal factors on weight 315.
- , influence of principal factors on wing area 317.
- , limits of 324.
- , —, absolute ceiling 330.
- , —, — endurance 333.
- , —, — high speed 328.
- , —, — range 332.
- Performance, limits of rate of climb 329.
- , — — speed range 324.
- , —, summary 264, 265.
- Period of oscillation, effect of  $M_q$  on 91.
- Pitching moment from tail and wings 30.
- moments 22.
- — and static stability 22.
- — at high speeds 42.
- —, contribution of airscrew to 34, 35.
- —, — — separate parts to 29.
- —, — to of body and minor parts 36.
- — — in circling flight 44.
- — — stalled flight 43.
- — — when c.g. is not on wing chord 32.
- Power absorbed by any propeller 321.
- at altitude 271.
- available 243.
- at altitudes, form for 248, 250.
- — — sea level and at altitudes 247, 248.
- — — —, form for 245.
- — — — — from special propeller 323.
- — — from ratio of thrust power 263.
- — — variation of r.p.m. with speed 261.
- required 239.
- — by estimating  $A$  directly 258.
- — — summarizing component drags 257.
- —, forms for 229.
- — in a true-banked turn 21.
- —, summary 256, 257.
- —, —, form for 264.
- Profile drag 232.
- coefficient 240.
- Propeller diameter, choice of 244.
- , equation for, values of  $K$  249.

- Propeller efficiency, variation in 247.  
 — and altitudes, choice of 320.  
 —, power absorbed by 321.
- Quadratic for  $\lambda$ , dimensionless form of 103.  
 Quartic equation for  $\lambda$  136.
- Radius of curvature, minimum 14, 15.  
 — — — of flight path 14.
- Range 332.  
 — of airplanes 305.
- Rapid incidence adjustment 96.
- Rate of roll, moments due to 70.
- References 221, 341.
- Roll and yaw, estimates of moments due to angular velocities of 67.  
 —, moments due to rate of 70.
- Rolling moment due to yawing 69.  
 — moments, aileron 83.  
 — motions, rapid damping of 110.
- Rotary derivatives, approximate formulæ for 71.  
 — —, calculations of, using chord axes 72.  
 — —, comparison between experiment and "strip" calculation 74.  
 — — — — model and full scale experiments 75.  
 — —, discussion of experiments on 74.  
 — — due to body, fin and rudder 73.  
 — —, experimental methods of measuring 73.  
 — —, influence of body, fin and rudder on 75.  
 — — in normal flight, summary 75.  
 — — in stalled flight 76.
- Rotation and oscillation experiments, comparison between 80.
- Rudder in normal flight 84.  
 — — stalled flight 85.
- Side-force, relation to side-slip 18.  
 Side-lip 58.  
 —, effect on body, fin and rudder 63.  
 —, effects of, measurements of on isolated wing 62.  
 — — —, omission in the assumptions regarding 61.  
 — in flat turn 20.  
 —, relation of side-force to 18.  
 — — to bank 19.  
 —, steady straight 18.  
 — with steady turn 107.
- Side-slips, large, effects of 67.
- Slots, wing tip, and ailerons 85.  
 — — —, auto-rotation 81.
- Speed, maximum 250, 328.  
 — range 324.
- Spin 204.  
 —, air yawing moment 217.  
 —, autorotation 208, 209.  
 — — about fixed axis 208.  
 — —, latent 209.  
 — —, rates 210.  
 —, centrifugal yawing moment 218.  
 —, effects of yaw on 215, 216.  
 —, experimental methods 205.  
 —, free of real aeroplanes 219.  
 — — — —, failure of ailerons and rudder to check 221.  
 — — — —, incidence 219, 220.  
 — — — —, load factor 220.  
 — — — —, radius 219.  
 — — — —, rate of descent 219.
- Spin, free of real aeroplanes, rotation rate 219.  
 — — — —, transition to flat spin 220.  
 —, notation and equations of motion 207.  
 —, pitching moments 210.  
 — — —, balance of 213.  
 — — —, centrifugal 210, 211.  
 —, relation between yaw and side-slip 216.  
 —, remaining degrees of freedom 214, 215.  
 —, theoretical calculations 206.
- Spiral motion, more accurate estimate of 113.  
 — —, slow 111.
- Stable aeroplane, statically, oscillation of 113.  
 — aeroplanes 103.
- Stability and control, relation between 28.  
 —, static, effect of position of center of gravity on 26.
- Stalled aeroplane, asymmetric motion 119.  
 — —, symmetric motion 118.  
 — flight, derivative  $L_r$  in 62.  
 — —, experimental results for  $M_q$  53.  
 — —, pitching moments in 43.  
 — —, rotary derivatives in 76.  
 — —, rudder in 85.
- Stalling speed in a true banked turn 20.
- Standard atmosphere, altitude-pressure-temperature table 242.
- Static stability and pitching moments 22.  
 — —, effect of position of center of gravity on 26.  
 — —, simplification by assuming 126.
- Step by step methods of solution 125.

- Strip hypothesis and experiments with yawing, comparison between 79.
- — — results of experiments with finite rates of roll, comparison between 78.
- Structural drag 233.
- Symbols 57, 122.
- Symmetric equations 129.
- — —, complementary function 152.
- — —, — — —, quartic for  $\lambda$  152.
- — —, — — —, values of  $\lambda$  and of ratio  $u_1, w_1, q_1$  154.
- — —, complete solutions and initial conditions 157.
- — —, complete solutions and initial conditions, conditions to which solutions apply 160.
- — —, complete solutions and initial conditions, conversion to ordinary units 162.
- — —, complete solutions and initial conditions, dimensionless form 160.
- — —, complete solutions and initial conditions, graphs on time 163.
- — —, complete solutions and initial conditions, in terms of other variables 163.
- — —, complete solutions and initial conditions, solutions discussed 161.
- — —, constants tabulated 151.
- — —, graphs discussed 164—168.
- — —, level flight 174.
- Symmetric equations, level flight, effect of airscrew on  $B, C, E$  in quartic for  $\lambda$  179.
- — —, — — —, effect of airscrew on damping of slow motion 180.
- — —, — — —, effect of airscrew on  $m_q$  and  $m_{\dot{w}}$  175.
- — —, — — —, effect of airscrew on  $m_u$  178.
- — —, — — —, effect of airscrew on  $m_w$  175.
- — —, — — —, effect of airscrew on  $x_u$  177.
- — —, — — —, effect of airscrew on  $x_u, z_u, z_w$  176.
- — —, — — —, effect of freeing elevators 181.
- — —, — — —, numerical values 180.
- — —, — — —, value of  $dT/dV$  for airscrew 176.
- — —, — — —, normal flight 168.
- — —, — — —, gliding flight, engine off 171.
- — —, — — —, large quadratic root 172.
- — —, — — —, numerical values 172.
- — —, — — —, quartic of  $\lambda$  169.
- — —, — — —, small quadratic root 173.
- — —, — — —, wind axes 170.
- — —, flight 5.
- — —, accelerated 13.
- — —, steady straight, forces involved 6.
- — —, motion of stalled aeroplane 118.
- — —, or pitching moments 22.
- Tail, functions of 24.
- — — in circling flight 44.
- True-banked steady turn 165.
- — — turn 20.
- — —, — — —, power required in a 21.
- — —, — — —, stalling speed in a 21.
- Turn, flat 19.
- — —, steady, true banked 105.
- — —, with side-slip 107.
- — —, true banked 20.
- Turns, steady, ascending and descending 108.
- Unstable aeroplane 95, 102.
- — —, statically, oscillation of 117.
- Volume coefficient 64.
- Whirling arm for measuring  $M_q$  48.
- Wind axes 71.
- Wing-tail interference 39.
- — — tip slots and ailerons 85.
- — — — — auto-rotation 81.
- Wings, contribution of to  $M_q$  46.
- Yaw and roll, estimates of moments due to angular velocities of 67.
- — —, moments due to rate of 67.
- Yawing moment due to yawing 69.
- — —, estimate of due to side-slip 61.
- — —, moments, aileron 84.

Printed by Universitätsdruckerei H. Stürtz A.G., Würzburg.





